Pertanika Journal of

SCIENCE & TECHNOLOGY

JST

VOL. 33 (5) AUG. 2025

PERTANIKA JOURNALS

A scientific journal published by Universiti Putra Malaysia Press

Pertanika Journal of Science & Technology
Pertanika Journal of Science & Technology

PERTANIKA JOURNAL OF SCIENCE & TECHNOLOGY

About the Journal

Overview

Pertanika Journal of Science & Technology is an official journal of Universiti Putra Malaysia. It is an open-access online scientific journal. It publishes original scientific outputs. It neither accepts nor commissions third party content.

Recognised internationally as the leading peer-reviewed interdisciplinary journal devoted to the publication of original papers, it serves as a forum for practical approaches to improve quality on issues pertaining to science and engineering and its related fields.

Pertanika Journal of Science & Technology currently publishes 6 issues a year (*January, March, April*, *July, August,* and *October*). It is considered for publication of original articles as per its scope. The journal publishes in **English** and it is open for submission by authors from all over the world.

The journal is available world-wide.

Aims and scope

Pertanika Journal of Science & Technology aims to provide a forum for high quality research related to science and engineering research. Areas relevant to the scope of the journal include: bioinformatics, bioscience, biotechnology and bio-molecular sciences, chemistry, computer science, ecology, engineering, engineering design, environmental control and management, mathematics and statistics, medicine and health sciences, nanotechnology, physics, safety and emergency management, and related fields of study.

History

Pertanika Journal of Science & Technology was founded in 1993 and focuses on research in science and engineering and its related fields.

Vision

To publish a journal of international repute.

Mission

Our goal is to bring the highest quality research to the widest possible audience.

Quality

We aim for excellence, sustained by a responsible and professional approach to journal publishing. Submissions can expect to receive a decision within 90 days. The elapsed time from submission to publication for the articles averages 180 days. We are working towards decreasing the processing time with the help of our editors and the reviewers.

Abstracting and indexing of Pertanika

Pertanika Journal of Science & Technology is now over 33 years old; this accumulated knowledge and experience has resulted the journal being abstracted and indexed in SCOPUS (Elsevier), Journal Citation Reports (JCR-Clarivate), EBSCO, ASEAN CITATION INDEX, Microsoft Academic, Google Scholar, and MyCite.

Citing journal articles

The abbreviation for Pertanika Journal of Science & Technology is *Pertanika J. Sci. & Technol.*

Publication policy

Pertanika policy prohibits an author from submitting the same manuscript for concurrent consideration by two or more publications. It prohibits as well publication of any manuscript that has already been published either in whole or substantial part elsewhere. It also does not permit publication of manuscript that has been published in full in proceedings.

Code of Ethics

The *Pertanika* journals and Universiti Putra Malaysia take seriously the responsibility of all of its journal publications to reflect the highest in publication ethics. Thus, all journals and journal editors are expected to abide by the journal's codes of ethics. Refer to *Pertanika*'s **Code of Ethics** for full details, or visit the journal's web link at http://www.pertanika.upm.edu.my/code_of_ethics.php

Originality

The author must ensure that when a manuscript is submitted to *Pertanika*, the manuscript must be an original work. The author should check the manuscript for any possible plagiarism using any program such as Turn-It-In or any other software before submitting the manuscripts to the *Pertanika* Editorial Office, Journal Division.

All submitted manuscripts must be in the journal's acceptable similarity index range:

≤ 20% – PASS; > 20% – REJECT.

International Standard Serial Number (ISSN)

An ISSN is an 8-digit code used to identify periodicals such as journals of all kinds and on all media–print and electronic.

Pertanika Journal of Science & Technology: e-ISSN 2231-8526 (Online).

Lag time

A decision on acceptance or rejection of a manuscript is reached in 90 days (average). The elapsed time from submission to publication for the articles averages 180 days.

Authorship

Authors are not permitted to add or remove any names from the authorship provided at the time of initial submission without the consent of the journal's Chief Executive Editor.

Manuscript preparation

For manuscript preparation, authors may refer to Pertanika's **INSTRUCTION TO AUTHORS**, available on the official website of *Pertanika*.

Editorial process

Authors who complete any submission are notified with an acknowledgement containing a manuscript ID on receipt of a manuscript, and upon the editorial decision regarding publication.

Pertanika follows a **double-blind peer-review** process. Manuscripts deemed suitable for publication are sent to reviewers. Authors are encouraged to suggest names of at least 3 potential reviewers at the time of submission of their manuscripts to *Pertanika*, but the editors will make the final selection and are not, however, bound by these suggestions.

Notification of the editorial decision is usually provided within 90 days from the receipt of manuscript. Publication of solicited manuscripts is not guaranteed. In most cases, manuscripts are accepted conditionally, pending an author's revision of the material.

The journal's peer review

In the peer-review process, 2 to 3 referees independently evaluate the scientific quality of the submitted manuscripts. At least 2 referee reports are required to help make a decision.

Peer reviewers are experts chosen by journal editors to provide written assessment of the **strengths** and **weaknesses** of written research, with the aim of improving the reporting of research and identifying the most appropriate and highest quality material for the journal.

Operating and review process

What happens to a manuscript once it is submitted to *Pertanika*? Typically, there are 7 steps to the editorial review process:

1. The journal's Chief Executive Editor and the Editor-in-Chief examine the paper to determine whether it is relevance to journal needs in terms of novelty, impact, design, procedure, language as well as presentation and allow it to proceed to the reviewing process. If not appropriate, the manuscript is rejected outright and the author is informed.

2. The Chief Executive Editor sends the article-identifying information having been removed, to 2 to 3 reviewers. They are specialists in the subject matter of the article. The Chief Executive Editor requests that they complete the review within 3 weeks.

   Comments to authors are about the appropriateness and adequacy of the theoretical or conceptual framework, literature review, method, results and discussion, and conclusions. Reviewers often include suggestions for strengthening of the manuscript. Comments to the editor are in the nature of the significance of the work and its potential contribution to the research field.

Pertanika Journal of Science & Technology
Pertanika Journal of Science & Technology

Pertanika Journal of Science & Technology
Pertanika Journal of Science & Technology

3. The Editor-in-Chief examines the review reports and decides whether to accept or reject the manuscript, invite the authors to revise and resubmit the manuscript, or seek additional review reports. In rare instances, the manuscript is accepted with almost no revision. Almost without exception, reviewers' comments (to the authors) are forwarded to the authors. If a revision is indicated, the editor provides guidelines for attending to the reviewers' suggestions and perhaps additional advice about revising the manuscript.

4. The authors decide whether and how to address the reviewers' comments and criticisms and the editor's concerns. The authors return a revised version of the paper to the Chief Executive Editor along with specific information describing how they have addressed' the concerns of the reviewers and the editor, usually in a tabular form. The authors may also submit a rebuttal if there is a need especially when the authors disagree with certain comments provided by reviewers.

5. The Chief Executive Editor sends the revised manuscript out for re-review. Typically, at least 1 of the original reviewers will be asked to examine the article.

6. When the reviewers have completed their work, the Editor-in-Chief examines their comments and decides whether the manuscript is ready to be published, needs another round of revisions, or should be rejected. If the decision is to accept, the Chief Executive Editor is notified.

7. The Chief Executive Editor reserves the final right to accept or reject any material for publication, if the processing of a particular manuscript is deemed not to be in compliance with the S.O.P. of *Pertanika*. An acceptance letter is sent to all the authors.

   The editorial office ensures that the manuscript adheres to the correct style (in-text citations, the reference list, and tables are typical areas of concern, clarity, and grammar). The authors are asked to respond to any minor queries by the editorial office. Following these corrections, page proofs are mailed to the corresponding authors for their final approval. At this point, **only essential changes are accepted**. Finally, the manuscript appears in the pages of the journal and is posted on-line.

Pertanika Journal of

SCIENCE & TECHNOLOGY

Vol. 33 (5) Aug. 2025

PERTANIKA JOURNALS

A scientific journal published by Universiti Putra Malaysia Press

PJST
Pertanika Journal of Science & Technology
AN INTERNATIONAL PEER-REVIEWED JOURNAL

EDITORIAL OFFICE
JOURNAL DIVISION
Putra Science Park
1st Floor, IDEA Tower II
UPM-MTDC Technology Centre
Universiti Putra Malaysia
43400 Serdang, Selangor Malaysia.

General Enquiry
Tel. No: +603 9769 1622
E-mail:
executive_editor.pertanika@upm.edu.my
URL: http://www.pertanika.upm.edu.my

PUBLISHER
UPM Press
Universiti Putra Malaysia
43400 UPM, Serdang, Selangor, Malaysia.
Tel: +603 9769 8855
E-mail: dir.penerbit@upm.edu.my
URL: http://penerbit.upm.edu.my

ABSTRACTING AND INDEXING OF PERTANIKA JOURNALS

Pertanika Journal of Science & Technology is indexed in Journal Citation Reports (JCR-Clarivate), SCOPUS (Elsevier), EBSCO, ASEAN Citation Index, Microsoft Academic, Google Scholar and MyCite.

Pertanika Journal of Science & Technology
Vol. 33 (5) Aug. 2025

Contents

Foreword

Welcome to the fifth issue of 2025 for the Pertanika Journal of Science and Technology (PJST)!

PJST is an open-access journal for studies in Science and Technology published by Universiti Putra Malaysia Press. It is independently owned and managed by the university for the benefit of the world-wide science community.

This issue contains 15 articles: four review articles; and the rest are regular articles. The authors of these articles come from different countries namely France, Indonesia, Malaysia, Morocco, Pakistan, Saudi Arabia and Spain.

Aseil Nadhim Kadhim and her teammates from Universiti Teknologi Malaysia Kuala Lumpur evaluated the gender classification ability of the You Only Look Once (YOLO) algorithm using deep learning. YOLO is one of the most accurate object detection models that can identify multiple objects in a video or image in real-time. In this study, various versions of YOLO (YOLOv3 to YOLOv9) were compared to find the most accurate and efficient model for gender classification. The research used a collection of 361 test images of male and female subjects in different scenarios, and the models' performance was measured using key metrics such as Precision, Recall, and F1-score. The results indicated that YOLOv9 was the most accurate (mAP = 97%) and precise (86.8%), making it the most effective for real-time applications. Despite its advancements, YOLOv9 still faces high computational demands and occasional misclassification in complex situations. More detailed information about this study is available on the page 2155.

A regular article titled "Screening and Isolation of Microalgae Collected from Tin Mining at Bangka Belitung Province with Remarks on Their UV-C Absorbance and Lead Remediation" examined the effect of growth media on microalgae isolated from water bodies at abandoned tin mining sites. The study also analyzed their sensitivity to UV-C spectrum and lead resistance. Samples from six locations were enriched in Bold Basal Medium (BBM) (pH 6.8) and Blue Green-11 (BG-11) (pH 7.4) media. They were maintained at 21°C and exposed to continuous light at 1,600 lux. The UV-C sensitivity of the cultures was measured using spectrophotometry at λ=230 nm, followed by growth rate assessment. The isolates were tested with lead concentrations of 0, 10, 100, and 200 ppm. The microalgae showed various absorbance peaks, indicating their ability to grow under UV-C wavelengths. Lead exposure affected the cell size, organelles, and growth of the microalgae. The different absorbance peaks suggest that the microalgae may produce beneficial metabolites as an adaptive response to harsh environments. Additional details of this study are available on page 2177.

A selected article titled "Volatile and Non-volatile Metabolites Profiling of the Chloroform Extract of Marine Sponge Clathria reinwardti via Mass Spectrometry" analyzed the metabolites in the chloroform extract of the marine sponge C. reinwardti using mass spectrometry. A sponge sample was collected from the east coast of Sulug Island, Sabah, Malaysia. Total phenolic and flavonoid contents were measured. The composition of these extracts was further examined through qualitative biochemical screening, Fourier transform infrared spectroscopy (FTIR), gas chromatography-mass spectrometry (GC-MS), and liquid chromatography-quadrupole time-of-flight mass spectrometry (LT-qTOF-MS) analyses. GC-MS analysis revealed various metabolites, including 2,5-bis(1,1-dimethylethyl) phenol, pentadecane, eicosane, tetracosane, and cholestanol, among others. LC-qTOF-MS analysis identified additional metabolites like thymine, hexadecasphinganine, hericene B, phylloquinone, 24-norcholesterol, palmitic amide, oleamide, solanidine, suillin, 9-thiastearic acid, and isoamijiol. These compounds are associated with various pharmacological activities, such as anti-inflammatory, antimicrobial, anti-diabetic, anticancer, antioxidant, anti-hemorrhagic, cytotoxic, neuroprotective, and chemopreventive effects. Therefore, the chloroform extract of C. reinwardti is a valuable source of metabolites. Complete information about this study is presented on the page 2279.

We anticipate that you will find the evidence presented in this issue to be intriguing, thought-provoking and useful in reaching new milestones in your own research. Please recommend the journal to your colleagues and students to make this endeavour meaningful.

All the papers published in this edition underwent Pertanika's stringent peer-review process involving a minimum of two reviewers comprising internal as well as external referees. This was to ensure that the quality of the papers justified the high ranking of the journal, which is renowned as a heavily-cited journal not only by authors and researchers in Malaysia but by those in other countries around the world as well.

We would also like to express our gratitude to all the contributors, namely the authors, reviewers and Editorial Board Members of PJST, who have made this issue possible.

PJST is currently accepting manuscripts for upcoming issues based on original qualitative or quantitative research that opens new areas of inquiry and investigation.

Editor-in-Chief
Luqman Chuah Abdullah

Pertanika J. Sci. & Technol. 33 (5): 2027 - 2047 (2025)

PERTANIKA JOURNALS

SCIENCE & TECHNOLOGY

Journal homepage: http://www.pertanika.upm.edu.my/

Using Deep Transfer Learning for Automated Identification of Susceptibility Vessel Signs in Patients with Acute Ischemic Stroke

Nur Lyana Shahfiqa Albashah[1,2]*, Ibrahima Faye[1], Fityanul Akhyar[2] and Ahmad Sobri Muda[3]

[1]Department of Fundamental and Applied Science, Universiti Teknologi Petronas, 32610 Bandar Seri Iskandar, Perak, Malaysia

[2]Faculty of Information and Communication Technology, Universiti Tunku Abdul Rahman, 31900 Kampar, Perak, Malaysia

[3]Putra Clinical Centre Neurovascular and Stroke, Hospital Sultan Abdul Aziz Shah, Faculty of Medical and Health Science, Universiti Putra Malaysia, 43400 Serdang, Selangor, Malaysia

ABSTRACT

Ischemic stroke, commonly caused by a blood clot obstructing the blood flow within brain vessels, requires accurate identification of the clot to determine appropriate treatment. Susceptibility-weighted imaging (SWI) is an imaging modality that effectively captures clots within the brain. The susceptibility vessel sign (SVS) visible on SWI images is crucial for influencing treatment outcomes. Traditionally, radiologists manually analyse the SVS, which is both challenging and time-consuming. This research aims to build an interactive deep learning (DL)-assisted method for identifying the SVS on the SWI in patients with acute ischemic stroke. Sixty-six images with SVS positive were used, and 66 images with SVS negative were used, with regions of interest extracted to create the training, validation, and test datasets. To increase the number of training samples, data augmentation was used. A deep convolutional neural network DenseNet121 was utilised to identify input images as either SVS positive or SVS negative. In terms of diagnostic performance using 5-fold cross validation, the DenseNet121 model achieved 96.92% sensitivity, 92.31% specificity, and 94.64% accuracy on the test dataset. These findings indicate that the DL methods might be advantageous for detecting the SVS on the SWI in patients with acute ischemic stroke.

Keywords: Brain stroke, DenseNet model, susceptibility vessel sign (SVS), SWI-MRI, transfer learning

ARTICLE INFO

Article history:
Received: 15 August 2024
Accepted: 29 April 2025
Published: 11 August 2025

DOI: https://doi.org/10.47836/pjst.33.5.01

E-mail addresses:
yanashahfiqa88@gmail.com (Nur Lyana Shahfiqa Albashah)
Ibrahima_faye@utp.edu.my (Ibrahima Faye)
fityanul@utar.edu.my (Fityanul Akhyar)
asobri@upm.edu.my (Ahmad Sobri Muda)
* Corresponding author

e-ISSN: 2231-8526

INTRODUCTION

Stroke is a severe medical condition that significantly impacts patients, both in terms of health and economic burden, especially during post-treatment care. Stroke survivors often require extensive and costly rehabilitation. Strokes can be categorised into two types: ischemic and hemorrhagic, with ischemic strokes accounting for approximately 85% of all cases (Sirsat et al., 2020). Ischemic strokes occur when a blockage obstructs a blood vessel in the brain, leading to oxygen deprivation and subsequent cell death. This results in functional impairments and delayed recovery. Therefore, rapid restoration of oxygen supply and minimisation of brain damage are crucial. In this context, brain imaging plays a vital role in diagnosing stroke types and guiding treatment strategies.

Magnetic resonance imaging (MRI) and computed tomography (CT) scans are commonly used for stroke diagnosis. Advanced imaging modalities, such as susceptibility-weighted imaging (SWI) and diffusion-weighted imaging (DWI), provide more precise localisation and assessment of the affected brain areas. The SWI, in particular, is highly effective in detecting small changes in magnetic properties between blood and tissue, enabling the identification of affected veins due to increased deoxygenated blood. Recent studies have reinforced the importance of the SWI in detecting thrombi, as the susceptibility vessel sign (SVS) has been linked to various stroke parameters, including risk factors and thrombus length, which are crucial for treatment planning.

Despite their advantages, existing brain imaging techniques have limitations. The perfusion-weighted imaging (PWI) requires contrast agents, which are unsuitable for patients with renal insufficiency. The DWI can be time-consuming and impractical for certain patients. The computed tomography angiography (CTA) is also prone to inaccuracies, such as false negatives due to vessel wall calcification and partial volume effects caused by clot thickness (Zhu et al., 2023). These limitations highlight the need for more efficient and reliable diagnostic methods.

Recent advancements in clot imaging and artificial intelligence (AI) have significantly improved clot detection and prediction. A systematic review of AI-based and conventional studies (Dumitriu LaGrange et al., 2023) highlighted several key findings. Deep learning (DL) has improved clot detection from non-contrast CT (NCCT) and MRI scans, achieving high sensitivity and specificity in large vessel occlusion (LVO) detection. Radiomics-based models have been developed for clot segmentation and classification, predicting thrombus composition and treatment response using machine learning techniques (Hanning et al., 2021; Hofmeister et al., 2020). Automated clot segmentation is a critical advancement, allowing rapid 3D reconstruction of clots to assist neuroradiologists in identifying clot location, extent, and composition (Mojtahedi et al., 2022). Moreover, AI-based clot detection software, such as MethinksLVO, can rapidly predict the LVO in ischemic stroke patients using the NCCT, reducing diagnostic time and improving early intervention (Olive-Gadea et al., 2020).

Automated detection of stroke characteristics, such as clot location and severity, can significantly enhance diagnostic efficiency. Currently, the SVS detection heavily relies on manual assessment by neurologists, which is time-consuming and subject to variability. The deep learning offers a promising solution by automating detection and improving accuracy. The DL models have demonstrated near-perfect accuracy in various medical applications (Tsochatzidis et al., 2019; Wessels & van der Haar, 2023). Convolutional neural networks (CNNs) have also been used to develop automated systems capable of detecting intracranial clots on non-contrast CT scans, further enhancing early stroke diagnosis. In the study, a Convolutional neural network (CNN) is used to classify input images as either hyperdense middle cerebral artery (MCA) sign (HMCAS)-positive or HMCAS-negative. The CNN, specifically the Xception architecture, is trained on augmented datasets to identify the presence of HMCAS on non-contrast CT scans in patients with acute ischemic stroke. The CNN demonstrated high diagnostic performance with 82.9% sensitivity, 89.7% specificity, and 86.5% accuracy in leave-one-case-out cross-validation. The study highlights the potential of the deep learning methods, like CNNs, to assist in the accurate identification of HMCAS, which is crucial for the management and treatment of acute ischemic stroke (Shinohara et al., 2020).

AI techniques, particularly machine learning, have been utilised to develop models capable of predicting the origin and composition of thrombi using the MRI data. For instance, a study employed gradient echo sequences (GRE) at 3T MRI to train a machine learning model that could predict atrial fibrillation (AF) as the thrombus origin (Chung et al., 2019). Additionally, the AI has been applied to analyse the SVS on the MRI, which is associated with increased red blood cell (RBC) content in the clot (Benson et al., 2021). This analysis aids in predicting the clot's response to treatments such as mechanical thrombectomy.

The AI-based radiomics plays a crucial role by extracting a vast number of quantitative features from the MRI scans to develop predictive models. These models can forecast treatment outcomes, including the likelihood of successful recanalisation and number of thrombectomy passes required (Dumitriu LaGrange et al., 2023). Moreover, the AI can integrate information from multiple MRI sequences to provide a comprehensive assessment of the thrombus and surrounding vascular anatomy, facilitating more informed treatment decisions. Overall, the AI applications in the MRI for clot imaging are transforming the field by enabling more accurate and detailed analyses, ultimately improving treatment planning and outcomes for stroke patients.

The classification of biomedical images, including stroke clot detection, is a substantial challenge due to the limited availability of annotated datasets and high computational cost of training deep learning models from scratch. Transfer learning has emerged as an effective solution, leveraging pre-trained deep learning models to enhance classification accuracy while reducing data requirements (Gunturu et al., 2024). By adapting pre-trained neural networks,

such as ResNet, DenseNet, and VGG, to domain-specific biomedical imaging tasks, the transfer learning significantly improves model performance while shortening training time.

In stroke detection, the transfer learning allows models trained on large general image datasets (e.g., ImageNet) to be fine-tuned on smaller, domain-specific datasets, such as the SWI-based clot images. This approach preserves critical features while requiring fewer labelled images, making it a powerful tool for detecting clots in the MRI scans. Studies have shown that fine-tuning deep convolutional networks on medical images achieves higher accuracy than training models from scratch, especially in cases with limited patient data.

This study aims to develop an automated detection system for the SVS identification in acute ischemic stroke using the transfer learning. To the best of our knowledge, this approach is novel as it integrates the SWI with the DL-based clot detection. The proposed system seeks to enhance stroke diagnosis by ensuring high accuracy and efficiency, leveraging state-of-the-art DL techniques in medical imaging. By incorporating the latest advancements in AI and deep learning, this research contributes to improving stroke detection, treatment planning, and overall patient outcomes.

LITERATURE REVIEW

Machine learning (ML) has recently provided a major breakthrough in the medical sector, particularly in stroke treatment. Diverse data on medicine can be processed by the ML, which, in many cases, identifies patterns and predicts them with astonishing accuracy. The first category pertains to stroke prevention, and the second one belongs to stroke diagnosis, whereas the third one is for treatment of strokes, while the fourth means outcome prediction in case of stroke.

Stroke Prevention

Preventing stroke is necessary to minimise the rates and impact of strokes. The ML techniques have demonstrated the potential for policy definition for risk factors and prediction of stroke-prone conditions. This section discusses research literature that has utilised the ML models to predict familial hypercholesterolemia (FH) and carotid-artery atherosclerosis, which are leading causes of stroke among individuals across the globe (Myers et al., 2019). The FH is an inherited condition that causes high cholesterol and a risk of premature heart disease or stroke. Performing early identification of the FH allows for the performance of health, promoting activities that reduce long-term cardiovascular risk. A study using the random forest (RF) algorithm is one of its notable examples to predict the FH. The method had to optimise the parameters and used a 5-fold cross-validation approach for stability assessment with respect to potential model overfitting. The study performed parameter optimisation and 5-fold cross-validation to ensure that the model has good performance. The precision was 0.85, and the recall was 0.45. Although the high

precision suggests solid performance, sub-performances seem to follow in their shadows, emphasising a possible area of concern. Hence, more effort is required for this model as it appears to be weak with respect to detecting the FH patients. Regardless, it illustrates the possibility of the ML to improve the detection of stroke risk-related genetic conditions, especially the RF. Carotid-artery atherosclerosis (CA), one of the main risk factors for ischemic stroke, represents plaque aggregation in carotids. Early recognition of the CA can lead to preventive management and reduce the risk of strokes. In a study (Bento et al., 2019), a support vector machine (SVM) was trained to classify individuals with the CA based on the MRI images. The SVM model performed with an accuracy of 97.6%, which indicated that the use of this algorithm could help in the identification of high-risk populations. The combination of the MRI images with the SVM results in a non-invasive diagnostic instrument for the CA, which has important clinical implications as it could enable early management and stroke prevention.

Stroke Diagnosis

A more accurate classification of the stroke subtypes, particularly the distinction between the ischemic and hemorrhagic strokes, which has implications for their treatment strategy, could lead to better patient outcomes. In this part, we discuss the results of the previous study of dividing stroke patients into subtypes and predicting outcomes using the ML techniques. In a stroke subtype classification study (Peixoto & Rebouças Filho, 2018), researchers used different ML techniques such as the SVM, Multi-layer Perceptron, and Minimal Learning Machines, together with the standard linear discriminant analysis as well as the structure co-occurrence matrix (SCM).

The objective was to differentiate between the ischemic and hemorrhagic strokes using imaging. Of the evaluated techniques, the SCM achieved the best performance, achieving an accuracy of 98%. This high level of accuracy emphasises the capacity of the SCM to accurately classify sub-types for all stroke types, thus becoming a valuable tool to help health professionals make reliable clinical decisions. For instance, Giacalone et al. (2018) predicted the final lesion for stroke patients with acute ischemic using raw perfusion MRI images. An SVM model is implemented in this study to measure brain stroke lesion extent and location prediction using the MRI data. The SVM model displayed satisfactory high accuracy (95%), and it could be predicted with precision. This type of prediction can be used to support therapeutic decisions or prognosis assessment.

Stroke Treatment

Stroke rehabilitation is a crucial part of treatment to improve physical and cognitive abilities in patients. The ML-based models have been employed to enhance rehabilitation exercises, in particular by utilising physiological signals and sensor technology for

personalised therapy designing and assessment. This section summarises studies that applied the ML techniques to optimise stroke rehabilitation, specifically in the areas of physiological stress identification and upper extremity function improvement. A study that focussed on trying to adapt the rehabilitation therapy to the physiological signals of patients organised this information into relaxed, medium-stressed, and over-stressed (Badesa et al., 2014). The physiological signals were classified using a number of the ML methods, the most significant results achieved by support vector machines with radial basis function (RBF) kernel. The SVM with RBF achieved an accuracy of 91.43%. The high accuracy indicates that the SVM with RBF can reliably interpret physiological signals, allowing the therapist to adjust the intensity and type of rehabilitation exercise in real time, thereby enhancing the effectiveness of the therapy. Another study focussed on improving upper extremity function post-rehabilitation, particularly targeting motor-specific responses. Traditional evaluation approaches, such as self-reporting, are often accurate but subjective (Bochniewicz et al., 2017). By using the sensor technology, accurate and objective data were collected to assess motor function. The study used the RF to classify the rehabilitation outcomes for control and stroke subjects. From the study, while the RF model was highly effective in distinguishing motor responses in healthy individuals, it faced challenges with the more variable and complex data from stroke patients. However, the sensor data and RF classification have greatly advanced beyond the traditional self-report method, whereby a more objective and detailed evaluation of rehabilitation progress may be obtained. Patients with stroke are frequently treated by thrombolysis, thrombectomy, or both and experience a highly variable outcome. Such fine-grained prognostication can help guide the choice of treatments and ultimately improve patient care. The ML techniques have been used with the clinical and imaging data to predict treatment response. In this section, studies are considered in predicting treatment outcomes using the ML and DL methods, especially focussing on the utilisation of the CTA images and diffusion tensor imaging (DTI). A study investigated the use of the DL for predicting functional outcomes after treatment in stroke from acquired computed tomography angiograms (Hilbert et al., 2019). The research employed the Resnet algorithm in order to analyse the CTA images and predict patient outcomes. This method was compared to traditional radiological biomarkers that were manually annotated by domain experts, who can introduce inter-observer variability. On 3 out of 4 cross-validation folds for functional outcomes, the model achieved an average AUC value of 0.71. The study results suggest that, compared with traditional radiological biomarkers, the DL model can more accurately predict outcomes and thus offers hope in improving the administration of stroke treatment. A further study using the ML explored the link between the DTI metrics and functional outcomes in a cohort of patients post-stroke. The axial diffusivity map as a key parameter was the central object of the study.

These maps were analysed, and the results were predicted using an SVM classifier. The SVM classifier had the highest accuracy rate, 82.8%, among imaging criteria in this current study. This result attests to the utility of the DTI metrics and SVM for forecasting outcomes, suggesting an effective approach used for assessing rehabilitation strategies.

Stroke Outcomes Prediction

The thrombus composition and stroke treatment response outcome may be influenced by the thrombotic material within a clot as well as its responsiveness to treatment. Radiomics of the clot, which examines connections between the thrombus composition and treatment response through sophisticated imaging techniques, is in increasing focus. The ML algorithms have demonstrated the potential to predict the composition of the thrombus and recognise specific stroke-related conditions. In this section, we summarise some representative studies that have used the ML for clot imaging in stroke treatment. Another was targeting prediction on the thrombus composition of clots using radiomics features extracted from the thrombi images (Hanning et al., 2021). The investigators applied nested five-fold cross-validation and used random-forest algorithms to classify the thrombus composition. At the end of this process, a receiver operating characteristic (ROC) curve value of 0.83 was obtained for red blood cell (RBC)-rich thrombi and another 0.84 for fibrin-rich thrombi by the random forest model, respectively. The high ROC value showed the random forest model to have differentiation power between the RBC-rich and fibrin-thrombi. Therefore, accurate prediction of the thrombus composition can help guide appropriate treatment strategies.

The identification of the LVO on the NCCT plays a key role in the decision-making process to identify which is going to be the right intervention for stroke patients. The proprietary MethinkLVO software created to aid in this identification had a sensitivity of 0.83 and specificity of 0.71 (Olive-Gadea et al., 2020). High sensitivity (92.7%) and specificity (99.8%) imply that the software is good at detecting the LVO to inform clinical decisions accurately with sufficiently low false discovery rate. A stunning result predicting the hyperdense middle cerebral artery (HMCA) in the NCCT showed the sensitivity and specificity were 0.83 (Xception model) and shown to be effective at HMCA identification, aiding in rapid diagnosis and intervention for acute stroke cases (Shinohara et al., 2020).

The SVS in susceptibility-weighted imaging has been linked with higher amounts of the RBC content within thrombi (Phuyal et al., 2024). A study by Tang et al. (2021) found clots without the SVS were fibrin-rich and less responsive to simple aspiration, requiring mechanical thrombolysis instead. In patients with the LVO treated with intravenous tissue plasminogen activator (TPA) alone, the presence of the SVS has similarly been identified as a predictor for better outcome thresholds (Tang et al., 2021). Although the SVS as a clot composition marker is extremely important, until now, no study has ever focussed on the

automatic detection of this sign based on the ML or DL. These gaps automatically denote an interesting direction in further development.

MATERIALS AND METHODS

This study comprises three main experimental phases. Phase 1 evaluates different pre-trained deep learning models using the Shinohara's method (Shinohara et al., 2020) to determine the best-performing architecture for the SVS detection, incorporating data augmentation. Phase 2 optimises the selected model by analysing the effects of augmentation strategies, learning rate, training epochs, resizing methods, and filtering techniques. Finally, Phase 3 validates the optimal configuration using the 5-fold cross-validation to ensure the generalisability of the developed model.

Experimental Setup

Phase 1: Deep Learning Model Selection

Step 1: Pre-Trained Models Evaluated. In this study, six prominent deep learning architectures were evaluated to identify the most effective model for the susceptibility-weighted Imaging (SWI) MRI scan analysis. The selected architectures are:

- Xception: This architecture utilises depthwise separable convolutions, which significantly reduce the number of parameters without compromising performance. The Xception has demonstrated superior accuracy in various image classification tasks, making it a strong candidate for medical image analysis (Faiz & Iqbal, 2022).
- ResNet50: Known for its residual learning framework, the ResNet50 addresses the vanishing gradient problem by incorporating skip connections. This design enables the training of deeper networks and has shown robust performance across diverse applications (Shen & Liu, 2017).
- DenseNet121: The DenseNet connects each layer to every other layer in a feed-forward fashion, promoting feature reuse and efficient gradient flow. This connectivity pattern leads to improved learning efficiency and has been effective in various computer vision tasks.
- MobileNet: Designed for mobile and embedded vision applications, the MobileNet employs depthwise separable convolutions to reduce computational complexity. Despite its lightweight nature, it achieves performance comparable to larger models, making it suitable for resource-constrained environments (Chen & Su, 2018).
- EfficientNetB0: The EfficientNet introduces a compound scaling method that uniformly scales network depth, width, and resolution. This balanced approach results in superior accuracy with fewer parameters, offering an efficient solution for image classification tasks (Utami et al., 2022).

- ConvNeXtLarge: As a modernised architecture, the ConvNeXtLarge builds upon standard convolutional networks by incorporating design elements from vision transformers. This integration aims to enhance performance while maintaining computational efficiency, making it a compelling choice for advanced image analysis (Hou et al., 2024).

Each of these architectures brings unique strengths to the table, and their performance was systematically evaluated to determine the most suitable model for our specific application.

Step 2: Implementation of the Method Inspired by Shinohara. Each pre-trained model was used as a feature extractor, replacing the final classification layers with a customised classifier. The classification head was designed as follows:

- Global average pooling layer
- Batch normalisation layer
- Dropout layer (0.3)
- Fully connected dense layer with sigmoid activation for binary classification

Step 3: Dataset and Preprocessing. All images with positive SVS are annotated by a neuroradiologist from Hospital Sultan Abdul Aziz Shah (HSAAS), Faculty of Medical and Health Science, Universiti Putra Malaysia (UPM), Malaysia. Data obfuscation, labelling and validation were done using padimedical system. The dataset comprises nine patients who exhibit the susceptibility vessel sign in the SWI MRI scans. Each SWI MRI scan contains 60 2D image slices. However, not all images contain positive signs of the SVS. The number of slices for each patient consisting of the SVS positive also varies. The total number of the SVS-positive images for this experiment is 66. For the training set taken from five patients, 30 images with the SVS positive and 30 images with the SVS negative are used. The validation set includes 19 images with the SVS positive and 19 images with the SVS negative, which is from two patients, while the testing dataset consists of 17 images with the SVS positive and 17 images with the SVS negative sign, which were obtained from another two patients. The images and data obtained initially are in the DICOM format, which is then converted into the JPEG format (672 × 672 pixels). All images with the positive SVS are taken into the dataset. Each full brain image with a SVS positive is cropped into various sizes of squares depending on the area of the SVS, ensuring that the information on the SVS is maximised in the background as shown in Figure 1 (the shape of the cropped area is square and being used as an input of classification), for the SVS negative is taken from the same image but in different position of the SVS positive. If the SVS positive is on the right side of the brain image, the SVS negative is taken from the left side of the brain, as shown in Figure 1. Each dataset (training, validation, and testing) are then organised

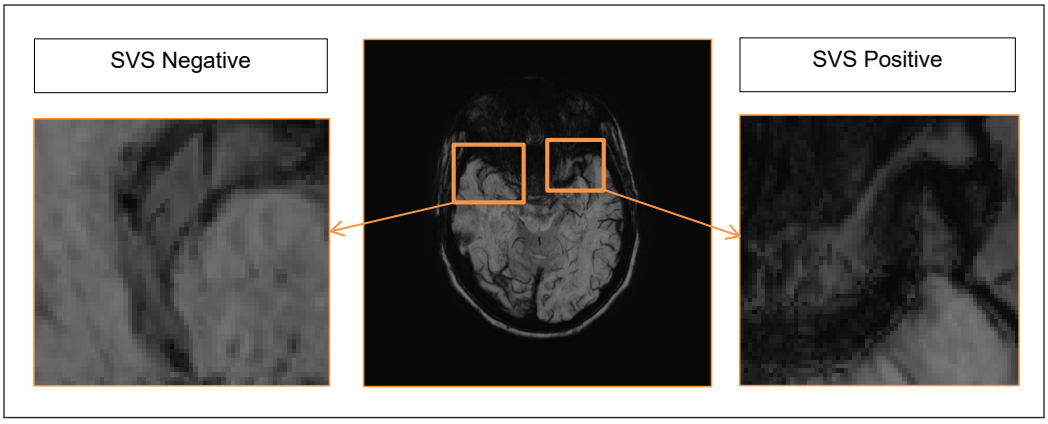

Figure 1. This is one of the image slices taken from acute ischemic stroke patients using the MRI modality with the SVS positive. This image is cropped into the negative SVS region and the positive SVS region that is used during the experiment
Note. MRI = Magnetic resonance imaging; SVS = Susceptibility vessel sign

into separate folders, which are further subdivided into images of the SVS positive and negative. Each of the images was resized to 240 × 240 using bilinear interpolation. Then, the filtering method was applied to reduce the noise. Data augmentation is employed to enable the model to understand various sets of features and expand the dataset size, thus mitigating overfitting. Each training set is augmented using random affine transformation, including shearing and rotation. The details of the image augmentation parameters are as follows: rotation within a range of 0 to 90 degrees in a step of 15 degrees, shearing at 0.2, zooming at 0.2, horizontal flipping, and vertical flipping. From this augmentation method, 300 augmented images were obtained for the training dataset.

Step 4: Model Training Configuration. For this study, each of the pre-trained models used this parameter as shown below:

- Optimiser: Adam with a fixed learning rate of 0.00001
- Batch size: 32
- 50 training epochs
- Loss function: Binary cross-entropy

Step 5: Evaluation Metrics and Model Selection. In this study, a few parameters are used to measure the efficiency and effectiveness of the classification model, using accuracy, sensitivity, and specificity derived from the confusion matrix. The calculation of each performance metric is as follows:

$$\text{Accuracy} = \frac{TP + TN}{TP + FP + TN + FN} \quad [1]$$

$$\text{Sensitivity} = \frac{\text{TP}}{\text{TP} + \text{FN}} \quad [2]$$

$$\text{Specificity} = \frac{\text{TN}}{\text{TN} + \text{FP}} \quad [3]$$

where, TP is true positive, TN is true negative, FP is false positive, and FN is false negative.The pre-trained model achieving the highest F1-score was selected for further experimentation in Phase 2.

Phase 2: Manual Hyperparameter Tuning of the Best Pre-Trained Model

After identifying the best-performing pre-trained model in Phase 1, an optimisation experiment was conducted using a manual hyperparameter tuning to examine the impact of augmentation strategies, learning rates, training epochs, resizing methods, and filtering techniques on the classification performance.

Experimental Configurations. The selected model was fine-tuned under different experimental conditions:

Step 1: Data Augmentation Strategies. The study analysed the impact of data augmentation on model performance by comparing two different training approaches:

1. **With Augmentation** – Various augmentation techniques were applied to enhance model generalisation and robustness. The applied transformations included:
   - Rotation: 0° to 90° with 15° step
   - Shear: 0.2
   - Zoom: 0.2
   - Horizontal and vertical flipping

   These augmentations were consistent with those used in **Phase 1** of the study.
2. **Without Augmentation** – The model was trained using the original dataset without any transformations, serving as a baseline for comparison.

The impact of augmentation was assessed based on model accuracy, generalisation capability, and sensitivity to variations in the input data.

Step 2: Learning Rate Variations (Manually Tuned). The study explored the impact of different manually tuned learning rates on the model performance. The following learning rate variations were tested:

- 10^{-3} (0.001) - A relatively high learning rate, allowing the model to converge quickly but with a potential risk of overshooting the optimal solution.
- 10^{-4} (0.0001) - A moderate learning rate, balancing convergence speed and stability.

- 10^{-6} (0.000001) - A very small learning rate, ensuring fine adjustments to the model's weight but potentially leading to slow convergence.

Step 3: Number of Training Epochs (Manually Tuned). The study investigated the effect of different training durations on the model performance by varying the number of training epochs. The following configurations were tested:

- 25 epochs – A shorter training duration to observe the model's initial learning progress and prevent overfitting.
- 50 epochs – A balanced approach, allowing the model to learn effectively while monitoring for potential overfitting.
- 70 epochs – A longer training duration to evaluate whether extended learning improves performance or leads to overfitting.

Early stopping was implemented based on the validation accuracy to determine the optimal number of epochs for achieving the best generalisation performance on test data.

Step 4: Resizing Methods. The study evaluated different image resizing techniques to determine their impact on model performance. The following interpolation methods were considered:

- Bilinear interpolation – Computes the pixel value using a weighted average of the four nearest neighbouring pixels, resulting in smoother images.
- Bicubic interpolation – Uses a more complex weighted average of 16 neighbouring pixels, producing sharper and higher-quality resized images.
- Nearest neighbour interpolation – Assigns the value of the nearest pixel without averaging, leading to a blocky appearance but preserving edges.

Each method was tested to assess its influence on image quality and the model's ability to detect the SVS effectively.

Step 5: Filtering Techniques. The study explored different image filtering techniques to assess their impact on model performance. The following filtering approaches were evaluated:

- No filtering – The raw images were used without any pre-processing.
- Median filter – Applied to reduce noise while preserving edges.
- Gaussian filter – Used for smoothing the images by reducing high-frequency noise.
- Combination of median and Gaussian filtering – Both techniques were applied sequentially to enhance image quality.

Each filtering method was analysed to determine its effectiveness in improving the model accuracy and generalisation.

Training and Evaluation Process. The Adam optimiser was employed for backpropagation across various manually selected learning rates to optimise the model's performance. Training was conducted for a range of epochs, with early stopping implemented to monitor validation accuracy and prevent overfitting. The best-performing configuration was identified based on the overall accuracy and generalisation performance evaluated on the test dataset.

Selection of the Optimal Configuration. After evaluating all experimental configurations, the optimal combination of augmentation techniques, image resizing, filtering methods, learning rate, and training epochs were selected based on the performance metrics. This final validated model was then subjected to 5-fold cross-validation in Phase 3 to ensure its robustness and generalisation capability.

Phase 3: 5-Fold Cross-Validation on the Optimal Configuration

Once the best model configuration was established, the 5-Fold Cross-validation was employed to validate its generalisability. The 5-Fold Cross-validation Strategy was implemented to evaluate the model's performance robustly. The dataset was randomly divided into five equal folds. In each iteration, one-fold was designated as the validation set, while the remaining four folds were used for training the model. This process was repeated five times, with each fold serving as the validation set exactly once. The final performance of the model was determined by calculating the mean performance across all five folds, providing a more reliable assessment of its generalisation capability.

RESULTS AND DISCUSSION

In this study, the performance of the multiple deep learning models for the detection of the SVS in the MRI scans was evaluated using the method proposed by Shinohara et al. (2020). The models assessed include the Xception, ResNet50, ConvNetXtXLarge, EfficientNet, MobileNet, and DenseNet. The performance of these models was analysed based on key classification metrics: accuracy, sensitivity, and specificity.

The results based on Table 1 indicate that the Xception achieved an accuracy of 52.94%, with a sensitivity of 1.00 and specificity of only 0.05. Similarly, the ResNet50, ConvNetXtXLarge, and EfficientNet all reported an accuracy of 50.00%, a perfect sensitivity score of 1.00, but a specificity of 0.00. This pattern suggests that these models overwhelmingly classified images as positive cases (SVS present), failing to correctly identify negative cases. Consequently, their high sensitivity came at the expense of specificity, making them ineffective for reliable classification in clinical settings. The DenseNet is better than the ResNet because the Densenet has the capability of feature reuse and better gradient flow (Padmakala & Uma Maheswari, 2024).

Table 1
Comparing performance metrics of the transfer learning models in the test dataset

Model	Accuracy	Sensitivity	Specificity
Xception	0.5294	1.00	0.05
ResNet 50	0.5000	1.00	0.00
ConvNetXtXLarge	0.5000	1.00	0.00
EfficientNetB0	0.5000	1.00	0.00
MobileNet	0.5588	0.7647	0.3529
DenseNet121	**0.5882**	**0.7647**	**0.4818**

Note. The bold data = The best results

The MobileNet demonstrated a relatively improved performance, achieving an accuracy of 55.88%, sensitivity of 0.7647, and specificity of 0.3529. Likewise, the DenseNet outperformed the other models by achieving the highest accuracy of 58.82%, with a sensitivity of 0.7647, and a specificity of 0.4818. These models showed a better balance between sensitivity and specificity, indicating that they were more capable of distinguishing between positive and negative cases than the other models. The Densenet model also shows outperformed in brain tumour detection because it is capable of handling small datasets compared to other models (Thimma Reddy & Balaram, 2024). The Densenet pre-trained model has also shown improvement in accuracy in the fundus medical images (Xu et al., 2018), breast cancer detection (Hamdy et al., 2021), chest disease (Iswahyudi et al., 2024), and others.

The results presented in Table 1 indicate that the Xception achieved an accuracy of 52.94%, with a sensitivity of 1.00 but a specificity of only 0.05. Similarly, the ResNet50, ConvNeXt-XLarge, and EfficientNet all reported an accuracy of 50.00%, a perfect sensitivity score of 1.00, but a specificity of 0.00. This pattern suggests that these models overwhelmingly classified images as positive cases (SVS present), failing to correctly identify negative cases. Consequently, their high sensitivity came at the expense of specificity, making them ineffective for reliable classification in clinical settings. The DenseNet outperforms the ResNet due to its ability to facilitate feature reuse and improve gradient flow (Padmakala & Uma Maheswari, 2024).

The MobileNet demonstrated relatively improved performance, achieving an accuracy of 55.88%, a sensitivity of 0.7647, and specificity of 0.3529. Likewise, the DenseNet outperformed the other models by achieving the highest accuracy of 58.82%, with a sensitivity of 0.7647, and specificity of 0.4818. These models exhibited a better balance between sensitivity and specificity, indicating that they were more effective in distinguishing between the positive and negative cases compared to the other models.

After that, in Phase 2, several experiments were conducted to compare the performance of the models with and without data augmentation, as well as to evaluate different resizing,

filtering methods, and other transfer learning models, as mentioned in Phase 2 in the methodology section. In Table 2, the results for without data augmentation are presented, comparing various learning rates and numbers of epochs. Our findings indicate that the best performance was achieved with a learning rate of 0.001 and 50 epochs, yielding an accuracy of 0.8235, with a specificity of 0.8235, a sensitivity of 0.8235, and a F1-score of 0.8235.

Then, performance improvement was observed after using the data augmentation method. As shown in Table 3, the highest performance in that case was achieved with a learning rate of 0.001 and 50 epochs, yielding an accuracy of 0.8824, with a specificity of 0.7647, sensitivity of 1.00, and F1-score of 0.8867.

Next, various resizing methods were evaluated using a learning rate of 0.001 and 50 epochs. The results in Table 4 indicate that bicubic interpolation achieved the highest accuracy of 0.8235 among the resizing methods. Nevertheless, when compared with the results from Table 3 (without any resizing), the performance without resizing was superior.

Furthermore, different filtering methods were compared. Table 5 shows that the best results were obtained without any filtering, achieving an accuracy of 0.7647, while the combination of the median and Gaussian filtering produced the lowest accuracy of 0.5.

In conclusion, the best model is the DenseNet121 model with data augmentation, with a learning rate of 0.001 and a number of epochs of 50. The DenseNet121 model obtained an average accuracy of 0.9464 when evaluated using the 5-Fold Cross-validation, as shown in Table 6. It also showed excellent sensitivity, specificity, and F1-score. The strong F1-score suggests that the model maintains a good balance between sensitivity and specificity, making it highly suitable for the SVS detection, which is supported by a value of a high AUC of 0.9728, shown in Figure 2.

Table 2
Comparing performance metrics of the DenseNet121 Model without augmentation with different learning rates (0.000001,0.00001, 0.001) and several epochs (25,50,70) in the test dataset

Learning rate	Epoch	Accuracy	Sensitivity	Specificity	F1-Score
0.000001	25	0.4706	0.8824	0.0588	0.625
0.000001	50	0.4118	0.1176	0.7059	0.1667
0.000001	70	0.5	0.1176	0.8824	0.1905
0.0001	25	0.6765	0.3529	1	0.5217
0.0001	50	0.5882	0.5882	0.5882	0.5882
0.0001	70	0.4412	0.1765	0.7059	0.24
0.001	25	**0.8235**	**0.8235**	**0.8235**	**0.8235**
0.001	50	0.6765	0.8824	0.4706	0.7317
0.001	70	0.7059	0.7647	0.6471	0.7222
0.000001	25	0.4706	0.8824	0.0588	0.625

Note. The bold data = The best results

Table 3
Comparing performance metrics of the DenseNet121 Model with augmentation with different learning rates (0.000001,0.00001, 0.001) and a number of epochs (25,50,70) in the test dataset

Learning rate	Epoch	Accuracy	Sensitivity	Specificity	F1-score
0.000001	25	0.3529	0.4074	0.6471	0.5
0.000001	50	0.4706	0.2353	0.7059	0.3077
0.000001	70	0.5882	0.8	0.2353	0.3636
0.0001	25	0.7353	0.8235	0.6471	0.767
0.0001	50	0.6176	0.3529	0.8824	0.48
0.0001	70	0.7647	0.6471	0.8824	0.7333
0.001	25	0.7941	0.8235	0.7647	0.8
0.001	**50**	**0.8824**	**0.7647**	**1**	**0.8667**
0.001	70	0.7647	0.7059	0.8235	0.75

Note. The bold data = The best results

Table 4
Comparing performance metrics of the DenseNet Model with augmentation among different resizing methods (bilinear, nearest, and bicubic) with a learning rate of 0.001 and the number of epochs of 50 in the test dataset

Resize method	Epoch	Accuracy	Sensitivity	Specificity	F1-score
Bilinear	50	0.7353	0.7647	0.7059	0.7429
Nearest	50	0.7059	0.6471	**0.7647**	0.6875
Bicubic	50	**0.8235**	**0.9412**	0.7059	**0.8421**

Note. The bold data = The best results

Table 5
Comparing performance metrics of the DenseNet121 Model with augmentation among different filtering methods (non-filtering, median, Gaussian, and median + Gaussian) with a learning rate of 0.001 and a number of epochs of 70 in the test dataset

Filtering method	Resize	Accuracy	Sensitivity	Specificity	F1-score
None	**None**	**0.7647**	**0.7647**	**0.7647**	**0.7647**
Gaussian	None	0.7059	0.7647	0.6471	0.7222
Median	None	0.7353	0.7059	0.7647	0.7273
Both	None	0.5	0	1	0

Note. The bold data = The best results

Table 6
Cross-validation using 5-fold cross-validation for the best model, the DenseNet121 with data augmentation, the learning rate is 0.001, and the number of epochs is 50

Transfer learning model	Avg. accuracy	Avg. sensitivity	Avg. specificity	Avg. F1-score
DenseNet	0.9464 ± .0393	0.9692 ± 0.0377	0.9231 ± .0487	0.9481 ± .0383

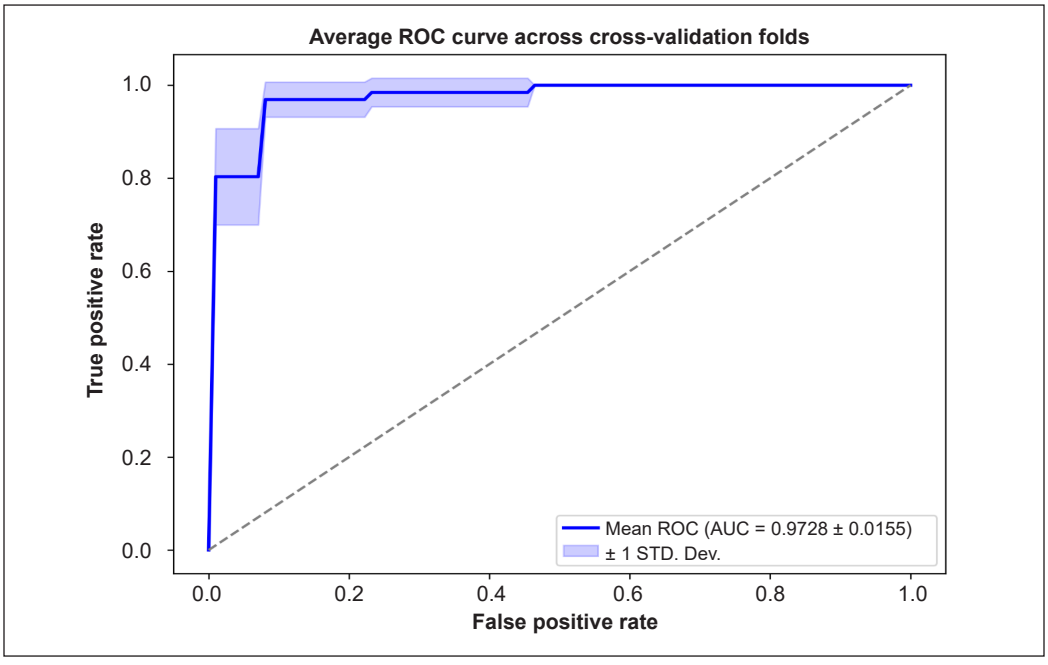

Figure 2. Receiver operating characteristic (ROC) curve in the test dataset using the best model-DenseNet121

CONCLUSION

This study presents the development of a deep learning model for the interactive identification of the SVS in brain stroke patients using the MRI data. A pre-trained DenseNet121 model was fine-tuned with augmented samples and trained using a learning rate of 0.001 for 50 epochs. Experimental results indicate that the data augmentation significantly improved the model performance, whereas image filtering techniques (e.g., median and Gaussian filters) did not yield further enhancement. These findings highlight the effectiveness of the augmentation in enhancing the SVS detection accuracy.

A comparative analysis of the ResNet50 and ConvNeXtXLarge revealed a significant discrepancy in classification performance. Both models achieved 100% sensitivity but 0% specificity, meaning they correctly identified all the SVS-positive cases but failed to classify the SVS-negative cases accurately. This suggests severe overfitting, where the models memorised features from the SVS-positive class rather than learning generalisable patterns. Several factors may have contributed to this issue, including the small dataset size, the complexity of the models, and insufficient regularisation.

The AUC score further confirms the model's strong classification ability. The DenseNet121 model achieved an AUC of 0.9728 (Figure 1), indicating excellent discriminative performance. However, despite this high AUC value, a meaningful comparison with human radiologists and existing AI-based stroke detection tools is

necessary to assess its clinical relevance. Additionally, external validation on independent datasets is required to ensure generalisability and robustness in real-world applications.

Furthermore, the DenseNet has also shown superior performance in brain tumour detection, as it is capable of handling small datasets more effectively than other models (Thimma Reddy & Balaram, 2024). Additionally, the DenseNet pre-trained model has demonstrated improved accuracy in various medical imaging applications, including fundus images (Xu et al., 2018), breast cancer detection (Hamdy et al., 2021), and chest disease diagnosis (Iswahyudi et al., 2024), among others.

Our study addresses the challenges posed by limited radiology data through employing the transfer learning, image augmentation, and various pre-processing techniques. Nevertheless, some limitations must be considered. The samples were extracted from a small region and manually delineated, whereas an automatic approach would be preferable. Additionally, the limited dataset size and potential data variability or class imbalance may have contributed to overfitting.

For future work, our approach is planned to be refined by developing an automatic segmentation method, improving accuracy through hyperparameter tuning, and exploring alternative strategies to enhance the model's robustness and generalisation performance. Furthermore, a comparative study with radiologists and existing AI models will be conducted to evaluate its clinical applicability and real-world effectiveness.

ACKNOWLEDGEMENTS

We would like to thank the radiology team at HSAAS, UPM, Malaysia, for their support in image annotation and clinical insights. We also acknowledge the Centre for Intelligent Signal and Imaging Research (CISIR), Universiti Teknologi PETRONAS (UTP), for their technical guidance and support throughout this study.

REFERENCES

Badesa, F. J., Morales, R., Garcia-Aracil, N., Sabater, J. M., Casals, A., & Zollo, L. (2014). Auto-adaptive robot-aided therapy using machine learning techniques. *Computer Methods and Programs in Biomedicine*, *116*(2), 123–130. https://doi.org/10.1016/j.cmpb.2013.09.011

Benson, J. C., Kallmes, D. F., Larson, A. S., & Brinjikji, W. (2021). Radiology-pathology correlations of intracranial clots: Current theories, clinical applications, and future directions. *American Journal of Neuroradiology*, *42*(9), 1558–1565. https://doi.org/10.3174/ajnr.A7249

Bento, M., Souza, R., Salluzzi, M., Rittner, L., Zhang, Y., & Frayne, R. (2019). Automatic identification of atherosclerosis subjects in a heterogeneous MR brain imaging data set. *Magnetic Resonance Imaging*, *62*, 18–27. https://doi.org/10.1016/j.mri.2019.06.007

Bochniewicz, E. M., Emmer, G., McLeod, A., Barth, J., Dromerick, A. W., & Lum, P. (2017). Measuring functional arm movement after stroke using a single wrist-worn sensor and machine learning.

Journal of Stroke and Cerebrovascular Diseases, *26*(12), 2880–2887. https://doi.org/10.1016/j.jstrokecerebrovasdis.2017.07.004

Chen, H.-Y., & Su, C.-Y. (2018). An enhanced hybrid MobileNet. In *9th International Conference on Awareness Science and Technology* (pp. 308–312). IEEE. https://doi.org/10.1109/ICAwST.2018.8517177

Chung, J. -W., Kim, Y. -C., Cha, J., Choi, E. -H., Kim, B. M., Seo, W. -K., Kim, G. -M, & Bang, O. Y. (2019). Characterization of clot composition in acute cerebral infarct using machine learning techniques. *Annals of Clinical and Translational Neurology*, *6*(4), 739–747. https://doi.org/10.1002/acn3.751

Dumitriu LaGrange, D., Hofmeister, J., Rosi, A., Vargas, M. I., Wanke, I., Machi, P., & Lövblad, K. -O. (2023). Predictive value of clot imaging in acute ischemic stroke: A systematic review of artificial intelligence and conventional studies. *Neuroscience Informatics*, *3*(1), 100114. https://doi.org/10.1016/j.neuri.2022.100114

Faiz, M. F. I., & Iqbal, M. Z. (2022). XceptionUnetV1: A lightweight DCNN for biomedical image segmentation. In L. Barolli, F. Hussain, & T. Enokido (Eds.), *Advanced information networking and applications* (pp. 23–32). Springer. https://doi.org/10.1007/978-3-030-99619-2_3

Giacalone, M., Rasti, P., Debs, N., Frindel, C., Cho, T. -H., Grenier, E., & Rousseau, D. (2018). Local spatio-temporal encoding of raw perfusion MRI for the prediction of the final lesion in stroke. *Medical Image Analysis*, *50*, 117–126. https://doi.org/10.1016/j.media.2018.08.008

Gunturu, V., Maiti, N., Toure, B., Kunekar, P., Banu, S. B., & Lenin, D. S. (2024). Transfer learning in biomedical image classification. In *International Conference on Advances in Computing, Communication and Applied Informatics* (pp. 1–5). IEEE. https://doi.org/10.1109/accai61061.2024.10601862

Hamdy, E., Zaghloul, M. S., & Badawy, O. (2021). Deep learning supported breast cancer classification with multi-modal image fusion. In *22nd International Arab Conference on Information Technology* (pp. 1–7). IEEE. https://doi.org/10.1109/ACIT53391.2021.9677099

Hanning, U., Sporns, P. B., Psychogios, M. N., Jeibmann, A., Minnerup, J., Gelderblom, M., Schulte, K., Nawabi, J., Broocks, G., Meyer, L., Krähling, H., Brehm, A., Wildgruber, M., Fiehler, J., & Kniep, H. (2021). Imaging-based prediction of histological clot composition from admission CT imaging. *Journal of Neurointerventional Surgery*, *13*(11), 1053–1057. https://doi.org/10.1136/neurintsurg-2020-016774

Hilbert, A., Ramos, L. A., van Os, H. J. A., Olabarriaga, S. D., Tolhuisen, M. L., Wermer, M. J. H., Barros, R. S., van der Schaaf, I., Dippel, D., Roos, Y. B. W. E. M., van Zwam, W. H., Yoo, A. J., Emmer, B. J., Lycklama à Nijeholt, G. J., Zwinderman, A. H., Strijkers, G. J., Majoie, C. B. L. M., & Marquering, H. A. (2019). Data-efficient deep learning of radiological image data for outcome prediction after endovascular treatment of patients with acute ischemic stroke. *Computers in Biology and Medicine*, *115*, 103516. https://doi.org/10.1016/j.compbiomed.2019.103516

Hofmeister, J., Bernava, G., Rosi, A., Vargas, M. I., Carrera, E., Montet, X., Burgermeister, S., Poletti, P. -A., Platon, A., Lovblad, K. -O., & MacHi, P. (2020). Clot-based radiomics predict a mechanical thrombectomy strategy for successful recanalization in acute ischemic stroke. *Stroke*, *51*(8), 2488-2494. https://doi.org/10.1161/STROKEAHA.120.030334

Hou, Q., Lu, C. -Z., Cheng, M. -M., & Feng, J. (2024). Conv2Former: A simple transformer-style ConvNet for visual recognition. In *IEEE Transactions on Pattern Analysis and Machine Intelligence* (Vol 46, No. 12, pp. 8274–8283). IEEE. https://doi.org/10.1109/TPAMI.2024.3401450

Iswahyudi, W., Farhan Ali Irfani, M., Dwi Mahandi, Y., Ari Elbaith Zaeni, I., Sendari, S., & Widiyaningtyas, T. (2024). Analyzing the effectiveness of MobileNetV2, Xception, and DenseNet for classifying chest diseases: Pneumonia, pneumothorax, and cardiomegaly. In *International Conference on Electrical Engineering and Computer Science* (pp. 251–255). IEEE. https://doi.org/10.1109/ICECOS63900.2024.10791269

Mojtahedi, M., Kappelhof, M., Ponomareva, E., Tolhuisen, M., Jansen, I., Bruggeman, A. A. E., Dutra, B. G., Yo, L., LeCouffe, N., Hoving, J. W., van Voorst, H., Brouwer, J., Terreros, N. A., Konduri, P., Meijer, F. J. A., Appelman, A., Treurniet, K. M., Coutinho, J. M., Roos, Y., van Zwam, W., … Marquering, H. (2022). Fully automated thrombus segmentation on CT images of patients with acute ischemic stroke. *Diagnostics*, *12*(3), 698. https://doi.org/10.3390/diagnostics12030698

Myers, K. D., Knowles, J. W., Staszak, D., Shapiro, M. D., Howard, W., Yadava, M., Zuzick, D., Williamson, L., Shah, N. H., Banda, J. M., Leader, J., Cromwell, W. C., Trautman, E., Murray, M. F., Baum, S. J., Myers, S., Gidding, S. S., Wilemon, K., & Rader, D. J. (2019). Precision screening for familial hypercholesterolaemia: A machine learning study applied to electronic health encounter data. *The Lancet Digital Health*, *1*(8), e393–e402. https://doi.org/10.1016/S2589-7500(19)30150-5

Olive-Gadea, M., Crespo, C., Granes, C., Hernandez-Perez, M., Pérez de la Ossa, N., Laredo, C., Urra, X., Carlos Soler, J., Soler, A., Puyalto, P., Cuadras, P., Marti, C., & Ribo, M. (2020). Deep learning based software to identify large vessel occlusion on noncontrast computed tomography. *Stroke*, *51*(10), 3133–3137. https://doi.org/10.1161/STROKEAHA.120.030326

Padmakala, S., & Uma Maheswari, S. (2024). Deep learning-based MRI analysis for brain tumor detection: Insights from ResNet and DenseNet models. In *8th International Conference on Electronics, Communication and Aerospace Technology* (pp. 1620–1626). IEEE. https://doi.org/10.1109/ICECA63461.2024.10800894

Peixoto, S. A., & Rebouças Filho, P. P. (2018). Neurologist-level classification of stroke using a Structural Co-Occurrence Matrix based on the frequency domain. *Computers and Electrical Engineering*, *71*, 398–407. https://doi.org/10.1016/j.compeleceng.2018.07.051

Phuyal, S., Paudel, S., Chhetri, S. T., Phuyal, P., Shrestha, S., & Maharjan, A. M. S. (2024). Susceptibility weighted imaging for detection of thrombus in acute ischemic stroke: A cross-sectional study. *Health Science Reports*, *7*(8), e2285. https://doi.org/10.1002/hsr2.2285

Shen, Z., & Liu, Y. (2017). A novel connectivity of deep convolutional neural networks. In *Chinese Automation Congress* (pp. 7779–7783). IEEE. https://doi.org/10.1109/CAC.2017.8244187

Shinohara, Y., Takahashi, N., Lee, Y., Ohmura, T., & Kinoshita, T. (2020). Development of a deep learning model to identify hyperdense MCA sign in patients with acute ischemic stroke. *Japanese Journal of Radiology*, *38*(2), 112–117. https://doi.org/10.1007/s11604-019-00894-4

Sirsat, M. S., Fermé, E., & Câmara, J. (2020). Machine learning brain stroke: A review. *Journal of Stroke and Cerebrovascular Diseases*, *29*(10), 105162. https://doi.org/10.1016/j.jstrokecerebrovasdis.2020.105162

Tang, S. Z., Sen, J., Goh, Y. G., & Anil, G. (2021). Susceptibility vessel sign as a predictor for recanalization and clinical outcome in acute ischaemic stroke: A systematic review and meta-analysis. *Journal of Clinical Neuroscience*, *94*, 159–165. https://doi.org/10.1016/j.jocn.2021.10.017

Thimma Reddy, B., & Balaram, V. V. S. S. S. (2024). MAFD: Model Agnostic Forest Densenet Approach for brain tumor detection. In R. R. Chillarige, S. Distefano, & S. S. Rawat (Eds.), *Advances in computational intelligence informatics* (pp. 295–306). Springer. https://doi.org/10.1007/978-981-97-4727-6_30

Tsochatzidis, L., Costaridou, L., & Pratikakis, I. (2019). deep learning for breast cancer diagnosis from mammograms—A comparative study. *Journal of Imaging*, *5*(3), 37. https://doi.org/10.3390/jimaging5030037

Utami, P., Hartanto, R., & Soesanti, I. (2022). The EfficientNet performance for facial expressions recognition. In *5th International Seminar on Research of Information Technology and Intelligent Systems* (pp. 756–762). IEEE. https://doi.org/10.1109/ISRITI56927.2022.10053007

Wessels, S., & van der Haar, D. (2023). Using a genetic algorithm to update convolutional neural networks for abnormality classification in mammography. In *Proceedings of the 12th International Conference on Pattern Recognition Applications and Methods* (pp. 790–797). SciTePress. https://doi.org/10.5220/0011648500003411

Xu, X., Lin, J., Tao, Y., & Wang, X. (2018). An improved DenseNet method based on transfer learning for fundus medical images. In *2018 7th International Conference on Digital Home* (pp. 137–140). IEEE. https://doi.org/10.1109/ICDH.2018.00033

Zhu, K., Bala, F., Zhang, J., Benali, F., Cimflová, P., Kim, B. J., McDonough, R., Singh, N., Hill, M. D., Goyal, M., Demchuk, A., Menon, B. K., & Qiu, W. (2023). Automated segmentation of intracranial thrombus on NCCT and CTA in patients with acute ischemic stroke using a coarse-to-fine deep learning model. *American Journal of Neuroradiology*, *44*(6), 641–648. https://doi.org/10.3174/ajnr.a7878

Pertanika J. Sci. & Technol. 33 (5): 2049 - 2068 (2025)

PERTANIKA JOURNALS

SCIENCE & TECHNOLOGY

Journal homepage: http://www.pertanika.upm.edu.my/

Review Article

Assessing the Role of Ontologies in Enhancing Various Modern Systems

Sarah Dahir[1]* and Abderrahim El Qadi[2]

[1]*Laboratory of Intelligent Systems and Applications, Faculty of Sciences and Technologies, Sidi Mohamed Ben Abdellah University, Fez 30000, Morocco*
[2]*Department of Applied Mathematics and Computer Engineering, National Graduate School of Arts and Crafts, Mohammed V University in Rabat 10000, Morocco*

ABSTRACT

Increasing the discoverability, accessibility, and understandability of data for both humans and machines is the ultimate objective of the Semantic Web (SW). Therefore, the purpose of this work is to survey and gain a clear understanding of the current state of the use of Linked Open Data (LOD) across a range of domains. We discovered that, of the four domains we evaluated, the two that use ontologies the most are machine learning (ML) and artificial intelligence (AI) in general. On the other hand, because it is a relatively new domain, the Metaverse uses ontologies the least. Despite ontologies' capacity to guarantee consistency in the virtual world, increase revenue, ensure inclusivity for people with disabilities, and save time. Additionally, the majority of domains are not utilizing SW to its full potential, and additional customization is required in light of each domain's unique challenges and traits. For instance, AI, cybersecurity, and the Metaverse have an unstructured nature and lack stability. Also, cybersecurity and the Metaverse lack consensus. In addition to this, the Metaverse is highly scalable. Another common difficulty of incorporating ontologies in general is choosing the right mapping technique as there are many. Given these domains' characteristics, Business Intelligence (BI) finds it easier to integrate them, whereas cybersecurity and the Metaverse find it more difficult. Lastly, dynamic ontologies are believed to make ontologies more appropriate and adaptable for domains lacking stability.

Keywords: Artificial intelligence, augmented reality, Business Intelligence, cybersecurity, ontology, Semantic Web

ARTICLE INFO

Article history:
Received: 12 December 2024
Accepted: 08 April 2025
Published: 11 August 2025

DOI: https://doi.org/10.47836/pjst.33.5.02

E-mail addresses:
sarah.dahir@usmba.ac.ma (Sarah Dahir)
a.elqadi@um5r.ac.ma (Abderrahim El Qadi)
* Corresponding author

e-ISSN: 2231-8526

INTRODUCTION

First and foremost, it is safe to confess that data is the ultimate fortune that anyone can capitalize on to succeed. Hence, Database Management Systems (DBMS) such as Oracle hang on their log files to be able to get back data if it gets corrupted or lost. As for businesses, they always have a history of data (in their data warehouse) to keep track of their evolution and build knowledge from it. It is also worth mentioning that the Facebook owner purchased WhatsApp and spent plenty of money on it even though it was not profitable, because he will gain something that is even more beneficial: data.

As for the SW, it is a main focus of Web 3.0 for many good reasons. Not only does it offer multiple Ontology Web Language (OWL) profiles that are centred on triples (subject, predicate, object), adding semantics to data. But it also allows us to claim data using SPARQL Protocol and Resource Description Framework (RDF) Query Language. Furthermore, it provides Named Entity Recognition (NER), e.g., France and Barack Obama. Moreover, it provides a wide range of axioms that can be tailored to our needs. For instance, there are: (i) fuzzy ontologies that consider the degree of membership of an instance to a class, and (ii) contextual ontologies that consider the degree of trust in a source when there are many. Additionally, OWL2 Description Logics (OWL2 DL) adds the ability to chain multiple properties thanks to (iii) property chain axioms. Also, one can use (vi) Semantic Web Rule Language (SWRL) to make decisions based on multiple conditions. In addition to that, SW requires the use of (v) reasoners to make inferences and check consistency. Last but not least, it allows the (vi) organization of ontologies into modules, which makes them easy to manage and reuse. Thus, offering Linked data to benefit from in diverse domains and for different purposes.

In recent years, ontologies have become a fundamental component of modern systems, aiding data organization, knowledge representation, and semantic interoperability across various domains. Worldwide, sectors have integrated ontologies to enhance system capabilities and improve decision-making. For example, the MITRE ATT&CK framework uses ontologies to categorize and analyse cyber threats, allowing organizations to better understand and mitigate potential attacks. Similarly, AI systems, such as Google's Knowledge Graph, leverage ontologies to create structured knowledge representations, improving search relevance and machine understanding.

This survey investigates how ontologies are incorporated into four different domains of information systems: AI, BI, cybersecurity, and the Metaverse. The choice to focus on these sectors stems from their pivotal role in the digital economy, where the complexity of data and the need for enhanced decision-making are rapidly growing. In cybersecurity, the increasing volume and sophistication of cyber threats demand structured knowledge frameworks for threat analysis. AI applications require ontologies to ensure semantic clarity and interpretability in decision-making models. Businesses rely heavily on data

integration and insights provided by BI systems, which are enhanced by ontologies. Lastly, the Metaverse, an emerging sector, necessitates interoperable virtual environments where ontologies can support digital asset management and rule-setting. This survey also determines which domains are more often introducing ontologies in their applications. Additionally, it examines how ontologies can enhance systems' performance and functionality despite challenges. Our survey shows the potential of ontologies to enhance modern systems by thoroughly examining various domains, addressing challenges, and proposing solutions. This study remains analytical, with no practical implementation. Further research is needed to validate and apply our findings.

BACKGROUND

Artificial Intelligence

Concerning AI, it is undeniably a huge success. Nevertheless, it has some liabilities. For example, it fails at predicting that « safe » is irrelevant to the query « dangerous cars », since « dangerous » and « safe » co-occur. Not only this, but AI systems require at times both an elevated number of iterations to start making correct predictions and a large scale of data for training.

One example of AI-powered systems is Chatbots. They are dialog systems (1,2). In order to answer a user's query: first, Natural Language Processing (NLP) is used to process it and extract keywords from it. Second, the keywords are matched to a knowledge base like Wikipedia, Frequently Asked Questions (FAQ), and manuals or a knowledge graph with nodes and edges. The edges may or may not be labelled. These Chatbots often assist disabled people by reading text for example, thereby enhancing daily activities and promoting inclusivity for people with disabilities. The drawbacks to building a chatbot are the difficulty of classifying the query especially when the utterance is long. Consequently, it is easy to be misled by the term frequency or the lack of certain terms that would best describe the user's intent. Also, it is hard to retrieve the right answer, and provide related information.

Another example of AI technologies is IBM Watson that uses Medical like Systematized Nomenclature of Medicine – Clinical Terms (SNOMED CT). The terminology consists of over 325,000 clinical concepts and is used in analysing medical records and suggesting treatment options. But such terminologies although organized in hierarchical way; they only define basic relationships, e.g., "part of", "is a". Also, they cannot be used for automated reasoning as they do not support reasoning engines like Hermit and Pallet.

AI systems that adhere to ethical standards and protect individual privacy are of need. Hence, Radanliev et al. (2024) explore innovative algorithmic techniques such as homomorphic encryption, which allows computations on encrypted data. They also explore federated learning that protects individuals' data privacy through training the model locally and sharing only the results with a central server. Last but not least, they dive into

differential privacy that consists of adding noise to data so as to make sure that individual data points cannot be identified. These methods limit breaches and misuse of AI systems, therefore allowing responsible AI deployment.

Cybersecurity

The Common Vulnerabilities and Exposures (CVE) identified 16,555 vulnerabilities in 2018. This was the highest number in the past 10 years. Later on, the increase in cyber-attacks during the pandemic and its remote working aftermath (Taylor, 2022) increased security attacks. This number kept rising every year and attained 24,000 in 2023, according to the National Vulnerability Database.

Multiple sources provide vulnerabilities to sensitize users; they come through when it comes to assisting them in vulnerability management. But, sources that gather and yield from all available and trustworthy sources are scarce (R. Syed, 2020). According to them, available ontologies in the domain are not enough for vetting vulnerabilities properly; like the Common Vulnerability Scoring System (CVSS) suggests.

One attempt to lessen security issues was made by Gao et al. (2023), who emphasize on swarms ability to solve cybersecurity.

Business Intelligence

Decision support Systems (DSS) aim at offering « the right information at the right time, with the right format (Turban et al., 2011). These systems can be classified into many categories, including data-driven DSS: data warehouse/BI (DW/BI) systems (Power, 2009) that allow decision making in companies through: First, the integration of data from various sources into a data lake (DL). These data include: (i) operational systems' data i.e., data from the information system (IS) or an Entreprise Resource Planification (ERP). They also include (ii) Client Relationship Management (CRM) data which are the company's strategy for client retention. The latter involves storing clients' phone numbers as well as their complaints and targeted or personalized marketing offers by sending e-mails to clients based on their age for example. Furthermore, they include (iii) external data like e-reputation data. Second, Extract, Transform, Load (ETL) these data into the DW. The latter could be split into many subject-oriented datasets called data marts. Third, the use of Online Analytical Processing (OLAP) tools to get reports and dash boards for decision making. These tools store data in cubes for dimensional modelling. They distinguish between quantitative facts (e.g., salesperson's quarterly target, product category's quarterly target, and regional quarterly target), and contextual dimensions (e.g., salesperson, product's category, region, time, and their hierarchies). Consequently, one can roll down to analyse a salesperson's quarterly target in a specific month or even a day. Alternatively, roll up to find that of a certain year. Also, users may drill up/down, i.e., move upwards or downwards in

the overall hierarchy of the cube and not only for a specific dimension but for all of them. Furthermore, one gets to aggregate many dimensions to check the quarterly target of a salesperson for a product in a certain month and a specific city. Users also get to slice for a two-dimensional view, e.g., sales per product and month. Alternatively, dice to extract a sub-cube that includes multiple dimensions. Hence, multidimensional databases (Kimball & Ross, 2013) are powerful compared to relational databases.

Metaverse

Augmented reality (AR) is valuable given that it yields a seamless integration of virtual environment in the real world objects (Marques et al., 2021). One main use of the Metaverse is allowing remote collaboration, which can be challenging since it involves vetting multiple aspects like team dynamics, task management, and communication, to name a few (Marques et al., 2021). Furthermore, the huge volume of interlinked data, especially when dealing with Mobile AR (MAR), makes appropriate filtering even more crucial to not overwhelm users using small screens. Yet, give them the ability to explore further links without having to switch to a different application. However, the heterogeneous nature of data in the Metaverse is yet another challenge.

One example of a virtual world is Decentraland. It is designed with its own set of data structures and protocols. This can hinder assets like skins and avatars from being transferred between different virtual environments or applications. In fact, the restrictive nature of such applications prevents the fluidity and scalability of the Metaverse, hindering the potential for a truly unified and open ecosystem.

As of now, many existing platforms lack the necessary accommodations for individuals with disabilities. To ensure that users with disabilities have equal access to virtual spaces, Radanliev et al. (2024) suggest a framework that enhances inclusivity for disabled people. For instance, disabled people can be allowed to customize their avatars to reflect their condition (e.g., adding a wheelchair). Another possibility for inclusivity would be creating interfaces that can accommodate people with different disabilities using assistive technologies like screen readers, voice commands, or haptic feedback devices for those with visual, auditory, or physical impairments.

METHODOLOGY

To identify relevant literature for this survey, a search method (Figure 1), which is commonly used in surveys within the scientific domain, was conducted. The method includes finding the right search strings (Table 1) to answer the following research questions (RQ):

RQ1: How and which domains are incorporating ontologies the most?

RQ2: How can the use of ontologies be optimized within each domain for enhanced results?

RQ3: How do the complexity and characteristics of specific fields impact the suitability and success of their integration?

As for the search engine, we used Google Scholar and filtered results to only get papers that were first and for most published between 2014 and 2024 and that contained one of the search strings from Table 1 along with « ontology », « Linked data », « Knowledge graph », « Semantic Web » in the title using the inclusion criterion « allintitle : », e.g., « allintitle : ontology natural language processing ».

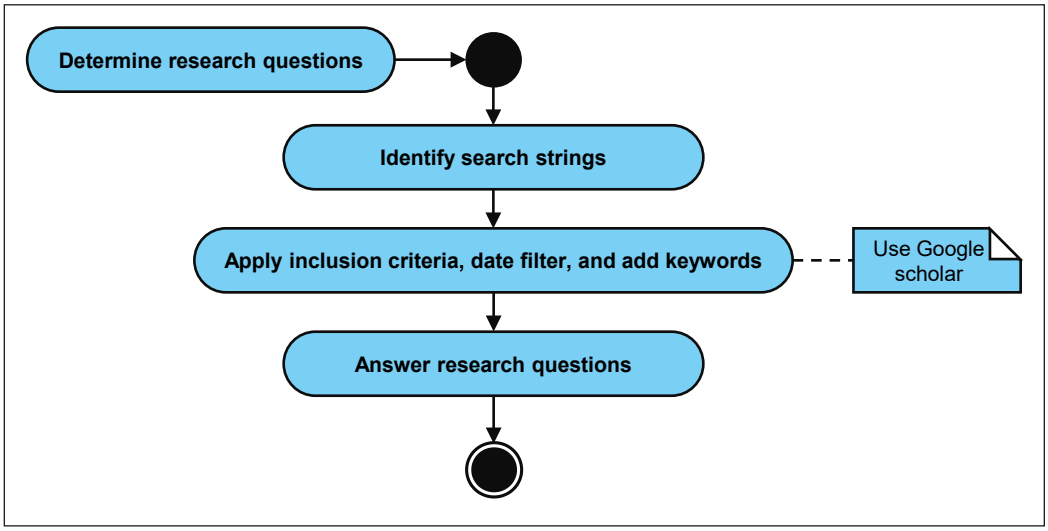

Figure 1. Methodology steps

Table 1
A comparison between the use of ontologies in different domains

Domain	Reference	Method	Purpose
AI	Ali et al. (2017)	Fuzzy ontologies and SWIRL rules	Sentiment analysis and decision making
	Nguyen et al. (2021)	NER	Classification of user entry in Chatbots
Cybersecurity	De Rosa et al. (2022)	Developing Ontologies	Circumventing attacks with an ontological representation instead of a syntactic one
	Mugwagwa et al. (2023)	Swarm ontologies	Identifying and mitigating threats
	K. Liu et al. (2022) Mitra et al. (2021); R. Syed (2020); Rastogi et al. (2021)	Developing ontologies	Gathering and sharing cybersecurity issues and solutions

Table 1 *(continue)*

Domain	Reference	Method	Purpose
	K. Liu et al. (2022)	Temporal-event ontologies	Representing dynamic knowledge through
BI	Antunes et al. (2022)	NER	Avoiding semantic mismatches in ETL
	Amaral and Guizzardi (2019); Moreira et al. (2015)	Representing multidimensional models in the form of ontologies by adding OWL DL's constraints in the DW	Better expressiveness
	Prat, Akoka, et al. (2012)	Uncovering relations through reasoner's inference	Better semantic expressiveness
	Prat, Akoka, et al. (2012); Prat, Megdiche, et al. (2012)	A domain ontology	Validating data's consistency within the DW
	Kurze et al. (2010)	Defining core concepts through an ontology	Insurance of interoperability between DW systems
Metaverse	Marques et al. (2021)	Developing an ontology	Facilitating remote collaboration
	Vlachos et al. (2024)	Combining existing cultural heritage ontologies	Ensuring interoperability

Note. AI = Artificial intelligence; BI: Business Intelligence; SWIRL = Semantic Web Inference Rule Language; NER = Named Entity Recognition; ETL = Extract, Transform, Load; OWL = Ontology Web Language; DL = Data lake; DW = Data warehouse

RESULTS

Artificial Intelligence

LOD could serve as training data. It was believed that their limits could be tackled by processing the training data to add and/or drop data based on LOD.

Also, by formalizing knowledge and relationships between concepts, ontologies enhanced AI systems' contextual understanding and ethical decision-making processes. In other words, ontologies could assist in embedding ethical standards within automated decision-making frameworks.

Ontologies in Sentiment Analysis

Ali et al. (2017) emphasized on the paramount importance of fuzzy ontologies as opposed to crisp ones in enhancing Intelligent Transportation Systems (ITS). They used tweets bigrams and trigrams' features to determine the degree of opinions' polarity for travellers. Also, they used SWRL rules to determine the reasons behind road congestion, for example. The authors' suggested system provided a 23% improvement in precision compared to using a classic ontology system. This leads to better decision-making for transport offices.

Nguyen et al. (2021) looked for the intent in the utterance by performing NER and classified queries into greeting, concepts, out of scope, comparison, and related knowledge. Consequently, classification issues are solved. Furthermore, they relied on relations between the provided answer and the meaning of the query to yield further knowledge. The authors' chatbot achieved an accuracy of 82% when tested on six types of queries.

Cybersecurity

De Rosa et al. (2022) suggested an ontology-based tool for tackling the rise in the number of attacks and presented knowledge gathered from external security sources. Their end goal was to opt for a semantic representation instead of a syntactic one.

Mugwagwa et al. (2023) used swarm ontology to sort out cybersecurity issues, given that the collective capabilities of swarms were higher than those of individual models in threat detection and bypass. They also developed a simulator to assess the role of ontologies in threat identification and mitigation.

K. Liu et al. (2022) outline the importance of knowledge graphs in cybersecurity. They gave vent to their possible applications given: (i) the asymmetric relationship between offence and defence in the security domain. Also, (ii) there has been a span in cyberspace to accommodate more fields, ranging from health to aviation and many more. Additionally, (iii) there is a shortage of cybersecurity experts. And (vi) the aggregation difficulty of heterogeneous data from open-source libraries and datasets into one model could be tackled by using, for instance, the Unified Cybersecurity Ontology (UCO). This ontology aggregates data from multiple cybersecurity standards and systems (Iannacone et al., 2015; Z. Syed et al., 2016). It therefore facilitates information sharing and exchange. However, ontologies were most effective when they were aimed towards a specific scenario. In other words, when they were application oriented, e.g., intrusion detection, malware categorization, vulnerability analysis, and threat actor analysis (Hooi et al., 2019; Pinkston et al., 2003; Sanagavarapu et al., 2021) (i.e., analysing his/her tools and level of expertise) rather than domain oriented (i.e., general). This specificity in ontologies was yet another issue since they might vary based on the field's specificities (e.g., health cybersecurity). Moreover, according to Sanagavarapu et al. (2021), ontologies should have been automatically enriched as this was a rapidly evolving domain. For instance, vulnerability management and prediction were highlighted in R. Syed (2020) as Syed developed a vulnerability ontology for cyber intelligence alert systems. Rastogi et al. (2021) established a malware knowledge graph for predicting malware attributes and sorting potential vulnerabilities. Their model achieved 80.4 for the hits@10 metric, which predicted the top 10 options for an information class. K. Liu et al. (2022) shed light on the need for representing dynamic knowledge through temporal and event subordination relations in cybersecurity knowledge graphs. Additionally, Mitra et al. (2021) suggested an ontology to vet out fake cybersecurity

intelligence, i.e., false or misleading information presented as threats or attacks by either malicious actors or unintentional errors and misinterpretations.

Social media was another source that could have been of paramount importance in vulnerability management. Truth be told, every social media per se yielded a mere tad number of ways to counter and hold out against attacks. But their combination had the potential to pay off. Hence, R. Syed (2020) took up benefitting from social media in an ontology along with other information from multiple other ontologies.

Business Intelligence

Given that data in a DL was heterogeneous, the same entity could have been in different formats and different presentations. So, in order to have a single version of truth (Antunes et al., 2022) and avoid semantic mismatches, NER could be used in the ETL phase to automate the process. Next, the determined entities along with their extracted properties could have been mapped to other ontologies to pinpoint their corresponding formalized entities' names and properties' names. This alignment of ontologies to have a common terminology (T-box) for knowledge building also benefited on the one hand, the interoperability between stakeholders or between DW/BI systems and other DSS (Kimball & Ross, 2013). On the other hand, it benefited the enrichment of data with semantic similarity (e.g., cat and kitten) and semantic relatedness (e.g., cat and dog). This enrichment offers new knowledge for decision makers. Additionally, at the DW level, the representation of multidimensional models in the form of ontologies by adding OWL DL's constraints allowed a higher level of expressiveness (Amaral & Guizzardi, 2019; Moreira et al., 2015). This semantic expressiveness would, in turn, help uncover relations through the reasoner's inference (Prat, Akoka, et al., 2012). For this purpose, an extra mapping layer was added between the ontological constraints within DW and the formal domain ontology, with the reasoner being used in the latter. As a result, users would get insight into other facts and hierarchical dimensions to use in semantic OLAP cubes. Alternatively, a domain ontology could be used to validate the data within the DW by checking its consistency and enforcing constraints (Prat, Akoka, et al., 2012; Prat, Megdiche, et al., 2012). On a similar note, users could take advantage of ontologies to interpret OLAP results and collaborate/share knowledge with other stakeholders. Last but not least, Kurze et al. (2010) guided the insurance of interoperability between DW systems by defining core concepts for data warehousing in an ontology.

Metaverse

According to Azuma et al. (2001), AR was not constrained to a particular type or a particular sense. Hence, it could be applied with all human senses (McGee, 1999; van Krevelen & Poelman, 2010) and could even substitute people's lacking senses (aka sensory substitution) (Carmigniani et al., 2011).

One more subpart of AR was diminished or mediated reality, which consisted on the removal of physical objects from the perceived environment (Azuma et al., 2001).

Marques et al. (2021) yielded an ontology to facilitate remote collaboration through structuring and understanding the scenarios of such collaborations.

Assuming that data without ontological structure and constraints might lack depth and consistency, Vlachos et al. (2024) combined existing cultural heritage ontologies for better AR in that domain, ensuring both interoperability and reusability across different projects and scenarios.

As for ethics and accessibility, particularly for disabled people, developing ontologies that were specific to the Metaverse, like MetaOntology, aimed at standardizing associated technologies and infrastructure. This formalization enhanced interoperability and accessibility, enabling users with disabilities to navigate and interact more effectively and within virtual environments.

From Figure 2, it could be seen that AI was the domain where ontologies were the most used in recent years and that BI was the domain that used them the least.

Based on Table 2, ML was up there in terms of taking advantage of ontologies to improve related applications. Moreover, deep learning and sentiment analysis were other sub-domains that benefited from ontologies the most.

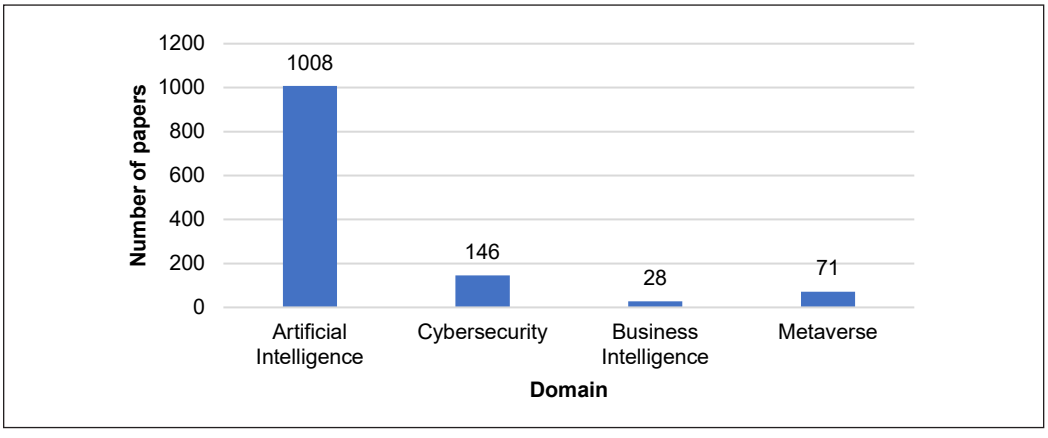

Figure 2. Number of English papers published between 2014 and 2024 and using in the title the keywords: Ontology/Linked Data/Semantic Web/Knowledge Graph, along with domain keywords

Table 2
Number of papers by sub domain using in the title: Ontology/Linked Data/Semantic Web/Knowledge Graph

Domain	Search string	Number of papers
Artificial intelligence	Artificial intelligence	94
	Deep learning	282
	Machine learning	484

Table 2 *(continue)*

Domain	Search string	Number of papers
	Opinion mining	27
	Sentiment analysis	152
	Natural language processing	116
	Chatbot	46
Cybersecurity	Cybersecurity	83
	Cyber security	63
Business Intelligence	Business Intelligence	26
Metaverse	Augmented reality	39
	Virtual reality	32

DISCUSSION

Comparison and Analysis

When it comes to AI, reasoners' inference would add more semantics to knowledge graphs. Thus, it benefits chatbot's capacity to classify user's input. Concerting healthcare AI, it is believed that by transforming SNOMED CT into an ontology with more advanced constraints like cardinality constraints (e.g., a patient has at most two diagnoses), and inverse properties (e.g., "has parent" and "has child"). Additionally, reasoners can infer new facts using defined axioms (e.g., disjointness and equivalence). For instance, they can find new connections. They can also detect logical inconsistencies such as contradictory definitions, redundant terms, and missing relationships. Furthermore, ontologies would allow advanced querying and improve interoperability by linking different datasets and allowing for more seamless integration across systems using Uniform Resource Identifiers (URIs).

As for Cybersecurity, ontologies are assumably great categorizers. This advantage leads to bettered reasoning (Abburu, 2012) and consideration of diverse implicit as well as explicit relations (DeStefano et al., 2016) for semantically boosted knowledge bases.

Assumably, SW remains by far the best choice if one has structured ontological data (like BI data) and is looking for semantic consistency across different areas of life (which is the case for BI for example). In other words, it is the best choice when the aim is to have a common vocabulary for a common understanding. This would also improve data integration through harmonizing data coming from different sources and ensuring its quality. One example of existing ontologies is Financial Industry Business Ontology (FIBO).

And concerning the Metaverse, matching ontologies can solve data heterogeneity. And URIs can allow access to real-time data despite their huge amount. Furthermore, a shared ontology can allow cross-world usage. For example, a wearable skin bought in Decentraland could be used by our created avatar in another Metaverse platform if both platforms agreed

upon the same ontology definitions. Consequently, instead of having to buy a new jacket or skin for each world, one can use the same wearables on different Metaverse platforms, making virtual items more valuable and interoperable. This, in turn, leads to easier content creation as creators can make wearables once and have them work across multiple virtual worlds, increasing their audience and revenue opportunities. Moreover, the ontology-based system could also suggest related or complementary assets based on semantic relationships defined in the ontology. For instance, if the creator selects a "cyberpunk jacket", the system might recommend other items such as "glowing gloves" or "high-tech boots". This would be time-saving and consistency-improving. But, this domain is new compared to the other ones, in this paper, which is why ontologies are underused in it despite their huge potential.

Our findings on the usefulness of ontologies in enhancing semantic interoperability, data integration, and decision-making are not limited solely to cybersecurity, AI, BI, and the Metaverse. In fact, similar principles and methodologies can be applied across a wide array of sectors (Gruber, 1993):

- Healthcare: Ontologies are extensively used in healthcare to standardize medical terminologies, integrate patient records, and support clinical decision-making. For example, the Unified Medical Language System (UMLS) organizes diverse biomedical vocabularies to facilitate data sharing and interoperability among Electronic Health Records (EHR) (Bodenreider, 2004; Noy & McGuinness, 2001). Also, the work by Kouremenou et al. (2024) presents a data modelling process aimed at achieving interoperability. The authors emphasize the importance of semantic and syntactic interoperability and address challenges such as compatibility issues and the need for global standards. Their approach contributes to resolving data management and exchange problems among healthcare entities, enhancing data accessibility and accuracy.
- Manufacturing and supply chain management: In manufacturing, ontologies help in structuring data from Internet of Things (IoT) devices and sensors, which can lead to more effective predictive maintenance, process optimization, and smart supply chain management. This approach enables better integration of heterogeneous data sources across production systems (Gómez-Pérez et al., 2004).
- Legal informatics: The legal field benefits from ontologies by systematizing complex legal information. They enable automated reasoning over case laws, regulations, and contractual documents, thereby supporting legal research and compliance monitoring.
- Education: Ontologies can support the development of adaptive learning systems by organizing educational content and tailoring it to individual learner profiles. This facilitates personalized learning and improved outcomes by mapping curricular standards to instructional materials.

- E-commerce: In e-commerce, ontologies are applied to enhance product categorization, semantic search, and recommendation engines. They enable more precise matching between customer queries and product offerings, ultimately leading to improved user experience and sales.
- Digital twins (DT): The study by Karabulut et al. (2024) offers a comprehensive review of how ontologies are utilized within DT, highlighting their role in knowledge representation, interoperability, and automated reasoning.

Incorporating ontological data representations aligns with the European Union's (EU) objectives of promoting digital transformation and establishing a Digital Single Market. It supports the EU's strategy for data-driven innovation and the development of interoperable digital public services. Moreover, the insights from these studies contribute to global discussions on data standardization and interoperability, influencing policies and practices beyond the EU.

Challenges and Open Issues

Although users opt for dynamic ontologies that include spatial, temporal, and event data to capture various dimensions of cyber threats and vulnerabilities; there is an absence of evaluation standards for dynamic ontologies (K. Liu et al., 2022).

Regarding BI, most related work studies use ontologies to limit heterogeneity and achieve interoperability while designing multidimensional models. But there is still a lack of papers that consider ontologies for the enrichment of DW with new interlinked data (Antunes et al., 2022). This enrichment would not only give a new ground on which users can build their decisions, but would also sort out semantic ambiguity, especially in complex domains (Bargui et al., 2011) like the healthcare domain. Moreover, to the best of our knowledge, even fewer studies were conducted on defining the architecture (T-box) of the DW to add instances (A-box) depending on the T-box. This is because full transformation of the DW would require further changes to the workflow and the tools used. For the time being, ontologies are rather used either to describe the DW's architecture (Szwed et al., 2015) or to support its design (X. Liu & Iftikhar, 2013). Concerning fuzzy and contextual ontologies, they are almost non-existent in the literature. Their use would drastically benefit the determination of valuable external sources from non-valuable ones right from the jump and would bring more accuracy to opinions' polarity on social media. Another possibility would be using ontologies, early on, for strategy modelling and metadata for guidance during information retrieval (IR) to automate the retrieval process and avoid retrieving irrelevant data for decision making.

As for the Metaverse, although it obtained a layered ontology from combining multiple ones (Vlachos et al., 2024). It can be less time-consuming, but it is hard to manage. Consequently, we will need to figure out ways to facilitate complex data management.

In general, ontologies can be challenging to incorporate for several reasons. First, they can be hard to create (Kiourtis et al., 2019). In fact, in order to build and maintain ontologies; a significant amount of manual intervention and expertise is needed to learn ontologies (Khadir et al., 2021) either from text or from relational databases. This process is time-consuming and impractical for resource-constrained domains. For more emphasize, ontologies are easier to incorporate when a domain is stable, as they can be hard to update if classification keeps changing. Second, ontologies have scalability and flexibility issues. This is specifically challenging when real-time data changes frequently or when we want to incorporate new concepts, due to their structured and rigid nature. To sort this out, tagging systems are often preferred (Höning, n.d.; Noy & McGuinness, 2001). Third, ontologies are hard to integrate because of the lack of standardization in some domains, as ontologies require a broad consensus across stakeholders to be effective. Fourth, incorporating ontologies in modern systems comes with the challenge of choosing adequate mapping techniques (Mavrogiorgou et al., 2020) to allow interoperability.

Table 3 indicates the domains vetting in which ontologies are easy/moderately easy/ hard to incorporate based on this survey.

Table 3
Classification of ontologies in terms of their ease of incorporation per domain

Ontology's ease of use	Domain	Domain's characteristics
Easy	BI	• Stability • Structured data • Consensus through common frameworks, e.g., OLAP, DW
Moderately easy	AI	• Lack of stability • Unstructured nature of some subfields like deep learning • Potential for flexibility; through combining ontologies with more flexible models like probabilistic reasoning or using probabilistic ontologies. These dynamic ontologies integrate ontological structures with probabilistic reasoning. This leads to better decision-making in scenarios with incomplete or ambiguous information
Hard	Cybersecurity	• Constantly evolving threats make ontologies hard to keep up-to-date • A lot of unstructured data, e.g., threat intelligence reports and network logs. These types of data can be hard to classify and manage within an ontology • Lack of consensus as some systems may priorities certain threats over others
	Metaverse	• Unstructured data • Dynamic virtual environment • Lack of consensus, as there is not much agreement on classification, given that many developers contribute to it • Scalability, as the domain's rapid growth and nature makes scaling ontologies hard

Note. BI = Business Intelligence; OLAP = Online Analytical Processing; DW = Data warehouse; AI = Artificial intelligence

Constructing ontologies for sectors such as cybersecurity, AI, BI, and the Metaverse presents several challenges:

- Data heterogeneity: Integrating diverse data formats and sources necessitates the development of robust mapping techniques to ensure consistency and interoperability.
- Dynamic environments: The rapidly evolving nature of these fields requires ontologies to be adaptable, accommodating continuous technological advancements, and emerging threats.
- Privacy and security concerns: Particularly in the Metaverse, safeguarding user data and ensuring secure interactions pose significant challenges. Biometric methods, while unique, are susceptible to misuse, highlighting the need for secure data handling practices.
- Decentralization issues: The lack of centralized authority in decentralized systems like the Metaverse complicates the establishment of uniform security standards and regulatory frameworks.

Future Directions

SW can be used interchangeably with AI to gain insight from the reasoner, for better anomaly or fraud detection, and for tweets' sentiments analysis in a fuzzy or a contextual way, to name a few use cases. Alternatively, it can be used along with AI to enrich data and make it more discoverable.

Ontologies can facilitate the distinction between threats, assess risks, scale vulnerabilities, and provide a step-by-step assistance tailored to every possible attack scenario or so. Nevertheless, it is believed that even if OWL DL is highly used as opposed to OWL Full. Critical domains like cybersecurity need the higher expressiveness of the full version of ontologies. Hence, more studies need to be done in that regard.

As for businesses, they may benefit from LOD in decision-making. Companies rely on DW and BI systems such as OLAP to make decisions. Using LOD prior to data marts would potentially add a lot of semantics that can lead to more accurate choices in the future. Especially, data warehouses consist, among other things, of operational systems' data and external data. The latter may help drastically when it comes to smartly assessing e-reputation, analysing social media, and studying the target population if incorporated with LOD. Dimensions bring context to the facts. So, using ontologies would bring more context that stakeholders were not even aware of. Users tend to create a bridge (i.e., an interoperability layer) between DW and the formal domain ontology, instead of fully transforming it into an ontology. Thus, we will not waste our time. It can also be used in DBMS and DL to avoid wasting space by creating only links to other ontologies. But before all that, it is worth digging deeper to investigate why BI is the least domain to benefit from ontologies, out of the four domains in this survey, despite their ease of incorporation in it.

Incorporating ontologies in Metaverse not only facilitates a common representation and classification of diverse data types but also bridges the gap between virtual entities and the physical world. Indeed, the Semantic Web serves as a valuable tool for advanced data exploitation, reasoning, and inference (Lampropoulos et al., 2020). This is specifically the case with emerging Metaverse technologies for context awareness through enriching our understanding of the difference between physical and virtual objects. However, do we need mere ontologies ensuring standardisation? Or are complex ontologies mandatory for adaptability, which is a key element in domains like the Metaverse?

Furthermore, ontologies can be used across various domains to boost expressiveness, reasoning, and create common knowledge. In fact, SW provides a wide range of features to choose from, and SPARQL to interrogate ontologies. Therefore, it should be used more often in various systems to boost their performance.

CONCLUSION

The Semantic Web leverages the capabilities of knowledge graphs by allowing them to be reusable and shareable using URIs. This enables internet-connected devices to understand, just like humans do, for ideal human-computer interaction and decision-making. It would also increase revenue and audience, amongst other things, across platforms in the Metaverse, for example. However, ontologies are constrained in systems and not fully taken advantage of as this would take either a bigger change in the architectures, as in BI. Alternatively, it would take their use early on in the process and not just as a complement. Additionally, critical domains like cybersecurity need thorough vetting and are very low in false tolerance. Hence, OWL Full would be better suited, thanks to its high expressiveness, despite it being computationally demanding. Furthermore, using dynamic ontologies more often can enhance systems given their diversity and the ability of each to encounter a certain issue. However, evaluation benchmarks for dynamic ontologies are lacking as of now. Finally, ontologies range from easy to hard to integrate depending on the domain in question. But again, dynamic ontologies have the potential to make them less difficult to incorporate as in AI.

It is believed that stakeholders such as cybersecurity professionals, AI developers, BI analysts, and Metaverse platform designers can benefit from this research by gaining insights into the integration of Semantic Web technologies to enhance systems' interoperability and security.

In the future, the focus will be on improving the MetaOntology's accessibility, inclusiveness, interoperability, and respect for user privacy:

- Months 1-2: Assessment and planning
    - Conduct a thorough review of existing the Metaverse platforms to identify accessibility shortcomings.

    - Evaluate current data collection practices within the Metaverse to identify potential privacy vulnerabilities.
- Months 3-5: Development of standards and guidelines
    - Create comprehensive standards that define accessibility features, such as customizable user interfaces, screen reader support, and alternative input methods.
    - Formulate robust privacy policies that outline data collection limitations, user consent mechanisms, and data protection measures.
    - Design a framework that facilitates seamless interaction between various Metaverse platforms, ensuring consistent user experiences.
- Months 6-8: Implementation and testing

ACKNOWLEDGEMENTS

We would like to thank the Laboratory of Intelligent Systems and Applications at the Faculty of Sciences and Technologies in Sidi Mohamed Ben Abdellah University for providing the technical support for this research.

REFERENCES

Abburu, S. (2012). A survey on ontology reasoners and comparison. *International Journal of Computer Applications*, *57*(17), 33-39.

Ali, F., Kwak, D., Khan, P., Islam, S. M. R., Kim, K. H., & Kwak, K. S. (2017). Fuzzy ontology-based sentiment analysis of transportation and city feature reviews for safe traveling. *Transportation Research Part C: Emerging Technologies*, *77*, 33-48. https://doi.org/10.1016/j.trc.2017.01.014

Amaral, G., & Guizzardi, G. (2019). On the application of ontological patterns for conceptual modeling in multidimensional models. In T. Welzer, J. Eder, V. Podgorelec, & A. Kamišalić Latifić (Éds.), *Advances in databases and information systems* (Vol. 11695, pp. 215-231). Springer. https://doi.org/10.1007/978-3-030-28730-6_14

Antunes, A. L., Cardoso, E., & Barateiro, J. (2022). Incorporation of ontologies in data warehouse/business intelligence systems — A systematic literature review. *International Journal of Information Management Data Insights*, *2*(2), 100131. https://doi.org/10.1016/j.jjimei.2022.100131

Azuma, R., Baillot, Y., Behringer, R., Feiner, S., Julier, S., & MacIntyre, B. (2001). Recent advances in augmented reality. *IEEE Computer Graphics and Applications*, *21*(6), 34-47. https://doi.org/10.1109/38.963459

Bargui, F., Ben-Abdallah, H., & Feki, J. (2011). A decision-making ontology for analytical requirements elicitation. In E. Gelenbe, R. Lent, & G. Sakellari (Éds.), *Computer and information sciences II* (pp. 495-501). Springer. https://doi.org/10.1007/978-1-4471-2155-8_63

Bodenreider, O. (2004). The Unified Medical Language System (UMLS): Integrating biomedical terminology. *Nucleic Acids Research*, *32*(suppl_1), D267-D270. https://doi.org/10.1093/nar/gkh061

Carmigniani, J., Furht, B., Anisetti, M., Ceravolo, P., Damiani, E., & Ivkovic, M. (2011). Augmented reality technologies, systems and applications. *Multimedia Tools and Applications*, *51*, 341-377. https://doi.org/10.1007/s11042-010-0660-6

De Rosa, F., Maunero, N., Nicoletti, L., Prinetto, P., & Trussoni, M. (2022). *Ontology for cybersecurity governance of ICT systems*. https://ceur-ws.org/Vol-3260/paper4.pdf

DeStefano, R. J., Tao, L., & Gai, K. (2016). Improving data governance in large organizations through ontology and linked data. In *IEEE 3rd International Conference on Cyber Security and Cloud Computing* (pp. 279-284). IEEE. https://doi.org/10.1109/CSCloud.2016.47

Gao, X., Xiao, G., Xie, K., Wang, W., Fu, Y., Chang, C., & Wang, Z. (2023). A framework of modeling and simulation based on swarm ontology for autonomous unmanned systems. *Applied Sciences*, *13*(16), 9297. https://doi.org/10.3390/app13169297

Gómez-Pérez, A., Fernández-López, M., & Corcho, O. (2004). *Ontological engineering: With examples from the areas of knowledge management, e-commerce and the Semantic Web* (1st ed.). Springer. https://doi.org/10.1007/b97353

Gruber, T. R. (1993). A translation approach to portable ontology specifications. *Knowledge Acquisition*, *5*(2), 199-220.https://doi.org/10.1006/knac.1993.1008

Höning, N. (n.d.). *Clay Shirky - "Ontology is overrated": A review*. https://www.nicolashoening.de/?twocents&nr=11

Hooi, E. K. J., Zainal, A., Maarof, M. A., & Kassim, M. N. (2019). *TAGraph: Knowledge graph of threat actor*. In *International Conference on Cybersecurity* (pp. 76-80). IEEE. https://doi.org/10.1109/ICoCSec47621.2019.8970979

Iannacone, M., Bohn, S., Nakamura, G., Gerth, J., Huffer, K., Bridges, R., Ferragut, E., & Goodall, J. (2015). Developing an ontology for cyber security knowledge graphs. In *Proceedings of the 10th Annual Cyber and Information Security Research Conference* (pp. 1-4). Associations for Computing Machinery. https://doi.org/10.1145/2746266.2746278

Karabulut, E., Pileggi, S. F., Groth, P., & Degeler, V. (2024). Ontologies in digital twins: A systematic literature review. *Future Generation Computer Systems*, *153*, 442-456. https://doi.org/10.1016/j.future.2023.12.013

Khadir, A. C., Aliane, H., & Guessoum, A. (2021). Ontology learning: Grand tour and challenges. *Computer Science Review*, *39*, 100339. https://doi.org/10.1016/j.cosrev.2020.100339

Kimball, R., & Ross, M. (2013). *The data warehouse toolkit: The definitive guide to dimensional modeling* (3rd ed.). Wiley.

Kiourtis, A., Mavrogiorgou, A., & Kyriazis, D. (2019). Constructing healthcare ontologies of any data format. In *eTELEMED 2019: The Eleventh International Conference on eHealth, Telemedicine, and Social Medicine* (pp. 43-48). IARIA Press.

Kouremenou, E., Kiourtis, A., & Kyriazis, D. (2024). A data modeling process for achieving interoperability. In H. N. Costin, R. Magjarević, & G. G. Petroiu (Éds.), *Advances in digital health and medical bioengineering* (Vol. 109, pp. 711-719). Springer. https://doi.org/10.1007/978-3-031-62502-2_80

Kurze, C., Gluchowski, P., & Bohringer, M. (2010). Towards an ontology of multidimensional data structures for analytical purposes. In *43rd Hawaii International Conference on System Sciences* (pp. 1-10). IEEE. https://doi.org/10.1109/HICSS.2010.485

Lampropoulos, G., Keramopoulos, E., & Diamantaras, K. (2020). Enhancing the functionality of augmented reality using deep learning, semantic web and knowledge graphs: A review. *Visual Informatics*, *4*(1), 32-42. https://doi.org/10.1016/j.visinf.2020.01.001

Liu, K., Wang, F., Ding, Z., Liang, S., Yu, Z., & Zhou, Y. (2022). *A review of knowledge graph application scenarios in cyber security*. arXiv. http://arxiv.org/abs/2204.04769

Liu, X., & Iftikhar, N. (2013). Ontology-based big dimension modeling in data warehouse schema design. In W. Abramowicz (Ed.), *Business information system* (Vol. 157, pp. 75-87). Springer. https://doi.org/10.1007/978-3-642-38366-3_7

Marques, B., Silva, S., Dias, P., & Santos, B. S. (2021). An ontology for evaluation of remote collaboration using augmented reality. In *Proceedings of the 19th European Conference on Computer-Supported Cooperative Work* (pp. 1-8). European Society for Socially Embedded Technologies. https://doi.org/10.18420/ecscw2021_p04

Mavrogiorgou, A., Kiourtis, A., & Kyriazis, D. (2020). Identification of IoT medical devices APIs through ontology mapping techniques. In P. Inácio, A. Duarte, P. Fazendeiro, & N. Pombo (Eds.), *5th EAI International Conference on IoT Technologies for HealthCare* (pp. 39-54). Springer. https://doi.org/10.1007/978-3-030-30335-8_4

McGee, M. K. (1999). *Integral perception in augmented reality* [Unpublished Doctoral dissertation]. Virginia Polytechnic Institute and State University.

Mitra, S., Piplai, A., Mittal, S., & Joshi, A. (2021). Combating fake cyber threat intelligence using provenance in cybersecurity knowledge graphs. In *IEEE International Conference on Big Data* (pp. 3316-3323). IEEE. https://doi.org/10.1109/BigData52589.2021.9671867

Moreira, J., Cordeiro, K., Campos, M. L. M., & Borges, M. (2015). Hybrid multidimensional design for heterogeneous data supported by ontological analysis: An application case in the Brazilian electric system operation. In *Workshop Proceedings of the EDBT/ICDT 2015 Joint Conference* (pp. 72-77). CEUR Workshop Proceedings.

Mugwagwa, A., Chibaya, C., & Bhero, E. (2023). A survey of inspiring swarm intelligence models for the design of a swarm-based ontology for addressing the cyber security problem. *International Journal of Research in Business and Social Science (2147-4478)*, *12*(4), 483-494. https://doi.org/10.20525/ijrbs.v12i4.2473

Nguyen, H. D., Tran, T.-V., Pham, X.-T., Huynh, A. T., & Do, N. V. (2021). Ontology-based integration of knowledge base for building an intelligent searching chatbot. *Sensors and Materials*, *33*(9), 3101-3123. https://doi.org/10.18494/SAM.2021.3264

Noy, N. F., & McGuinness, D. L. (2001). *Ontology development 101: A guide to creating your first ontology*. Knowledge Systems Laboratory Stanford University.

Pinkston, J., Undercoffer, J., Joshi, A., & Finin, T. (2003). *A target-centric ontology for intrusion detection*. https://ebiquity.umbc.edu/_file_directory_/papers/626.pdf

Power, D. J. (2009). *Decision support basics*. Business Expert Press.

Prat, N., Akoka, J., & Comyn-Wattiau, I. (2012). Transforming multidimensional models into OWL-DL ontologies. In *Sixth International Conference on Research Challenges in Information Science* (pp. 1-12). IEEE. https://doi.org/10.1109/RCIS.2012.6240451

Prat, N., Megdiche, I., & Akoka, J. (2012). Multidimensional models meet the semantic web: Defining and reasoning on OWL-DL ontologies for OLAP. In *Proceedings of the Fifteenth International Workshop on Data Warehousing and OLAP* (pp. 17-24). Association for Computing Machinery. https://doi.org/10.1145/2390045.2390049

Radanliev, P., De Roure, D., Novitzky, P., & Sluganovic, I. (2024). Accessibility and inclusiveness of new information and communication technologies for disabled users and content creators in the Metaverse. *Disability and Rehabilitation: Assistive Technology*, *19*(5), 1849-1863. https://doi.org/10.1080/17483107.2023.2241882

Rastogi, N., Dutta, S., Christian, R., Gridley, J., Zaki, M., Gittens, A., & Aggarwal, C. (2021). *Predicting malware threat intelligence using KGs*. https://www.semanticscholar.org/paper/Predicting-malware-threat-intelligence-using-KGs-Rastogi-Dutta/0b4d8612f4d2cd69b6eade7f01f023fcca2e16cc

Sanagavarapu, L. M., Iyer, V., & Reddy, R. (2021). *A deep learning approach for ontology enrichment from unstructured text*. arXiv. https://doi.org/10.48550/arXiv.2112.08554

Syed, R. (2020). Cybersecurity vulnerability management: A conceptual ontology and cyber intelligence alert system. *Information and Management*, *57*(6), 103334. https://doi.org/10.1016/j.im.2020.103334

Syed, Z., Padia, A., Finin, T., Mathews, L., & Joshi, A. (2016). *UCO: A unified cybersecurity ontology*. In *The Workshops of the Thirtieth AAAI Conference on Artificial Intelligence* (pp. 195-202). Association for the Advancement of Artificial Intelligence.

Szwed, P., Komnata, W., & Dymek, D. (2015). DWARM: An ontology of data warehouse architecture reference model. In S. Kozielski, D. Mrozek, P. Kasprowski, B. Małysiak-Mrozek, & D. Kostrzewa (Éds.), *Beyond databases, architectures and structures* (Vol. 521, pp. 222-232). Springer. https://doi.org/10.1007/978-3-319-18422-7_20

Taylor, A. (2022, February 17). There's a huge surge in hackers holding data for ransom, and experts want everyone to take these steps. *Fortune*. https://fortune.com/2022/02/17/ransomware-attacks-surge-2021-report/

Turban, E., Sharda, R., & Delen, D. (2011). *Decision support and business intelligence systems* (9th ed.). Pearson Education India.

van Krevelen, D. W. F., & Poelman, R. (2010). A survey of augmented reality technologies, applications and limitations. *International Journal of Virtual Reality*, *9*(2), 1-20. https://doi.org/10.20870/IJVR.2010.9.2.2767

Vlachos, A., Perifanou, M., & Economides, A. A. (2024). A review of ontologies for augmented reality cultural heritage applications. *Journal of Cultural Heritage Management and Sustainable Development*, *14*(2), 160-174. https://doi.org/10.1108/JCHMSD-06-2021-0110

Pertanika J. Sci. & Technol. 33 (5): 2069 - 2095 (2025)

PERTANIKA JOURNALS

SCIENCE & TECHNOLOGY

Journal homepage: http://www.pertanika.upm.edu.my/

Modified Cuckoo Search Algorithm Using Sigmoid Decreasing Inertia Weight for Global Optimization

Kalsoom Safdar[1,2], Khairul Najmy Abdul Rani[1,3], Siti Julia Rosli[1,3], Mohd Aminudin Jamlos[1,3]* and Muhammad Usman Younus[4,5]

[1]Faculty of Electronic Engineering and Technology, Universiti Malaysia Perlis, 02600 Arau, Perlis, Malaysia
[2]Department of Computer Science and Information Technology, University of Jhang, 35200, Jhang, Pakistan
[3]Advanced Communication Engineering, Centre of Excellence, Universiti Malaysia Perlis, 01000 Kangar, Perlis, Malaysia
[4]Department of Computer Science and Information Technology, Baba Guru Nanak University, 39120 Nankana Sahib, Pakistan
[5]Ecole Math´ematiques, Informatique, T´el´ecommunications de Toulouse, Universit´e de Toulouse, 31000 de Toulouse, France

ABSTRACT

Cuckoo Search (CS) is an evolutionary computational (EC) algorithm inspired by the behavior of a cuckoo bird, introduced by Yang and Deb in 2009 to solve various engineering-intensive optimization problems. However, this metaheuristic algorithm, CS, still suffers from premature convergence, mainly due to multimodal problems leading to local trap problems. This research introduces an adaptive swarm-based optimization approach to the CS algorithm, using the sigmoid decreasing inertia weight (DIW), which produces the modified Cuckoo Search using decreasing inertia weight (MCS-DIW) algorithm to tackle local trap problems. The paper shows that the proposed MCS-DIW depicts a better-controlled mechanism by adding the DIW with Lévy flight, for balanced exploration and exploitation in the global search domain. Moreover, this study presents an inclusive, experimental analysis of the widely used set of standardized benchmark test problems released by the Institute of Electrical and Electronics Engineers (IEEE) Congress on Evolutionary Computation (CEC) benchmark along with selected mathematical test functions to assess the performance of the MCS algorithm. The MCS-DIW algorithm is compared with other swarm intelligence (SI) algorithms to validate, including the original CS algorithm, Whale Optimization Algorithm (WOA), Sine Cosine Algorithm (SCA), and Search Sparrow Algorithm (SSA). The compiled simulation

ARTICLE INFO

Article history:
Received: 31 December 2024
Accepted: 29 April 2025
Published: 11 August 2025

DOI: https://doi.org/10.47836/pjst.33.5.03

E-mail addresses:
kalsoombajwa11@gmail.com (Kalsoom Safdar)
khairulnajmy@unimap.edu.my (Khairul Najmy Abdul Rani)
sitijulia@unimap.edu.my (Siti Julia Rosli)
mohdaminudin@unimap.edu.my (Mohd Aminudin Jamlos)
usman.younus@bgnu.edu.pk (Muhammad Usman Younus)
* Corresponding author

e-ISSN: 2231-8526

findings showed that the modified proposed CS algorithm, in most cases, performed better in attaining a low mean global minimum value, high convergence rate, and low central processing unit (CPU) processing time compared to other counterparts. The dynamic adjustment of inertia weight enhances optimization performance with an initial high inertia weight (e.g., 0.9) and promotes exploration, gradually decreasing to 0.2 for better exploitation. This proposed MCS-DIW approach provides faster convergence and has been proven to mitigate premature convergence. It reduces the number of iterations by 30-40% and achieves lower fitness values (e.g., 10-2) than static inertia weight, which often stabilizes at higher values (e.g., 10-1). In sum, the proposed MCS-DIW algorithm is proven to mitigate the local trap problems via an improved capability in searching for the global optimum.

Keywords: Cuckoo Search Algorithm, exploration, exploitation, inertia weight, local trap problem, premature convergence, swarm intelligence

INTRODUCTION

Optimization plays an essential role in engineering to solve critical problems, such as communication routing, system design, image reconstruction, network operations, and energy loss (A. Chakraborty & Kar, 2017; Saka et al., 2013). These problems depend upon the minimization or maximization of the given objective functions. Subsequently, proper assessment for algorithmic validation is required, including accuracy, convergence rate, and computational time of the designed system (Sekyere et al., 2024; Zangana et al., 2024). It also ensures efficient problem-solving mechanisms in complex systems under diverse constraints, including energy consumption (Adeyelu et al., 2024), communication limitations, image reconstruction errors (Habeb et al., 2024), and environmental factors related to the diverse changes in the search space. Accordingly, it emphasizes reliability, adaptability, and precision of algorithmic performance (Abualigah et al., 2024).

Moreover, metaheuristic algorithms provide guiding mechanisms to the new trending EA toward solving diverse optimization problems related to engineering (Luo et al., 2024). Generally, the term "metaheuristic" is composed of two Greek words covering two verbs, which are "to find" and "beyond, in an upper level". Moreover, metaheuristics can be defined based on two significant tactics: intensification and diversification (Abdul Rani et al., 2017; Adeyeye & Akanbi, 2024; Brezočnik et al., 2018; Saka et al., 2013). Additionally, intensification intends to choose the best optimal solution while searching for the best existing solution. However, diversification intends to explore the given search region efficiently, often by randomization (Brezočnik et al., 2018). Subsequently, modern evolutionary metaheuristic optimization algorithms such as SSA, Genetic Algorithm (GA) (Sohail, 2023), WOA (Mahmood et al., 2023), SCA, Ant Lion Optimization (ALO), and Particle Swarm Optimization (PSO) are aimed at carrying out a global search for three main reasons: solving diverse and large problems, getting faster convergence, and providing

robustness (Abdul Rani & Malek, 2011; Kwakye et al., 2024; Massat, 2018; Xue et al., 2023). Moreover, algorithmic efficiency can be considered the key attribute of metaheuristic algorithms. Accordingly, they started imitating the optimal features of nature, and mainly, they opted for the natural selection method using the fittest selection criteria, which can be seen in biology-based systems that have evolved over millions of years through natural selection (Adeyeye & Akanbi, 2024; Kwakye et al., 2024) .

Nowadays, some innovative researchers have introduced many nature-inspired optimization algorithms, for example, the Differential Evolution (DE) algorithm developed by Strom and Prince, functioned on crossover, selection and mutation operations using evolving populations. PSO inspired by fish and birds' schooling behavior (S. Chakraborty et al., 2023; Shi & Eberhart, 1998). However, Simulated Annealing (SA) uses a metal annealing mechanism (Chen et al., 2024). Comparatively, the Bat-inspired algorithm has an echolocation capability to sense the distance between its surroundings. Besides, Ant and Bee's algorithms worked through their foraging behavior using pheromone and concentration as a chemical messenger to control the given problem efficiently (Umar et al., 2024).

Though the CS algorithm is a nature-inspired, swarm intelligence-based evolutionary algorithm (EA) introduced by Yang and Deb in 2009 (Huang & Zhou, 2024). Basically, the CS algorithm used a cuckoo bird’s brood reproductive approach to increase their population. In addition, the CS algorithm is more prevalent and computationally efficient in discovering optimum solutions than its counterparts because it has fewer parameters than other nature-inspired algorithms. Moreover, the CS algorithm provides a potential solution using random groups of cuckoos inspired by the cuckoo’s brood parasitism that obligates the behavior of laying eggs in a habitat to the host nest. In this regard, recent research on CS algorithms provides different evolutionary mechanisms for better local and globally optimal solutions using nature-inspired optimization techniques, which provide solutions regarding different complex optimization-related engineering problems. However, its simplicity and balancing mechanism in exploration and exploitation provide ease in regenerating a better solution for various optimization problems (Abdul Rani & Malek, 2011; Aziz, 2022; Mohammed et al., 2023; Yang et al., 2024).

According to the above discussion, this paper aimed to propose an optimized variant of the Modified Cuckoo Search (MCS) algorithm using the sigmoid DIW, yielding MCS-DIW to solve premature convergence and local trap problems. This proposed MCS-DIW algorithm ensures better exploration to efficiently find the global optimal solution. This research investigated a detailed parametric study, which aimed to fine-tune different parameters of the proposed algorithm. Afterwards, the anticipated strategy is validated using several different mathematical benchmark functions. Moreover, the performance of the MCS-DIW algorithm has been verified using different SI algorithms, including original

CS, SCA, WOA, and SSA. Hence, it has been observed that the MCS-DIW algorithm outperformed for most of the testing functions compared to its counterparts.

The organization of this research paper is as follows: Section 2 deliberates research materials and methods along with previous advancements using the different improved/ modified variants of the CS algorithm and the increasing and decreasing inertia weight by shedding light on their innovative contributions to providing efficient algorithms. Moreover, it briefly discusses the proposed methodology using the proposed research design, including the implementation strategy and its working principles. Subsequently, Section 3 exhibits experimental techniques used for the simulation setup. Furthermore, Section 4 presents results and discussions, which provide the interpretation regarding the performance of a series of empirical experimental results using different benchmark functions. Finally, Section 5 concludes the overall findings of this paper.

MATERIALS AND METHODS

The proposed research involves modifying the CS algorithm to improve its performance for complex optimization tasks. The modified CS variant's effectiveness is thoroughly tested using a set of standard mathematical benchmark test functions, which includes unimodal and multimodal problems. Significant performance metrics such as computational efficiency, accuracy, and convergence rate are evaluated to validate the improvements associated with exploration and exploitation capabilities. Furthermore, the materials include benchmark mathematical functions like Ackley, Rosenbrock, Rastrigin, and Sphere, to test and evaluate the optimization performance. MATLAB-2020a is used to implement and simulate the modified CS algorithm.

However, this paper provides Wilcoxon and Friedman statistical analyses of a proposed modified variant of the CS algorithm using the sigmoid DIW. The major objective of conducting this research is to modify and improve the CS algorithm to enhance the performance and competency of the conventional CS algorithm for better exploration to find the global best fitness value in the given problem region. In this regard, a parametric study was conducted to fine-tune the internal parameters of the original CS algorithm. Afterwards, the effectiveness of the proposed MCS-DIW algorithm is evaluated through empirical simulations using seven different well-known mathematical benchmark functions compared with a few chosen SI algorithms, including original CS, SCA, WOA, and SSA.

Research Design

A step-by-step flowchart of the proposed research design is depicted in Figure 1. The flowchart outlines the steps of the MCS-DIW algorithm, incorporating the proposed modification along the overall research optimization process. The process begins with a feasibility study to initialize parameters, define iterations, and determine test function

dimensions. Subsequently, the CS algorithm parameters are fine-tuned to identify the optimal configuration and the maximum number of iterations for enhanced performance. Here is a detailed breakdown of each step:

Feasibility study of CS algorithm : A preliminary investigation is conducted to evaluate the feasibility and potential performance of the basic CS algorithm for the task at hand.

Fine-tune and evaluate the original CS algorithm's internal parameters through parametric studies : The original CS algorithm is fine-tuned and assessed using various population numbers and fraction probability values. These parametric studies will determine the best internal parameters to use for the MCS algorithm in the later stage.

Formulate a MCS algorithm and generate a random population or host nest using increasing inertia weight (IIW) and DIW : The CS algorithm is modified in two versions by introducing both IIW and DIW in generating a random host nest (population) to improve the optimizer's performance in exploring and exploiting potential global optimal solutions.

Validate the solution of the proposed MCS-IIW and MCS-DIW algorithms : The process checks the validity of the global optimal solution of both MCS-IIW and MCS-DIW algorithms iteratively. If the solution is invalid, the process returns to the previous step, fine-tuning and re-evaluating both MCS-IIW and MCS-DIW algorithms. If the solution is valid, the process will proceed until the existing number of iterations reaches the maximum number of iterations. After achieving the maximum number of iterations, the method identifies the best fitness value of both MCS-IIW and MCS-DIW, corresponding to the global optimum solution (best nest). Simulate and compare both MCS-DIW and MCS-IIW algorithms with the original CS algorithm. Finally, the proposed MCS-DIW is compared with other chosen SI algorithms, which include the SCA, WOA, and SSA.

Hence, this flowchart represents a typical process for optimizing solutions using an enhanced version of the CS algorithm with inertia weight, iterating through different potential solutions until the optimal one is found and validating the process along the

way (Figure 1). The final step compares the performance of this algorithm against other optimization-related algorithms.

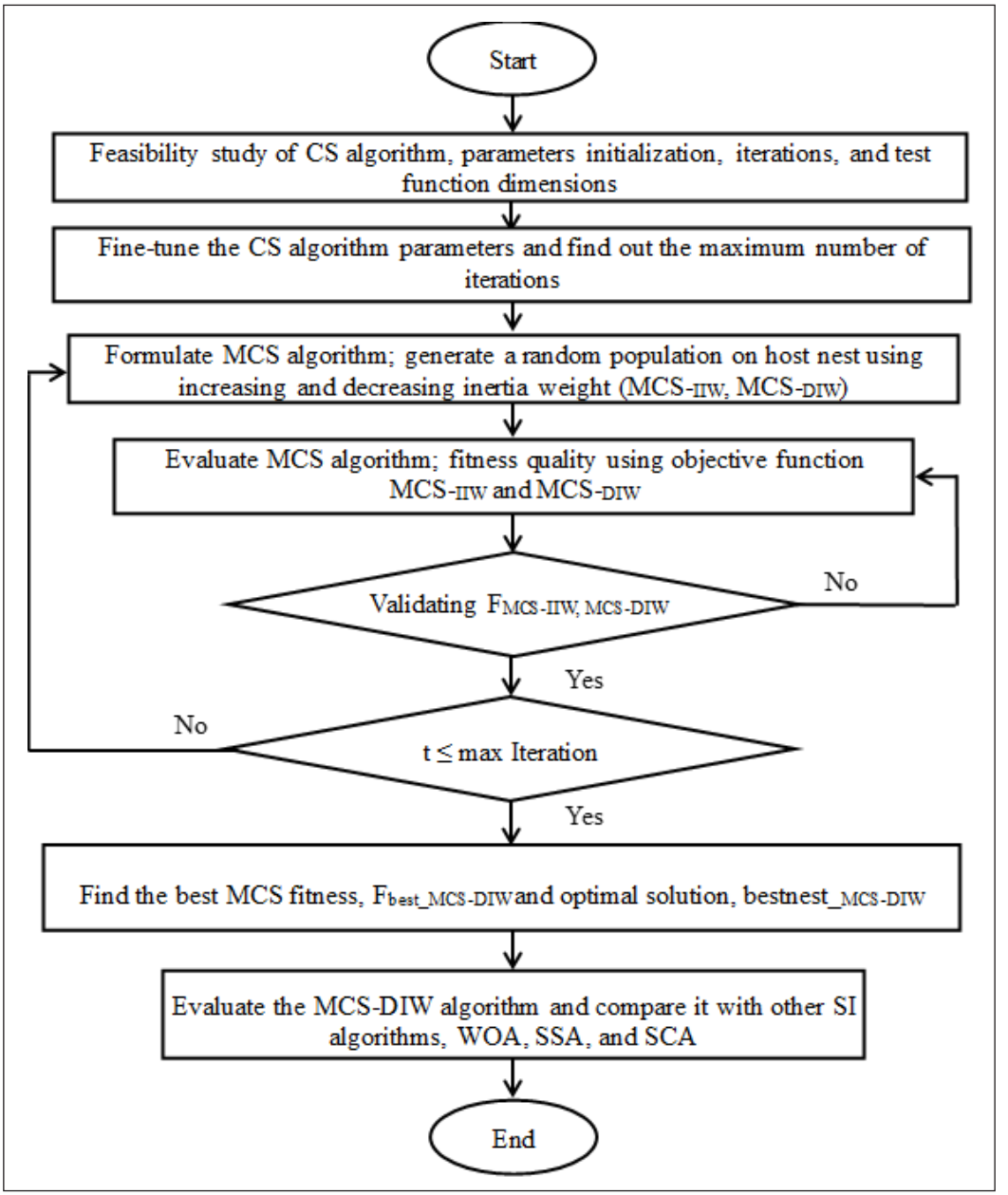

Figure 1. Research flowchart

Note. CS = Cuckoo Search; MCS = Modified Cuckoo Search; MCS-$_{IIW}$ = Modified Cuckoo Search using increasing inertia weight; MCS-$_{DIW}$ = Modified Cuckoo Search using decreasing inertia weight; SI = Swarm intelligence; WOA = Whale Optimization Algorithm; SSA = Search Sparrow Algorithm; SCA = Sine Cosine Algorithm

Modified Variant of CS Using Inertia Weight

The advanced nature-inspired optimization method known as the CS algorithm is motivated by the brood parasitism nature of cuckoo birds, who laid their eggs in the nests of other birds (Joshi et al., 2017; Meena et al., 2024). The CS algorithm, introduced by Yang and Deb in 2009, uses a local search mechanism to fine-tune solutions along with a combination of Lévy flight for global exploration (Almufti et al., 2025; Mareli & Twala, 2018). The algorithm begins by using a population of possible solutions for each representing a nest. Lévy flight, a kind of random walk that permits both tiny and large steps, strike a compromise between exploration and exploitation to produce new candidate solutions (Tian et al., 2024). A new one is substituted if an opted strategy doesn't increase the population's overall fitness. The population is updated iteratively by this method. This breeding behavior along Lévy flight is being applied to improve the efficiency of CS and solve the various optimization problems (Ahmad et al., 2025; Cuong-Le et al., 2021).

Inertia Weight

The idea of an inertia weight was initiated to maintain a balance between the exploration and exploitation mechanisms and eliminate the need for maximum iterations, I_{max}. It is an innovative enhancement of the CS optimization algorithm that integrates the concept of inertia weight commonly utilized in metaheuristic algorithms. The addition of inertia weight introduces an adaptive parameter that modulates the magnitude of step changes during the search, enhancing the exploration and exploitation abilities of the algorithm. Alongside, by incorporating inertia weight, the algorithm dynamically balances the trade-off between local exploitation and global exploration, allowing for smoother convergence and improved convergence accuracy (Choudhary et al., 2023). This novel extension holds significant promise for enhancing the performance of Cuckoo Search in various optimization tasks across diverse domains. The inertia weight (w) ensured a controlled transition of the cuckoos by adding the weight to the contribution of the previous solution (Zdiri et al., 2021). Eq. [1] uses the Lévy flight to offer the new optimal solution using the inertia weight, which is mathematically shown in the following equation. Updated CS algorithm, Lévy flight equations using inertia weight.

$$X_i^{(t+1)} = w * x_i^t + \alpha \cdot Le'vy(\lambda) \quad [1]$$

$$Le'vy(\lambda) \sim \frac{u}{|v|^{1/\lambda}} \quad [2]$$

In Eq. [2], u and v are drawn from normal distributions. The following equations represent the weight update mechanism, typically used in optimization algorithms like

MCS or similar swarm intelligence method. The weight W_k shown in Eq. [3] dynamically changes over iterations to ensure stability to explore and exploit during the search process.

Moreover, Eq. (3) (Y. Zheng et al., 2003) is utilized by DIW and IIW in Eq. [4] (Y. Zheng et al., 2003). Subsequently, the value of u is defined in Eq. [5] (Y. Zheng et al., 2003). Accordingly, as shown in Table 1, which provides all the parameters used in the inertia weight equations.

$$W_k = \frac{W_{Start} - W_{end}}{\left(1+e^{-u*(k-n*iter)}\right)} + W_{end} \quad [3]$$

$$W_k = \frac{W_{Start} - W_{end}}{\left(1+e^{u*(k-n*iter)}\right)} + W_{end} \quad [4]$$

$$u = 10^{(\log(iter)-2} \quad [5]$$

W_k is calculated as a combination of the initial weight W_{start} and the final weight W_{end}, modulated by a sigmoid function. Further the term $e^{-u*(k-n*iter)}$ defines the rate of decay, where k is the existing iteration and n_{iter} is the total number of iterations. This ensures that W_k transitions smoothly from W_{start} to W_{end} as iterations progress.

Moreover, in Eq. [5], the parameter $u = 10^{(\log(iter)-2}$ adapts the decay rate based on the current iteration. It fine-tunes how quickly the weight shifts from exploration (higher weights) to exploitation (lower weights) as the algorithm progresses.

Table 1
Parameters details for the inertia weight equations

Symbol	Name
$X_i^{(t+1)}$	A new solution for the *ith* cuckoo at iteration t + 1
x_i^t	Current solution
α	Scaling factor step size
$Le´vy(\lambda)$	Represents the Lévy flight distribution
W	Inertia weight
W_{start}	Starting inertia weight at the given run
W_{end}	Ending inertia weight at the given run
U	Constant to adjust the shape of the function
N	Constant to set the duration of the function

Later, this weight scheduling mechanism allows the algorithm to focus on early-stage global exploration by assigning higher weights and gradually shifting towards local exploitation in later stages, improving convergence to the optimum solution. This adaptive

weight adjustment improves the CS algorithm's balance between finding diverse solutions and refining the best solutions over iterations.

MCS Algorithm – Pseudocode

The pseudocode of the proposed MCS algorithm is provided below. Previously, the inertia weights were implemented using constant (Sekyere et al., 2024) and dynamic (Nickabadi et al., 2011) values for all possible solutions and dimensions used for the complete search domain. In Eq. [1], the fitness function f(X) is evaluated for each solution X to determine its quality using inertia weight. The goal is to maximize or minimize this fitness, depending on the optimization problem. Conversely, dynamic values used two different increasing and decreasing approaches. For increasing, a small value of inertia weight will increase linearly or nonlinearly to a linearly increasing large value. For decreasing, a large value of inertia weight will decrease linearly or nonlinearly to a linearly small value. A large value of inertia weight will foster the possibility of global search convergence, and a small value of inertia weight has more potential for local search than a large value of inertia weight. As provided, the following MCS algorithm, where the modification is performed at step no. 07 using Eq. [1, 2] to add inertia weight to get the fastest convergence compared to the original CS algorithm.

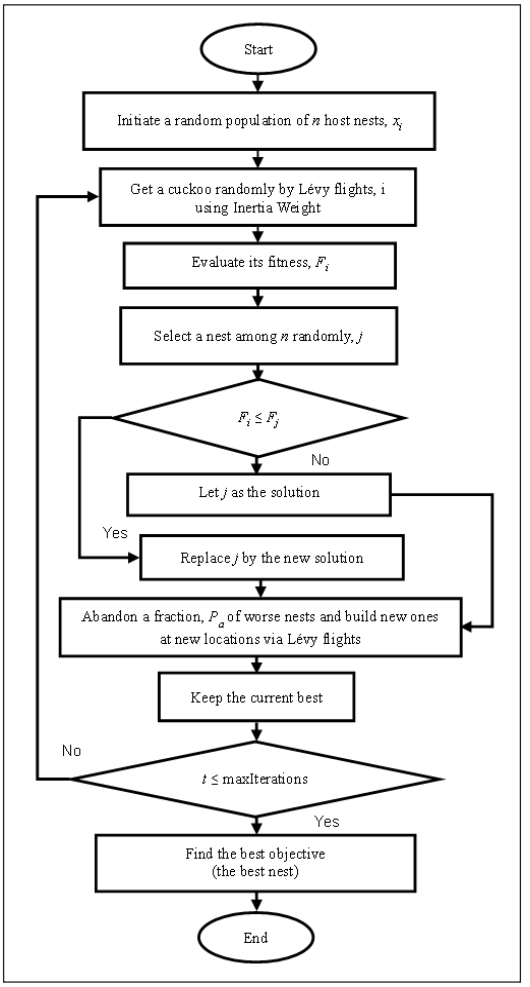

Figure 2. Modified Cuckoo Search Algorithm flow chart

Note. n = Population; t = Iteration; x_i = Host nest; x_j = Random nest; F = Fitness value; P_a = Discovery probability

The nature-inspired modified cuckoo search MCS-DIW metaheuristic algorithm begins by initializing the population nests, which are randomly distributed candidate solutions among the given search space. The next step shows exploration and exploitation using a random walk mechanism, generating new solutions using Lévy flights by adding inertia weight (Figure 2).

Furthermore, the bio inspired optimization strategy of cuckoo species is based on the brood parasitic behavior , which employs random walk using Lévy flight and discovery mechanism to find global optimal solution efficiently.

In addition to enhancing the modified variant of the CS algorithm, the inertia weight is applied to the random walk solution to improve the performance of MCS-DIW. Using the inertia weight, the fitness value of each new solution is assessed repeatedly each time the new and better solution is replaced with the existing one if the performance of the new solution is better than the existing solution. This scenario mimics the strategy of the host bird cuckoo search involving detecting and eliminating foreign eggs. This step is repeated continuously according to the given condition until the stopping criterion is met, including achieving convergence and reaching the maximum number of iterations. In this regard, the first step of modified cuckoo search algorithm includes the definition of objective function and parameter initialization, such as maximum iterations *t*, host nest *n*, discovery probability *Pa*, and the parameters given in the Table 1. In the next step, the control enters the main loop to evaluate the fitness value of each host nest (solution) using the given objective function. Accordingly, inertia weight given in Eq. [1, 2] will be updated dynamically to ensure smooth transition to find the global optima over the given iterations. Further, the control enters a nested For loop to generate a new solution using Lévy flight with controlled step size using inertia weight. Subsequently, the latest fitness value will be evaluated to see if it is better than the existing solution. Under the upper and lower bound conditional check, the better optimal fitness value will be replaced with the existing one to enhance diversity. In other words, the new random solutions will be replaced with the fraction of nests (solutions) as the discovery probability *Pa* is determined. This process of global best selection will be executed until it reaches the maximum number of iterations. Lastly, found the optimal solution. Hence, it has proven that combining MCS-DIW with better selection, randomization with inertia weight, and nest replacement provides an efficient solution to the given problems, ensuring rapid optimal convergence and balanced exploitation and exploration.

Modified Cuckoo Search Algorithm

1. Start
2. Objective function $f(x), x = (x_1, x_2, x_d)^T$
3. Generate, initial population of *n* host nests,
4. $x_i, i = 1,2,3, \ldots n$
5. while *t* < max iteration or stopping criterion
6. Get a cuckoo randomly by Lévy flight
7. **Evaluate its quality/fitness F_i using DIW for each nest Eq. [1, 2]**

8. Select a nest randomly from n (say, j)
9. if $F_i \leq F_j$
10. Replace j with a new solution
end if
11. A fraction, P_a of worst nests are abandoned, and new ones are reconstructed
12. Keep the best solutions (or nests with quality solutions)
13. Rank the solutions and find the current best
14. end while
15. Postprocess results and visualization
16. End

Data Analysis and Interpretation Techniques

To validate the efficiency of the proposed MCS algorithm, real-time performance will be analyzed, and tests will be carried out to identify the improvements. Thus, unimodal and multimodal-based objective functions were used to test the working of the MCS algorithm. Table 2 demonstrates eight out of 23 classical sets of test functions used for the MCS algorithm performance analysis (Cheraghi et al., 2023).

Table 2
Selected eight test functions (Mareli & Twala, 2018)

Problems	Name	Range
F1	Rosenbrock's function	[-2.048, -2.048]
F2	Ackley's function	[-32.768,32.768]
F3	Griewanks's function	[-600,600]
F4	Rastrigin's function	[-5.12,5.12]
F5	Nocontinuous Rastrigin's function	[-5.12,5.12]
F6	Schewfel's function	[-500,-500]
F7	Weierstrass's function	[-0.5,-0.5]
F8	E_Scaffer's F6 function	[-100,100]

The selected test functions encompass a range of optimization landscapes, each posing unique challenges to optimization algorithms. Additionally, the evaluation extends to include the Rotated Elliptic, Rotated Bent Cigar, and Rotated Discus functions (Ghiaskar et al., 2024; Thaher et al., 2024; W. Zheng et al., 2023). The formulas, domains, and ranges of these functions are meticulously defined to provide a consistent basis for comparison.

Further, these benchmark functions facilitate a comprehensive assessment, allowing for thoroughly validating the proposed methods' performance across various optimization landscapes. By subjecting the proposed methods to these standardized tests, the research

aims to establish their effectiveness, efficiency, and adaptability in solving real-world optimization problems (Bharambe et al., 2024; Liu et al., 2022; Wei & Niu, 2022). This validation and verification process highlights the robustness and practical applicability of the proposed method, providing a credible foundation for its integration into optimization tasks.

Experimental Techniques

Experimental Setup

An experimental setup was deployed to validate the effectiveness of the proposed MCS algorithm. Eight different categories of mathematical benchmark functions were used to test the efficiency of the proposed algorithm. Accordingly, MATLAB R2020a was used for coding on a Core (TM) 1.61 GHz system for simulation experiments.

Parametric Study

The parametric study is performed using optimization test functions. In this regard, the original cuckoo search algorithm was tested using different values, including population and probability.

Simulation Findings

The findings of all the initial results are presented in this section. In this regard, 23 optimization mathematical test functions are used to fine-tune the internal parameters of the original CS algorithm, where the F1 to F3 test functions were unimodal. In contrast, the F4 to F16 test functions were multimodal. Accordingly, Figure 3 depicts the comparison of different mathematical test functions, including F1 to F23, using 500 iterations, where the original CS algorithm exhibited the fast convergence curve in four out of 23 test functions, namely, the F6, F12, F13, and F22 test functions. In most evaluations, the convergence exhibited higher performance in F6, F12, F13, and F22 compared with the adjusted benchmark functions and the original CS algorithm. Moreover, to fine-tune the internal parameters, the population is set to 30 and the fraction probability is set to 0.5, running for 3000 iterations. The resultant functions show faster convergence with more exploration of the given problem. A comparison was performed with other Swarm Intelligence (SI) algorithms to ensure a fair evaluation of the metaheuristics.

Furthermore, the analysis of the abovementioned comparison shows that the CS algorithm performed better in four out of 23 functions, including F6, F12, F13, and F22, respectively. As shown in Figure 4 (a), the selected test functions demonstrated the algorithm's performance using logarithmic fitness values to minimize the objective function using 3000 iterations. These resultant functions are compared further to get the

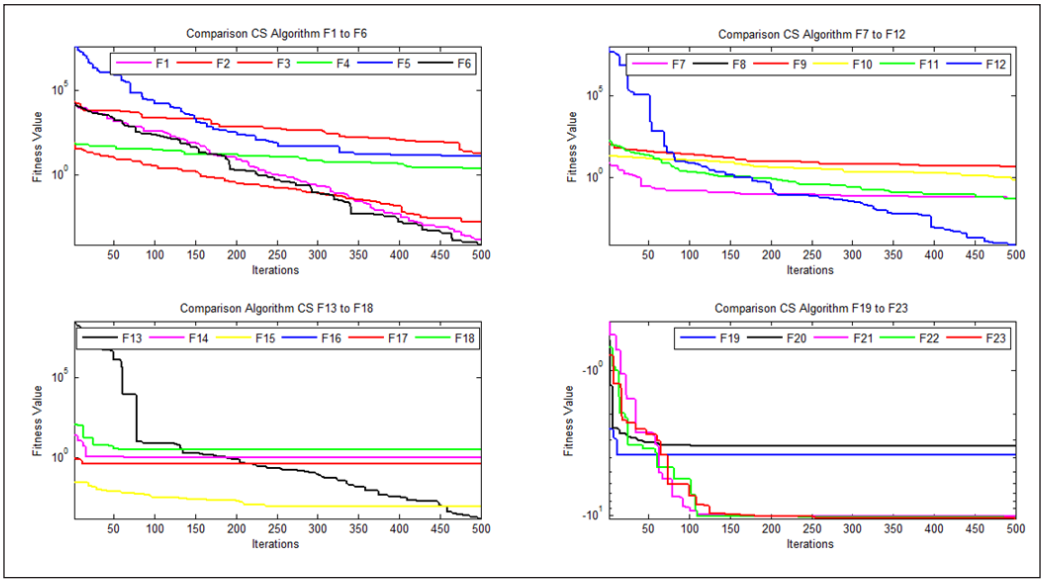

Figure 3. Convergence curve of the original Cuckoo Search (CS) Algorithm using the 23 different mathematical test functions for F1 to F23

best optimal solution to fine-tune the internal parameters. Additionally, the results show that F6 is being explored more deeply in the search area than F12, F13, and F22. Hence, the F6 function indicates a black line depicting the fastest convergence among all other test functions, achieving the lowest fitness value within the fewest iterations.

Subsequently, as depicted in Figures 4 (b) and (c), the CEC benchmark functions were evaluated using the proposed MCS algorithm, along with the original CS algorithm, over 500 iterations. Where the performance of MCS is better as compared to the original CS algorithm, this ensures the fastest convergence to find the global optimal solution.

Figure 5 shows the convergence curves with different population values assigned 10, 20, 30, 40, and 50, with a fraction probability value of 0.5 using the F6 test function because F6 outperformed in the above shown Figures 3 and 4 out of 23 mathematical test functions. The fitness value is plotted against the different number of iterations out of 3000 iterations. The results show that as the size of the population decreases, the convergence rate becomes higher. In contrast, an appropriate selection of population size is to balance the solution quality and computational efficiency. Additionally, the given scenario illustrates that the population size of 10 depicts a higher computational cost for the best optimization problem compared to other population values.

Moreover, the probability parameter is also critical in controlling the balance between exploration and exploitation in the algorithm using the F6 test function. For this scenario, a range of probability values (0.1, 0.25, 0.5, 0.75, and 1) has been compared to estimate the better performance of the CS algorithm optimization c=0.5 (red line) achieves the best

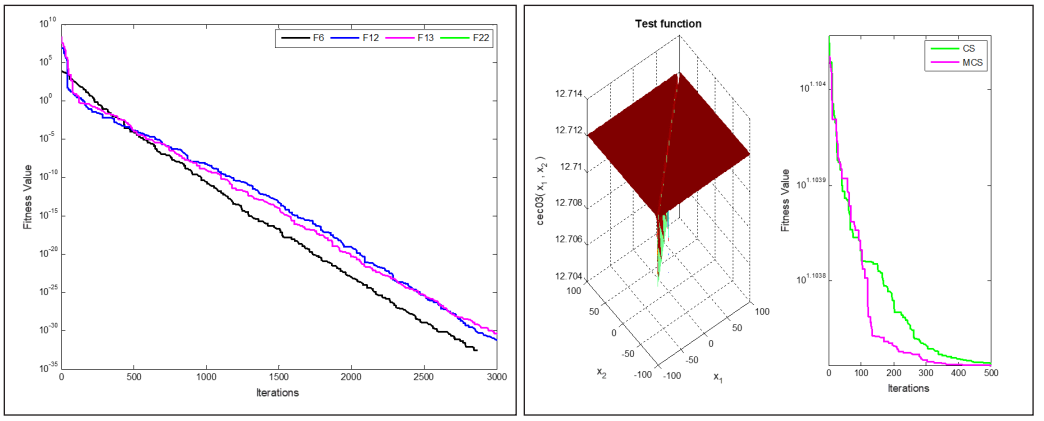

(a) (b)

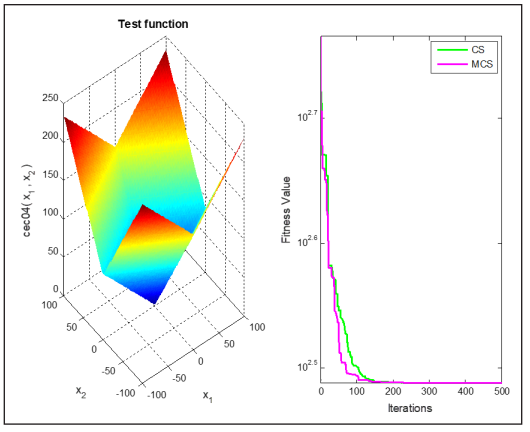

(c)

Figure 4. Convergence curve of the original Cuckoo Search (CS) Algorithm using the best test functions along Congress on Evolutionary Computation (CEC) benchmark functions
Note. MCS = Modified Cuckoo Search

overall performance, combining fast convergence with a low final fitness value. Lower probabilities, while slower, may still be useful for problems requiring more extensive exploration. Thus, the fraction probability of 0.5 had the lowest global optimal solutions compared to different values (Figure 6).

RESULTS AND DISCUSSION

First, a comparison between increasing and decreasing sigmoid inertia weight has been performed using Eqs. (3) and (4), as shown in Figure 7, using the specifications listed in

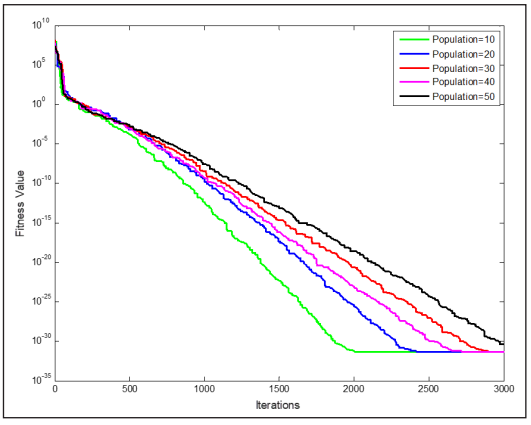

Figure 5. Comparison of parametric results with different values of population in the Cuckoo Search Algorithm

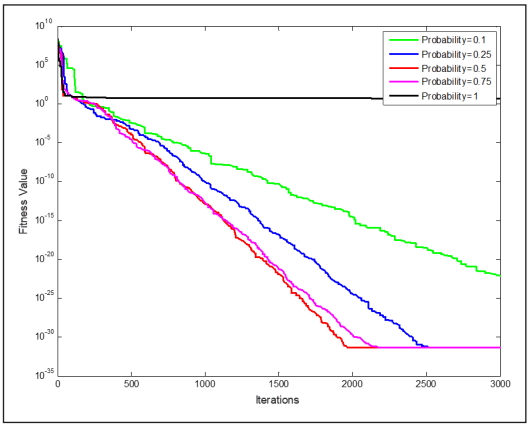

Figure 6. Comparison of parametric results with different values of fraction probability in Cuckoo Search Algorithm

Table 3 for the performance comparison of both increasing and decreasing inertia weight. The MCS algorithm using the DIW performed better than the MCS algorithm using the IIW to attain faster convergence after 1300 iterations (Figure 7).

The MCS-DIW outperforms both MCS-IIW and CS in terms of achieving the lowest fitness value and fastest CPU time due to its dynamic adjustment of the inertia weight. Subsequently, the Big O computational complexity of the proposed MCS-DIW

Table 3
Parameters of the proposed Modified Cuckoo Search Algorithm

Serial no.	Name	Values
1.	Population	10
2.	Probability	0.5
3.	W-Start	400
4.	W-End	200
5.	Iterations	2000

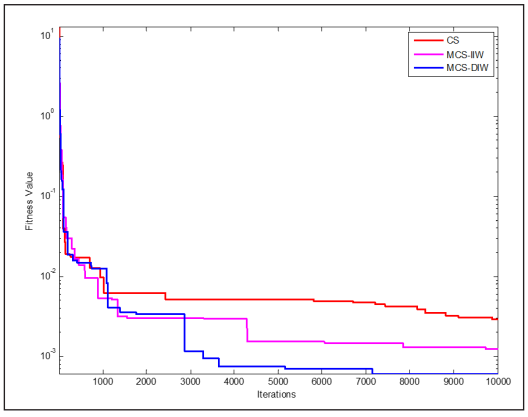

Figure 7. Comparison between original Cuckoo Search (CS) with proposed Modified Cuckoo Search (MCS) Algorithm
Note. MCS-IIW = Modified Cuckoo Search using increasing inertia weight; MCS-DIW = Modified Cuckoo Search using decreasing inertia weight

algorithm using the additional computation of decreasing inertia weight remains the same as compared to the original CS algorithm, which is $O(n \times Maxiter)$, where n represents the number of nests, and *MaxIter* is the maximum number of iterations. The proposed MCS-DIW algorithm also improves the convergence stability, global search efficiency, and solution accuracy. Thus, the modified algorithm is computationally richer and more robust compared to the original CS algorithm. Ensuring improved convergence and better global search behavior with manageable computational load.

Furthermore, as shown in Figure 7, the MCS-DIW (blue line) consistently reaches lower fitness values faster and stabilizes below 10^{-2} approaching 10^{-3}, whereas MCS-IIW (magenta line) plateaus earlier at a higher fitness value, and CS (red line) converges more slowly and stagnates around 10^{-1}. The key advantage of MCS-DIW lies in its adaptive inertia weight mechanism, where the inertia weight decreases over time starting high (e.g., around 0.9) to promote exploration in the early stages, allowing the algorithm to traverse large areas of the search space and avoid local minima. As iterations progress, the inertia weight decreases (e.g., down to 0.2), which helps the algorithm focus on exploitation, refining solutions in promising regions for more precise optimization. This dynamic control prevents premature convergence and ensures that MCS-DIW maintains a balance between exploration and exploitation, resulting in faster convergence to lower fitness values with fewer iterations, which in turn reduces CPU time. In contrast, MCS-IIW has a more static inertia weight adjustment, and CS lacks adaptive mechanisms, leading to slower and less efficient performance.

The results depicted in Figure 7 demonstrate the superior performance of the MCS-DIW algorithm (blue line) compared to MCS-IIW (magenta line) and CS (red line). The

MCS-DIW reaches a significantly lower fitness value of approximately 10^{-3} within 2800 to 7100 iterations, whereas MCS-IIW stabilizes at a fitness value near 10^{-1}, and CS plateaus around one after approximately 1000 iterations out of a total of 10000 iterations. In terms of efficiency, MCS-DIW requires fewer iterations and thus achieves faster CPU time as it converges more quickly toward an optimal solution. In contrast, MCS-IIW and CS take longer to converge and stabilize at suboptimal fitness values, highlighting the advantage of MCS-DIW's dynamic inertia weight in both accuracy and computational efficiency.

Furthermore, the proposed MCS-DIW and original CS, SSA, SCA, and WOA have been compared using four selected optimization test functions, as shown in Figures 8-11. Performance indicators are provided in Tables 4 and 5 for comparison purposes.

Moreover, Figures 8-11 show the results of 4 different mathematical benchmark test functions, including (a) F4, (b) F5, (c) F7, and (d) F9, using different SI algorithms, including MCS-DIW, CSA, WOA, and SSA, to emphasize the significance of balancing between exploration and exploitation to attain accuracy and robustness in optimization related problems. These different swarm intelligence algorithms showed various convergence rates for objective function minimization using the logarithmic scale fitness values against 2000 iterations for each of the four selected functions.

Subsequently, in Figure 8, using the F4 function, the proposed MCS-DIW algorithm has significantly outperformed as compared to other selected SI algorithms and demonstrated by the magenta line, achieving the fastest convergence by the lowest fitness value ~10^{-20} against 2000 iterations and continued to improve the exploration process capabilities along

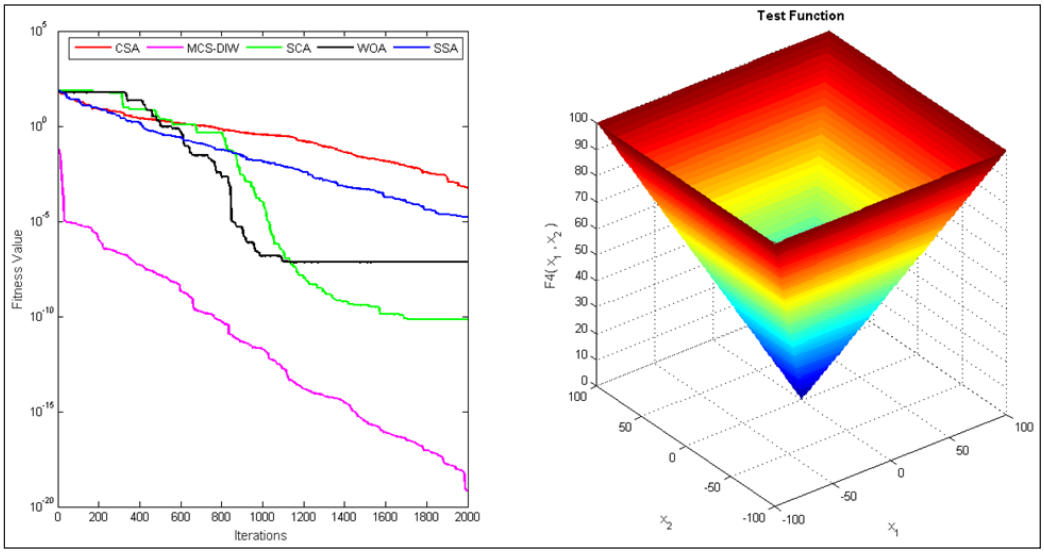

Figure 8. Comparison of the Modified Cuckoo Search using Decreasing Inertia Weight (MCS-DIW) algorithm with Cuckoo Search Algorithm (CSA), Sine Cosine Algorithm (SCA), Search Sparrow Algorithm (SSA), and Whale Optimization Algorithm (WOA) using the test function F4

deep exploitation to find the global optimal value over time. Afterwards, the SCA showed a green line illustrating a slower convergence rate using the moderate fitness value, ~10^{-5}, with early stagnation of the overall search space. Next, the WOA represents a black line and stagnates quickly with ~10^{-2} fitness values over 800 iterations, which depicts a local trap problem and premature convergence. The blue line represents SSA, reflecting an imbalance between exploitation and exploration with slower convergence than MCS and SCA. Hence, SSA reaches ~10^{-3} fitness values over 1200 iterations. Besides, the original CS algorithm represents a red line along its fine-tuned parameters and showed better performance than WOA and SSA around 1500 iterations, achieving the fitness value of ~10^{-4}. However, the red line demonstrates the original CS algorithm depicted, which showed a slower convergence rate as compared to the proposed MCS-DIW algorithm. Additionally, it has shown intermediate performance and is less efficient than the MCS-DIW and SCA algorithms, along with limited exploration capability to find the global optimal value.

In Figure 9, using the F5 function to minimize the objective function, the proposed MCS-DIW algorithm has maintained a good balance between exploration and exploitation to find the global optimal solution as compared to other selected SI algorithms. It has been demonstrated by the magenta line, achieving the fastest convergence by the final lowest fitness value ~10^{-20} by approximately 200 iterations, and it has continued to improve the exploration process capabilities along deep exploitation to find the global optimal value over time by reaching ~10^{-5} against 1000 iterations and drops to ~10^{-15} fitness value. Accordingly, it efficiently achieves the global optimal value compared to the other selected SI algorithms.

Besides, the blue line represents SSA, reflecting a gradual imbalance between exploitation and exploration with slower convergence than MCS and CS. Hence, SSA reaches ~10^{-2} fitness values without further improvements with 500 iterations, leading to suboptimal solutions. Afterwards, the SCA showed a green line exhibiting an initial rapid convergence rate but got trapped in local search space early. As a result, it only reached the moderate fitness value, ~10^{-3} with 200 iterations, with early stagnation of the overall search space, and afterwards there were no significant improvements.

Subsequently, the red line demonstrates that the original CS algorithm depicts a slower convergence rate using the moderate fitness value, ~10^{-12}, with early stagnation of the overall search space over 1500 iterations. Over 500 iterations, the fitness values have been improving from ~10^{-4} to ~10^{-8} at 1000 iterations. However, the original CS algorithm is a bit slower as compared to the modified variant in reaching the global optimal level.

Next, the WOA represents a black line and stagnates quickly with ~10^{-1} fitness value over 200 iterations, which depicts a local trap problem and premature convergence. Hence, the proposed MCS-DIW provides satisfactory results to find the global optimal solution as compared to early stagnation and limited optimization potential of SCA, SSA, and WOA comparative variants.

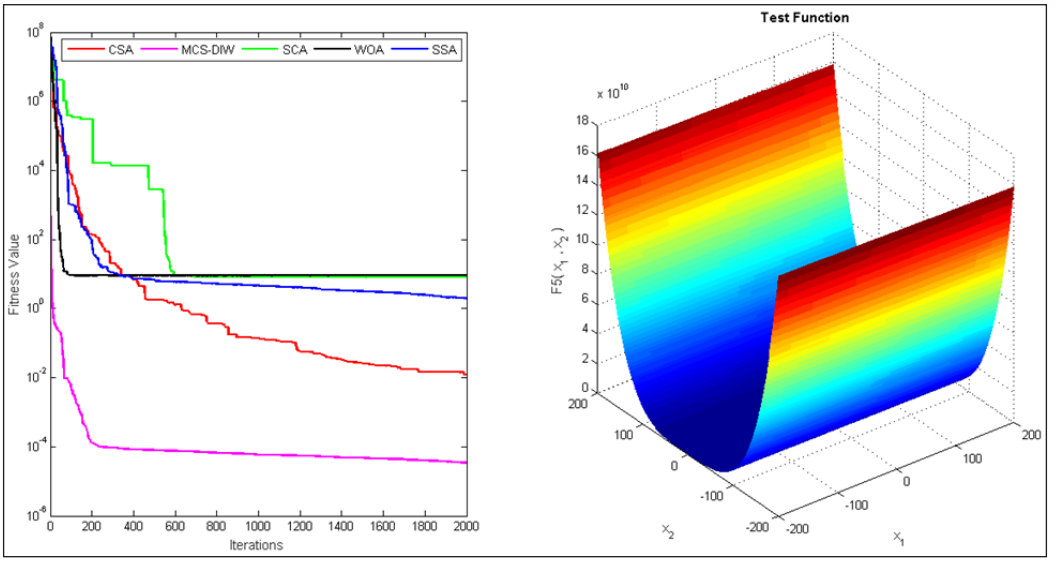

Figure 9. Comparison of the Modified Cuckoo Search using decreasing inertia weight (MCS-DIW) alg1orithm with Cuckoo Search Algorithm (CSA), Sine Cosine Algorithm (SCA), Search Sparrow Algorithm (SSA), and Whale Optimization Algorithm (WOA) using the test function F5

In Figure 10, using the F7 function to minimize the objective function, the proposed MCS-DIW algorithm has maintained a good balance between exploration and exploitation to find the global optimal solution as compared to other selected SI algorithms. It has been demonstrated by the magenta line, achieving the fastest convergence by the lowest fitness value ~10^{-14} by approximately 600 iterations and drops to ~10^{-4} fitness value by 200 iterations. Accordingly, it efficiently achieves the global optimal value compared to the other selected SI algorithms by keeping a balance between exploration and exploitation.

Besides, the blue line represents SSA, again reflecting an imbalance between exploitation and exploration with higher fitness values and slower convergence. Hence, SSA reaches ~10^{-3} fitness values without further improvements with 1000 iterations, leading to early suboptimal solutions. Afterwards, the SCA showed a green line exhibiting an initial rapid convergence rate but got trapped in the local search space early. As a result, it has comparatively demonstrated effective but less robust and slower performance, providing a fitness value of ~10^{-12} with 1200 iterations.

Subsequently, the red line demonstrates that original CS algorithm depicts a slower convergence rate using the moderate fitness value, ~10^{-10}, with moderate performance over 1800 iterations. Still, according to the results, it is less efficient than MCS-DIW and SCA. Next, the WOA represents a black line and stagnates quickly with ~10^{-2} fitness values throughout the iterations, which depicts a local trap problem and premature convergence.

Hence, the proposed MCS-DIW provides satisfactory results with the lowest fitness value to find the global optimal solution as compared to other selected SI algorithms.

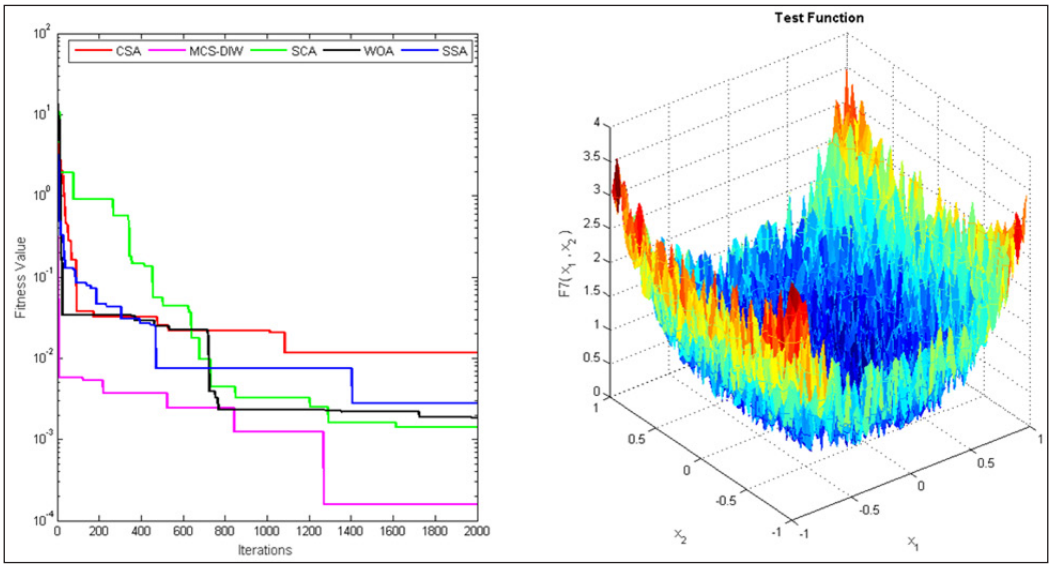

Figure 10. Comparison of the Modified Cuckoo Search using decreasing inertia weight (MCS-DIW) algorithm with Cuckoo Search Algorithm (CSA), Sine Cosine Algorithm (SCA), Search Sparrow Algorithm (SSA), and Whale Optimization Algorithm (WOA) using the test function F7

In Figure 11, using the F9 function to minimize the objective function, the proposed MCS-DIW algorithm has maintained a good balance between exploration and exploitation to find the global optimal solution compared to other selected SI algorithms. It has been demonstrated by the magenta line, achieving the fastest convergence by the lowest fitness value ~10^{-4} by approximately 1200 iterations and exhibiting steady improvement. Accordingly, it efficiently achieves the global optimal value compared to the other selected SI algorithms by balancing exploration and exploitation.

Besides, the blue line represents SSA, exhibiting slower convergence and limited exploration capabilities. Hence, SSA reaches ~10^{-2} fitness values without further improvements with 1200 iterations, leading to early suboptimal solutions. Afterwards, the SCA showed a green line exhibiting an initial rapid convergence rate of around 1000 iterations but got trapped in local search space early. As a result, it has demonstrated an effective but less robust and slower performance, providing a fitness value of ~10^{-2}.

Subsequently, the red line demonstrates the original CS algorithm depicts a slower convergence rate using the moderate fitness value, ~10^{-3}, with moderate performance over 1500 iterations, but according to the results, it is showing better performance as compared to SCA, SSA, and WOA. Next, the WOA represents a black line; it is less effective as it

stagnates quickly with ~10^{-1} fitness value with 600 iterations without further improvements, which depicts a local trap problem and premature convergence.

Hence, the proposed MCS-DIW provides satisfactory results with the lowest fitness value to find the global optimal solution as compared to other selected SI algorithms.

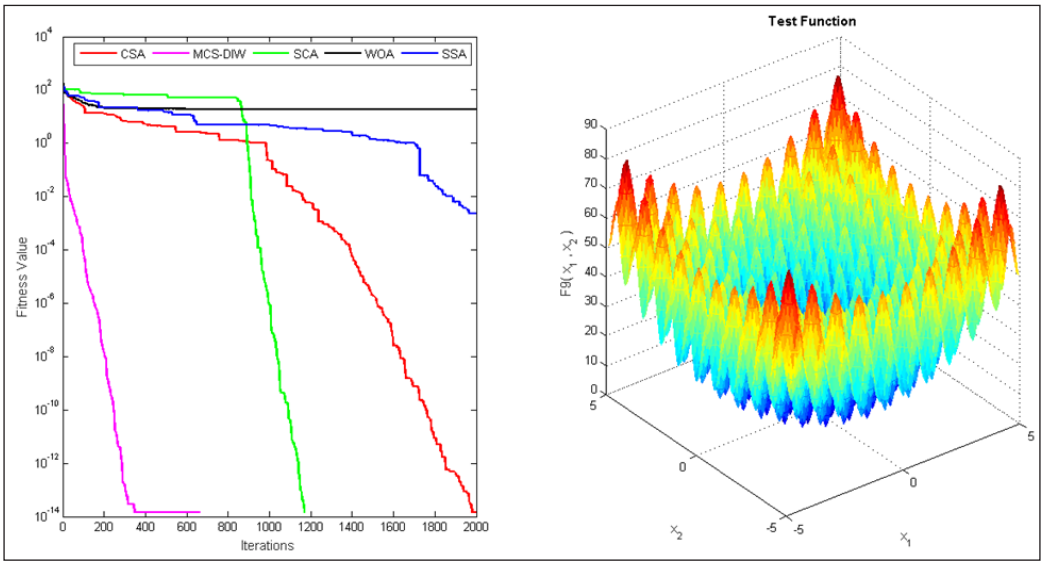

Figure 11. Comparison of the Modified Cuckoo Search using decreasing inertia weight (MCS-DIW) algorithm with Cuckoo Search Algorithm (CSA), Sine Cosine Algorithm (SCA), Search Sparrow Algorithm (SSA), and Whale Optimization Algorithm (WOA) using the test function F9

Additionally, the mean and standard deviation (Std) comparison results are provided in Table 4, where all the comparative SI algorithms' results are compared using 2000 iterations and the 4 selected mathematical test functions. This comparison showed that the proposed MCS-DIW provides better mean values compared to other selected algorithms.

Furthermore, Table 5 depicts the best cost values and CPU processing time comparison, and comparatively, the proposed algorithm showed efficiency with less time compared to the selected SI algorithms.

To validate the proposed MCS-DIW's effectiveness, Figure 12 depicts the statistical analysis results for the Wilcoxon and Friedman statistical tests, where the final fitness values of the different optimization SI algorithms along proposed MCS-DIW have been evaluated. The proposed MCS-DIW showed a better convergence with significantly lower fitness values than the other comparative swarm intelligence algorithms.

Table 6 indicates that the Wilcoxon results provide p-values < 0.05, indicating that the proposed MCS-DIW significantly outperforms its counterparts.

Table 4
Mean and standard deviation global minimum comparison

Test functions	MCS-DIW mean/std.	CS mean/std.	SCA mean/std.	WOA mean/std.	SSA mean/std.	Iterations
F4	150.5354/ 37.02811	211.1881/ 56.34211	519.586/ 33.1708	190.4882/ 12.4564	635.3371/ 38.45453	2000
F5	23802.9639/ 28.5646	58123.004/ 40.5653	1207313.7257/ 39.87865	69099.5753/ 39.65743	173143.7317/ 17.45434	2000
F7	0.058221/ 0.03221	0.12902/ 0.10902	1.1749/ 1.1130	0.11596/ 0.12484	0.19193/ 0.12184	2000
F9	0.035221/ 0.05822	0.22602/ 0.12902	1.1479/ 1.1749	0.12596/ 0.11596	0.18292/ 0.19193	2000

Note. CS = Cuckoo Search; MCS-DIW = Modified Cuckoo Search using decreasing inertia weight; WOA = Whale Optimization Algorithm; SCA = Sine Cosine Algorithm; SSA = Search Sparrow Algorithm; std. = Standard deviation

Table 5
Best cost and CPU processing time comparison

Problems	MCS-DIW best cost/ CPU time consumption	CS best cost/ CPU time consumption	SCA best cost/ CPU time consumption	WOA best cost/ CPU time consumption	SSA best cost/ CPU time consumption	Iterations
F4	1.9557e-114/ 0.57213	2.8581e-17/ 1.4351	0/ 0.14198	1.1235e19/ 1.7858	0.45196/ 0.35833	2000
F5	1.0788e-88/ 0.5828	1.4398e-09/ 1.7483	0/ 0.16401	1.9121e08/ 1.6112	0.00053215/ 0.38028	2000
F7	0.005398912.1/ 4	0.0093989/ 10.0351	0.01339591.267/ 3	6.1368/ 4.9487	1.8422/ 2.761	2000
F9	0.0068648/ 1.3327	0.010044/ 1.2569	0/ 0.12485	0.0097856/ 0.43367	0.082626/ 0.33124	2000

Note. CS = Cuckoo Search; MCS-DIW = Modified Cuckoo Search using decreasing inertia weight; WOA = Whale Optimization Algorithm; SCA = Sine Cosine Algorithm; SSA = Search Sparrow Algorithm; CPU = Central processing unit

Table 6
Test Wilcoxon results for MCS-DIW

Comparative algorithms	Wilcoxon Statistic	*p*-value
MCS-DIW vs CS	0.0	0.0023
MCS-DIW vs SCA	0.0	0.0017
MCS-DIW vs WOA	1.0	0.0034
MCS-DIW vs SSA	0.0	0.0028

Note. MCS-DIW = Modified Cuckoo Search using decreasing inertia weight; CS = Cuckoo Search; SCA = Sine Cosine Algorithm; WOA = Whale Optimization Algorithm; SSA = Search Sparrow Algorithm

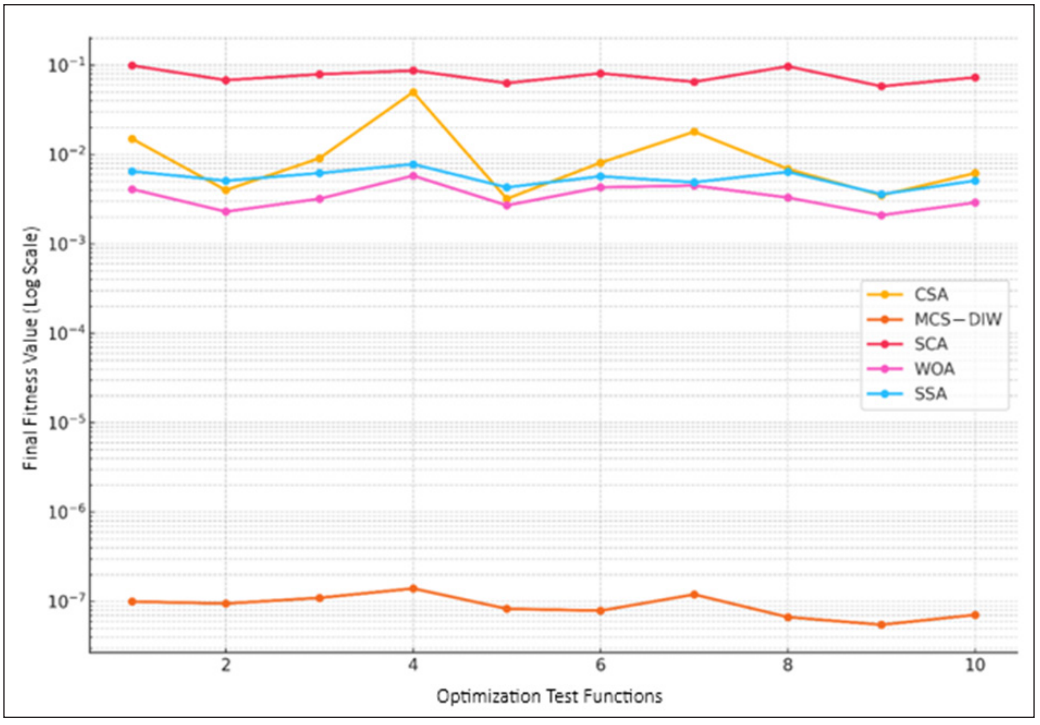

Figure 12. Comparison of the Modified Cuckoo Search using decreasing inertia weight (MCS-DIW) Algorithm with original Cuckoo Search, Sine Cosine Algorithm (SCA), Search Sparrow Algorithm (SSA), and Whale Optimization Algorithm (WOA) using the 10 different optimization test functions
Note. CSA = Cuckoo Search Algorithm

The results shown in Table 7 indicate better performance of the proposed MCS-DIW as the *p*-value ($p < 0.05$) is extremely low compared to other comparative swarm intelligent algorithms, ensuring the effectiveness of the proposed algorithm.

Table 7
Friedman statistical result

Statistical test	**Test value**	***p*-value**
Friedman Test	38.32	9.63×10^{-8}

CONCLUSION AND FUTURE WORKS

This research paper provides an improved variant of the MCS algorithm, proposed using the sigmoid DIW to avoid premature convergence. Extensive investigations are conducted to validate the performance of the MCS-DIW algorithm using optimization test functions. The performance of the MCS-DIW algorithm is compared with a few different SI algorithms, such as original CS, SCA, WOA, and SSA. The simulation experiments show that the

performance, stability, robustness, and convergence speed of the MCS-DIW algorithm surpasses other SI counterparts. In sum, the MCS-DIW algorithm can effectively overcome the local trap problem through its enhanced exploration capacity to find the best global optimum. The proposed research significantly improved the performance of MCS-IW by utilizing fewer tuning parameters and providing the fastest convergence compared to its counterparts. Additionally, MCS-IW's local optima escaping ability ensured strong global search capabilities. However, due to the heavy reliance on the randomized nature of nest and Lévy flight replacements, there exists a problem of inconsistency and population diversity; additional modifications are required to handle the inconsistencies and constrained optimization problems effectively. In this regard, a more in-depth analysis of the proposed MCS-DIW algorithm will be executed in both single-objective (SO) and multi-objective (MO) real-world engineering problems, such as power system optimization, neural network training, image reconstruction, data clustering, data classification, and error minimization. Moreover, the MCS-IW algorithm will be integrated with other swarm intelligence algorithms to hybridize the capabilities to find the maximum global optima. However, the efficiency of the proposed algorithm can be improved by implementing quantum-inspired techniques, parallel computing, and constraint-handling advanced mechanisms to enhance the performance of large-scale optimization tasks for better balancing between exploration and exploitation.

ACKNOWLEDGEMENTS

This research was funded by the Fundamental Research Grant Scheme (FRGS) under a grant number of FRGS/1/2019/ICT02/UNIMAP/02/7.

REFERENCES

Abdul Rani, K. N., Abdulmalek, M., Rahim, H. A., Chin, N. S., & Abd Wahab, A. (2017). Hybridization of strength pareto multiobjective optimization with modified cuckoo search algorithm for rectangular array. *Scientific Reports*, *7*, 46521. https://doi.org/10.1038/srep46521

Abdul Rani, K. N., & Malek, F. (2011). Preliminary study on cuckoo search parameters for symmetric linear array geometry synthesis. In *TENCON 2011-2011 IEEE Region 10 Conference* (pp. 568–572). IEEE. https://doi.org/10.1109/TENCON.2011.6129169

Abualigah, L., Ababneh, A., Ikotun, A. M., Zitar, R. A., Alsoud, A. R., Khodadadi, N., Ezugwu, A. E., Hanandeh, E. S., & Jia, H. (2024). A survey of cuckoo search algorithm: Optimizer and new applications. In L. Abualigah (Ed.), *Metaheuristic optimization algorithms: Optimizers, analysis, and applications* (pp. 45–57). Morgan Kaufmann. https://doi.org/10.1016/B978-0-443-13925-3.00018-2

Adeyelu, A. A., John, Z. S., Uga-Otor, S., Elusakin, O. E., & Godwin, I. R. (2024). An adaptation of Cuckoo Search Algorithm in maximizing energy efficiency of Dynamic Source Routing Algorithm for Mobile AdHoc Network. *International Journal of Computer Applications*, *186*(9), 29-36.

Adeyeye, O. J., & Akanbi, I. (2024). Optimization in systems engineering: A review of how data analytics and optimization algorithms are applied. *Computer Science and IT Research Journal*, *5*(4), 809–823. https://doi.org/10.51594/csitrj.v5i4.1027

Ahmad, T., Sulaiman, M., Bassir, D., Alshammari, F. S., & Laouini, G. (2025). Enhanced numerical solutions for fractional PDEs using Monte Carlo PINNs coupled with cuckoo search optimization. *Fractal and Fractional*, *9*(4), 225. https://doi.org/10.3390/fractalfract9040225

Almufti, S. M., Marqas, R. B., Asaad, R. R., & Shaban, A. A. (2025). Cuckoo search algorithm: Overview, modifications, and applications. *International Journal of Scientific World*, *11*(1), 1-9.

Aziz, R. M. (2022). Cuckoo search-based optimization for cancer classification: A new hybrid approach. *Journal of Computational Biology*, *29*(6), 565–584. https://doi.org/10.1089/cmb.2021.0410

Bharambe, U., Ramesh, R., Mahato, M., & Chaudhari, S. (2024). Synergies Between natural language processing and swarm intelligence optimization: A comprehensive overview. In J. Valadi, K. P. Singh, M. Ojha, & P. Siarry (Eds.), *Advanced machine learning with evolutionary and metaheuristic techniques* (pp. 121–151). Springer. https://doi.org/10.1007/978-981-99-9718-3_6

Brezočnik, L., Fister, I., & Podgorelec, V. (2018). Swarm intelligence algorithms for feature selection: A review. *Applied Sciences*, *8*(9), 1521. https://doi.org/10.3390/app8091521

Chakraborty, A., & Kar, A. K. (2017). Swarm intelligence: A review of algorithms. In S. Patnaik, X. S. Yang, & K. Nakamatsu (Eds.), *Nature-inspired computing and optimization: Theory and applications* (Vol. 10, pp. 475–494). Springer. https://doi.org/10.1007/978-3-319-50920-4_19

Chakraborty, S., Saha, A. K., Ezugwu, A. E., Agushaka, J. O., Zitar, R. A., & Abualigah, L. (2023). Differential evolution and its applications in image processing problems: A comprehensive review. *Archives of Computational Methods in Engineering*, *30*, 985–1040. https://doi.org/10.1007/s11831-022-09825-5

Chen, J., Xia, R., You, J., Yao, Q., Dai, Y., Zhang, J., Yao, J., & Guo, Y. (2024). Automatic optimal design of field plate for silicon on insulator lateral double-diffused metal oxide semiconductor using simulated annealing algorithm. *IET Power Electronics*, *17*(4), 487–493. https://doi.org/10.1049/pel2.12658

Cheraghi, N., Miri, M., & Rashki, M. (2023). An adaptive artificial neural network for reliability analyses of complex engineering systems. *Applied Soft Computing*, *132*, 109866. https://doi.org/10.1016/j.asoc.2022.109866

Choudhary, S., Sugumaran, S., Belazi, A., & Abd El-Latif, A. A. (2023). Linearly decreasing inertia weight PSO and improved weight factor-based clustering algorithm for wireless sensor networks. *Journal of Ambient Intelligence and Humanized Computing*, *14*, 6661-6679. https://doi.org/10.1007/s12652-021-03534-w

Cuong-Le, T., Minh, H.-L., Khatir, S., Wahab, M. A., Tran, M. T., & Mirjalili, S. (2021). A novel version of Cuckoo search algorithm for solving optimization problems. *Expert Systems with Applications*, *186*, 115669. https://doi.org/10.1016/j.eswa.2021.115669

Ghiaskar, A., Amiri, A., & Mirjalili, S. (2024). Polar fox optimization algorithm: A novel meta-heuristic algorithm. *Neural Computing and Applications*, *36*, 20983–21022. https://doi.org/10.1007/s00521-024-10346-4

Habeb, A. A. A. A., Taresh, M. M., Li, J., Gao, Z., & Zhu, N. (2024). Enhancing medical image classification with an advanced feature selection algorithm: A novel approach to improving the cuckoo search algorithm by incorporating Caputo fractional order. *Diagnostics*, *14*(11), 1191. https://doi.org/10.3390/diagnostics14111191

Huang, S., & Zhou, J. (2024). An enhanced stability evaluation system for entry-type excavations: Utilizing a hybrid bagging-SVM model, GP and kriging techniques. *Journal of Rock Mechanics and Geotechnical Engineering*, *17*(4), 2360-2373. https://doi.org/10.1016/j.jrmge.2024.05.024

Joshi, A. S., Kulkarni, O., Kakandikar, G. M., & Nandedkar, V. M. (2017). Cuckoo search optimization - A review. *Materials Today: Proceedings*, *4*(8), 7262–7269. https://doi.org/10.1016/j.matpr.2017.07.055

Kwakye, B. D., Li, Y., Mohamed, H. H., Baidoo, E., & Asenso, T. Q. (2024). Particle guided metaheuristic algorithm for global optimization and feature selection problems. *Expert Systems with Applications*, *248*, 123362. https://doi.org/10.1016/j.eswa.2024.123362

Liu, C., Wang, J., Zhou, L., & Rezaeipanah, A. (2022). Solving the multi-objective problem of IoT service placement in fog computing using cuckoo search algorithm. *Neural Processing Letters*, *54*, 1823–1854. https://doi.org/10.1007/s11063-021-10708-2

Luo, X., Chen, J., Yuan, Y., & Wang, Z. (2024). Pseudo gradient-adjusted particle swarm optimization for accurate adaptive latent factor analysis. In *IEEE Transactions on Systems, Man, and Cybernetics: Systems* (Vol. 54, No. 4, pp. 2213-2226). IEEE. https://doi.org/10.1109/TSMC.2023.3340919

Mahmood, S., Bawany, N. Z., & Tanweer, M. R. (2023). A comprehensive survey of whale optimization algorithm: Modifications and classification. *Indonesian Journal of Electrical Engineering and Computer Science*, *29*(2), 899-910. http://doi.org/10.11591/ijeecs.v29.i2.pp899-910

Mareli, M., & Twala, B. (2018). An adaptive Cuckoo search algorithm for optimisation. *Applied Computing and Informatics*, *14*(2), 107–115. https://doi.org/10.1016/j.aci.2017.09.001

Massat, M. B. (2018). A promising future for AI in breast cancer screening. *Applied Radiology*, *47*(9), 22–25.

Meena, K. S., Singh, S. S., & Singh, K. (2024). Cuckoo search optimization-based influence maximization in dynamic social networks. *ACM Transactions on the Web*, *18*(4), 1–25. https://doi.org/10.1145/3690644

Mohammed, B. A., Zhuk, O., Vozniak, R., Borysov, I., Petrozhalko, V., Davydov, I., Borysov, O., Yefymenko, O., Protas, N., & Kashkevich, S. (2023). Improvement of the solution search method based on the cuckoo algorithm. *Eastern-European Journal of Enterprise Technologies*, *2*(4 (122)), 23-30. https://doi.org/10.15587/1729-4061.2023.277608

Nickabadi, A., Ebadzadeh, M. M., & Safabakhsh, R. (2011). A novel particle swarm optimization algorithm with adaptive inertia weight. *Applied Soft Computing*, *11*(4), 3658–3670. https://doi.org/10.1016/j.asoc.2011.01.037

Saka, M. P., Doğan, E., & Aydogdu, I. (2013). Analysis of swarm intelligence–based algorithms for constrained optimization. In X.-S. Yang, R. Xiao, & M. Karamanoglu (Eds.), *Swarm intelligence and bio-inspired computation: Theory and applications* (pp. 25–48). Elsevier. https://doi.org/10.1016/B978-0-12-405163-8.00002-8

Sekyere, Y. O. M., Effah, F. B., & Okyere, P. Y. (2024). An enhanced particle swarm optimization algorithm via adaptive dynamic inertia weight and acceleration coefficients. *Journal of Electronics and Electrical Engineering*, *3*, 53–67. https://doi.org/10.37256/jeee.3120243868

Shi, Y., & Eberhart, R. C. (1998). Parameter selection in particle swarm optimization. In V. W. Porto, N. Saravanan, D. Waagen, & A. E. Eiben (Eds.), *Evolutionary Programming VII: 7th International Conference* (Vol. 1447, pp. 591–600). Springer. https://doi.org/10.1007/BFb0040810

Sohail, A. (2023). Genetic algorithms in the fields of artificial intelligence and data sciences. *Annals of Data Science*, *10*, 1007–1018. https://doi.org/10.1007/s40745-021-00354-9

Thaher, T., Sheta, A., Awad, M., & Aldasht, M. (2024). Enhanced variants of crow search algorithm boosted with cooperative based island model for global optimization. *Expert Systems with Applications*, *238*(Part A), 121712. https://doi.org/10.1016/j.eswa.2023.121712

Tian, Y., Zhang, D., Zhang, H., Zhu, J., & Yue, X. (2024). An improved cuckoo search algorithm for global optimization. *Cluster Computing*, *27*, 8595-8619. https://doi.org/10.1007/s10586-024-04410-w

Umar, S. U., Rashid, T. A., Ahmed, A. M., Hassan, B. A., & Baker, M. R. (2024). Modified Bat Algorithm: A newly proposed approach for solving complex and real-world problems. *Soft Computing*, *28*, 7983–7998. https://doi.org/10.1007/s00500-024-09761-5

Wei, J., & Niu, H. (2022). A ranking-based adaptive cuckoo search algorithm for unconstrained optimization. *Expert Systems with Applications*, *204*, 117428. https://doi.org/10.1016/j.eswa.2022.117428

Xue, X., Shanmugam, R., Palanisamy, S., Khalaf, O. I., Selvaraj, D., & Abdulsahib, G. M. (2023). A hybrid cross layer with Harris-hawk-optimization-based efficient routing for wireless sensor networks. *Symmetry*, *15*(2), 438. https://doi.org/10.3390/sym15020438

Yang, Q., Wang, Y., Zhang, J., & Gao, H. (2024). An adaptive operator selection cuckoo search for parameter extraction of photovoltaic models. *Applied Soft Computing*, *166*, 112221. https://doi.org/10.1016/j.asoc.2024.112221

Zangana, H. M., Sallow, Z. B., Alkawaz, M. H., & Omar, M. (2024). Unveiling the collective wisdom: A review of swarm intelligence in problem solving and optimization. *Inform: Jurnal Ilmiah Bidang Teknologi Informasi Dan Komunikasi*, *9*(2), 101–110. https://doi.org/10.25139/inform.v9i2.7934

Zdiri, S., Chrouta, J., & Zaafouri, A. (2021). An expanded heterogeneous particle swarm optimization based on adaptive inertia weight. *Mathematical Problems in Engineering*, *2021*(1), 4194263. https://doi.org/10.1155/2021/4194263

Zheng, W., Si, M., Sui, X., Chu, S., & Pan, J. (2023). Application of a parallel adaptive Cuckoo Search algorithm in the rectangle layout problem. *CMES-Computer Modeling in Engineering and Sciences*, *135*(3), 2173-2196. https://doi.org/10.32604/cmes.2023.019890

Zheng, Y.-L., Ma, L.-H., Zhang, L.-Y., & Qian, J.-X. (2003). Empirical study of particle swarm optimizer with an increasing inertia weight. In *The 2003 Congress on Evolutionary Computation* (pp. 221–226). IEEE. https://doi.org/10.1109/CEC.2003.1299578

Pertanika J. Sci. & Technol. 33 (5): 2097 - 2124 (2025)

PERTANIKA JOURNALS

SCIENCE & TECHNOLOGY

Journal homepage: http://www.pertanika.upm.edu.my/

Optimizing Carbon Footprint Estimation in Residential Construction: A Comparative Analysis of Regression Trees and ANFIS for Enhanced Sustainability

Rufaizal Che Mamat[1]*, Azuin Ramli[2] and Aminah Bibi Bawamohiddin[3]

[1]Centre of Green Technology for Sustainable Cities, Department of Civil Engineering, Politeknik Ungku Omar, Jalan Raja Musa Mahadi, 31400 Ipoh, Perak, Malaysia
[2]Centre of Research and Innovation Excellence, Politeknik Ungku Omar, Jalan Raja Musa Mahadi, 31400 Ipoh, Perak, Malaysia
[3]Department of Information Technology and Telecommunications, Politeknik Ungku Omar, Jalan Raja Musa Mahadi, 31400 Ipoh, Perak, Malaysia

ABSTRACT

This study evaluates the predictive accuracy of Regression Trees (RTrees) and Adaptive Neuro-Fuzzy Inference Systems (ANFIS) for estimating the carbon footprint in residential construction projects. The results indicate that the ANFIS significantly outperforms the RTrees in predictive accuracy, achieving a reduction in Root Mean Square Error (RMSE) by 84.3% in the production stage (from 0.53174 to 0.08346) and by 40.4% in the operational stage (from 0.13865 to 0.08265). These improvements underscore the effectiveness of the ANFIS in capturing complex nonlinear relationships in carbon footprint data. Despite its superior accuracy, the ANFIS exhibits higher computational costs, requiring an average training time of 76.2 s, compared to 12.4 s for the RTrees. These findings highlight the trade-offs between accuracy and computational efficiency, providing valuable insights for selecting machine learning models in sustainable construction. The study concludes that integrating hybrid approaches or ensemble learning could further enhance predictive performance while maintaining efficiency.

Keywords: ANFIS, carbon emission, machine learning, regression trees, sustainable construction

ARTICLE INFO

Article history:
Received: 28 January 2025
Accepted: 29 April 2025
Published: 11 August 2025

DOI: https://doi.org/10.47836/pjst.33.5.04

E-mail addresses:
rufaizal.cm@gmail.com (Rufaizal Che Mamat)
azuin.ramli@puo.edu.my (Azuin Ramli)
aminahbibi@puo.edu.my (Aminah Bibi Bawamohiddin)
* Corresponding author

INTRODUCTION

The construction industry significantly contributes to global greenhouse gas emissions, accounting for approximately 39% of the world's final energy consumption and 37% of energy-related carbon dioxide

e-ISSN: 2231-8526

(CO_2) emissions in 2021 (Chen et al., 2023). These figures underscore the urgent need for a transformative shift towards sustainable practices within the sector. A critical component of this transformation is the ability to accurately predict a project's carbon footprint, enabling stakeholders to identify areas for improvement and implement effective strategies to minimize emissions (Mahapatra et al., 2021). This study focuses on developing and comparing advanced machine learning models to enhance the accuracy of carbon footprint predictions in residential construction projects.

Over the past decade, machine learning has emerged as a powerful tool in various industries, including construction, for its ability to analyze large datasets and uncover complex relationships between variables. Comprehensive, traditional methods of carbon footprint estimation, such as life cycle assessment (LCA), are often time-consuming and prone to errors due to data uncertainties (Marsh et al., 2023). Integrating machine learning techniques offers a promising solution to these challenges by providing more precise and efficient predictions, thus supporting the construction industry's shift toward sustainability.

While several studies have explored the application of machine learning in carbon footprint prediction, there is a noticeable gap in comparative analyses of different models within the context of residential construction. Previous research has primarily focused on individual methodologies, such as support vector regression (Farghaly et al., 2020; Hasan et al., 2025; Mamat et al., 2025) and artificial neural networks (Sergeev et al., 2022; Yao et al., 2024). However, a direct comparison of different machine learning approaches remains underexplored, particularly in their ability to predict carbon footprints in residential projects. Machine learning methodologies face significant limitations that can impede their effectiveness across diverse applications.

A major challenge is the dependency on large, high-quality datasets (Gong et al., 2023). Insufficient data can result in governance failures (Vinayak & Ahmad, 2023) and poor decision-making (Kim, 2024). Machine learning models also struggle with generalizability, particularly in applications like carbon emission prediction, where diverse data is necessary (Yiming et al., 2024). Additionally, imbalanced datasets (Jia et al., 2024), which are common in atmospheric studies, complicate model training. Conceptual and statistical limitations, such as unmodeled dependencies (Pillai et al., 2023), further exacerbate these issues. Addressing these challenges requires robust data governance, diverse training sets, advanced techniques, and increased awareness of ML's inherent limitations.

This study aims to address the existing gap in the literature by rigorously comparing the performance of two widely recognized machine learning models: RTrees and ANFIS. The primary objective is to determine the most accurate and efficient model for predicting carbon footprints in residential construction. Through an in-depth evaluation of the predictive capabilities of the RTrees and ANFIS, this research provides stakeholders with a valuable tool to mitigate the environmental impacts associated with construction

activities. Moreover, this study contributes significantly to the growing body of knowledge by offering a comprehensive analysis of the strengths and limitations inherent in both models, thus providing actionable insights for future research directions. The importance of this research lies in its potential to refine carbon footprint prediction methods, which is critical to achieving sustainability goals in the construction sector. The anticipated outcomes are expected to influence policy formulation and practical applications, facilitating the reduction of the environmental footprint of residential buildings. Ultimately, this study supports ongoing efforts to promote a more sustainable built environment by advancing the integration of machine learning techniques into real-world construction practices.

MATERIALS AND METHODS

This study employs a robust and systematic methodological framework to critically evaluate the performance of the RTrees and ANFIS in predicting the carbon footprint of residential construction projects. The methodology is meticulously designed to ensure the reliability and reproducibility of the results. The main phases of the approach include data collection, preprocessing, model development, performance evaluation, and a comprehensive comparative analysis. Each stage is carefully aligned with the study's core objectives to thoroughly assess the models' predictive capabilities, facilitating a nuanced understanding of their effectiveness in the context of carbon footprint prediction in the construction sector.

Computational Cost and Deployment Considerations

The computational cost and hardware-software requirements for deploying the machine learning models were carefully assessed to evaluate their practicality in real-world applications. The training and testing processes were conducted on a system equipped with an Intel Core i7-12700K processor, 32GB Random Access Memory (RAM), and an NVIDIA RTX 3080 graphics processing unit (GPU). The software environment included MATLAB R2023a and Python 3.9, with essential libraries such as Scikit-Learn and TensorFlow. While the RTrees demonstrated lower computational overhead, requiring an average training time of 12.4 s, ANFIS exhibited significantly higher resource demand, with an average training time of 76.2 s. This discrepancy highlights the trade-off between computational efficiency and predictive accuracy. The implementation of the ANFIS on large-scale datasets may necessitate high-performance computing resources, increasing deployment costs. Additionally, licensing costs for proprietary software such as MATLAB may pose financial constraints for small-scale projects. To mitigate these challenges, cloud-based solutions and GPU acceleration strategies can be explored to enhance model scalability and accessibility.

Data Sources and Process

This study utilizes data from a residential construction project featuring a reinforced concrete structure. The dataset was generated using Autodesk Revit Architecture 2018, which enabled the creation of a detailed 3D building model to estimate material quantities and their associated properties. A hybrid approach combining manual calculations and automated tools was applied to assess the carbon emissions at various stages of the building's life cycle using LCA. Manual calculations were based on the Inventory of Carbon and Energy (ICE) database, which provides standardized embodied carbon and energy coefficients for construction materials. To enhance the accuracy of the carbon footprint estimations, two additional databases, GaBi and Ecoinvent, were integrated into the One Click LCA software, ensuring a comprehensive assessment of emissions.

For transportation-related emissions, factors such as material transportation distances, vehicle types, and fuel consumption rates were incorporated using One Click LCA to estimate the carbon footprint associated with logistics. The operational energy consumption of the building was determined using actual electricity consumption data collected over an extended period, ensuring real-world applicability.

The dataset consists of 1,000 instances, each with 20 features, representing key variables such as material types, transportation distances, energy consumption rates, and demolition waste. To ensure robust model training, the dataset was pre-processed to remove inconsistencies, handle missing values, and standardize features for better comparability. Following standard machine learning practices, the dataset was split into 80% training data (800 instances) and 20% testing data (200 instances) to allow for model evaluation on unseen data. To provide clarity, Table 1 presents a structured summary of the dataset, including the number of records, feature categories, and the train-test distribution.

Table 1
Dataset features and train-test split

Feature category	Description	Number of features	Variables
Material properties	Embodied carbon, weight, volume	6	Concrete, steel, wood, glass, plastic, bricks, cement, sand
Transportation	Distance, vehicle type, fuel consumption	4	Truck, excavator, cranes, backhoe
Operational energy	HVAC usage, lighting, and electricity consumption	5	kWh consumption
Demolition waste	Material recycling rate, landfill emissions	5	Concrete waste, metals, glass, plastic, bricks, cement, sand
Total records	Number of data points	1,000	-
Train-test split	Training (80%), testing (20%)		800 train, 200 test

Note. HVAC = Heating, ventilation, and air conditioning

System Boundaries

The unit process in LCA is primarily determined by the system boundaries defined for the study. In this study, the system boundaries are clearly outlined in Figure 1. One Click LCA was employed to facilitate efficient material mapping. The environmental impacts of various building materials across different life cycle stages were assessed using a combination of three key databases. Initial manual calculations were conducted using the Inventory of ICE database. In contrast, software-based calculations were performed using One Click LCA, which integrates the GaBi and Ecoinvent databases. This study evaluates the carbon footprint across four life cycle phases, focusing on the stages within the system boundaries presented in Figure 1. These phases include: (1) Construction, which encompasses material production, transportation, and on-site construction activities. The transportation component considers fuel consumption, the number of vehicles, and material quantities. (2) Operations involve using heating, ventilation, and air conditioning (HVAC) systems, lighting, water supply, and equipment. (3) Demolition, which addresses the environmental impacts associated with the destruction and renovation of the building.

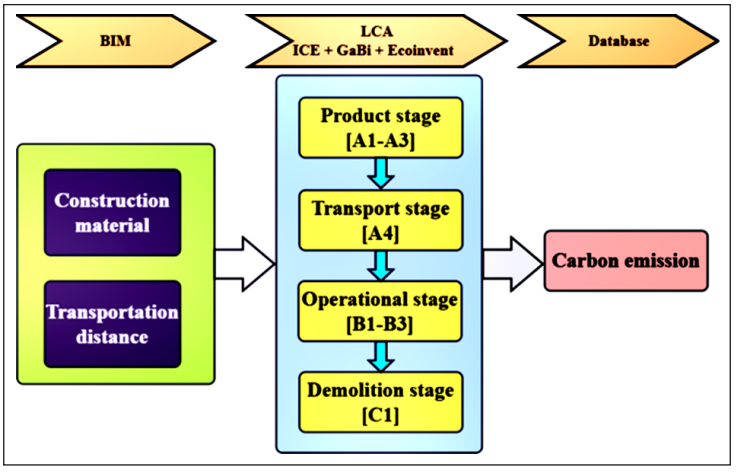

Figure 1. Boundaries of the system within the unit process
Note. BIM = Building Information Modeling; LCA = Life cycle assessment; ICE = Inventory of Carbon and Energy; GaBi and Ecoinvent = Proprietary names of databases

Building Information Modeling

This study presents a case study of a bungalow-type residential building constructed with a reinforced concrete structure in Taman Rapat Setia Baru, Ipoh, Malaysia. The building's structural design is depicted in Figure 2, which serves as the focal point for the contextual analysis. The total built area is approximately 614 m², featuring a 2.5-meter-high Dutch gable roof and 200 mm-thick concrete stone walls. Additionally, a fired clay

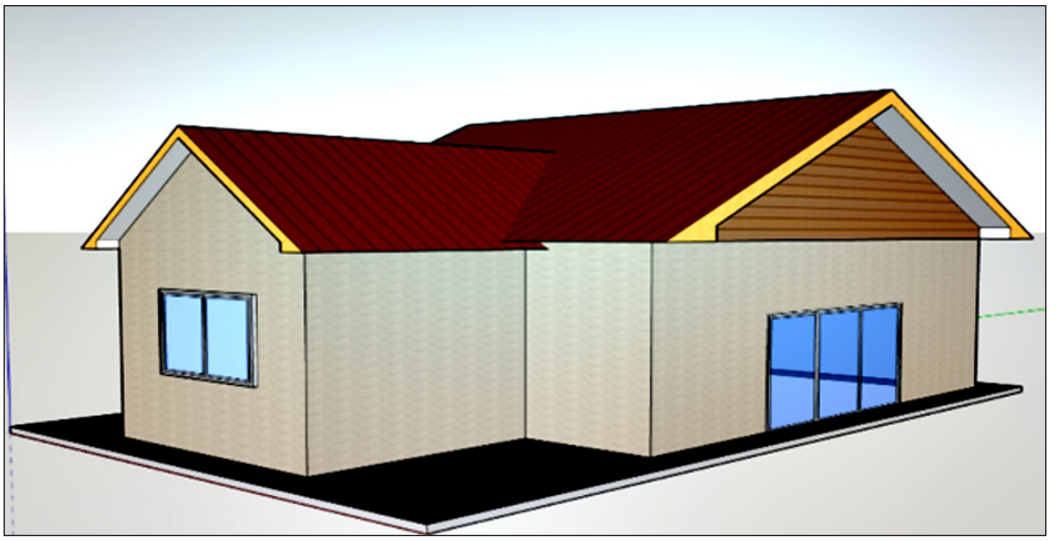

Figure 2. Three-dimensional architectural model of the case study

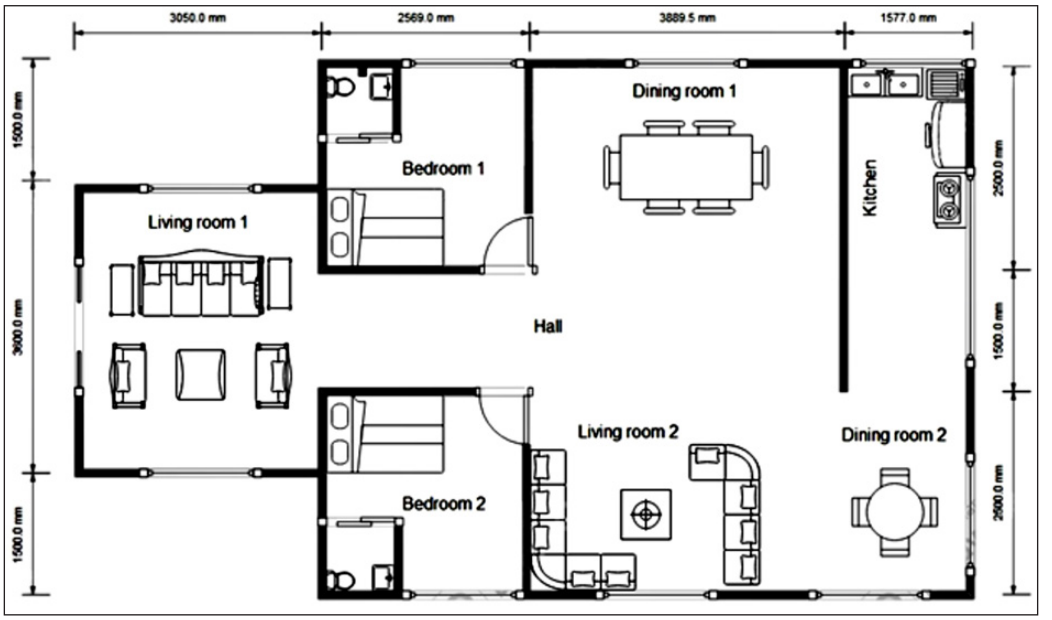

Figure 3. Floor plan

brick parapet wall enhances the overall structural integrity. The architectural plans were meticulously developed in AutoCAD (Figure 3), which were then imported into Autodesk Revit Architecture 2018 to create detailed 3D models and integrate specific building parameters. Architectural and structural components were simulated using the building information modeling (BIM) through Autodesk Revit to enable precise floor plans and

comprehensive building designs. Enscape, a real-time rendering tool integrated with Revit, further enhanced the visualization process, providing high-fidelity renderings with a single click, as demonstrated in the 3D visualization shown in Figure 2.

Life Cycle Assessment Database

The integral element of the LCA is carefully selecting a suitable life cycle database. This study employs an LCA database embedded with carbon emission rates, leveraging BIM to extract data on construction materials. Using the GaBi software, the study simulates the lifecycle impacts based on material quantities, energy consumption by construction equipment, fuel usage and time in transportation, and operational energy demands. The GaBi's database is distinguished by its global industrial life cycle data coverage. Furthermore, the ICE database enriches the analysis by providing embodied energy and carbon metrics. At the same time, the Ecoinvent dataset delivers a comprehensive cradle-to-gate inventory spanning energy production, material extraction, chemicals, metals, agriculture, and logistics, ensuring rigorous and holistic environmental assessment.

Data Pre-Processing

The dataset underwent an extensive pre-processing phase to ensure optimal conditions for model development. This phase included meticulous data cleaning to resolve inconsistencies, such as managing missing values and outliers, and feature standardization to render variables directly comparable. Standardization was a pivotal step in enhancing the efficiency and accuracy of the machine learning algorithms. This stratified division was selected to achieve a balance between maximizing the data available for model training and ensuring rigorous evaluation of unseen data. The training set supported model construction and parameter tuning, while the testing set served as an independent benchmark for validating model performance.

Model Architecture and Implementation

The architecture of the proposed models, the RTrees and ANFIS, has been expanded in detail to enhance clarity and reproducibility. The RTrees model follows a hierarchical decision-making structure where data is recursively partitioned into nodes based on entropy or variance reduction. The root node is selected based on the most informative feature, and branches are generated until a stopping criterion, such as a minimum leaf size, is reached. A pruning mechanism is applied to prevent overfitting. Figure 4 illustrates the RTrees workflow, highlighting its feature-splitting process.

In contrast, the ANFIS model integrates fuzzy logic with a multi-layer artificial neural network (ANN) to capture nonlinear relationships within the dataset. The five-layer

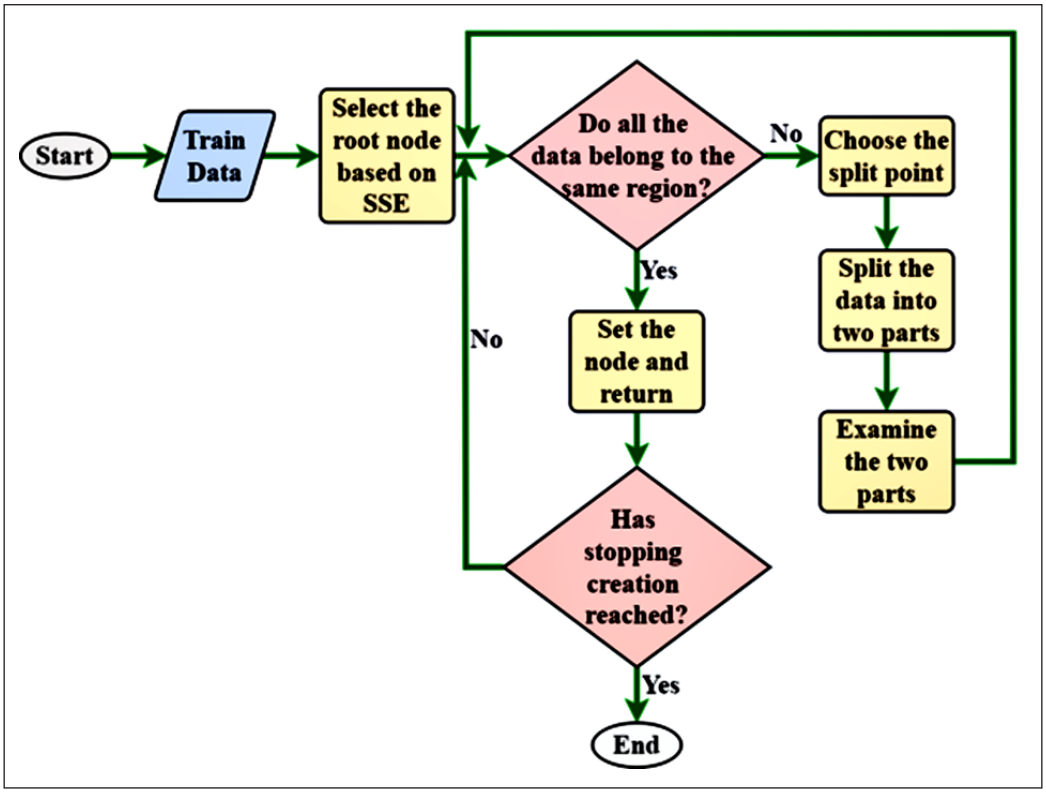

Figure 4. Regression tree flow diagram

architecture of the ANFIS consists of (1) fuzzification, where crisp input variables are converted into fuzzy membership functions, (2) rule inference, where Sugeno-type fuzzy rules are applied, (3) normalization, where rule strength is adjusted, (4) defuzzification, which maps fuzzy results to a continuous output, and (5) final summation, which aggregates rule-based outputs to provide the final prediction. The training process employs a hybrid optimization approach combining the gradient descent method and the least squares estimator (LSE) to adjust membership function parameters iteratively. Figure 5 presents a structured visualization of the ANFIS model, illustrating the connectivity between layers. These expanded descriptions provide a deeper understanding of the predictive models used in this study, supporting their effective implementation in carbon footprint estimation.

To enhance clarity and reproducibility, we have included a detailed step-by-step explanation of the RTrees model used for carbon footprint estimation in residential construction, as shown in Figure 6. The implementation begins with data preprocessing, where missing values are handled, numerical variables are normalized, and categorical variables are encoded. The dataset is divided into 80% training and 20% testing sets to ensure a fair evaluation. Once the data is prepared, the regression tree model is constructed

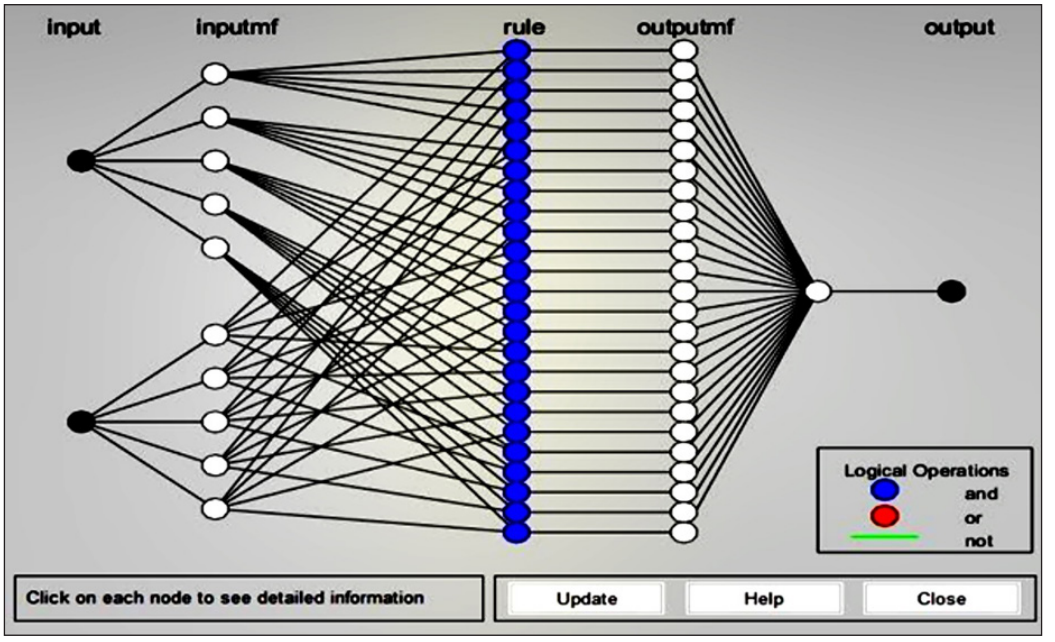

Figure 5. The foundational principle of the Adaptive Neuro-Fuzzy Inference Systems (ANFIS) architecture

using a recursive partitioning approach. The root node is selected based on the optimal splitting criterion, typically minimizing variance within child nodes. The dataset is progressively divided into smaller subsets until a stopping condition is met, such as reaching a minimum leaf size. After the initial tree construction, a pruning process is applied to eliminate branches that do not contribute to improved performance, reducing overfitting and enhancing model generalization. Following the model training, the RTrees model is evaluated using key performance metrics, including the RMSE, Mean Squared Error (MSE), and Mean Absolute Percentage Error (MAPE). The final trained model is then applied to predict carbon footprint values across different life cycle stages of construction, providing insights into emission trends.

The ANFIS model integrates fuzzy logic with artificial neural networks to enhance predictive accuracy in carbon footprint estimation. The ANFIS implementation begins with data preprocessing, where input variables such as material usage, transportation distances, energy consumption, and demolition waste are normalized to ensure consistency, as shown in Figure 7. Unlike RTrees, which rely on decision trees, ANFIS employs a fuzzy inference system (FIS) to model nonlinear relationships within the dataset. During the model development phase, triangular membership functions are used to define fuzzy rules, allowing the system to interpret input variables more effectively. The training employs a hybrid optimization technique, combining the gradient descent method with the least squares estimator to adjust membership function parameters iteratively. This adaptive

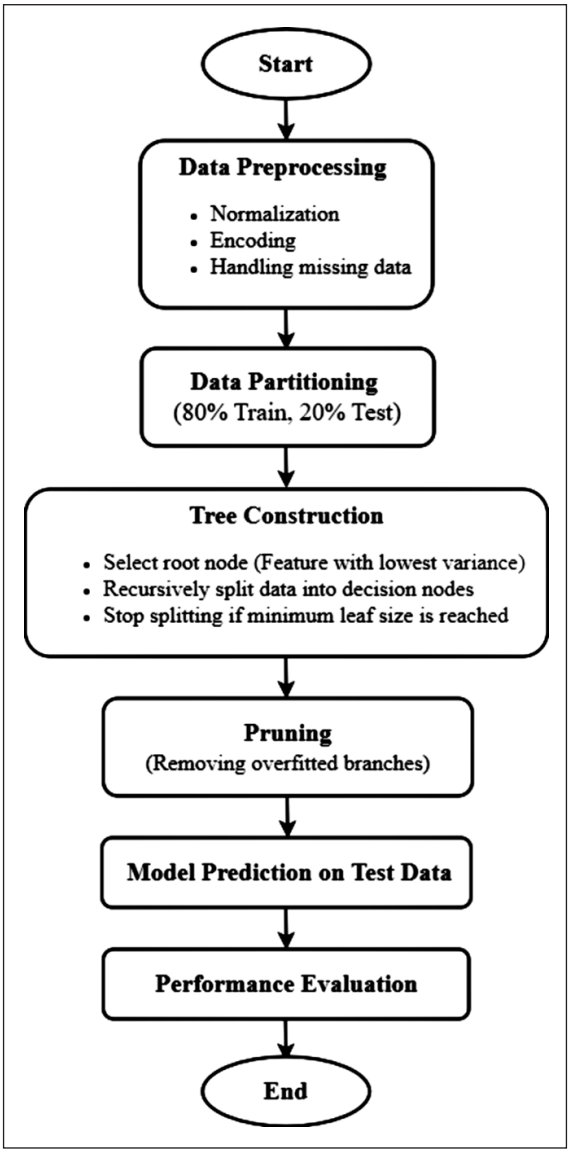

Figure 6. Regression trees implementation

learning process refines the model's generalization ability across different construction scenarios. After training, the ANFIS model is tested on the reserved dataset, and its predictive accuracy is assessed using RMSE, MSE, and MAPE. The ability of ANFIS to capture complex patterns in carbon emissions makes it particularly useful for analyzing environmental impacts at various construction stages. By leveraging the strengths of fuzzy logic and neural networks, the model provides a robust framework for estimating carbon footprints with high precision.

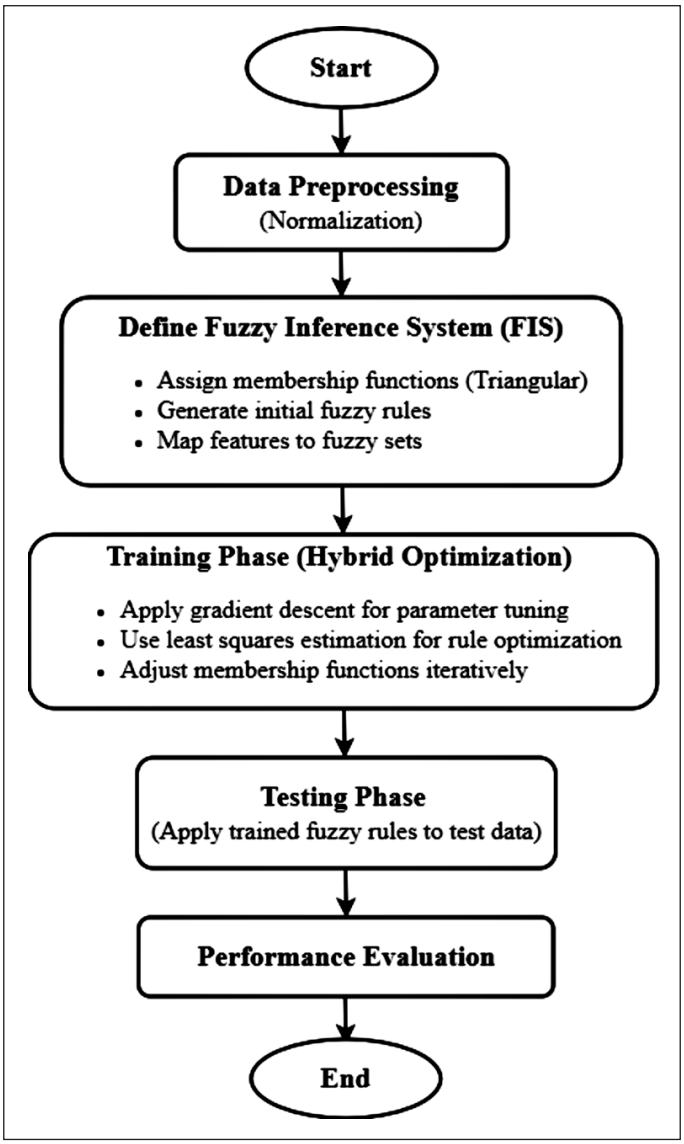

Figure 7. Adaptive neuro-fuzzy inference system implementation

Regression Trees

The divergence between statistical modeling and machine learning lies in their methodologies and objectives. The statistical models employ explicit mathematical equations to represent relationships between variables, estimating population parameters from sample data (Selvan & Balasundaram, 2021). In contrast, the machine learning autonomously extracts predictive patterns from data, bypassing the need for predefined rules or assumptions (Ramon et al., 2024). Both frameworks utilize training and testing

datasets, but machine learning incorporates hyperparameter tuning via validation datasets, enhancing its capacity to analyze both small and large datasets with superior predictive accuracy. Its ability to learn directly from historical data makes it a powerful tool for data-driven predictions. Regression trees, among the diverse machine learning methodologies, especially the classification and regression trees (CART) technique, are recognized for their transparency, minimal preprocessing requirements, and resilience to outliers and incomplete data (Mienye & Jere, 2024). Unlike traditional approaches, CART models can analyze relationships without data normalization, making them particularly suitable for complex, multifaceted datasets.

This study leverages the regression tree analysis to estimate carbon emissions within LCA boundaries, focusing on parameters such as construction material usage and transportation distances. The model was implemented in MATLAB using the fine tree algorithm, which systematically partitions the data based on key lifecycle features of construction projects. Figure 4 visualizes the structure and decision-making process of the regression tree. To optimize the model's performance, hyperparameter tuning was conducted, with particular attention in refining the minimum leaf size for terminal nodes, thereby enhancing the model's predictive capabilities.

The regression trees provide a robust alternative to linear methods, excelling in modeling non-linear and intricate relationships by leveraging decision trees to predict continuous response variables. The methodology partitions data recursively into smaller, homogeneous regions, assigning each region a constant value equal to the average response. This recursive partitioning, performed in a top-down greedy manner, optimizes splits to minimize the sum of squares error, as formalized in Equation 1:

$$minimize\left\{SSE = \sum_{i \in R_1}\left(x_i - \hat{y}_{R_1}\right)^2 + \sum_{i \in R_2}\left(x_i - \hat{y}_{R_2}\right)^2 + \right\} \quad [1]$$

In this context, x_i represents the actual carbon emissions, and $\hat{y}_{R_1}$ and $\hat{y}_{R_2}$ signify the predicted emissions for regions 1 and 2, respectively. The regression trees are particularly useful for exploratory data analysis due to their simplicity and interpretability. However, they are prone to overfitting, which can limit their generalization capabilities and predictive accuracy when compared to more advanced machine learning techniques.

Adaptive Neuro-Fuzzy Inference Systems

The adaptive neuro-fuzzy inference system is a cutting-edge neuro-fuzzy architecture that models complex and nonlinear systems (Chopra et al., 2021). The ANFIS uniquely integrates the adaptive learning capabilities of neural networks with the interpretability

of fuzzy logic, leveraging Sugeno's first-order adaptive fuzzy inference model (Mamat, Kasa, & Razali, 2019). Its hybrid optimization methodology, combining gradient descent and least-squares algorithms, enables precise parameter adjustment, making it a powerful tool for capturing and modeling sophisticated system behaviors (Karaboga & Kaya, 2019).

This study implemented the ANFIS model using MATLAB to address the complexities and uncertainties associated with carbon footprint data. By integrating the strengths of fuzzy logic and neural networks, ANFIS is particularly effective for modeling nonlinear and uncertain systems such as carbon footprint prediction. The model was meticulously fine-tuned by adjusting the membership functions, which are crucial for defining the degree of membership of data points within specific fuzzy sets.

A triangular membership function was selected due to its simplicity and computational efficiency, which are especially advantageous when working with large datasets or real-time applications. Unlike more complex functions, such as Gaussian or bell-shaped, triangular membership functions require fewer parameters, thereby reducing computational overhead and preserving flexibility for modeling uncertainties. This simplicity also enhances the interpretability of fuzzy rules, a key factor in ensuring the model's practicality in the construction industry. To improve predictive accuracy, the ANFIS model employed an iterative learning process to optimize the parameters of the triangular membership functions. The model refined these functions through repeated training cycles to better capture the complex patterns in carbon footprint data, leading to more reliable and accurate predictions. As shown in Figure 5, the ANFIS architecture comprises five distinct layers. The following equations determine the outputs of the first layer:

$$L1_i = \mu_{Ai}(x), \qquad i = 1,2 \tag{2}$$

$$L1_i = \mu_{Bi}(y), \qquad i = 3,4 \tag{3}$$

where, x is the input to node i, and A_i represents the linguistic function label. The terms $\mu_{Ai}(x)$ and $\mu_{Bi}(y)$ are Gaussian membership functions defined as:

$$\mu_{Ai}(x) = \exp\left[-\left(\frac{x - c_i}{a_i}\right)^2\right] \tag{4}$$

where, a_i and c_i are the deviation and centre parameters of the membership function, respectively. The outputs of the second layer are computed as:

$$L2_i = w_i = \mu_{Ai}(x)\mu_{Bi}(y), \qquad i = 1,2 \tag{5}$$

where w_i represents the strength of the rules. The third layer outputs are given by:

$$L3_i = \overline{w_i} = \frac{w_i}{w_1 + w_2}, \qquad i = 1,2 \qquad [6]$$

where, $\overline{w_i}$ are the normalized weights. In the fourth layer, the outputs are calculated as:

$$L4_i = \overline{w_i}(p_i x + q_i y + r_i), \qquad i = 1,2 \qquad [7]$$

where, p_i, q_i and r_i are known as consequent parameters. Finally, the output of the fifth layer, which represents the model's final output, is computed by summing the inputs as:

$$L5_i = \sum_{i=1}^{2} \overline{w_i}(p_i x + q_i y + r_i), \qquad i = 1,2 \qquad [8]$$

The ANFIS structure thus involves two types of parameters: premise parameters $\{a_i, c_i\}$ and consequent parameters $\{p_i, q_i, r_i\}$. These parameters are jointly optimized. ANFIS employs a hybrid algorithm for parameter optimization: the least-squares method is used to optimize the consequent parameters while keeping the premise parameters fixed, and the gradient descent method then tunes the premise parameters using the previously optimized consequent parameters.

Model Parameters and Hyperparameter Settings

To ensure reproducibility and enhance the interpretability of the models used in this study, Table 2 presents the key parameters and hyperparameter settings applied in the RTrees and ANFIS models. These parameters were selected based on an extensive hyperparameter tuning process to optimize prediction accuracy while maintaining computational efficiency. For the RTrees model, main parameters such as minimum leaf size, maximum tree depth, and pruning strategy were adjusted to minimize overfitting and enhance generalization. In contrast, the ANFIS model was fine-tuned by selecting appropriate membership functions, optimization algorithms, and epoch iterations to achieve the best trade-off between accuracy and computational efficiency.

These parameters were determined through experimental tuning to achieve optimal performance across all construction lifecycle stages. The results indicate that while RTrees excel in computational efficiency, ANFIS provides superior accuracy due to its adaptive learning process. The selected configurations allow for a balanced evaluation of both

Table 2
Model parameters and hyperparameter settings

Parameter	RTrees value	ANFIS value
Minimum leaf size	5	Not applicable
Maximum tree depth	15	Not applicable
Pruning method	Cost complexity	Not applicable
Membership function	Not applicable	Triangular
Optimization algorithm	Not applicable	Gradient descent and least squares
Number of epochs	Not applicable	100
Learning rate	Not applicable	0.01

Note. RTrees = Regression trees; ANFIS = Adaptive Neuro-Fuzzy Inference Systems

models, ensuring that the findings contribute valuable insights into machine learning applications for carbon footprint prediction in construction.

Model Evaluation Metrics

To evaluate the predictive accuracy of the machine learning models, this study utilized four widely recognized evaluation metrics: RMSE, MSE, MAPE, and mean squared logarithmic error (MSLE), as defined in Equations 9–12. These metrics are well-documented in the literature, and their detailed formulations and interpretations can be found in the corresponding references (Liu et al., 2022; Mamat, Kasa, Razali, et al., 2019). The evaluation metrics are defined as follows:

$$RMSE = \sqrt{\frac{\sum_{i=1}^{N}(y_i - x_i)^2}{N}} \quad [9]$$

$$MSE = \frac{1}{N}\sum_{i=1}^{N}(x_i - y_i)^2 \quad [10]$$

$$MAPE = \frac{1}{N}\sum_{i=1}^{N}\left|\frac{x_i - y_i}{y_i}\right| \times 100\% \quad [11]$$

$$MSLE = \frac{1}{N}\sum_{i=1}^{N}(\log(y_i + 1) - \log(x_i + 1))^2 \quad [12]$$

where, x_i are the simulated carbon emission values, y_i are the predicted carbon emission values, and N is the number of simulations.

RESULTS AND DISCUSSION

This study sought to evaluate and compare the performance of the RTrees and ANFIS in predicting carbon footprints across various stages of residential construction. Given the construction sector's significant contribution to global greenhouse gas emissions, developing precise and efficient carbon footprint estimation tools is imperative for advancing sustainability initiatives. This analysis provides a comprehensive assessment of each model's accuracy and robustness, highlighting their potential for enhancing predictive capabilities in the construction industry.

Performance of the RTrees in the Carbon Footprint Estimation

This section evaluates the RTrees model's performance across different LCA stages in residential construction. The primary focus is on the model's ability to predict carbon footprints with particular attention to the RMSE and MSE metrics across production, transportation, operation, and demolition stages (Table 3). During the production stage, the RTrees showed a training RMSE of 0.53174 and MSE of 0.51424, but test errors were significantly higher (RMSE = 4.57221, MSE = 4.44606), indicating possible overfitting issues during model training. This tendency for overfitting was observed in complex datasets, particularly where training data diversity is lacking (Heydari & Stillwell, 2024; Mamat et al., 2021). The notable discrepancy in test errors highlights difficulties in accurately predicting carbon emissions, suggesting the necessity for refining training methodologies to improve reliability across all stages.

In contrast, the transportation stage exhibited a more consistent generalization with lower discrepancies between the training and testing errors (training RMSE = 0.49223, test RMSE = 3.65314). Operational and demolition stages, however, reflected the model's limitations in capturing variable emissions effectively, with the operational stage showing a rise in test RMSE to 2.10647 despite a low training RMSE of 0.13865. The demolition

Table 3
The statistical error metric for the RTrees model

LCA stages	Cross validation fold	Leaf size	Training		Test	
			RMSE	MSE	RMSE	MSE
Production	50	2	0.53174	0.51424	4.57221	4.44606
Transportation	30	4	0.49223	0.44707	3.65314	3.30173
Operational	15	4	0.13865	0.11793	2.10647	3.90404
Demolition	10	8	0.06312	0.06104	3.00541	4.05205
Total carbon emission	50	4	0.17177	0.16086	3.13147	4.12267

Note. RTrees = Regression trees; LCA = Life cycle assessment; RMSE = Root Mean Square Error; MSE = Mean Squared Error

stage presented a similar pattern with a low training RMSE of 0.06312 but a higher test RMSE (3.00541), underscoring challenges in predicting variability inherent in demolition processes. These findings highlight the RTrees' tendency to overfit training data, especially in the LCA stages characterized by high variability. Future enhancements could include integrating ensemble methods or hybrid models to address these limitations and boost predictive accuracy (Seghetta & Goglio, 2020; Yıldız & Beyhan, 2025).

ANFIS Model Performance in the Carbon Footprint Estimation

This section examines the performance of the ANFIS across various LCA stages in residential construction. Performance metrics, including the RMSE and MSE, were utilized for both training and testing phases, as detailed in Table 4. The ANFIS demonstrated high accuracy during training, particularly in the production and operational stages (RMSE = 0.08346 and 0.08265, respectively). However, it exhibited significant increases in test errors across all stages, with the operational stage test RMSE escalating to 5.55423. This pronounced discrepancy between the training and testing performance suggests potential overfitting, which is a common issue with models trained on highly variable data sets (Srivastava et al., 2023; Yelghi, 2024).

Table 4
The error statistic for ANFIS using triangular membership functions

LCA stages	Training		Test	
	RMSE	MSE	RMSE	MSE
Production	0.08346	0.03974	3.90782	4.33421
Transportation	0.03172	0.03557	4.74549	5.04436
Operational	0.08265	0.00644	5.55423	1.39193
Demolition	0.02485	0.03573	4.14777	3.50365
Total of carbon emission	0.05213	0.02618	4.32182	3.80569

Note. ANFIS = Adaptive Neuro-Fuzzy Inference Systems; LCA = Life cycle assessment; RMSE = Root Mean Square Error; MSE = Mean Squared Error

The model's limited ability to generalize beyond the training data highlights the need for refining the ANFIS framework to improve its robustness. Proposed methods include incorporating regularization techniques and expanding the training dataset to enhance the model's exposure to diverse construction scenarios, thereby improving its predictive accuracy for carbon emissions (Dosdoğru, 2019). Moreover, the consistent overperformance of ANFIS in training relative to testing across stages indicates the model's sensitivity to the specific characteristics of the training data. This necessitates further investigation into the model's parameter tuning and the adoption of ensemble techniques, which could mitigate the observed overfitting and support more reliable carbon footprint predictions.

Comparative Performance of the RTrees and ANFIS in the Carbon Footprint Prediction

This section presents a comparative analysis of the RTrees and ANFIS models in estimating the carbon emissions during various stages of the residential construction life cycle. The comparison utilizes the RMSE and MAPE values, detailed in Figures 9 and 10, to assess the models' relative strengths and weaknesses. ANFIS consistently outperforms RTrees in percentage-based accuracy (MAPE), especially notable in the production and transportation stages. As illustrated in Figure 8, this superior performance in the production stage is clearly visible, with ANFIS showing a consistently lower MAPE than RTrees. This superior performance is attributed to ANFIS's ability to handle complex nonlinear relationships within the dataset, providing a more accurate prediction of carbon emissions (Rajab, 2019). Conversely, RTrees demonstrate better adaptability in managing logarithmic errors (MSLE) in larger datasets, suggesting a potential advantage in scenarios where precise handling of small logarithmic discrepancies is crucial (Gu et al., 2016).

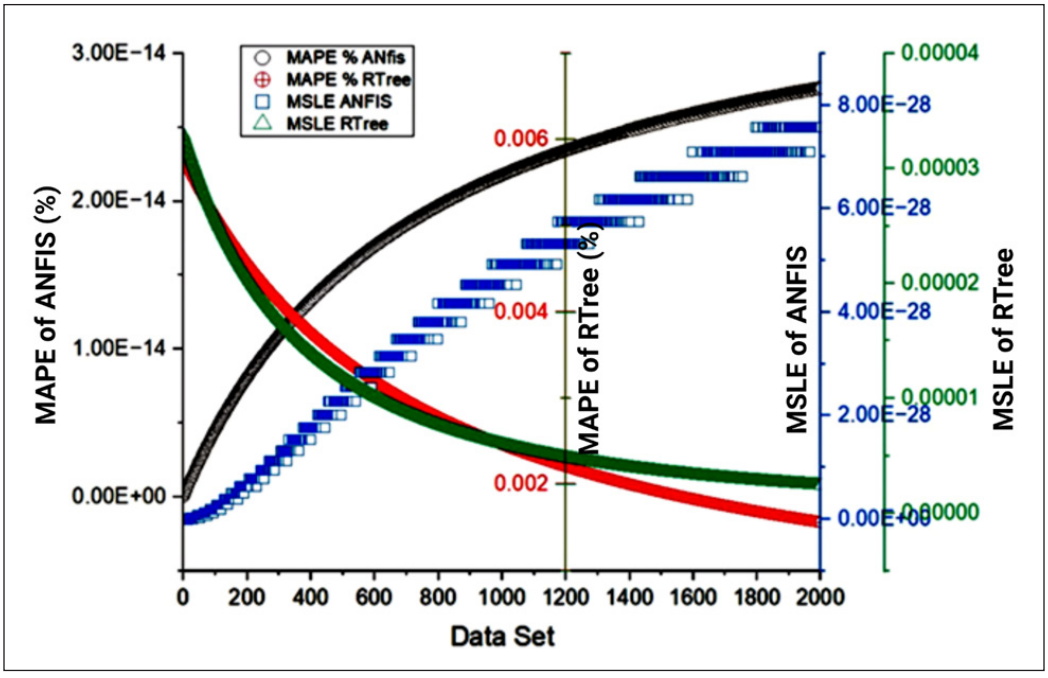

Figure 8. Performance of ANFIS and RTrees in production stage
Note. ANFIS = Adaptive Neuro-Fuzzy Inference Systems; RTree = Regression tree; MAPE = Mean Absolute Percentage Error; MSLE = Mean Squared Logarithmic Error

During the transportation stage, ANFIS showed a significant decline in MAPE, stabilizing at a lower value compared to RTrees, which gradually improved but stabilized

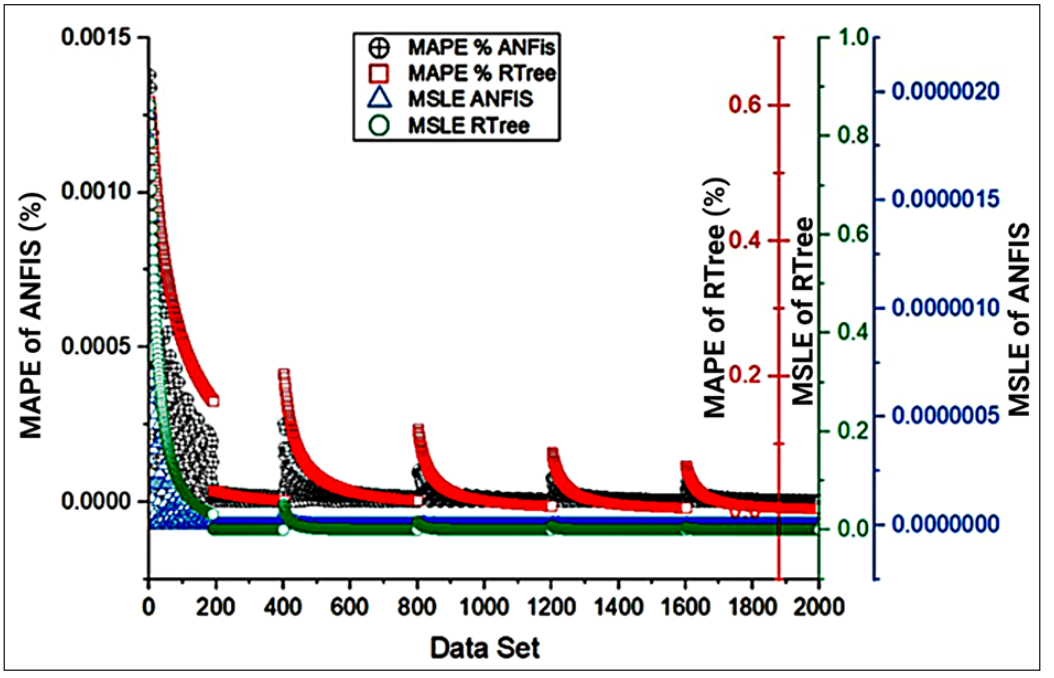

Figure 9. Comparative analysis of ANFIS and RTree in the transportation stage
Note. ANFIS = Adaptive Neuro-Fuzzy Inference Systems; RTree = Regression tree; MAPE = Mean Absolute Percentage Error; MSLE = Mean Squared Logarithmic Error

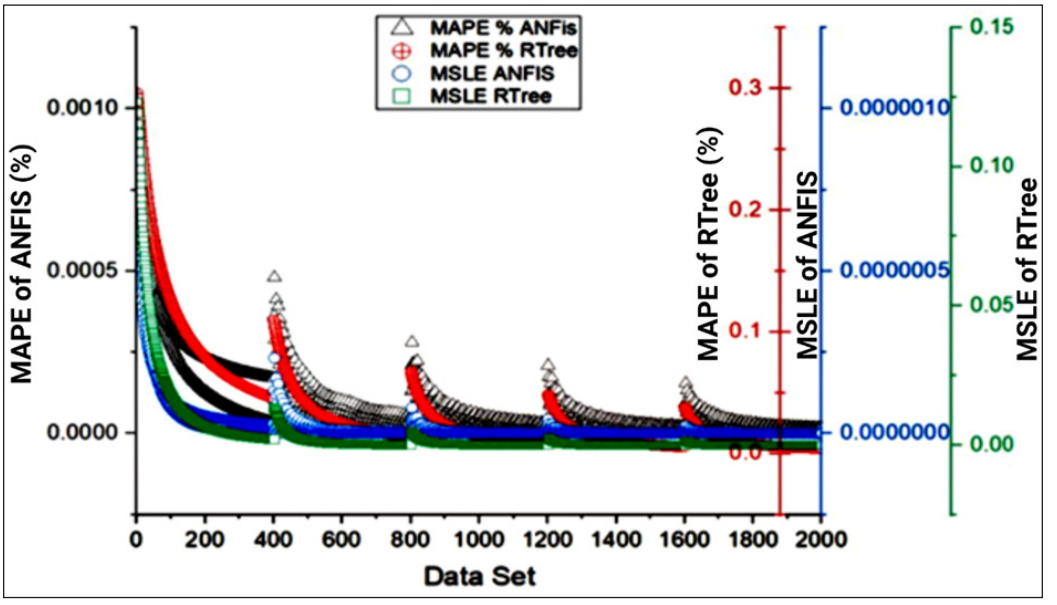

Figure 10. Operational stage performance of ANFIS and RTree
Note. ANFIS = Adaptive Neuro-Fuzzy Inference Systems; RTree = Regression tree; MAPE = Mean Absolute Percentage Error; MSLE = Mean Squared Logarithmic Error

at a higher MAPE (Figure 9). This trend underscores ANFIS's enhanced ability to minimize percentage-based prediction errors as the dataset size increases. Both models exhibited relatively low and comparable MSLE, indicating their effectiveness in managing small logarithmic errors in carbon emissions related to transportation. In the operational stage, while both models' MAPE values converged as dataset size increased, indicating an overall improvement in predictive accuracy with larger training datasets, RTrees marginally outperformed ANFIS, suggesting a slightly better capability in minimizing percentage-based errors in this specific phase (Figure 10).

Given these observations, the choice between the RTrees and ANFIS should be guided by the specific requirements of the project. The ANFIS is recommended for scenarios requiring high accuracy in percentage error minimization, whereas the RTrees may be preferred for its simplicity and effectiveness in managing logarithmic errors, particularly in large-scale applications where computational efficiency and interpretability are prioritized.

Impact of Dataset Size on Model Accuracy

This section investigates how the size of the dataset influences the accuracy of the RTrees and ANFIS models in estimating the carbon emissions, as depicted in Figures 11 and 12. Figure 12 provides a granular view of this trend, showing how both the MAPE and the MSLE for the ANFIS and RTrees stabilize as the dataset size increases, confirming that larger datasets contribute to more consistent model performance. Both models demonstrate improved accuracy with the expansion of the dataset, though they exhibit distinct performance trends. RTrees showed a rapid improvement in the MAPE as dataset size increased, indicating enhanced performance with larger data volumes (Figure 11). This trend suggests that the RTrees are particularly effective when processing extensive datasets, making them suitable for large-scale carbon emission estimation projects where data abundance can significantly influence predictive accuracy.

Conversely, while the ANFIS excels with smaller datasets, its generalization does not significantly improve as data volume increases. This finding is particularly relevant for scenarios demanding fine-grained accuracy in small-scale environments, where its hybrid neuro-fuzzy architecture effectively captures subtle nonlinear patterns in the carbon emission dynamics (Dzakiyullah et al., 2018). However, this strength also highlights a potential limitation in scaling to larger datasets without compromising predictive accuracy, a crucial factor for applications involving diverse and extensive inputs. Interestingly, both models maintained relatively low and stable MSLE values regardless of dataset size, suggesting their robust ability to manage small logarithmic errors effectively. This consistency is crucial for applications that require precise logarithmic error handling, such as detailed environmental impact assessments, where even minor inaccuracies can lead to significant deviations in policy planning and environmental compliance.

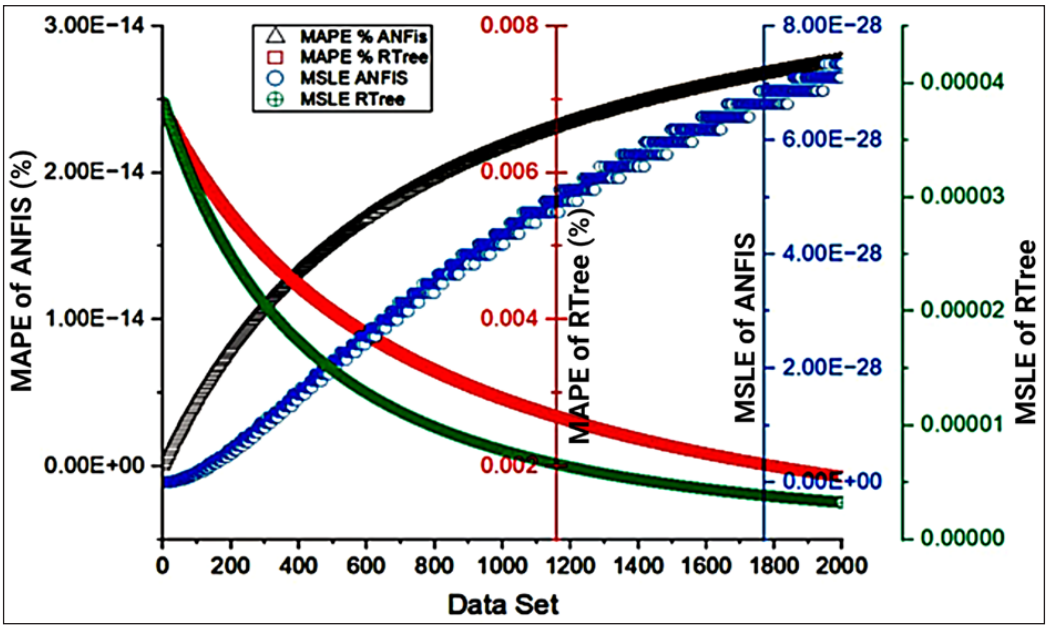

Figure 11. Performance of ANFIS and RTree in demolition stage
Note. ANFIS = Adaptive Neuro-Fuzzy Inference Systems; RTree = Regression tree; MAPE = Mean Absolute Percentage Error; MSLE = Mean Squared Logarithmic Error

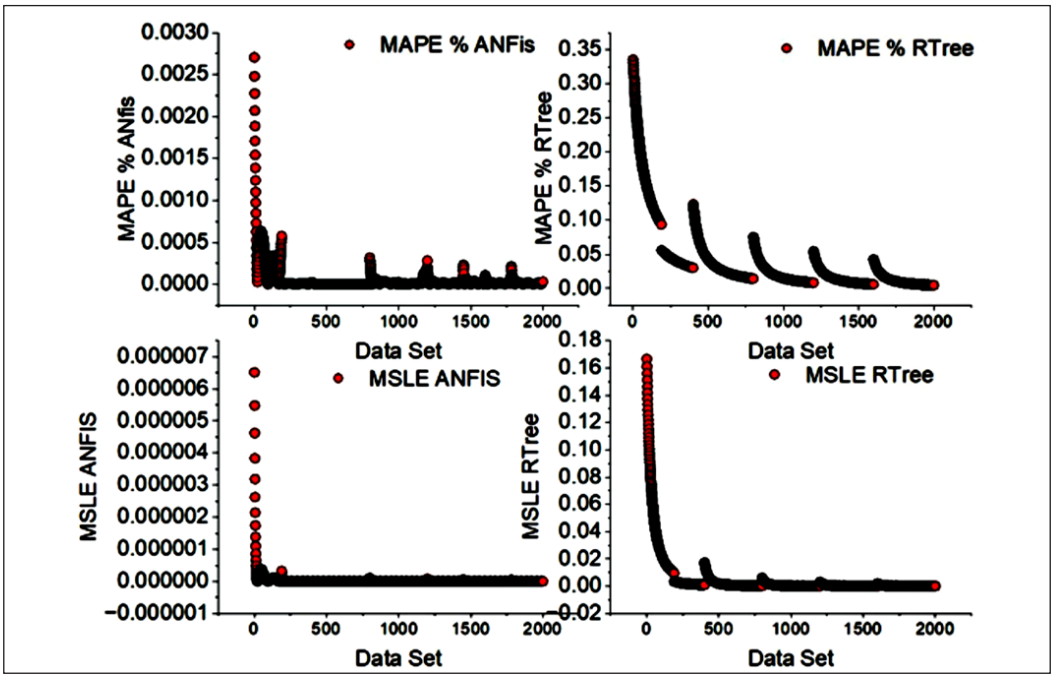

Figure 12. Overall carbon emission prediction accuracy of models
Note. ANFIS = Adaptive Neuro-Fuzzy Inference Systems; RTree = Regression tree; MAPE = Mean Absolute Percentage Error; MSLE = Mean Squared Logarithmic Error

The findings from this analysis emphasize the importance of selecting a machine learning model that aligns with specific data characteristics and project requirements. While the ANFIS may be preferred for smaller, more detailed datasets where high precision is necessary, the RTrees offers a robust option for broader applications where data volume and complexity are higher. These insights should guide the strategic selection of predictive models in construction projects to optimize carbon footprint assessments across various life cycle stages.

Computational Time Analysis

This section evaluates the computational efficiency of the RTrees and ANFIS models by measuring the time required for training and testing across various construction lifecycle stages, as detailed in Table 5. This analysis is crucial for assessing the practicality of deploying these models in real-world applications. The RTrees demonstrated a significantly lower training time than the ANFIS, indicating its computational efficiency and suitability for scenarios where quick model deployment is essential. However, despite the ANFIS's higher training times, which are attributable to its complex iterative optimization process, it consistently provided more accurate predictions, as shown in the enhanced carbon footprint estimation accuracy.

Table 5
Computational time for model training and testing

Model	Training time (s)	Testing time (s)
RTrees	12.4	1.8
ANFIS	76.2	2.5

Note. RTrees = Regression trees; ANFIS = Adaptive Neuro-Fuzzy Inference Systems

The testing times for both models were also analyzed, with the ANFIS showing greater stability across different datasets. This suggests that while the ANFIS requires more time to train, its predictions are reliable and consistent, making it suitable for applications where prediction accuracy is prioritized over computational speed. These results highlight a fundamental trade-off between the computational efficiency and predictive accuracy. The RTrees, with its quicker training times, offers an advantageous solution for applications needing rapid updates with less computational resource usage. Conversely, the higher accuracy of the ANFIS justifies its longer computational times, particularly in complex predictive tasks where precision is crucial.

Comprehensive Performance Evaluation

This section delivers a thorough evaluation of the RTrees and ANFIS models using multiple performance metrics: the RMSE, MSE, MAPE, and MSLE, which provide a comprehensive view of prediction accuracy, error distribution, and their capabilities in the carbon footprint estimation across various construction lifecycle stages (Table 6). The analysis demonstrated that the ANFIS consistently outperforms the RTrees in all error measures, achieving lower

Table 6
Performance metrics of RTrees and ANFIS models

Model	RMSE	MSE	MAPE (%)	MSLE
RTrees	0.5317	0.5142	8.23	0.0451
ANFIS	0.0834	0.0826	2.17	0.0598

Note. RTrees = Regression trees; ANFIS = Adaptive Neuro-Fuzzy Inference Systems; RMSE = Root Mean Square Error; MSE = Mean Squared Error; MAPE = Mean Absolute Percentage Error; MSLE = Mean Squared Logarithmic Error

RMSE, MSE, and MAPE values, which are particularly notable in the production and operational stages. This superior accuracy of the ANFIS underscores its effectiveness in precise carbon footprint predictions, where handling complex nonlinear relationships is essential for achieving high precision in sustainable construction practices.

Despite its lower performance in certain error metrics, the RTrees showed relatively better management of small logarithmic errors (MSLE), indicating its potential advantage in applications where handling of logarithmic discrepancies is critical. This makes the RTrees a viable alternative, offering computational efficiency with stable logarithmic error management, which is beneficial for large-scale applications or scenarios where rapid predictions are essential.

Comparison with Existing Studies

To assess the effectiveness of the proposed machine learning models, this study compares its results with previous research on carbon footprint estimation in construction. Several studies have investigated machine learning-based approaches for predicting the carbon emissions, yet direct comparisons between the RTrees and ANFIS models remain limited. For instance, Mamat et al. (2025) applied the Gaussian process regression (GPR), achieving an RMSE of 0.211 and a MAPE of 3.01%, which is significantly higher than the ANFIS model in this study (RMSE = 0.0834, MAPE = 2.17%). This demonstrates the superior accuracy of the ANFIS model in handling nonlinear relationships in carbon footprint estimation. Similarly, Kwon and Kim (2023) employed the deep neural networks (DNNs), obtaining an RMSE of 0.195 with relatively lower computational costs (16.5 sec training time), indicating that deep learning models can also achieve competitive performance in this domain.

However, when considering computational efficiency, the RTrees model in this study offers a significant advantage. With a training time of only 12.4 s, the RTrees outperform the ANFIS (76.2 s) and other deep learning models, such as the LSTMs (145 s) (Shao & Ning, 2023), in terms of speed, making them suitable for applications where rapid predictions are required. Nevertheless, this efficiency comes at the cost of higher error rates (RMSE

= 0.5317, MAPE = 8.23%), suggesting that while the RTrees provide a fast alternative, they may not be the best choice for high-accuracy applications.

Table 7 presents a comparative summary of various models used in previous studies alongside the results obtained in this research. These comparisons highlight that while the ANFIS achieves superior accuracy, it requires longer training time compared to the RTrees and DNN-based approaches. Meanwhile, the RTrees exhibit faster training and prediction times but with slightly higher errors compared to deep learning-based methods. Overall, this study contributes to the literature by demonstrating that the ANFIS offers a highly accurate solution for the carbon footprint estimation, particularly for complex, nonlinear datasets. However, the RTrees remain a viable alternative for applications requiring faster computation with reasonable accuracy. Future work should explore hybrid models that integrate the strengths of both the ANFIS and RTrees to achieve both efficiency and accuracy.

Table 7
Comparison of model performance with existing studies

Study	Model used	RMSE	MAPE (%)	Computational time (sec)
This study	ANFIS	0.0834	2.17	76.2 (train)
This study	RTrees	0.5317	8.23	12.4 (train)
Mamat et al. (2025)	GPR	0.211	3.01	110 (train)
Kwon and Kim (2023)	DNN	0.195	3.77	16.5 (train)
Shao and Ning (2023)	LSTM	4.984	0.024	145 (train)

Note. ANFIS = Adaptive Neuro-Fuzzy Inference Systems; RTrees = Regression trees; GPR = Gaussian Process Regression; DNN = Deep neural networks; LSTM = Long Short-Term Memory; RMSE = Root Mean Square Error; MAPE = Mean Absolute Percentage Error

Limitations and Future Considerations

While this study demonstrates the effectiveness of the RTrees and ANFIS in predicting the carbon footprint of residential construction, several limitations exist. The dataset, though comprehensive, is limited to a specific region, potentially affecting generalizability. Additionally, the ANFIS requires high computational power, making real-time applications challenging. The RTrees, though computationally efficient, exhibit lower predictive accuracy in complex scenarios. Another limitation is the lack of interpretability in the ANFIS, which may hinder industry adoption. Moreover, policy and environmental factors are not explicitly integrated into the models, limiting their adaptability to evolving sustainability regulations. Future research should focus on expanding datasets, optimizing computational efficiency, incorporating explainable AI techniques, and integrating policy-based factors to enhance model reliability. Additionally, real-time data from smart construction monitoring systems

could further refine predictions. Addressing these challenges will improve machine learning applications for sustainable construction.

CONCLUSION

This study critically evaluated the predictive performance of the RTrees and ANFIS in estimating the carbon emissions across the life cycle stages of residential construction. The results demonstrate that the ANFIS consistently delivers higher predictive accuracy compared to the RTrees, with RMSE improvements exceeding 80% in key life cycle stages such as the production and operation. This superior performance makes the ANFIS an effective tool for precise carbon footprint estimation, aiding decision-makers in developing sustainable mitigation strategies. However, the higher computational demands of the ANFIS highlight the importance of balancing accuracy and processing efficiency in real-world applications. The findings emphasize the need for hybrid modeling approaches that combine the strengths of the RTrees and ANFIS to achieve both accuracy and efficiency. Future research should explore ensemble learning techniques, cloud-based deployment strategies, and real-time carbon footprint monitoring to enhance model applicability in the construction sector. These improvements align with evolving sustainability goals, paving the way for more data-driven decision-making in reducing environmental impacts.

ACKNOWLEDGEMENTS

The project has been financially supported by the TVET Applied Research Grant Scheme (Grant No. T-ARGS/2024/BK01/00076) from the Department of Polytechnic and Community College Education, Malaysian Ministry of Higher Education.

REFERENCES

Chen, L., Zhao, Y., Xie, R., Su, B., Liu, Y., & Renfei, X. (2023). Embodied energy intensity of global high energy consumption industries: A case study of the construction industry. *Energy*, *277*, 127628. https://doi.org/10.1016/j.energy.2023.127628

Chopra, S., Dhiman, G., Sharma, A., Shabaz, M., Shukla, P., & Arora, M. (2021). Taxonomy of Adaptive Neuro-Fuzzy Inference System in modern engineering sciences. *Computational Intelligence and Neuroscience*, *2021*(1), 6455592. https://doi.org/10.1155/2021/6455592

Dosdoğru, A. T. (2019). Improving weather forecasting using de-noising with maximal overlap discrete wavelet transform and GA based neuro-fuzzy controller. *International Journal on Artificial Intelligence Tools*, *28*(3), 1950012. https://doi.org/10.1142/S021821301950012X

Dzakiyullah, N. R., Saleh, C., Rina, F., & Fitra, A. R. (2018). Estimation of carbon dioxide emission using Adaptive Neuro-Fuzzy Inference System. *Journal of Engineering and Applied Sciences*, *13*(6), 5196 - 5202.

Farghaly, H. M., Ali, A. A., & Abd El-Hafeez, T. (2020). Building an effective and accurate associative classifier based on support vector machine. *Sylwan*, *164*(3), 39-56.

Gong, Y., Liu, G., Xue, Y., Li, R., & Meng, L. (2023). A survey on dataset quality in machine learning. *Information and Software Technology*, *162*, 107268. https://doi.org/10.1016/j.infsof.2023.107268

Gu, Y., Wylie, B. K., Boyte, S. P., Picotte, J., Howard, D. M., Smith, K., & Nelson, K. J. (2016). An optimal sample data usage strategy to minimize overfitting and underfitting effects in regression tree models based on remotely-sensed data. *Remote Sensing*, *8*(11), 943. https://doi.org/10.3390/rs8110943

Hasan, M. S., Tarequzzaman, M., Moznuzzaman, M., & Juel, M. A. A. (2025). Prediction of energy consumption in four sectors using support vector regression optimized with genetic algorithm. *Heliyon*, *11*(2), e41765. https://doi.org/10.1016/j.heliyon.2025.e41765

Heydari, Z., & Stillwell, A. S. (2024). Comparative analysis of supervised classification algorithms for residential water end uses. *Water Resources Research*, *60*(6), e2023WR036690. https://doi.org/10.1029/2023WR036690

Jia, W., Lu, M., Shen, Q., Tian, C., & Zheng, X. (2024). Dual generative adversarial networks based on regression and neighbor characteristics. *PLOS One*, *19*(1), e0291656. https://doi.org/10.1371/journal.pone.0291656

Karaboga, D., & Kaya, E. (2019). Adaptive network based fuzzy inference system (ANFIS) training approaches: A comprehensive survey. *Artificial Intelligence Review*, *52*, 2263-2293. https://doi.org/10.1007/s10462-017-9610-2

Kim, E.-S. (2024). Can data science achieve the ideal of evidence-based decision-making in environmental regulation? *Technology in Society*, *78*, 102615. https://doi.org/10.1016/j.techsoc.2024.102615

Kwon, O. I., & Kim, Y. I. (2023). Review of machine learning for building energy prediction. *Journal of the Architectural Institute of Korea*, *39*(5), 133-140. https://doi.org/10.5659/JAIK.2023.39.5.133

Liu, Y., Zhang, W., Yan, Y., Li, Z., Xia, Y., & Song, S. (2022). An effective rainfall–ponding multi-step prediction model based on LSTM for urban waterlogging points. *Applied Sciences*, *12*(23), 12334. https://doi.org/10.3390/app122312334

Mahapatra, S. K., Schoenherr, T., & Jayaram, J. (2021). An assessment of factors contributing to firms' carbon footprint reduction efforts. *International Journal of Production Economics*, *235*, 108073. https://doi.org/10.1016/j.ijpe.2021.108073

Mamat, R. C., Kasa, A., & Razali, S. F. M. (2019). The applications and future perspectives of adaptive neuro-fuzzy inference system in road embankment stability. *Journal of Engineering Science and Technology Review*, *12*(5), 75-90.

Mamat, R. C., Kasa, A., Razali, S. F. M., Samad, A. M., Ramli, A., & Yazid, M. R. M. (2019). Application of artificial intelligence in predicting ground settlement on earth slope. In *AIP Conference Proceedings* (Vol. 2138, No. 1, p. 040015). AIP Publishing. https://doi.org/10.1063/1.5121094

Mamat, R. C., Ramli, A., & Bawamohiddin, A. B. (2025). A comparative analysis of gaussian process regression and support vector machines in predicting carbon emissions from building construction activities. *Journal of Advanced Research in Applied Mechanics*, *131*(1), 185 - 196. https://doi.org/10.37934/aram.131.1.185196

Mamat, R. C., Ramli, A., Samad, A. M., Kasa, A., Razali, S. F. M., & Omar, M. B. H. C. (2021). Artificial neural networks in slope of road embankment stability applications: A review and future perspectives. *International Journal of Advanced Technology and Engineering Exploration*, *8*(75), 304-319. https://doi.org/10.19101/IJATEE.2020.762127

Marsh, E., Allen, S., & Hattam, L. (2023). Tackling uncertainty in life cycle assessments for the built environment: A review. *Building and Environment*, *231*, 109941. https://doi.org/10.1016/j.buildenv.2022.109941

Mienye, I. D., & Jere, N. (2024). A survey of decision trees: Concepts, algorithms, and applications. In *IEEE Access* (Vol. 12, pp. 86716-86727). IEEE. https://doi.org/10.1109/ACCESS.2024.3416838

Pillai, R., Sharma, N., & Gupta, R. (2023). Fine-tuned EfficientNetB4 transfer learning model for weather classification. In *2023 3rd Asian Conference On Innovation In Technology* (pp. 1-6). IEEE. https://doi.org/10.1109/ASIANCON58793.2023.10270698

Rajab, S. (2019). Handling interpretability issues in ANFIS using rule base simplification and constrained learning. *Fuzzy Sets and Systems*, *368*, 36-58. https://doi.org/10.1016/j.fss.2018.11.010

Ramon, Y., Martens, D., Evgeniou, T., & Praet, S. (2024). Can metafeatures help improve explanations of prediction models when using behavioral and textual data? *Machine Learning*, *113*, 4245-4284. https://doi.org/10.1007/s10994-021-05981-0

Seghetta, M., & Goglio, P. (2020). Life cycle assessment of seaweed cultivation systems. In K. Spilling (Ed.), *Biofuels from algae: Methods and protocols* (Vol. 1980, pp. 103-119). Humana. https://doi.org/10.1007/7651_2018_203

Selvan, C., & Balasundaram, S. R. (2021). Data analysis in context-based statistical modeling in predictive analytics. In *Handbook of research on engineering, business, and healthcare applications of data science and analytics* (pp. 96-114). IGI Global. https://doi.org/10.4018/978-1-7998-3053-5.ch006

Sergeev, A., Buevich, A., Shichkin, A., Baglaeva, E., Subbotina, I., & Sergeeva, M. (2022). Comparing the types of artificial neural networks to predict the carbon dioxide concentration changes. In *AIP Conference Proceedings* (Vol. 2425, No. 1, p. 110007). AIP Publishing. https://doi.org/10.1063/5.0081641

Shao, C., & Ning, J. (2023). Construction and application of carbon emission prediction model for China's textile and garment industry based on improved WOA-LSTM. *Journal of Beijing Institute of Fashion Technology*, *43*(4), 73-81. https://doi.org/10.16454/j.cnki.issn.1001-0564.2023.04.010

Srivastava, A. K., Rathore, J. S., & Shrivastava, S. (2022). Efficacy of ANN and ANFIS as an AI technique for the prediction of COF at finger pad interface in manipulative tasks. In A. Kumar, M. Zunaid, K. A. Subramanian, & H. Lim (Eds.), *Recent Advances in Materials, Manufacturing and Thermal Engineering* (pp. 13-21). Springer. https://doi.org/10.1007/978-981-19-8517-1_2

Vinayak, N., & Ahmad, S. (2023). Sample size estimation for effective modelling of classification problems in machine learning. In I. Woungang, S. K. Dhurandher, K. K. Pattanaik, A. Verma, & P. Verma (Eds.), *Advanced Network Technologies and Intelligent Computing* (Vol. 1798, pp. 365-378). Springer. https://doi.org/10.1007/978-3-031-28183-9_26

Yao, X., Zhang, H., Wang, X., Jiang, Y., Zhang, Y., & Na, X. (2024). Which model is more efficient in carbon emission prediction research? A comparative study of deep learning models, machine learning models,

and econometric models. *Environmental Science and Pollution Research*, *31*, 19500-19515. https://doi.org/10.1007/s11356-024-32083-w

Yelghi, A. (2024). Estimation single output with a hybrid of ANFIS and MOPSO_HS. *Sakarya University Journal of Computer and Information Sciences*, *7*(1), 112-126. https://doi.org/10.35377/saucis...1414742

Yıldız, M. E., & Beyhan, F. (2025). Prediction of cooling load via machine learning on building envelope design parameters. *Journal of Building Engineering*, *100*, 111724. https://doi.org/10.1016/j.jobe.2024.111724

Yiming, L., Junhan, Y., Zhang, Z., Peiqi, X., & Nianxiong, L. (2024). A comparative study of machine learning algorithm models for predicting carbon emissions of residential buildings in cold zones. *Journal of Tsinghua University*, *64*(10), 1734-1745. https://doi.org/10.16511/j.cnki.qhdxxb.2024.22.031

Pertanika J. Sci. & Technol. 33 (5): 2125 - 2153 (2025)

PERTANIKA JOURNALS

SCIENCE & TECHNOLOGY

Journal homepage: http://www.pertanika.upm.edu.my/

Review Article

A Systematic Review of AI-Integrated Tools in ESL/EFL Education

Sadaf Manzoor[1,2]*, Hazri Jamil[3], Muhammad Nawaz[4], Muhammad Shahbaz[5] and Shahzad Ul Hassan Farooqi[6]

[1]*School of Educational Studies, Universiti Sains Malaysia, 11800 Penang, Malaysia*
[2]*Dow Institute of Health Professionals Education (General Education), Dow University of Health Sciences, 75280 Karachi, Pakistan*
[3]*School of Educational Studies, Universiti Sains Malaysia, 11800 Penang, Malaysia*
[4]*School of Languages, Literacies and Translation, Universiti Sains Malaysia, 11800 Penang, Malaysia*
[5]*Government College Women University Sialkot, Kutchehry Road, 51310 Sialkot, Pakistan*
[6]*Department of English, College of Education, Almajmaah University, 11952 AlZulfi, Saudi Arabia*

ABSTRACT

Artificial intelligence (AI) tools have demonstrated sophisticated capabilities, offering immediate support in various fields, including English as a Second Language/English as a Foreign Language (ESL/EFL) education. Delivering immediate support, the AI tools promptly answer queries and provide helpful explanations in various fields. EFL/ESL educators still have varied sentiments about the AI's noteworthy capacities and impressive skills in accomplishing different tasks in the second language teaching domain. The twofold purpose of this review is to identify recent publications pertinent to the AI integration in ESL education, with a focus on methodology, commonly used AI applications, pedagogical approaches, and sampling strategies. Secondly, it aims to understand the most frequently used keywords and countries with the highest number of publications. In conducting the exploration, guidelines based on Shaffril et al. (2021) were followed, including the seven steps: review protocol, formulation of research question, systematic searching strategies, quality appraisal, data extraction, data synthesis, and data demonstration. The review involved 921 articles from the Scopus, Web of Science (WoS), and ScienceDirect databases, from which 25 articles were selected for comprehensive analysis based on relevance, following systematic review protocols. The selection criteria included pertinent keywords, field of study, and an emphasis on the studies that focused on the AI-integration in the ESL/EFL education. Finally, the review synthesised the

ARTICLE INFO

Article history:
Received: 17 May 2024
Accepted: 17 April 2025
Published: 28 August 2025

DOI: https://doi.org/10.47836/pjst.33.5.05

E-mail addresses:
mesadafmanzoor@gmail.com (Sadaf Manzoor)
hazri@usm.my (Hazri Jamil)
memuhammadnawaz@gmail.com (Muhammad Nawaz)
m.shahbaz@gcwus.edu.pk (Muhammad Shahbaz)
s.farooqi@mu.edu.sa (Shahzad Ul Hassan Farooqi)
* Corresponding author

e-ISSN: 2231-8526

findings of 25 articles. The results revealed that the recent studies have integrated the AI-applications in the ESL/EFL contexts, which predominantly emphasised a varied range of AI-based applications. Particularly, ChatGPT and Wordtune are listed as the key sources for language augmentation. The research studies focused on the pedagogical implications for ESL students and teachers to enhance language teaching and learning practices. The AI tools enhance the ESL/EFL education by improving writing skills through real-time grammar feedback, personalised content suggestions, and automated assessments, fostering learner autonomy, and engagement. The results showed the most frequently used keywords and countries with more publications. Despite being confined to the most recent literature available, this review highlights gaps in the AI-driven ESL education, offering valuable insights for future research on the AI's pedagogical applications.

Keywords: AI integration, AI-tools, ESL/EFL, learning, systematic review, teaching

INTRODUCTION

AI encompasses the ability to perform tasks traditionally associated with human intellect (Britannica, 2025; Oxford University Press, n.d.). The AI is currently reshaping and leading institutions and workplaces towards transformation (Liang et al., 2021). This transformative process is also evident in ESL/EFL education. Barrot (2023) emphasises that language learners can improve their writing skills and text editing by integrating the AI-based tools. By using tools like ChatGPT, students can improve their grammar, sentence structures, and overall clarity in their writing (Zhang & Aslan, 2021). Learners can also review their work and decide to accept or reject the modifications made by ChatGPT. While the tool poses challenges to traditional writing, it concurrently fosters new possibilities and methods for teaching and learning writing skills. By recognising the constraints of the AI tools, educators can stimulate learners' creative thinking, guiding them to perceive writing as both an intellectual pursuit and a means of personal development. In addition to these tools, current research has focussed on the influence of the AI writing assistants, with a particular emphasis on teaching English as a foreign language (TEFL) domain, notably, studies including Kurniati and Fithriani (2022), Wang et al. (2022), and Zhao (2022), propose that the AI-integrated applications can play a crucial role in advancing students' writing abilities. Despite the constraints of the AI-driven tools, they allow learners to engage in creative thinking (Liu et al., 2022; Lund et al., 2023; Qadir, 2022). The prevailing literature narrowly encompasses the entire function of the AI tools in augmenting writing skills, including grammar and syntax. Thus, it becomes imperative to discover the classification of the AI applications and their specific approaches in addressing the AI applications in the EFL/ESL context.

Broadly, AI plays a significant role in enhancing learning contexts based on the individual needs of students (H. Gao, 2021). It helps the students engage in autonomous learning (Liang et al., 2021). It allows the learners to manage self-paced learning

conveniently, providing flexibility, instant feedback, and assistance with minimal teacher involvement (Keerthiwansha, 2018). The AI creates a relaxed learning atmosphere for the learners to engage in conversation with machines, providing opportunities for repetitive tasks and language drills. For instance, conversational Chatbots or virtual role-playing platforms offer the learners a relaxed environment to practice real-life interactions, thereby facilitating greater language fluency (N.-Y. Kim, 2019). Educators benefit from the AI-based tools and systems for the development of an intelligent and up-to-date learning and teaching system (Li & Du, 2017). Thus, this systematic review aims to fill the gap by exploring the comprehensive role of the AI applications in the ESL/EFL education, with a focus on their pedagogical and methodological implications.

LITERATURE REVIEW

Current technological breakthroughs, particularly in the field of artificial intelligence, spotlight their impact on everyday life and education. The surge in research on the integration of AI in ESL education is evident. Both ChatGPT and Wordtune have emerged as essential tools in the ESL/EFL contexts, enhancing writing skills by providing automated feedback on grammar, syntax, and style. This integration helps learners build accuracy and fluency in their writing (Kirmani, 2022; Zhao, 2023). These researchers predominantly explore the AI tools or the AI-based applications that utilise specific particular AI methods or classifications (Pikhart, 2020). Recent research (Chen et al., 2023; Moussalli & Cardos, 2020) reveal that language learners have a positive reception towards the integration of the AI technologies in language learning. The AI's ability to deliver instant responses and introduce flexibility and ease into teaching and learning environments is highlighted. Utilising the AI empowers the learners to be involved in an independent and feasible learning experience (Srinivasan, 2022). Concerning language skills, the focus in the AI-based computer-assisted learning (CAL) revolves around writing (Liang et al., 2021). Sharadgah and Sa'di (2022), in their overview of studies on AI in English Language Teaching (ELT) education from 2015 to 2021, shed light on existing gaps. These gaps include inherent challenges associated with body language, gestures, emotions, expressions, and translation. Additionally, the review underscored the dearth of descriptions of teaching resources utilised in the AI-based learning and teaching, as well as uncertainties surrounding the scope of what falls within the domain of the AI. Hence, there is a compelling need for more in-depth investigations across various AI teaching tools (Y. Gao et al., 2021), and considerable research progress still needs to be made. Furthermore, concerns have been raised regarding the readiness of English language teachers to incorporate the AI tools into the teaching process (Kessler, 2021). Therefore, there is a strong need for more research related to the AI integration in various teaching and learning contexts. Ethical concerns also arise regarding privacy and over-reliance on the AI tools. Additionally, there is a risk that over-dependence on the AI

tools may reduce students' active engagement in the learning process (J. Kim et al., 2020; Kessler, 2021; Kirmani, 2022).

While ongoing reports on the AI teaching tools and expression recognition are underway, more studies are needed to bridge the substantial gaps in the field. Moreover, issues regarding ethical considerations in the AI research pertinent to teachers and learners are also being discussed (J. Kim et al., 2020). Further inquiry and training should address the impending challenges and obstacles, including the pedagogical focus and practical growth of the AI applications in advancing language education and their effective utilisation (Jin & Zhuo, 2025). One of the most debatable topics today regarding AI is ChatGPT and its features for writing essays, poems, stories, and letters (Dergaa et al., 2023). Studies aim to identify and discuss the potential benefits of ChatGPT in the field of ESL education, particularly in writing skills. Since its launch in November 2022, ChatGPT has achieved significant success and become one of the most renowned AI tools. The Generative Pre-trained Transformer (GPT) has ushered in a paradigm shift, transforming conventional learning and teaching methodologies for writing (Kirmani, 2022). In a broad context, the AI writing tools analyse written text and provide instant feedback on everything from grammar to the overall structure (Hosseini et al., 2023). Within a concise two-month timeframe, OpenAI's technologies have reached a significant milestone by exceeding 100 million users (Williams, 2023). The AI writing assistant ChatGPT has effectively modernised conventional teaching and learning processes and enhanced writing abilities. Kirmani's analysis (2022) highlights ChatGPT as an advanced language model technology.

The AI plays a pivotal role in the implementation of adapted teaching and learning, as highlighted by Z. Huang et al. (2021). The AI-based applications can create personalised situational learning, allowing these systems to offer tailored teaching and learning activities, analyse students' development, and automatically adjust instructions as needed. Based on the big data, the AI can comprehensively record the learners' data and provide data presentation support to teachers, enabling them to adapt their teaching pedagogies accordingly (X. Yang, 2020). Past studies in the field of Natural Language Processing (NLP) have taken varied approaches, including Esit (2011)'s research related to delivering feedback to learners. This research imparts insights to researchers and teachers on how textual aspects influence the learners' performance (Monteiro & Kim, 2020). Additionally, it explores the utilisation of different devices to optimise and positively impact learning outcomes (Pérez-Paredes et al., 2019). The results of previous studies reveal a general lack of knowledge about these technologies among educators, resulting in their underutilisation. Pérez-Paredes et al. (2019) suggested that language instructors need to be trained in the necessities and advantages of these tools through skills development training related to the NLP technologies.

Therefore, these methodological gaps emphasise the need for future research to provide clear guidelines for the AI integration in teaching practices. In addition to these concerns,

the AI tools differ in their educational focus and impact. While studies such as those by Sharadgah and Sa'di (2022) focus on writing skills, other researchers, like J. Kim et al. (2020), explore the AI's impact on speaking and oral communication, illuminating the diverse applications of the AI in language education. In summary, although the AI tools like Wordtune and ChatGPT have shown potential in enhancing the ESL/EFL education, noticeable gaps persist in understanding their full potential and pedagogical implications. Therefore, this review aims to address these gaps by providing a systematic exploration of the current AI integration in education.

The initial database search and subsequent screening process were conducted to ensure the inclusion of relevant studies. Table 1 outlines the Scopus search string along with the applied screening criteria during the selection process.

Table 1
Search string (Scopus)

Initial search/ topic	**Search items/strings**	**Document found**
Artificial intelligence/ ChatGPT/ Writing skills	TITLE-ABS-KEY (artificial AND intelligence) OR (ai) AND (LIMIT-TO (SUBJAREA , "SOCI") OR LIMIT-TO (SUBJAREA , "ARTS")) AND (LIMIT-TO (DOCTYPE , "ar")) AND (LIMIT-TO (LANGUAGE , "English")) AND (LIMIT-TO (EXACTKEYWORD , "Education") OR LIMIT-TO (EXACTKEYWORD , "Teaching") OR LIMIT-TO (EXACTKEYWORD , "Artificial Intelligence (AI)")) AND (LIMIT-TO (EXACTSRCTITLE , "International Journal Of Artificial Intelligence In Education") OR LIMIT-TO (EXACTSRCTITLE , "International Journal Of Emerging Technologies In Learning") OR LIMIT-TO (EXACTSRCTITLE , "Computers And Education") OR LIMIT-TO (EXACTSRCTITLE , "Education And Information Technologies"))	195
Screening Process Learning setting, educational level, and focus on ESL/ EFL	TITLE-ABS-KEY (ai) AND (chatgpt) AND (assistant) AND (english) AND (teaching) AND (education) AND (LIMIT-TO (SUBJAREA , "SOCI")) AND (LIMIT-TO (DOCTYPE , "ar") OR LIMIT-TO (DOCTYPE , "cp")) AND (LIMIT-TO } (EXACTSRCTITLE , "Education And Information Technologies") OR LIMIT-TO (EXACTSRCTITLE , "Computers And Education Artificial Intelligence") OR LIMIT-TO (EXACTSRCTITLE , "Journal Of Applied Learning And Teaching") OR LIMIT-TO (EXACTSRCTITLE , "Cogent Education") OR LIMIT-TO (EXACTSRCTITLE , "International Journal Of Educational Technology In Higher Education") OR LIMIT-TO (EXACTSRCTITLE , "International Journal Of Educational Research") OR LIMIT-TO (EXACTSRCTITLE , "Technology Knowledge And Learning"))	28

In the Web of Science database, an initial keyword-based search generated a large number of documents. These results were subsequently refined using specific filters such as research area, document type, publication title, and enriched cited references.

Table 2 displays the number of documents retrieved at each stage of the screening and refinement process.

Table 2
Search string (Web of Science)

Topic	Search items/string	Documents found
Artificial intelligence	ALL=(AI OR ARTIFICIAL INTELLIGENCE AND ESL AND EFL)	119
Refined by: 1) Research area 2) Document type 3) Publication title 4) Enriched cited references	ALL=(Artificial Intelligence or AI and English and ESL and EFL)	56

The search strategy applied to ScienceDirect followed a topic-wise approach, using specific keywords to locate relevant studies. The number of documents retrieved was then refined by applying inclusion criteria. Table 3 presents the search strings used for each topic, along with the corresponding number of documents initially found and those retained after refinement.

Table 3
Search string (ScienceDirect)

Topic	String	Documents found
Artificial intelligence / /English language	"AI", "ARTIFICIAL INTELLIGENCE", "AI TOOLS", "ENGLISH"	607
Refined by Subject areas, article type, publication title, and subject areas	"AI", "ARTIFICIAL INTELLIGENCE", "AI TOOLS", "ENGLISH"	23

For Google Scholar, the articles were identified using relevant keywords, and a handpicking technique was used to shortlist the studies.

METHODOLOGY

The exploration of pertinent literature was conducted through Scopus, WoS, and ScienceDirect research databases. Insights were drawn from relevant literature in the domain of the AI-integrated writing assistance (Ippolito et al., 2022), and a set of research keywords was systematically identified. This study initiated a detailed examination of the

identification and retrieval of existing literature related to the AI tools. The data were refined systematically through the application of relevant criteria. To execute this process, leading databases, including Scopus, WoS, Google Scholar, and ScienceDirect, were utilised.

Review Protocol

This stage highlights the review protocol in which the researcher plans how selected studies are considered suitable and pertinent for the review (Shaffril et al., 2021). By spotlighting the research questions of the study, the researcher ensured that all the studies included in the review were relevant; further filtering was conducted for the final selection. To maintain relevance, inclusion criteria were established to ensure a focus on studies that directly explore the impact of the AI tools on the ESL/EFL teaching practices, prioritising those that involve the AI-driven language models and writing tools. The second criterion was based on the integration of the AI applications in the ESL/EFL education. Therefore, studies that lacked a focus on the AI integration in the ESL/EFL education were ultimately excluded. Referring to publication or reporting standards, several studies were considered eligible based on the criteria set forth in Table 4. A detailed review of the literature is included in the discussion section. To establish guidelines, the current study followed the guidelines outlined by Shaffril et al. (2022). These guidelines suggest that establishing a protocol and referring to different plans can assist researchers in presenting a systematic literature review (SLR) in a transparent, referrable, and replicable manner (Mengist et al., 2020).

Table 4
Inclusion and exclusion criteria

Criteria	Eligibility	Exclusion
Language and educational area / teaching learning	Should have "AI" or "Artificial intelligence "as a basic component in title	Published in a language other than English
Specific focus on ESL/EFL education	Mainly address about ESL/EFL	Book reviews, editorials, chapters, and non-journal articles
Type of literature	Written and published in English	Published by the same author on different databases

Note. ESL = English as a Second Language; EFL = English as a Foreign Language

Formulation of Research Questions

The following research questions will guide the entire research procedure. The approach used and synthesised data are based on the main items in these questions. Researchers emphasise that formulating a research question should not be too general in order to reduce the volume of searched articles (Burgers et al., 2019; Johnson & Hennessy, 2019).

Q1: What methodologies and AI applications are most prevalent in recent studies on the AI integration in the ESL/EFL education, and how do they impact pedagogy and sampling?

Q2: What are the most frequently used keywords, and countries with more publications?

Searching Strategies

In this phase, a rationale for the search strategy was established. The initial step involved "identification" based on keywords to retrieve potential articles. This identification pinpointed diverse journals that focus on the integration of AI in ESL/EFL education. This task was performed through three prominent databases: WoS, Scopus, Google Scholar, and ScienceDirect. Given the significance and depth of the topic, the preliminary search produced more than a thousand papers, as no filters were employed at this initial stage. However, later in the process, the authors applied filters focusing on the research questions. Therefore, the implementation of a three-step process based on Shaffril et al. (2018) was employed. These steps include a) identification, b) screening, and c) eligibility. The search strategy varied for each search engine, as the filters were adjusted to refine the varying degrees of irrelevant data in the chosen databases.

Identification

During the identification process, suggested keywords were added to the ScienceDirect, Scopus, and WoS databases; however, for Google Scholar, the keywords remained the same. Consequently, the use of keywords such as “AI”, “ESL/EFL”, and “education” resulted in the identification of 921 studies. The keywords were refined through iterative searches, focusing on combinations that directly addressed the integration of the AI tools in the ESL/EFL contexts, which resulted in a more manageable dataset of 107 potential articles.

Screening

The second step of the process, screening, involves collecting relevant papers based on predefined inclusion and exclusion criteria. Both manual and automated techniques can be utilised, employing database options and functions to filter search results according to the study's requirements. In this study, the researchers applied both manual methods and database filters to select suitable papers, choosing published studies with a focus on the AI in the ESL/EFL context. Given the study's emphasis on English-language sources, articles were selected from studies in the Social Sciences, Arts, and Humanities. As the filtration process continued, the focus remained primarily on the teaching and learning domains.

Eligibility

In this stage, the titles, abstracts, and other key sections of the papers were reviewed to assess the eligibility of the studies. Through this process, the authors excluded 820 articles. Consequently, 107 articles were deemed broadly relevant. After further reviewing these articles with a focus on the EFL/ESL context, AI, and English language education, an additional 82 articles were excluded for not meeting the selection criteria. Ultimately, only 25 articles met the criteria and proceeded with the quality appraisal process (Figure 1).

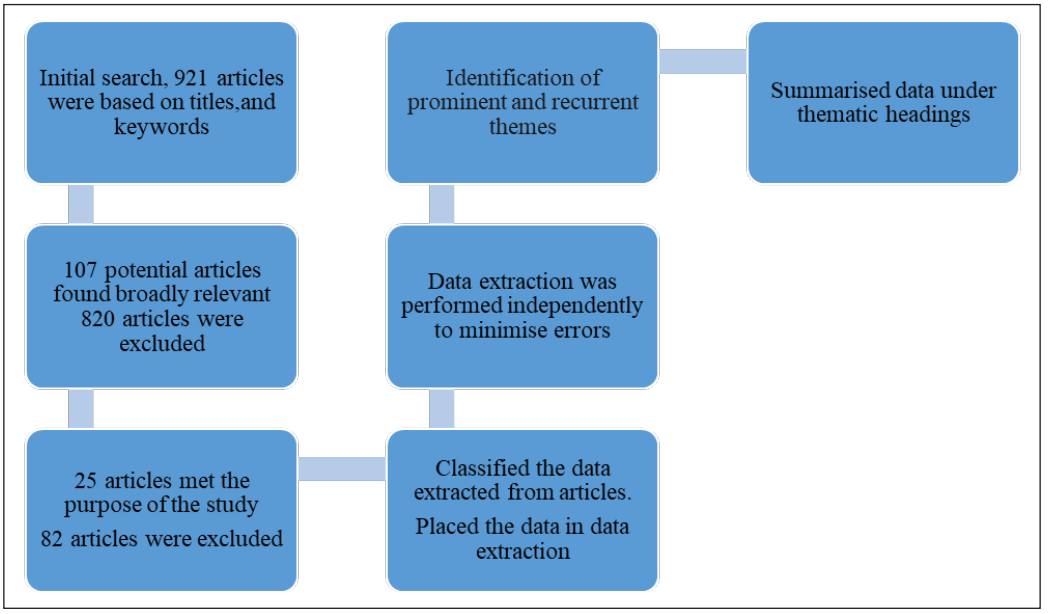

Figure 1. Systematic review process

Quality Appraisal

The articles that have passed the eligibility stage require careful scrutiny to make sure the absence of bias in the quality of the review methodology (Higgins et al., 2019). Each article underwent a rigorous quality appraisal using established guidelines (Shaffril, 2021) to ensure the relevance and reliability of the studies included in the review. At this stage, duplicate articles, articles written in languages other than English, book reviews, editorials, non-journal articles, and papers outside the predetermined focus of the study were removed. To minimise selection bias, the authors established inclusion and exclusion criteria before the extraction stage, as indicated in Table 4. This filtering process ultimately identified 25 articles pertinent to the study.

Data Extraction

At this stage, prior to the final selection of papers, the authors arbitrarily chose five papers and conducted a collaborative review with a qualified assistant to ensure inter-rater reliability in making the inclusion and exclusion decisions. Discrepancies between reviewers were addressed through discussion, ensuring the reliability and consistency of the data extraction process. Each paper was read in its entirety and independently to minimise errors in subsequent stages (Charrois, 2015; Gomersall et al., 2015). Following this, inter-rater reliability was established by identifying connections and noting changes in the extracted data. The selected articles include both the experimental and theoretical studies. For data extraction, the authors discussed thematic concepts and applied established coding, which evolved into broader themes. Ultimately, the information from the 25 papers was categorised under specific headings.

Data Synthesis

The authors and a knowledgeable partner analysed the records by comparing subjects across categories within the articles. This approach facilitated the creation of a systematic review, allowing the authors to reflect on changes in the collected data. Over a two-month period, the authors and expert collaboratively analysed the findings, ultimately formulating a comprehensive summary of the data, as illustrated in the Appendix.

Data Demonstration

It is crucial to use a flow diagram for a systematic literature review (SLR). For this purpose, the current study utilises a tailored flow diagram (Figure 1) introduced by Shaffril et al. (2019). Tables and figures are employed to present data from the findings of the selected articles, along with tables that highlight key statements and main focuses. Additionally, a separate table is used to display the selection and exclusion criteria, providing a comprehensive overview of the current study. Tables were used to visualise the key findings, such as the frequency of the AI applications, and the geographical distribution of the research studies. By following a rigorous, multi-step methodology, this systematic review ensured that only high-quality and relevant, reliable studies were included. The findings from this process offer a comprehensive understanding of the AI integration in ESL/EFL education, which will be discussed in the following sections.

Predefined criteria guided the selection of studies. Table 4 presents the inclusion and exclusion criteria used in the review.

After screening and analysing the selected studies, key thematic areas were identified based on their methodological focus, AI applications, pedagogical approaches, and sampling strategies. Table 5 presents the major themes extracted from the reviewed articles.

Table 5
Themes

No.	Authors	Methodological focus	AI applications	Pedagogical focus	Sampling focus
1	Annamalai et al. (2023)	Questionnaire and interviews	AI Chatbots	Enhancing English language learning	ESL students
2	Mizumoto and Eguchi (2023)	Quantitative research approaches	ChatGPT AI Language Model	Writing evaluation and feedback	Non-native English speakers
3	Fathi et al. (2024)	Mixed method	AI-speaking Chatbot Andy	EFL students speaking WTC	EFL learners
4	Darwin et al. (2024)	Semi-structured interviews	AI-technologies	Enhancing critical thinking skills	EFL Master's degree students
5	Annamalai et al. (2023)	Interviews	AI Chatbots	Motivation to learn English	Undergraduate ESL learners
6	Abdelatif and Siddiqui (2021)	Close-ended questionnaire	Various AI Tools in EFL teaching	Integration and utilisation of AI tools in English language teaching	ESL faculty members from languages and translation
7	Mohammadkarimi (2023)	Questionnaire and interviews	AI- tools	Equipping teachers with AI tools	67 EFL teachers
8	An et al. (2023)	Questionnaire and interviews	Various AI-driven technologies	AI integration EFL teaching practices and learning outcomes	EFL teachers
9	Du and Gao (2022)	Interviews	AI-based applications in EFL studies	Factors influence adoption of AI tools /EFL teachers' perceptions	17 experts
10	Liu et al. (2024)	Recordings and interviews	GAI ChatGPT and Bing Chat	Students' multimodal writing process	Two groups of EFL writers
11	Moorhouse (2024)	In-depth-individual and group interviews	Generative AI tools, specifically ChatGPT	Readiness of language teachers to use GAI tools in their professional work.	Ten beginning teachers and seventeen first-year English language teachers

Table 5 *(continue)*

No.	Authors	Methodological focus	AI applications	Pedagogical focus	Sampling focus
12	Jiang (2022)	Comprehensive overview	Automatic Evaluation Systems Neural Machine Translation Tools, (ITSs) AI Chatting Robots, IVE, Affective Computing (AC) in ITSs	Impact of AI on teaching and learning.	Existing literature
13	Alshumaimeri and Alshememry (2023)	Systematic review	The review covers a wide range of AI technologies/methodologies	Understanding AI influences in ESL education	Scholarly articles, studies and papers
14	Anggoro and Pratiwi (2023)	Overview	Quizizz GAI	Promoting independent learning	ESL students and teachers
15	Zhao (2023)	Tech review	Writing assistant (Wordtune)	Facilitating ESL learners in the writing process	Not specified
16	Jeon (2021)	Semi-structured interviews	Customised Chatbots, Google Dialog flow	ESL learners motivation to learn English	Thirty-six Korean primary school learners
17	Al-Garaady and Albuhairy (2023)	Statistical analysis, *F*-score and *p*-value	LLM ChatGPT	Focus on identifying writing errors/ effectiveness of ChatGPT	EFL learners
18	Madhavi et al. (2023)	Non-ICT with traditional and ICT-AI speaking test	Several AI and ICT tools and resources	Specific focus on speaking skills or spoken communication	100 students /ICT and non-ICT
19	Fleckenstein et al. (2024)	Inventory lime survey	ChatGPT	Students' text or writing skills	Pre-service teachers
20	Sun et al. (2021)	Deep learning assisted approach	AI module to create a modern tool program	Enhancing English language teaching efficiency	Online English teaching system

Table 5 *(continue)*

No.	Authors	Methodological focus	AI applications	Pedagogical focus	Sampling focus
21	Sharadgah and Sa'di (2022)	Systematic literature review from 2015 to 2021	Range of AI approaches including NLP, MLNN	To highlight the positive impact of AI approaches on ESL language optimization	The study examined 200 articles, retaining 64
22	Al Mahmud (2023)	Pre-posttest writing samples/	Wordtune, an AI-powered writing tool and Grammarly	Impact of Wordune on EFL learners writing quality	ESL students
23	Kohnke et al. (2023)	Semi-structured interviews	GAI tools in English language teaching	Identification of digital competencies and pedagogical knowledge required for integrating GAI in education	Twelve higher education English language teachers in Hong Kong
24	Moulieswaran and Prasantha Kumar (2023)	Utilising survey instruments with a 5-point Likert Scale	AI-assisted language learning (AI-ALL)	Problems faced by ESL learners regarding AI-assisted language learning and teaching	The study includes 81 engineering stream students
25	Alharbi (2023)	Pre-test Post-test	Machine Translation/Google Translate	Writing skills	234 university EFL students

Note. AI = Artificial intelligence; ESL = English as a Second Language; EFL = English as a Foreign Language; WTC = Willingness to communicate; GAI = General Ability Index; ITSs = Intelligent Tutoring Systems; IVE = Immersive virtual environment; AC = Affective computing; LLM = Large language model; ICT = Information and Communication Technology; NLP = Natural Language Processing; MLNN = Multilayer neural network; ALL = Adaptive language learning

RESULTS

The 25 studies provide significant insights into the integration of the AI tools in the ESL/EFL education, focusing on methodological trends, diverse AI applications, and their broader pedagogical impact.

Q1: What is the methodological focus, most commonly used AI applications, sampling focus, and pedagogical focus in the AI-integrated teaching and learning in the ESL/EFL studies?

The results of the reviewed studies revealed the following themes:

Methodological Focus

Figure 2 illustrates the primary methodological focus of the 25 reviewed studies. Most of the studies examine the effectiveness of AI technologies in relation to English language acquisition for ESL/EFL learners, encompassing a range of methodologies within the context of ESL/EFL education.

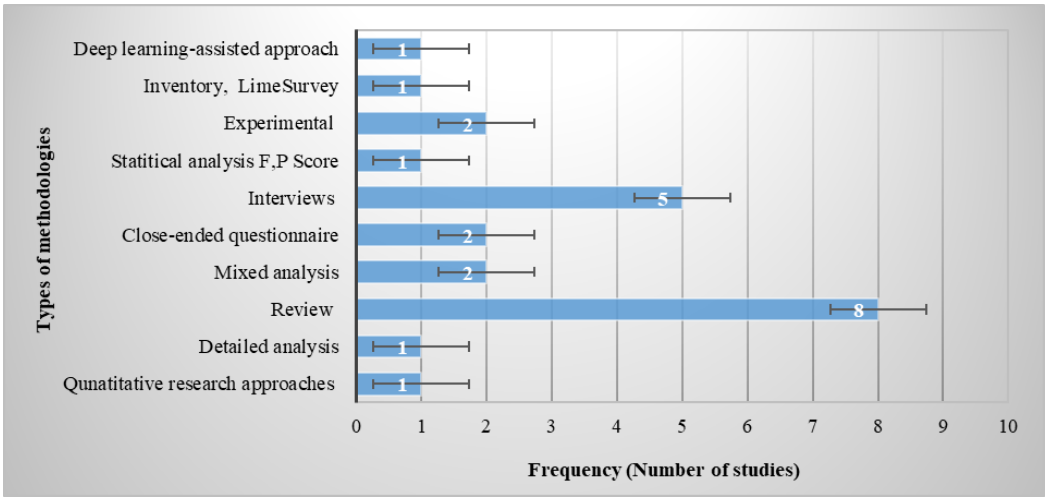

Figure 2. Methodological focus

The reviewed studies include various strategies that integrate AI tools into the classroom. Most studies aimed to understand and explore the benefits of the AI tools in the ESL/EFL classes. These strategies employed a range of approaches, including qualitative techniques, mixed-method designs, and quantitative analyses, to provide a deeper understanding of the AI and GAI-based tools and applications. Among the studies, literature reviews were the most common methodology (f = 8), followed by interviews (f = 5), experimental studies

(f = 2), close-ended questionnaires (f = 2), quantitative research (f = 1), class-based activities (f = 1), statistical analysis (f = 1), detailed analysis (f = 1), mixed-method analyses (f = 2), and inventories or surveys (f = 1). Most studies utilised qualitative methods, such as interviews and reviews, indicating a strong emphasis on understanding the practical use of the AI tools and learner experiences in the ESL/EFL context.

AI Applications

Figure 3 illustrates the most commonly used AI applications and trends in research regarding the AI integration in ESL/EFL education, including Chatbots, ChatGPT, Wordtune, AI-speaking chatbots, GAI, Bing, and Wordtune.

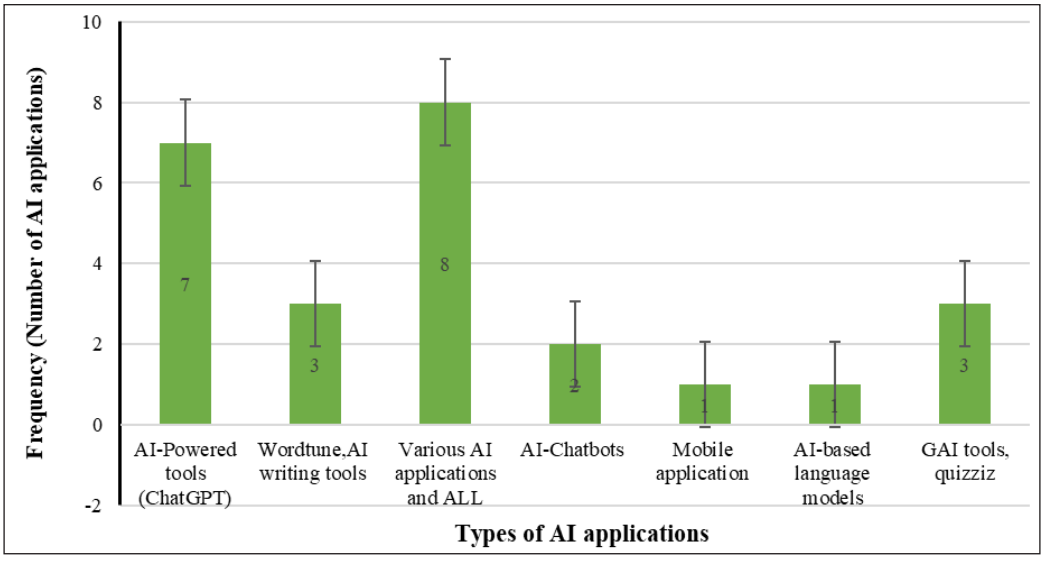

Figure 3. Most commonly used AI Applications in ESL/EFL studies
Note. AI = Artificial intelligence; ALL = Adaptive language learning; GAI = Generative artificial intelligence

The studies explored various AI applications, including AI chatbots, AI-powered ChatGPT, and AI-based language learning models. Researchers also identified tools such as Wordtune and Quizizz. A few studies examined AI-assisted tools, including the NLP, neural networks (NN), and machine learning (ML), highlighting the broad scope of the artificial intelligence and GAI in English language teaching. The integration of various AI applications was the most popular research topic in the ESL/EFL education (f = 7). The ChatGPT emerged as the second most frequently used AI application (f = 6), followed by Wordtune and other AI writing tools (f = 3). Additionally, the GAI and Quizizz were employed with equal frequency (f = 3). Conversely, the AI-based language models, mobile applications, tailored chatbots, AI-based social robots, and cloud computing appeared in

only one study each (f = 1). Consequently, the ChatGPT was frequently used to support writing, grammatical accuracy, and syntax accuracy, while the Wordtune was employed to enhance coherence and fluency in students' written tasks.

Pedagogical Focus

Pedagogical focus presents the number of review studies focussing on different pedagogical themes within the ESL/ELT education. Figure 4 illustrates those involving the AI integration particularly.

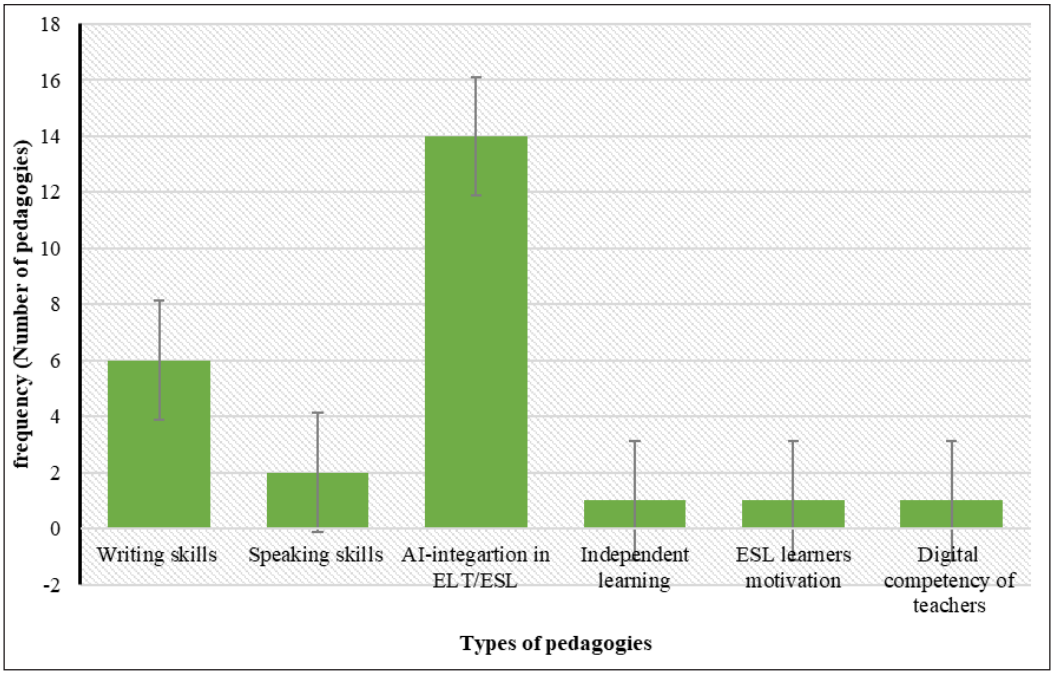

Figure 4. Pedagogical focusses of review studies
Note. AI = Artificial intelligence; ELT = English language teaching; ESL = English as a second language

The studies revealed a primary focus on the incorporation of the AI-based applications in the ESL/EFL instruction (f = 14). The second most common pedagogical focus was on writing skills (f = 6). One study explored the digital competency and proficiency of the ESL/EFL instructors in integrating the AI tools within the teaching and learning contexts (f = 1). Additionally, some studies highlighted recent advancements in the GAI within the educational landscape and explored the enhancement of speaking skills using the GAI tools in English-speaking classes (f = 2). It is evident that the AI integration has been extensively investigated in a general context to understand the tools, applications, and their importance in the English language teaching and learning. Ultimately, the studies emphasised a strong

association between the AI and writing skills. A few studies also examined topics such as independent learning (f = 1) and the ESL students' motivation (f = 1). The emphasis on the writing skills within the AI applications stems from the real-time feedback and ease with which the AI can provide automated, individualised assistance on writing style, structure, and grammar. This not only streamlines the learning process but also makes writing a prime area for the AI integration in the ESL/EFL contexts.

Sampling Focus

The studies employed diverse sampling strategies as displayed in Figure 5.

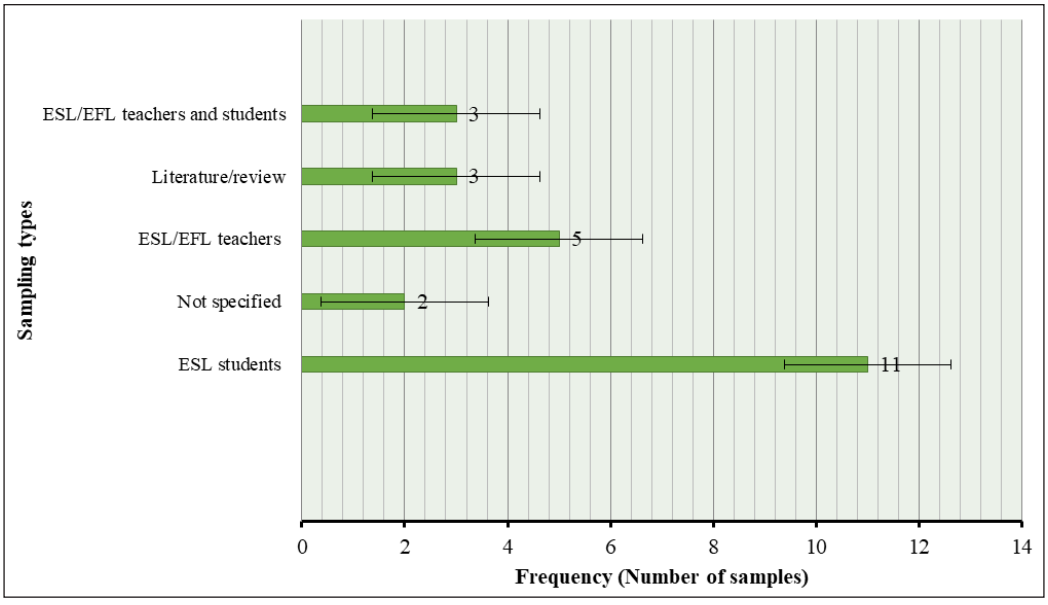

Figure 5. Sampling focus of review studies
Note. ESL = English as a second language; EFL = English as a foreign language

Empirical studies involving the ChatGPT collected data from 17 experts, although a few studies (f = 2) did not specify sample details. Other studies included male and female students, higher education language teachers from Hong Kong, and technical students from India. One study (f = 1) focussed on an English course using questionnaires for the data collection. Similarly, 67 primary-level students from Korea and 100 EFL students participated in some studies as samples

Nevertheless, the ESL students represent the highest sampling focus category, indicating (f = 11), while the ESL/EFL teachers (f = 5) constitute the second most common sampling focus in the AI-based studies. Some studies (f = 3) used extant literature as the primary data source in the context of the AI-based applications in the English language teaching,

whereas the comparison between teachers and students (f = 3) appeared to be less prevalent. Thus, research involving teachers typically raised issues regarding digital literacy and the challenges of the AI adoption, while studies focussed on students highlighted how the AI applications affected learning outcomes, engagement, and performance.

Q2: What are the most frequently used keywords, and countries with more publications?

Keywords with Greater Frequency

The authors identified 3,894 words as the main keywords. The minimum threshold to determine the keywords with higher frequency was set at nine for the co-occurrence of author keywords. As a result, 24 keywords were grouped into five categories.

Table 6 presents the frequently occurring keywords across the reviewed studies, grouped by thematic relevance.

Table 6
Keywords with greater frequency

Groups	Keywords
Group 1	Artificial intelligence technologies (29), Artificial intelligence in education (21), ChatGPT (39), Chatbots (29), AI systems (28)
Group 2	Teaching (105), Interactive learning environment (24), Learning system (92), Natural language processing system (115), Innovation (38)
Group 3	Education (103), Education computing (53), Computer-aided instruction (81), Feedback (11), Educational technology (24), Technology (49)
Group 4	Teaching and learning (9), Machine learning (240), Virtual reality (24), English teaching (10), Students (203)

Table 6 illustrates the most influential keywords. The most frequently used keywords by researchers included artificial intelligence, machine learning, students, natural language processing systems, and teaching. From 2018 to 2024, the artificial intelligence in the English language teaching has primarily been associated with addressing digital transformation. However, terms like AI, learning systems, artificial intelligence technology, and ChatGPT have emerged as recent keywords in the studies.

The analysis of 25 articles, based on question two, is discussed below.

Figure 6 illustrates the countries with the highest number of publications in the selected field.

Figure 6 shows the countries with more publications were the United States (f = 90), China (f = 62), United Kingdom (f = 31), Taiwan (f = 26), Australia (f = 19), Canada (f = 18), Spain (f = 16), Brazil (f = 13), Greece (f = 13), Germany (f = 11), Hong Kong (f = 10), Saudi Arabia (f = 10), France (f = 8), Malaysia (f = 7), Morocco (f = 7), the Netherlands (f = 7), South Korea (f = 7), Turkey (f = 7), India (f = 6), Indonesia (f = 6),

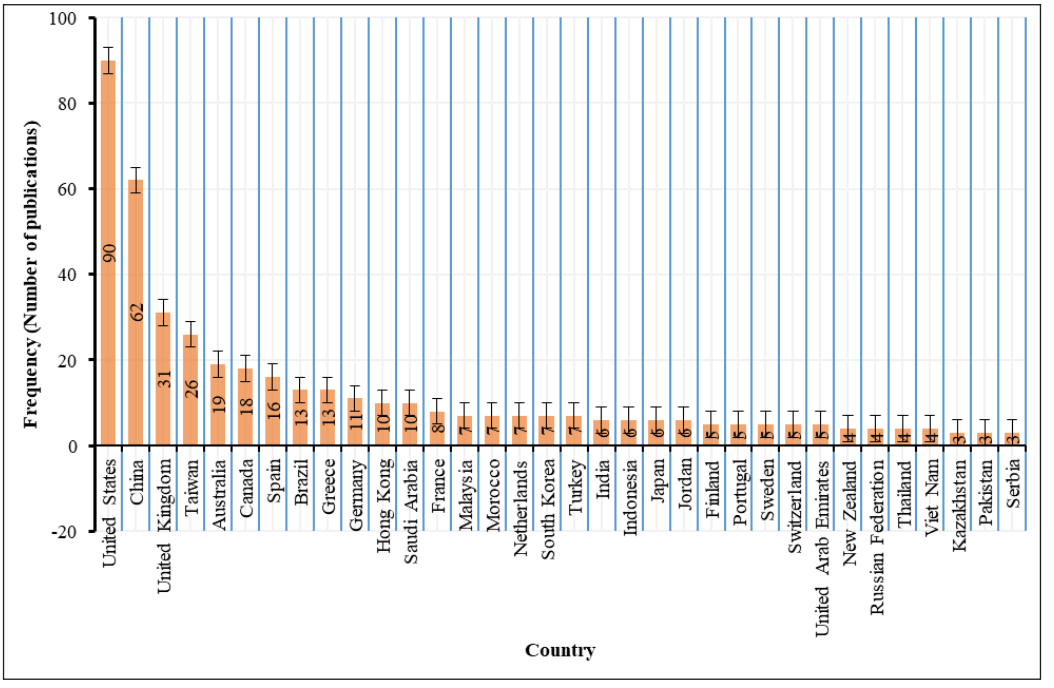

Figure 6. *Countries* with more publications

Japan (f = 6), Jordan (f = 6), Finland (f = 5), Portugal (f = 5), Sweden (f = 5), Switzerland (f = 5), and New Zealand (f = 4). However, various countries remained less productive in terms of publications with a number less than 5 (Figure 5). In light of publication trends, the dominance of the United States and China in the AI research can be attributed to their substantial investments in educational innovation and technology, as well as the widespread implementation of the AI within their education systems. These findings provide a comprehensive overview of trends in the AI integration in the ESL/EFL education, offering valuable insights into the applications, methodologies, and pedagogical aspects that have attracted the most scholarly attention.

DISCUSSION

The review found that the AI tools predominantly enhance writing skills in the ESL/EFL contexts, with the ChatGPT and Wordtune being the most frequently used applications. This aligns with the research question exploring the most used AI applications and their methodological focus. Similarly, the second research question aimed to identify the most used keywords and countries with the highest number of publications. Initial database searches on the topic yielded 921 documents, as no filters were initially applied to the publication years. This number was subsequently reduced to 107 potential articles based

on relevance, after applying the inclusion and exclusion criteria. Following a rigorous selection process, 25 articles remained for a blinded review (Table 6).

Through the systematic analysis, the research pinpoints the methodological focus, pedagogical focus, AI tools or applications, and sampling focus. Recent studies have sought to understand and explore the benefits of the AI tools in the ESL/EFL classes. Many studies emphasised the general integration of the AI tools in the English language teaching, with a specific focus on writing skills as the second most common pedagogical area. Researchers also explored topics like teachers' digital competency and speaking skills. A few studies investigated diverse topics, highlighting the evolving nature of the AI technology in the ESL education. Consistent with Sharadgah and Sa'di (2022), this review also noted that writing skills remain the dominant focus of the AI tools in the ESL/EFL education, highlighting the AI's role in providing real-time feedback and tailored support.

This review highlighted that teachers could incorporate the AI tools, such as the Wordtune for peer review exercises or the ChatGPT, to create conversational practice, thereby encouraging collaboration among the learners. In this context, concentrated pedagogical focusses included 'motivation of learners', 'independent learning', 'parental involvement and role', and 'traditional versus ChatGPT-based instruction'. Furthermore, these methodologies employed approaches based on qualitative techniques, mixed-method designs, and quantitative analysis. The most used methodology was 'review', aimed at providing a deeper understanding of artificial intelligence or GAI-based tools and applications. However, some studies encompassed a range of methodologies within the context of ESL/EFL education.

The United States and China had the most publications, indicating their significant involvement in research on the AI integration in ESL education. These findings align with K. Huang et al. (2023), who concluded that the United States and Arizona State University are actively engaged in studies on AI-based language education. However, according to the Business of Apps data, the United States is the second top country for using and downloading AI applications. Both China and the United States are further advanced in terms of resources, technological innovation, and educational development, which positions them as leaders in the AI integration within language education. Additionally, the most frequently used keywords in the ESL/EFL context were 'artificial intelligence,' 'machine learning,' 'students,' and 'natural language processing systems'. In addition, the findings also revealed that over-reliance on the AI tools may limit the learners' chances to engage in critical thinking and creativity. Moreover, privacy concerns arise with applications like ChatGPT that collect user data.

Incorporating the AI tools into everyday ESL/EFL classroom practices can facilitate differentiated learning by providing individual support. The AI applications can offer personalised feedback on writing tasks while also simulate real-time conversations to help

the learners enhance their speaking skills according to their individual learning needs. Future research should investigate the use of the AI tools in enhancing oral communication skills, especially within immersive learning environments like virtual or augmented reality, which could provide a more realistic learning experience. It would also be valuable to explore how AI can support educators in creating more interactive and dynamic lessons, offering insights into the integration of AI in facilitating real-time student progress. In conclusion, the AI tools such as ChatGPT and Wordtune have shown great effectiveness in enhancing writing skills; however, there is still much unexplored potential for the AI to revolutionise other facets of language learning. Addressing ethical issues will be essential, as it will equip teachers with the necessary skills for the successful integration of AI in ESL/EFL education.

CONCLUSION

This review addressed two key research questions: the methodological focus and most used AI applications in the ESL/EFL education, as well as the frequently used keywords and geographical distribution of publications. The findings indicated that the AI tools, primarily ChatGPT and Wordtune, have had a significant impact on writing skills, with an emphasis on qualitative methodologies in the reviewed studies. The surge in research publications in the field highlights the depth and academic value of the artificial intelligence tools in ESL/EFL education. This review also noted that, with the help of selected studies for the current research, the initial emphasis was on education in general, but over time, this focus has expanded to include diverse pedagogical approaches. Despite the positive impact, the AI is still considered insufficient and requires more research in the domain of English language teaching. This inadequacy is evident in the results, which emphasise the importance of AI for learners of English as a second language. The focus should be on providing training to teachers to effectively utilise these applications in their instruction. It is also evident that proficiency in using the AI-based applications is a necessary skill for both the learners and educators to achieve future success. Recent studies have emphasised the need for more research related to the AI-based language learning in real-life classroom settings (H. Yang & Kyun, 2022). Researchers widely concur with the impact of the AI applications and tools after COVID-19; however, the ELT/ESL research still demands systematic investigation. Several obstacles persist in the educational process due to the evolving nature of AI and GAI, which validates the need for more empirical research to address various issues and assist language teachers.

Considering the limitations of the current study, specific exploration with clear objectives necessitates more in-depth research on the AI technologies in the ESL/EFL education. One limitation of this review is its focus on the latest studies, which may have excluded valuable insights from earlier research. Additionally, the review primarily focussed on the AI's role

in writing, with less attention given to other language skills such as speaking and listening. For educators, these findings suggest that the AI tools can significantly improve language instruction by offering personalised feedback and promoting self-directed learning. For researchers, there remains an urgent need to explore the AI's scope in education, particularly by investigating its impact on speaking skills and facilitating classroom interactions. Future research should examine the AI's role in improving oral communication and listening skills among the ESL/EFL students. Additionally, more empirical studies are needed to evaluate the lasting impact of the AI integration on overall language proficiency and address the ethical concerns associated with the AI use in education. As the AI technology advances, its integration into the ESL/EFL education presents promising opportunities and effective approaches to language learning.

ACKNOWLEDGEMENTS

The corresponding author would like to express her sincere gratitude to Mr. Muhammad Nawaz from the School of Languages, Literacies and Translation, Universiti Sains Malaysia (USM), for his intellectual guidance and active role in data extraction and analysis, which significantly enriched this study. Special thanks are also extended to Professor Dr. Hazri Jamil, the research supervisor at the School of Educational Studies, USM, for his unwavering academic guidance, insightful feedback, and motivational support throughout the research process.

REFERENCES

Abdelatif, K., & Siddiqui, A. (2021). Incorporating artificial intelligence (AI) tools in EFL classes at King Khalid University (KKU). *Journal of Tianjin University Science and Technology*, *54*(10), 197-221. https://doi.org/10.17605/OSF.IO/N7QSF

Al Mahmud, F. (2023). Investigating EFL students' writing skills through artificial intelligence: Wordtune application as a tool. *Journal of Language Teaching and Research*, *14*(5), 1395-1404. https://doi.org/10.17507/jltr.1405.28

Al-Garaady, J., & Albuhairy, M. M. (2023). ChatGPT's capabilities in spotting and analyzing writing errors experienced by EFL learners. *Arab World English Journal*, *9*(CALL), 3-17. https://doi.org/10.24093/awej/call9.1

Alharbi, W. (2023). The use and abuse of artificial intelligence-enabled machine translation in the EFL classroom: An exploratory study. *Journal of Education and e-Learning Research*, *10*(4), 689-701. https://doi.org/10.20448/jeelr.v10i4.5091

Alshumaimeri, Y. A., & Alshememry, A. K. (2023). The extent of AI applications in EFL learning and teaching. In *IEEE Transactions on Learning Technologies* (Vol. 17, pp. 653-663). IEEE. https://doi.org/10.1109/TLT.2023.3322128

An, X., Chai, C. S., Li, Y., Zhou, Y., & Yang, B. (2023). Modeling students' perceptions of artificial intelligence-assisted language learning. *Computer Assisted Language Learning*, 1-22. https://doi.org/10.1080/09588221.2023.2246519

Annamalai, N., Eltahir, M. E., Zyoud, S. H., Soundrarajan, D., Zakarneh, B., & Al Salhi, N. R. (2023). Exploring English language learning via Chabot: A case study from a self-determination theory perspective. *Computers and Education: Artificial Intelligence*, *5*, 100148. https://doi.org/10.1016/j.caeai.2023.100148

Anggoro, K. J., & Pratiwi, D. I. (2023). Fostering self-assessment in English learning with a generative AI platform: A case of Quizizz AI. *Studies in Self-Access Learning Journal*, *14*(4), 489-501. https://doi.org/10.37237/140406

Barrot, J. S. (2023). Using ChatGPT for second language writing: Pitfalls and potentials. *Assessing Writing*, *57*, 100745. https://doi.org/10.1016/j.asw.2023.100745

Britannica. (2025). *Artificial intelligence*. https://www.britannica.com/technology/artificial-intelligence/Reasoning

Burgers, C., Brugman, B. C., & Boeynaems, A. (2019). Systematic literature reviews: Four applications for interdisciplinary research. *Journal of Pragmatics*, *145*, 102-109. https://doi.org/10.1016/j.pragma.2019.04.004

Charrois, T. L. (2015). Systematic reviews: What do you get to know to get started? *Canadian Journal of Hospital Pharmacy*, *68*(2), 144-148. https://doi.org/10.4212/cjhp.v68i2.1440

Chen, B., Zhu, X., & del Castillo, H. F. D. (2023). Integrating generative AI in knowledge building. *Computers and Education: Artificial Intelligence*, *5*, 100184. https://doi.org/10.1016/j.caeai.2023.100184

Dergaa, I., Chamari, K., Zmijewski, P., & Saad, H. B. (2023). From human writing to artificial intelligence generated text: Examining the prospects and potential threats of ChatGPT in academic writing. *Biology of Sport*, *40*(2), 615-622. https://doi.org/10.5114/biolsport.2023.125623

Du, Y., & Gao, H. (2022). Determinants affecting teachers' adoption of AI-based applications in EFL context: An analysis of analytic hierarchy process. *Education and Information Technologies*, *27*, 9357-9384. https://doi.org/10.1007/s10639-022-11001-y

Esit, Ö. (2011). Your verbal zone: An intelligent computer-assisted language learning program in support of Turkish learners' vocabulary learning. *Computer Assisted Language Learning*, *24*(3), 211-232. https://doi.org/10.1080/09588221.2010.538702

Gao, H. (2021). Reform of college English teaching model under the background of artificial intelligence. In *Journal of Physics: Conference Series* (Vol. 1744, No. 4, p. 042161). IOP Publishing. https://doi.org/10.1088/1742-6596/1744/4/042161

Gao, Y., Tao, X., Wang, H., Gang, Z., & Lian, H. (2021). Artificial intelligence in language education: Introduction of *Readizy*. *Journal of Ambient Intelligence and Humanized Computing*. https://doi.org/10.1007/s12652-021-03050-x

Gomersall, J. S., Jadotte, Y. T., Xue, Y., Lockwood, S., Riddle, D., & Preda, A. (2015). Conducting systematic reviews of economic evaluations. *International Journal of Evidence-Based Healthcare*, *13*(3), 170-178. https://doi.org/10.1097/xeb.0000000000000063

Higgins, J. P. T., López-López, J. A., Becker, B. J., Davies, S. R., Dawson, S., Grimshaw, J. M., McGuinness, L. A., Moore, T. H. M., Rehfuess, E. A., Thomas, J., & Caldwell, D. M. (2019). Synthesising quantitative evidence in systematic reviews of complex health interventions. *BMJ Global Health*, *4*(Suppl 1), e000858. https://doi.org/10.1136/bmjgh-2018-000858

Hosseini, M., Resnik, D. B., & Holmes, K. (2023). The ethics of disclosing the use of artificial intelligence tools in writing scholarly manuscripts. *Research Ethics*, *19*(4), 449-465. https://doi.org/10.1177/17470161231180449

Huang, K., Sun, K., Xie, E., Li, Z., & Liu, X. (2023). *T2I-CompBench: A comprehensive benchmark for open-world compositional text-to-image generation*. https://openreview.net/forum?id=weHBzTLXpH

Huang, Z., Shen, Y., Li, J., Fey, M., & Brecher, C. (2021). A survey on AI-driven digital twins in Industry 4.0: Smart manufacturing and advanced robotics. *Sensors*, *21*(19), 6340. https://doi.org/10.3390/s21196340

Ippolito, D., Yuan, A., Coenen, A., & Burnam, S. (2022). *Creative writing with an AI-powered writing assistant: Perspectives from professional writers*. *arXiv. https://doi.org/10.48550/arXiv.2211.05030*

Jeon, J. (2021). Exploring AI chatbot affordances in the EFL classroom: Young learners' experiences and perspectives. *Computer Assisted Language Learning*, *37*(1-2), 1-26. https://doi.org/10.1080/09588221.2021.2021241

Jiang, R. (2022). How does artificial intelligence empower EFL teaching and learning nowadays? A review on artificial intelligence in the EFL context. *Frontiers in Psychology*, *13*, 1049401. https://doi.org/10.3389/fpsyg.2022.1049401

Jin, K., & Zhuo, H. H. (2025). Integrating AI planning with natural language processing: A combination of explicit and tacit knowledge. *ACM Transactions on Intelligent Systems and Technology*. https://doi.org/10.1145/3729236

Johnson, B. T., Hennessy, E. A. (2019). Systematic reviews and meta-analyses in the health sciences: Best practice methods for research syntheses. *Social Science and Medicine*, *233*, 237–251. https://doi.org/10.1016/j.socscimed.2019.05.035

Keerthiwansha, N. W. B. S. (2018). Artificial intelligence education (AIEd) in English as a second language (ESL) classroom in Sri Lanka. *International Journal of Conceptions on Computing and Information Technology*, *6*(1), 31-36.

Kessler, G. (2021). Current realities and future challenges for CALL teacher preparation. *CALICO Journal*, *38*(3), i–xx. https://doi.org/10.1558/cj.21231

Kim, J., Merrill, K., Xu, K., & Sellnow, D. D. (2020). My teacher is a machine: Understanding students' perceptions of AI teaching assistants in online education. *International Journal of Human-Computer Interaction*, *36*(20), 1902–1911. https://doi.org/10.1080/10447318.2020.1801227

Kim, N.-Y. (2019). A study on the use of artificial intelligence chatbots for improving English grammar skills. *Journal of Digital Convergence*, *17*(8), 37-46. https://doi.org/10.14400/JDC.2019.17.8.037

Kirmani, A. R. (2022). Artificial intelligence enabled science poetry. *ACS Energy Letters*, *8*(1), 574-576. https://doi.org/10.1021/acsenergylett.2c02758

Kohnke, L., Moorhouse, B. L., & Zou, D. (2023). Exploring generative artificial intelligence preparedness among university language instructors: A case study. *Computers and Education: Artificial Intelligence*, *5*, 100156. https://doi.org/10.1016/j.caeai.2023.100156

Kurniati, E. Y., & Fithriani, R. (2022). Post-graduate students' perceptions of Quillbot utilization in English academic writing class. *Journal of English Language Teaching and Linguistics*, *7*(3), 437-451. https://doi.org/10.21462/jeltl.v7i3.852

Li, D., & Du, Y. (2017). *Artificial intelligence with uncertainty*. CRC Press. https://doi.org/10.1201/9781315366951

Liang, J.-C., Hwang, G.-J., Chen, M.-R. A., & Darmawansah, D. (2021). Roles and research foci of artificial intelligence in language education: An integrated bibliographic analysis and systematic review approach. *Interactive Learning Environments, 31(7), 4270-4296*. https://doi.org/10.1080/10494820.2021.1958348

Liu, M., Zhang, L. J., & Biebricher, C. (2024). Investigating students' cognitive processes in generative AI-assisted digital multimodal composing and traditional writing. *Computers and Education*, *211*, 104977. https://doi.org/10.1016/j.compedu.2023.104977

Lund, B. D., Wang, T, Mannuru, N. R., Nie, B., Shimray, S., & Wang, Z. (2023). ChatGPT and a new academic reality: Artificial intelligence-written research papers and the ethics of the large language models in scholarly publishing. *Journal of the Association for Information Science and Technology*, *74*(5), 570–581. https://doi.org/10.1002/asi.24750

Madhavi, E., Sivapurapu, L., Koppula, V., Rani, P. B. E., & Sreehari, V. (2023). Developing learners' English-speaking skills using ICT and AI tools. *Journal of Advanced Research in Applied Sciences and Engineering Technology*, *32*(2), 142-153. https://doi.org/10.37934/araset.32.2.142153

Mengist, W., Soromessa, T., & Legese, G. (2020). Ecosystem services research in mountainous regions: A systematic literature review on current knowledge and research gaps. *Science of the Total Environment*, *702*, 134581. https://doi.org/10.1016/j.scitotenv.2019.134581

Mohammadkarimi, E. (2023). Teachers' reflections on academic dishonesty in EFL students' writings in the era of artificial intelligence. *Journal of Applied Learning and Teaching*, *6*(2), 105-113. https://doi.org/10.37074/jalt.2023.6.2.10

Monteiro, K., & Kim, Y. (2020). The effect of input characteristics and individual differences on L2 comprehension of authentic and modified listening tasks. *System*, *94*, 102336. https://doi.org/10.1016/j.system.2020.102336

Moorhouse, B. L. (2024). Beginning and first-year language teachers' readiness for the generative AI age. *Computers and Education: Artificial Intelligence*, *6*, 100201. https://doi.org/10.1016/j.caeai.2024.100201

Moulieswaran, N., & Prasantha Kumar, N. S. (2023). Investigating ESL learners' perception and problem towards artificial intelligence (AI)-assisted English language learning and teaching. *World Journal of English Language*, *13*(5), 290. https://doi.org/10.5430/wjel.v13n5p290

Moussalli, S., & Cardoso, W. (2020). Intelligent personal assistants: Can they understand and be understood by accented L2 learners? *Computer Assisted Language Learning*, *33*(8), 865–890. https://doi.org/10.1080/09588221.2019.1595664

Oxford University Press. (n.d.). *Artificial intelligence*. https://global.oup.com/academic/category/science-and-mathematics/computer-science/artificial-intelligence/?cc=my&lang=en&

Pérez-Paredes, P., Guillamón, C. O., de Vyver, J. V., Meurice, A., Jiménez, P. A., Conole, G., & Hernándezd, P. S. (2019). Mobile data-driven language learning: Affordances and learners' perception. *System*, *84*, 145–159. https://doi.org/10.1016/j.system.2019.06.009

Pikhart, M. (2020). Intelligent information processing for language education: The use of artificial intelligence in language learning apps. *Procedia Computer Science*, *176*, 1412–1419. https://doi.org/10.1016/j.procs.2020.09.151

Shaffril, H. A. M., Krauss, S. E., & Samsuddin, S. F. (2018). A systematic review on Asian's farmers' adaptation practices towards climate change. *Science of the Total Environment*, *644*, 683-695. https://doi.org/10.1016/j.scitotenv.2018.06.349

Shaffril, H. A. M., Samah, A. A., Samsuddin, S. F., & Ali, Z. (2019). Mirror-mirror on the wall, what climate change adaptation strategies are practiced by the Asian's fishermen of all? *Journal of Cleaner Production*, *232*, 104–117. https://doi.org/10.1016/j.jclepro.2019.05.262

Shaffril, H. A. M., Samsuddin, S. F., & Samah, A. A. (2021). The ABC of systematic literature review: The basic methodological guidance for beginners. *Quality and Quantity*, *55*, 1319-1346. https://doi.org/10.1007/s11135-020-01059-6

Sharadgah, T. A., & Sa'di, R. A. (2022). A systematic review of research on the use of artificial intelligence in English language teaching and learning (2015–2021): What are the current effects? *Journal of Information Technology Education: Research*, *21*, 337–377. https://doi.org/10.28945/4999

Srinivasan, V. (2022). AI & learning: A preferred future. *Computers and Education: Artificial Intelligence*, *3*, 100062. https://doi.org/10.1016/j.caeai.2022.100062

Wang, X., Pang, H., Wallace, M. P., Wang, Q., & Chen, W. (2022). Learners' perceived AI presences in AI-supported language learning: A study of AI as a humanized agent from community of inquiry. *Computer Assisted Language Learning*, *37*(4), 814-840. https://doi.org/10.1080/09588221.2022.2056203

Williams, T. (2023). *Turnitin announces AI detector with '97 per cent accuracy'*. Times Higher Education. https://www.timeshighereducation.com/news/turnitin-announces-ai-detector-97-cent-accuracy

Yang, H., & Kyun, S. (2022). The current research trend of artificial intelligence in language learning: A systematic empirical literature review from an activity theory perspective. *Australasian Journal of Educational Technology*, *38*(5), 180–210. https://doi.org/10.14742/ajet.7492

Yang, X. (2020). Research on integration method of AI teaching resources based on learning behaviour data analysis. *International Journal of Continuing Engineering Education and Life Long Learning*, *30*(4), 492-508. https://doi.org/10.1504/IJCEELL.2020.110930

Zhang, K., & Aslan, A. B. (2021). AI technologies for education: Recent research and future directions. *Computers and Education: Artificial Intelligence*, *2*, 100025. https://doi.org/10.1016/j.caeai.2021.100025

Zhao, X. (2022). Leveraging artificial intelligence (AI) technology for English writing: Introducing Wordtune as a digital writing assistant for EFL writers. *RELC Journal*, *54*(3), 890-894. https://doi.org/10.1177/00336882221094089

Zhao, X. (2023). Leveraging artificial intelligence (AI) technology for English writing: Introducing Wordtune as a digital writing assistant for EFL writers. *RELC Journal*, *54*(3), 890-894. https://doi.org/10.1177/00336882221094089

APPENDIX

The list of 25 articles is as follows:

Abdelatif, K., & Siddiqui, A. (2021). Incorporating artificial intelligence (AI) tools in EFL classes at King Khalid University (KKU). *Journal of Tianjin University Science and Technology*, *54*(10), 197-221. https://doi.org/10.17605/OSF.IO/N7QSF

Al Mahmud, F. (2023). Investigating EFL students' writing skills through artificial intelligence: Wordtune application as a tool. *Journal of Language Teaching and Research*, *14*(5), 1395-1404. https://doi.org/10.17507/jltr.1405.28

Al-Garaady, J., & Albuhairy, M. M. (2023). ChatGPT's capabilities in spotting and analyzing writing errors experienced by EFL learners. *Arab World English Journal*, *9*(CALL), 3-17. https://doi.org/10.24093/awej/call9.1

Alharbi, W. (2023). The use and abuse of artificial intelligence-enabled machine translation in the EFL classroom: An exploratory study. *Journal of Education and e-Learning Research*, *10*(4), 689-701. https://doi.org/10.20448/jeelr.v10i4.5091

Alshumaimeri, Y. A., & Alshememry, A. K. (2023). The extent of AI applications in EFL learning and teaching. In *IEEE Transactions on Learning Technologies* (Vol. 17, pp. 653-663). IEEE. https://doi.org/10.1109/TLT.2023.3322128

An, X., Chai, C. S., Li, Y., Zhou, Y., & Yang, B. (2023). Modeling students' perceptions of artificial intelligence-assisted language learning. *Computer Assisted Language Learning*, 1-22. https://doi.org/10.1080/09588221.2023.2246519

Anggoro, K. J., & Pratiwi, D. I. (2023). Fostering self-assessment in English learning with a generative AI platform: A case of Quizizz AI. *Studies in Self-Access Learning Journal*, *14*(4), 489-501. https://doi.org/10.37237/140406

Annamalai, N., Eltahir, M. E., Zyoud, S. H., Soundrarajan, D., Zakarneh, B., & Al Salhi, N. R. (2023). Exploring English language learning via Chabot: A case study from a self-determination theory perspective. *Computers and Education: Artificial Intelligence*, *5*, 100148. https://doi.org/10.1016/j.caeai.2023.100148

Darwin., Rusdin, D., Mukminatien, N., Suryati, N., Laksmi, E. D., & Marzuki. (2024). Critical thinking in the AI era: An exploration of EFL students' perceptions, benefits, and limitations. *Cogent Education*, *11*(1), 2290342. https://doi.org/10.1080/2331186X.2023.2290342

Du, Y., & Gao, H. (2022). Determinants affecting teachers' adoption of AI-based applications in EFL context: An analysis of analytic hierarchy process. *Education and Information Technologies*, *27*, 9357-9384. https://doi.org/10.1007/s10639-022-11001-y

Fathi, J. Rahimi, M., Derakhshan, A. (2024). Improving EFL learners' speaking skills and willingness to communicate via artificial intelligence-mediated interactions, *System*, *121*, 103254. https://doi.org/10.1016/j.system.2024.103254

Fleckenstein, J., Meyer, J., Jansen, T., Keller, S. D., Köller, O., & Möller, J. (2024). Do teachers spot AI? Evaluating the detectability of AI-generated texts among student essays. *Computers and Education: Artificial Intelligence*, *6*, 100209. https://doi.org/10.1016/j.caeai.2024.100209

Jeon, J. (2021). Exploring AI chatbot affordances in the EFL classroom: Young learners' experiences and perspectives. *Computer Assisted Language Learning*, *37*(1-2), 1-26. https://doi.org/10.1080/09588221.2021.2021241

Jiang, R. (2022). How does artificial intelligence empower EFL teaching and learning nowadays? A review on artificial intelligence in the EFL context. *Frontiers in Psychology*, *13*, 1049401. https://doi.org/10.3389/fpsyg.2022.1049401

Kohnke, L., Moorhouse, B. L., & Zou, D. (2023). Exploring generative artificial intelligence preparedness among university language instructors: A case study. *Computers and Education: Artificial Intelligence*, *5*, 100156. https://doi.org/10.1016/j.caeai.2023.100156

Liu, M., Zhang, L. J., & Biebricher, C. (2024). Investigating students' cognitive processes in generative AI-assisted digital multimodal composing and traditional writing. *Computers and Education*, *211*, 104977. https://doi.org/10.1016/j.compedu.2023.104977

Madhavi, E., Sivapurapu, L., Koppula, V., Rani, P. B. E., & Sreehari, V. (2023). Developing learners' English-speaking skills using ICT and AI tools. *Journal of Advanced Research in Applied Sciences and Engineering Technology*, *32*(2), 142-153. https://doi.org/10.37934/araset.32.2.142153

Mizumoto, A., & Eguchi, M. (2023). Exploring the potential of using an AI language model for automated essay scoring. *Research Methods in Applied Linguistics*, *2*(2), 100050. https://doi.org/10.1016/j.rmal.2023.100050

Mohammadkarimi, E. (2023). Teachers' reflections on academic dishonesty in EFL students' writings in the era of artificial intelligence. *Journal of Applied Learning and Teaching*, *6*(2), 105-113. https://doi.org/10.37074/jalt.2023.6.2.10

Moorhouse, B. L. (2024). Beginning and first-year language teachers' readiness for the generative AI age. *Computers and Education: Artificial Intelligence*, *6*, 100201. https://doi.org/10.1016/j.caeai.2024.100201

Moulieswaran, N., & Prasantha Kumar, N. S. (2023). Investigating ESL learners' perception and problem towards artificial intelligence (AI)-assisted English language learning and teaching. *World Journal of English Language*, *13*(5), 290. https://doi.org/10.5430/wjel.v13n5p290

Qadir, J. (2022). *Engineering education in the era of ChatGPT: Promise and pitfalls of generative AI for education*. TechRxiv. https://doi.org/10.36227/techrxiv.21789434.v1

Shaffril, M. H. A., Samsuddin, S. F. & Samah, A. A. (2021). The ABC of systematic literature review: The basic methodological guidance for beginners. *Quality and Quantity*, *55*, 1319-1346. https://doi.org/10.1007/s11135-020-01059-6

Sharadgah, T. A., & Sa'di, R. A. (2022). A systematic review of research on the use of artificial intelligence in English language teaching and learning (2015–2021): What are the current effects? *Journal of Information Technology Education: Research*, *21*, 337–377. https://doi.org/10.28945/4999

Sun, Z., Anbarasan, M., & Praveen Kumar, D. (2021). Design of online intelligent English teaching platform based on artificial intelligence techniques. *Computational Intelligence*, *37*(3), 1166-1180. https://doi.org/10.1111/coin.12351

Pertanika J. Sci. & Technol. 33 (5): 2155 - 2176 (2025)

PERTANIKA JOURNALS

SCIENCE & TECHNOLOGY

Journal homepage: http://www.pertanika.upm.edu.my/

Face Detection and Gender Classification by YOLO Algorithm

Aseil Nadhim Kadhim*, Syahid Anuar and Saiful Adli Ismail

Fakulti Teknologi dan Informatik Razak, Universiti Teknologi Malaysia Kuala Lumpur, Jalan Sultan Yahya Petra, 54100 Kuala Lumpur, Malaysia

ABSTRACT

Gender classification is a fundamental computer vision problem used in a wide range of applications in surveillance and marketing. The work in this paper is to determine the gender classification ability of the You Only Look Once (YOLO) algorithm using deep learning. YOLO is one of the most accurate object detection models that can detect multiple objects in a video or picture in real-time. In this work, various versions of YOLO (YOLOv3 to YOLOv9) were compared to determine the most accurate and efficient model for gender classification. The work utilized a collection of 361 test images of male and female subjects in different scenarios of their settings, and the models' performance was gauged in terms of key metrics of Precision, Recall, and F1-score. The analysis of performance also confirmed that YOLOv9 was even better compared to its counterparts, registering a mean average precision (mAP) of 97%, a Precision of 86.8%, a Recall of 86.1%, and an F1-score of 86.54%. The processing time of the model was 0.332 seconds per picture, or a frame per second (FPS) of 3.00. The confusion matrix also recorded 157 true positives (TP), 25 false negatives (FN), 23 false positives (FP), and 156 true negatives (TN), a reflection of a highly balanced classification performance. The results confirm that YOLOv9 is highly accurate and efficient to use in gender classification in practical applications.

Keywords: Face detection, gender classification, object detection, YOLO

ARTICLE INFO

Article history:
Received: 18 October 2024
Accepted: 17 April 2025
Published: 28 August 2025

DOI: https://doi.org/10.47836/pjst.33.5.06

E-mail addresses:
n-20@graduate.utm.my (Aseil Nadhim Kadhim)
syahid.anuar@utm.my (Syahid Anuar)
saifuladli@utm.my (Saiful Adli Ismail)
* Corresponding author

INTRODUCTION

Gender classification is one of the most important applications of computer vision in surveillance, security, and marketing (Xiao et al., 2020). The gender is automatically classified in terms of a human's face features (Varnima & Ramachandran, 2020) using deep learning to be more accurate and efficient (Jabraelzadeh et al., 2023; Tilki et

e-ISSN: 2231-8526

al., 2021). Unlike traditional methods that apply hand-coded features, more recent deep learning methods, such as YOLO, enable gender classification in real-time straight from pictures (Sonthi et al., 2023). YOLO is a widely used object detection approach that can identify multiple objects in a single picture. The more recent versions of YOLO, such as YOLOv9, execute face detection and gender classification in a single step of inference without separate preprocessing procedures. This enhances processing time, in addition to improving precision in classification (Tejaswi et al., 2023). There have been various studies that have explored gender recognition using deep learning, noting that models that employ convolutional neural networks (CNN) in face feature processing work (Azhar et al., 2022). This study compares different versions of YOLO in gender classification based on a set of tagged face pictures. The aim is to determine the most efficient YOLO model that can be applied in gender classification in a way that is applicable in real-time and in a diverse range of situations (Ayo et al., 2022).

RELATED WORKS

With the increasing use of artificial intelligence in various sectors, face detection and gender identification between men and women pose primary challenges in security, surveillance, and data analysis. Gender identification is of crucial significance in various situations, such as in identity recognition systems, behavioral analysis, and enhancing the user experience in smart services. From a security aspect, face detection and gender identification models of high efficiency need to be developed, mainly in areas of public use such as airports and stations (Awan et al., 2021; Ayo et al., 2022; Singh et al., 2021). Several models of gender identification in real-time via CNN have been put forward (Xiao et al., 2020). The traditional method of CNN is separated into two key stages (Sumi et al., 2021) and has evolved in different ways, i.e., R-CNN, Fast-RCNN, and Faster-RCNN. Although CNN is found to be extremely efficient in gender detection, it is also afflicted with a set of serious limitations, i.e., (1) multiple stages of training, (2) high memory and computational demands, and (3) slower detection compared to other methods, rendering detection speed enhancement a necessity (Raman et al., 2023; Ramya et al., 2022). On the contrary, YOLO models have gained immense popularity in face detection and gender recognition due to their high efficiency and speed. As compared to CNN-based approaches, YOLO processes one entire picture in a one-time step, in keeping with the "You Only Look Once" method, rendering it much more efficient (Raman et al., 2023; Ramya et al., 2022). Given these advantages, this work is focused on comparing and evaluating different YOLO models to determine the most efficient one to apply in real-time face detection and gender recognition. The latest one, YOLOv9, is selected here because it is more computationally efficient compared to previous versions of YOLO. However, challenges in gender classification accuracy in public places persist. Hence, it is important to evaluate YOLO models in such an environment

(Sonthi et al., 2023). Consequently, this work attempts to compare various implementations of YOLO to determine the most appropriate model for face detection in real-time in actual applications (Jabraelzadeh et al., 2023).

Face Detection

Face detection is a fundamental computer vision problem, and various methods of making it more accurate and efficient have been proposed (Sonthi et al., 2023). Even though face recognition is one of computer vision's fundamental challenges, there have been proposals in the literature to process face features. The face detection is a beginning point in this process, given that it facilitates gender identification using face-based properties (Tejaswi et al., 2023).

Gender Classification

Gender classification is a crucial aspect of social interaction in most intelligent applications, i.e., human-machine interaction (Ayo et al., 2022; Azhar et al., 2022). The most effective method of gender classification is face image analysis, and face detection is a fundamental starting process in gender classification (Awan et al., 2021; Singh et al., 2021). Research has extensively explored various gender classification methods, of which face-based methods predominate (Mittal et al., 2023). The face detection coupled with gender classification is of interest in scientific research (Jabraelzadeh et al., 2020; Shet et al., 2022). This study is distinct in using face feature analysis in gender identification (Shen et al., 2021), one of the most accurate yet practical approaches in real applications (Al-Bayati & Abood, 2023; Alsaif et al., 2023; Srinivasan, 2023).

Detection Algorithms

Object detection and classification models can be divided into two groups of interest: one is region-based classification using CNN, and the other is one-stage models like YOLO. The models using CNN follow a two-stage approach of classification (Dutta et al., 2022; Ullah, 2020). However, despite their accuracy, there also lie certain limitations of CNN models, such as multiple processes of training and high demands on computation, thus making it slower compared to other approaches (Nepal & Eslamiat, 2022; Srikar & Malathi, 2022). YOLO, on the other hand, detects and classifies in a single step without a separate phase of classification. The combined approach enhances speed in addition to precision, making YOLO more suitable in real-time applications (Eşer & Hardalaç, 2021; F. Wang et al., 2023; Gan et al., 2023; Jiang et al., 2022; Thakuria & Erkinbaev, 2023; W. Wang et al., 2023; Zhang et al., 2020). Due to its efficiency, YOLO is widely used in face detection and gender classification, where real-time performance is essential.

Research Goal

This study seeks to assess YOLO models in gender classification, i.e., whether a detected face is male or female. Considering that existing studies affirm YOLO's speed over CNN, this work aims to compare various versions of YOLO to determine the most accurate and efficient of these models in real-time applications for gender classification.

MATERIALS AND METHODS

This study attempts to determine the effectiveness of YOLO-based deep learning models in face detection and gender recognition. Compared to methods that use separate face detection and classification networks, YOLO brings the two processes in one system, making it more efficient and capable of real-time processing. The primary objective of this work is to find the best YOLO model for gender classification in terms of its accuracy, inference time, and resource requirements.

The methodology is a sequential process of ordered processes that encompasses data collection, image preprocessing, augmentation, model training, evaluation, and comparative analysis. The work is divided into two major phases: first, YOLO models are used to detect faces to accurately detect and cut faces out of pictures. Then, in phase two, the same YOLO model is used to classify gender directly, in which each face is automatically categorized as male or female without applying an external classifier. This integrated approach ensures a seamless and optimized classification process, making YOLO a robust solution for real-time gender classification.

Data Collection

The dataset for this study was collected from the students at the University of Babylon, Iraq, ensuring diverse real-world conditions to enhance model robustness. Images were captured under various lighting conditions (sunlight, cloudy, backlighting) and different facial angles (frontal, side, tilted) to improve detection accuracy. The dataset includes individuals with and without head coverings, varying age groups, and diverse facial expressions. Partial occlusions due to environmental factors were also considered to simulate real-world challenges. A total of 140 images were collected, ensuring the trained model's reliability across different scenarios. Figure 1 shows examples of photos of people's faces.

Image Processing and Data Segmentation with Augmentation

A systematic preprocessing and augmentation strategy was applied to optimize the dataset for training and evaluation. Initially, the dataset consisted of 140 high-quality images captured most within the university campus, encompassing diverse lighting conditions, facial orientations, and real-world variations. To standardize input dimensions, all images

Figure 1. Examples of student photos taken in various settings: (a) Normal frontal face image, (b) Natural light angle, (c) Heavy occlusion (e.g., glasses or mask), (d) Side light angle, (e) Overlapping group of students, and (f) Backlight angle

were resized to 640 × 640 pixels and converted to grayscale, with pixel values normalized within the 0 to 1 range for consistency in model interpretation. Facial features were emphasized by cropping each image to retain 25 to 75% of both horizontal and vertical regions, minimizing background interference. Additionally, images were segmented into a 2 × 2 grid (four equal parts) to enhance localized feature extraction, improving the precision of face detection and gender classification.

To further enhance model generalization and prevent overfitting, 25% of the dataset underwent augmentation, incorporating horizontal and vertical flipping, cropping adjustments, hue modifications (+25° to -25°), brightness variations (±25%), and Gaussian blurring (up to 2.5 pixels) to introduce controlled noise. The Static Crop function was also utilized to generate more variations by flipping images over specific areas and axes to enrich the dataset even further Figure 2.

As a result of expansion and segmentation, the dataset was increased to 361 images to give a more representative and diverse set of training. The final dataset was divided into three groups: 316 for training to learn to better optimize the YOLO model, 30 for validating to set hyperparameters and to prevent overfitting, and 15 for final testing to verify generalization performance. The new structured data preprocessing approach significantly improved gender recognition using YOLO to be more resilient in various practical situations Figure 3.

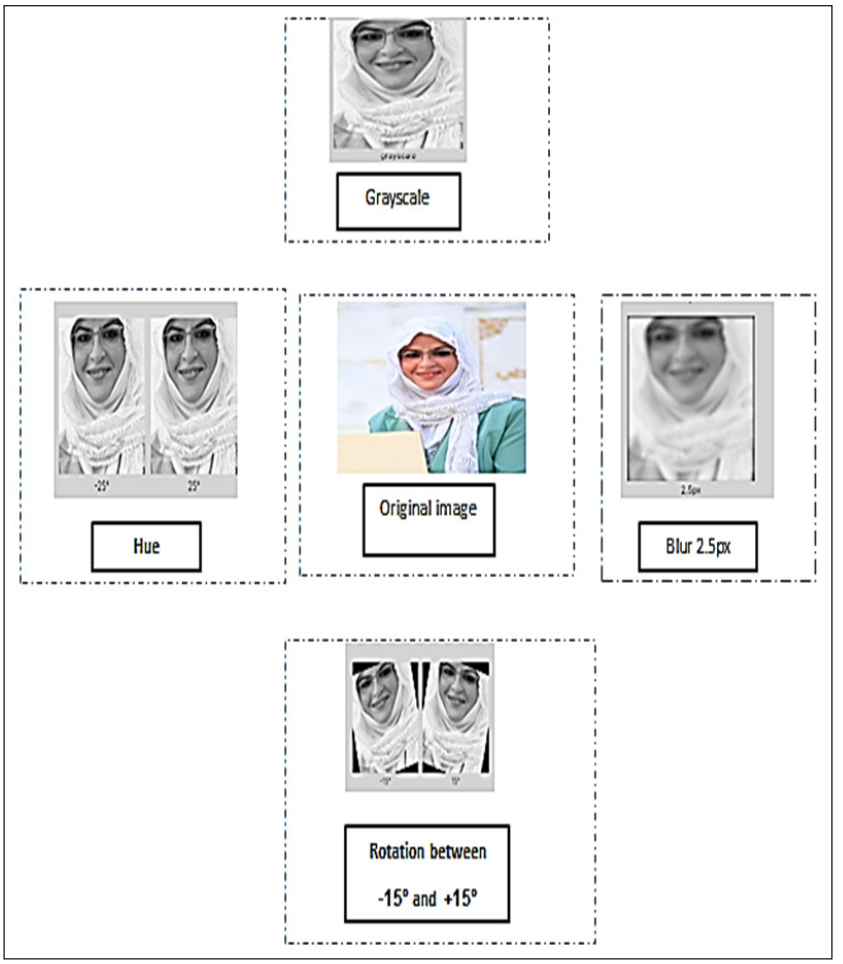

Figure 2. Image processing and data set segmentation

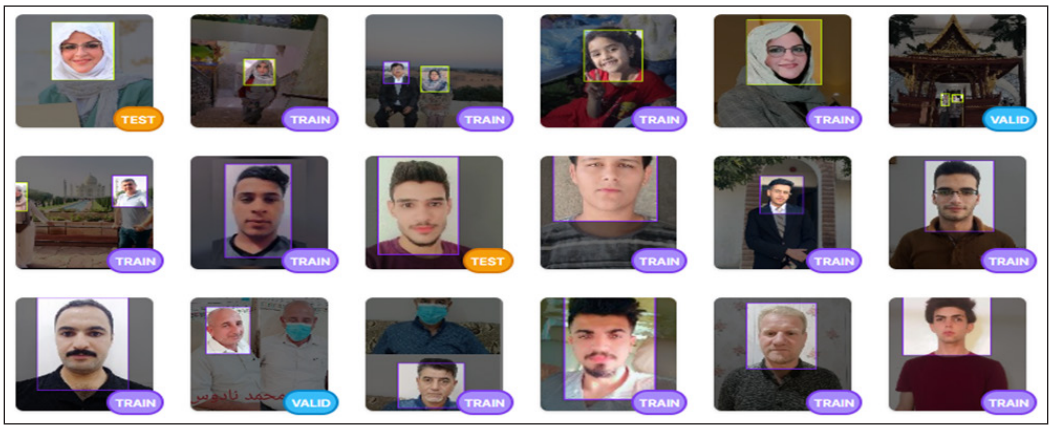

Figure 3. Augmented training set and distributed

YOLOv9 Network Architecture

YOLOv9 represents a milestone in one-stage object detection models that is intended to find a balance between speed and accuracy in real-time applications. As per benchmark tests, YOLOv9 can process between 5 and 160 frames per second (FPS), depending on hardware specifications and input resolution (Figure 4). Overview of the proposed research process, including training and testing phases using YOLO-based gender classification. (Acharya, 2024a; Boesch, 2024). The network architecture is structured into three primary components:

- Internal Network: Handles data preprocessing and feature extraction.
- Core Network: Obtains high-level representations to facilitate object recognition.
- Main Network: Carries out end detection and classification processes.

Key enhancements:

- Object detection in real-time: Maintains high detection speed without sacrificing precision.
- Programmable Gradient Information (PGI) integration: A stand-alone process in YOLOv9 that allows smooth flow of information and reduces loss of features to support better model efficacy and accuracy.
- Cross Stage Partial Network (CSPNet): Improves computational efficiency and reduces memory requirements by splitting features into two streams and merging them afterwards.
- Generalized Efficient Layer Aggregation Network (GELAN): An advanced version of ELAN that enhances computational efficiency, reduces resource use, and enhances accuracy and inference time.
- ELAN (Efficient Layer Aggregation Network): Enhances information flow within the network, reducing feature loss and improving deep learning.
- Improved performance: Outperforms state-of-the-art models on datasets like MS COCO, excelling in accuracy, speed, and overall efficiency for real-time gender classification (C.-Y. Wang et al., 2024).

Here is a step-by-step process of detection using the YOLOv9 model:

1. Input Processing: The model segments input images into a grid of cells, each responsible for detecting objects within its assigned region.
2. Bounding Box Prediction: YOLOv9 generates bounding boxes for detected objects, defining their position using x, y (center point), width, and height.

3. Object Classification: Each bounding box is assigned a classification probability, determining the likelihood that it belongs to a specific class.
4. Non-Maximum Suppression: To refine detections, redundant bounding boxes are filtered based on confidence scores, ensuring accurate localization.
5. Post-Processing: After suppression, the most reliable bounding boxes are retained, enabling precise real-time detection (Boesch, 2024; C.-Y. Wang et al., 2024).

YOLOv9 integrates PGI for reliable gradient generation and deep feature retention, while GELAN optimizes parameters, accuracy, and inference speed for enhanced efficiency (Boesch, 2024; C.-Y. Wang et al., 2024) as shown in Figure 5.

Training Platform and Parameter Settings

This study applied transfer learning with the use of the YOLOv9 algorithm in gender identification, leveraging its object detection in real-time. Training was done using Google Colab on a Tesla T4 GPU to provide high processing capability. To ensure that it was working to its optimal capacity, it was trained for 300 epochs at a batch size of 16 samples per iteration and an input image size of 640 × 640 pixels. The learning rate was initially set to 0.001 and was dynamically adjusted during training to facilitate better convergence and model stability.

Model Establishment and Assessment Indicators

Establishment of Model

After dataset preprocessing (as described in the methodology), the YOLOv9 model was trained using the allocated training set and optimized through validation. The final model performance was then assessed on the test set to ensure its effectiveness in gender classification. The evaluation process and performance results are illustrated in Figure 4.

Model Evaluation

For quantification, the Complete Intersection Over Union (CIOU) loss function was employed. The difference between the calibration and prediction squares was analyzed effectively (Zheng et al., 2020) with A representing the calibration bin, B representing the prediction bin, and L1 representing the distance. It shows the specifications based on the model's predicted and validation bins required for computing the CIOU. The diagonal length, or L2, is the separation between the centroids of minimum-Square Rectangle A and B.

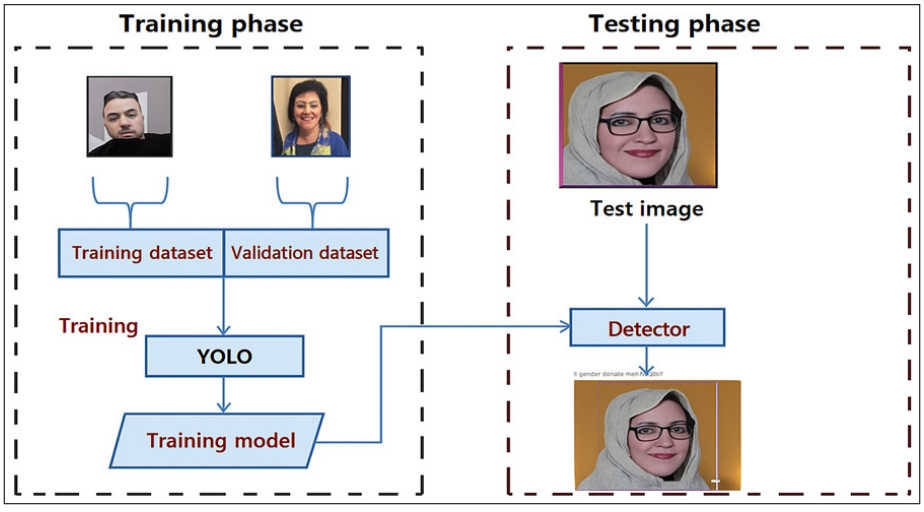

Figure 4. Process of the suggested research

A visual representation of the CIOU computation between the ground truth and the model prediction box is shown in Figure 6. The blue box represents the prediction box, while the calibration box is represented by the yellow box.

CIOU was calculated as follows (Equation 1):

$$Loss_{CIou}=1-IOU+\frac{L1^2}{L2^2}+\alpha v \quad [1]$$

where α is the balancing component among the loss brought on by Intersection over Union (IOU) and V, and v is the aspect ratio similarity between boxes A and B. The study employed the following metrics F1 score, recall, precision, and mAP to evaluate model performance in an impartial and consistent manner. Accuracy, which is determined by dividing the total number of detected targets by the number of correct targets, is the most commonly used evaluation index. In general, accuracy increases detection efficacy. While high precision is necessary for grading, it is not usually indicative of genius. Therefore, to assess comprehensiveness, mAP, recall, and F1 are shown. This section displays the calculations for the mAP, F1, recall, precision, and F1 outcomes (Achary, 2024b):

$$\text{Precision}, p=\frac{\text{TP}}{\text{TP+FP}}\times 100\% \quad [2]$$

$$\text{Recall}, \text{R}=\frac{\text{TP}}{\text{TP+FN}}\times 100\% \quad [3]$$

$$\text{Average Precision}, \text{AP}=\text{P}\int_0^1.(\text{r})\text{dr} \quad [4]$$

$$\text{Mean Average Precision, mAP} = \frac{1}{n} \sum_{i=1}^{n} AP1 \quad [5]$$

$$\text{F1 score, F1} = 2 \times \frac{P \times R}{P + R} \quad [6]$$

False negative (FN) refers to the total number of gender-related objects that were not identified or ignored. In contrast, false positive (FP) represents the percentage of objects that

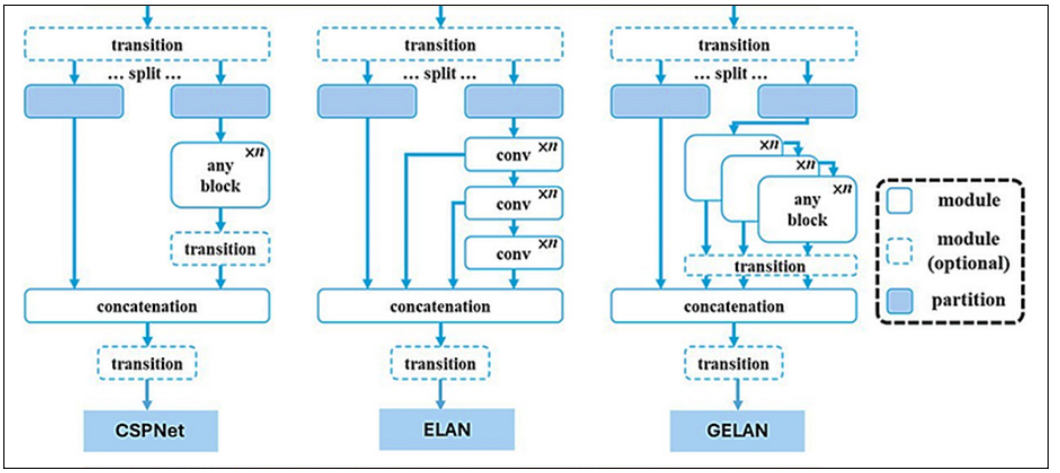

Figure 5. Architecture of YOLOv9 network (Yaseen, 2024)
Note. CSPNet = Cross Stage Partial Network; ELAN = Efficient Layer Aggregation Network; GELAN = Generalized Efficient Layer Aggregation Network

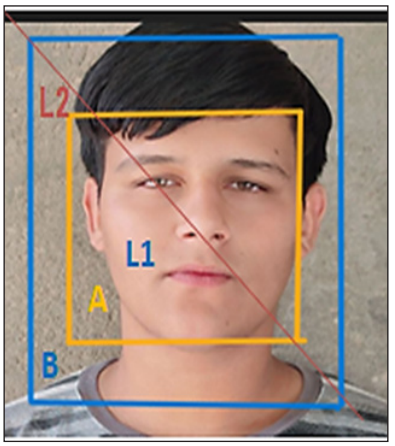

Figure 6. The prediction box
Note. A = Calibration (ground truth) box; B = Predicted box by the model; L1 = Euclidean distance between the centroids of boxes A and B; L2 = Diagonal length of the smallest enclosing box covering both A and B (used for Complete Intersection Over Union [CIOU] calculation)

were misidentified as gender. True positive (TP) refers to the number of objects correctly identified as a gender.

RESULTS AND DISCUSSION

Training Dataset of YOLO Models

Figure 7 shows an example of the complete pipeline used for gender classification and gender recognition results. The red color represents the category designated for men, and the blue color represents the category designated for women. During testing of images using YOLO models, it was discovered that the YOLOv9 algorithm achieved the highest detection accuracy.

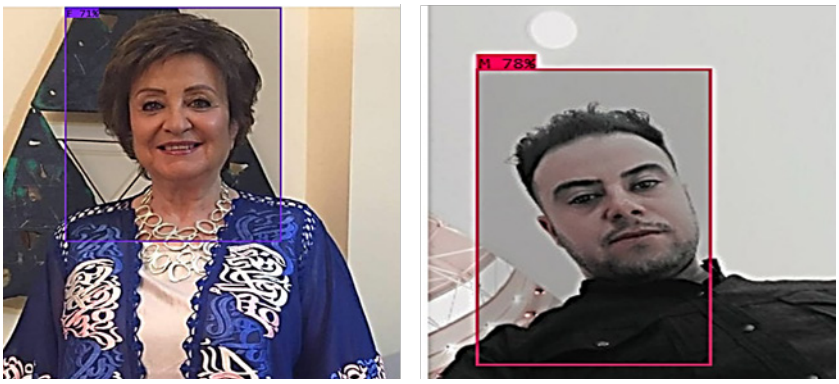

Figure 7. Results of the real-time gender classification

Using the YOLOv9 algorithm, gender detection has achieved accuracy rates of up to 97%. Figure 8 illustrates the mAP values for this model. Overall, YOLOv9 surpasses YOLOv8 and other YOLO versions in terms of speed, accuracy, and scalability. This performance enhancement is attributed to advancements in model architecture, improved training techniques, and the integration of new features such as PGI and GELAN.

The loss curves of YOLOv9 in Figure 9 reflect a constantly improving performance coupled with stabilization of models during learning. Both Box Loss and Object Loss exhibit a steep decline that is subsequently followed by stabilization, indicating improving precision in object localization. Similarly, Class Loss reduces steeply in early training stages and plateaus at a low value, suggesting the strength of the model in gender classification. The patterns also suggest YOLOv9's capability of learning in a more efficient manner and having a high performance, making it a reliable model for gender classification.

The loss curves of YOLOv8 in Figure 10 exhibit progressive learning and stabilization during training. Box Loss and Object Loss decline steeply in earlier epochs and stabilize to smaller values, suggesting improved object localization. Similarly, Class Loss also drops

steeply and remains low, demonstrating effective gender classification. However, compared to YOLOv9, YOLOv8 displays slightly more oscillations, suggesting potential instability in a number of its phases. The results verify that even though YOLOv8 is efficient in learning and has a faster convergence, YOLOv9 is a better model due to its higher stability and overall performance in gender classification.

The loss curves of YOLOv7 in Figure 11 exhibit a smooth improvement in performance during training, though there is a visible oscillation. Both Box Loss and Object Loss decrease steeply initially, after that there is a slower stabilization, indicating improvement in object localization though there is a lack of stability. Class Loss has high fluctuations prior to stabilization, suggesting gender classification to be less stable in learning compared to newer models. Compared to YOLOv8 and YOLOv9, YOLOv7 is more volatile in loss values, suggesting less stable convergence. These trends highlight that while YOLOv7 achieves reasonable performance, YOLOv9 remains the most stable and accurate model for gender classification.

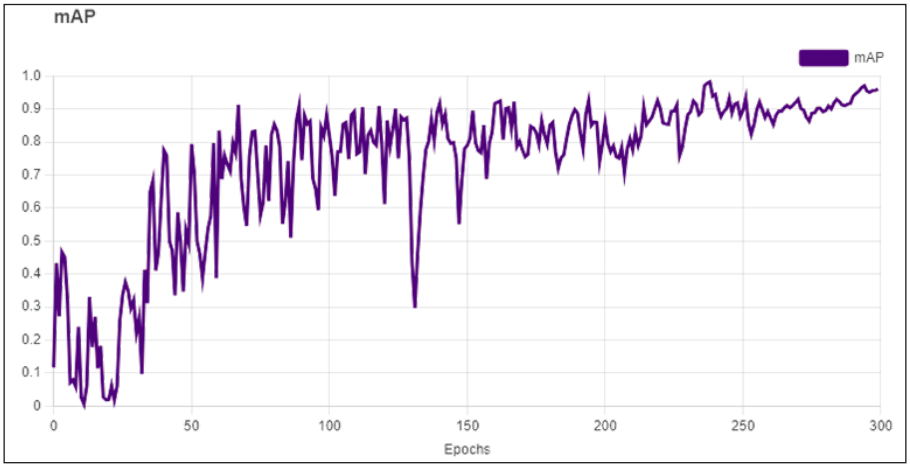

Figure 8. Mean average precision (mAP) accuracy of the YOLOv9 model for gender detection

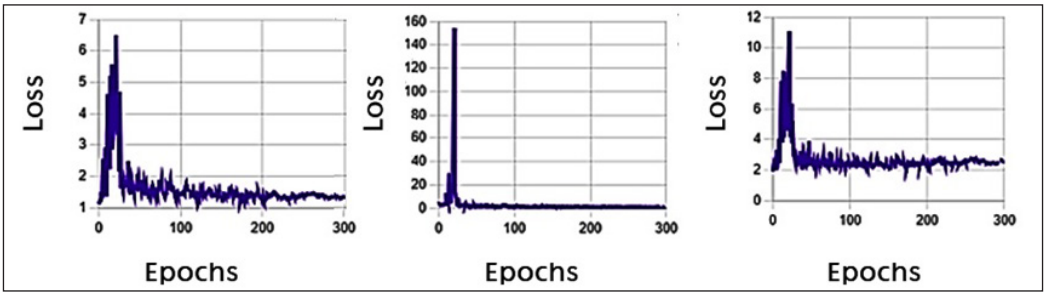

(a) (b) (c)

Figure 9. Loss curve of the Yolov9 model training: (a) Box Loss; (b) Class Loss; (c) Object Loss

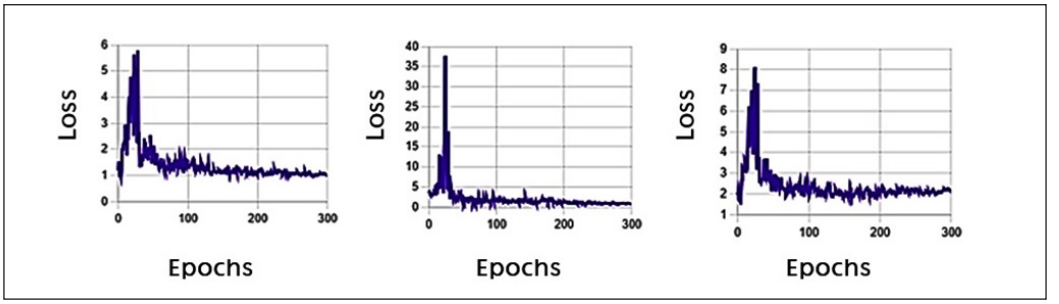

(a) (b) (c)

Figure 10. Loss curve of the Yolov8 model training: (a) Box Loss; (b) Class Loss; (c) Object Loss

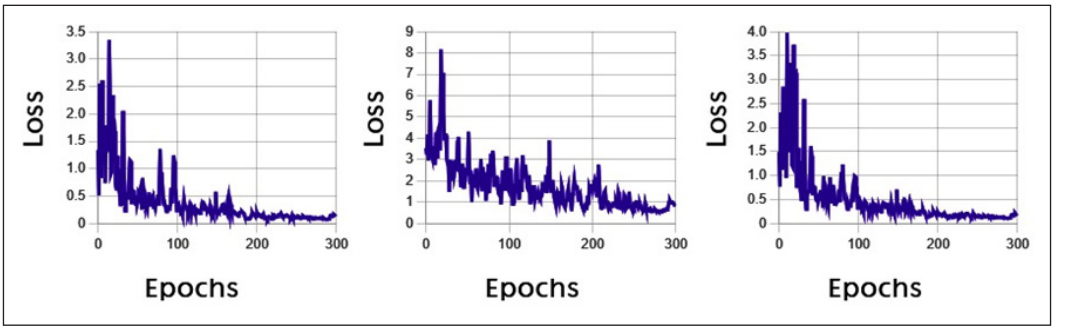

(a) (b) (c)

Figure 11. Loss curve of the YOLOv7 model training: (a) Box Loss; (b) Class Loss; (c) Object Loss

The loss curves of YOLOv5 in Figure 12 display a steep initial decline in Object Loss and Box Loss, subsequently levelling off, suggesting improvement in localization. The Class Loss oscillates to stabilize, suggesting learning progressively. However, compared to YOLOv9, YOLOv5 displays higher variance and a slower convergence rate, justifying its lower stability and accuracy in gender classification.

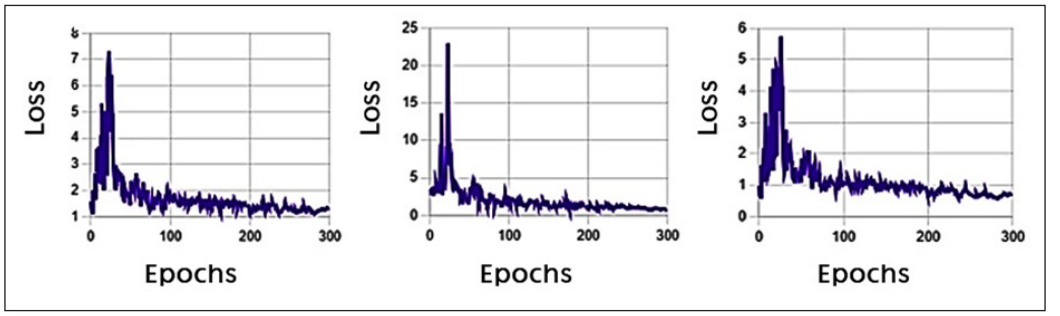

(a) (b) (c)

Figure 12. Loss curve of the Yolov5 model training: (a) Object Loss; (b) Class Loss; (c) Box Loss

The loss curves of YOLOv4 in Figure 13 display a steep initial decline in Object Loss and Box Loss, after which they stabilize over time. Class Loss steeply drops but oscillates before it eventually converges, indicating a moderate learning efficiency. YOLOv4 is more variant and slower to converge than YOLOv9, validating that it is less accurate and more unstable in gender classification.

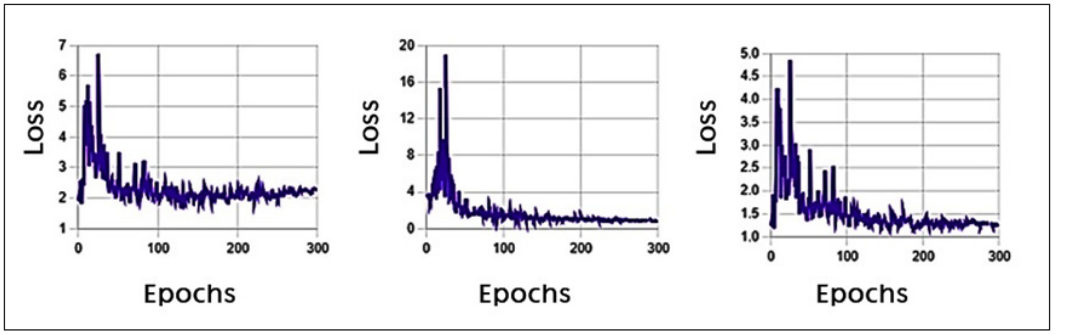

(a) (b) (c)

Figure 13. Loss curve of the Yolov4 model training: (a) Object Loss; (b) Class Loss; (c) Box Loss

The loss curves of YOLOv3 Figure 14 indicate a steep initial decline coupled with apparent oscillations, more evidently in Class Loss, indicating unstable learning. Object Loss and Box Loss take a slower time to converge compared to newer models of YOLO. The patterns confirm that YOLOv3 is of lower precision and stability, hence less accurate in gender classification.

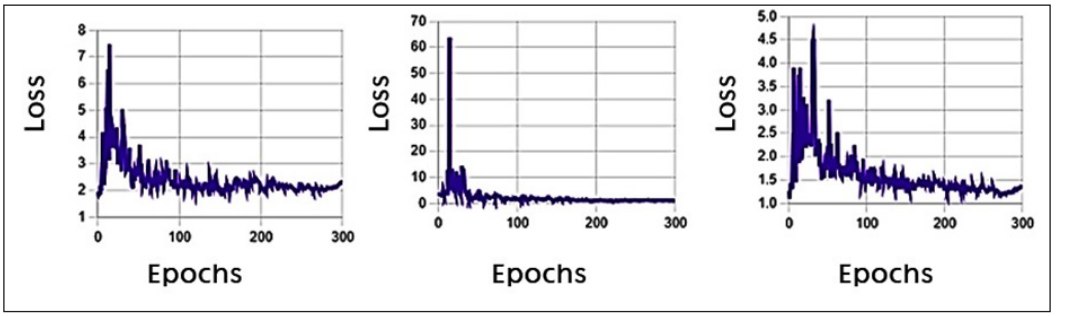

(a) (b) (c)

Figure 14. Loss curve of the Yolov3 model training: (a) Object Loss; (b) Class Loss; (c) Box Loss

Comparison of Models

The results demonstrate a progressive improvement in the performance of YOLO models, from YOLOv3 to YOLOv9, with newer versions exhibiting enhanced accuracy, inference speed, and training efficiency. YOLOv9 achieved the highest mAP (97%) with the fastest

inference time (0.332 seconds per image, FPS = 3.00), making it the most efficient for real-time applications. YOLOv8 (mAP = 96.2%) followed closely, offering the best balance between precision and recall (F1-score = 91.82%), ensuring reliable classification with minimal errors. YOLOv7 (mAP = 94.4%) performed well but was slightly less efficient than the more recent versions. In terms of inference speed, the latest versions demonstrated superior performance, with YOLOv9 being the fastest (0.332 seconds per image, FPS = 3.00), followed by YOLOv8 (0.379 seconds, FPS = 2.63). In contrast, older models such as YOLOv3 and YOLOv4 exhibited significantly slower inference times (0.759 and 0.648 seconds, respectively), making them less suitable for real-time applications requiring immediate processing. Regarding training time, YOLOv9 required the shortest duration (1:45:00 hours) compared to YOLOv3 (4:00:00 hours), reflecting advancements in algorithm optimization and architectural efficiency as shown in Table 1. These findings confirm that YOLOv9 is the most effective and reliable model for gender classification, followed by YOLOv8 as the optimal balance between accuracy and performance, while older versions demonstrate lower efficiency, making them less suitable for modern, high-performance applications, as shown in Figure 15.

The analysis of error rates across YOLO models confirms YOLOv9 as a highly reliable model, achieving a strong balance between precision and recall. While YOLOv8 recorded the lowest total error count (FP + FN = 29), YOLOv9 (FP = 23, FN = 25, total errors = 48) demonstrated superior stability and consistency, making it highly effective in maintaining classification accuracy. Additionally, YOLOv9's structure is highly optimized to limit false positives compared to older models, resulting in fewer incorrect detections. In contrast, YOLOv3 was associated with the highest error rate (FP + FN = 59), a reflection of inferior reliability. The results point to YOLOv9 to be a highly efficient model of high detection strength that is a competitive candidate for real-time classification, as shown in Figure 16 and Table 2.

Table 1
Performance comparison among different YOLO models

Target detection networks	mAP (%)	Precision (%)	Recall (%)	F1 score (%)	Inference time per image	Frames per second	Training time
YOLO v3	83.0	84.3	82.4	83.32	0.759	1.31	4:00:00 sec
YOLO v4	89.6	85.1	86.6	85.84	0.648	1.54	3:25:00 sec
YOLOv5	84.1	87.7	83.4	85.49	0.604	1.65	3:11:00 sec
YOLOv7	94.4	87.9	85.3	86.58	0.427	2.34	2:15:00 sec
YOLOv8	96.2	88.7	95.2	91.82	0.379	2.63	2:00:00 sec
YOLOv9	97	86.8	86.1	86.54	0.332	3.00	1:45:00 sec

Note. YOLO = You Only Look Once; mAP = Mean average precision

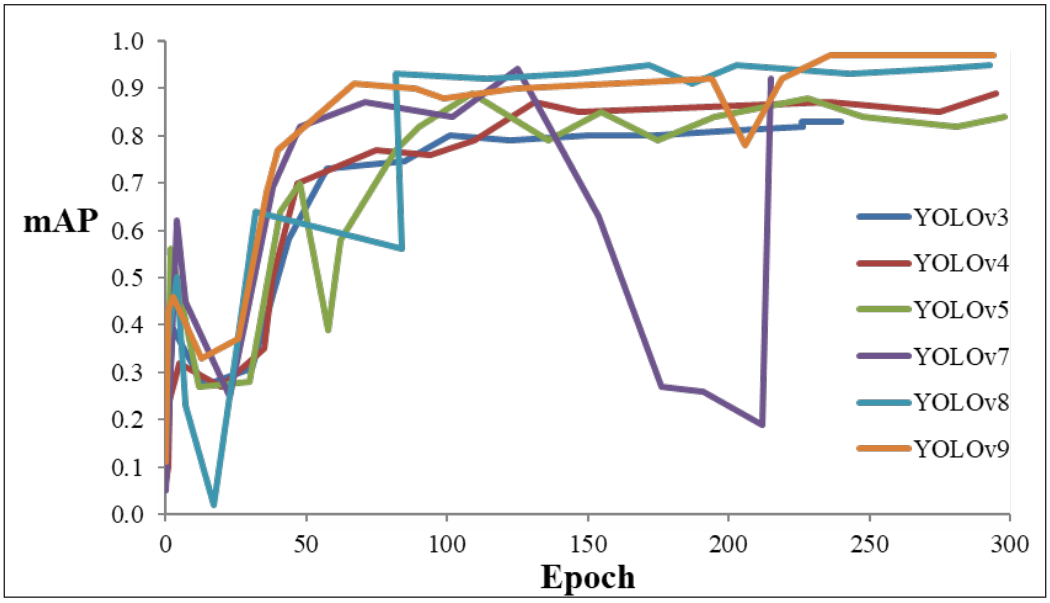

Figure 15. Mean average precision (mAP) accuracy of You Only Look Once (YOLO) models for gender detection

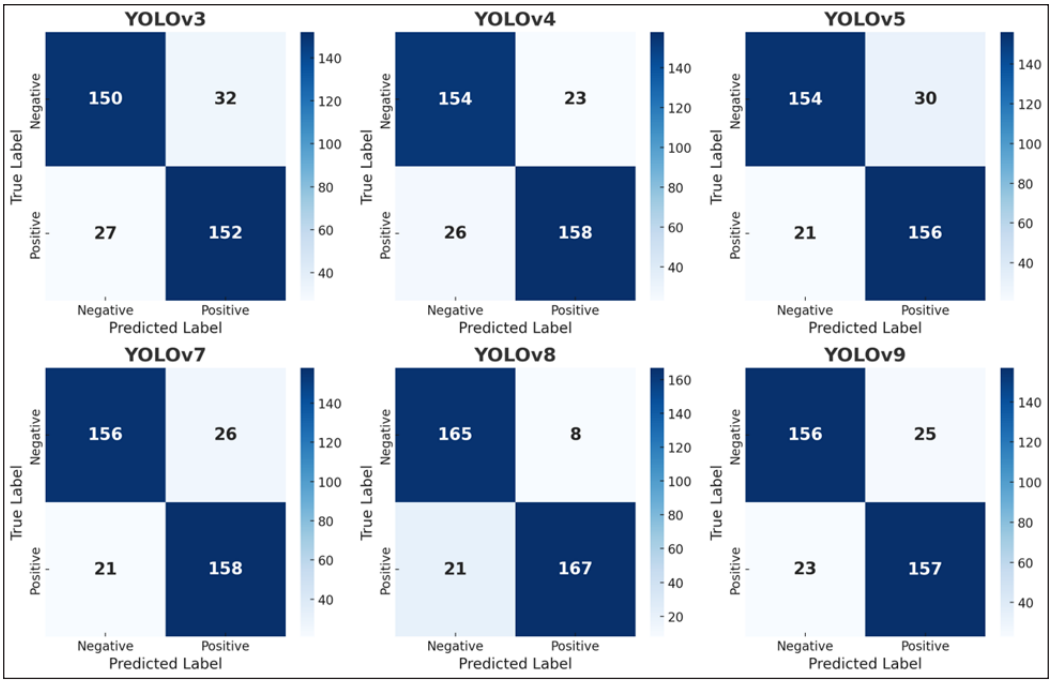

Figure 16. Confusion matrix analysis for the You Only Look Once (YOLO) models

Table 2
Confusion matrix analysis for the You Only Look Once (YOLO) models

Model	True positives (TP)	False negatives (FN)	False positives (FP)	True negatives (TN)
YOLO v3	152	32	27	150
YOLO v4	158	26	23	154
YOLOv5	156	30	21	154
YOLOv7	158	26	21	156
YOLOv8	167	8	21	165
YOLOv9	157	25	23	156

Used PyTorch Grad-CAM to visualize the most responsible areas in the YOLOv9 decision-making process in classifying gender. The results revealed that the model is primarily observing eyes and mouth, both of which are biological features used in classifying between genders. This proves that YOLOv9 relies on patterns learned that are in agreement with human vision, contributing to its classification accuracy.

In addition to that, Canny Edge Detection with OpenCV has been employed in analyzing structural features that are recognized by the model as critical. The outcome indicates that YOLOv9 is heavily dependent on the sharp edges of faces, particularly the jawline edge, eyebrow curve edge, and nose and mouth edges. This is a pointer that the model classifies based on patterns in face architecture and is quite sensitive to image quality changes, lighting conditions, and complexity of the environment.

The results revealed that Grad-CAM approximately 31.48% of the image consists of very active regions, which confirms that the model is focusing on significant face features such as eyes and mouth. Canny Edge Detection analysis, on the other hand, revealed that 5.70% of the image consists of sharp edges around the jawline, eyebrows, and mouth, which confirms that in its classification process, YOLOv9 is largely reliant on structural face features.

Although YOLOv9 is good at recognizing large-scale face features and effectively analyzing visual patterns for classifying gender. This reliance implies that the model's classification performance would be susceptible to low lighting conditions, noise, or distractions in the scene. The results, as observed in Figure 17, present a full picture of YOLOv9's feature selection mechanism and confirm that its decision process is both edge-dependent and biologically meaningful.

A one-way analysis of variance (ANOVA) was conducted using Python's SciPy library to determine if different YOLO models (YOLOv3 to YOLOv9) varied in their performance statistically. Five trial results for each model were utilized to provide consistency in results in terms of mean average precision (mAP) values. The analysis also confirmed statistically significant differences ($F = 8993.63$, $P < 0.05$), implying that observed gains in

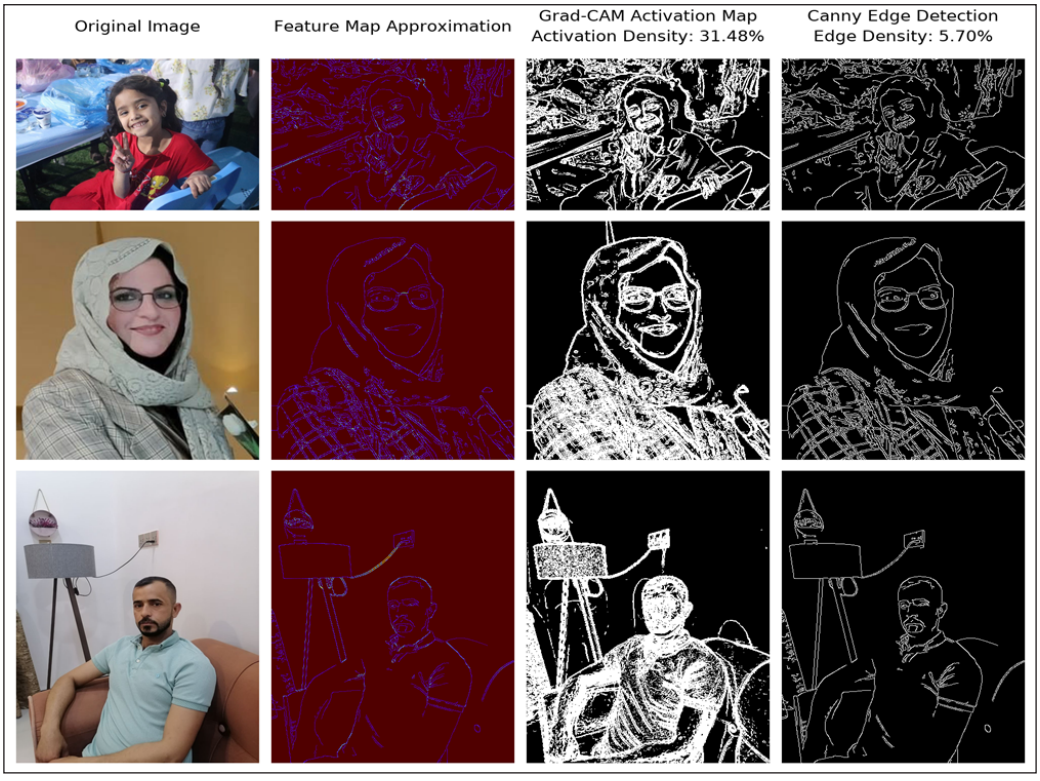

Figure 17. Feature visualization and model analysis for the YOLOv9 in gender classification

YOLOv9 and YOLOv8 are not a function of random variance but a genuine improvement in performance. The results affirm that architectural advances in newer versions of YOLO have been a primary force in detection precision, as shown in Table 3.

Table 3
Mean average precision (mAP) values across five trials for YOLO models

YOLOv9 (mAP %)	YOLOv8 (mAP %)	YOLOv7 (mAP %)	YOLOv5 (mAP %)	YOLO v4 (mAP %)	YOLO v3 (mAP %)	Epoch
97.3	96.4	93.9	84.4	89.2	83.0	1
96.9	96.1	94.2	84.1	89.8	82.8	2
97.1	95.8	94.1	83.8	89.1	83.1	3
97.2	96.3	94.5	84.3	88.9	82.9	4
97	96.2	94.4	84.1	89.6	83.0	5

Practical Applications and Future Directions

YOLOv9's real-time performance (FPS = 3.00) is ideal for applications that need quick decision-making, e.g., automated surveillance, biometric identification, and AI-based

customer engagement. Deployment is still a challenge, though, mainly in terms of computational requirements and privacy-sensitive settings. Future research must explore optimization techniques, i.e., quantization and model pruning, to enable it to be used in low-power embedded systems.

While YOLOv9 is highly performing, pairing it with a more accurate approach would also increase classification precision and credibility. Further enhancement would be introduced by expanding examinations using real-world datasets to enable flexibility in different demographic and environmental settings.

CONCLUSION

This study showed a progressive improvement of the YOLO models (YOLOv3–YOLOv9) in gender classification, of which YOLOv9 was found to be most accurate (mAP = 97%) and most precise (86.8%) in nature, making it most efficient for use in real-time. Despite its advancement, YOLOv9 is also afflicted with high computational demands and misclassification in complex situations. The efforts in the coming times must be focused on optimization strategies and fusion of higher-accurate methods to enhance robustness and flexibility in a diverse set of real-world applications.

ACKNOWLEDGEMENTS

The authors would like to thank Universiti Teknologi Malaysia for their academic support throughout the completion of this research.

REFERENCES

Acharya, A. (2024a). *YOLOv9: SOTA object detection model explain*ed. Encord. https://encord.com/blog/yolov9-sota-machine-learning-object-dection-model/

Acharya, A. (2024b). *Comparative analysis of YOLOv9 and YOLOv8 using custom dataset on encord active*. Encord. https://encord.com/blog/performanceyolov9-vs-yolov8-custom-dataset/

Al-Bayati, R. E., & Abood, Z. M. (2023). Comparison between gait recognizing algorithms. *Mustansiriyah Journal of Pure and Applied Sciences*, *1*(1), 133–139.

Alsaif, O. I., Hasan, S. Q., & Maray, A. H. (2023). Using a structural model for human gait gender recognition. *IAES International Journal of Artificial Intelligence*, *12*(2), 974–983. https://doi.org/10.11591/ijai.v12.i2.pp974-983

Awan, M. J., Raza, A., Yasin, A., Shehzad, H. M. F., & Butt, I. (2021). The customized convolutional neural network of face emotion expression classification. *Annals of the Romanian Society for Cell Biology*, *25*(6), 5296–5304.

Ayo, F. E., Mustapha, A. M., Braimah, J. A., & Aina, D. A. (2022). Geometric analysis and YOLO algorithm for automatic face detection system in a security setting. In *Journal of Physics: Conference Series* (Vol. 2199, No. 1, p. 012010). IOP Publishing. https://doi.org/10.1088/1742-6596/2199/1/012010

Azhar, M., Ullah, S., Ullah, K., Rahman, K. U., Khan, A., Eldin, S. M., & Ghamry, N. A. (2022). Real-time dynamic and multi-view gait-based gender classification using lower-body joints. *Electronics*, *12*(1), 118. https://doi.org/10.3390/electronics12010118

Boesch, G. (2024). *YOLOv9: Advancements in real-time object detection*. Viso.ai. https://viso.ai/computer-vision/yolov9/

Dutta, A., Atik, A., Bhadra, M., Pal, A., Khan, M.A., & Chakraborty, R. (2022). Detection of objects using a fast R-CNN-based approach. In B. Das, R. Patgiri, S. Bandyopadhyay, & V. E. Balas (Eds.), *Modeling, simulation and optimization: Proccedings of CoMSO 2021*. Springer. https://doi.org/10.1007/978-981-19-0836-1_21

Eşer, E. E., & Hardalaç, F. (2021, December 9-11). *Performance of YOLO on a custom dataset of infrared laser images* [Paper presentation]. 1st International Conference on Informatics and Computer Science, Ankara, Turkey. https://webupload.gazi.edu.tr/upload/1104/2022/6/11/1f03cadc-5320-4546-86fb-c36b37c86b77-guncel_2021-1st-international-conference-on-informatics-and-computer-science_isbn.pdf

Gan, N., Wan, F., Lei, G., Xu, L., Xu, C., Xiong, Y., & Zhou, W. (2023). YOLO-CID: Improved YOLOV7 for X-ray contraband image detection. *Electronics*, *12*(17), 3636. https://doi.org/10.3390/electronics12173636

Jabraelzadeh, P., Charmin, A., & Ebadpore, M. (2020). Providing a hybrid method for face detection, gender recognition, facial landmarks localization and pose estimation using deep learning to improve accuracy. *Journal of Artificial Intelligence in Electrical Engineering*, *8*(32), 1–14.

Jabraelzadeh, P., Charmin, A., & Ebadpour, M. (2023). Providing a hybrid method for face detection and gender recognition by a transfer learning and fine-tuning approach in deep convolutional neural networks and the Yolo algorithm. *International Journal of Nonlinear Analysis and Applications*, *14*(1), 2373–2381. https://doi.org/10.22075/ijnaa.2022.26099.3661

Jiang, P., Ergu, D., Liu, F., Cai, Y., & Ma, B. (2022). A review of YOLO algorithm developments. *Procedia Computer Science*, *199*, 1066–1073. https://doi.org/10.1016/j.procs.2022.01.135

Mittal, S., Thakral, K., Majumdar, P., Vatsa, M., & Singh, R. (2023). Are face detection models biased? In *IEEE 17th International Conference on Automatic Face and Gesture Recognition* (pp. 1–7). IEEE. https://doi.org/10.1109/FG57933.2023.10042564

Nada, A. M. A., Alajrami, E., Al-Saqqa, A. A., & Abu-Naser, S. S. (2020). Age and gender prediction and validation through single user images using CNN. *International Journal of Academic Engineering Research*, *4*(8), 21-24.

Nepal, U., & Eslamiat, H. (2022). Comparing YOLOV3, YOLOV4 and YOLOV5 for autonomous landing spot detection in faulty UAVs. *Sensors*, *22*(2), 464. https://doi.org/10.3390/s22020464

Raman, V., ELKarazle, K., & Then, P. H. (2023). Artificially generated facial images for gender classification using deep learning. *Computer System Science and Engineering*, *44*(2), 1341-1355. https://doi.org/10.32604/csse.2023.026674

Ramya, R., Anandh, A., Muthulakshmi, K., & Venkatesh, S. (2022). Gender recognition from facial images using multichannel deep learning framework. In P. P. Sarangi, M. Panda, S. Mishra & B. S. P Mishra (Eds.), *Machine learning for biometrics: Concepts, algorithms and learning* (pp. 105–128). Academic Press. https://doi.org/10.1016/B978-0-323-85209-8.00009-2

Shen, T. W., Wang, D., Cheung, K. W. K., Chan, M. C., Chiu, K. H., & Li, Y. K. (2021). A real-time single-shot multi-face detection, landmark localization, and gender classification. In *Proceedings of the 2021 3rd International Conference on Image Processing and Machine Vision* (pp. 1–4). Association for Computing Machinery. https://doi.org/10.1145/3469951.3469952

Shet, A. V., Chinmay, B. S., Shetty, A. A., Shankar, T., Hemavathy, R., & Ramakanth, P. (2022). Face detection and recognition in near infra-red image. In *6th International Conference on Computation System and Information Technology for Sustainable Solutions* (pp. 1–6). IEEE. https://doi.org/10.1109/CSITSS57437.2022.10026378

Singh, A., Rai, N., Sharma, P., Nagrath, P., & Jain, R. (2021). Age, gender prediction and emotion recognition using convolutional neural network. In *Proceedings of the International Conference on Innovative Computing and Communication* (pp. 1–11). https://doi.org/10.2139/ssrn.3833759

Sonthi, V. K., Sikka, R., Anusha, R., Devi, P. B. S., Kamble, S. K., & Pant, B. (2023). A deep learning technique for smart gender classification system. In *3rd International Conference on Advance Computing and Innovative Technologies in Engineering* (pp. 983–987). IEEE. https://doi.org/10.1109/ICACITE57410.2023.10182683

Srikar, M., & Malathi, K. (2022). An improved moving object detection in a wide area environment using image classification and recognition by comparing You Only Look Once (YOLO) algorithm over Deformable Part Models (DPM) algorithm. *Journal of Pharmaceutical Negative Results*, *13*(Special Issue 4), 1701–1707. https://doi.org/10.47750/pnr.2022.13.S04.204

Srinivasan, L. (2023). Automatic gait gender classification using convolutional neural networks. In *Proceedings of the 2023 Fifth International Conference on Image Processing and Machine Vision* (pp. 34–40). Association for Computing Machinery. https://doi.org/10.1145/3582177.3582184

Sumi, T. A., Hossain, M. S., Islam, R. U., & Andersson, K. (2021). Human gender detection from facial images using convolution neural network. In M. Mahmud, M. S. Kaizer, N. Kasabov, K. Iftekharudin, & N. Zhing (Eds.), *Applied Intelligence and Informatics: First International Conference* (Vol. 1435, pp. 188–203). Springer. https://doi.org/10.1007/978-3-030-82269-9_15

Tejaswi, K., Mokshith, D., Kumar, C. M., & Kumar, M. (2023). Facial expression recognition using YOLO. In *International Conference on Research Methodologies in Knowledge Management, Artificial Intelligence and Telecommunication Engineering* (pp. 1–8). IEEE. https://doi.org/10.1109/RMKMATE59243.2023.10369028

Thakuria, A., & Erkinbaev, C. (2023). Improving the network architecture of YOLOV7 to achieve real-time grading of canola based on kernel health. *Smart Agricultural Technology*, *5*, 100300. https://doi.org/10.1016/j.atech.2023.100300

Tilki, S., Dogru, H. B., Hameed, A. A., Jamil, A., Rasheed, J., & Alimovski, E. (2021). Gender classification using deep learning techniques. *Manchester Journal of Artificial Intelligence and Applied Sciences*, *2*(1), 126–131.

Ullah, M. B. (2020). CPU based YOLO: A real time object detection algorithm. In *IEEE Region 10 Symposium* (pp. 552–555). IEEE. https://doi.org/10.1109/TENSYMP50017.2020.9230778

Varnima, E. K., & Ramachandran, C. (2020). Real-time gender identification from face images using You Only Look Once (YOLO). In *4th International Conference on Trends in Electronics and Informatics* (pp. 1074–1077). IEEE. https://doi.org/10.1109/ICOEI48184.2020.9142989

Wang, C.-Y., Yeh, I.-H., & Liao, H.-Y. M. (2024). YOLOv9: Learning what you want to learn using programmable gradient information. In A. Leonardis, E. Ricci, S. Roth, T. Sattler, & G. Varol (Eds.), Computer *vision – ECCV 2024: Lecture notes in computer science* (Vol. 15089, pp. 1-21). Springer. https://doi.org/10.1007/978-3-031-72751-1_1

Yaseen, M. (2024). *What is YOLOv9: An in-depth exploration of the internal features of the next-generation object detector*. arXiv. https://doi.org/10.48550/arXiv.2409.07813

Wang, F., Jiang, J., Chen, Y., Sun, Z., Tang, Y., Lai, Q., & Zhu, H. (2023). Rapid detection of Yunnan Xiaomila based on lightweight YOLOV7 algorithm. *Frontiers in Plant Science*, *14*, 1200144. https://doi.org/10.3389/fpls.2023.1200144

Wang, W., Chen, J., Huang, Z., Yuan, H., Li, P., Jiang, X., Wang, X., Zhong, C., & Lin, Q. (2023). Improved YOLOV7-based algorithm for detecting foreign objects on the roof of a subway vehicle. *Sensors*, *23*(23), 9440. https://doi.org/10.3390/s23239440

Xiao, M., Xiao, N., Zeng, M., & Yuan, Q. (2020). Optimized convolutional neural network-based object recognition for humanoid robot. *Journal of Robotics and Automation*, *4*(1), 122–130. https://doi.org/10.36959/673/363

Zheng, Z., Wang, P., Liu, W., Li, J., Ye, R., & Ren, D. (2020). Distance-IoU loss: Faster and better learning for bounding box regression. In *Proceedings of the AAAI Conference on Artificial Intelligence* (Vol. 34, No. 07, pp. 12993–13000). Association for the Advancement of Artificial Intelligence Publishing. https://doi.org/10.1609/aaai.v34i07.6999

Pertanika J. Sci. & Technol. 33 (5): 2177 - 2205 (2025)

PERTANIKA JOURNALS

SCIENCE & TECHNOLOGY

Journal homepage: http://www.pertanika.upm.edu.my/

Screening and Isolation of Microalgae Collected from Tin Mining at Bangka Belitung Province with Remarks on Their UV-C Absorbance and Lead Remediation

Feni Andriani[1,3,5], Yasman[1,3], Arya Widyawan[2] and Dian Hendrayanti[1,4]*

[1]*Biology Department, Faculty of Mathematics and Natural Sciences, Universitas Indonesia, Depok, 16424 West Java, Indonesia*

[2]*Plant Protection Department, College of Food and Agriculture Sciences, King Saud University, 11451 Riyadh, Saudi Arabia*

[3]*Metabolomic and Chemical Ecology Research Group, Biology Department, Faculty of Mathematics and Natural Sciences, Universitas Indonesia, Depok, 16424 West Java, Indonesia*

[4]*Microbial Systematic and Prospecting Research Group, Biology Department, Faculty of Mathematics and Natural Sciences, Universitas Indonesia, Depok, 16424 West Java, Indonesia*

[5]*Biology Department, Faculty of Mathematics and Natural Sciences, Universitas Riau, Pekanbaru, 28293 Riau, Indonesia*

ABSTRACT

Microalgae inhabit mining sites, performing specific adaptations to survive the stress conditions. This study aimed to investigate the effect of growth media on the microalgae isolated from water bodies at abandoned tin mining sites and analyse their sensitivity to ultraviolet-C (UV-C) spectrum and lead resistance. Samples from six locations were enriched in Bold Basal Medium (BBM) (pH 6.8) and Blue Green-11 (BG-11) (pH 7.4) media, and the grown cultures were kept in a cold room at a temperature of 21°C, provided with continuous light (1,600 lux). The UV-C sensitivity of the cultures was observed with spectrophotometry at λ=230 nm, followed by growth rate measurement. The isolate was subjected to lead concentrations of 0, 10, 100, and 200 ppm. The results showed that the diversity of the microalgae in the BBM was higher than in BG-11, with 7 and 3 species, respectively. Most microalgae grown in BBM were coccoid green algae, while diatoms and cyanobacteria were in BG-11. All cultures developed from enrichment step showed UV-C absorption, and the fastest growth was performed by Ulu River (UL) culture. Isolate coccoid green algae UL4 had sensitivity to the UV-C spectrum and survived high lead concentrations up to 200 ppm. This character, plus the capability to survive in high lead concentration, made UL4 a potential candidate for a bioremediation agent. Phylogenetic analysis based on the 18S rRNA

ARTICLE INFO

Article history:
Received: 22 October 2024
Accepted: 29 April 2025
Published: 28 August 2025

DOI: https://doi.org/10.47836/pjst.33.5.07

E-mail addresses:
andrianifeni98@gmail.com (Feni Andriani)
yasman.si@sci.ui.ac.id (Yasman)
ayanto@ksu.edu.sa (Arya Widyawan)
dian.hendrayanti@sci.ui.ac.id (Dian Hendrayanti)
* Corresponding author

e-ISSN: 2231-8526

gene showed that the strain UL4 is nested within the clade of *Chlorococcum* spp. It is of interest for future research to investigate the involvement of secondary metabolites as a mechanism for UL4 survival in stress conditions.

Keywords: Algal media, Bangka Belitung, green algae, lead remediation, UV-C tolerance

INTRODUCTION

Microalgae are autotrophic microorganisms which are found in aquatic, terrestrial, and aerial environments (Sahoo & Baweja, 2015). The potential of the microalgae in various fields has been acknowledged. Species such as *Chlorella* and *Spirulina* have been widely developed as health and beauty supplements because of their active ingredients, like polyunsaturated fatty acid (PUFA) and β-1,3-glucan (Koyande et al., 2019). Another species like *Scenedesmus obliquus* and *Chlamydomonas reinhardtii* are developed for biofuel due to their high lipid content. In waste treatment, *Chlorella* sp. is used for bioremediation agent to reduce ammonia and palm oil waste (Shuba & Kifle, 2018). The application of algae in many fields is a long journey from sampling, isolating, and culturing potential species, producing biomass, until algal productions.

Muntok City, the capital of West Bangka Regency, Bangka Belitung Islands Province, has been established as a tin mining site since 1707 (Swastiwi et al., 2017). Due to the expansion of the tin mining areas, Haryati and Dariah (2019) estimated the production of carbon dioxide emissions in Bangka Belitung would reach 36,908,808 t carbon dioxide (CO_2) in 2040. The high CO_2 emission thinned the ozone layer, thereby increasing ultraviolet (UV) radiation on the Earth's surface. The excessive exposure to the UV radiation, especially the UV-C radiation, which has high energy, could affect the survival ability, growth rate, distribution, motility, and even death of the microorganisms (Tekiner et al., 2019). Therefore, the microalgae that live in extreme areas, such as tin mining sites, must be able to adapt to the UV-C radiation.

Several studies reported that the microalgae survived and thrived in mining areas. Gomes et al. (2021) reported the discovery of *Spirogyra, Mouegotia*, *Chlorella*, and diatoms, like *Pinnularia*, *Navicula*, and *Eunotia*, in the copper and silver mining area at Sao Domingo, Portugal. Another research by Senhorinho et al. (2018) discovered several species, including *Chlorococcum*, *Desmodesmus*, and *Cocomyxa*, in an abandoned mining site in Canada. Water sample observations conducted around the tin mining sites in West Bangka Regency by Rachman (2019) revealed that the microalgae diversity was dominated by the diatoms such as *Thalassiothrix*, *Chaetoceros*, and *Rhizosolenia*. Besides diatoms, Rachman (2019) also found dinoflagellates such as *Protoperidinium* and *Pyrophacus*. Previously, Bidayani (2017) found *Chroococcus* and *Uroglena* as the dominant microalgae in the reuse of a tin mining pit.

Several studies showed that the UV-C light-adapted microalgae could produce advantageous metabolites. For example, *Dunaliella salinea*, *Chlorella vulgaris*, and *Pavlova lutheri*, which produced high sterols and lipids that are useful for biofuel production (Ahmed & Schenk, 2017; Carino & Vital, 2022; Ghezelbash et al., 2023). Another potential of the microalgae living in extreme conditions was investigated by Gauthier et al. (2020) and Senhorinho et al. (2018). Both reported that the microalgae which were exposed to heavy metals, ultraviolet-B (UV-B) radiation, and high salinity had the potential to generate advantageous metabolite compounds such as antibacterials and antioxidants.

The microalgae that have been living in the Muntok tin mine since the mining's existence more than a hundred years ago could develop a strategy to adapt to the UV exposure. One of the strategies is producing specific metabolites that not only protect cells from UV radiation but also reduce other environmental stresses, such as high concentrations of heavy metals. The metal-binding protein metallothioneins have roles for transporting toxic metals from the cytosol into other organelles (Balzano et al., 2020). Metallothionein-2 transplastomic *Chlamydomonas reinhardtii* showed higher resistance to the UV-B exposure than the wild type. The addition of metals (zinc, cadmium, and copper) to the growth medium of MT2 transgenic *C. reinhardtii* is related to the survival of the cells (Zhang et al., 2005).

The water bodies in the Bangka Belitung tin mining area were contaminated with heavy metals, dominated by lead. Some research, such as Miranda et al. (2018), reported the lead content in the sediment of River Pakil was 12.96 mg/kg, while Tawa et al. (2019) found lead content in the waters of Kelabat Bay was 0.2624-0.5713 mg/L. Exploration of the lead-tolerant microalgae in the tin mining area of Bangka Belitung becomes important to get information on the diversity of indigenous microalgae and their potential. Moreover, isolation of the UV-C and lead-tolerant microalgae could be viewed as one of the solutions to the environmental problems.

Algal growth media play an important role in the success of algal isolation and culture. Differences in nutrients of the algal growth media influence the kind of microalgal species, their growth rate, and metabolite production. Synthetic media, such as BBM and BG-11, are widely used as both medium enrichment and growth medium for an established culture (Andersen, 2005; Badr & Fouad, 2021).

Bold Basal Medium was introduced by Bischoff and Bold in 1963 for isolating soil microalgae. Several characteristics of the BBM include high metal element content, pH 6.4-6.8, and a lack of vitamins (Andersen, 2005). The BBM is a generic medium for the green microalgae, and many species have been cultured in the BBM, such as *Chlorella* spp. (Blair et al., 2014), *Scenedesmus* spp. (Habibi et al., 2019), *Micractinium* spp., and *Chlamydomonas* spp. (Lloyd et al., 2021).

On the other hand, the BG-11 medium was developed by Allen and Stanier in 1968. This medium was developed from the artificial medium No. 11 created by Hughes et al. in 1958. The BG-11 medium was created for culturing the freshwater, saltwater, and soil

cyanobacteria (Andersen, 2005; Rippka, 1979). Cyanobacteria, such as *Synechococcus elongatus* PCC7942 (Yang et al., 2015) and *Synechocystis* sp. (Yan et al., 2014), can be cultured in the BG-11.

The aims of this research were to investigate the effect of growth media and the existence of UV-C-tolerant microalgae communities from Muntok tin mining. Besides, we also evaluated the potential of a microalgal isolate for lead resistance.

MATERIALS AND METHODS

Sample Collection and Enrichment

Samples were collected from fresh and brackish waters around the abandoned tin mining site located in the Muntok Subdistrict, West Bangka Belitung Regency, Bangka Belitung Province, Indonesia, in January and February 2022. Six sampling sites were selected based on a purposive sampling method, which were Pait (PA) and Ketok (KE) abandoned mining sites, Belo River (BE), Pancur River (PC), Pantai Baru Beach (PB), and Ulu River (UL) (Figure 1). From each location, a 100 ml water sample was collected approximately 5 cm below the surface and transferred into polyethylene terephthalate (PET) plastic

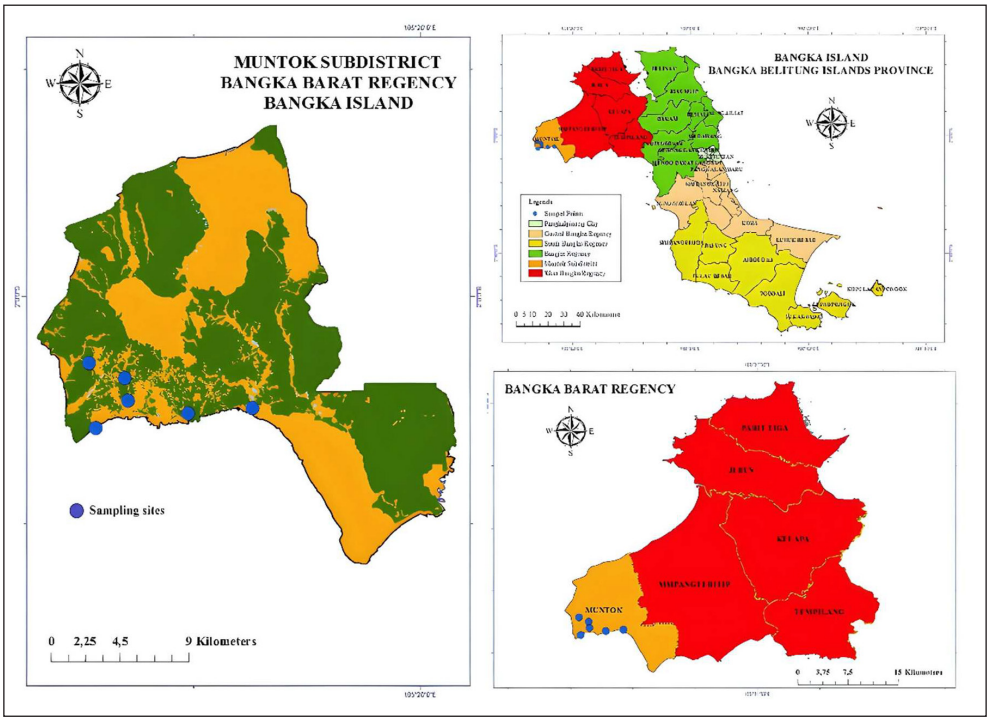

Figure 1. Research locations map. The coordinate points of Pait (PA): -2.06826, 105.19686; Belo River (BE): -2.06491, 105.23462; Ketok (KE): -2.03884, 105.13849; Ulu River (UL): -2.06079, 105.16154; Pancur River (PC): -2.04750, 105.15974; and Pantai Baru Beach (PB): -2.07589, 105.14210

bottles. The collected samples were stored in a refrigerator (4°C) before being transported to the Microalgae Culture Preparation Laboratory, Department of Biology, Faculty of Mathematics and Natural Sciences, Universitas Indonesia, West Java Province. At the laboratory, samples were immediately subjected to the enrichment process.

All samples were enriched using the BBM and BG-11 media in a 48-well microplate. The BBM and BG-11 media were prepared according to Andersen (2005) and Stanier et al. (1971), respectively. The pH value was adjusted to 6.8 for the BBM and 7.4 for the BG-11 by adding 0.1 M sodium hydroxide (NaOH, Merck, USA). The media were sterilised using an autoclave (TOMY SX 700, Japan) at a temperature of 121°C, with an air pressure of 1 atm. The enriched samples in a well microplate were placed on a culture storage rack (Figure 2) at a temperature of approximately 21°C, under continuous light for two to three weeks. Observations were carried out once a week. Any growing microalgae from the enrichment step were re-cultured with addition of fresh BBM (50 ml volume per 100 ml Erlenmeyer flask; triplicate) and observed for 14 days. At the end of the observation, the most stable culture was selected and used for the UV-C absorption experiment. The stable culture was designated qualitatively based on the homogeneity of biomass and colour as determined by the Hexadecimal (HEX) Colour Codes (https://www.colour-hex.com/). The entire process was carried out in an aseptic process.

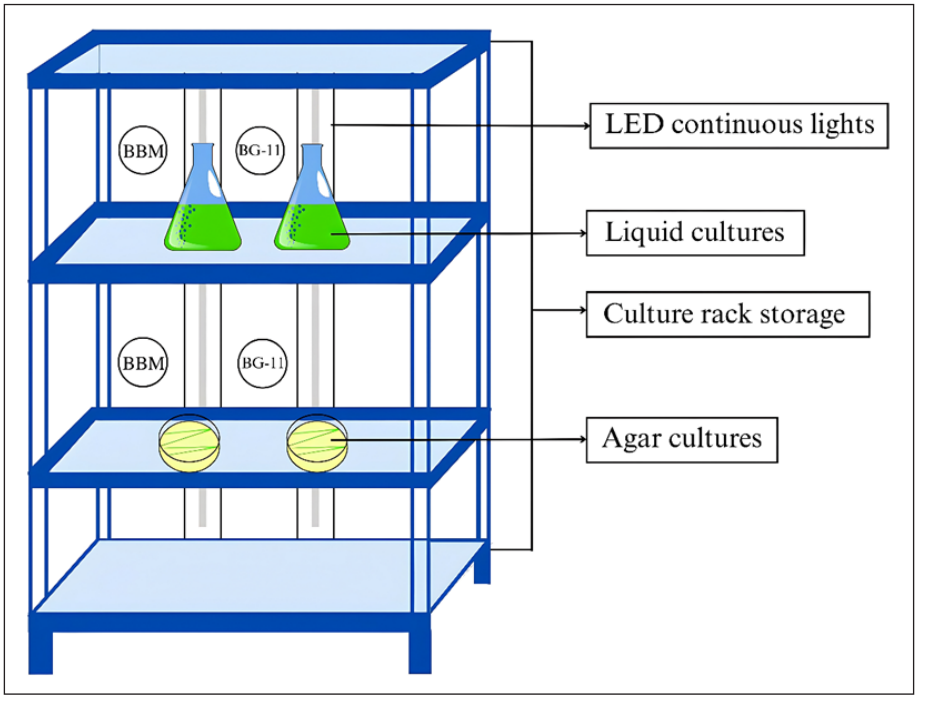

Figure 2. Culture storage setup for the microalgae enrichment and cultivation
Note. BBM = Bold Basal Medium; BG-11 = Blue Green-11; LED = Light emitting diode

Microalgal Observation

The observation of the microalgae was conducted using a binocular light microscope (Leica DM 500 Microscope, Germany) equipped with the LAS EZ software (version 3.4.0) for documentation. Culture sampling for the morphological observation was carried out in a transfer box following an aseptic procedure. Representative samples were taken from the liquid cultures using a sterilised Pasteur pipette, placed on a glass slide, and covered with a coverslip (Govindan et al., 2021). For the agar culture, one colony was taken using a sterilised loop and then placed on glass slides with a single drop of sterilised aquabidest. Morphological characters were observed, including the cell shape and size, colour, chloroplast type, number of pyrenoids, presence of flagella and sheath, and other cells' ornaments. Identification was performed using a determination key (Rosen & Mareš, 2016; Wehr et al., 2014) and other references (Komárek et al., 2014; Puilingi et al., 2022; Tan et al., 2016). Information from the AlgaeBase was also used (https://www.algaebase.org/).

Measurements of UV-C Sensitivity and Microalgal Growth Rate

For the growth rate experiment, a total of 20% of the inoculum from the stock of the selected culture was transferred at the exponential phase to different 500 ml flasks, each containing 200 ml BBM or BG-11 medium (Blanco-Vieites et al., 2022). Experiments were performed with three replications. The experiment cultures were then placed in the culture rack previously described. Daily manual agitation was performed to ensure homogeneous distribution of nutrients.

Growth rate observations were conducted using the optical density measurement method with a spectrophotometer (Genesys 105 UV-VIS Spectrophotometer, Thermo Fisher Scientific, USA). The wavelength was determined using the culture absorbance sensitivity, which ranged from 200 to 800 nm. After repeated observations, the wavelength of 230 nm (OD_{230}) was selected for growth measurement. The experiment was carried out for 20 days and the microalgal culture growth was observed every 2 days (Susanti et al., 2021). The specific growth rate was calculated using the formula as follows:

$$Specific\ growth\ rate\ (\mathrm{K}')(\mu/day) = \frac{Ln\ (\frac{N2}{N1})}{t2 - t1}$$

where, Ln = Constant (3.22); N1 = Biomass time t1; and N2 = Biomass at time t2 (Krzemińska et al., 2014).

Isolation and DNA Extraction, Amplification, and Sequencing

Isolation and purification of the microalgae were carried out using the streak and serial dilution methods (Sandeep et al., 2019) using the BBM and BG-11 liquid and agar media (2.5% Bacto™ Agar, Becton Dickinson, Canada). The biomass of the isolate was collected by centrifugation, and 1 mg was subjected to DNA extraction using the DNeasy Plant Mini Kit (Promega, USA) according to the manufacturer's instructions. Concentration and purification of extracted DNA were measured with a nanophotometer (Implen, Germany).

The amplification of the 18S rRNA gene was carried out using the thermal cycler (Techne TC-3000G, USA) with forward primer of 18SF (5'-CCTGGTTGATCCTGCCAG-3') and 18SR (5'-WTGATCCTTCYGCAGGTTCA-3') (Wan et al., 2011). The reaction was performed in a total volume of 25 µl, having 12.5 µl of Dream Taq Green (ThermoFisher, Germany) master mix, 1 µl of each primer, 2 µl of DNA template, and 8.5 µl of nuclease-free water. Polymerase chain reaction (PCR) was initiated with denaturation (94°C, 3 min), followed by 30 cycles of denaturation (94°C, 1 min), annealing (59°C, 1 min), elongation (72°C, 1 min), and finished by terminal extension (72°C, 10 min).

The amplicons were sent to Macrogen (Singapore) for sequencing. The result sequenced forward, and reverse fragments were checked using the software package Chromas 2.6.2 (Technelysium.com). The 18S rRNA gene sequences obtained were run through the Basic Local Alignment Search Tool nucleotide (BLASTn) programme from GenBank to check species identity with reference sequences before reconstructing the phylogenetic tree.

Lead Resistant Experiment

A total of 1.34 g of lead (II) chloride ($PbCl_2$) (Merck, USA) was dissolved in 1 L of distilled water (Zehra et al., 2018). The lead solution is then sterilised using an autoclave before use. To prevent lead precipitation due to the sterilisation process, the lead solution was filtered using a filter paper (Whatman 934-AH, diameter 47 mm). The lead medium was diluted to concentrations of 10, 100, and 200 ppm. The growth rate of the microalgae at various lead concentrations was measured using a wavelength of 680 nm (OD_{680}).

The culture biomass dry weight was measured to observe the influence of lead. At the end of the growth observation, the culture biomass was harvested using centrifugation at 4,427 x *g* for 15 min. The wet biomass was placed in an evaporating basin and dried using an oven (Jisico, Korea) until a constant weight was achieved. The dried biomass was measured using an analytical balance (Precisa XT-200, Swiss). The weight difference between the empty evaporating basin and the dish with dry biomass measured the biomass weight.

Data Analysis

Data analysis was conducted both qualitatively and quantitatively. The qualitative analysis was performed for morphological observations and colour, while the quantitative analysis

was performed for optical density, specific growth rate, and dry biomass. All data were transformed into tables and graphics using Microsoft Excel 2021. The statistical analysis was run using a *t*-test in comparing the growth rates of culture in the BBM and BG-11 media, while analyses of variance (ANOVA) ($P<0.05$) was used to compare the growth rate of the isolate at various lead concentrations. The correlation analysis (r) was conducted to measure the relationship between lead concentration and dry biomass.

The phylogenetic tree was inferred by using the maximum likelihood method and the Tamura-Nei model (Tamura & Nei, 1993). The tree with the highest log likelihood (-5576.57) is shown. The percentage of trees on which the associated taxa clustered together is shown above the branches. Initial tree(s) for the heuristic search were obtained automatically by applying the Neighbour-Join and BioNJ algorithms to a matrix of pairwise distances estimated using the Tamura-Nei model and then selecting the topology with the superior log likelihood value. The tree is drawn to scale, with branch lengths measured in the number of substitutions per site. This analysis involved 22 nucleotide sequences. There was a total of 1,656 positions in the final dataset. Evolutionary analyses were conducted in MEGA11 (Tamura et al., 2021).

RESULTS

Observation of Microalgal Growth in the BBM and BG-11 Media

Most microalgae grown in KE, BE, PC, and PB samples were unicellular coccoid green microalgae, while in the UL sample, filamentous cyanobacteria were present. Diatoms appeared in three samples: PA, BE, and UL. Overall, the BE sample had the most diverse microalgae. Diatom, coccoid green algae, and filamentous cyanobacteria were found in both the BBM and BG-11 (Figure 3 and 4). However, coccoid cyanobacteria were the only population found in the BBM. Most microalgae grown in the BBM were unicellular coccoid green algae (Figure 4 F, G, H, I, J, L, M), while in the BG-11 were diatoms (Figure 3 A, B, C). The growth of algae in the BBM flourished more than in the BG-11 (Table 1).

Table 1
List of species grown in the BBM and BG-11 as a result of enrichment

Medium	List of species	Morphology characteristics	References
Blue Green No. 11 (BG-11)	*Nitzschia* sp. (Figure 3 A-C)	Two chloroplasts with a yellow-brown shape at the cell edge. Lancet and sometimes rectangular. Solitary and sometimes a colony. Cell size varied. L: 38–110 µm and W: 9–11 µm.	Puilingi et al., (2022); Tan et al., (2016)
	Pseudanabaena sp. (Figure 3 E-F)	Cylindrical septate without a heterocyst. Cell size varied. L= 7.04-12.83 µm.	Rosen and Mareš (2016); Yusof et al. (2017)

Table 1 *(continue)*

Medium	List of species	Morphology characteristics	References
	Chlorella sp. (Figure 3 D)	Cup-shaped chloroplast with or without pyrenoid Elliptical or rounded with cell size varying from 2-10 µm.	Shubert and Gartner (2015)
Bold Basal Medium (BBM)	*Chlorella* sp. (Figure 4 A, G, L, M)	(See *Chlorella* in BG-11)	
	Pseudanabaena sp. (Figure 4 A, C)	(See *Pseudanabaena* in BG-11)	
	Nitzschia sp. (Figure 4F)	(See *Nitzschia* in BG-11)	
	Nostoc sp. (Figure 4 E, N)	Long filament with heterocyst and akinete. Cell size varied from 5-10 µm.	Rosen and Mareš (2016); Videau and Cozy (2019)
	Pinnularia sp. (Figure 4 B, C)	Linear shaped with curved end. Cell size varied. L= 28-64 µm; W = 5-12 µm.	Xu et al. (2024)
	Chlorococcum sp. (Figure 4 F)	Cell spherical and solitary. Parietal with one pyrenoid. Cell size varied from 5-15 µm.	Hodač et al. (2015); Shubert and Gartner (2015)
	Coccomyxa sp. (Figure 4 H)	Cell ellipse to cylindrical. Parietal chloroplast with pyrenoid.	Hodač et al. (2015); Shubert and Gartner (2015)

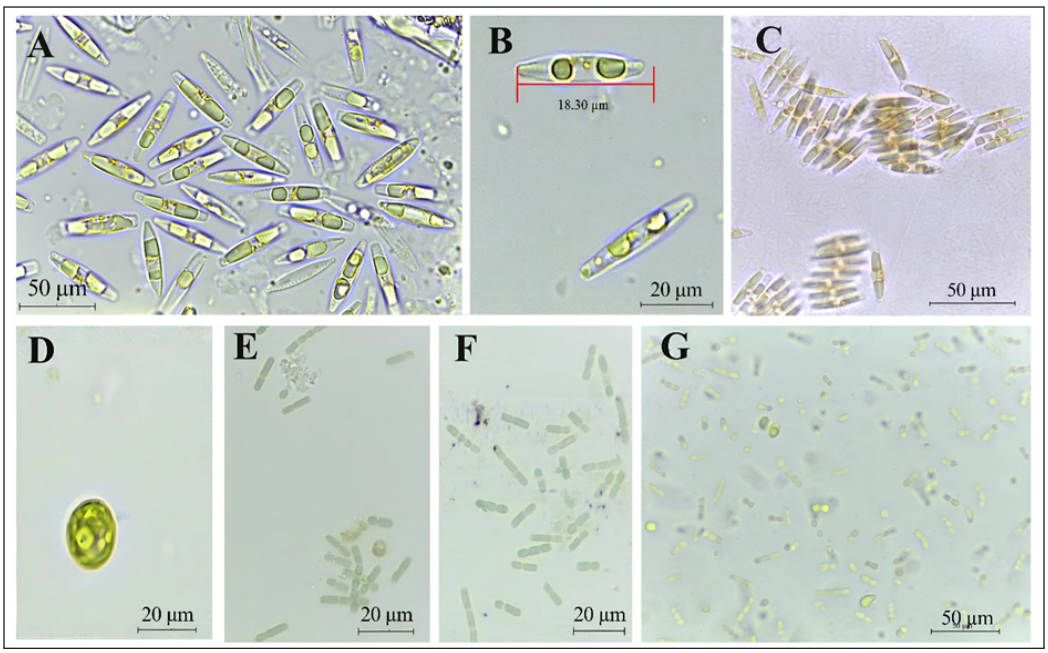

Figure 3. Diversity of the microalgae from six locations in the Blue Green-11 medium
Note. Diatom (A, B, C), coccoid green algae (D), and filamentous cyanobacteria (E, F, G)

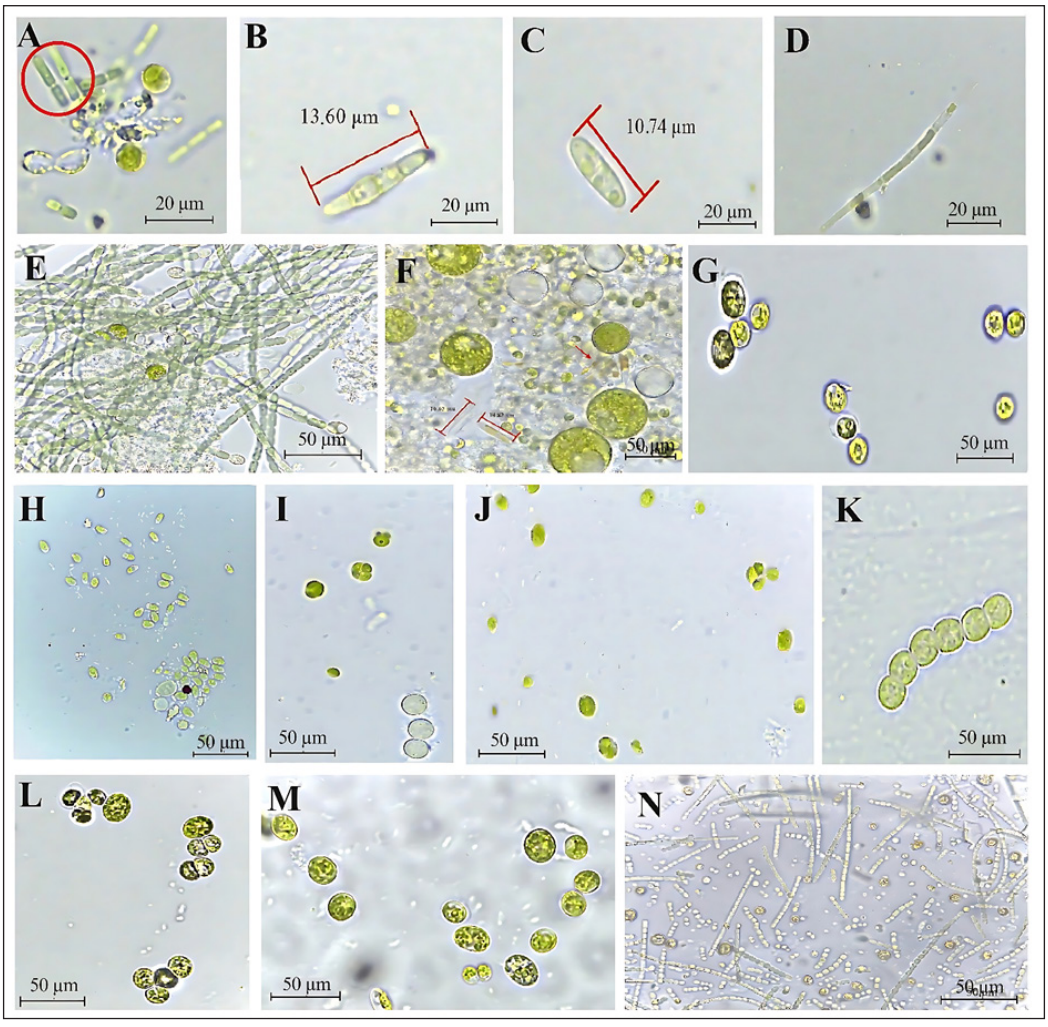

Figure 4. Diversity of the microalgae from six locations in the Bold Basal Medium
Note. Coccoid green algae (A, F, G, I, J, L, M), filamentous cyanobacteria (A, D, E, K, N), unicellular microalgae (B, C), and diatoms (F)

UV-C Spectrum Sensitivity and Growth Rate

Colour changes of six (mix) cultures during incubation were systematically documented (Figure 5). The colour began to change at day 12. The UL and KE cultures changed into yellow-green (HEX #9ACD32), while the others were light green (HEX #90EE90). At day 15, the colours of the UL, PA, and PC cultures changed to avocado green (HEX #A568203). At the end of the experiment (day 21), the colour of UL and KE cultures changed to golden brown (HEX #996515), and the biomass clumped.

Figure 5. Colour change of six cultures at day 15. The first day (top) and after 15 days (bottom). PA, UL, PC culture biomass changed to avocado green (HEX #A568203) and the KE culture biomass changed to yellow green (HEX #9ACD32)
Note. PA = Pait; UL = Ulu River; PC = Pancur River; KE = Ketok

The UV sensitivity analysis was conducted on the UL (mix) culture because, under standard laboratory conditions, the culture showed optimum growth compared to other cultures. Spectrum analysis from T0 up to T10 days old culture showed that different peaks were observed in culture media BBM and BG-11 (Table 2) (Figure 6). However, the peak

Table 2
Wavelength peaks of UL (mix) culture in the BBM and BG-11

Time observation (d)	Wavelengths (nm)	
	BBM	BG-11
T0	230, 340, 640	230
T1	220, 240, 440, 680	230
T2	220, 240, 360, 680	230, 340
T3	240, 440, 680	230, 360, 680
T4	210, 230, 360, 440, 680	230, 360, 680
T5	230, 440, 680	230, 340, 440, 680
T6	230, 440, 680	230, 360, 440, 680, 740
T7	230, 360, 440, 480, 680	230, 340, 440, 680, 740
T8	230, 440, 680	230, 440, 680, 760
T9	230 320, 440, 680,780	230, 440, 480, 680
T10	230, 440, 600, 680	230, 440, 680, 760

Note. UL = Ulu River; BBM = Bold Basal Medium; BG-11 = Blue Green-11

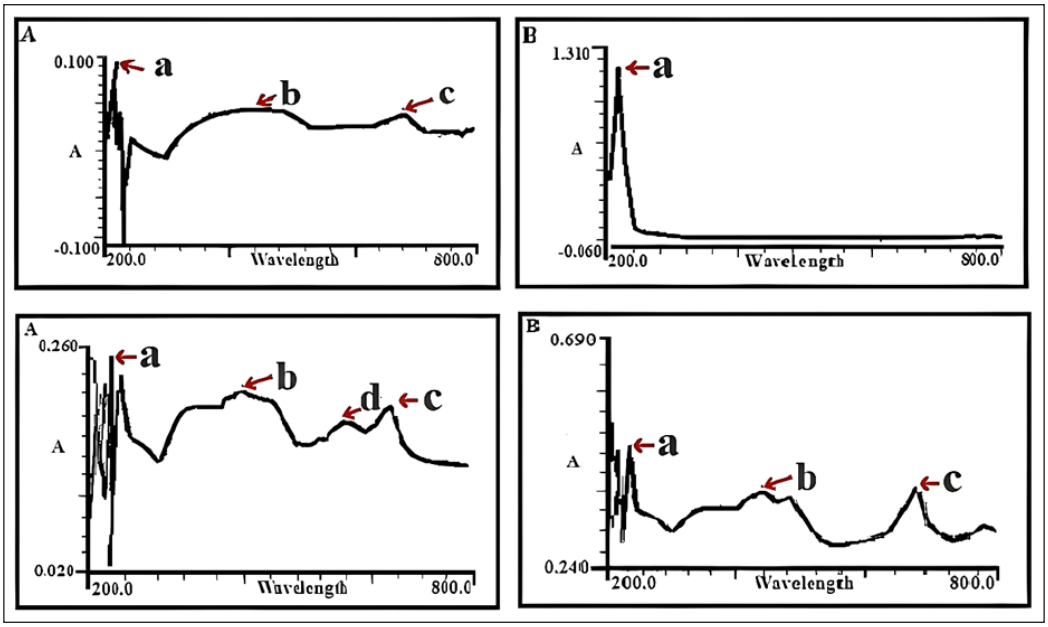

Figure 6. Absorbance wavelength sensitivity test of the UL culture at T0 (top) and T10 (bottom)
Note. (A) Bold Basal Medium (BBM); (B) Blue Green-11 (BG-11) medium; (a) wavelength 230 nm, (b) wavelength 440-480 nm, (c) wavelength 680 nm, and (d) wavelength 600 nm

at λ=230 nm was considered as an indicator for the UV sensitivity (International Agency for Research on Cancer [IARC], 2012). The peak was consistently observed from T0 up to T10 in media growth BG-11, while the same peak was observed consistently from T4- T10. Moreover, this peak indicated the presence of the UV-tolerant microalgae in the UL culture. The growth of the UV-tolerant microalgae in the UL culture on the BBM was predicted to be faster compared to the BG-11, as indicated by the colour change (Figure 7A). The BBM culture entered the stationary phase on day 16 and steadily decreased at day 20. Meanwhile, the BG-11 culture was still in log phase until the end of the observation. The average specific growth rate of the UL culture on the BBM media was 0.027 μ/day, while on the BG-11 was 0.018 μ/day (Figure 7B).

Morphological and Molecular Identification of the Isolate UL4

The morphological observations showed that the cell of the isolate (coded as UL4) was unicellular, round in shape, 6-14 μm in length, and non-motile. The shape of the chloroplast was cup-shaped, and a single pyrenoid was located at the periphery of the cell. The cell size ranged from 6 to 12 μm. The vegetative cell reproduced by autospore formation, but sometimes cell division occurred (Figure 8).

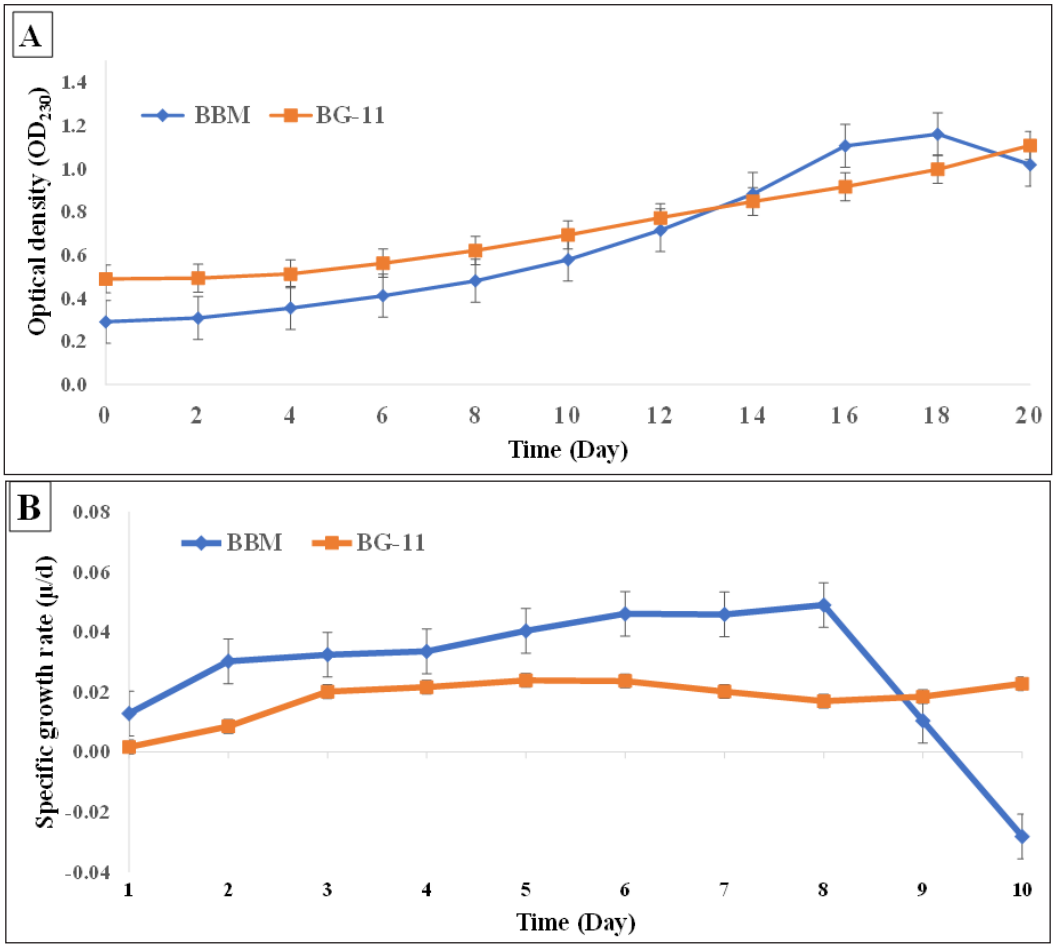

Figure 7. The growth curves (A) and specific growth rate (B) of the UL culture in Bold Basal Medium (BBM) and Blue Green-11 (BG-11) at 230 nm wavelength.
Note. *T*-test analysis on the mean of specific growth rate data showed there was no significant difference between growth on the BBM and BG-11 (p>0.05). However, *t*-test analysis on day 20 (T10) showed a significant difference in growth rate between the BBM and BG-11 (p = 0.02)

The length of the UL4 forward and reverse sequences was 491 and 533 bp, respectively. The whole sequence of the 18S rRNA gene using 18F-18R primers should be 1,500 bp (Figure 9), but the capability of the sequence reading machine was limited to 500-600 bp. Therefore, there was a gap between the F- and R-sequences after the sequence's continuity. The phylogenetic analyses of the isolate UL4 were conducted using the partial sequence (1,024 bp). Tree reconstructions were performed using the neighbour joining (NJ), maximum parsimony (MP), and maximum likelihood methods. *Neospongiococcum macropyrenoidosa* and *Neospongiococcum vacuolatum* were used as outgroups. Bootstrap of 1,000 was set up for all trees. The isolate UL4 was always placed within the big

clades, consisting of *Chlorococcum* spp., *Neospongiococcum gelatinosum*, *Pleurastrum rubrioleum*, and *Macrochloris radiosa*. The nodes in NJ/MP/ML trees that separated the UL4 clade from other aforementioned OTUs were supported by the 93/100/99 bootstrap values. Only ML phylogenetic trees are shown here (Figure 10). Other tree analyses can be seen upon request.

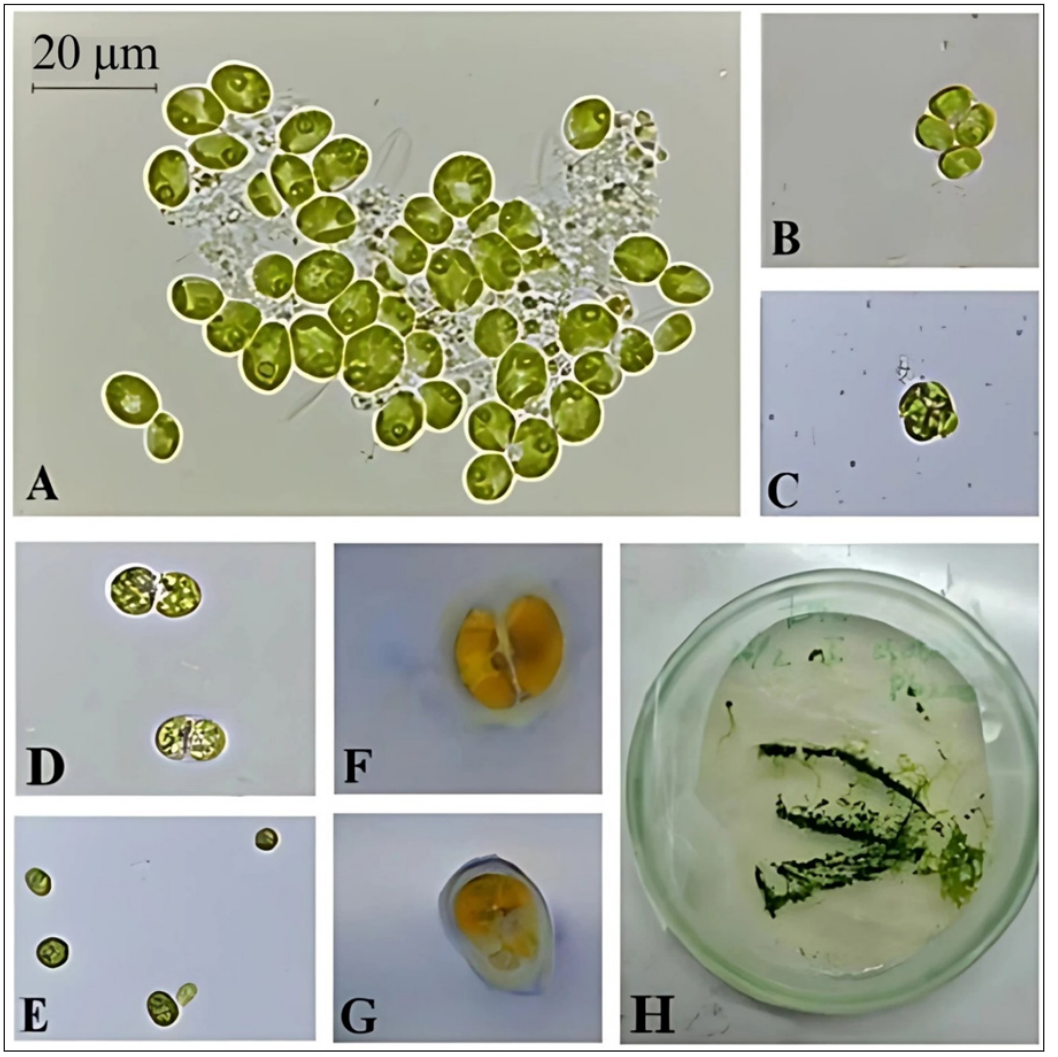

Figure 8. The morphology of the UL4 in different life stages. (A) Mature cells (18 days old); (B-C) Autospores; (D) Cell division; (E) Young cells (2-7 days old); (F-G) Old cells (age ± 245 days); (H) The isolate UL4 in the Bold Basal Medium agar
Note. Figures B-H without scale. All documentation was taken under a light microscope with 1,000× magnification

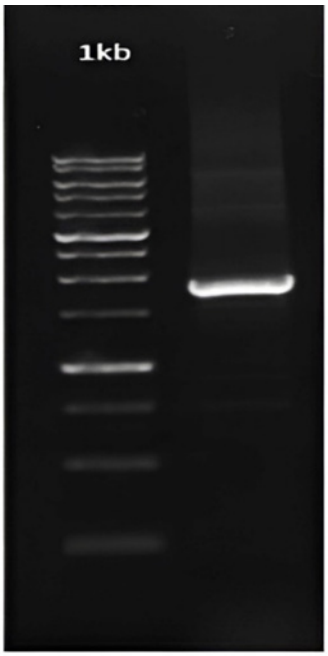

Figure 9. Polymerase chain reaction amplification of the UL4

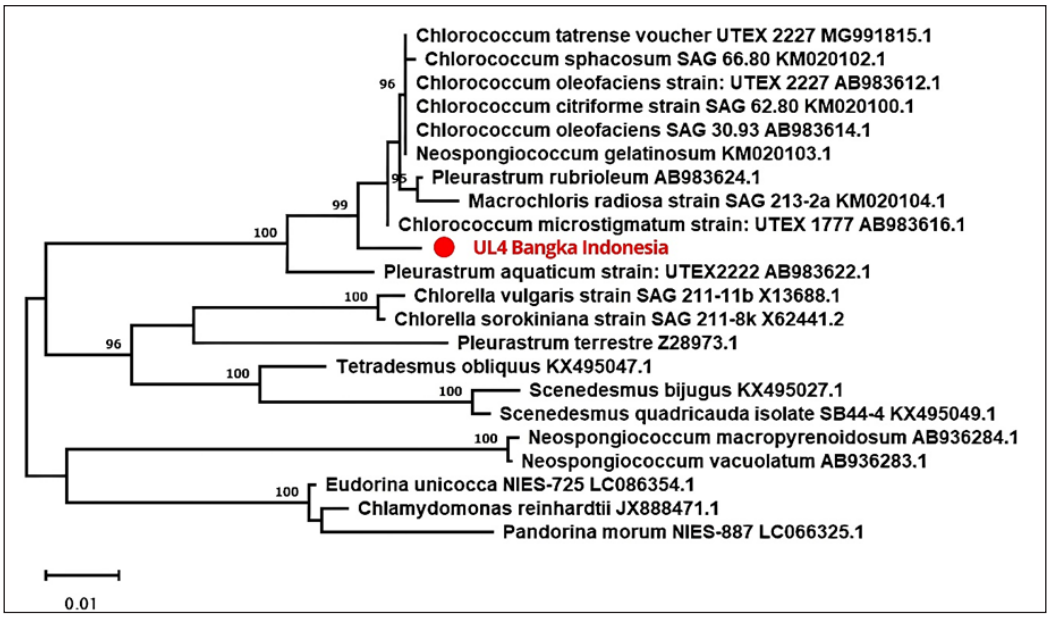

Figure 10. Phylogenetic tree of the UL4 inferred from the Maximum Likelihood method

Effects of Various Lead Concentrations

The morphology of the UL4 grown in various lead concentrations showed changes in the cell shape and size (Figure 11). Compared to the control, the cell on 10-200 ppm lead either enlarged or decreased (Table 3).

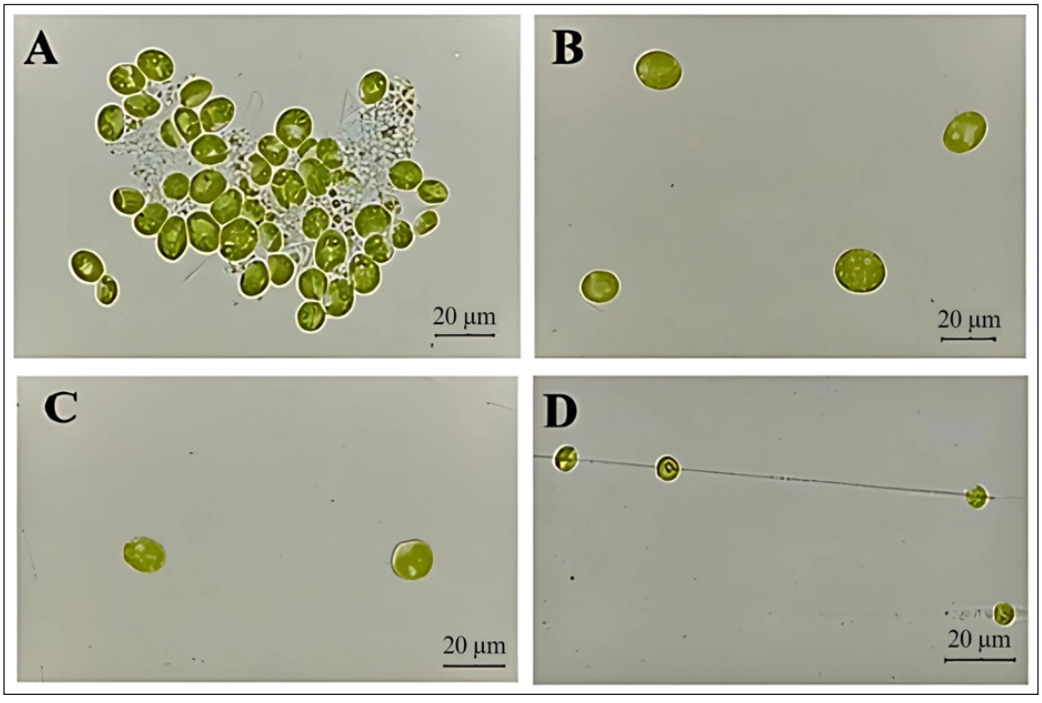

Figure 11. The mtorphological observations of the UL4 isolate under various lead concentrations after 22 days of incubation (T8): (A) 0 ppm, (B) 10 ppm, (C) 100 ppm, and (D) 200 ppm

Table 3
Effect of lead on total cell count and cell size of the isolate UL4

Lead concentrations (ppm)	Total cell (unit)	Cell size (µm)
0	273	11.26
10	87	13.86
100	63	5.02
200	34	4.58

The lead also changes the colour of the culture. The control culture showed avocado green (HEX#3A5702), while at 10 and 100 ppm, the cultures appeared olive green (HEX#446702) and dark green (HEX#568203) respectively, and at 200 ppm, the colour changed to yellowish green (HEX#9DC209) (Figure 12).

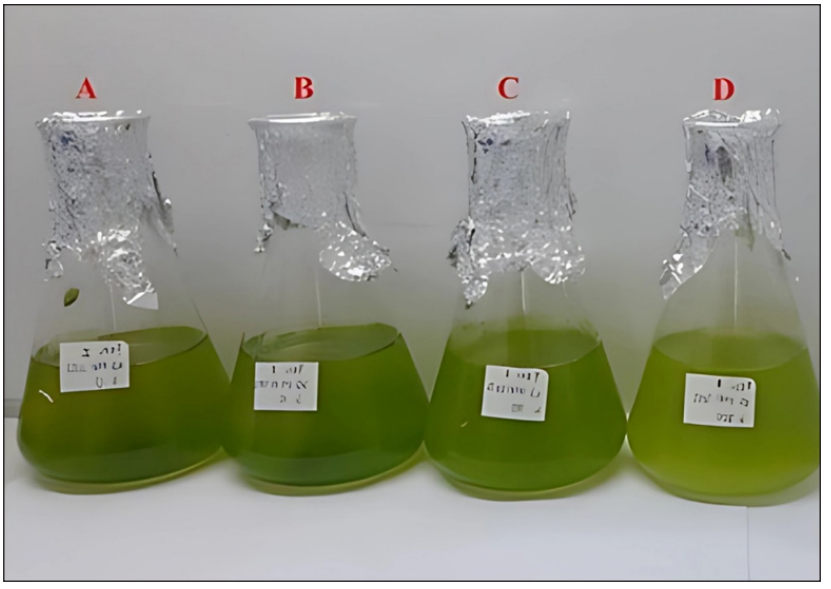

Figure 12. Colour differences of the UL4 cultivation in various lead concentrations at day 18
Note. (A) 0 ppm, (B) 10 ppm, (C) 100 ppm, and (D) 200 ppm

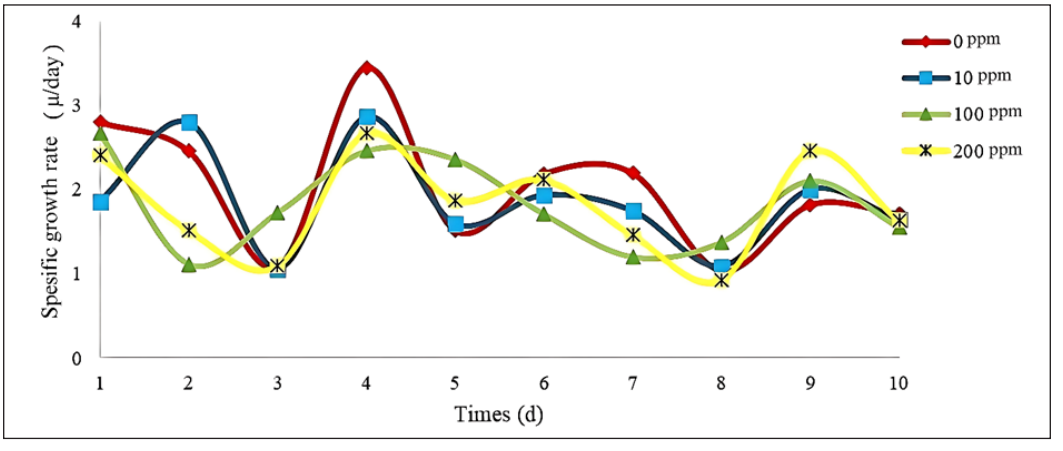

Figure 13. Specific growth rates of the UL4 culture based on optical density values. The optical density value was taken at a wavelength of 680 nm (OD_{680})
Note. Analyses of variance test showed $P > 0.05$

Lead also affected the growth of the UL4. The specific growth rates (µ/day) for the control (K0), 10 ppm (K10), 100 ppm (K100), and 200 ppm (K200) were 2.027 ± 0.75, 1.860 ± 0.60, 1.827 ± 0.54, and 1.814 ± 0.59, respectively. Although the growth rates varied among different lead concentrations, these variations were not statistically significant (ANOVA, *P*>0.05) (Figure 13).

Furthermore, the average of the dry biomass data showed that the lead affected the production of the UL4 biomass (Table 4). The highest biomass production was in the control group (1.7877 g/ml), whereas the lowest was in the 200-ppm lead treatment (0.3608 mg/L). These results indicated that increased lead concentrations caused a decrease in the biomass. The correlation analysis (r) showed an r value of -0.8. This indicated a strong negative relationship between concentration and dry weight; as the concentration of the metal increased, the production of dry weight decreased.

Table 4
Comparison of dry biomass weight of the UL4 isolates

Concentrations (ppm)	Dry biomass weight (g/mL)		
	Sample 1	Sample 2	Average
0	1.5903	1.9851	1.7877 ± 0.2
10	0.8323	1.3869	1.1096 ± 0.3
100	0.4695	0.9809	0.7252 ± 0.3
200	0.2993	0.4223	0.3608 ± 0.08

Note. Data were shown as mean ± standard deviation ($P > 0.05$) ($r = -0.8$)

DISCUSSION

The Different Microalgae Communities in the BG-11 and BBM

The BG-11 and BBM media could be used as the enrichment media to initiate the growth of the microalgae from the tin mining sites in West Bangka, Bangka Belitung. The coccoid green algae, filamentous green algae, and coccoid cyanobacteria, and diatoms were germinated after three weeks of incubation. Unfortunately, the initial observations of fresh samples could not be carried out because of the long lapse (4-6 weeks) from the time the sample was taken until the sample arrived at the laboratory. More microalgae exist in their natural habitat than those that germinate in the laboratory. While considering the lack of initial observation, the enrichment results in this study could provide a (limited) picture of the microalgae that exist in West Bangka. The presence of the green algae and diatoms in the mining sites has been reported by Gomes et al. (2021), who found *Chlorella* sp., *Chlamydomonas* sp., *Pinnularia* sp., and *Navicula* sp. in river flows around the copper and silver mining sites in São Domingos, Portugal. Additionally, the occurrence of filamentous and coccoid cyanobacteria in the mining sites was also documented by Damatac II and Cao (2022) in the mining sites around Acupan, Philippines.

The growth of many microalgae (7 species) on the BBM, while only three in the BG-11, can be predicted considering that the nutrient composition in the BBM was richer than the BG-11, especially the phosphorus content. Badr and Fouad (2021) reported that more

microalgae from Nile River water samples grew in the BBM (27 species) compared to the BG-11 (25 species). According to Badr and Fouad (2021), the high phosphorus (P) nutrient in the BBM supported a broader range of microalgal species compared to the BG-11. In this study, the phosphorus concentration in the final BBM medium was 1.711 mM, which was derived from 17.5 g/L potassium phosphate (KH_2PO_4, Merck, USA) and 7.5 g/L di-potassium hydrogen phosphate (K_2HPO_4, Merck, USA) stock solutions, respectively, whereas the BG-11 contained 0.229 mM phosphorus, which was derived from a 2 g/500 ml K_2HPO_4 stock solution. Previous studies also reported that high phosphorus could increase the algal diversity due to high nutrient sources, which supported the microalgae growth and reduced competition among species (Felisberto et al., 2011; Smith & Schindler, 2009). Furthermore, Felisberto et al. (2011) also discovered that high phosphorus supported the green algae diversity because the green algae could assimilate and accumulate P faster.

Although the BG-11 was specifically designed for cyanobacteria (Rippka, 1979), other species such as the diatoms and green algae could also grow in this medium. This study found the diatom *Nitzschia* sp. and a coccoid green alga. The cultivation of the diatoms in the BG-11 was reported previously by Sahin et al. (2019), who cultivated the marine diatom *Nanofrustulum shiloi*, and by Machado et al. (2021), who cultured the freshwater diatom *Nitzschia palea*. Additionally, the culture of the green algae in the BG-11 was documented by Purkayastha et al. (2017), who cultured *Chlorella elipsodea*.

The Culture Selection and Absorption Scanning

The selection of the UL cultures for the UV-C wavelength absorption experiments uses colourimetry. The use of colour to identify the culture conditions and microalgae growth has been extensively studied. For example, Salgueiro et al. (2022) used a Red–Green–Blue (RGB) colour palette to identify the growth of *Chlorella vulgaris*, while Castillo et al. (2023) used HEX colour pellets to observe the astaxanthin pigmentation in *Haematococcus pluvialis*. In this study, HEX colour pellets were used for the qualitative observation of the microalgal growth.

The variations of the culture colours indicated some cell conditions, such as pigment composition (Sarrafzadeh et al., 2015) and cell death (Indrayani et al., 2023). The green colour implied the dominance of the chlorophyll pigment, which reflected cell growth (Tang et al., 2023). The yellow colour indicated nutrient depletion (Fierdaus et al., 2015) and pigment alterations due to the metabolic processes (Alkhamis et al., 2022). Meanwhile, the brown colour indicated cell deterioration due to the nutrient deficiencies or contamination (Rinawati et al., 2020). Based on the colour, we documented that the UL culture grew faster and therefore chose it as the testing culture.

The ultraviolet visible (UV-Vis) scanning of the UL culture revealed absorption peaks at various wavelengths, including the UV-C range (200-280 nm). The appearance

of absorption peaks in the UV-C range indicated the presence of molecules that absorbed light, including the pigment molecules. The discovery of the UV wavelength absorption peaks was aligned with the study by Post and Larkum (1993), who found that maximal absorption occurred in the macroalga *Prasiola crispa* at a wavelength in the UV-B range (295 nm). According to Post and Larkum (1993), the UV-B absorption peaks were related to the presence of pigments such as chlorophyll and carotenoids as protective agents. Another pigment, such as sporopollenin, mycosporine-like amino acid (MAAs), and syctonemin, were also detected in the range of 280-315 nm (Dionisio-Sese, 2010).

Furthermore, Post and Larkum (1993) stated that the high UV-absorbing pigments appeared due to the high UV exposure in their habitat. Tin mining activities had increased the risk of UV exposure due to the reduction of vegetation and excavation activities. Excessive exposure to UV radiation led to the destruction of chloroplasts, mitochondria, and DNA (Holzinger & Lütz, 2006). Some of the species discovered in this study, such as *Anabaena* and *Nitzschia* from PA, UL, and BE samples, were recognised to survive the UV exposure. *Anabaena* produces syctonemin, mycosporine-glycine, porphyra, and shinorine to adapt to the UV-C exposure (Dionisio-Sese, 2010; Singh, 2008). On the other hand, *Nitzschia* adapted by changing the antioxidant, protein, and pigment levels.

Besides chlorophyll and carotenoid, the microalgae adapted to the UV radiation by forming xanthophyll and phycobiliprotein (Dionisio-Sese, 2010). According to Croce and van Amerongen (2014), phycobiliproteins were detected in the range of 560-680 nm, while xanthophyll was detected in the range of 400-450 nm. In this research, the absorption peaks at 400-480, 600, and 680 nm were documented (Table 2). The presence of these peaks at different wavelengths in the UL culture indicated the diversity of pigments contained in the various microalgal species in the UL culture.

The Absorbance of the UL Culture in the UV-C Spectrum

The absorbance observations of the UL cultures at the UV wavelengths showed differences in the maximum absorbance values between the BG-11 and BBM media. The cultures grown in the BBM medium exhibited a higher average absorbance value. A high absorbance value indicated a high concentration of substances that absorb light (Pratiwi & Nandiyanto, 2022). Although the specific types of substances or pigments at a wavelength of 230 nm were not investigated in this study, several studies reported that the pigments from the phenolic group, such as anthocyanins (Aleixandre-Tudo & du Toit, 2018), the photosynthetic pigments like scytonemin, tetramethoxyscytonemin, and dimethoxyscytonemin (Simeonov & Michaelian, 2017), as well as the MAAs (Garcia-Pichel & Castenholz, 1993), were absorbed at a wavelength of 230 nm.

The differences in the concentration of substances might have been caused by the variations in the growth rates of the microalgae or differences in the types of microalgae

present in the two media (Dionisio-Sese, 2010). Growth rate observations indicated that the microalgae grew more optimally in the BBM medium compared to the BG-11 medium. We also found the different microalgae that are present in the BBM and BG-11. For example, in the BBM, the microalgae were dominated by the green algae, while in the BG-11, the microalgae were dominated by the diatoms.

The higher growth in the BBM medium compared to the BG-11 medium might have been due to differences in the concentrations of the components of the media. The slower growth of microalgae in the BG-11 medium was also reported by Idenyi et al. (2016), who compared the growth of *Chlorella* in BG-11 and Bristol's Modified Medium (BMM). Idenyi et al. (2016) stated that high nitrogen concentrations resulted in slower growth. High nitrogen content could have decreased growth for some microalga species due to stress, which triggered a response leading to decreased protein levels affecting the photosynthesis process (Courchesne et al., 2009; Ördög et al., 2012). Furthermore, Ördög et al. (2012) explained that high nitrogen concentrations also triggered a decrease in the amount of chlorophyll a and b pigments.

Although there was no UV light treatment during the cultivation process, the UV-absorbing substances showed increased and decreased absorbance values. Variations in the absorbance values might be caused by the microalgae's population and adaptation mechanisms to nutritional changes and laboratory conditions. This result suggested that the UV-absorbing substances not only functioned to absorb UV radiation but also served other roles such as the abiotic stress and even involved in the remediation. Dionisio-Sese (2010) and Simeonov and Michaelian (2017) mentioned that the MAAs not only played a photoprotective role but also helped against thermal stress. Another UV absorption pigment, the phycocyanin, also played roles as a chelator for heavy metal remediation (Kalita & Baruah, 2023).

The Effect of Various Lead Concentrations on the UL4 Isolate

Lead influenced cell size, growth, and biomass, ultimately causing the death of the microalgae. This study discovered that the addition of metals could have increased the cell size. The increase in cell size after metal addition was also reported by Nishikawa et al. (2003), who discovered the increase in *Chlamydomonas acidophila* after being exposed to 20 μM cadmium. The increases in cell size were attributed to several factors, including the deposition of metal ions in the vacuole, which increased the vacuole size, cytoplasmic vesiculation, and an increase in starch as a response to stress protection conditions (Bauenova et al., 2021; La Rocca et al., 2009).

High lead concentration led to a decrease in the cell size. The decrease in cell size after the metal treatment was previously reported by Qiu et al. (2006), who cultivated *Chlorococcum AZHB* at copper and cadmium concentrations ranging from 0 to 200 ppm. The result showed that at a 200-ppm concentration of copper and cadmium, the cell size

of the microalgae decreased. The decrease in the cell size due to metal addition was also reported for *Koliella antarctica* (La Rocca et al., 2009). The cells of *K. antarctica* experienced loss of chloroplast shape, irregular thylakoid distribution, and cell lysis due to the addition of 5 ppm cadmium (La Rocca et al., 2009). The irregular cell shape and cell death of the UL4 in 200 ppm lead treatment were observed.

Besides affecting the cell morphology, lead influenced the growth of the microalgae. The growth of the microalgae decreased in alignment with the high concentrations of lead. The reduction in growth was indicated by decreases in the growth rate and dry weight. According to Dao and Beardall (2016), lead (Pb^{2+}) ions produce greater stress, resulting in alterations in antennae and central reactions in photosystem II, which inhibit photosynthesis, thereby decreasing the growth and biomass production of the algae.

The decrease in the specific growth rate of the UL4 isolate due to lead exposure was also reported by Teoh and Wong (2018), who cultured *Chlorella* sp. at a lead concentration of 0-100 mg/L. Their results showed that higher lead concentrations led to a lower specific growth rate. A decrease in the growth rate of the green algae due to an increase in lead concentration was also previously reported in *Chlorella sorokiniana* (Carfagna et al., 2013). Although the specific growth rate measurements in this research did not show a significant difference, there was still a difference in growth rates between the treatment and control. The control had the highest growth rate (2.027 μ/days), whereas at the 200-ppm lead concentration, the growth rate was 1.814 μ/days.

Additionally, Nanda et al. (2021) reported a decreased biomass production following lead treatment in *Chlorella sorokiniana UNIND6*. Their results showed that *C. sorokiniana* produced 0.78 g/L of dry biomass, whereas the control produced 1.2 g/L. Similarly, this research also observed less dry biomass after lead treatment. The control produced an average dry biomass of 1.787 g, whereas the 200-ppm lead treatment yielded an average of 0.608 g. According to Zeng et al. (2024), the decrease in the biomass was caused by lead metals binding with various compounds that disrupted the microalgal metabolite production, including proteins, thereby inhibiting growth.

CONCLUSION

There were different microalgae communities between the BG-11 and BBM. In the BG-11, the microalgae were dominated by diatoms and cyanobacteria, while in the BBM, there was a greater variety of green algae. The microalgae exhibited various absorbance peaks, demonstrating their ability to grow under the UV-C wavelengths. Lead treatment affected the microalgae cell size, organelle, and growth. The various absorbance peaks indicated that the microalgae may produce advantageous metabolites as an adaptive mechanism to a severe environment. Further investigation was needed regarding the species' molecular analysis, types of UV-C wavelength compounds, and their roles in lead bioremediation.

ACKNOWLEDGEMENT

This research was funded by Hibah Riset Universitas Indonesia in 2023 (Grant no: PENG-001/UN2.RST/PPM.00.00/2023).

REFERENCES

Ahmed, F., & Schenk, P. M. (2017). UV–C radiation increases sterol production in the microalga *Pavlova lutheri*. *Phytochemistry*, *139*, 25–32. https://doi.org/10.1016/j.phytochem.2017.04.002

Aleixandre-Tudo, J. L., & du Toit, W. (2018). The role of UV-visible spectroscopy for phenolic compounds quantification in winemaking. In R. L. Solís-Oviedo & Á. de la Cruz Pech-Canul (Eds.), *Frontiers and new trends in the science of fermented food and beverages*. IntechOpen. https://doi.org/10.5772/intechopen.79550

Alkhamis, Y. A., Mathew, R. T., Nagarajan, G., Rahman, S. M., & Rahman, M. M. (2022). pH induced stress enhances lipid accumulation in microalgae grown under mixotrophic and autotrophic condition. *Frontiers in Energy Research*, *10*, 1033068.

Andersen, R. A. (Ed.). (2005). *Algal culturing techniques* (1st ed.). Academic Press.

Badr, A. A., & Fouad, W. M. (2021). Identification of culturable microalgae diversity in the River Nile in Egypt using enrichment media. *African Journal of Biological Sciences*, *3*(2), 50–64.

Balzano, S., Sardo, A., Blasio, M., Chahine, T. B., Dell'Anno, F., Sansone, C., & Brunet, C. (2020). Microalgal metallothioneins and phytochelatins and their potential use in bioremediation. *Frontiers in Microbiology*, *11*, 517. https://doi.org/10.3389/fmicb.2020.00517

Bauenova, M. O., Sadvakasova, A. K., Mustapayeva, Z. O., Kokociński, M., Zayadan, B. K., Wojciechowicz, M. K., Balouch, H., Akmukhanova, N. R., Alwasel, S., & Allakhverdiev, S. I. (2021). Potential of microalgae *Parachlorella kessleri* Bh-2 as bioremediation agent of heavy metals cadmium and chromium. *Algal Research*, *59*, 102463. https://doi.org/10.1016/j.algal.2021.102463

Bidayani, E. (2017). *Study kelimpahan dan keanekaragaman mikroalga di perairan kolong bekas tambang timah Desa Lubuk Lingkuk dan Desa Laut Kecamatan Lubuk Besar Kabupaten Bangka Tengah* [Study of the abundance and diversity of microalgae in the waters of the former tin mine basin in Lubuk Lingkuk Village and Laut Village, Lubuk Besar District, Central Bangka Regency]. https://repository.ubb.ac.id/id/eprint/2634/

Bischoff, H. W., & Bold, H. C. (1963). *Some soil algae from enchanted rock and related algal species* (Vol. 4). University of Texas.

Blair, M. F., Kokabian, B., & Gude, V. G. (2014). Light and growth medium effect on *Chlorella vulgaris* biomass production. *Journal of Environmental Chemical Engineering*, *2*(1), 665–674. https://doi.org/10.1016/j.jece.2013.11.005

Blanco-Vieites, M., Suárez-Montes, D., Delgado, F., Álvarez-Gil, M., Battez, A. H., & Rodríguez, E. (2022). Removal of heavy metals and hydrocarbons by microalgae from wastewater in the steel industry. *Algal Research*, *64*, 102700. https://doi.org/10.1016/j.algal.2022.102700

Carfagna, S., Lanza, N., Salbitani, G., Basile, A., Sorbo, S., & Vona, V. (2013). Physiological and morphological responses of lead or cadmium exposed *Chlorella sorokiniana* 211-8K (Chlorophyceae). *SpringerPlus*, *2*, 147. https://doi.org/10.1186/2193-1801-2-147

Carino, J. D. G., & Vital, P. G. (2022). Characterization of isolated UV-C-irradiated mutants of microalga *Chlorella vulgaris* for future biofuel application. *Environment, Development and Sustainability*, *25*, 1258–1275.

Castillo, A., Finimundy, T. C., Heleno, S. A., Rodrigues, P., Fernandes, F. A., Pereira, S., Lores, M., Barros, L., & Garcia-Jares, C. (2023). The generally recognized as safe (GRAS) microalgae *Haematococcus pluvialis* (wet) as a multifunctional additive for colouring and improving the organoleptic and functional properties of foods. *Food and Function*, *14*(13), 6023–6035. https://doi.org/10.1039/D3FO01028G

Courchesne, N. M. D., Parisien, A., Wang, B., & Lan, C. Q. (2009). Enhancement of lipid production using biochemical, genetic and transcription factor engineering approaches. *Journal of Biotechnology*, *141*(1-2), 31–41. https://doi.org/10.1016/j.jbiotec.2009.02.018

Croce, R., & van Amerongen, H. (2014). Natural strategies for photosynthetic light harvesting. *Nature Chemical Biology*, *10*, 492-501. https://doi.org/10.1038/nchembio.1555

Damatac II, A. M., & Cao, E. P. (2022). Identification and diversity assessment of cyanobacterial communities from some mine tailing sites in Benguet Province, Philippines using isolation-dependent and isolation-independent methods. *Environment, Development and Sustainability*, *24*, 1166–1187.

Dao, L. H. T., & Beardall, J. (2016). Effects of lead on two green microalgae *Chlorella* and *Scenedesmus*: Photosystem II activity and heterogeneity. *Algal Research*, *16*, 150–159. https://doi.org/10.1016/j.algal.2016.03.006

Dionisio-Sese, M. L. (2010). Aquatic microalgae as potential sources of UV-screening compounds. *Philippine Journal of Science*, *139*(1), 5–16.

Felisberto, S. A., Leandrini, J. A., & Rodrigues, L. (2011). Effects of nutrients enrichment on algal communities: An experimental in mesocosms approach. *Acta Limnologica Brasiliensia*, *23*(2), 128–137. https://doi.org/10.1590/S2179-975X2011000200003

Fierdaus, M., & Kristiawan, O. (2015). The influence of media composition on the growth of *Scenedesmus* sp. microalgae in varied media. *Scientific Contributions Oil and Gas*, *38*(3), 225–232. https://doi.org/10.29017/SCOG.38.3.550

Garcia-Pichel, F., & Castenholz, R. W. (1993). Occurrence of UV-absorbing, mycosporine-like compounds among cyanobacterial isolates and an estimate of their screening capacity. *Applied and Environmental Microbiology*, *59*(1), 163–169.

Gauthier, M. R., Senhorinho, G. N. A., & Scott, J. A. (2020). Microalgae under environmental stress as a source of antioxidants. *Algal Research*, *52*, 102104. https://doi.org/10.1016/j.algal.2020.102104

Ghezelbash, F., Purakbar, L., Agh, N., & Khodabandeh, S. (2023). The effect of salinity, UV-C, UV-B irradiation stress on the growth, fatty acid and lipid class composition in *Dunaliella salina*. *Aquaculture Sciences*, *11*(20), 72–84.

Gomes, P., Valente, T., Albuquerque, T., Henriques, R., Flor-Arnau, N., Pamplona, J., & Macías, F. (2021). Algae in acid mine drainage and relationships with pollutants in a degraded mining ecosystem. *Minerals*, *11*(2), 110. https://doi.org/10.3390/min11020110

Govindan, N., Bhuyar, P., Feng, H. X., Ab. Rahim, M. H., Maniam, G. P., Sundararaju, S., & Muniyasamy, S. (2021). Evaluation of microalgae's plastic biodeterioration property by a consortium of *Chlorella* sp. and *Cyanobacteria* sp. *Journal of Environmental Research, Engineering and Management*, *77*(3), 86–98. https://doi.org/10.5755/j01.erem.77.3.25317

Habibi, A., Nematzadeh, G. A., Shariati, F. P., Amrei, H. D., & Teymouri, A. (2019). Effect of light/dark cycle on nitrate and phosphate removal from synthetic wastewater based on BG11 medium by *Scenedesmus* sp. *3 Biotech*, *9*, 150. https://doi.org/10.1007/s13205-019-1679-7

Haryati, U., & Dariah, A. (2019). Carbon emission and sequestration on tin mined land: A case study in Bangka Belitung Province. In *IOP Conference Series: Earth and Environmental Science* (Vol. 393, No. 1, p. 012097). IOP Publishing. https://doi.org/10.1088/1755-1315/393/1/012097

Hodač, L., Brinkmann, N., Mohr, K. I., Arp, G., Hallmann, C., Ramm, J., Spitzer, K., & Friedl, T. (2015). Diversity of microscopic green algae (Chlorophyta) in calcifying biofilms of two karstic streams in Germany. *Geomicrobiology Journal*, *32*(3-4), 275–290. https://doi.org/10.1080/01490451.2013.878418

Holzinger, A., & Lütz, C. (2006). Algae and UV irradiation: Effects on ultrastructure and related metabolic functions. *Micron*, *37*(3), 190–207. https://doi.org/10.1016/j.micron.2005.10.015

Idenyi, J. N., Ebenyi, L. N., Ogah, O., Nwali, B. U., & Ogbanshi, M. E. (2016). Effect of different growth media on the cell densities of freshwater microalgae isolates. *IOSR Journal of Pharmacy and Biological Sciences*, *11*(3), 24–28.

Indrayani, I., Ramadani, N. Z., Mawaddah, N., Kaseng, E. S., Sukainah, A., Putra, R. P., Hambali, A., Fadilah, R., Nurmila., & Ardiansyah. (2023). Influence of different culture media and light intensity on the growth and biomass productivity of a newly isolated *Chlorella* sp. UNM-IND1 from Waepella hot spring, South Sulawesi, Indonesia. *AACL Bioflux*, *16*(3), 1508-1518.

International Agency for Research on Cancer. (2012). *Radiation: Volume 100 D – A review of human carcinogens*. IARC.

Kalita, N., & Baruah, P. P. (2023). [Cyanobacteria as a potent platform for heavy metals biosorption: Uptake, responses and removal mechanisms. *Journal of Hazardous Materials Advances*, *11*, 100349. https://doi.org/10.1016/j.hazadv.2023.100349

Komárek, J., Kaštovský J., Mareš J., & Johansen J. R. (2014). Taxonomic classification of cyanoprokaryotes (cyanobacterial genera) 2014, using a polyphasic approach. *Preslia*, *86*, 295–335.

Koyande, A. K., Chew, K. W., Rambabu, K., Tao, Y., Chu, D.-T., & Show, P.-L. (2019). Microalgae: A potential alternative to health supplementation for humans. *Food Science and Human Wellness*, *8*(1), 16–24. https://doi.org/10.1016/j.fshw.2019.03.001

Krzemińska, I., Pawlik-Skowrońska, B., Trzcińska, M., & Tys, J. (2014). Influence of photoperiods on the growth rate and biomass productivity of green microalgae. *Bioprocess and Biosystems Engineering*, *37*, 735-741. https://doi.org/10.1007/s00449-013-1044-x

La Rocca, N., Andreoli, C., Giacometti, G. M., Rascio, N., & Moro, I. (2009). Responses of the Antarctic microalga *Koliella antarctica* (Trebouxiophyceae, Chlorophyta) to cadmium contamination. *Photosynthetica*, *47*(3), 471–479. https://doi.org/10.1007/s11099-009-0071-y

Lloyd, C., Tan, K. H., Lim, K. L., Valu, V. G., Fun, S. M. Y., Chye, T. R., Mak, H. M., Sim, W. X., Musa, S. L., Ng, J. J. Q., Nordin, N. S. B., Md Aidzil, N. B., Eng, Z. Y. W., Manickavasagam, P., & New, J. Y. (2021). Identification of microalgae cultured in Bold's Basal medium from freshwater samples, from a high-rise city. *Scientific Reports*, *11*, 4474. https://doi.org/10.1038/s41598-021-84112-0

Machado, M., Vaz, M. G. M. V., Bromke, M. A., Rosa, R. M., Covell, L., de Souza, L. P., Rocha, D. I., Martins, M. A., Araújo, W. L., Szymański, J., & Nunes-Nesi, A. (2021). Metabolic stability of freshwater *Nitzschia palea* strains under silicon stress associated with triacylglycerol accumulation. *Algal Research*, *60*, 102554. https://doi.org/10.1016/j.algal.2021.102554

Miranda, F., Kurniawan, K., & Adibrata, S. (2018). Kandungan logam berat timbal (Pb) dan kadmium (Cd) pada sedimen di perairan sungai Pakil Kabupaten Bangka [The content of heavy metals lead (Pb) and cadmium (Cd) in sediment in the waters of the Pakil River, Bangka Regency]. *Akuatik: Jurnal Sumberdaya Perairan*, *12*(2), 84-92.

Nanda, M., Jaiswal, K. K., Kumar, V., Vlaskin, M. S., Gautam, P., Bahuguna, V., & Chauhan, P. K. (2021). Micro-pollutant Pb (II) mitigation and lipid induction in oleaginous microalgae *Chlorella sorokiniana* UUIND6. *Environmental Technology and Innovation*, *23*, 101613. https://doi.org/10.1016/j.eti.2021.101613

Nishikawa, K., Yamakoshi, Y., Uemura, I., & Tominaga, N. (2003). Ultrastructural changes in *Chlamydomonas acidophila* (Chlorophyta) induced by heavy metals and polyphosphate metabolism. *FEMS Microbiology Ecology*, *44*(2), 253–259. https://doi.org/10.1016/s0168-6496(03)00049-7

Ördög, V., Stirk, W. A., Bálint, P., van Staden, J., & Lovász, C. (2012). Changes in lipid, protein and pigment concentrations in nitrogen-stressed *Chlorella minutissima* cultures. *Journal of Applied Phycology, 24*, 907–914. https://doi.org/10.1007/s10811-011-9711-2

Post, A., & Larkum, A. W. D. (1993). UV-absorbing pigments, photosynthesis and UV exposure in Antarctica: Comparison of terrestrial and marine algae. *Aquatic Botany*, *45*(2-3), 231-243.

Pratiwi, R. A., & Nandiyanto, A. B. D. (2022). How to read and interpret UV-VIS spectrophotometric results in determining the structure of chemical compounds. *Indonesian Journal of Educational Research and Technology*, *2*(1), 1-20. https://doi.org/10.17509/ijert.v2i1.35171

Puilingi, C. G., Tan, S. N., Maeno, Y., Leaw, C. P., Lim, P. T., Yotsu-Yamashita, M., Terada, R., & Kotaki, Y. (2022). First record of the diatom *Nitzschia navis-varingica* (Bacillariophyceae) producing amnesic shellfish poisoning-toxins from Papua New Guinea. *Toxicon*, *216*, 65–72. https://doi.org/10.1016/j.toxicon.2022.06.016

Purkayastha, J., Bora, A., Gogoi, H. K., & Singh, L. (2017). Growth of high oil yielding green alga *Chlorella ellipsoidea* in diverse autotrophic media, effect on its constituents. *Algal Research*, *21*, 81–88. https://doi.org/10.1016/j.algal.2016.11.009

Qiu, C. E., Kuang, Q. J., Bi, Y. H., Liu, G. X., & Hu, Z. Y. (2006). Response of *Chlorococcum* sp. AZHB to copper and cadmius stress. *Bulletin of Environmental Contamination and Toxicology*, *77*, 772-778. https://doi.org/10.1007/s00128-006-1130-8

Rachman, A. (2019). Struktur komunitas fitoplankton di area tambang timah dan perairan sekitar Kabupaten Bangka Barat [Phytoplankton community structure in the waters around the coastal tin mining of West Bangka]. *Jurnal Teknologi Lingkungan*, *20*(2), 189-204. https://doi.org/10.29122/jtl.v20i2.2938

Rinawati, M., Sari, L. A., & Pursetyo, K. T. (2020). Chlorophyll and carotenoids analysis spectrophotometer using method on microalgae. In *IOP Conference Series: Earth and Environmental Science* (Vol. 441, No. 1, p. 012056). IOP Publishing. https://doi.org/10.1088/1755-1315/441/1/012056

Rippka, R., Deruelles, J., Waterbury, J. B., Herdman, M., & Stanier, R. Y. (1979). Generic assignments, strain histories and properties of pure cultures of cyanobacteria. *Microbiology*, *111*(1), 1–61.

Rosen, B. H., & Mareš, J. (2016). *Catalog of microscopic organisms of the Everglades, Part 1—The cyanobacteria*. United States Geological Survey.

Sahin, M. S., Khazi, M. I., Demirel, Z., & Dalay, M. C. (2019). Variation in growth, fucoxanthin, fatty acids profile and lipid content of marine diatoms *Nitzschia* sp. and *Nanofrustulum shiloi* in response to nitrogen and iron. *Biocatalysis and Agricultural Biotechnology*, *17*, 390-398. https://doi.org/10.1016/j.bcab.2018.12.023

Sahoo, D., & Baweja, P. (2015). General characteristics of algae. In D. Sahoo & J. Seckbach (Eds.), *The algae world* (Vol. 26, pp. 3-29). Springer.

Salgueiro, J. L., Pérez, L., Sanchez, Á., Cancela, Á., & Míguez, C. (2022). Microalgal biomass quantification from the non-invasive technique of image processing through red–green–blue (RGB) analysis. *Journal of Applied Phycology*, *34*, 871-881. https://doi.org/10.1007/s10811-021-02634-6

Sandeep, K. P., KumaraguruVasangam, K. P., Kumararaja, P., Syama Dayal, J., Sreekanth, G. B., Ambasankar, K., & Vijayan, K. K. (2019). Microalgal diversity of a tropical estuary in south India with special reference to isolation of potential species for aquaculture. *Journal of Coastal Conservation*, *23*, 253-267. https://doi.org/10.1007/s11852-018-0655-4

Sarrafzadeh, M. H., La, H.-J., Seo, S.-H., Asgharnejad, H., & Oh, H.-M. (2015). Evaluation of various techniques for microalgal biomass quantification. *Journal of Biotechnology*, *216*, 90–97. https://doi.org/10.1016/j.jbiotec.2015.10.010

Senhorinho, G. N. A., Laamanen, C. A., & Scott, J. A. (2018). Bioprospecting freshwater microalgae for antibacterial activity from water bodies associated with abandoned mine sites. *Phycologia*, *57*(4), 432–439. https://doi.org/10.2216/17-114.1

Shuba, E. S., & Kifle, D. (2018). Microalgae to biofuels: 'Promising' alternative and renewable energy, review. *Renewable and Sustainable Energy Reviews*, *81*(Part 1), 743–755. https://doi.org/10.1016/j.rser.2017.08.042

Shubert, E., & Gärtner, G. (2015). Nonmotile coccoid and colonial green algae. In *Freshwater algae of North America* (2nd ed., pp. 315–373). Academic Press. https://doi.org/10.1016/B978-0-12-385876-4.00007-4

Simeonov, A., & Michaelian, K. (2017). *Properties of cyanobacterial UV-absorbing pigments suggest their evolution was driven by optimizing photon dissipation rather than photoprotection*. arXiv. https://doi.org/10.48550/arXiv.1702.03588

Singh, S. P., Sinha, R. P., Klisch, M., & Häder, D.-P. (2008). Mycosporine-like amino acids (MAAs) profile of a rice-field cyanobacterium *Anabaena doliolum* as influenced by PAR and UVR. *Planta*, *229*, 225–233. https://doi.org/10.1007/s00425-008-0822-1

Smith, V. H., & Schindler, D. W. (2009). Eutrophication science: Where do we go from here? *Trends in Ecology and Evolution*, *24*(4), 201-207. https://doi.org/10.1016/j.tree.2008.11.009

Stanier, R. Y., Kunisawa, R., Mandel, M., & Cohen-Bazire, G. (1971). Purification and properties of unicellular blue-green algae (order Chroococcales). *Bacteriological Reviews*, *35*(2), 171-205. https://doi.org/10.1128/br.35.2.171-205.1971

Susanti, H., Rahman, D. Y., Praharyawan, S., & Susilaningsih, D. (2021). Characterization and identification of tropical lipid-producing microalgae isolated from abandoned kaolin and tin mine site in Belitung Island, Indonesia. *Journal of Hunan University Natural Sciences*, *48*(10), 571-576.

Swastiwi, A. W., Nugraha, S. A., & Purnomo, H. (2017). *Lintas sejarah perdagangan timah di Bangka Belitung abad 19-20* [A cross-history of tin trade in Bangka Belitung in the 19th- 20th centuries]. Balai Pelestraian Nilai Budaya.

Tamura, K., & Nei, M. (1993). Estimation of the number of nucleotide substitutions in the control region of mitochondrial DNA in humans and chimpanzees. *Molecular Biology and Evolution*, *10*(3), 512–526. https://doi.org/10.1093/oxfordjournals.molbev.a040023

Tamura, K., Stecher, G., & Kumar, S. (2021). MEGA11: Molecular Evolutionary Genetics Analysis Version 11. *Molecular Biology and Evolution*, 38(7), 3022–3027. https://doi.org/10.1093/molbev/msab120

Tan, S. N., Teng, S. T., Lim, H. C., Kotaki, Y., Bates, S. S., Leaw, C. P., & Lim, P. T. (2016). Diatom *Nitzschia navis-varingica* (Bacillariophyceae) and its domoic acid production from the mangrove environments of Malaysia. *Harmful Algae*, *60*, 139-149. https://doi.org/10.1016/j.hal.2016.11.003

Tang, D. Y. Y., Chew, K. W., Ting, H.-Y., Sia, Y.-H., Gentili, F. G., Park, Y.-K., Banat, F., Culaba, A. B., Ma, Z., & Show, P. L. (2023). Application of regression and artificial neural network analysis of Red-Green-Blue image components in prediction of chlorophyll content in microalgae. *Bioresource Technology*, *370*, 128503. https://doi.org/10.1016/j.biortech.2022.128503

Tawa, D. A., Afriyansyah, B., Ihsan, M., & Nugraha, M. A. (2019). Biokonsentrasi timbal (Pb) pada hepatopankreas, insang dan daging *Penaeus merguiensis* di Teluk Kelabat bagian luar [Bioconcentration of lead (Pb) in hepatopancreas, gills and flesh of *Penaeus merguiensis* in outer Kelabat Bay]. *Jurnal Kelautan Tropis*, *22*(2), 109-117.

Tekiner, M., Ak, İ., & Kurt, M. (2019). Impact of UV-C radiation on growth of micro and macro algae in irrigation systems. *Science of The Total Environment*, *672*, 81-87. https://doi.org/10.1016/j.scitotenv.2019.03.460

Teoh, M.-L, & Wong, S.-W. (2018). Influence of lead on growth and physiological characteristics of a freshwater green alga *Chlorella* sp. *Malaysian Journal of Science*, *37*(2), 82-93. https://doi.org/10.22452/mjs.vol37no2.1

Videau, P., & Cozy, L. M. (2019). *Anabaena* sp. strain PCC 7120: Laboratory maintenance, cultivation, and heterocyst induction. *Current Protocols in Microbiology*, *52*(1), e71. https://doi.org/10.1002/cpmc.71

Wan, M., Rosenberg, J. N., Faruq, J., Betenbaugh, M. J., & Xia, J. (2011). An improved colony PCR procedure for genetic screening of *Chlorella* and related microalgae. *Biotechnology Letters*, *33*, 1615-1619. https://doi.org/10.1007/s10529-011-0596-6

Wehr, J. D., Sheath, R. G., & Kociolek, J. P. (Eds.). (2014). *Freshwater algae of North America: Ecology and classification*. Academic Press. https://doi.org/10.1016/C2010-0-66664-8

Xu, S.-M., Liu, B., Rioual, P., Yi, M.-Q., & Ma, Y.-D. (2024). A new freshwater species of *Pinnularia* (Bacillariophyta) from Hunan Province, China. *PhytoKeys*, *237*, 179-189. https://doi.org/10.3897/phytokeys.237.116946

Yan, H., Han, Z., Zhao, H., Zhou, S., Chi, N., Han, M., Kou, X, Zhang, Y., Xu, L. Tian, C., & Qin, S. (2014). Characterization of calcium deposition induced by *Synechocystis* sp. PCC6803 in BG11 culture medium. *Chinese Journal of Oceanology and Limnology*, *32*, 503-510. https://doi.org/10.1007/s00343-014-3150-2

Yang, C.-C., Wen, R. C., Shen, C. R., & Yao, D.-J. (2015). Using a microfluidic gradient generator to characterize BG-11 medium for the growth of cyanobacteria *Synechococcus elongatus* PCC7942. *Micromachines*, *6*(11), 1755-1767.

Yusof, T. N., Rafatullah, M., Ismail, N., Zainuddin, Z., & Lalung, J. (2017). Application of selected Malaysian wild plant leaves as potential control of cyanobacterial bloom. *International Journal of Research and Environment Science*, *3*(1), 10-19. https://doi.org/10.20431/2454-9444.0301002

Zehra, S., Gul, I. H., & Hussain, Z. (2018). Liquid crystal based optical platform for the detection of Pb^{2+} ions using $NiFe_2O_4$ nanoparticles. *Results in Physics*, *9*, 1462-1467. https://doi.org/10.1016/j.rinp.2018.04.063

Zeng, Y., Chen, X., Zhu, J., Long, D., Jian, Y., Tan, Q., & Wang, H. (2024). Effects of Cu (II) on the growth of *Chlorella vulgaris* and its removal efficiency of pollutants in synthetic piggery digestate. *Toxics*, *12*(1), 56.

Zhang, Y.-K., Shen, G.-F., & Ru, B.-G. (2005). Survival of human metallothionein-2 transplastomic *Chlamydomonas reinhardtii* to ultraviolet B exposure. *Acta Biochimica et Biophysica Sinica*, *38*(3), 187-193. https://doi.org/10.1111/j.1745-7270.2006.00148.x

Pertanika J. Sci. & Technol. 33 (5): 2207 - 2236 (2025)

PERTANIKA JOURNALS

SCIENCE & TECHNOLOGY

Journal homepage: http://www.pertanika.upm.edu.my/

Review Article

A Systematic Literature Review on Factors Affecting the Compatibility of Natural Fibre as Cement Board Reinforcement

Hasniza Abu Bakar, Lokman Hakim Ismail*, Emedya Murniwaty Samsudin, Nik Mohd Zaini Nik Soh, Siti Khalijah Yaman and Hannifah Tami

Faculty of Civil Engineering and Built Environment, Universiti Tun Hussein Onn Malaysia, 86400 Parit Raja, Batu Pahat, Johor Darul Takzim, Malaysia

ABSTRACT

The compatibility of natural fibres in cement composite is a significant concern, primarily due to their inherent incompatibility with the cement matrix. Fibre's intrinsic extractive presence cannot be used solely as a primary material for cement board (CB). Therefore, this study aims to conduct a systematic literature review (SLR) to identify the main factors that affect the compatibility between natural fibre and CB products. The review processes were based on Preferred Reporting Items for Systematic Reviews and Meta-Analyses (PRISMA) and were conducted through identification, screening, eligibility, and data extraction procedures. From an intensive literature review, the compatibility of natural fibre with cement was determined to be primarily influenced by its chemical composition. As such, this aspect must be thoroughly examined before producing fibre-cementitious composites due to the varying chemical arrangement of the chemical composition of natural fibres, ranging from cellulose content (22-79.3%), followed by hemicellulose (6.9-48%) and lignin (2.44-29%). Previous studies have revealed that cellulose is the primary structural component of cell walls. The elevated cellulose content in processed fibre mainly influences its strength. This is accomplished by employing treated fibres that eliminate contaminants, leading to void circular cavities or increased pore dimensions. Notably, the approach elevates the cellulose content, diminishes the fibre diameter, augments the tensile strength, and concurrently improves the performance of the CB. The analysis of variance (ANOVA) test demonstrated a significant *P*-value of less than 0.05 ($P < 0.05$), suggesting that the increase in cellulose content significantly affects the tensile

ARTICLE INFO

Article history:
Received: 10 November 2024
Accepted: 17 April 2025
Published: 28 August 2025

DOI: https://doi.org/10.47836/pjst.33.5.08

E-mail addresses:
hasniza@uthm.edu.my (Hasniza Abu Bakar)
lokman@uthm.edu.my (Lokman Hakim Ismail)
emedya@uthm.edu.my (Emedya Murniwaty Samsudin)
nikzaini@uthm.edu.my (Nik Mohd Zaini Nik Soh)
khalijah@uthm.edu.my (Siti Khalijah Yaman)
hannifah@uthm.edu.my (Hannifah Tami)
* Corresponding author

e-ISSN: 2231-8526

strength of the fibre. Therefore, this study reveals the importance of cellulose content and its impact on the performance of CB. Thus, it can be concluded that natural fibre possesses considerable potential as a sustainable material for CB composite reinforcement.

Keywords: Compatibility, cement board reinforcement, natural fibre

INTRODUCTION

Over the past few decades, cement has rapidly increased its use of wood as a natural fibre reinforcement. According to Aras et al. (2022), wood is one of the raw materials used to make CB. Nowadays, the use of CB has gained interest among construction practitioners in Malaysia as one of the industrial building systems (IBS) components. The application of CB in construction projects as IBS components, such as wall siding, façades, and roof panels (Hasan et al., 2021b). The United Nations (2022) highlights the growing focus on green building initiatives to enhance resource efficiency, reduce waste, and promote a circular economy. However, the use of wood as a fibre reinforcement raises forest resource demand (Maynet et al., 2021). Previously, asbestos fibres (Momoh & Osofero, 2020) and synthetic fibres (Futami et al., 2021; Mawardi et al., 2022) were generally used for building construction material. But the use of these cement composites poses risks to health exposure (Momoh & Osofero, 2020), discharging plenty of carbon dioxide, high cost, and not biodegradable (Futami et al., 2021; Hasan et al., 2021b). To address these issues, non-wood materials can be used with cement matrices for construction materials. Therefore, most of the researchers are now investigating new alternatives to other non-wood lignocellulose materials such as palm fibres (Abrha et al., 2024), kenaf fibres (Amel et al., 2020; Amiandamhen & Osadolor, 2020; Malik et al., 2021), coconut and oil palm fibres (Futami et al., 2021), rice husk fibres (Jiang et al., 2020; Xie & Li, 2021), pineapple fibres (Syduzzaman et al., 2020), coir fibre (Budiman et al. 2021; K. J. Rao et al., 2024; Kochova, Gauvin, et al., 2020; Stapper et al., 2021; Zhang et al., 2022), empty fruit bunches (EFB) fibres (Iskandar et al., 2021; Maynet et al., 2023; Peter et al., 2020; Ridzuan et al., 2023), bamboo fibres (Taiwo et al., 2024), and others to replace wood fibres in the natural fibre composite products.

On top of that, the construction industries are going to turn to the implementation of cement-based products in green building materials and construction technology to meet the Sustainable Development Goals (SDGs). Previous research has explored the natural fibre in polymer composites for the production of micro-perforated panels, particle boards, and medium-density fibre boards (Rao & Ramakrishna, 2022). The utilization of natural fibre in cement composites is very less compared with epoxy composites, however, few researchers enhancing composite products as fibre reinforcement that can be used for indoor and outdoor building materials like concrete (Futami et al., 2021; Houda et al.,

2024), fibre cement flat sheets (Taiwo et al., 2024), roof tile (Rao et al., 2024; Momoh & Osofero, 2020), brick (Momoh & Osofero, 2020), cement boards (Budiman et al., 2021; Maynet et al., 2023; Peter et al., 2020; Ridzuan et al., 2023), building claddings and facades (Momoh & Osofero, 2020).

Furthermore, the issue of compatibility is a significant challenge in the manufacturing of fibre-cement products (Aras et al., 2022; Hasan et al., 2020, 2021; Xie & Li, 2021). The aspect of compatibility between natural fibres and cement has been emphasised in numerous studies that examined the utilisation of bio-composites. Based on research by Hasan et al. (2021), the cement becomes compatible with the fibre if there is no or little disturbance during the chemical reaction of cement board formations. Conversely, the cement could be incompatible with wood or fibre substances if any imperfection occurred during the CB fabrication process, especially at the hardening stage of the cement. El Hamri et al. (2024) indicate that the presence of hemicellulose, starch, sugar, tannins, and lignin in fibre-cement composites leads to compatibility issues that significantly hinder the cement hydration process. Consequently, this primarily influences the mechanical strength of fibre-cement composites (Hasan et al., 2020; Maynet et al., 2021). Furthermore, to improve the compatibility between the fibre and the cementitious material, it is essential to perform fibre modification before its application (Jiang et al., 2020; Maynet et al., 2021). The modifications were made to improve board properties by removing certain extractives to expedite the cement setting and hardening process (El Hamri et al., 2024). Therefore, it is important to identify the key factors of compatibility between the fibre and cement that can significantly impede the hardening process. The significance of these aspects is paramount in the production of cement composites. According to recent research, there is insufficient comprehensive information regarding the primary factors influencing the compatibility of natural fibre as a reinforcement in composite materials.

This systematic review was performed in accordance with the guidelines outlined in the Preferred Reporting Items for Systematic Reviews and Meta-Analyses (PRISMA) checklist. A SLR serves as a robust method for acquiring comprehensive insights into the most relevant research findings pertaining to a specific inquiry (Alaloul et al., 2021). SLR is a systematic approach that thoroughly identifies and integrates relevant research while adhering to structured, transparent, and reproducible methods at every stage of the process. The review procedures, encompassing identification, screening, eligibility, and data extraction, have not been sufficiently addressed. This gap highlights concerns about transparency and bias in traditional literature review practices. Moreover, numerous authors often select articles that support their research findings (Shaffril et al., 2020). Such a system would present a significant challenge for future scholars in replicating the study, validating the interpretations, or assessing the study's comprehensiveness. The present study seeks to perform an SLR that specifically examines the compatibility of natural fibre with

cement, addressing the identified gap in the existing literature. During the review process, the authors focused on the primary research question: "What are the factors affecting the compatibility of natural fibre in a cement matrix?". The primary emphasis of this paper is on the key factors that influence the performance of CB. Therefore, this study aimed to find the main factor that contributes to the compatibility between natural fibres and cement in the cement board, which primarily influences the fibre's strength and simultaneously improves the performance of the CB.

METHODOLOGY

Systematic Literature Review

The SLR was performed by examining electronic databases and bibliographies of published research and reviews (Mhd Noor et al., 2023). This method was used as a comprehensive tool based on the PRISMA framework diagram. Previously, PRISMA was frequently employed in the field of environmental management. Nevertheless, since its introduction, the review approach has garnered much attention and has been widely utilised by many researchers. For instance, Thompson et al. (2025) applied the method in the field of civil engineering, and Alaloul et al. (2021) utilised it in the context of construction materials investigations. Meanwhile, according to Shaffril et al. (2021), PRISMA's primary focus is on randomised trials, and it may also serve as a guide for systematic reviews in any field of research that incorporates intervention evaluations. The current study employed the PRISMA framework, which encompasses three distinct domains of inquiry: environmental science, material sciences, and engineering. The analysis utilised two main scholarly databases as recommended by Thompson et al. (2025), which are Scopus and the Web of Science (WoS). The databases were selected because both are the most prominent databases in the context of an SLR. The advantages of these resources include advanced search tools, extensive coverage, rigorous quality control measures for articles, and a multidisciplinary focus that includes studies on environmental management and related fields (Gusenbauer & Haddaway, 2020).

Systematic Review Process

The current research utilised three systematic methodologies to gather pertinent publications: identification, screening, eligibility, and data abstraction, as recommended by Shaffril et al. (2020, 2021). This study effectively used these methodologies to identify and integrate relevant research in order to facilitate a systematic and clear SLR. The SLR method consists of four distinct phases, as outlined by Shaffril et al. (2021): (i) identification, (ii) screening, (iii) eligibility, and (iv) data extraction. Figure 1 illustrates the four phases of the SLR method utilised in the paper.

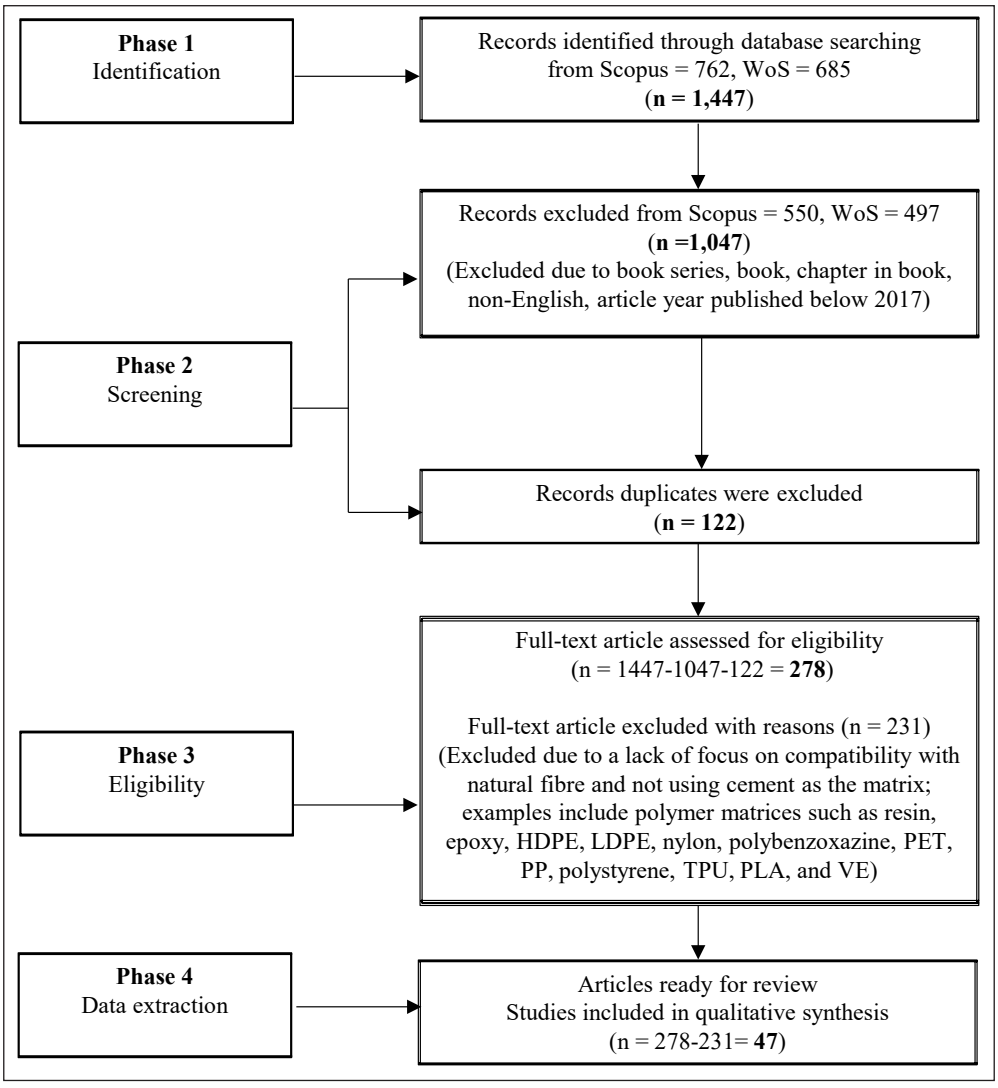

Figure 1. PRISMA diagram (Alaloul et al., 2021)
Note. PRISMA = Preferred Reporting Items for Systematic Reviews and Meta-Analyses; WoS = Web of Science; HDPE = High-density polyethylene; LDPE = Low-density polyethylene; PET = Polyethylene terephthalate; PP = Polypropylene; TPU = Thermoplastic polyurethane; PLA = Polylactic acid; VE = Vinyl ester

Phase 1: Identification

The initial stage consisted of identifying the keywords used in the search process. Three primary keywords were identified according to the defined research questions: compatibility, natural fibre, and CB. To enhance the richness of these keywords, a thorough search for synonyms, related phrases, and variations was performed. This was accomplished by utilising an online thesaurus, specifically thesaurus.com, and referencing the keywords used

in prior research. Additionally, the keywords recommended by Scopus were considered, and input from experts in the field was solicited. This procedure involved the examination of several terms associated with CB, including composite, bio-composite, biocomposite, cement composite, cement board, cementboard, cement-bonded board, particleboard, particle board, cement-bonded, cement-based product, fiberboard, and fibre board. The search functions employed for processing keyword combinations comprised field code functions, phrase searching, wildcards, truncation, and Boolean operators within Scopus databases (Table 1). A total of 762 records were identified through database searching in Scopus, while 685 records were identified in Web of Science, covering a duration of 6 years. The search methodology utilised a human approach known as "handpicking" from reputable databases, including Google Scholar. The search efforts yielded a total of 1,447 potential articles from the selected databases, as depicted in Figure 1.

Table 1
The search string used for the systematic review process

Database	String
Scopus	TITLE-ABS-KEY ((*"compatibility"*) AND (*"natural fib*"*) AND (*"composite*"* OR *"biocomposite*"* OR *"bio composite*"* OR *"bio-composite*"* OR *"cement"* OR *"cement composite*"* OR *"cementboard*"* OR *"cement board*"* OR *"cement bonded board*"* OR *"particleboard*"* OR *"particleboard*"* OR *"cement bonded"* OR *"cement-bonded"* OR *"cement based product*"* OR *"fib*board*"* OR *"fib* board*"*))
Web of Science	(("compatibility") AND ("natural fib*") AND ("composite*" OR "biocomposite*" OR "bio composite*" OR "bio-composite*" OR "cement" OR "cement composite*" OR "cementboard*" OR "cement board*" OR "cement bonded board*" OR "particleboard*" OR "particle board*" OR "cement bonded" OR "cement-bonded" OR "cement based product*" OR "fib*board*" OR "fib* board*"))

Phase 2: Screening

The second step in the process was screening, wherein publications were evaluated for their inclusion or exclusion from the study. The process was executed using either database assistance or manual screening performed by the authors. The inclusion or exclusion of articles was determined by a specific set of criteria, as detailed in Table 2. By the notion of "research field maturity" highlighted by Kraus et al. (2020), this study has restricted the screening procedure to encompass only publications published from 2020 onwards. Furthermore, the selection of this timeline was based on the number of published papers required for a comprehensive review. The authors decided to focus on empirical research publications, as these provide the necessary source data for an in-depth examination. It

is worth noting that, to prevent any potential misinterpretation, only texts written in the English language were taken into consideration. Given that the purpose of the SLR pertains to material studies, the selection of material science, environmental science, and engineering as the subject areas was deemed to enhance the likelihood of obtaining a greater number of articles relevant to the study. At this juncture, among the pool of 1,047 articles deemed suitable for review, a cumulative count of 122 items exhibiting duplication was excluded.

Table 2
Inclusion and exclusion criteria

Criterion	Inclusion	Exclusion
Timeline	2020 and 2025	< 2020
Document type	Articles	Book chapter, book series
Language	English	Non-English
Subject area	Material science, Environmental science, Engineering	

Phase 3: Eligibility

The third phase entails the assessment of eligibility, during which all the articles were obtained for further analysis. The authors conducted a manual examination of the remaining papers to assess their relevance, employing methods such as reading the title, abstract, or the complete text. The initial review of the abstracts was followed by a comprehensive examination of all the articles to identify relevant themes or factors influencing the compatibility of natural fibres. Following the completion of the evaluation process, a cumulative count of 231 articles was deemed ineligible for inclusion due to their lack of emphasis on the compatibility of natural fibre, CB, or cement composite. These articles were excluded due to a lack of focus on the compatibility of natural fibre and insufficient emphasis on the use of cement, including polymer matrices such as resin, epoxy, and others.

Phase 4: Data Extraction

The final round of the evaluation process for data extraction yielded a total of 47 articles.

RESULTS

Descriptive Information

Based on the provenance of the articles, out of the 47 articles, a significant portion, nine papers (19%), originated from Malaysia. This was followed by the Netherlands, which contributed six papers (13%), and four papers (9%) were from the United Kingdom and Hungary, as illustrated in Figure 2. The interest might be ascribed to the abundant availability of significant quantities of natural fibres within these nations.

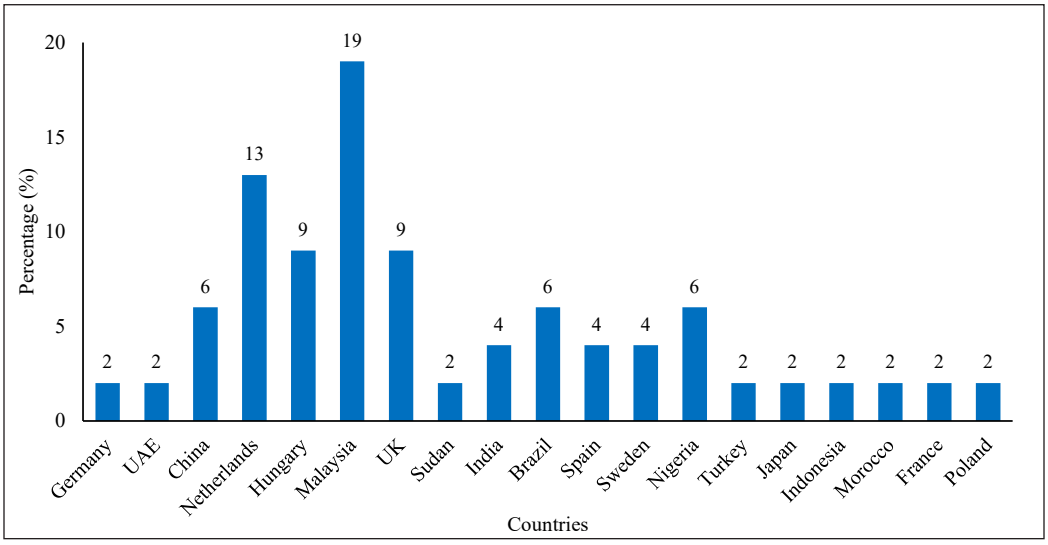

Figure 2. Distribution of research based on origin
Note. UAE = United Arab Emirates; UK = United Kingdom

Factors Affecting the Compatibility of Natural Fibre as CB Reinforcement

The present study involved the examination of 47 specifically chosen items, leading to the identification of two primary factors: (1) Fibre strand and (2) CB. Subsequently, each factor was categorised into three sub-factors, as shown in Table 3. The main research question

Table 3
Factors affecting the compatibility of natural fibre in cement board

No.	Authors	Type of natural fibre	Fibre strand			Cement board		
			Fibre properties	Fibre treatment	Cement hydration	Density	Cement–fibre ratio	Water content
1	Kochova, Caprai, et al. (2020)	Wood fibre	√		√			√
2	Kochova, Gauvin, et al. (2020)	Coir fibre	√					
3	Amel et al. (2020)	Kenaf fibre			√		√	
4	Jiang et al. (2020)	Straw fibre		√	√			√
5	Peter et al. (2020)	EFB fibre		√		√	√	√
6	Hasan et al. (2020)	Hungarian plant	√		√			
7	Bonnet-Masimbert et al. (2020)	Oil palm fibre	√	√	√			

Table 3 *(continue)*

No.	Authors	Type of natural fibre	Fibre strand			Cement board		
			Fibre properties	Fibre treatment	Cement hydration	Density	Cement–fibre ratio	Water content
8	Owoyemi et al. (2020)	*Gmelina arborea* (Roxb.)		√		√	√	
9	Momoh and Osofero (2020)	Oil palm fibre	√		√			
10	Momoh et al. (2020)	Oil palm broom	√	√				
11	Sahu and Gupta (2020)	-		√				
12	Najeeb et al. (2020)	Pineapple leaf fibres	√					
13	Amiandamhen and Osadolor (2020)	Kenaf fibres					√	
14	Berger et al. (2020)	Spruce wood	√		√			
15	Mirski et al. (2020)	Sawdust				√		
16	Mucsi et al. (2020)	Coconut husk, Reed straw				√		
17	Xie and Li (2021)	Rice straw fibre	√	√	√			
18	Adelusi et al. (2021)	Corn Cob, *G. arborea* Sawdust		√		√		
19	Futami et al. (2021)	EFB fibre	√					
20	Maynet et al. (2021)	EFB fibre		√	√			√
21	Iskandar et al. (2021)	EFB fibre	√	√				
22	Malik et al. (2021)	Kenaf fibre	√					
23	Hasan et al. (2021b)	Wood fibre	√			√	√	√
24	Hasan et al. (2021a)	Lignocellulosic fibre		√	√	√		
25	Stapper et al. (2021)	Coir fibre		√				
26	Amiandamhen et al. (2021)	*Ceiba pentandra* (L.) Gaertn. and *G. arborea* (Roxb.)					√	
27	Vitrone et al. (2021)	Lignocellulosic fibre	√					
28	Kabir et al. (2021)	Hemp fibre	√					
29	Castellano et al. (2021)	Opuntia fibre	√	√				
30	Budiman et al. (2021)	Coconut coir	√	√		√		
31	Wu et al. (2022)	*Miscanthus* x *giganteus*	√					
32	Zhang et al. (2022)	Coir fibre	√		√			√
33	Aras et al. (2022)	Olive oil fibre				√	√	
34	Chougan et al. (2022)	Wheat straw						√
35	Maynet et al. (2023)	EFB fibre	√	√	√	√	√	

Table 3 *(continue)*

No.	Authors	Type of natural fibre	Fibre strand			Cement board		
			Fibre properties	Fibre treatment	Cement hydration	Density	Cement–fibre ratio	Water content
36	Lima et al. (2023)	Malva fibre	√		√			
37	Ridzuan et al. (2023)	EFB fibre				√	√	√
38	Song et al. (2023)	Hemp fibers	√					
39	El Hamri et al. (2024)	Cedar Sawdust	√			√		
40	Kolajo et al. (2024)	EFB fibre		√				
41	Silva et al. (2024)	Eucalyptus fibers	√		√			
42	Taiwo et al. (2024)	Bamboo fibre	√					
43	Azmi et al. (2024)	-		√		√	√	
44	K. J. Rao et al. (2024)	Coir fibre	√					
45	Abrha et al. (2024)	Palm fibre	√					
46	Aaron and Carsten (2024)	Softwood fibre	√		√			
47	Fioroni et al. (2025)	Bamboo fibre, pine fibre	√					
	Total		**29**	**17**	**15**	**13**	**10**	**8**

Note. EFB = Empty fruit bunches

addressed in this SLR was "What are the factors affecting the compatibility of natural fibre in the cement matrix?" The study's results identified two primary factors, along with six sub-factors: fibre properties, treatment, cement hydration, density, cement-to-fibre ratio, and water content. These factors collectively provided insights into the research question. Furthermore, the primary factors emphasised in this study pertain to the evaluation of fibre strands about CB performance. Therefore, the priority of this study was to focus on the highest scoring factor, fibre properties (29), as the main criterion, compared to fibre treatment (17) and cement hydration (15), which were not elaborated.

Properties of Natural Fibre as CB Reinforcement

Generally, the most important factors considered by many to influence the strength of composites as construction materials are the mechanical and physical properties of EFB fibre (Bonnet-Masimbert et al., 2020). Nonetheless, in actuality, the chemical properties play the most crucial role in enhancing the compatibility between fibre and cement. A fluid matrix effectively restricts sugar levels at the fibre's surface without interfering with the cement hydration, which, in turn, enhances the properties of the interface (Bonnet-Masimbert et al., 2020). Previous researchers have conducted distinct studies on the chemical, physical,

and mechanical properties of fibres, as illustrated in Table 4. Currently, there is insufficient discourse concerning how the interaction of chemical, physical, and mechanical properties of natural fibre influences the performance of CB. Therefore, this study aims to identify the key factors in fibre properties that enhance the compatibility of CB composites.

Table 4 provides a detailed review of articles examining the chemical, physical, and mechanical properties of fibre strands. The tabulated information showed that chemical composition (CC), scanning electron micrograph (SEM), and tensile (T) are the main fibre properties tested, with 18, 14, and 8 articles, respectively, addressing each property. However, there is limited number of studies that investigate the impact of fibre properties that are significant for supplementary testing, including micro duplet (MD), moisture content (MC), attenuated total reflection (ATR), Fourier Transformed Infrared Spectroscopy (FTIR), thermogravimetric analysis (TGA), X-Ray diffraction (XRD), energy dispersive X-ray (EDX) and pull out (PO). Therefore, this paper focused on recent studies regarding CC, SEM, and T properties, which are important for future researchers or industries when fabricating CB.

Table 4
Articles reviewed for fibre properties

References	**Fibre properties**										
	Chemical properties	**Physical properties**								**Mechanical properties**	
	CC	**SEM**	**MD**	**MC**	**ATR**	**FTIR**	**TGA**	**XRD**	**EDX**	**T**	**PO**
Momoh et al. (2020)		√		√				√		√	
Kochova, Caprai, et al. (2020)	√	√									
Kochova, Gauvin, et al. (2020)	√	√				√		√	√	√	√
Peter et al. (2020)	√	√									
Hasan et al. (2020)		√									
Bonnet-Masimbert et al. (2020)	√	√				√				√	√
Momoh and Osofero (2020)	√	√									
Najeeb et al. (2020)	√				√		√	√	√	√	
Futami et al. (2021)	√	√	√							√	
Iskandar et al. (2021)		√				√				√	
Xie and Li (2021)	√	√				√					
Hasan et al. (2021b)		√				√	√				
Vitrone et al. (2021)	√										
Kabir et al. (2021)	√	√									
Castellano et al. (2021)	√										

Table 4 *(continue)*

References	Fibre properties										
	Chemical properties		Physical properties							Mechanical properties	
	CC	SEM	MD	MC	ATR	FTIR	TGA	XRD	EDX	T	PO
Budiman et al. (2021)	√										
Wu et al. (2022)						√		√			
Zhang et al. (2022)				√							
Maynet et al. (2023)	√	√		√						√	
Lima et al. (2023)	√										
Song et al. (2023)	√	√				√		√			
El Hamri et al. (2024)	√										
Silva et al. (2024)	√										
Abrha et al. (2024)											√
Aaron and Carsten (2024)	√									√	
Fioroni et al. (2025)	√					√					
Total	**18**	**14**	1	3	1	8	2	5	2	**8**	3

Note. CC = Chemical composition; SEM = Scanning electron micrograph; T = Tensile; MD = Micro duplet; MC = Moisture content; ATR = Attenuated total reflection; FTIR = Fourier Transformed Infrared Spectroscopy; TGA = Thermogravimetric analysis; XRD = X-Ray diffraction; EDX = Energy dispersive X-ray; PO = Pull out

Effect on the Chemical Properties of Natural Fibre as CB Reinforcement

The properties of natural fibres are mainly influenced by the chemical composition of the plant sources from which they are derived (Malik et al., 2021; Xie & Li, 2021). Fibre properties such as hemicellulose, cellulose, lignin and other impurities significantly influence the normal setting process and contribute to the prolonged setting time of the cement matrix (El Hamri et al., 2024; Hasan et al., 2021b; Maynet et al., 2023). The presence of residual oil disrupts the binding agent, preventing the immediate use of natural fibre in the cement matrix (Maynet et al., 2021). Research by Hasan et al. (2020), Maynet et al. (2021), and Wu et al. (2022) indicates that plant fibres, which are composed of various chemical compounds, including sugar and tannin, play a significant role in inhibiting the hydration of wood fibre and cement, thereby affecting the strength. This finding is in agreement with that reported by Silva et al. (2024), that untreated eucalyptus fibres produced higher impurities, hemicellulose (65.6%), lignin (23%) and extractive (10.9%). The amount and types of fibre extractives in contact with the cement matrix water can potentially inhibit the hydration of the cement composite setting. Similarly, Ridzuan et al. (2023) discovered that untreated fibre yielded lower results, falling below the minimum standard requirement for the physical and mechanical properties of a standard CB. This research obtained low

results for thickness swelling (TS, 1.82%), modulus of elasticity (MOE, 1398 N/mm^2), modulus of rupture (MOR, 3.51 N/mm^2) and internal bonding (IB, 0.164 N/mm^2) due to incompatibility between the cement and the untreated fibre. Consequently, raw fibre needs to be processed to remove the impurities due to its original conditions, which might cause difficulties in establishing good bonding between the fibre-cement matrix and produce low performance of CB.

Cellulose serves as the primary component in the cell wall of natural fibre, contributing to its toughness (Momoh & Osofero, 2020; Xie & Li, 2021). Additionally, cellulose functions as a crucial element that affects the mechanical properties of fibres and their interaction with matrices. Moreover, hemicellulose and lignin, which serve as bonding agents for cellulose, are non-crystalline and dissolve within the cement paste (Bonnet-Masimbert et al., 2020; Hasan et al., 2021a; Kabir et al., 2021; Kochova, Caprai, et al., 2020). Figure 3 illustrates the chemical composition of the natural fibre identified in previous research. It has been demonstrated that cellulose constitutes the primary component of the chemical composition of natural fibres, ranging from 33-78.5%, followed by hemicellulose (6.9-37.3%), lignin (2.6-36%) and others (0.1-6.1%). This finding proved that the values of composition indicated that cellulose content possesses the highest percentage and suggesting its potential use in the composite. This statement was agreed by Maynet et al. (2023) and Futami et al. (2021) that high cellulose is crucial for fibre reinforcement in cement board materials and acts as a viable alternative to wood fibre in cement boards. Fioroni et al. (2025) proved that higher cellulose content (87%) of bamboo fibre produced high performance of cement composites (MOE, 7710 N/mm^2 and MOR, 16.50 N/mm^2). Therefore, the cellulose content contributes to the structural integrity and stiffness of the composite. This is particularly beneficial in construction materials like cement boards, where rigidity is essential for structural performance.

Besides, the chemical composition of fibre is influenced by various factors such as age, location, growth stage, environment, and land conditions (Malik et al., 2021). Sahu and Gupta (2020) indicated that the inconsistency in natural fibre properties arises from factors such as their origin, climate, and growth duration. Similarly, Momoh and Osofero (2020) stated that other factors that have an impact include the age of the fibre source, diverse experimental techniques, various fibre sources, and treatments. Previous studies have shown that different varieties of plants yield different properties of the fabricated CB. Studies by Najeeb et al. (2020) proved that pineapple leaf fibre (PALF)-Yankee leaf fibre had a higher cellulose content compared to Josapine's PALF. The cellulose of PALF- Yankee leaf fibre and Josapine's PALF was 47.74 and 33%, respectively. This finding proved that different types of PALF resulted in different chemical compositions. Similar studies by El Hamri et al. (2024) highlighted that the challenges in the advancement of wood-cement composites for different wood species compatibility with cement constituents and their inhibitory impact on cement hydration. Other than that, findings from Momoh and Osofero (2020) proved that

the removal of impurities on the different parts of the oil palm tree through pre-treatment resulted in different chemical compositions. The results proved that EFB fibre contained higher cellulose, 38-65%, compared to oil palm frond (OPF) fibre and oil palm trunk (OPT) fibre, which were 40-50% and 29-47%, respectively. Meanwhile, different treatments also significantly affect the chemical composition of fibre. Xie and Li (2021) demonstrated that various treatments led to different conclusions, with twice-bleached rice straw fibres (RF4) achieving an optimal cellulose content of 78.5%, surpassing other treatments, such as steam explosion, hydrogen peroxide immersion, and bleaching. In summary, determining the chemical composition of natural fibres after treatment is essential for optimizing their properties, ensuring quality, and expanding their potential applications. Therefore, it is very important to determine the chemical composition of natural fibres after the treatment process before they can be used for the next stage.

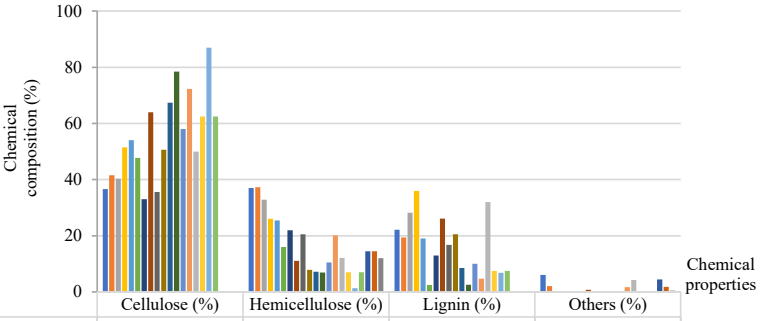

	Cellulose (%)	Hemicellulose (%)	Lignin (%)	Others (%)
Kochova et al. (2020)-Coir fibre	36.6	37	22.2	6.1
Kochova et al. (2020)-Spruce fibre	41.6	37.3	19.4	2.1
Peter et al. (2020)-EFB fibre	40.35	32.82	28.26	
Momoh and Osofero (2020)-EFB fibre	51.5	26	36	
Bonnet-Masimbert et al. (2020)-Oil palm fibre	54	25.5	19	
Najeeb et al. (2020)-PALF, Yankee	47.74	15.98	2.44	
Najeeb et al. (2020)-PALF, Josapine	33	22	13	
Aaron and Carsten (2024) -Softwood fibre	64	11.1	26.1	0.8
Xie and Li (2021)-Rice straw fibre, RF1	35.6	20.5	16.8	
Xie and Li (2021)-Rice straw fibre, RF2	50.6	7.9	20.5	
Xie and Li (2021)-Rice straw fibre, RF3	67.4	7.2	8.5	0.1
Xie and Li (2021)-Rice straw fibre, RF4	78.5	6.9	2.6	
Castellano et al. (2021)-Opuntia fibre	58	10.5	10	
Song et al. (2023) - Hemp fibre	72.3	20.15	4.7	1.7
Anas et al. (2024)-Cedar sawdust	50	12.1	32	4.24
Lima et al (2023)-Malva fibre	62.5	7	7.5	
Carlos et al. (2025)-Bamboo fibre	87	1.38	6.8	
Lima et al. (2023)-Malva fibre	62.5	7	7.5	
Budiman et al. (2021)-Coir fibre (untreated)		14.5		4.5
Budiman et al. (2021)-Coir fibre (cold water)		14.5		1.8
Budiman et al. (2021)-Coir fibre (hot water)		12		0.5

Figure 3. Main percentages of chemical composition of the natural fibres
Note. EFB = Empty fruit bunches; PALF = Pineapple fibre

Effect on the Physical Properties of Natural Fibre as CB Reinforcement

Many researchers used surface morphology analysis (SEM) to observe changes on the fibre surface after pre-treatment. A study conducted by Peter et al. (2020) investigated how the impurities attached to the surface of untreated EFB fibre influenced the bonding characteristics between EFB fibre and the cement matrix. Similar studied by Maynet et al. (2023), that mentioned high amount of silica body were attached on the fibre surface before treatment, as shown in Figure 4a. While, Figure 4b shows that natural impurities and silica bodies were eliminated from the fibre's surface, leading to an increased pore size and a rougher surface after sodium hydroxide (NaOH) pre-treatment (Bonnet-Masimbert et al., 2020). In summary, the consensus among previous studies suggests that the removal of impurities (silica bodies) from the fibre surface results in the formation of empty circular craters or larger pore sizes (Bonnet-Masimbert et al., 2020; Peter et al., 2020), an increase in cellulose content (Maynet et al., 2023), reduced fibre's diameter (Maynet et al., 2021), improved tensile strength (Maynet et al., 2023) and better compatibility between fibre and cement matrix (Xie & Li, 2021).

Nonetheless, a high chemical concentration or an excessive solution would certainly degrade the fibre. Research done by Jiang et al. (2020) proved that the fibre begins to sustain damage and deform at a concentration of 4% NaOH and affected of the boundary layers of the EFB fibre, leading to a deterioration of the fibre particles, as illustrated in Figure 4c. Furthermore, based on findings from Kabir et al. (2021), it was observed that high concentrations of NaOH treatment (6-10%) led to a weakening and breakage of hemp fibre, as illustrated in Figure 4d. In addition, the application of hot water treatment at a temperature of 100°C for a duration of 2 h resulted in damage to the fibre, attributed to excessive delignification and radial cracking (Momoh et al., 2020).

Additionally, Maynet et al. (2021) indicated that the diameter of the fibre influenced its properties, in which when the diameter was decreased, the strength of the fibre also increased. Previous findings stated that fibre diameter in range 0.03 to 0.57 mm as shown in Table 5. Others than that, the physical properties of natural fibres that consist of length (1-200 mm), moisture content (5-43.51%), and density (0.07-1.51 g/cm^3). Nevertheless, moisture content should be a priority, but lack of research were not included these properties. Maynet et al. (2021) proved that 5% moisture content produced CB with meet the minimum standard for physical properties with density CB of 1309 kg/m^3 and TS value of 0.65%. They argued that the moisture content of the fibre must be controlled at approximately ±5%. It is because the interaction between natural fibres and the material matrix and fibres can be influenced by fibre hydrophilicity and hydrophobicity.

Recent findings by Maynet et al. (2023) revealed that the length of the fibres significantly influences the strength of the CB composite. EFB fibres at different lengths were utilised according to the mesh retained sizes of R7M (5 mm), R14M (3 mm), and R30M (1 mm).

The findings show that the ideal fibre length recommended for the fabrication of CB composites is the processed fibres that retain on the R14M sieve, averaging 3 mm in length. Nonetheless, shorter particles tend to bypass significant voids and irregularities in CB, whereas longer fibre lengths, particularly those retained at R7M, result in a composite with lower density, which consequently increases the number of voids. The result from this study agrees with Momoh and Osofero (2020) who commended the fibre length of 3 cm and should not be greater than 50 mm since longer lengths create "balling" of the fibres in cement matrix. Therefore, the potential natural fibres physical properties for the suitability in cement board primarily influence by diameter fibre in range 0.03 to 0.57 mm, fibre length of 3 mm and moisture content of 5%, would significantly enhanced the interlocking at the interface in CB composite.

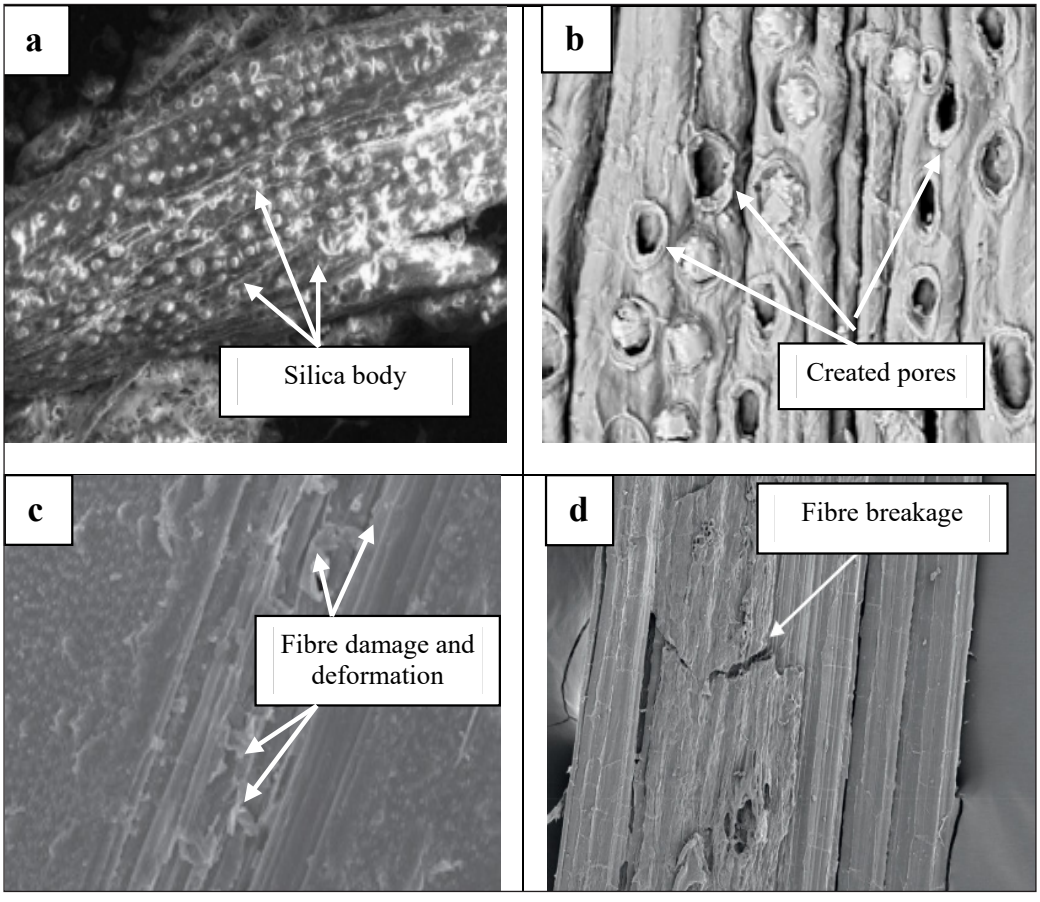

Figure 4. Scanning electron microscope images: (a) Silica body on the fibre surface before treatment (empty fruit bunches [EFB] fibre); (b) Pore or empty circular crater on the fibre surface after treatment (EFB fibre); (c) Fibre damage and deformation; and (d) Fibre breakage - 8% sodium hydroxide (Hemp fibre)
Source: Bonnet-Masimbert et al. (2020), Jiang et al. (2020), Kabir et al. (2021), and Maynet et al. (2023)

Table 5
Physical properties of different natural fibres

Type of fibre	Physical properties				References
	Diameter (mm)	Length (mm)	Moisture content (%)	Density (g/cm^3)	
Coir fibre	-	40-50	-	-	Kochova, Gavin, et al. (2020)
	-	1-2	-	-	Budiman et al. (2021)
	0.20-0.50	8	-	0.07	Zhang et al. (2022)
	0.10-0.20	150-200	10.50	1.40	K. J. Rao et al. (2024)
Spruce wood	-	-	-	-	Kochova, Caprai, et al. (2020)
Oil palm fibre	-	60	-	0.70-1.51	Bonnet-Masimbert et al. (2020)
	-	-	-	-	Momoh et al. (2020)
EFB fibre	-	3	-	-	Momoh and Osofero (2020)
	0.22-0.57	17-47.70	13-43.51	-	Peter et al. (2020)
	-	1, 3, 5	5	-	Maynet et al. (2023)
	-	-	-	-	Iskandar et al. (2021)
Pineapple leaf fibre	-	-	-	-	Najeeb et al. (2020)
Rice straw fibre	0.06-0.07	0.354-0.578	-	-	Xie and Li (2021)
Hemp fibre	0.25	4.23	-	1.34	Song et al. (2023)
Bamboo fibre	0.03	5.30	-	-	Taiwo et al. (2024)
Palm fibre	0.171	12	-	0.723	Abrha et al. (2024)

Note. EFB = Empty fruit bunches

Effect on the Mechanical Properties of Natural Fibre as CB Reinforcement

Previous studies demonstrated that natural fibre can serve as reinforcement for CB based on its mechanical strength. Figure 5 shows the previous findings on tensile strength, which ranges from 200-663 N/mm^2. Findings from Momoh and Osofero (2020), and Xie and Li (2021) showed that the elimination of contaminants from EFB fibre through pre-treatment improved the chemical composition. Momoh and Osofero (2020) showed that EFB fibre possesses the highest cellulose content after it has undergone NaOH treatment. This study also revealed that a higher cellulose content correlates with enhanced strength in treated fibre. Similar with Bonnet-Masimbert et al. (2020) confirmed that fibre treatment such as NaOH solution (2, 4, 6, 10%), Silane (1, 3%) and hot water (1-2 hr soaking time) improved fibre surface by indicating the presence of empty circular craters or larger pore sizes, significantly improve the tensile strength of the fibres. This study resulted in the tensile strength of oil palm fibre improving, ranging from 220 to 395 N/mm^2 at 2-4% NaOH, respectively. Furthermore, the tensile strength of 3% silane treatment increased compared to 1% silane, with achieved optimal values of 484 and 316 N/mm^2, respectively.

Meanwhile, hot water treatment one soaking hour higher than 2 hour at strength value of 404 and 347 N/mm^2. The reason of an increament of strength due to fibre treatment that successfully removes impurities, hemicellulose, lignin, and waxy substances from fibre surfaces, exposing more cellulose fibrils with higher tensile strength and improving mechanical properties.

A prior study by Najeeb et al. (2020) demonstrated that different types of plants possessed different properties. The percentages of cellulose of PALF-Yankee leaf fibre and Josapine's PALF, which were 47.74 and 33%, produced different tensile strength results of 390 and 295 N/mm^2, respectively. The strength of Yankee's PALF is higher than Josapine's PALF due to higher crystallinity, which enhances the strength of the fibre. Furthermore, a higher concentration of chemicals or an overly prolonged treatment would certainly degrade the fibre (Bonnet-Masimbert et al., 2020). Their findings show that tensile strength decreased from 6-10% NaOH (334-288 N/mm^2). In a similar sense, hot water treatment at 100°C with 2 hours of soaking time may also result in fibre degradation due to severe delignification and radial cracking, causing the tensile strength of the fibre to decrease (Momoh et al., 2020) and fibre to fracture (Kabir et al., 2021). Therefore, exposure to higher chemical concentrations, temperature, and prolonged soaking durations can be considered to hurt the tensile strength of the fibre due to lignocellulose degradation and surface rupture.

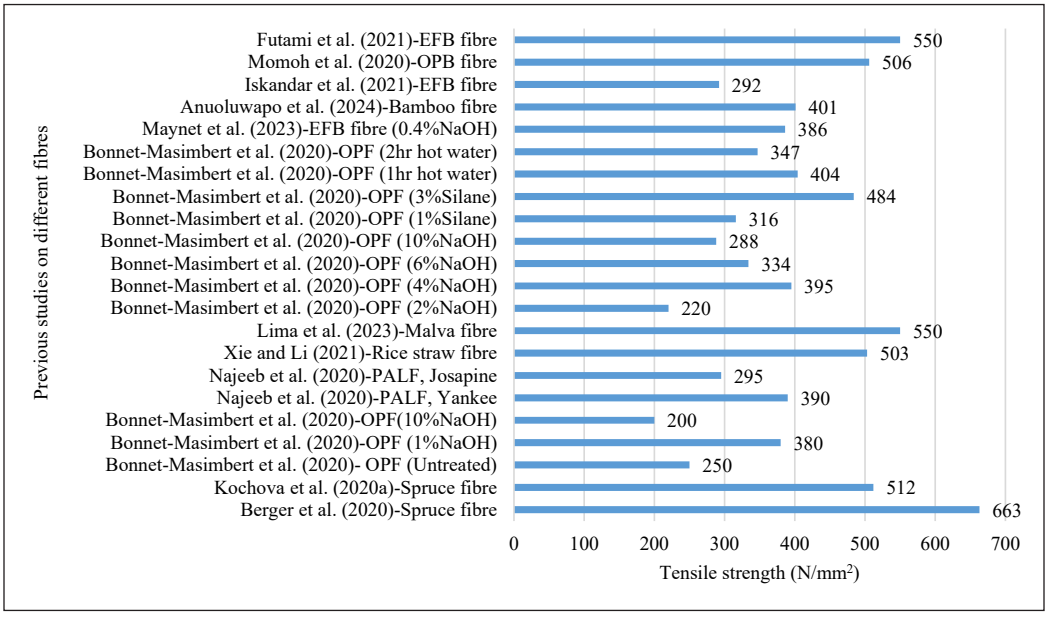

Figure 5. The fibre strength of natural fibre
Note. EFB = Empty fruit bunches; OPB = Oil palm broom; OPF = Oil palm fibre ; PALF = Pineapple fibre; NaOH = Sodium hydroxide

Relationship Between Chemical, Physical and Mechanical Properties of Natural Fibre Towards CB Reinforcement

As mentioned earlier, cellulose serves as the primary structural component in cell walls. Consequently, numerous findings reported that pre-treatment of fibre is effective in removing impurities, increasing the cellulose content, improving the tensile strength and simultaneously enhancing the compatibility between fibre and cement matrix (Iskandar et al., 2021; Maynet et al., 2023). Najeeb et al.'s (2020) research found that PALF-Yankee leaf fibre had a higher cellulose content (47.74%) than Josapine's PALF (33%), and tensile strength measurements were 390 and 295 N/mm^2. The reason for the strength of Yankee's PALF was higher than that of Josapine's PALF because of its elevated crystallinity, which contributes to the higher strength of the fibre. As a summary, higher crystallinity generally correlates with higher tensile strength due to the more organised and deformation-resistant nature of crystalline regions.

Furthermore, the percentage of cellulose examined by Kochova, Gauvin, et al. (2020), Peter et al. (2020), Xie and Li (2021), Castellano et al. (2021), El Hamri et al. (2024), Aaron and Carsten (2024), fall within the ranges reported by earlier studies, specifically, 37, 40, 57, 58, 50, 64%, respectively. All of these compositions prove the potential for outstanding fibre strength of cellulose. Nonetheless, researchers including Bonnet-Masimbert et al. (2020), Momoh et al. (2020), Futami et al. (2021), Iskandar et al. (2021), Maynet et al. (2023) and Taiwo et al. (2024), merely cited the chemical composition values from previous studies, with the tensile strength was found to be within a favourable range of 220-550 N/mm^2. Therefore, a lack of study reported that both chemical composition and tensile strength are necessary to be determined. Somehow, it can predict earlier the performance of cement board.

As such, higher cellulose content holds great significance, as this material is the most robust and stiffest in organic fibres. In contrast, hemicellulose lacks the same impactful properties due to its solubility in water and high water absorption. Meanwhile, lignin primarily serves as a bonding agent, functioning as the matrix within this cellulose composite. Moreover, the impact of cellulose on fibre strength is illustrated in Figure 6. The figure shows that the elimination of natural impurities and silica bodies from the fibre's surface leads to the formation of larger pore sizes and rougher surfaces. This, in turn, enhances cellulose content, reduces fibre diameter, increases tensile strength, and simultaneously improves the compatibility between fibre and the cement matrix. Research conducted by Bonnet-Masimbert et al. (2020), and Xie and Li (2021) confirmed this finding, indicating that the presence of empty circular craters or larger pore sizes can improve the tensile strength of the fibres. Table 6 shows the findings from a one-way analysis of variance (ANOVA) examining the relationship between cellulose content and fibre tensile strength. Since the p-value was below 0.05, the ANOVA test indicates a statistically significant result.

Thus, it can be concluded that the increase in cellulose content has influenced the fibre's tensile strength. The reason is that higher cellulose content contributes to better strength and simultaneously higher compatibility of fibre when incorporated in the cement matrix as a form of reinforcement. The relatively low tensile strength can be attributed to the lower content of cellulose in untreated fibre. This demonstrates the importance of cellulose content, as it is the primary molecule in the cell wall of natural fibre and plays a crucial role in providing toughness, thereby enabling the full potential of the fibre to be harnessed.

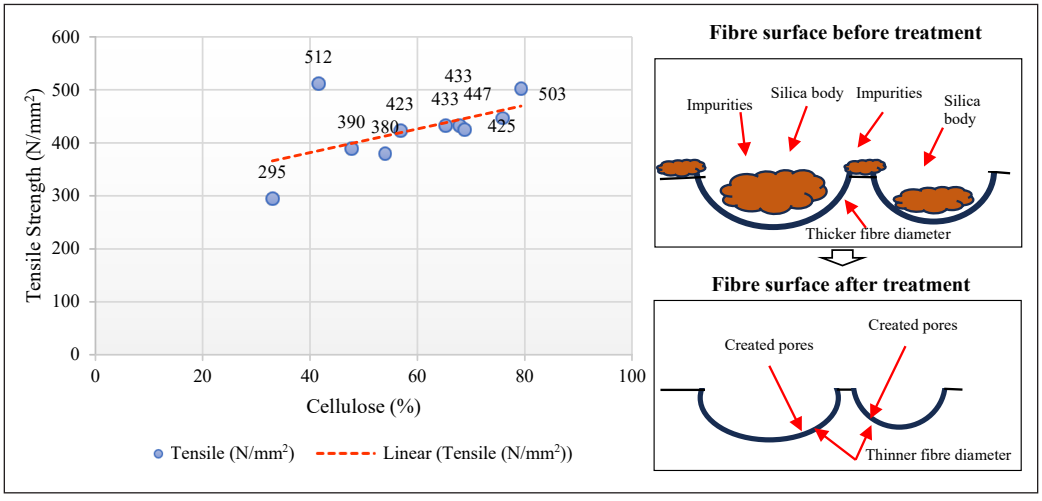

Figure 6. Effect of cellulose on the fibre strength as a reinforcement for cement board

Table 6
Analysis of variance test for the effect of cellulose on the fibre strength as a reinforcement for cement board

Source of variation	SS	df	MS	*F*	*P*-value	*F* crit
Between groups	666435.3	1	666435.3	329.0484	5.16E-13	4.413873
Within groups	36456.14	18	2025.341			
Total	702891.4	19				

Future Perspectives on Improving the Drawbacks of Natural Fibre

Fibre Surface Modification of Natural Fibre

Fibre surface modification improves fibre integrity in cement composites (Momoh & Osofero, 2020). Factors like extractives hinder cement hydration, setting, and strength development, affecting the physical and mechanical properties (Hasan et al., 2021b, 2020; Momoh et al., 2020). According to Iskandar et al. (2021), Bonnet-Masimbert et al. (2020) and Aruna et al. (2020) have addressed the improvement of fibre cement compatibility through surface treatment of fibre, such as physical and chemical treatments. Figure 7 (a-f)

shows the effect of fibre treatment, such as hot water, alkaline, thermal, and untreated, on the physical (TS, water absorption [WA], and density) and mechanical properties (MOE, MOR, IB) of CB. Ridzuan et al. (2023) proved that untreated fibre produced low performance of physical and mechanical properties of cement board with optimum value of TS (1.82%), density (1313 kg/m^3), MOE (1398 N/mm^2), MOR (3.51 N/mm^2), and IB (0.164 N/mm^2).

Previous studies were mainly conducted on the chemical method, such as Maynet et al. (2023) and Peter et al. (2020) used a lower concentration of NaOH (0.4 and 1%), resulting in physical and mechanical properties below the minimum requirement. However, the study indicates that heat thermal pre-treatment of the fibre significantly eliminates residual and impurities compared to NaOH pre-treatment with optimum value of MOE (4699 N/mm^2), MOR (9.1 N/mm^2) and IB (0.53 N/mm^2). Therefore, low concentrations are not suggested, but high concentrations of chemical treatments can damage fibres, affecting their mechanical properties and affecting the health implications.

However, the knowledge of the impact of physical treatments like hot water treatment on the compatibility of cement composites is limited. Adelusi et al. (2021) found that pre-treatment of maize cob and sawdust fibre with hot water at 100°C for an hour produced stronger, stiffer, and more stable cement boards, resulting in higher MOE and MOR values of 10,797 and 8.42 N/mm^2, respectively, and lowest TS and WA after 24 hours (0.3-1.15%). This is due to many void spaces being filled, which helps achieve a thorough and homogenous mix of the cement bonded board. Similar to Owoyemi et al. (2020), who conducted a study using hot water treatment at 90°C for 30 minutes, produced the highest MOE value of 4164 N/mm^2. The study reveals that higher cement and corn cob particle mixing ratios improve composite board resistance, stiffness, and breaking strength. Therefore, surface modification treatment can enhance surface roughness, remove impurities, and incorporate new functional groups to improve bonding between the fibre surface and the matrix.

In conclusion, hot water treatment is seen as the right approach to improve the drawbacks of natural fibre as a cement board reinforcement. This treatment has good potential from other methods in some benefits, such as being non-chemical or environmentally friendly, cheaper than alkalization and salinization (Momoh et al., 2020; Stapper et al., 2021), increasing mechanical properties and improving thermal stability (Nordin et al., 2020).

Compatibility Method of Fibre and Cement Matrix

The combination of materials in cement can lead to degradation of natural fibres, causing disintegration within the cement matrix and reducing the structural integrity of composites. Silva et al. (2024) highlight that plant fibers' incompatibility with cement is due to dissolved extractives' impact on cement hydration and the presence of numerous hydroxyl groups in cell walls, which negatively affect the physical and mechanical properties of the composites. According to Amel et al. (2020), Aaron and Carsten (2024), and Silva et

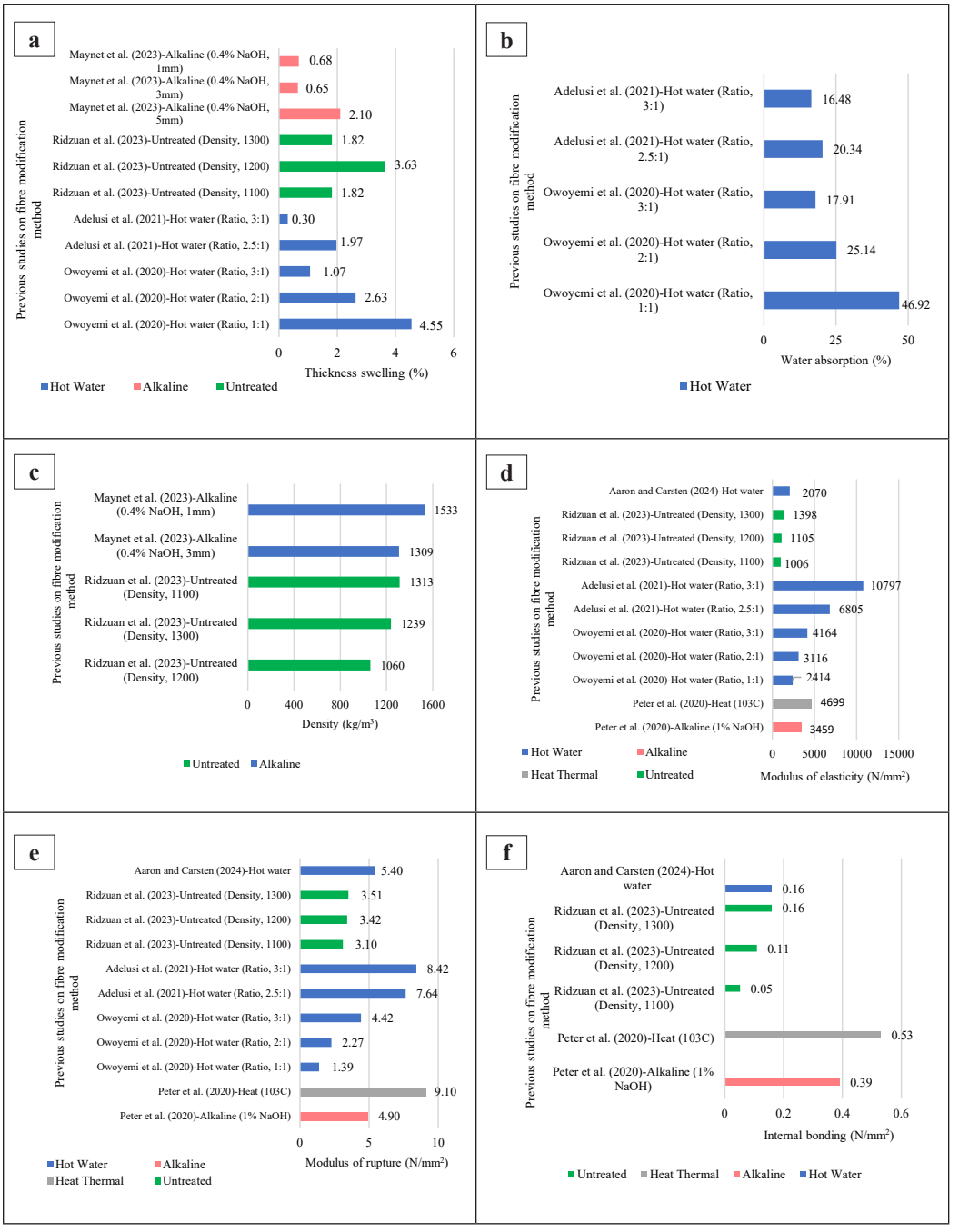

Figure 7. Effect of fibre treatment on the physical and mechanical properties of cement board: (a) Thickness swelling; (b) Water absorption; (c) Density; (d) Modulus of elasticity; (e) Modulus of rupture; (f) Internal bonding

al. (2024), a hydration test was conducted to assess the compatibility of wood particles or fibres on the setting of cement. Their findings show that increased fibre content influences the hydration of anhydrous cement.

Previous studies have shown that fibre treatments such as cold water (Kochova, Caprai, et al., 2020), NaOH (Bonnet-Masimbert et al., 2020; Jiang et al., 2020; Lima et al., 2023; Maynet et al., 2023), and hot water (Aaron & Carsten, 2024) produced medium inhibition grade (Table 7). This phenomenon is due to the poor setting of fibre treatment,

Table 7
Effect of fibre treatment on the compatibility of fibre-cement matrix

References	Type of fibre	Treatment / Concentration	T (°C)	H (hr)	*I* (%)	Grade of inhibition
Kochova, Caprai, et al. (2020)	Spruce wood wool	CW-A	-	-	85	Medium
		CW-B	-	-	75	Medium
Amel et al. (2020)	Kenaf fibre	-	67.8	6	-	-
Jiang et al. (2020)	Straw fibre	3%NaOH (4hours)	15.8	1.5	91.72	-
Bonnet-Masimbert et al. (2020)	Oil palm fibre	1 NaOH	-	-	91.5	Medium
		10% NaOH	-	-	93.2	Medium
Xie and Li (2021)	Rice straw fibres	S (97.5OPC-2.5RF1)	-	-	2.606	Low
		S (95OPC-5RF1)	-	-	25.58	Medium
		S (92.5OPC-7.5RF1)	-	-	112.68	Extreme
		S (90OPC-10RF1)	-	-	Infinate	Extreme
		S+HPA (95OPC-5RF22	-	-	0.027	Low
		S+HPA (92.5OPC-7.5RF2)	-	-	1.168	Low
		S+HPA (90OPC-10RF2)	-	-	14.55	Medium
		S+HPA+B 1x (95OPC-5RF3)	-	-	0.027	Low
		S+HPA+B 1x (90OPC-10RF3)	-	-	1.943	Low
		S+HPA+B 2x (95OPC-5RF4)	-	-	0.02	Low
		S+HPA+B 2x (90OPC-10RF4)	-	-	2.222	Low
Lima et al. (2023)	Malva fibre	5% NaOH (30 min)	-	-	80	Medium
Maynet et al. (2023)	EFB fibre	U	45.9	10.5	-	-
		0.4% NaOH (24 hr)	47	11.2	-	-
Aaron and Carsten (2024)	Softwood fibre	HW (5 hr)	-	-	18.1	Medium
Silva et al. (2024)	Eucalyptus fibers	NB	36	-	34.52	Medium

Note. CW = Cold water; NaOH = Sodium hydroxide; S = Steam; HPA = Hydrogen peroxide aqueous; B = Bleaching; U = Untreated; HW = Hot water; NB = Non bleached; RF = Rice straw fibers; OPC = Ordinary Portland cement

which causes an amount and types of fibre extractives in contact with the cement matrix that can potentially disintegrate within the cement matrix or inhibit hydration. They have shown that the interfacial bond strength between wood fibres and cement matrix can be increased with fibre treatment. Nevertheless, Silva et al. (2024) mentioned that untreated Eucalyptus fibres also produced moderate inhibition of the cementitious matrix. This happened due to the type of fibre, which had fewer impurities, resulting in better inhibition of the composite. Similar findings with Lima et al. (2023) resulted in a high concentration of 5% NaOH solution. Soaking for 30 minutes produced a medium inhibition grade for Malva fibre. Similar to Xie and Li (2021), who found that adding rice straw (RF1) from 2.5-10 wt.% significantly slowed cement hydration. It may be due to a high amount of impurities, which reduces and delays the hydration process, forming a thin permeable layer around the cement grains. Other than that, a shorter length of the treated fibre produced a higher hydration temperature. Maynet et al. (2023) found that cement mixed with EFB fibre increased the hydration rate for R14M, reaching 44.9°C for treated fibre and 43.8°C for untreated fibre. Shorter treated fibres improved interfacial bond, load transfer, and crack resistance. Therefore, the treated fibre removes impurities, resulting in increased cellulose content, improved strength, and significantly enhanced hydration rate.

In conclusion, many factors contribute to the incompatibility caused by the various chemical compositions affecting the hydration of cement setting. Therefore, this hydation test can be used to assess the suitability of compatibility for cement-fibre composite before production, either under low, medium, or extreme inhibition grade. Furthermore, inhibition index is a suitable method for evaluating the compatibility of fibre and cement matrix before the CB fabrication process (Hasan et al., 2021b; Maynet et al., 2021). Thus, mostly previous researcher have not studied the chemical composition with the performance of physical and mechanical CB. Therefore, this pre-checking of the hydration test could know the suitability of fibre and predict the performance of CB before it can be proceeded to the fabrication.

CONCLUSION

The compatibility of natural fibre with cement is primarily determined by the properties of the fibre. Through an intensive literature review, the physical, chemical and mechanical properties of natural fibre influence to the performance of the cement board. The potential natural fibres physical properties for the suitability in cement board are primarily influence by diameter fibre in range 0.03 to 0.57 mm, fibre length of 3 mm and moisture content of 5%, would significantly enhanced the interlocking at the interface in CB composite. Meanwhile, the chemical composition contains of cellulose is the main factor of the structural component in cell walls and its contribure the compatibility in the CB composite. During the fibre treatment could eliminates an impurities, resulting in empty circular craters or larger pore sizes. Notably, it increases the cellulose content, decreases the fibre diameter,

enhances the mechanical strength of tensile, and simultaneously improves the performance of the CB. Furthermore, there are still lacking of study on the effect of hot water treatment on the hydration rate of the EFB fibre-cement mix. This pre-checking of the hydration test could know the suitability of fibre and predict the performance of cement board before it can be proceeded to the fabrication. In summary, natural fibre is promising as a sustainable construction material for reinforcing cement matrices, potentially replacing synthetic fibres and asbestos for CB reinforcement.

ACKNOWLEDGEMENTS

The authors gratefully acknowledged support from the Malaysian Ministry of Higher Education (MOHE) and Universiti Tun Hussein Onn Malaysia (UTHM) through FRGS-RACER grant No. K159.

REFERENCES

Aaron K. M., & Carsten, M. (2024). Basalt grid reinforcement of cement-bonded particleboards. *Construction and Building Materials*, *410*, 134168. https://doi.org/10.1016/j.conbuildmat.2023.134168

Abrha, S. F., Shiferaw, H. N., & Kanakubo, T. (2024). Bridging behavior of palm fiber in cementitious composite. *Journal of Composite Science*, *8*(9), 361. https://doi.org/10.3390/jcs8090361

Adelusi, E. A., Olaoye, K. O., Adelusi, F. T., & Adedokun, S. A. (2021). Physico-mechanical properties of cement-bonded boards produced from mixture of corn cob particles and *Gmelina arborea* sawdust. *Journal of Forest and Environmental Science*, *37*(1), 79-89, https://doi.org/10.7747/JFES.2021.37.1.79

Alaloul, W. S., Salaheen, M. A., Malkawi, A. B., Alzubi, K., Al-Sabaeei, A. M., & Musarat, M. A. (2021). Utilising of oil shale ash as a construction material: A systematic review. *Construction and Building Materials*, *299*, 123844. https://doi.org/10.1016/j.conbuildmat.2021.123844

Amel, B. A., Paridah, M. T., Rahim, S., & Hussein, A. S. (2020). Effects of kenaf bast fibre and silica fume content on bending strength and dimensional stability of cement bonded kenaf composite boards. *Journal of Engineering Science and Technology*, *15*(2), 1124–1138.

Amiandamhen, S. O., & Osadolor, S. O. (2020). Recycled waste paper–cement composite panels reinforced with kenaf fbres: Durability and mechanical properties. *Journal of Material Cycles and Waste Management*, *22*, 1492-1500. https://doi.org/10.1007/s10163-020-01041-2

Amiandamhen, S. O., Agwu, C. U., & Ezenwaegbu, P. N. (2021). Ezenwaegbu, evaluation of cement-bonded particleboards produced from mixed sawmill residues, *Journal of the Indian Academy of Wood Science*, *18*(1), 14–19. https://doi.org/10.1007/s13196-021-00273-5

Aras, U., Kalaycıoğlu, H., Yel, H., & Kuştaş, S. (2022). Utilisation of olive mill solid waste in the manufacturing of cement-bonded particleboard, *Journal of Building Engineering*, *49*, 104055. https://doi.org/10.1016/j.jobe.2022.104055

Azmi, N. H, Nik Soh, N. M. Z., & Abu Bakar, H. (2024). The compatibility of cement bonded fibreboard through dimensional stability analysis: A review. *Pertanika Journal of Science and Technology*, *32*(5), 1979-1996. https://doi.org/10.47836/pjst.32.5.03

Berger, F., Gauvin, F., & Brouwers, H. J. H. (2020). The recycling potential of wood waste into wood-wool/cement composite. *Construction and Building Materials*, *260*, 119786. https://doi.org/10.1016/j.conbuildmat.2020.119786

Bonnet-Masimbert, P. A., Gauvin, F., Brouwers, H. J. H., & Amziane, S. (2020). Study of modifications on the chemical and mechanical compatibility between cement matrix and oil palm fibres. *Results in Engineering*, *7*, 100150. https://doi.org/10.1016/j.rineng.2020.100150

Budiman, I., Sumarno, A., Triastuti, Prasetyo, A. M., Maidina, Widodo, E., Akbar, F., Subiyanto, B., & Nugroho, A. (2021). The properties of cement boards reinforced with coconut coir fiber (*Cocos nucifera*) as building materials. In *IOP Conference Series: Earth and Environmental Science* (Vol. 762, No. 1, p. 012074). IOP Publishing. https://doi.org/10.1088/1755-1315/762/1/012074

Castellano, J., Marrero, M. D., Ortega, Z., Romero, F., Benitez, A. N. & Ventura, M. R. (2021). *Opuntia* spp. fibre characterisation to obtain sustainable materials in the composites field. *Polymers*, *13*(13), 2085. https://doi.org/10.3390/polym13132085

Chougan, M., Ghaffar, S. H., Sikora, P., Mijowska, E., Kukułka, W., & Stephan, D. (2022). Boosting Portland cement-free composite performance via alkali-activation and reinforcement with pre-treated functionalised wheat straw. *Industrial Crops and Products 178*, 114648. https://doi.org/10.1016/j.indcrop.2022.114648

El Hamri, A., Mouhib, Y., Ourmiche, A., Chigr, M., & El Mansouri, N. E. (2024). Study of the effect of cedar sawdust content on physical and mechanical properties of cement boards. *Molecule*, *29*(18), 4399. https://doi.org/10.3390/molecules29184399

Fioroni, C. A., Kadivar, M., do Amaral, L. M., Ezugwu, E. K., Calabria-Holley, J., & Savastano Junior, H. (2025). Sol-gel treated pulp and accelerated carbonation curing: A novel approach for high-performance bamboo fibre cement composites. *Construction and Building Materials*, 458, 139487. https://doi.org/10.1016/j.conbuildmat.2024.139487

Futami, E., Shafigh, P., Katman, H. Y., & Ibrahim, Z. (2021). Recent progress in the application of coconut and palm oil fibres in cement-based materials, *Sustainability*, *13*(22), 12865. https://doi.org/10.3390/su132212865

Gusenbauer, M. & Haddaway, N. R. (2020). Which academic search systems are suitable for systematic reviews or meta-analyses? Evaluating retrieval qualities of Google Scholar, PubMed, and 26 other resources. *Research Synthesis Methods*, *11*(2), 181–217. https://doi.org/10.1002/jrsm.1378

Hasan, K. M. F., Brahmia, F. Z., Bak, M., Peter, G. H., Levente, D., & Tibor, A. (2020). Effects of cement on lignocellulosic fibres. In R. Nemeth, P. Redemacher, C. Hansman, M. Bak, & M. Bader (Eds.), *9th Hardwood Proceedings Part I: With Special Focus on "An Underutilized Resource: Hardwood Oriented Research"* (pp. 99–103). University of Sopron Press.

Hasan, K. M. F., Horváth, P. G., & Alpár, T. (2021a). Lignocellulosic fiber cement compatibility: A state of the art review. *Journal of Natural Fibers*, *19*(13), 5409-5434. https://doi.org/10.1080/15440478.2021.1875380

Hasan, K. M. F., Horváth, P. G., & Alpár, T. (2021b). Development of lignocellulosic fiber reinforced cement composite panels using semi-dry technology, *Cellulose*, *28*, 3631–3645. https://doi.org/10.1007/s10570-021-03755-4

Houda, H., Mehrez, I., Gheith, R., & Jemni, A. (2024). Enhancing concrete properties with agave Americana fiber reinforcement. *ACS Omega*, *9*(8), 8743–8753. https://doi.org/10.1021/acsomega.3c03687

Iskandar, W. M. E., Ong, H. R., Rahman Khan, M. M., Ramli, R., & Mohamed Halim, R. (2021). Influence of ultrasound on alkaline treatment of empty fruit bunch fibre: Preliminary study. In *IOP Conference Series: Materials Science and Engineering* (Vol. 1092, No. 1, p. 012002). IOP Publishing. https://doi.org/10.1088/1757-899x/1092/1/012002

Jiang, D., An, P., Cui, S., Sun, S., Zhang, J., & Tuo, T. (2020). Effect of modification methods of wheat straw fibers on water absorbency and mechanical properties of wheat straw fiber cement-based composites. *Advances in Materials Science and Engineering*, *2020*, 8392935. https://doi.org/10.1155/2020/8392935

Kabir, M. M., Alhaik, M. Y., Aldajah, S. H., Lau, K. T., Wang, H., & Islam, M. M. (2021). Effect of hemp fibre surface treatment on the fibre-matrix interface and the influence of cellulose, hemicellulose, and lignin contents on composite strength properties. *Advances in Materials Science and Engineering*, *2021*, 9753779, https://doi.org/10.1155/2021/9753779

Kochova, K., Caprai, V., Gauvin, F., Schollbach, K., & Brouwers, H. J. H. (2020). Investigation of local degradation in wood stands and its effect on cement wood composites. *Construction and Building Materials*, *231*, 117201. https://doi.org/10.1016/j.conbuildmat.2019.117201

Kochova, K., Gauvin, F., Schollbach, K., & Brouwers, H. J. H. (2020). Using alternative waste coir fibres as a reinforcement in cement-fibre composites. *Construction and Building Materials*, *231*, 117121. https://doi.org/10.1016/j.conbuildmat.2019.117121

Kolajo, T. E., Fowowe, A. O., & Adefowope, G. (2024). Production of the structural layer of wall panels using fibres obtained from stalk of oil palm empty fruit bunch wastes. *Adeleke University Journal of Engineering and Technology*, *7*(1), 139-146.

Kraus, S., Breier, M., & Dasí-Rodríguez, S. (2020). The art of crafting a systematic literature review in entrepreneurship research. *International Entrepreneurship and Management Journal*, *16*, 1023-1042. https://doi.org/10.1007/ s11365-020-00635-4

Lima, T. E. S., Tambara Ju´nior, L. U. D., Nascimento, L. F. C., Demosthenes, L. C. C., Monteiro, S. N., & Azevedo, A. R. G. (2023). Evaluation of the feasibility application of Malva fibers in cement-basedcomposites. *Journal of Materials Research and Technology*, *23*, 6274-6286. https://doi.org/10.1016/j.jmrt.2022.11.014

Malik, K., Ahmad, F., & Gunister, E. (2021). A review on the kenaf fiber reinforced thermoset. *Applied Composite Materials*, *28*, 491-528. https://doi.org/10.1007/s10443-021-09871-5

Mawardi, I., Aprilia, S., Faisal, M., Ikramullah., & Rizal, S. (2022). An investigation of thermal conductivity and sound absorption from binderless panels made of oil palm wood as bio-insulation materials. *Results in Engineering*, *13*, 100319. https://doi.org/10.1016/j.rineng.2021.100319

Maynet, W. A., Samsudin, E. M., & Nik Soh, N. M. Z. (2023). Effects of fibre length on the physical properties of oil palm empty fruit bunch cement board (OPEFB-CB). *Pertanika Journal of Science and Technology*, *31*(3), 1279–1290. https://doi.org/10.47836/pjst.31.3.09

Maynet, W., Samsudin, E. M., & Nik Soh, N. M. Z. (2021). Physical and mechanical properties of cement board made from oil palm empty fruit bunch fibre: A review. In *IOP Conference Series: Materials*

Science and Engineering (Vol. 1144, No. 1, p. 012008). IOP Publishing. https://doi.org/10.1088/1757-899x/1144/1/012008

Mhd Noor, M. T., Shahar, H. K., Baharudin, M. R., Syed Ismail, S. N., Abdul Manaf, R., Md Said, S., Ahmad, J., & Sri Ganesh, M. (2023). A systematic review on an optimal dose of disaster preparedness intervention utilizing Health Belief Model Theory. *Pertanika Journal of Science and Technology*, *31*(1), 149-159. https://doi.org/10.47836/pjst.31.1.10

Mirski, R., Dukarska, D., Derkowski, A., Czarnecki, R., & Dziurka, D. (2020). By-products of sawmill industry as raw materials for manufacture of chip-sawdust boards. *Journal of Building Engineering*, *32*, 101460. https://doi.org/10.1016/j.jobe.2020.101460

Momoh, E. O., & Osofero, A. I. (2020). Recent developments in the application of oil palm fibers in cement composites. *Frontiers of Structural and Civil Engineering*, *14*(1), 94-108. https://doi.org/10.1007/s11709-019-0576-9

Momoh, E. O., Osofero, A. I., & Menshykov, O. (2020). Physicomechanical properties of treated oil palm-broom fibers for cementitious composites. *Journal of Materials in Civil Engineering*, *32*(10). https://doi.org/10.1061/(asce)mt.1943-5533.0003412

Mucsi, Z. M., Hasan, K. M. F., Horvath, P. G., Bak, M., Koczan, Z., & Alpar, T. (2020). Semi-dry technology mediated lignocellulosic coconut and energy reed straw reinforced cementitious insulation panels. *Journal of Building Engineering*, *57*, 104825. https://doi.org/10.1016/j.jobe.2022.104825

Najeeb, M. I., Sultan, M. T. H., Andou, Y., Shah, A. U. M., Eksiler, K., Jawaid, M., & Ariffin, A. H. (2020). Characterisation of lignocellulosic biomass from Malaysian's yankee pineapple ac6 toward composite application. *Journal of Natural Fibers*, *18*(12), 2006-2018. https://doi.org/10.1080/15440478.2019.1710655

Owoyemi, J. M., Ogunrinde, O. S., & Oyeleye, I. O. (2020). Physical and mechanical properties of cement bonded strand board produced from *Gmelina arborea* (Roxb.) harvesting residues. *African Journal of Agricultural Research*, *16*(7), 976-982. https://doi.org/10.5897/ajar2020.14809

Peter, P., Nik Soh, N. M. Z., Akasah. Z. A., & Mannan, M. A. (2020). Durability evaluation of cement board produced from untreated and pre-treated empty fruit bunch fibre through accelerating ageing. In *IOP Conference Series: Materials Science and Engineering* (Vol. 713, No. 1, p. 012019). IOP Publishing. https://doi.org/10.1088/1757-899X/713/1/012019

Rao, P. R., & Ramakrishna, G. (2022). Oil palm empty fruit bunch fiber: Surface morphology, treatment, and suitability as reinforcement in cement composites - A state of the art review. *Cleaner Materials*, *6*, 100144. https://doi.org/10.1016/j.clema.2022.100144

Rao, K. J., Sastri, M. V. S. S., Swetha, T., & Poojita, C. (2024). Optimizing roofing efficiency: Utilizing GGBS and coir fibre in cement tile production. In *IOP Conference Series: Earth and Environmental Science* (Vol. 1409, No. 1, p. 012014). IO Publishing. https://doi.org.10.1088/1755-1315/1409/1/012014

Ridzuan, M. N., Abu Bakar, H., Samsudin, E. M., Nik Soh, N. M. Z., & Ismail, L. H. (2023). Effects of density variation on the physical and mechanical properties of empty fruit bunch cement board (EFBCB). *Pertanika Journal of Science and Technology*, *31*(3), 1157-1172. https://doi.org/10.47836/pjst.31.3.02

Sahu, P., & Gupta, M. K. (2020). A review on the properties of natural fibres and its bio-composites: Effect of alkali treatment. *Proceedings of the Institution of Mechanical Engineers, Journal of Materials, Part L: Design and Applications*, *234*(1), 198-217. https://doi.org/10.1177/1464420719875163

Shaffril, H. A. M., Ahmad, N., Samsuddin, S. F., Abu Samah, A., & Hamdan, M. E. (2020). Systematic literature review on adaptation towards climate change impacts among indigenous people in the Asia Pacific regions. *Journal of Cleaner Production*, *258*, 120595. https://doi.org/10.1016/j.jclepro.2020.120595

Shaffril, H. A. M., Samsuddin, S. F., & Abu Samah, A. (2021). The ABC of systematic literature review: The basic methodological guidance for beginners. *Quality and Quantity*, *55*, 1319-1346. https://doi.org/10.1007/s11135-020-01059-6

Silva, D. W., Bufalino, L., Alves Junior, A. T., Scatolino, M. V., Batista, F. G., de Medeiros, D. T., Mendes, L. M., & Tonoli, G. H. D. (2024). Impact of accelerated aging cycles on the performance of extruded cement-based composites reinforced with non-bleached eucalyptus fibers. *Environmental Science and Pollution Research*, *31*, 35789-35799. https://doi.org/10.1007/s11356-024-33665-4

Song, H., Liu, T., Gauvin, F., & Nrouwers, H, J. H. (2023). Improving the interface compatibility and mechanical performances of the cementitious composites by low-cost alkyl ketene dimer modified fibers. *Construction and Building Materials*, *395*, 132186. https://doi.org/10.1016/j.conbuildmat.2023.132186

Stapper, J. L., Gauvin, F., & Brouwers, H. J. H. (2021). Influence of short-term degradation on coir in natural fibre-cement composites. *Construction and Building Materials*, *306*, 124906. https://doi.org/10.1016/j.conbuildmat.2021.124906

Syduzzaman, M., Al Faruque, M. A., Bilisik, K., & Naebe, M. (2020). Plant-based natural fibre reinforced composites: A review on fabrication, properties and applications. *Coatings*, *10*(10), 973. https://doi.org/10.3390/coatings10100973

Taiwo, A. S., Ayre, D. S., Khorami, M., & Rahatekar, S. S. (2024). Optimizing the mechanical properties of cement composite boards reinforced with cellulose pulp and bamboo fibers for building applications in low-cost housing estates. *Materials*, *17*(3), 646. https://doi.org/10.3390/ma17030646

Thompson, D., Augarde, C., & Osorio, J. P. (2025). A review of chemical stabilisation and fibre reinforcement techniques used to enhance the mechanical properties of rammed earth. *Discover Civil Engineering*, *2*, 27. https://doi.org/10.1007/s44290-025-00184-1

United Nations. (2022). *Report of the secretary-general on the work of the organization*. https://www.un.org/annualreport/2022/index.html

Vitrone, F., Ramos, D., Ferrando, F., & Salvad, J. (2021). Binderless fiberboards for sustainable construction – Materials, production methods and applications. *Journal of Building Engineering*, *44*, 102625. https://doi.org/10.1016/j.jobe.2021.102625

Wu, F., Yu, Q., & Brouwers, H. J. H. (2022). Long-term performance of bio-based miscanthus mortar. *Construction and Building Materials*, *324*, 126703. https://doi.org/10.1016/j.conbuildmat.2022.126703

Xie, X. & Li, H. (2021). compatibility between rice straw fibers with different pre-treatments and ordinary Portland cement. *Materials*, *14*(21), 6402. https://doi.org/10.3390/ma14216402

Zhang, X. X., Ji, Y. L., Pel, L., Sun, Z. P., & Smeulders, D. (2022). Early-age hydration and shrinkage of cement paste with coir fibers as studied by Nuclear Magnetic Resonance. *Construction and Building Materials*, *336*, 127460. https://doi.org/10.1016/j.conbuildmat.2022.127460

Pertanika J. Sci. & Technol. 33 (5): 2237 - 2258 (2025)

PERTANIKA JOURNALS

SCIENCE & TECHNOLOGY

Journal homepage: http://www.pertanika.upm.edu.my/

Extraction and Characterisation of Leaf Fibres from *Pandanus atrocarpus, Pandanus amaryllifolius,* and *Ananas comosus*

Syahril Amin Hashim[1], Been Seok Yew[1,2]*, Fwen Hoon Wee[3], Ireana Yusra Abdul Fatah[1], Nur Haizal Mat Yaakob[1] and Muhamad Nur Fuadi Pargi[1]

[1]*Faculty of Innovative Design and Technology, Universiti Sultan Zainal Abidin, Gong Badak, 23100 Kuala Nerus, Terengganu, Malaysia*

[2]*Microfabrication, Sensor, Electronic and Computer System RG, Universiti Sultan Zainal Abidin, Gong Badak, 23100 Kuala Nerus, Terengganu, Malaysia*

[3]*Faculty of Electronic Engineering Technology, Universiti Malaysia Perlis, 02600 Arau, Perlis, Malaysia*

ABSTRACT

Pandanus atrocarpus, *Pandanus amaryllifolius*, and *Ananas comosus* plants are abundantly found in Malaysia. This study reports on the water retting extracting leaf fibres method, the morphology, chemical structure (functional groups), thermal stability, and dielectric properties of the *P. atrocarpus*, *P. amaryllifolius*, and *A. comosus* leaf fibres. Morphological analysis showed that the average diameter of leaf fibres is 445.5 µm for *P. atrocarpus*, 226.3 µm for *P. amaryllifolius*, and 311.2 µm for *A. comosus*. The presence of hemicellulose, cellulose, and lignin in the leaf fibres was detected in Fourier transform infrared (FTIR) spectra. Thermogravimetric analysis (TG) indicates that the leaf fibres are thermally stable up to a temperature of 220°C. Differential thermogravimetric (DTG) and differential scanning calorimetry (DSC) curves revealed a consistent thermal behaviour of the leaf fibres, where hemicellulose and cellulose decomposed at 275.0 and 355.3°C, respectively. Incorporation of the leaf fibres from *P. atrocarpus*, *P. amaryllifolius*, and *A. comosus* into epoxy composites enhanced the dielectric properties performance of epoxy. Overall, the findings from this study suggest that the leaf fibres from *P. atrocarpus*, *P. amaryllifolius*, and *A. comosus* are potentially useful for diversifying polymerisation for high-frequency applications.

ARTICLE INFO

Article history:
Received: 18 November 2024
Accepted: 29 April 2025
Published: 28 August 2025

DOI: https://doi.org/10.47836/pjst.33.5.09

E-mail addresses:
syahrilamin@unisza.edu.my (Syahril Amin Hashim)
bseokyew@unisza.edu.my (Been Seok Yew)
fhwee@unimap.edu.my (Fwen Hoon Wee)
ireanayusra@unisza.edu.my (Ireana Yusra Abdul Fatah)
haizal@unisza.edu.my (Nur Haizal Mat Yaakob)
mohamadnurfuadi@unisza.edu.my (Muhamad Nur Fuadi Pargi)
* Corresponding author

Keywords: *Ananas* comosus, leaf fibres, *Pandanus amaryllifolius*, *Pandanus atrocarpus*

INTRODUCTION

The utilisation of lignocellulosic fibres from plants as alternatives to synthetic fibres has gained significant attention due to their sustainability and renewability (Samuel et al., 2022; Yadav & Singh, 2022). Lignocellulosic

fibres consist of cellulose and amorphous constituents such as hemicelluloses, lignin, and impurities on the surface of the fibre, like pectin, waxes, and greases (Rana et al., 2021; Rao et al., 2023; Weerappuliarachchi et al., 2020). Cellulose is composed of linear macromolecular glucose chains in the form of microfibrils arranged in the plant cell wall. Hemicellulose contains microfibrils, which strengthen the fibres' structure, whereas lignin provides rigidity and decay resistance (Banagar et al., 2024; Diyana et al., 2024; Feng et al., 2024). There are four classifications of lignocellulosic fibres, namely leaf fibre, bast fibre, seed fibre, and agricultural residues. Incorporating lignocellulosic fibres has improved the strength and durability of composite materials, adsorbent fibres, and textile fibres (Diah et al., 2024; Elfaleh et al., 2023; Habibi et al., 2020; Meng et al., 2019; Owonubi et al., 2021; Yadav & Singh, 2022).

Pandanaceae family includes about 600 species and grows throughout the tropics of Asia. *Pandanus atrocarpus* (known as screw pine) and *Pandanus amaryllifolius* (known as fragrant pandan) are easily found and grow abundantly in Malaysia. *Pandanus atrocarpus* naturally grows in swampy and riverbank habitats. It has long, narrow, and sheathing leaves with parallel veins structure and spiny edges. *Pandanus atrocarpus* leaves have been widely used as thatching roofs and producing handicrafts. *Pandanus amaryllifolius* is widely planted at home as its scented leaves are commonly used in food and beverage flavouring (Azahana, Wikneswari, Noraini, Nordahlia et al., 2015; Hamdan et al., 2018; Hashim et al., 2023; Mohamed et al., 2018b). It has a similar long, narrow and parallel vein structure of leaves. In contrast, *Ananas comosu*s (pineapple) is a fruit-bearing plant. Despite belonging to Bromeliaceae family, it shares similar leaf characteristics with both *P. atrocarpus* and *P. amaryllifolius*, but it has waxy leaf surface. Traditionally, fibres are extracted from pineapple leaves to produce rope and textiles (Sethupathi et al., 2024).

Natural fibres can be incorporated as reinforcement in polymer composites, enhancing their tensile strength and thermal stability. Recent research emphasises the significance of *P. amaryllifolius* and *A. comosu*s leaf fibres compared to *P. atrocarpus*. Diyana et al. (2021, 2024) reported that *P. amaryllifoliu*s fibres contain high cellulose content (48.79%). Its fibres have been incorporated into polymer composites and yield impressive tensile strength up to 45.61 MPa (Diyana et al., 2021, 2024; Sari et al., 2019). Similarly, *A. comosus* fibres exhibit excellent tensile strength (up to 1620 MPa) and thermal stability, which have been commercially used as reinforcement in composites and the textile industry (Gaba et al., 2021; Hamzah et al., 2021; Mohd Ali et al., 2020; Neves et al., 2023; Prado & Spinacé, 2019; Santos et al., 2021; Sethupathi et al., 2024; Todkar & Patil, 2019). In contrast, the current research of *P. atrocarpus* leaf fibres primarily reports on their mechanical properties (Chin et al., 2018; Kuan et al., 2017; Mohamed et al., 2018a; Mohd Zain et al., 2024). It is essential to broaden the investigation on the characteristics of fibres extracted from *P. atrocarpus* leaf.

Natural fibres extracted from plants are potentially useful as conductive fillers for dielectric material. Dielectric material is used in high-frequency applications, commonly wireless and satellite communications, to suppress electromagnetic interference (EMI). Practically, metal is utilised to suppress EMI, but it is heavy, costly, and prone to corrosion, thus limiting its practical application. Consequently, polymeric-based dielectric material or conducting polymer is preferred as an alternative dielectric material to metal in EMI suppression. Polymeric-based dielectric material exhibits advantages such as being lightweight, highly flexible, and having excellent corrosion resistance (Wei et al., 2020; Yao et al., 2021; Zhang et al., 2018). However, it has low thermal conductivity, which causes poor heat dissipation efficiency (Chen et al., 2024). Polymer typically exhibits a single polarisation orientation within its molecules. To improve its thermal conductivity, conductive fillers such as metal, ceramic, and carbon are incorporated into polymer composites. The interaction of the conductive filler particles and polymer matrix facilitates polarisation behaviour, thus improving the overall dielectric properties and thermal conductivity (Gong et al., 2019; Kwon et al., 2021; Vallés et al., 2019; Wang et al., 2021; Yao et al., 2021; Zheng et al., 2024).

Natural fibers like *P. atrocarpus*, *P. amaryllifolius*, and *A. comosus* could serve as alternative conductive fillers to enhance the flow of electrical charges in the polymer composites for high-frequency applications (Al-Oqla et al., 2015; Tang et al., 2024). It is worth highlighting that while natural fibres can modify the properties of the polymer composites, they cannot entirely substitute polymer as the matrix. Studies have reported that natural fibres can be used to partially substitute the polymer matrix to reduce cost and enhance the properties of polymer composites. Polymer matrix has excellent adhesiveness and is generally used as a binding agent in composites, while natural fibres are used as fillers (Alazzawi et al., 2024; Elfaleh et al., 2023; Hao et al., 2018; Khalid et al., 2021; Sahari et al., 2013).

Since the species and growing environment may contribute to a diverse range of properties in the natural fibres, characterisation is crucial to investigate the quality and performance of the fibres. In this study, characterisation of the extracted fibres from the mature leaves of *P. atrocarpus*, *P. amaryllifolius*, and *A. comosus* was performed. The water retting method was carried out to extract the leaf fibres from the plants. The morphological properties, functional structure, and thermal properties of the extracted leaf fibres were analysed using scanning electron microscopy (SEM), Fourier transform infrared spectroscopy (FTIR), simultaneous thermogravimetric analyser (STA), and differential scanning calorimetry (DSC). An open-ended coaxial line method was used to measure the dielectric properties of the epoxy composites incorporated with extracted leaf fibres. Notably, the micromechanical characterisation is excluded in this study as the emphasis was placed on dielectric properties, as these parameters are crucial for high-frequency dielectric applications (Reddy et al., 2022; Singh et al., 2024; Xiong et al., 2025).

MATERIALS AND METHODS

Collection of Fibres

The collection of *P. atrocarpus*, *P. amaryllifolius*, and *A. comosus* leaves was conducted based on the maturity, age, and size in Kuala Nerus (Terengganu, Malaysia), as shown in Figure 1. It can be observed that *P. atrocarpus* and *P. amaryllifolius* leaves have parallel veins, while *A. comosus* has waxy surface leaves. The leaves of these plants were harvested from mature plants aged around 1 to 2 years, measuring approximately 5 cm in width.

(a)

(b)

(c)

Figure 1. (a) *Pandanus atrocarpus* plant and its leaf (parallel veins); (b) *Pandanus amaryllifolius* plant and its leaf (parallel veins); and (c) *Ananas comosus* plant and its waxy surface leaf

Extraction of Leaf Fibres Using Water Retting

The water retting method was performed to extract the fibres from *P. atrocarpus*, *P. amaryllifolius*, and *A. comosus* leaves. The water retting method introduces moisture and natural enzymatic reaction that results from rotting bacteria and fungi for fibre extraction from the leaves. Water retting is a standard and preferred for its effectiveness in producing high-quality fibres (Diyana et al., 2021; Feleke et al., 2023; Plakantonaki et al., 2024). The stalks of *P. atrocarpus* and *P. amaryllifolius* leaves were separately soaked in stagnant water to undergo the water retting process at a room temperature of 20–25°C for 8 weeks (56 days), whereas the water retting process of *A. comosus* leaves was carried out for 4 weeks (28 days). The stagnant water emitted an unpleasant odour, and clean water needed to be replaced frequently (approximately every 2 to 3 days) during the water retting process. During the entire procedure, it became evident that the water retting process caused the soft tissue or gummy elements in the leaf stalk to dissolve and break down. The degumming of fibres from the retted leaf stalk is shown in Figure 2(a). This, in turn, facilitated the manual extraction of fibres by scraping and peeling them from the retted stalk of leaves, as shown in Figure 2(b). The extracted fibres were cleaned to

remove impurities and allowed to dry in a dehydrator at a temperature of 70°C for 12 hours. The extracted *P. atrocarpus*, *P. amaryllifolius*, and *A. comosus* leaf fibres are presented in Figures 2(c), 2(d), and 2(e), respectively.

In this study, water retting at standard room temperature (20–25°C) was found to be less efficient than at the optimal range of 30–32°C, slowing microbial activity and requiring longer stagnant time. However, extending the stagnant time can yield high-quality fibres. Conversely, water retting at 30–32°C produced fibres that were light, hard, and less durable (Aisyah et al., 2016; Różańska et al., 2023). *Pandanus atrocarpus* and *P. amaryllifolius* leaves require a longer stagnant time to dissolve the gummy elements of the leaves than *A. comosus* leaves. This is due to the structural differences in the leaves. The parallel vein structure of the *P. atrocarpus* and *P. amaryllifolius* leaves strengthens their durability. In contrast, *A. comosus* leaves have a less robust structure. Additionally, the sample collection involves mature and non-decorticated leaves, thus increasing the duration of stagnant water required to soften and dissolve the elements of the leaves during the water retting process.

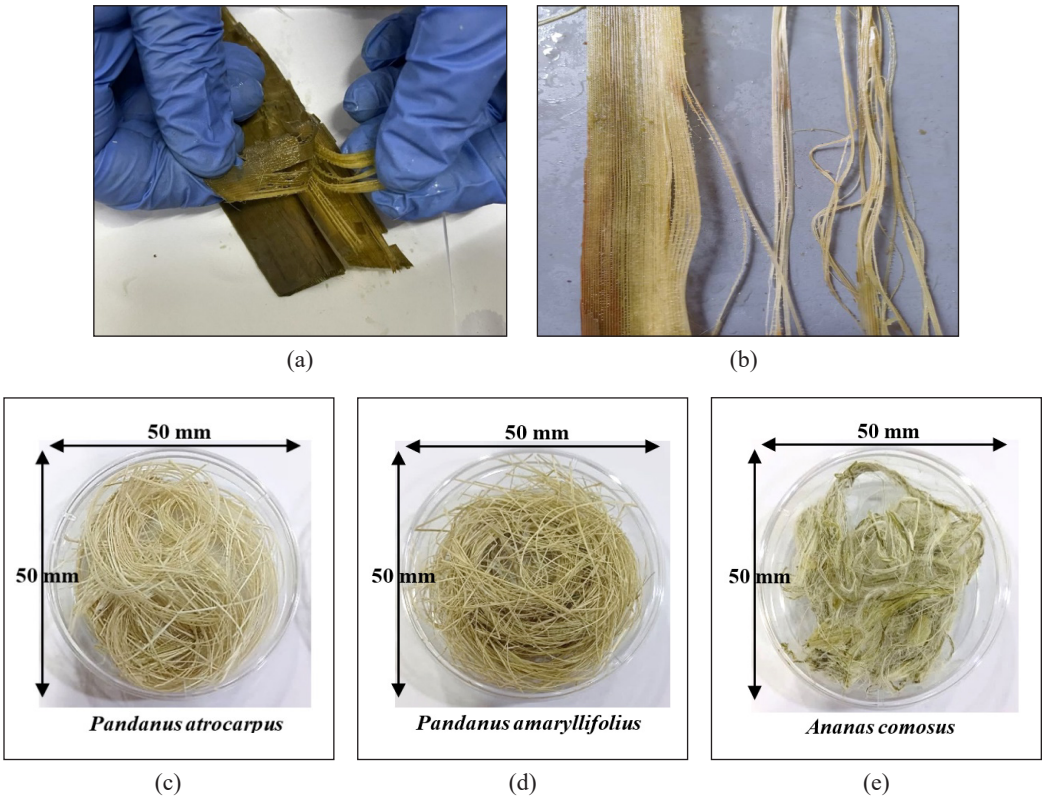

Figure 2. (a) Degumming the fibres from retted leaf stalk (*Pandanus atrocarpus*); (b) peeling of fibre; (c) extracted *P. atrocarpus* leaf fibres; (d) extracted *Pandanus amaryllifolius* leaf fibres; (e) extracted *Ananas comosus* leaf fibres

Fibre Morphology and Diameter

The longitudinal fibre morphology and diameter of the leaf fibres were observed using Thermo Scientific Quattro Environmental Scanning Electron Microscope (ESEM, USA). The sample fibres were coated with a layer of 8 nm platinum using a G20 Ion Sputter Coater (GSEM Co., Ltd., South Korea) prior to characterisation to avoid electrostatic charges. The samples' fibres were observed at a magnification of 100×. The average diameter was randomly measured at different positions of each image, and the average value was determined.

FTIR Spectroscopy Analysis

The infrared spectrum with percentage transmittance (%T) versus wavelength (cm^{-1}) was obtained by using a PerkinElmer Spectrum Two™ FTIR Spectrometer (USA) in attenuated total reflectance (ATR) mode within the range of 4000–450 cm^{-1}.

Thermogravimetric Analysis (TGA) and Derivative Thermogravimetry (DTG)

The thermal stability of the leaf fibres was analysed through TGA and DTG using NETZSCH STA 2500 Regulus Simultaneous Thermal Analyser (Germany). Samples of 10 mg were scanned from 30 to 600°C. The heating rate temperature was 10°C/min with a constant nitrogen flow of 50 ml/min to avoid thermal oxidation**.**

DSC

NETZSCH DSC 3500 Sirius DSC (Germany) was used to scrutinise the thermal transitions of the samples. Samples with a weight of 5–10 mg were heat scanned at a temperature range of 30–600°C under 40 ml/min nitrogen airflow and 10°C/min heating rate.

Open-Ended Coaxial Line Method

An open-ended coaxial line method was used to measure the dielectric constant, dielectric loss factor and electrical conductivity over a wide microwave frequency range of 300 MHz-20 GHz at room temperature. For the open-ended coaxial line method, the dimension of the materials under test (MUT) must be > 20 mm and infinite thickness ≤ 5 mm to meet the requirement of open-ended coaxial probe dielectric properties measurement, to minimise the fringing field effect. The measurement apparatus includes an open-ended coaxial probe, an Agilent 85070E Dielectric Probe Kit (USA) and an Agilent E8362B PNA Series Network Analyser (USA). The MUTs were prepared by mixing the sample fibres with D.E.R.™ 331 epoxy resin and hardener (Euro Chemo-Pharma Sdn. Bhd., Malaysia). The extracted fibres were ground into short fibres using an IKA A10 Analytical Mill (Germany). It is recommended to ensure the fibre size is below 500 μm to minimise the risk of agglomeration and ensure better dispersion within the resin matrix (Callister

& Rethwisch, 2011). The composition of the MUT is 10% fibre to 90% matrix to avoid agglomeration, and is fabricated in a 50 mm diameter disposable petri dish with a thickness of 5 mm. Figure 3(a) presents the *P. atrocarpus* composite, Figure 3(b) shows the *P. amaryllifolius* composite, and Figure 3(c) displays the *A. comosus* composite, respectively.

The dielectric properties are presented in the form of complex permittivity (ε), dielectric constant (ε'), and dielectric loss factor (ε''), where $\varepsilon = \varepsilon' + \varepsilon''$. ε' refers to the material's capacity to store electromagnetic (EM) energy, whereas ε'' indicates the ability to convert the stored EM energy into heat dissipation (heat loss). ε'' is always greater than zero and is much smaller than ε'. The ratio of heat dissipation to stored EM energy in a lossy material is known as the dissipation factor or tangent delta (tan δ), where tan $\delta = \varepsilon''/\varepsilon'$ (Keysight Technologies, 2016).

Dielectric loss in materials measures energy dissipation as heat when an alternating electric field is applied. This loss is influenced by the material's dielectric properties and its conductivity. The relationship between dielectric loss and conductivity is $\sigma = 2\pi f \varepsilon_o \varepsilon''$, where σ is the conductivity (S/m), ε_o is the free space permittivity (8.854×10^{-12} F/m), f is the frequency (Hz), ε" is the dielectric loss factor (Bouaamlat et al., 2020; Mittal et al., 2016). Materials with high conductivity will have higher dielectric losses, leading to more heat dissipation. This is crucial in applications like EMI shielding, where both the dielectric properties and conductivity of the material determine its effectiveness in absorbing and dissipating EM energy.

(a)

(b)

(c)

Figure 3. (a) *Pandanus atrocarpus* composite, (b) *Pandanus amaryllifolius* composite, and (c) *Ananas comosus* composite

RESULTS AND DISCUSSION

Fibre Morphology and Diameter

Samples of *P. atrocarpus*, *P. amaryllifolius*, and *A. comosus* leaf fibres were picked randomly to observe the longitudinal fibre morphology and to determine the average fibre diameter. It was observed that there is a presence of longitudinal streaks in the *P. atrocarpus*, *P. amaryllifolius*, and *A. comosus* leaf fibres' structure. The longitudinal fibre morphology showed that these fibres exhibit an arrangement of vertical alignments that follow the direction of the fibre axis, attributed to the compactly aligned microfibrils bonded together by lignin, pectin, and other non-cellulosic materials (Azahana, Wickneswari, Noraini, Nurnida et al., 2020; Donaldson et al., 2016; Hashim et al., 2023). The vascular bundle structure in

P. atrocarpus and *P. amaryllifolius* fibres can be easily detected and observed at 100× and 300× magnification, appearing as rectangular arrangements in the leaf fibres, contributing to the hydrophilic behaviour in the cellulosic fibres. It was observed that *P. atrocarpus* leaf fibres have a rougher surface texture than *P. amaryllifolius* and *Ananas comosus* leaf fibres. The fibre diameter of *P. atrocarpus* ranges from 421.0 to 458.7 µm, with average fibre diameter of 445.5 µm; whereas for *P. amaryllifolius*, the diameter ranges from 194.3 to 291.6 µm, with average fibre diameter of 226.3 µm; and for *A. comosus*, the diameter ranges from 258.5 to 393.9 µm, with average fibre diameter of 311.2 µm. The fibre diameters were measured randomly to account for the natural variability and irregularities in the fibres. The measured diameter of the natural fibres sample in this study aligns with findings from other research, supporting the consistency of these findings (Diyana et al., 2024; Gnanasekaran et al., 2022; Mohamed et al., 2018a; Neves et al., 2023; Kuan & Lee, 2014). The fibres' morphology of *P. atrocarpus*, *P. amaryllifolius*, and *A. comosus* leaves are presented in Figure 4.

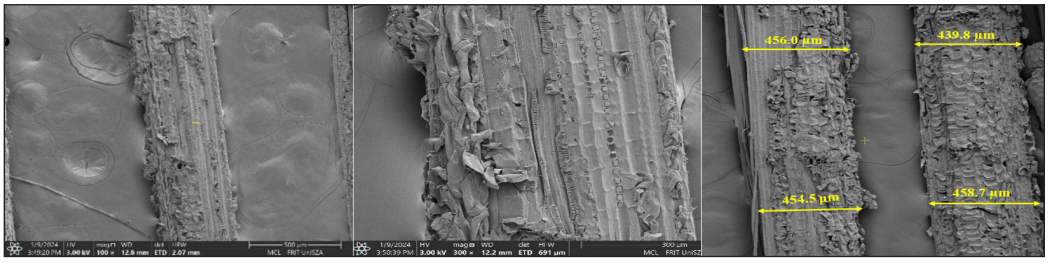

(a)

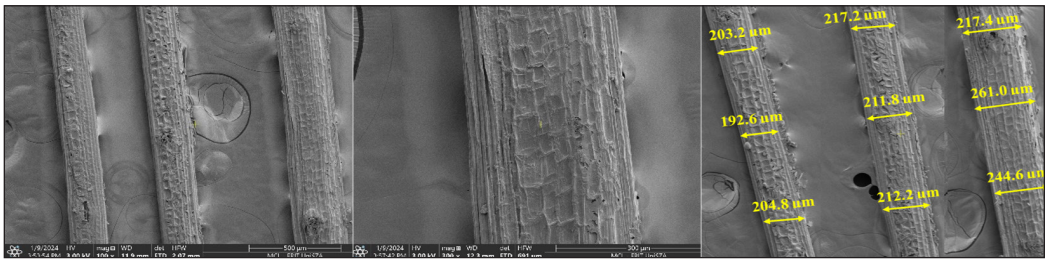

(b)

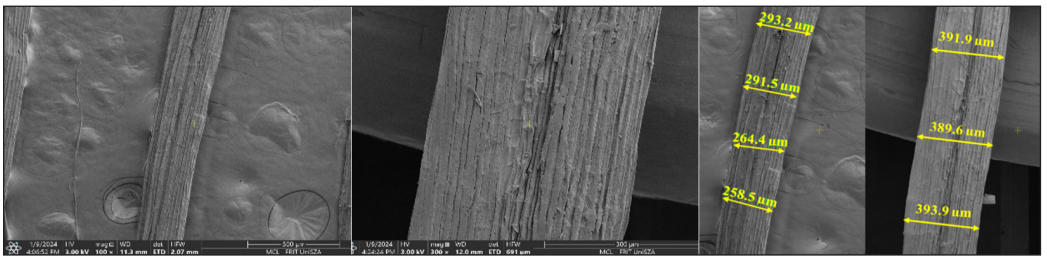

(c)

Figure 4. Scanning electron microscopy view of leaf fibres morphology (100× and 300× magnification) and diameter: (a) *Pandanus atrocarpus*, (b) *Pandanus amaryllifolius*, and (c) *Ananas comosus*

FTIR Spectra Analysis

The FTIR spectra depicted in Figure 5 have been attributed to the lignocellulosic-based materials and verified the existence of cellulose, hemicellulose, and lignin in the *P. atrocarpus*, *P. amaryllifolius*, and *Ananas comosus* leaf fibres. The presence of the O-H stretching vibrations was observed at broad absorption peaks of 3330.88, 3340.21, and 3334.08 cm^{-1}, respectively, for *P. atrocarpus*, *P. amaryllifolius*, and *A. comosus* leaf fibres, which correlates to the hydrophilic hydroxyl group (OH) in cellulose, hemicellulose and lignin (Diyana et al., 2021; Shaker et al., 2020). The existence of cellulose and hemicellulose was confirmed by the absorption peaks observed at 2916.80, 2917.19, and 2916.53 cm^{-1}, corresponding to the alkanes C-H stretching (Ikhuoria et al., 2017; Ilyas et al., 2019; Yew et al., 2019). The sharp and intense C-H stretching peak observed in *P. atrocarpus* leaf fibre FTIR spectra implies that cellulose and hemicellulose are most dominant in *P. atrocarpus* leaf fibre compared to *P. amaryllifolius* and *A. comosus* leaf fibres (Md Salim et al., 2021).

The absorption peaks observed at 1731.20, 1729.51, and 1726.40 cm^{-1} correspond to carbonyl C=O stretching vibrations of aliphatic carboxylic acids, acetyl and ketone groups in cellulose, hemicellulose and lignin (Alemdar & Sain, 2008; Diyana et al., 2021; Salem et al., 2021; Sheltami et al., 2012). The vibration of aromatic C=C further identifies

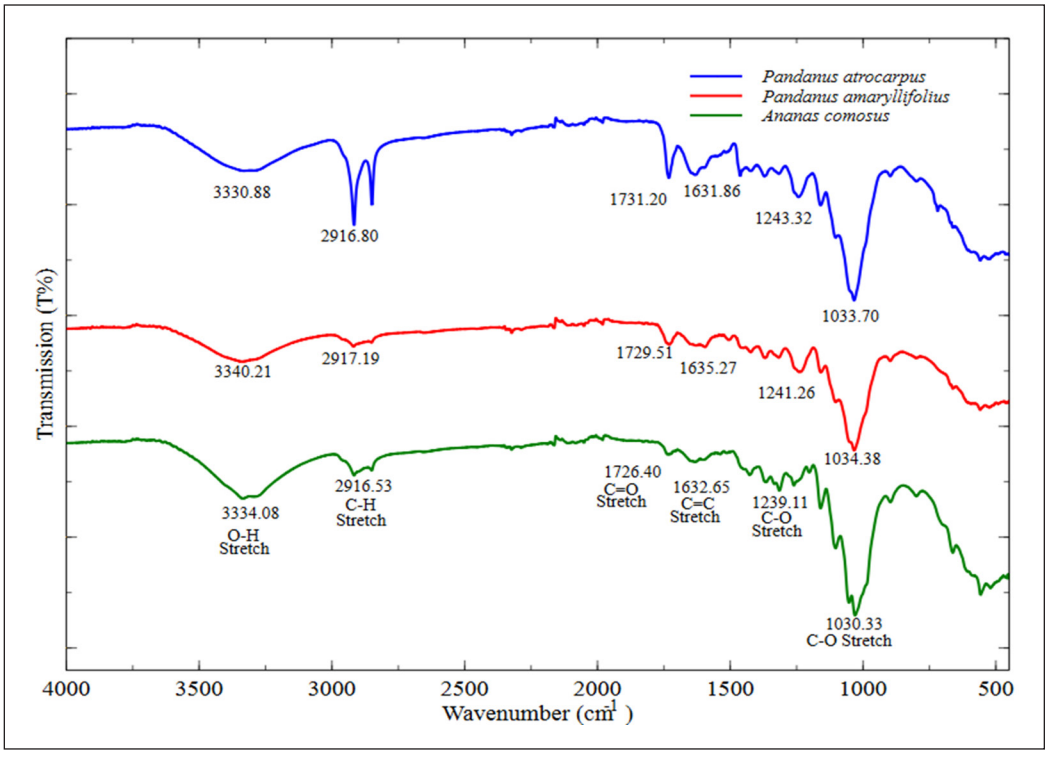

Figure 5. Fourier-transformed infrared spectra of the sample fibres

the presence of lignin rings functional groups detected at peaks 1631.86, 1635.27, and 1632.65cm^{-1} (Shi et al., 2019). The aromatic ester linkage CO stretching vibration in ferulic carboxylic group, phenylpropanoids and p-coumaric acids in lignin and hemicellulose were observed at the absorption peaks of 1243.32, 1241.26, and 1239.65 cm^{-1}. The existence of C-O stretching corresponds to xylan-rich polysaccharide in cellulose and hemicellulose was further confirmed with the appearance of peaks at 1033.70, 1034.38, and 1030.33cm^{-1} (Banagar et al., 2024; Diyana et al., 2021; Gaba et al., 2021).

Thermal Analysis

TGA and DTG

The thermal decomposition of natural fibre involves the dehydration, emission of volatile components, and weight loss due to lignocellulosic components degradation (Azwa et al., 2013; Yew et al., 2019). The degradation takes place in the following sequences: hemicellulose, cellulose, lignin, and the rest of the constituents (Tamanna et al., 2021). Figures 6(a) and 6(b) present the TG and DTG curves of the *P. atrocarpus*, *P. amaryllifolius*, and *A. comosus* leaf fibres. The curves showed that these samples' fibre degrade through four distinct stages in the following ranges: (I) from 30 to 120°C, (II) 120 to 220°C, (III) 220 to 390°C, and (IV) 390 to 600°C.

From Figures 6(a) and 6(b), the initial degradation occurs at range I, which marks the beginning of the weight loss in the sample fibres as the fibres were heated. The weight loss was attributed to the hydrophilic behaviour of the sample fibres, where evaporation of moisture and volatile contents occurred. The volatile contents tend to migrate to the fibre surface along with the movement of the water molecules from the internal parts to the outer surface of the fibre during the evaporation process. The moisture of the sample fibres was completely evaporated around 120°C with low mass loss of 7.27, 7.32, and 6.54%, respectively, for *P. atrocarpus*, *P. amaryllifolius*, and *A. comosus* leaf fibres.

The second stage of thermal degradation (Range II) started at temperatures above 120°C and was thermally stable until 220°C for all leaf fibres, where no significant peak of degradation is observed in both TG and DTG curves (Diyana et al., 2021; Ilyas et al., 2019; Ishak et al., 2012). At this stage, the average weight loss is about 0.6%, which is induced by the removal of impurities, waxes and inorganic components of volatile extractives from the fibres.

The third stage of thermal decomposition occurs at range III (200 to 390°C), corresponding to the degradation of hemicellulose and cellulose, resulting in significant mass loss up to 72%. As can be observed for *P. atrocarpus* and *P. amaryllifolius* fibres, two DTG peaks were observed on range III, which correspond to the degradation of hemicellulose that took place between 220 and 320°C. In contrast, the sharp DTG peaks can be observed at 320 to 390°C, corresponding to the degradation of cellulose. Hemicellulose structure is

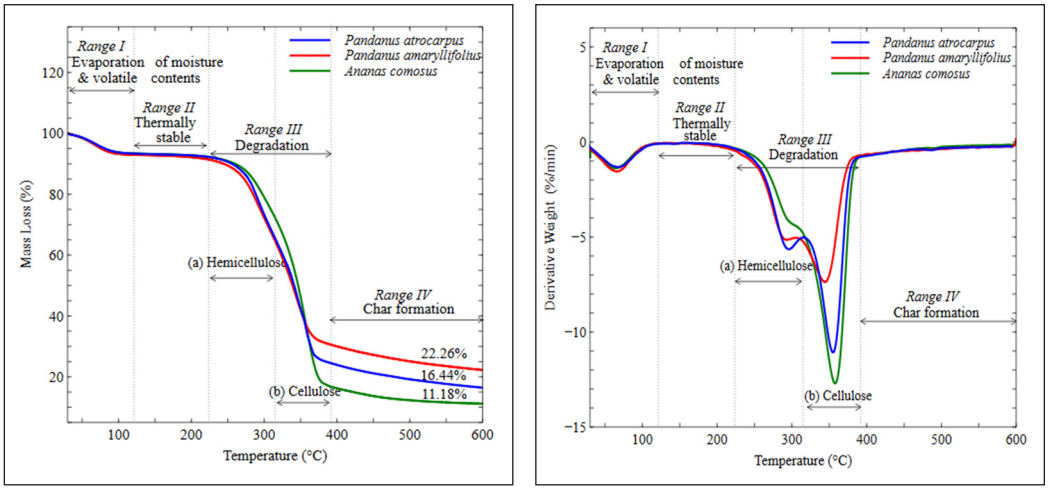

(a) (b)

Figure 6. (a) Thermogravimetry thermogram of weight loss as a function of temperature, and (b) derivative thermogravimetric curve of the rate of weight loss as a function of time

amorphous, which is less thermally stable and easily degrades to a volatile state at lower temperatures compared to cellulose. Cellulose structure is highly crystalline and thermally stable due to its microfibril chain cell wall. The highest peak of decomposition temperature in DTG occurred at 359.0, 355.9, and 344.2°C for *P. atrocarpus*, *P. amaryllifolius*, and *A. comosus* leaf fibre, respectively, attributed to the cellulose degradation.

The fourth stage decomposition that occurs up to 600°C at range IV corresponds to the degradation of lignin and the rest of the constituents in the sample fibres. The final residual is carbonaceous impurities, known as char. Char residue is 16.44, 22.26, and 14.04% respectively for *P. atrocarpus*, *P. amaryllifolius*, and *A. comosus* leaf fibres. The amount of residual weight obtained at the end of the combustion process in *P. amaryllifolius* was greater than that of *P. atrocarpus* and *A. comosus* leaf fibres. This indicates the highest thermal stability, attributed to a higher composition of char, suggesting improved fire resistance capability of the fibre, thus providing insulation against further thermal degradation. Furthermore, the char residue formation could be attributed to the presence of inorganic materials and silicon dioxide within the natural fibre. These components only degrade at extremely high temperatures exceeding 1,500°C (Diyana et al., 2024; Sahari et al., 2013).

DSC Analysis

Natural fibre constituents (hemicellulose, cellulose, and lignin) are sensitive to temperature. When these fibre constituents are subjected to heat, separate peaks of decomposition can be detected. DSC is useful in assessing the thermal stability and composition of the natural fibres. DSC measures the temperature at which decomposition occurs. Higher

decomposition temperatures indicate better thermal stability and resistance to degradation, thus higher quality fibres (Acharya et al., 2024; PerkinElmer, 2011). Figure 7 shows the DSC curves of fibres from *P. atrocarpus*, *P. amaryllifolius*, and *A. comosus* leaves upon heating. The DSC curves clearly showed three distinct peaks. The presence of each peak represents the temperature at which the maximum rate of weight loss occurs, indicating the critical temperature at which the fibre composition decomposes.

The DSC curves showed a large and broad endothermic peak at the temperature range of 30–120°C (Range I), which indicates the removal of moisture by evaporation (volatilisation) in the intercellular region of the *P. atrocarpus*, *P. amaryllifolius*, and *A. comosus* leaf fibres. At the temperature range of 220–390°C (Range III), there were two peaks detected in the DSC curves. The exothermic peaks at a temperature range of 220–320°C represent the degradation of hemicellulose, where hemicellulose decomposed and produced char residue. Hemicellulose is an amorphous structure constituent that tends to absorb water as it consists of hydroxyl groups, which degrade earlier than cellulose and lignin. Cellulose is a crystalline structure constituent that possesses higher thermal stability than hemicellulose; thus, it exhibits higher degradation temperature. The endothermic peaks at a temperature range of 320–390°C represent the degradation of cellulose with the formation of volatiles. The extended temperature ranges from 390 to 600°C (Range IV) signifies the presence of lignin. The lignin curve showed a broad exothermic peak. Lignin possesses aromatic rings with many chemical branches. As a result, degradation

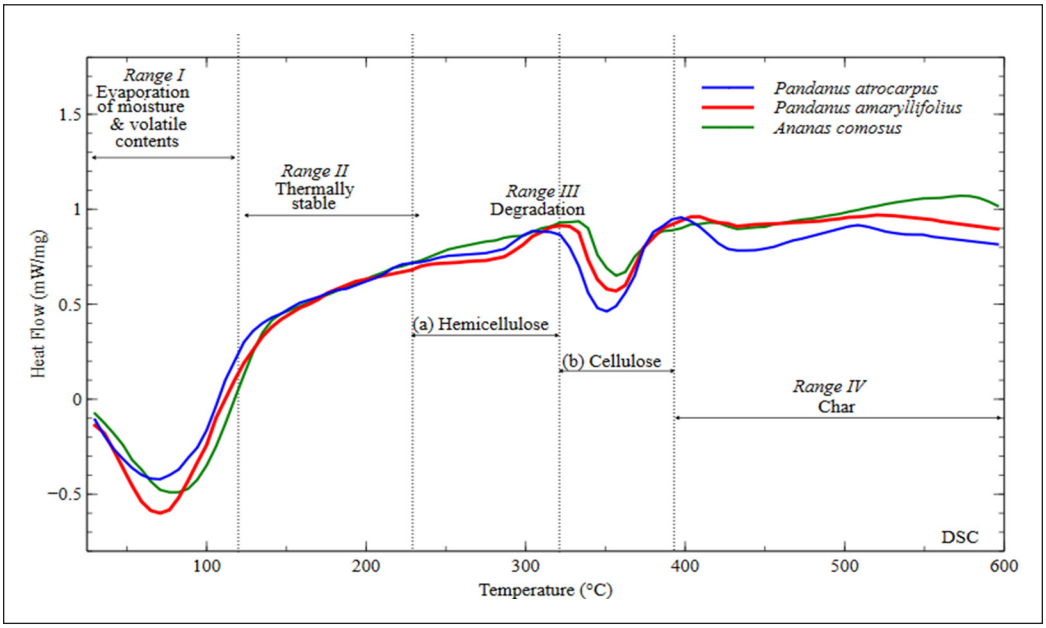

Figure 7. Differential scanning calorimetry curves of *Pandanus atrocarpus*, *Pandanus amaryllifolius*, and *Ananas comosus* leaf fibres

of lignin occurs over a broad temperature range. It might be attributed to the cracking of some functional groups in cellulose residue.

The DSC curves of the three leaf fibres corresponded well with their DTG curves. Hemicellulose and cellulose peaks in DSC curves appeared at around 275.0 and 355.3°C, respectively. The highest peak of decomposition temperature in DTG curves occurred at 359.0, 355.9, and 344.2°C for *P. atrocarpus*, *P. amaryllifolius*, and *A. comosus* leaf fibres, respectively, attributed to the cellulose degradation. These findings from the DSC curves in Figure 7 align with the DTG curves shown in Figure 6(b), where similar temperatures were observed for hemicellulose and cellulose.

Dielectric Properties

Figure 8(a) presents the dielectric constant, ε', of the epoxy and composites filled with the sample fibres. It can be observed that over a wide range of frequencies up to 20 GHz, the ε' of all composites is inversely proportional to the frequency at room temperature, with the ε' trend decreasing as the frequency of the electromagnetic field increases. The ε' is more significant at lower frequencies because the dipoles within the material have ample time to align with the alternating electric field, resulting in a higher dielectric constant. Conversely, at higher frequencies, the rapid oscillations of the electric field prevent the dipoles from fully orienting, thus leading to a decrease in the ε' (Hassan & Ah-yasari, 2019). Figures 8(b)-(d), respectively, present the graphs of dielectric loss factor (ε''), dissipation factor (tan δ), and conductivity (σ) versus frequency for all epoxy composites. Similar trends in the behaviour of ε'', tan δ, and σ were observed. At lower frequencies, the mechanism of energy dissipation in the epoxy composites increases with frequency as the polarization of the dipoles in the material is more effective in the electromagnetic field. This leads to higher energy dissipation as the dipoles continuously reorient themselves with the changing field, which increases the dielectric losses and conductivity, thus dissipating more heat. At higher frequencies (7.5 GHz onwards), the rapid oscillations of the electric field prevent the dipoles from fully aligning, leading to a decrease in these parameters. As a result, the ability of the dipoles to reorient decreases, leading to lower energy dissipation and a decrease in the ε''.

The comparative analysis using a two-sample t-test reveals statistically significant differences in the dielectric properties between the composites of *P. atrocarpus*, *P. amaryllifolius*, and *A. comosus* and epoxy. The p-values for all comparisons are less than the significance level of 0.05, and the t-scores are beyond the critical value of ±1.96, indicating that the results are statistically significant at the 95% confidence level. From the comparative analysis, epoxy without natural fibre filler shows slightly poorer dielectric properties compared to composites filled with *P. atrocarpus*, *P. amaryllifolius*, and *A. comosus* leaf fibres. While the relative differences indicate that epoxy has a higher dielectric constant in

each case (2.03% for *P. atrocarpus* composite, 1.92% for *P. amaryllifolius* composite, and 3.43% for *A. comosus* composite), these relative differences reflect that epoxy has better insulating properties, thus resulting in a higher dielectric constant in terms of heat storage. Consequently, its ability to dissipate heat is poorer, leading to a lower ε'', tan δ, and σ.

When natural fibre fillers are added to epoxy, their chemical composition, which includes hemicellulose, cellulose, and lignin, captures and attracts charges due to interactions of polar molecules and displacement currents in the electromagnetic field. Hemicellulose contributes to flexibility and bonding within the epoxy composite, allowing the flow of

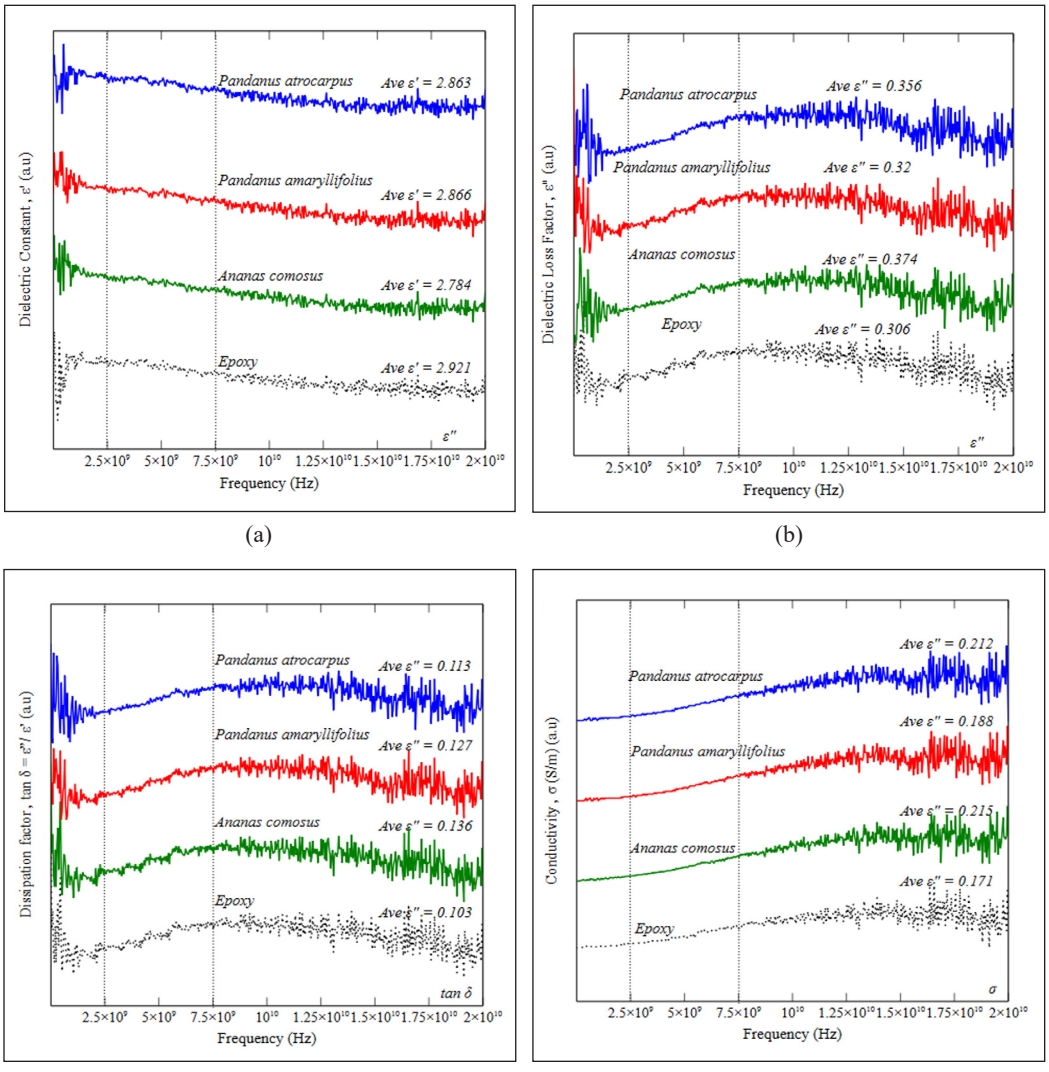

Figure 8. (a) The dielectric constant (ε'), (b) dielectric loss factor (ε''), (c) dissipation factor (tan δ), and (d) conductivity (σ,) of the epoxy and composites filled with the sample fibres

displacement currents through the amorphous regions. The molecular structure of cellulose contributes to orientation polarization, thereby enhancing the material's ability to store and dissipate energy when subjected to an electromagnetic field. Lignin, with its complex aromatic structure, contributes to char formation and improves thermal stability, providing insulation against further thermal degradation (Rowlandson et al., 2020). Together, the fibres from *P. atrocarpus*, *P. amaryllifolius*, and *A. comosus* improve the overall dielectric behaviour of the epoxy composite by increasing orientation polarization, capturing charges, and promoting interaction with the electromagnetic field. It was observed that *A. comosus* composite exhibits higher relative differences in dielectric properties than *P. atrocarpus* and *P. amaryllifolius* composites. This can be attributed to the thermal stability of the *A. comosus* fibres that decompose more readily under thermal conditions, as confirmed by lowest mass residue and sharp peaks in TG and DSC curves, The differences in thermal stability between the natural fibres can influence the composite's overall dielectric response, as materials with different thermal stability can exhibits different polarization behaviours when subjected to an electromagnetic field (Airinei et al., 2021; Neto et al., 2021; Neves et al., 2023; Yusof et al., 2023).

CONCLUSION

The leaf fibres extracted from *P. atrocarpus*, *P. amaryllifolius*, and *A. comosus* plants, exhibit potentially useful characteristics for a variety of high frequency applications as dielectric material for antennas, microwave circuits, and in electromagnetic interference (EMI) suppression to remove noise and improve signal quality. The fibres exhibit unique morphological features determined via SEM analysis. FTIR spectra reveal the existence of hemicellulose, cellulose and lignin constituents. Thermogravimetric analysis indicates that the fibres possess thermal stability up to 220°C. The consistent thermal behaviour was observed in both DTG and DSC curves, which further highlights the decomposition temperature peaks for hemicellulose and cellulose. The dielectric properties of the epoxy composites filled with natural fibres demonstrate better performance compared to epoxy. The addition of the *P. atrocarpus*, *P. amaryllifolius*, and *A. comosus* leaf fibres in the composites facilitates polarizations in the polymer composites. This approach aligns well with Sustainable Development Goals (SDGs) by encouraging innovation in sustainable materials by reducing the dependency on polymers (SDG 9), promoting greener and environmentally friendly materials (SDG 12), minimizing carbon footprint (SDG 13). To effectively use these natural fibres as fillers for polymer composites, it is crucial to address further their limitations on thermal stability, moisture resistance, and compatibility with the polymer matrix. This can be achieved through chemical treatments, surface modifications, or hybridization with compatibilizers to enhance the properties of natural fibres.

ACKNOWLEDGEMENTS

The research conducted in this study was financially supported by Universiti Sultan Zainal Abidin, Malaysia, under the grant number UniSZA/2022/DPU2.0/25.

REFERENCES

Acharya, P., Pai, D., Bhat, K. S., & Mahesha, G. T. (2024). Thermomechanical and morphological characteristics of cellulosic natural fibers and polymer based composites: A review. *Chemistry Africa*, *7*(10), 5149–5174. https://doi.org/10.1007/s42250-024-01157-0

Airinei, A., Asandulesa, M., Stelescu, M. D., Tudorachi, N., Fifere, N., Bele, A., & Musteata, V. (2021). Dielectric, thermal and water absorption properties of some EPDM/flax fiber composites. *Polymers, 13*(15), 2555. https://doi.org/10.3390/polym13152555

Al-Oqla, F. M., Sapuan, S. M., Anwer, T., Jawaid, M., & Hoque, M. E. (2015). Natural fiber reinforced conductive polymer composites as functional materials: A review. *Synthetic Metals*, *206*, 42–54. https://doi.org/10.1016/j.synthmet.2015.04.014

Alazzawi, S., Mahmood, W. A., & Shihab, S. K. (2024). Comparative study of natural fiber-reinforced composites for sustainable thermal insulation in construction. *International Journal of Thermofluids*, *24*, 100839. https://doi.org/10.1016/j.ijft.2024.100839

Alemdar, A., & Sain, M. (2008). Isolation and characterization of nanofibers from agricultural residues—Wheat straw and soy hulls. *Bioresource Technology*, *99*(6), 1664–1671. https://doi.org/10.1016/j.biortech.2007.04.029

Azahana, A., Wickneswari, R., Noraini, T., Nordahlia, A. S., Solihani, N. S., & Nurnida, M. K. (2015). Notes on *Pandanus atrocarpus* Griff and *P. tectorius* Parkinson in Peninsular Malaysia. In *AIP Conference Proceedings* (Vol. 1678, No. 1, p. 0200023). AIP Publishing. https://doi.org/10.1063/1.4931208

Azahana, A., Wickneswari, R., Noraini, T., Nurnida, K., Solehani, S., & Dahlia, A. S. (2020). Leaf anatomical and micromorphological adaptation of *Pandanus immersus* Ridley and *Pandanus tectorius* Parkinson. *Malayan Nature Journal*, *72*(3), 341–347.

Azwa, Z. N., Yousif, B. F., Manalo, A. C., & Karunasena, W. (2013). A review on the degradability of polymeric composites based on natural fibres. *Materials and Design*, *47*, 424–442. https://doi.org/10.1016/j.matdes.2012.11.025

Banagar, A. R., Patel, G. R. R., Srinivasa, C. V., Dhanalakshmi, S., Hemaraju, & Ramesh, B. T. (2024). Extraction and characterization of hemicellulose and lignin contents of areca fiber. *Journal of the Indian Academy of Wood Science*, *21*(1), 112–122. https://doi.org/10.1007/s13196-024-00330-9

Bouaamlat, H., Hadi, N., Belghiti, N., Sadki, H., Bennani M. N., Abdi, F., Lamcharfi, T., Bouachrine, M., & Abarkan, M. (2020). Dielectric properties, ac conductivity, and electric modulus analysis of bulk ethylcarbazole-terphenyl. *Advances in Materials Science and Engineering*, *2020*(1), 8689150. https://doi.org/10.1155/2020/8689150

Callister, W. D., & Rethwisch, D. (2011). *Materials science and engineering: An introduction*. John Wiley & Sons, Inc.

Chen, Q., Yang, K., Feng, Y., Liang, L., Chi, M., Zhang, Z., & Chen, X. (2024). Recent advances in thermal-conductive insulating polymer composites with various fillers. *Composites Part A: Applied Science and Manufacturing*, *178*, 107998. https://doi.org/10.1016/j.compositesa.2023.107998

Chin, S. C., Tong, F. S., Doh, S. I., Gimbun, J., Foo, Y. K., & Siregar, J. P. (2018). Potential external strengthening of reinforced concrete beam using natural fiber composite plate. *Applied Mechanics and Materials*, *878*, 41–48. https://doi.org/10.4028/www.scientific.net/AMM.878.41

Diah, S. B. M., Abdullah, S. H. Y. S., Seok, Y. B., Fatah, I. Y. A., Rahman, N. I. A., Hafizulhaq, F., & Alias, N. N. (2024). Towards sustainable food packaging: A review of thermoplastic starch (TPS) as a promising bioplastic material, its limitations, and improvement strategies with bio-fillers and essential oils. *Journal of Advanced Research in Fluid Mechanics and Thermal Sciences*, *119*(1), 80–104. https://doi.org/10.37934/arfmts.119.1.80104

Diyana, Z. N., Jumaidin, R., Selamat, M. Z., Alamjuri, R. H., & Yusof, F. A. M. (2021). Extraction and characterization of natural cellulosic fiber from *Pandanus amaryllifolius* leaves. *Polymers*, *13*(23), 4171. https://doi.org/10.3390/polym13234171

Diyana, Z. N., Jumaidin, R., Selamat, M. Z., Suan, M. S. M., Hazrati, K. Z., Yusof, F. A. M., Ilyas, R. A., & Eldin, S. M. (2024). Effect of *Pandanus amaryllifolius* fibre on physio-mechanical, thermal and biodegradability of thermoplastic cassava starch/beeswax composites. *Journal of Polymers and the Environment*, *32*(3), 1406–1422. https://doi.org/10.1007/s10924-023-03039-x

Donaldson, L., Nanayakkara, B., & Harrington, J. (2016). Wood growth and development. In B. Thomas, B. G. Murray & D. J. Murphy (Eds.), *Encyclopedia of applied plant sciences* (2nd ed., Vol. 1, pp. 203–210). Academic Press. https://doi.org/10.1016/B978-0-12-394807-6.00114-3

Elfaleh, I., Abbassi, F., Habibi, M., Ahmad, F., Guedri, M., Nasri, M., & Garnier, C. (2023). A comprehensive review of natural fibers and their composites: An eco-friendly alternative to conventional materials. *Results in Engineering*, *19*, 101271. https://doi.org/10.1016/j.rineng.2023.101271

Feleke, K., Thothadri, G., Tufa, H. B., Rajhi, A. A., & Ahmed, G. M. S. (2023). Extraction and characterization of fiber and cellulose from ethiopian linseed straw: Determination of retting period and optimization of multi-step alkaline peroxide process. *Polymers*, *15*(2), 469. https://doi.org/10.3390/polym15020469

Feng, Y., Hao, H., Lu, H., Chow, C. L., & Lau, D. (2024). Exploring the development and applications of sustainable natural fiber composites: A review from a nanoscale perspective. *Composites Part B: Engineering*, *276*, 111369. https://doi.org/10.1016/j.compositesb.2024.111369

Gaba, E. W., Asimeng, B. O., Kaufmann, E. E., Katu, S. K., Foster, E. J., & Tiburu, E. K. (2021). Mechanical and structural characterization of pineapple leaf fiber. *Fibers*, *9*(8), 51. https://doi.org/10.3390/fib9080051

Gnanasekaran, S., Ahamad Nordin, N. I. A., Jamari, S. S., & Shariffuddin, J. H. (2022). Isolation and characterisation of nanofibrillated cellulose from N36 *Ananas comosus* leaves via ball milling with green solvent. *Industrial Crops and Products*, *178*, 114660. https://doi.org/10.1016/j.indcrop.2022.114660

Gong, M., Sun, S.-G., Sun, L., Tian, A.-Q., & Li, Q. (2019). Simulation and experimentation of wide frequency electromagnetic shielding coating used for carbon fiber composite materials of track vehicles. *International Journal of Modern Physics B*, *33*(1–3), 1940020. https://doi.org/10.1142/S0217979219400204

Habibi, M., Selmi, S., Laperrière, L., Mahi, H., & Kelouwani, S. (2020). Post-impact compression behavior of natural flax fiber composites. *Journal of Natural Fibers*, *17*(11), 1683–1691. https://doi.org/10.1080/15440478.2019.1588829

Hamdan, M. H. M., Siregar, J. P., Bachtiar, D., Rejab, M. R. M., & Cionita, T. (2018). Mechanical properties of mengkuang leave fiber reinforced low density polyethylene composites. In S. M. Sapuan, H. Ismail & E. S. Zainudin (Eds.), *Natural fibre reinforced vinyl ester and vinyl polymer composites—Development, characterization and applications* (pp. 181–196). Woodhead Publishing. https://doi.org/10.1016/B978-0-08-102160-6.00009-3

Hamzah, A. F. A., Hamzah, M. H., Che Man, H., Jamali, N. S, Siajam, S. I., & Ismail, M. H. (2021). Recent updates on the conversion of pineapple waste (*Ananas comosus*) to value-added products, future perspectives and challenges. *Agronomy*, *11*(11), 1630. https://doi.org/10.3390/agronomy11112221

Hao, L. C., Sapuan, S. M., Hassan, M. R., & Sheltami, R. M. (2018). Natural fiber reinforced vinyl polymer composites. In S. M. Sapuan, H. Ismail & E. S. Zainudin (Eds.), *Natural fibre reinforced vinyl ester and vinyl polymer composites—Development, characterization and applications* (pp. 27–70). Woodhead Publishing. https://doi.org/10.1016/B978-0-08-102160-6.00002-0

Hashim, S. A., Yew, B. S., Fatah, I. Y. A., Wee, F. H., & Abdullah, N. A. (2023). Leaf anatomical characteristics of the *Pandanus immersus* Ridley virgin fibres using Field Emission Scanning Electron Microscope (FESEM). *Malayan Nature Journal*, *75*(2), 267–278.

Hassan, D., & Ah-yasari, A. H. (2019). Fabrication and studying the dielectric properties of (polystyrene-copper oxide) nanocomposites for piezoelectric application. *Bulletin of Electrical Engineering and Informatics*, *8*(1), 52–57. https://doi.org/10.11591/eei.v8i1.1019

Ikhuoria, E. U., Omorogbe, S. O., Agbonlahor, O. G., Iyare, N. O., Pillai, S., & Aigbodion, A. I. (2017). Spectral analysis of the chemical structure of carboxymethylated cellulose produced by green synthesis from coir fibre. *Ciencia e Tecnologia Dos Materiais*, *29*(2), 55–62. https://doi.org/10.1016/j.ctmat.2016.05.007

Ilyas, R. A., Sapuan, S. M., Ibrahim, R., Abral, H., Ishak, M. R., Zainudin, E. S., Asrofi, M., Atikah, M. S. N., Huzaifah, M. R. M., Radzi, A. M., Azammi, A. M. N., Shaharuzaman, M. A., Nurazzi, N. M., Syafri, E., Sari, N. H., Norrrahim, M. N. F., & Jumaidin, R. (2019). Sugar palm (*Arenga pinnata (Wurmb.) Merr)* cellulosic fibre hierarchy: A comprehensive approach from macro to nano scale. *Journal of Materials Research and Technology*, *8*(3), 2753–2766. https://doi.org/10.1016/j.jmrt.2019.04.011

Ishak, M. R., Sapuan, S. M., Leman, Z., Rahman, M. Z. A., & Anwar, U. M. K. (2012). Characterization of sugar palm (*Arenga pinnata*) fibres tensile and thermal properties. *Journal of Thermal Analysis and Calorimetry*, *109*, 981–989. https://doi.org/10.1007/s10973-011-1785-1

Keysight Technologies. (2016). *Measuring dielectric properties using Keysight's materials measurement solutions*. https://www.keysight.com/zz/en/assets/7018-03896/brochures/5991-2171.pdf

Khalid, M. Y., Al Rashid, A., Arif, Z. U., Ahmed, W., Arshad, H., & Zaidi, A. A. (2021). Natural fiber reinforced composites: Sustainable materials for emerging applications. *Results in Engineering*, *11*, 100263. https://doi.org/10.1016/j.rineng.2021.100263

Kuan, H. T. N., & Lee, M. C. (2014). Tensile properties of *Pandanus atrocarpus* based composites. *Journal of Applied Science and Process Engineering*, *1*(1), 39–44. https://doi.org/10.33736/jaspe.158.2014

Kuan, H. T. N., Lee, M. C., Khan, A. A., & Sawawi, M. (2017). The low velocity impact properties of pandanus fiber composites. *Materials Science Forum*, *895*, 56–60. https://doi.org/10.4028/www.scientific.net/MSF.895.56

Kwon, Y. J., Park, J. B., Jeon, Y. P., Hong, J. Y., Park, H. S., & Lee, J. U. (2021). A review of polymer composites based on carbon fillers for thermal management applications: Design, preparation, and properties. *Polymers*, *13*(8), 1–15. https://doi.org/10.3390/polym13081312

Md Salim, R., Asik, J., & Sarjadi, M. S. (2021). Chemical functional groups of extractives, cellulose and lignin extracted from native *Leucaena leucocephala* bark. *Wood Science and Technology*, *55*, 295–313. https://doi.org/10.1007/s00226-020-01258-2

Meng, F., Wang, G., Du, X., Wang, Z., Xu, S., & Zhang, Y. (2019). Extraction and characterization of cellulose nanofibers and nanocrystals from liquefied banana pseudo-stem residue. *Composites Part B: Engineering*, *160*, 341–347. https://doi.org/10.1016/j.compositesb.2018.08.048

Mittal, G., Rhee, Y. K., & Park, J. S. (2016). The effects of cryomilling CNTs on the thermal and electrical properties of CNT/PMMA composites. *Polymers*, *8*(5), 169. https://doi.org/10.3390/polym8050169

Mohamed, W. Z. W., Baharum, A., Ahmad, I., Abdullah, I., & Zakaria, N. E. (2018a). Effects of fiber size and fiber content on mechanical and physical properties of mengkuang reinforced thermoplastic natural rubber composites. *BioResources*, *13*(2), 2945–2959. https://doi.org/10.15376/biores.13.2.2945-2959

Mohamed, W. Z. W., Baharum, A., Ahmad, I., Abdullah, I., & Zakaria, N. E. (2018b). Mengkuang fiber reinforced thermoplastic natural rubber composites: Influence of rubber content on mechanical properties and morphology. *Malaysian Journal of Analytical Sciences*, *22*(5), 906–913. https://doi.org/10.17576/mjas-2018-2205-19

Mohd Ali, M., Hashim, N., Abd Aziz, S., & Lasekan, O. (2020). Pineapple (*Ananas comosus*): A comprehensive review of nutritional values, volatile compounds, health benefits, and potential food products. *Food Research International*, *137*, 109675. https://doi.org/10.1016/j.foodres.2020.109675

Mohd Zain, N., Aris, M. A., Ja'afar, H., & Awang, R. A. (2024). Characterization of electrical and mechanical properties of *Pandanus atrocarpus* flexible organic-based substrate for microwave communication in ISM applications. *Journal of Materials Science: Materials in Electronics*, *35*, 1694. https://doi.org/10.1007/s10854-024-13453-z

Nabilah Huda A. H., Ramlah, M. T., Aida Isma, M. I., Siti Aishah, G., Nor Munirah, A., & Che Man, H. (2016). Polysulfone membrane nutrients reclamation tests for nutrients reclamation of kenaf retted wastewater. *Jurnal Teknologi*, *78*(1–2), 59–63. https://doi.org/10.11113/jt.v78.7261

Neto, J. S. S., de Queiroz, H. F. M., Aguiar, R. A. A., & Banea, M. D. (2021). A review on the thermal characterisation of natural and hybrid fiber composites. *Polymers*, *13*(24), 4425. https://doi.org/10.3390/polym13244425

Neves, P., dos Santos, V., Tomazello-Filho, M., Cabral, M. R., & Junior, H. S. (2023). Leaf anatomy and fiber types of Curaua (*Ananas comosus* var. *erectifolius*). *Cellulose*, *30*, 3429–3439. https://doi.org/10.1007/s10570-023-05107-w

Owonubi, S. J., Agwuncha, S. C., Malima, N. M., Shombe, G. B., Makhatha, E. M., & Revaprasadu, N. (2021). Non-woody biomass as sources of nanocellulose particles: A review of extraction procedures. *Frontiers in Energy Research*, *9*, 608825. https://doi.org/10.3389/fenrg.2021.608825

PerkinElmer. (2011). *Characterization of single fibers for forensic applications using high speed DSC*. https://perkinelmer.cl/wp-content/uploads/2018/05/Characterization-of-Single-Fibers-for-Forensic-Applications-Using-High-Speed-DSC.pdf

Plakantonaki, S., Kiskira, K., Zacharopoulos, N., Belessi, V., Sfyroera, E., Priniotakis, G., & Athanasekou, C. (2024). Investigating the routes to produce cellulose fibers from agro-waste: An upcycling process. *ChemEngineering*, *8*, 112. https://doi.org/10.3390/chemengineering8060112

Prado, K. S., & Spinacé, M. A. S. (2019). Isolation and characterization of cellulose nanocrystals from pineapple crown waste and their potential uses. *International Journal of Biological Macromolecules*, *122*, 410–416. https://doi.org/10.1016/j.ijbiomac.2018.10.187

Rana, A. K., Frollini, E., & Thakur, V. K. (2021). Cellulose nanocrystals: Pretreatments, preparation strategies, and surface functionalization. *International Journal of Biological Macromolecules*, *182*, 1554–1581. https://doi.org/10.1016/j.ijbiomac.2021.05.119

Rao, J., Lv, Z., Chen, G., & Peng, F. (2023). Hemicellulose: Structure, chemical modification, and application. *Progress in Polymer Science*, *140*, 101675. https://doi.org/10.1016/j.progpolymsci.2023.101675

Reddy, P. L., Deshmukh, K., & Pasha, S. K. K. (2022). Dielectric properties of epoxy/natural fiber. In S. M. Rangappa, J. Parameswaranpillai, S. Siengchin, & S. Thomas (Eds.), *Handbook of epoxy/fiber composites* (pp. 575–609). Springer. https://doi.org/10.1007/978-981-19-3603-6_23

Rowlandson, J. L., Woodman, T. J., Tennison, S. R., Edler, K. J., & Ting, V. P. (2020). Influence of aromatic structure on the thermal behaviour of lignin. *Waste and Biomass Valorization*, *11*, 2863–2876. https://doi.org/10.1007/s12649-018-0537-x

Różańska, W., Romanowska, B., & Rojewski, S. (2023). The quantity and quality of flax and hemp fibers obtained using the osmotic, water-, and dew-retting processes. *Materials*, *16*(23), 7436. https://doi.org/10.3390/ma16237436

Sahari, J., Sapuan, S. M., Zainudin, E. S., & Maleque, M. A. (2013). Mechanical and thermal properties of environmentally friendly composites derived from sugar palm tree. *Materials and Design*, *49*, 285–289. https://doi.org/10.1016/j.matdes.2013.01.048

Salem, K. S., Naithani, V., Jameel, H., Lucia, L., & Pal, L. (2021). Lignocellulosic fibers from renewable resources using green chemistry for a circular economy. *Global Challenges*, *5*(2), 2000065. https://doi.org/10.1002/gch2.202000065

Samuel, B. O., Sumaila, M., & Dan-Asabe, B. (2022). Manufacturing of a natural fiber/glass fiber hybrid reinforced polymer composite ($P_xG_yE^z$) for high flexural strength: An optimization approach. *The International Journal of Advanced Manufacturing Technology*, *119,* 2077–2088. https://doi.org/10.1007/s00170-021-08377-5

Santos, D. I., Martins, C. F., Amaral, R. A., Brito, L., Saraiva, J. A., Vicente, A. A., & Moldão-Martins, M. (2021). Pineapple (*Ananas comosus* L.) by-products valorization: Novel bio ingredients for functional foods. *Molecules*, *26*(11), 3216. https://doi.org/10.3390/molecules26113216

Sari, N. H., Sanjay, M. R., Arpitha, G. R., Pruncu, C. I., & Siengchin, S. (2019). Synthesis and properties of pandanwangi fiber reinforced polyethylene composites: Evaluation of dicumyl peroxide (DCP) effect. *Composites Communications*, *15*, 53–57. https://doi.org/10.1016/j.coco.2019.06.007

Sethupathi, M., Khumalo, M. V, Skosana, S. J., & Muniyasamy, S. (2024). Recent developments of pineapple leaf fiber (PALF) utilization in the polymer composites—A review. *Separations*, 11(8), 245. https://doi.org/10.3390/separations11080245

Shaker, K., Waseem Ullah Khan, R. M., Jabbar, M., Umair, M., Tariq, A., Kashif, M., & Nawab, Y. (2020). Extraction and characterization of novel fibers from *Vernonia elaeagnifolia* as a potential textile fiber. *Industrial Crops and Products*, *152*, 112518. https://doi.org/10.1016/j.indcrop.2020.112518

Sheltami, R. M., Abdullah, I., Ahmad, I., Dufresne, A., & Kargarzadeh, H. (2012). Extraction of cellulose nanocrystals from mengkuang leaves (*Pandanus tectorius*). *Carbohydrate Polymers*, *88*(2), 772–779. https://doi.org/10.1016/j.carbpol.2012.01.062

Shi, Z., Xu, G., Deng, J., Dong, M., Murugadoss, V., Liu, C., Shao, Q., Wu, S., & Guo, Z. (2019). Structural characterization of lignin from *D. sinicus* by FTIR and NMR techniques. *Green Chemistry Letters and Reviews*, *12*(3), 235–243. https://doi.org/10.1080/17518253.2019.1627428

Singh, P. P., Dash, A. K., & Nath, G. (2024). Dielectric characterization analysis of natural fiber based hybrid composite for microwave absorption in X-band frequency. *Applied Physics A*, *130*, 171. https://doi.org/10.1007/s00339-024-07331-y

Tamanna, T. A., Belal, S. A., Shibly, M. A. H., & Khan, A. N. (2021). Characterization of a new natural fiber extracted from Corypha taliera fruit. *Scientific Reports*, *11*, 7622. https://doi.org/10.1038/s41598-021-87128-8

Tang, D., Qu, R., Xiang, H., He, E., Hu, H., Ma, Z., Liu, G., Wei, Y., & Ji, J. (2024). Highly stretchable composite conductive fibers (SCCFs) and their applications. *Polymers*, *16*(19), Article 2710. https://doi.org/10.3390/polym16192710

Todkar, S. S., & Patil, S. A. (2019). Review on mechanical properties evaluation of pineapple leaf fibre (PALF) reinforced polymer composites. *Composites Part B: Engineering*, *174*, 106927. https://doi.org/10.1016/j.compositesb.2019.106927

Vallés, C., Zhang, X., Cao, J., Lin, F., Young, R. J., Lombardo, A., Ferrari, A. C., Burk, L., Mülhaupt, R., & Kinloch, I. A. (2019). Graphene/polyelectrolyte layer-by-layer coatings for electromagnetic interference shielding. *ACS Applied Nano Materials*, *2*(8), 5272–5281. https://doi.org/10.1021/acsanm.9b01126

Wang, Z., Meng, G., Wang, L., Tian, L., Chen, S., Wu, G., Kong, B., & Cheng, Y. (2021). Simultaneously enhanced dielectric properties and through-plane thermal conductivity of epoxy composites with alumina and boron nitride nanosheets. *Scientific Reports*, *11*, 2495. https://doi.org/10.1038/s41598-021-81925-x

Weerappuliarachchi, J. W. M. E. S., Perera, I. C., Gunathilake, S. S., Thennakoon, S. K. S., & Dassanayake, B. S. (2020). Synthesis of cellulose microcrystals (CMC)/nylon 6,10 composite by incorporating CMC isolated from *Pandanus ceylanicus. Carbohydrate Polymers*, *241*, 116227. https://doi.org/10.1016/j.carbpol.2020.116227

Wei, H., Cheng, L., & Shchukin, D. (2020). Effect of porous structure on the microwave absorption capacity of soft magnetic connecting network Ni/Al_2O_3/Ni film. *Materials*, *13*(7), 1764. https://doi.org/10.3390/ma13071764

Xiong, R., Hu, Y., Xia, A., Huang, K., Yan, L., & Chen, Q. (2025). A high-temperature and wide-permittivity range measurement system based on ridge waveguide. *Sensors*, *25*(2), 541. https://doi.org/10.3390/s25020541

Yadav, V., & Singh, S. (2022). A comprehensive review of natural fiber composites: Applications, processing techniques and properties. *Materials Today: Proceedings*, *56*(5), 2537–2542. https://doi.org/10.1016/j.matpr.2021.09.009

Yao, Y., Jin, S., Zou, H., Li, L., Ma, X., Lv, G., Gao, F., Lv, X., & Shu, Q. (2021). Polymer-based lightweight materials for electromagnetic interference shielding: A review. *Journal of Materials Science*, *56*(11), 6549–6580. https://doi.org/10.1007/s10853-020-05635-x

Yew, B. S., Muhamad, M., Mohamed, S. B., & Wee, F. H. (2019). Effect of alkaline treatment on structural characterisation, thermal degradation and water absorption ability of coir fibre polymer composites. *Sains Malaysiana*, *48*(3), 653–659. https://doi.org/10.17576/jsm-2019-4803-19

Yusof, N. A. T., Zainol, N., Aziz, N. H., & Karim, M. S. A. (2023). Effect of fiber morphology and elemental composition of *Ananas comosus* leaf on cellulose content and permittivity. *Current Applied Science and Technology*, *23*(6), 1–12. https://doi.org/10.55003/cast.2023.06.23.002

Zhang, L., Bi, S., & Liu, M. (2018). Lightweight electromagnetic interference shielding materials and their mechanisms. In M.-G. Han (Ed.), *Electromagnetic materials and devices*. IntechOpen. https://doi.org/10.5772/intechopen.82270

Zheng, S., Wang, Y., Wang, X., & Lu, H. (2024). Research progress on high-performance electromagnetic interference shielding materials with well-organized multilayered structures. *Materials Today Physics*, *40*, 101330. https://doi.org/10.1016/j.mtphys.2024.101330

Pertanika J. Sci. & Technol. 33 (5): 2259 - 2277 (2025)

PERTANIKA JOURNALS

SCIENCE & TECHNOLOGY

Journal homepage: http://www.pertanika.upm.edu.my/

Strategic Talent Development: Development of Training Model for Enhancing Competencies for Technology Transfer Professionals

Sofia Adrianna Ridhwan Lim[1,2], Samsilah Roslan[2]*, Gazi Mahabubul Alam[2] and Mohd Faiq Abd Aziz[3]

[1]SIRIM Berhad, Persiaran Dato' Menteri, Box 7035, Section 2, 40700 Shah Alam, Selangor, Malaysia
[2]Department of Foundation of Education, Faculty of Educational Studies, Universiti Putra Malaysia, 43400 Serdang, Selangor, Malaysia
[3]Department of Professional Development and Continuing Education, Faculty of Educational Studies, Universiti Putra Malaysia, 43400 Serdang, Selangor, Malaysia

ABSTRACT

Science, technology, and innovation (STI) often struggle to achieve successful commercial exploitation, resulting in failures during technology commercialization, which highlights the critical gap between research and market implementation. Bridging this gap through effective technology commercialization involves disseminating scientific discoveries to industries capable of commercialization, which is crucial. Technology Transfer Professionals (TTP) serve as crucial intermediaries in the process of technology transfer and commercialization. Despite their importance, there is still a significant gap in understanding the specific skill sets and competencies required to enhance their effectiveness. This study seeks to bridge that gap by identifying the key elements necessary to design a specialized training model uniquely tailored to the needs of TTP, moving beyond traditional, generic employee training approaches. Utilizing the Fuzzy Delphi Method (FDM), the study presents a training model that functions as a strategic talent management tool for both organizations and government agencies. It equips TTP with a focused development program to enhance its credibility, effectiveness, and impact in engaging with diverse stakeholders throughout the innovative ecosystem. By incorporating these findings into professional development initiatives and organizational strategies, the model, which encompasses technical, interpersonal, knowledge-based, and entrepreneurial competencies, aims to enhance technology transfer and commercialization outcomes. Ultimately, this approach strengthens individual TTP capabilities while reinforcing the broader innovation ecosystem at both national and global levels, serving as a catalyst for a more connected, resilient, and innovation-driven global economy.

Keywords: Commercialization, Technology transfer (TT), Technology Transfer Professional (TTP), training model

ARTICLE INFO

Article history:
Received: 06 December 2024
Accepted: 04 June 2025
Published: 28 August 2025

DOI: https://doi.org/10.47836/pjst.33.5.10

E-mail addresses:
sofia@sirim.my (Sofia Adrianna Ridhwan Lim)
samsilah@upm.edu.my (Samsilah Roslan)
gazi.mahabubul@upm.edu.my (Gazi Mahabubul Alam)
mohdfaiq@upm.edu.my (Mohd Faiq Abd Aziz)
* Corresponding author

e-ISSN: 2231-8526

INTRODUCTION

Innovation is the precursor to driving economic development nationwide. Perhaps, all countries, including Malaysia, are confronted with the issues of how to position the innovation reservoir for economic growth and its sustainability (Wang et al., 2024). Research institutes, the entities that actively conduct research and development (R&D) activities, which are led by R&D professionals, including universities, research institutions and private R&D companies, are vigorous agents of producing R&D in STI. Therefore, allocating a substantial budget to R&D expenditure represents an optimistic approach to R&D investment. Research consistently suggests that increased upstream R&D investment correlates with enhanced downstream innovation performance (Jiang et al., 2024), which can significantly contribute to technology commercialization and pave the way for successful research pathways. The R&D landscape in Malaysia has expanded significantly over the past decade, with output in categories such as publications, articles, and reviews increasing by 7.2%. In comparison, other countries have reported lower growth rates: Australia at 4.6%, China at 4.2%, and Singapore at 3.6% (Kasim et. al., 2021). According to the Global Innovation Index (GII), Malaysia ranks 33rd among the 133 world economies in 2024, based on its innovation capabilities, which are measured by 80 indicators of innovation inputs and outputs (Figure 1). While Malaysia performs relatively well in terms of innovation inputs, ranking 28th, it lags in innovation outputs, ranking 41st (World Intellectual Property Organization [WIPO], 2024). This discrepancy suggests that while the country excels at developing R&D, it struggles to effectively translate these innovations into commercial outcomes, highlighting a potential bottleneck in technology transfer and commercialization. This gap in exploiting innovation for downstream applications may be contributing to slower and less efficient technology transfer processes.

Innovation can be defined as a process that integrates science, technology, economics, and management to achieve novelty. It spans from the initial emergence of an idea to its eventual commercialization through production, exchange, and consumption. Other scholars describe innovation as the generation of new ideas and their implementation in the form of new products, processes, or services, contributing to dynamic economic growth, increased employment, and the generation of profit for innovative enterprises (Kogabayev & Maziliauskas, 2017).

Dissemination of innovation from the research institutions to potential and capable industries is defined as technology transfer. The advantages of turning the scientific discoveries into commercial potential which referred as innovation, includes (i) leveraging R&D outcome and intellectual assets, (ii) enhance the accessibility of R&D outcome to broad range of industries through technology adoption, (iii) align with government initiative on technology commercialization of local innovation, (iv) accelerate the productivity outcome via utilization of innovation including digital transformation, (v) intensify

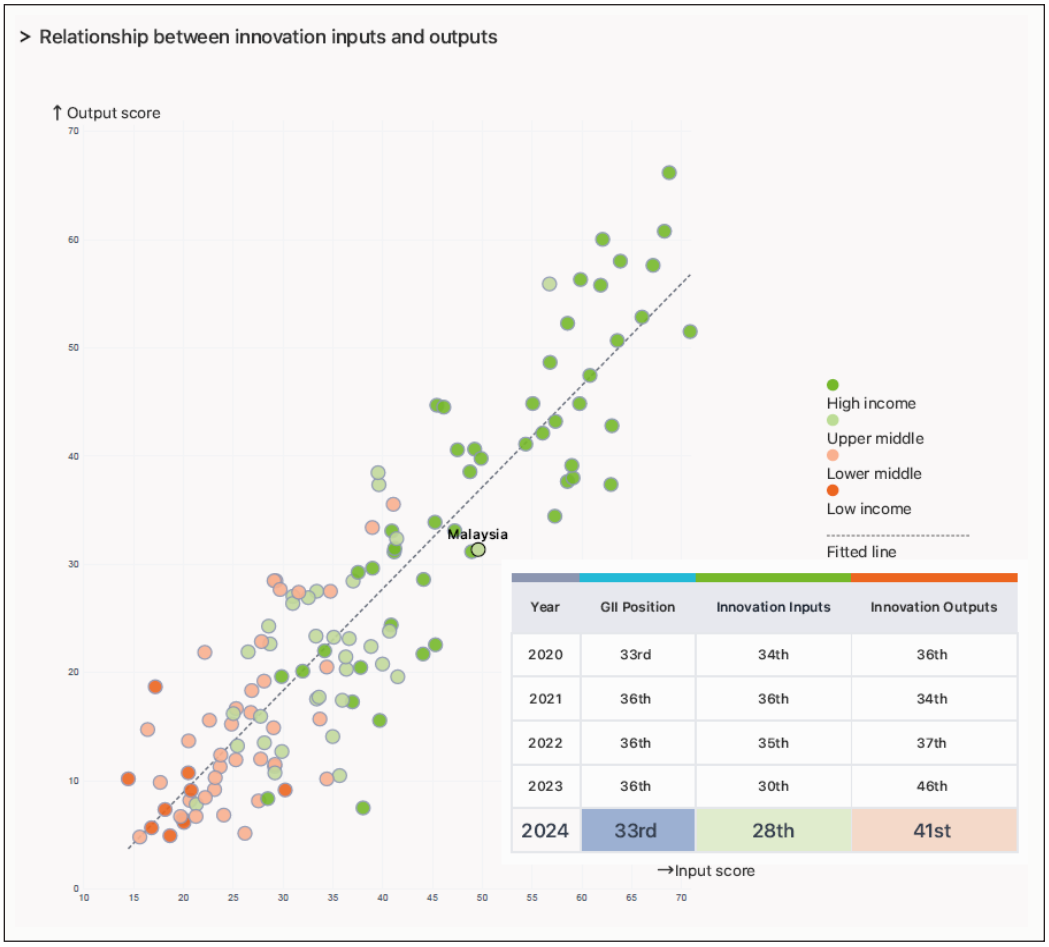

Figure 1. Global Innovation Index 2024 (*Source:* WIPO, 2024)

industrial competition among local and international, and (vi) accelerate economic growth and social development of the communities.

For research institutions to play an active role in creating innovation, TTP is required to effectively perform its role as a professional mediator between research institutions and industries. TTP, also known as a technology transfer officer, is an employee who works in the field of technology transfer and commercialization to transform the research output into commercial value to enhance the innovation-driven and economic growth of the country. Despite numerous studies exploring the issues and challenges associated with technology transfer, the question of which skillsets and competencies are necessary for TTP remains unanswered (Boguszewicz-Kreft et al., 2021; Mom et al., 2012; Soares & Torkomian, 2021; Takata et al., 2022). This issue has been recognized as part of broader challenges since the early 2000s, where concerns over the competency of staff include insufficient

training and capability (Jensen & Thursby, 2001; Manap et al., 2017; Mom et. al., 2012; Swamidass & Vulasa, 2009). TTP is required to employ a diverse skill set and competencies to achieve goals set in technology transfer and commercialization. This includes setting goals amidst high uncertainty, translating scientific discoveries into business-viable, and initiating stakeholder engagement. Cunningham and O'Reilly (2018) have emphasized the diverse and varied nature of TTP capabilities, highlighting the importance of identifying the specific skill sets and competencies that contribute to effective technology transfer.

Our study aims to address this gap by investigating the essential components required to be integrated into the training model, which can enhance the impact and efficiency of TTP. Through expert views and consensus, the critical components of competencies were identified for training. Our goal is to improve the effectiveness of TTP by developing a comprehensive training model that includes a series of important components. This strategic approach aims to ensure the delivery of purposeful, successful, and impactful training programs for TTP through a systematic methodology.

THEORETICAL FRAMEWORK

This study focuses on talent management and human resource development to form a pathway to the key variables examined, namely, the Talent DNA Model and McLagan's Model of Human Resource Development (HRD). In the Talent DNA model, Shravanthi and Sumanth (2008) proposed a talent management framework designed to create a strategic roadmap for achieving organizational objectives. The model is built around the concept of DNA, which comprises three key components: identifying critical roles, defining the competencies required for those roles, and recognizing the necessary talent. This cycle is supported by the development of a comprehensive competency database, which provides a structured mechanism for making informed and accurate talent-related decisions (Omotunde & Alegbeleye, 2021). The relevance of the Talent DNA model to this study lies in its emphasis on identifying and integrating role-specific skills and capabilities, thereby guiding the design and development of competencies required for the TTP. These components are critical for shaping an effective training model. To ensure a comprehensive approach, the study also incorporates McLagan's HRD Model, which categorizes competencies into four essential domains: technical, business, intellectual, and interpersonal. These competency areas form a well-rounded foundation for HRD professionals and support both individual and organizational growth. The integration of McLagan's model provides a structured lens for categorizing and defining the competencies needed within the proposed framework. Accordingly, this study recognizes the Talent DNA model and McLagan's HRD model as the key theoretical underpinnings of the study, with both models serving as foundational theories while the Sequential Iterative Model (SIM) serves as supporting model. The theoretical framework developed based on these models is presented in Figure 2.

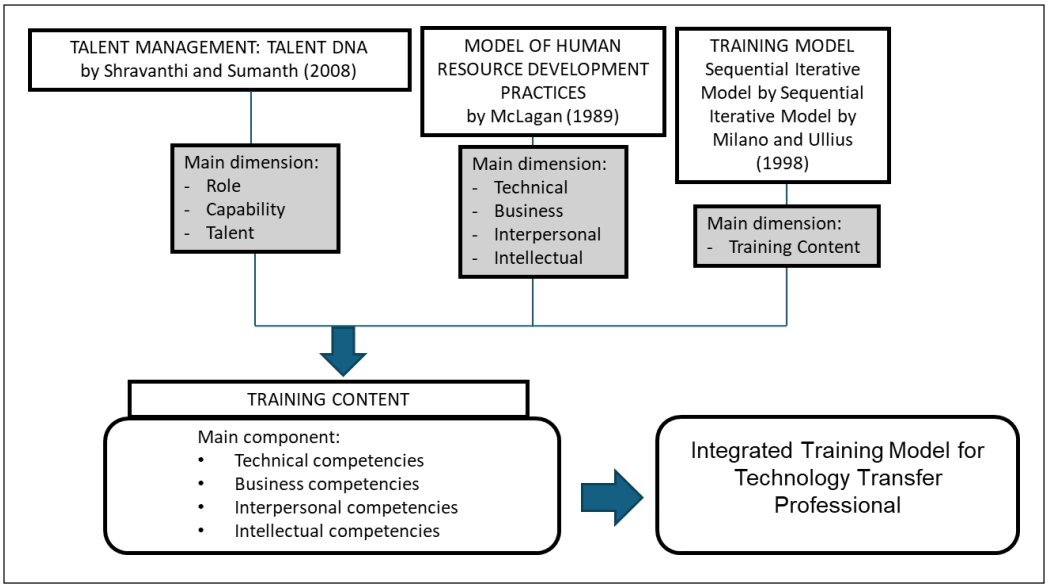

Figure 2. Theoretical framework

METHODOLOGY

This study utilized a quantitative method, specifically FDM, to obtain consensus from experts on the components necessary for a training model for TTP. The FDM was chosen for its ability to systematically gather expert opinions and achieve consensus. Experts were selected through purposive sampling to ensure appropriateness and adherence to criteria recommended by scholars for maximizing result accuracy (Jamil & Noh, 2020; Mohd @ Ariffin & Md Rami, 2023; Siraj et al., 2021). Criteria included a minimum of a bachelor's degree, at least five years of experience in technology transfer and commercialization, and successful commercialization of at least five technologies to companies. According to Berliner (2004), individuals with more than five years of experience are considered skilled in their field, while Gambatese (2008) emphasized the importance of high academic qualifications for experts. The FDM typically requires a minimum of 10 experts to ensure high uniformity in opinions (Adler & Ziglio, 1996; Jones & Twiss, 1978). Therefore, this study involved 14 experts obtaining a consensus on the important components to integrate into the TTP training model.

FDM incorporates principles from fuzzy set theory, representing an evolution from the traditional Delphi method and offering efficiencies in time, cost, and procedural handling through survey questionnaires (Yusoff et al., 2021). It comprises two main components: the triangular fuzzy number and the defuzzification process. To represent expert opinions, a triangular fuzzy number represented as m_1, m_2, m_3 was employed. This format creates a fuzzy scale similar to the Likert scale, enabling the conversion of linguistic variables

into fuzzy numerical values. The scale uses odd-numbered levels to indicate degrees of agreement, where higher fuzzy values reflect greater precision and accuracy in the data (Jamil et al., 2024). Figure 3 illustrates the summary of methodology for this study.

The 7-point Likert scale strengthens methodological accuracy as higher Likert scales are reported to enhance precision and reliability of the data (Mohd et al., 2018). Table 1 illustrates the 7-point Likert scale used in this study to represent the fuzzy values.

The questionnaire development in this study draws upon insights from a literature review and a series of interviews with experts conducted in earlier phases (Jamil et al., 2014; Mohd @ Ariffi & Md Rami, 2023). According to Skulmoski et al. (2007), the development of research instruments such as questionnaires should integrate findings from literature reviews, pilot studies, and expert input, tailored specifically to the research area (Okoli & Pawlowski, 2004; Yusof et al., 2021). The questionnaire then underwent validation procedures, including assessments of language and content validity, with input from field experts. This study encompasses four competencies and their respective items (Table 2), identified as essential for TTP to effectively facilitate technology transfer and commercialization.

Table 1
The 7-point Likert scale

Scale	Linguistic variable	Fuzzy scale
1	Extremely disagree	(0.9,1.0,1.0)
2	Strongly disagree	(0.7,0.9,1.0)
3	Disagree	(0.5,0.7,0.9)
4	Partially agree	(0.3,0.5,0.7)
5	Agree	(0.1,0.3,0.5)
6	Strongly agree	(0.0,0.1,0.3)
7	Extremely agree	(0.0,0.0,0.1)

Source: Jamil and Nooh (2020)

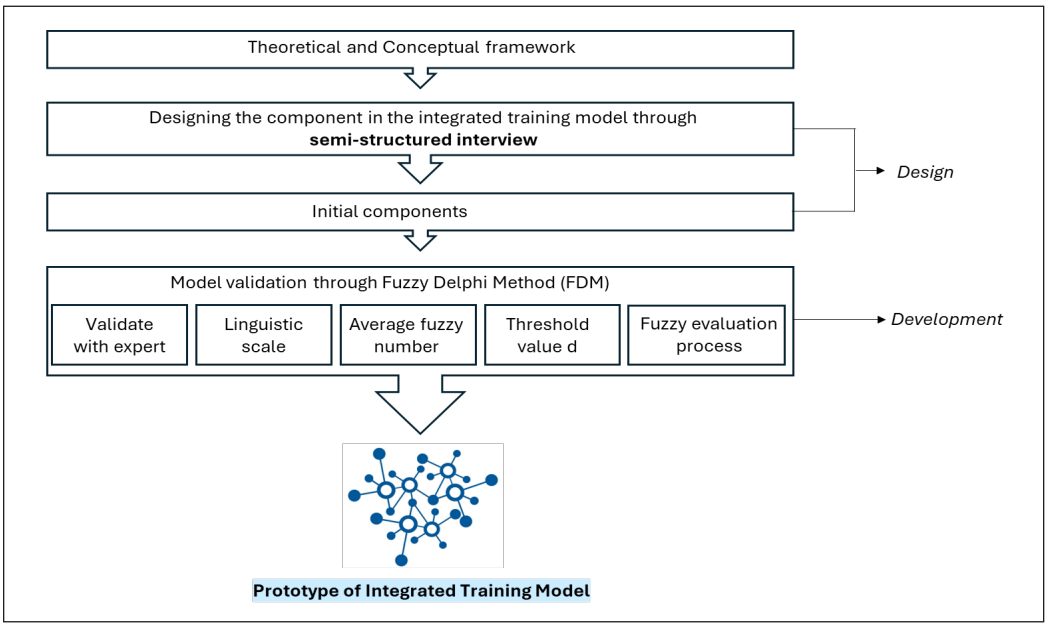

Figure 3. Summary of methodology

Table 2
Components in the training model for Technology Transfer Professionals

No.	Component/ Element	Items	Literature review
1	Technical competency	A1. Science, technology, and innovation (STI) A2. Technology assessment and profiling A3. Technology valuation A4. Intellectual property (IP) management and IP strategy A5. Regulatory requirements A6. Conduct, analyze, present, and evaluate market research whenever necessary A7. Due diligence and company profiling	Fasi (2022); Khademi et. al. (2014); Mom et. al. (2012); Sachani (2020); Soares and Torkomian (2021); Takata et. al. (2022)
2	Interpersonal competency	C1. Communication skills C2. Negotiation skills C3. Networking and sustaining relationships C4. Project management skills C5. Problem-solving skills C6. Teamwork skills C7. Generic interpersonal skills	
3	Knowledge competency	D1. Commercialization knowledge D2. Legal literacy knowledge D3. Marketing strategy knowledge D4. Finance knowledge D5. Investment knowledge which covers investment-worthy to prove the technology can be incorporated into a product or service, investment outcomes, and investment risk D6. Industry knowledge includes: i. Identify and exploit new opportunities ii. Knowledge of industrial competition iii. Compliance with regulation iv. Knowledge of commercial security	
4	Entrepreneurship competency	E1. Respond and manage several uncertain situations E2. Development of a market-viable proof of concept, identify and convince promising stakeholders, and effectively execute the transfer to industries. E3. Envision the commercial value of innovations and technologies and convince potential stakeholders.	

Note. The authors' comprehension derived from prior interviews with subject matter experts

DATA ANALYSIS

The data analysis of the FDM is conducted systematically using Microsoft Excel software, as advocated by leading scholars in the field (Jamil et al., 2014; Jamil & Noh, 2020; Ramlie et al., 2014; Yusoff et al., 2021). The analysis adheres to established FDM guidelines, which specify that the threshold value (d) should not exceed 0.2 (Chen, 2000; Cheng & Lin, 2002). Moreover, it ensures that the percentage of expert agreements meets or exceeds 75% (Chu & Hwang, 2008) and that the fuzzy score (A_{max}) equals or exceeds 0.5.

In the ranking process, components are prioritized based on their fuzzy score values, with higher scores indicating greater consensus among experts. A detailed explanation of these conditions is as follows:

(a) Condition 1: Triangular Fuzzy Numbers – Threshold value (d) is ≤ 0.2

Expert consensus is achieved when the resultant value is 0.2 or less. Components and items with values of 0.2 or lower are considered accepted, indicating consensus among experts. This determination is based on the following formula:

$$d(\vec{m},\vec{n}) = \sqrt{\frac{1}{3}[(m_1 - n_1)^2 + (m_2 - n_2)^2 + (m_3 - m_3)^2]}$$

(b) Condition 2: Expert agreement percentage is ≥ 75%

This criterion follows the principles of the traditional Delphi method, where the percentage value is determined based on the number of items with a threshold value (d) not exceeding 0.2. Each item meeting or falling below this threshold (d ≤ 0.2) is accepted and converted to a percentage value based on the traditional Delphi method (Mohd @ Ariffin & Md Rami, 2023).

(c) Condition 3: Defuzzification value – Fuzzy score (A) value is ≥ 0.5

This condition determines the fuzzy score value based on the α-cut, which is set at 0.5. A fuzzy score (A) value below 0.5 indicates that the item is rejected based on the consensus of the experts. Conversely, a value of 0.5 or above indicates acceptance of the item. Further steps to determine the position or ranking of items involve prioritizing items based on their fuzzy score values, with the highest A value assigned the first position or rank. The determination of the value A score is based on the following formula:

$$A = \frac{1}{3}(m_1 + m_2 + m_3)$$

RESULTS

Demographic Information

Experts' demographic information is shown in Table 3. The majority of the experts possessed a Ph.D., obtained years of experience working in technology transfer and commercialization, and 64% are certified Registered Technology Transfer Professional (RTTP).

Technical Competency

Based on the findings presented in Table 4, items A1, A2, A4, and A7 have garnered consensus among experts. These items were evaluated against the three conditions stipulated in the FDM:

Table 3
Experts' demographic information

Expert	Years of experience in technology transfer and commercialization (Years)	Professional certification	Academic qualification
FDM1	30	-	Doctoral degree
FDM2	16	RTTP	Doctoral degree
FDM3	6	RTTP	Doctoral degree
FDM4	10	RTTP	Doctoral degree
FDM5	45	RTTP	Master's degree
FDM6	7	RTTP	Doctoral degree
FDM7	15	RTTP	Doctoral degree
FDM8	10	-	Doctoral degree
FDM9	17	RTTP	Master's degree
FDM10	7	RTTP	Doctoral degree
FDM11	7	-	Doctoral degree
FDM12	14	-	Doctoral degree
FDM13	21	-	Doctoral degree
FDM14	18	RTTP	Master's degree

Note. FDM = Fuzzy Delphi Method; RTTP = Registered Technology Transfer Professional

Table 4
Findings of the expert consensus on technical

Technical competency	Value d of item	Value d of element	Percentage of expert agreement on the item (%)	Fuzzy score (A_{max})	Position/ Ranking	Expert consensus
A1	0.153	0.138	79	0.860	4	Accept
A2	0.111		86	0.914	1	Accept
A3	0.192		57	0.817	-	Reject
A4	0.111		86	0.914	1	Accept
A5	0.162		64	0.850	-	Reject
A6	0.147		64	0.836	-	Reject
A7	0.089		86	0.871	3	Accept

a threshold value ≤ 0.2, expert agreement exceeding 75%, and a defuzzification value (α-cut) of 0.5 or higher. Conversely, other items were rejected due to their failure to meet the required threshold of expert agreement exceeding 75%. The accepted items were subsequently ranked in order of priority, as depicted in Table 5, highlighting their significance for integration into the training model for TTP.

Table 5
Ranking of items for technical

Ranking	Items	Item code
1	Technology assessment and profiling	A2
2	IP management and IP strategy	A4
3	Due diligence and company profiling	A7
4	STI	A1

Note. IP = Intellectual property; STI = Science, technology, and innovation

Interpersonal Competency

Based on the findings presented in Table 6, all items have garnered consensus among experts. These items were evaluated against the three conditions stipulated in the FDM: a threshold value ≤ 0.2, expert agreement exceeding 75%, and a defuzzification value (α-cut) of 0.5 or higher. The items were subsequently ranked in order of priority, as depicted in Table 7, highlighting their significance for integration into the training model for TTP.

Table 6
Findings of expert consensus on interpersonal

Interpersonal competency	Value d of item	Value d of element	Percentage of expert agreement on the item (%)	Fuzzy score (A_{max})	Position/ Ranking	Expert consensus
C1	0.078	0.101	93	0.933	1	Accept
C2	0.087		93	0.926	4	Accept
C3	0.087		93	0.926	3	Accept
C4	0.138		86	0.879	7	Accept
C5	0.078		93	0.933	1	Accept
C6	0.120		93	0.905	5	Accept
C7	0.120		93	0.905	5	Accept

Knowledge Competency

Based on the findings presented in Table 8, items D1, D3, D4, and D6 have garnered consensus among experts. These items were evaluated against the three conditions stipulated in the FDM: a threshold value ≤ 0.2, expert agreement exceeding 75%, and a defuzzification value (α-cut) of 0.5 or higher. Conversely, other items were rejected due to their failure to meet the required threshold of expert agreement exceeding 75%. The accepted items were subsequently ranked in order of priority, as depicted in Table 9, highlighting their significance for integration into the training model for TTP.

Table 7
Ranking of items for interpersonal

Ranking	Items	Item code
1	Communication skills	C1
2	Problem-solving skills	C5
3	Networking and sustaining the relationship	C3
4	Negotiation skills	C4
5	Teamworking skills	C6
6	Generic interpersonal skills	C7
7	Project management skills	C4

Entrepreneurship Competency

Based on the findings presented in Table 10, all items have garnered consensus among experts. These items were evaluated against the three conditions stipulated in the FDM:

a threshold value ≤ 0.2, expert agreement exceeding 75%, and a defuzzification value (α-cut) of 0.5 or higher. The items were subsequently ranked in order of priority, as depicted in Table 11, highlighting their significance for integration into the training model for TTP.

Table 8
Findings of expert consensus on knowledge

Knowledge competency	Value d of item	Value d of element	Percentage of expert agreement on the item (%)	Fuzzy score (A_{max})	Position/ Ranking	Expert consensus
D1	0.062	0.134	100	0.938	1	Accept
D2	0.147		64	0.836		Reject
D3	0.113		86	0.893	3	Accept
D4	0.166		79	0.795	4	Accept
D5	0.199		64	0.788		Reject
D6	0.115		86	0.900	2	Accept

Table 9
Ranking of items for knowledge

Ranking	Items	Item code
1	Commercialization knowledge	D1
2	Industry knowledge	D6
3	Marketing strategy knowledge	D3
4	Finance knowledge	D4

Table 10
Findings of expert consensus on entrepreneurship

Entrepreneurship competency	Value d of item	Value d of element	Percentage of expert agreement on the item (%)	Fuzzy score (A_{max})	Position/ Ranking	Expert consensus
E1	0.153	0.143	79	0.860	3	Accept
E2	0.138		86	0.879	1	Accept
E3	0.138		86	0.879	1	Accept

Table 11
Ranking of items for entrepreneurship

Ranking	Items	Item code
1	Development of a market-viable proof of concept, identify and convince promising stakeholders, and effectively execute the transfer to industries.	E2
2	Envision the commercial value of innovations and technologies and convince potential stakeholders.	E3
3	Respond and manage several uncertain situations in bridging commercialization gaps.	E1

DISCUSSION

Through the analysis of FDM, the researcher has identified several elements and items that should be integrated into the training model for TTP. This study represents a novel contribution by offering a comprehensive model specifically focused on TTP as a human capital system designed to optimize the utilization of individual talents for achieving maximum returns for their organization (Kibui et al., 2014). Furthermore, through a holistic perspective, enhancing technology transfer and commercialization within organizations contributes to governmental goals, thereby fostering economic growth and advancing a globally competitive, innovation-driven economy. The research output, namely the training model for TTP, serves as a pivotal component of a talent management tool designed to systematically attract, identify requisite competencies, develop, engage through appropriate training programs, retain, and strategically deploy TTP that transmit substantial value to the organization. This value may manifest in their high potential for future roles or in their critical contributions to business operations (Brantnell & Baraldi, 2022; Chau et al., 2017).

The training model developed in this study differs significantly from the professional certification known as the RTTP, which is organized by the Alliance of Technology Transfer Professionals (ATTP). According to ATTP (2025), RTTP is an internationally recognized standard that certifies the professional competence and experience of technology transfer practitioners working in universities, industry, and government laboratories, based on a proven track record of real-world achievements. It requires individuals to demonstrate mastery of domain-specific knowledge and a specific achievement in technology transfer and commercialization. The RTTP framework leverages a specialized model that has been integrated with existing national systems across several countries. It emphasizes core competencies essential for RTTP designation, including entrepreneurial leadership, governance, and project management, as well as strategic and business acumen.

In contrast, the training model proposed in this study is designed specifically for end users such as novice or early-career TTP. It emphasizes applied learning, proactive role development, and is aligned with the latest advancements and best practices in the field of technology commercialization. Unlike RTTP, which necessitates prior experience and accomplishments, this model addresses the foundational capacity-building needs of beginner TTPs, who are not yet eligible for RTTP certification. By providing structured, competency-based training early in their careers, this model plays a crucial role in bridging the gap between entry-level practice and professional recognition. It serves as an essential stepping stone, equipping novice TTPs with the knowledge, skills, and confidence needed to advance toward future RTTP certification and excel in the field of technology transfer and commercialization.

Based on the findings, the components encompassing technical, interpersonal, knowledge, and entrepreneurial competencies are identified as critical prerequisites for

effectively equipping TTP to perform tasks in technology transfer and commercialization activities in the Malaysian framework. Each component includes specific items acknowledged by experts as crucial for training TTP. Therefore, these components have been integrated into the training model as a research output of the overall study to guide the development of future training programs. Competency refers to the capability of TTP to effectively address complex demands within a specific context by mobilizing knowledge, skills, attitudes, and values. It comprises behavioral patterns necessary for TTP to perform tasks and functions effectively. Within the competencies, it pertains to the functional knowledge, skills, and attributes required for technology transfer and commercialization activities (Brantnell & Baraldi, 2022).

According to the findings, technical competency requires TTP to be competent in (i) STI, (ii) technology assessment and profiling to ensure its commercial potential, (iii) IP management and IP strategy, and (iv) due diligence and company profiling. These items are crucial to be part of the training model as TTP often encounters a diversity of technological developments created by researchers, and it may lead to distinct patterns of IP protection and managing the overall commercialization pathway (Soares & Torkomian, 2021). In today's rapidly advancing technological landscape, technological revolution boosts numerous advancements observed in health, agriculture, energy, and global development. Hence, TTP must adeptly navigate these challenges. According to Comacchio et al. (2012), TTPs' technical expertise allows them to effectively translate scientific language and transform intellectual knowledge into practical applications. This capability not only increases the potential for commercial exploitation and reduces information asymmetry during negotiations with firms, but also has significant international relevance. By bridging the gap between research and industry across different innovation systems, this function of TTP can facilitate cross-border technology commercialization, support international R&D collaborations, and contribute to the global diffusion of innovation, thereby accelerating technological adoption globally. This activity involves several pathways besides the linear process, including invention disclosure, technology assessment, patenting, and licensing to potential and capable firms or industry (Hayter et al., 2020).

In interpersonal competency, the finding reveals that all items are important to integrate in the training model for TTP, this includes (i) communication skill, (ii) problem-solving skill, (iii) networking and sustaining the relationship, (iv) negotiation skill, (v) team working skill, (vi) generic interpersonal skill, and (vii) project management skill. This study defines interpersonal skills as TTP's special skills and abilities for effective interaction. These skill sets are crucial for TTP to acquire and master, as they serve as professional mediators between institutions and industry (Mom et al., 2012; Sachani, 2020; Takata et al., 2022). TTP needs to translate scientific language into business language effectively. As technology advances, every stakeholder within the ecosystem, whether technology provider,

technology recipient, investor, policymaker, or consumer, has their distinct mission and vision. Therefore, the roles and responsibilities of TTP today are increasingly complex due to the diverse interests within the ecosystem, particularly in concluding commercialization agreements. Interpersonal competency is critically important for TTPs operating in a global context, as it enables them to navigate cross-cultural environments effectively and build strong, collaborative relationships across international boundaries.

For knowledge competency, several items are important to be integrated in the training model, and they include (i) commercialization knowledge, (ii) industry knowledge, (iii) marketing strategy knowledge, and (iv) finance knowledge. In this study, knowledge is defined as the intellectual aspects of TTP, which relate to knowledge and skills for thinking and processing information related to technology transfer and commercialization. This component is crucial for TTP to navigate the entirety of the technology transfer and commercialization process—from its inception to its conclusion. By effectively managing stages such as technology and market positioning, identifying suitable licensees or partners for technology transfer and commercialization, and delineating potential commercialization pathways, TTP can significantly enhance the likelihood of achieving successful outcomes. This minimizes the risk of misjudgment at any stage of the process and ensures more effective technology transfer and commercialization, not only at the national level but also within the global innovation landscape. The knowledge and awareness related to these activities are deemed crucial for the business environment of technology transfer and commercialization strategic decisions (Mom et al., 2012). With this knowledge, it would be straightforward for TTP to identify opportunities at various stages, given the evolving nature of technology-related knowledge. TTP may encounter risks associated with a lack of knowledge and awareness in technology transfer and commercialization, as noted by scholars. Research has shown that this deficiency has led universities in the United Kingdom to misjudge their approach to spin-offs in technology transfer engagements (Lambert, 2003; Mom et al., 2012).

Entrepreneurship competency has been remarked as the evolving component that TTP should have today. It comprises the elements of (i) developing a market-viable proof of concept, identifying and convincing promising stakeholders, and effectively executing the transfer to industries, (ii) envisioning the commercial value of innovations and technologies, and convincing potential stakeholders, and (iii) responding to and managing several uncertain situations. In this study, entrepreneurship is defined as the behavioral patterns of TTP that progressively look at the opportunities in technology transfer and commercialization. Recent studies have shown that entrepreneurial behavior is influenced by the emerging roles of TTP and the function of research institutions, including universities (Fasi, 2022; Takata et. al., 2022). In the Malaysian framework, the government emphasizes that scientific inventions should benefit the community, thereby contributing to economic growth. With the commercialization gap widening, TTPs play a crucial role in

facilitating researchers in technological development. This includes persuading businesses of the commercial viability of innovations and ensuring that inventions can penetrate the market and meet manufacturability standards. This process often involves consultations and collaboration with research engineers to scale up the technology effectively. The aspect of commercialization strategies is important for TTP as it observes technology risk management, how to transform inventions into marketable products, and how to identify the best commercialization pathway for specific technologies or innovations. At the global level, entrepreneurial-minded TTPs play a pivotal role in accelerating international technology transfer, enabling cross-border innovation, and driving the development of competitive, innovation-led economies worldwide. This study defines entrepreneurship competency as one of the components for sustainable business practices that lead to shaping the future of technology innovation. Today, the role of TTP has evolved to encompass not only facilitating technological development but also validating innovations for practicality and commercial viability (Sachani, 2020; Takata et al., 2022) to ensure the technology succeeds in penetrating the market. This dual responsibility aims to mitigate the risk of business sustainability failures for firms.

In response to the evolving role of TTP today, research underscores the importance of developing a training model focused on professional work in technology transfer and commercialization. This initiative aligns with the increasingly complex and diverse responsibilities of TTP today. As professional mediators, the organization and government must support TTP through offering tailored training programs that enhance their credibility and reputation in professional engagements with stakeholders, while bolstering their skills, competencies, and intelligence. Given the importance of the training program's content and modules, there is a distinct need to create a specialized training model tailored for TTP, as identified by Giday and Elantheraiyan (2023). This model should cater not only to novice TTP but also to experienced professionals who seek to enhance their competencies in technology transfer and commercialization.

CONCLUSION

This study contributes a novel perspective to the research on training model development for TTP by presenting a structured model as a key research output. It identifies and integrates four essential competency components into the model: (i) technical competency, (ii) interpersonal competency, (iii) knowledge competency, and (iv) entrepreneurship competency. Each component includes specific items that will serve as essential elements—or module content of training programs—requiring training for TTP to enhance their competency and skill set in executing their roles effectively. Its focused approach ensures the training is highly relevant, addresses specific needs, and bridges practical gaps, thereby enhancing the training's effectiveness and meeting the unique requirements of TTP.

From a theoretical perspective, this model represents a significant advancement in talent development, HRD, and the broader field of technology transfer and commercialization. It is purposefully designed to address the evolving roles and responsibilities of TTP, integrating core competencies that are essential in today's innovation landscape.

This training model contributes to talent management in both HRD and technology transfer and commercialization, practically and theoretically. It serves as a reference tool for strategizing key components essential for effective succession management through guiding the organization in forecasting the TTP needs. Moreover, this study identifies critical components to integrate into the training model, aimed at equipping TTP with essential modules to engage in technology transfer and commercialization activities proficiently. It is a recognized model among Malaysian organizations with Technology Transfer Offices (TTOs), demonstrating its applicability across universities, research institutions, agencies, and ministries. As institutions globally confront similar challenges in bridging the gap between research and market, this model provides a scalable and adaptable framework for enhancing the talent management of TTP ecosystems, which could extend its impact beyond Malaysia.

RECOMMENDATIONS

For future research, it is recommended to develop a dedicated training module grounded in the training model proposed in this study. This approach will support the creation of high-quality content, ensure consistency across the training program, and effectively achieve intended outcomes aligned with best practices. The training program also has the potential to empirically measure performance outcomes for TTP, including the number of technology licensing activities, commercialization success rates, startup creation, and enhanced industry-academic collaborations. The model is further strengthened by a comprehensive evaluation framework that incorporates pre- and post-training assessments, participant feedback, and longitudinal tracking of key performance indicators. These metrics not only reflect the development of individual competencies but also validate the model's broader contribution to fostering a more dynamic, resilient, and innovation-driven economy.

ACKNOWLEDGEMENTS

We extend our heartfelt appreciation to the technology transfer and commercialization experts from diverse ministries, universities, and agencies, both local and international, for their invaluable contributions to this study. Their generous allocation of time and effort amidst busy schedules underscores their dedication and support, significantly enhancing the quality and depth of our research. Their active involvement was pivotal in offering insights and perspectives essential for advancing our understanding of technology transfer and commercialization processes. We sincerely acknowledge their cooperation and unwavering commitment throughout the study.

REFERENCES

Adler, M., & Ziglio, E. (Eds.) (1996). *Gazing into the Oracle: The Delphi method and its application to social policy and public health*. Jessica Kingsley Publisher.

Alliance of Technology Transfer Professionals. (2025). *ATTP – Global standards in knowledge and technology transfer*. https://attp.global/

Berliner, D. C. (2004). Describing the behavior and documenting the accomplishments of expert teachers. *Bulletin of Science, Technology and Society*, *24*(3), 200-212. https://doi.org/10.1177/0270467604265535

Boguszewicz-Kreft, M., Arvanitis, A., Karatzas, K., Antonelli, G., & Simonetti, B. (2021). Technology transfer steps towards the commercialization of research results for universities. *WSB Journal of Business and Finance*, *55*(1), 26-39. https://doi.org/10.2478/wsbjbf-2021-0003

Brantnell, A., & Baraldi, E. (2022). Understanding the roles and involvement of technology transfer offices in the commercialization of university research. *Technovation*, *115*, 102525. https://doi.org/10.1016/j.technovation.2022.102525

Chau, V. S., Gilman, M., & Serbanica, C. (2017). Aligning university–industry interactions: The role of boundary spanning in intellectual capital transfer. *Technological Forecasting and Social Change*, *123*, 199–209. https://doi.org/10.1016/j.techfore.2016.03.013

Chen, C.-T. (2000). Extensions of the TOPSIS for group decision-making under fuzzy environment. *Fuzzy Sets and Systems*, *114*(1), 1–9. https://doi.org/10.1016/S0165-0114(97)00377-1

Cheng, C.-H., & Lin, Y. (2002). Evaluating the best main battle tank using fuzzy decision theory with linguistic criteria evaluation. *European Journal of Operational Research*, *142*(1), 174-186. https://doi.org/10.1016/S0377-2217(01)00280-6

Chu, H.-C., & Hwang, G.-J. (2008). A Delphi-based approach to developing expert systems with the cooperation of multiple experts. *Expert Systems with Applications*, *34*(4), 2826–2840. https://doi.org/10.1016/j.eswa.2007.05.034

Comacchio, A., Bonesso, S., & Pizzi, C. (2012). Boundary spanning between industry and university: The role of technology transfer centres. *The Journal of Technology Transfer*, *37*, 943-966. https://doi.org/10.1007/s10961-011-9227-6

Cunningham, J. A., & O'Reilly, P. (2018). Macro, meso and micro perspectives of technology transfer. *The Journal of Technology Transfer*, *43*, 545-557. https://doi.org/10.1007/s10961-018-9658-4

Fasi, M. A. (2022). An overview on patenting trends and technology commercialization practices in the university Technology Transfer Offices in USA and China. *World Patent Information*, *68*, 102097. https://doi.org/10.1016/j.wpi.2022.102097

Giday, D. G., & Elantheraiyan, P. (2023). A study on the effect of training on employee performance in the case of Mekelle City, Tigray, Ethiopia. *Social Sciences and Humanities Open*, *8*(1), 100567. https://doi.org/10.1016/j.ssaho.2023.100567

Hayter, C. S., Rasmussen, E., & Rooksby, J. H. (2020). Beyond formal university technology transfer: Innovative pathways for knowledge exchange. *The Journal of Technology Transfer*, *45*, 1-8. https://doi.org/10.1007/s10961-018-9677-1

Jamil, M. R. M., Idris, N., Aris, N. M., Razalli, A. R., Zalli, M. M. M., Othman, M. S., Hosshan, H., & Noh, N. M. (2024). Crafting a blueprint for enhancing emotional well-being in special education post-pandemic: A fuzzy Delphi approach. *International Journal of Advanced and Applied Sciences*, *11*(11), 99-111. https://doi.org/10.21833/ijaas.2024.11.011

Jamil, M. R. M., & Noh, N. R. M. (2020). *Kepelbagaian metodologi dalam penyelidikan reka bentuk dan pembangunan* [Diversity of methodologies in design and development research]. Qaisar Prestige Resources.

Jamil, M. R. M., Siraj, S., Hussin, Z., Noh, N. M., & Sapar, A. A. (2014). *Pengenalan asas kaedah Fuzzy Delphi dalam penyelidikan rekabentuk dan pembangunan* [Basic introduction to the Fuzzy Delphi method in design and development research]. Minda Intelek.

Jensen, R., & Thursby, M. (2001). Proofs and prototypes for sale: The licensing of university inventions. *American Economic Revi*ew, *91*(1), 240–259. https://doi.org/10.1257/aer.91.1.240

Jiang, C., Li, S., & Shen, Q. (2024). Science and technology evaluation reform and universities' innovation performance. *Technology in Society*, *78*, 102614. https://doi.org/10.1016/j.techsoc.2024.102614

Jones, H., & Twiss, B. C. (1978). *Forecasting technology for planning decisions*. Macmillan Press.

Kasim, A. M., Chang, L. W., Norpi, N. M., Kasim, N. H. A., & Hashim, A. (2021). Enhancing research mechanisms and institutional processes in Malaysia: A case study of Universiti Malaya (UM). *Journal of Research Management and Governance*, *4*(1), 10-23. https://doi.org/10.22452/jrmg.vol4no1.2

Khademi, T., Parnian, A., Garmsari, M., Ismail, K., & Lee, C. T. (2014). Role of technology transfer office/centre of universities in improving the commercialization of research outputs: A case study in Malaysia. In *Knowledge Management International Conference* (pp. 538–542). Universiti Utara Malaysia Press. https://doi.org/10.13140/2.1.2122.9443

Kibui, A. W., Gachunga, H., & Namusonge, G. S. (2014). Role of talent management on employees retention in Kenya: A survey of state corporations in Kenya: Empirical review. *International Journal of Science and Research*, *3*(2), 414–424.

Kogabayev, T., & Maziliauskas, A. (2017). The definition and classification of innovation. *HOLISTICA - Journal of Business and Public Administration*, *8*(1), 59–72. https://doi.org/10.1515/hjbpa-2017-0005

Lambert, R. (2003). *Lambert Review of business-university collaboration: Final report*. Her Majesty's Treasury.

Manap, A., Ismail, N., & Sidek, S. (2017). The roles of technology transfer offices to facilitate intellectual property commercialisation in the university: Issues and challenges. *The Social Sciences*, *12*(6), 919–924.

McLagan, P. A. (1989). Models for HRD practice. *Training and Development Journal*, *41*(9), 49–59.

Milano, M., & Ullius, D. (1998). *Designing powerful training: The sequential-iterative model* (1st ed.). Pfeiffer.

Mohd @ Ariffin, J. A., & Md Rami, A. A. (2023). Application of the Fuzzy Delphi Method to identify middle leaders' competencies in crisis management. *Management Research Journal*, *12*(1), 26–37. https://doi.org/10.37134/mrj.vol12.1.3.2023

Mohd, R., Siraj, S. & Hussin, Z. (2018). Aplikasi kaedah Fuzzy Delphi dalam pembangunan modul pengajaran pantun Melayu berasaskan maksud al-Quran mengenai keindahan flora, fauna dan langit Tingkatan 2

[Fuzzy Delphi method application in developing model of Malay poem based on the meaning of the Quran about flora, fauna and sky in Form 2]. *Jurnal Pendidikan Bahasa Melayu*, *8*(2), 57-67.

Mom, T. J. M., Oshri, I., & Volberda, H. W. (2012). The skills base of technology transfer professionals. *Technology Analysis and Strategic Management*, *24*(9), 871-891. https://doi.org/10.1080/09537325.2012.718663

Okoli, C., & Pawlowski, S. D. (2004). The Delphi method as a research tool: An example, design considerations and applications. *Information and Management*, *42*(1), 15-29. https://doi.org/10.1016/j.im.2003.11.002

Omotunde, O. I., & Alegbeleye, G. O. (2021). Talent management practices and job performance of librarians in university libraries in Nigeria. *The Journal of Academic Librarianship*, *47*(2), 102319. https://doi.org/10.1016/j.acalib.2021.102319

Ramlie, H. A., Hussin, Z., Jamil, M. R. M., Sapar, A. A., Siraj, S., & Noh, N. R. M. (2014). Aplikasi teknik Fuzzy Delphi terhadap keperluan aspek 'Riadhah Ruhiyyah' untuk profesionalisme perguruan Pendidikan Islam [Application of Fuzzy Delphi technique to the needs of 'Riadhah Ruhiyyah' aspects for the professionalism of Islamic Education teachers]. *The Online Journal of Islamic Education*, *2*(2), 53-72.

Sachani, S. S. (2020). Best of both worlds: A career in technology transfer and business development. *Developmental Biology*, *459*(1), 30-32. https://doi.org/10.1016/j.ydbio.2019.10.025

Shravanthi, S., & Sumanth, G. (2008). Talent DNA model. *Journal of Human Resource Management*, *22*(1), 78-85.

Siraj, S., Abdullah, M. R. T. L. A., & Rozkee, R. M. (2021). *Pendekatan penyelidikan rekabentuk dan pembangunan: Aplikasi kepada penyelidikan pendidikan* [Design and development research approaches: Applications to educational research]. Penerbit Universiti Pendidikan Sultan Idris.

Skulmoski, G. J., Hartman, F. T., & Krahn, J. (2007). The Delphi method for graduate research. *Journal of Information Technology Education*, *6*(1), 1-21.

Soares, T. J., & Torkomian, A. L. V. (2021). TTO's staff and technology transfer: Examining the effect of employees' individual capabilities. *Technovation*, *102*, 102213. https://doi.org/10.1016/j.technovation.2020.102213

Swamidass, P. M., & Vulasa, V. (2009). Why university inventions rarely produce income? Bottlenecks in university technology transfer. *The Journal of Technology Transfer*, *34*, 343-363. https://doi.org/10.1007/s10961-008-9097-8

Takata, M., Nakagawa, K., Yoshida, M., Matsuyuki, T., Matsuhashi, T., Kato, K., & Stevens, A. J. (2022). Nurturing entrepreneurs: How do technology transfer professionals bridge the Valley of Death in Japan? *Technovation*, *109*, 102161. https://doi.org/10.1016/j.technovation.2020.102161

Wang, W., Hu, B., Liu, J., & Yang, Z. (2024). Can antitrust policy promote enterprise innovation? Evidence from Zhongguancun Science and Technology Park. *Heliyon*, *10*(9), e30341. https://doi.org/10.1016/j.heliyon.2024.e30341

World Intellectual Property Organization. (2024). *Global Innovation Index 2024: Unlocking the promise of social entrepreneurship* (17th ed.). WIPO. https://doi.org/10.34667/tind.50062

Yusoff, A. F. M., Hashim, A., Muhamad, N., & Wan Hamat, W. N. (2021). Application of Fuzzy Delphi technique to identify the elements for designing and developing the e-PBM PI-Poli module. *Asian Journal of University Education*, *17*(1), 292-304.

Pertanika J. Sci. & Technol. 33 (5): 2279 - 2298 (2025)

PERTANIKA JOURNALS

SCIENCE & TECHNOLOGY

Journal homepage: http://www.pertanika.upm.edu.my/

Volatile and Non-Volatile Metabolites Profiling of the Chloroform Extract of Marine Sponge *Clathria reinwardti* via Mass Spectrometry

Wan Huey Chan[1,2], Muhammad Dawood Shah[2]*, Yoong Soon Yong[3,4], Rossita Shapawi[2], Nurzafirah Mazlan[2], Cheng Ann Chen[2], Wei Sheng Chong[2] and Fikri Akmal Khodzori[2]

[1]*Marine Science Programme, Faculty of Science and Natural Resources, Universiti Malaysia Sabah, Jalan UMS, 88400 Kota Kinabalu, Sabah, Malaysia*

[2]*Higher Institution Centre of Excellence, Borneo Marine Research Institute, Universiti Malaysia Sabah, Jalan UMS, 88400 Kota Kinabalu, Sabah, Malaysia*

[3]*R&D Quality Department, Osmosis Nutrition Sdn Bhd, Jalan Nilam 3, Bandar Nilai Utama, 71800 Nilai, Negeri Sembilan, Malaysia*

[4]*China-ASEAN College of Marine Sciences, Xiamen University Malaysia, Jalan Sunsuria, Bandar Sunsuria, 43900 Sepang, Selangor, Malaysia*

ABSTRACT

Metabolites are organic molecules produced by metabolic processes in living organisms and are responsible for various cellular functions. They are obtained from both terrestrial and marine organisms. Among marine organisms, sponges are an important source of metabolites. *Clathria reinwardti* Vosmaer is a demosponge belonging to the order Poecilosclerida and the family Microcionidae. The study aims to profile the metabolites of the chloroform extract of the marine sponge *C. reinwardti* using mass spectrometry analysis. A sponge sample was collected from the east coast of Sulug Island, Sabah, Malaysia. Total phenolic and flavonoid contents were determined. The composition of these extracts was further elucidated through qualitative biochemical screening, Fourier transform infrared spectroscopy (FTIR), gas chromatography-mass spectrometry (GC-MS), and liquid chromatography-quadrupole time-of-flight mass spectrometry (LT-qTOF-MS) analyses. The extracts displayed total phenolic and flavonoid content values. The qualitative biochemical screening tests indicated the presence of alkaloids and steroids. The GC-MS analysis indicated the presence of different metabolites of various natures, which include 2,5-bis(1,1-dimethylethyl) phenol,

ARTICLE INFO

Article history:
Received: 14 January 2025
Accepted: 18 May 2025
Published: 28 August 2025

DOI: https://doi.org/10.47836/pjst.33.5.11

E-mail addresses:
chanwanhuey@gmail.com (Wan Huey Chan)
dawoodshah@ums.edu.my (Muhammad Dawood Shah)
yongys@osmosis.com.my (Yoong Soon Yong)
rossita@ums.edu.my (Rossita Shapawi)
nurzafirah@ums.edu.my (Nurzafirah Mazlan)
chengann@ums.edu.my (Cheng Ann Chen)
chong@ums.edu.my (Wei Sheng Chong)
mfakmal@ums.edu.my (Fikri Akmal Khodzori)
* Corresponding author

pentadecane, octacosane, eicosane, tetracosane, and cholestanol. The LC-qTOF-MS analysis indicated the presence of thymine, C16 sphinganine, hericene B, phylloquinone, 24-norcholesterol, palmitic amide, oleamide, solanidine, suillin, 9-thiastearic acid, and isoamijiol. The detected metabolites have been reported to have different pharmacological activities such as anti-inflammatory, antimicrobial, anti-diabetic, anti-cancer, antioxidant, anti-haemorrhagic, cytotoxic, neuroprotective, and chemopreventive. The finding highlights that the chloroform extract of *C. reinhardt* is an important source of metabolites with potential benefits to humans and animals, particularly in the aquaculture industry. Further isolation, purification, and characterization of the detected metabolites are needed for future studies.

Keywords: *Clathria reinhardt,* GC-MS, LC-QTOF-MS analysis, marine sponge, metabolites, seafood security

INTRODUCTION

Metabolites are small organic molecules resulting from various metabolic processes within living organisms (Lu et al., 2017). These molecules have various functions, including the formation of cellular structures, energy sources, signalling molecules, defence, and inter-organism interactions (Altaf-Ul-Amin et al., 2018). Metabolites have received much attention in biomedical research because of their potential therapeutic applications and diverse pharmacological properties (Qiu et al., 2023). They have exhibited various biological activities, including antimicrobial, antioxidant, anticancer, and anti-inflammatory (Hamzalioğlu & Gökmen, 2016).

Metabolites can be obtained from both terrestrial and marine sources. From the history of marine metabolites research, marine invertebrates, such as sponges, sea slugs, and soft corals, have been the major contributors to the novel source of natural bioactive compounds for the current trend in drug discovery (Varijakzhan et al., 2021). Among marine organisms, sponges are one of the richest sources of pharmacological metabolites such as alkaloids, terpenoids, steroids, phenolics, and flavonoids. Over 5,300 different bioactive products are known from marine sponges and their associated microorganisms, along with more than 200 new metabolites to be reported annually (Laport et al., 2009). Several drugs originated from sponges that had entered clinical trials and been approved. For instance, the development of cytarabine (Ara-C) for cancer treatment and vidarabine as an antiviral agent (Mayer et al., 2010).

Among the diverse types of marine sponges, *Clathria reinwardti* is the targeted sponge in this study. The *C. reinwardti* Vosmaer is classified under the phylum Porifera and the family Microcionidae. These sponges exhibit branching and sprawling morphologies that extend horizontally, resembling the intricate structure of branching tree roots (Ashok et al., 2019). Apart from their morphology, they also display orange colours, ranging from vibrant, bright, salmon-like orange colors to dark and dull brown-yellowish tones (Figure 1).

The *C. reinwardti* marine sponge has been documented in various regions, including Vietnam (Tai et al., 2021; Trang et al., 2022), Thailand (Dechsakulwatana et al., 2022), Indonesia (Sugrani et al., 2019), India (Venkateshwar et al., 2005), Singapore (S. C. Lim, 2008), and Malaysia (Ocean Biodiversity Information System [OBIS], n.d.).

Figure 1. Underwater photograph of *Clathria reinwardti* at the sampling site of Sulug Island, North Borneo, Sabah, Malaysia

To the author's knowledge, only a handful of authors have published on the composition of the bioactive compounds of *C. reinwardti*, with the reported metabolites limited to a maximum of seven compounds (Tai et al., 2021; Trang et al., 2022; Venkateshwar et al., 2005). In these studies, nuclear magnetic resonance spectroscopy (NMR) was mainly used to analyze the compounds. However, the inherent limitations of NMR spectroscopy, such as low sensitivity and the inability to quantitatively analyze trace compounds, may result in fewer compounds being detected (Wang et al., 2021), leading to a limited metabolite profile.

To date, no studies have been conducted on the metabolite profiling of *C. reinwardti* specifically in Sabah, in the Coral Triangle region. Filling this research gap is crucial because it is known that variations in location and environmental parameters affect the composition of bioactive compounds in marine sponges (Melawaty & Pasau, 2015). Therefore, this study is important to contribute to the fundamental understanding of *C. reinwardti* and serve as a reference for identifying the main compounds. Consequently, the study aims to evaluate the metabolite profile of chloroform extracts from *C. reinwardti* in Borneo waters using GC-MS and LC-qTOF-MS analyses.

METHODOLOGY

Chemicals and Reagents

The chemicals and reagents utilized to conduct this study include chloroform, n-hexane, catechin, folin-ciocalteau solution, hydrochloric acid (HCl), iodine, potassium iodide (KI), sulphuric acid (H_2SO_4), benzene, ammonia, sodium hydroxide (NaOH), acetone, high-performance liquid chromatography (HPLC)-grade methanol, distilled water, and Toyobo MagExtractor-Genome-Kit. The chemicals and reagents were purchased from Sigma Chemicals (Sigma-Aldrich Corporation, USA), Merck (USA), and J. T. Baker (Avantor, USA).

Sample Collection

Approximately 1 kg of *C. reinwardti* was collected in September 2023 from a site located on the east coast of Sulug Island, Sabah, Malaysia (5.9571°N, 115.9963°E) at a depth of 15 m. Concurrently, *in-situ* water parameters were measured using a YSI water quality meter (Professional Plus Multiparameter, Xylem Analytics, USA): water temperature (29.5°C), pH (7.69), salinity (31.31 ppt), dissolved oxygen (89%), total dissolved solids (31,330 mg/L), and turbidity (0.12 NTU). The necessary permits for sample collection in Sabah were obtained from the Sabah Biodiversity Centre (SaBC) (License No.: JKM/MBS.1000-2/13 JLD. 2(47)), the Sabah Parks Research Permit (Application: SPRP-220; Letter Ref. No.: TTS 100-6/2 Jld. 30), and the Department of Fisheries (DoF) (License No.: JPIN/BPP:100-24 Klt.7 (102).

Following collection, the samples were carefully placed in labeled zip-lock bags, cleaned, and rinsed with distilled water, and subsequently stored in a -80°C freezer for further analysis facilitation. The sample was deposited at the Borneo Marine Research Institute, Universiti Malaysia Sabah Herbarium, and assigned the voucher specimen number IPMB-Pf 01.00002. Additionally, DNA isolation from the collected sample was performed for identification purposes.

Extraction

The *C. reinwardti* sample was dried at room temperature and then ground into fine powder using a heavy-duty grinder. The powdered sample was extracted with HPLC-grade methanol, chloroform, and distilled water in a 1:10:10:10 (w/v/v) ratio using the orbital shaking method at 27°C for 72 hr. The extract was then filtered with a metal mesh, a cheesecloth strainer, and Whatman filter paper (125 mm) before separation with a separatory funnel. Three layers were formed, including the chloroform layer known as the non-polar layer (lowest layer), which was collected as chloroform crude extract. In contrast, the macromolecule layer and polar layer (mixture of methanol and distilled water layer) were discarded as a sea salt removal approach. The extract was dried with a rotary evaporator before lyophilization using a freeze dryer to obtain the crude extract. Subsequently, the crude extracts were then stored at a temperature of -80^{o}C for further analysis, and the extraction yield was calculated using Equation 1 (Yong et al., 2018).

$$Extraction\ yield\ (\%) = \frac{Mass\ of\ the\ extract\ obtained\ \times 100\%}{Mass\ of\ the\ dry\ material\ taken\ for\ extraction} \quad [1]$$

Determination of Total Phenolic and Flavonoid Contents

The total phenolic content (TPC) of the diluted extract was determined with the Folin-Ciocalteau method (Velioglu et al., 1998), while the total flavonoid content (TFC) was evaluated using the aluminum chloride colorimetric method (Zou et al., 2004).

Qualitative Metabolites Screening

The qualitative metabolite screening of the chloroform crude extract of *C. reinwardti* was conducted to assess the presence of different metabolites, including alkaloids, anthraquinones, saponins, and steroids (Harborne, 1998).

FTIR Analysis

The FTIR analysis was performed using a Bruker Alpha II Compact FTIR Spectrophotometer (Bruker, Germany). The crude chloroform extract was placed directly in contact with the test crystal window surface during data acquisition. Identification of the chemical class present was analyzed based on the FTIR spectrum range of previous studies (Nandiyanto et al., 2019).

GC-MS Analysis

About 1 µl of the hexane-reconstituted sample was injected into an HP-5MS capillary column (30 m × 0.25 mm with a film thickness) using a GC-MS system (Agilent Technologies, USA). Helium (99.999%) was used as a carrier gas at a constant flow rate of 1.0 ml/min. The injector temperature was set at 250°C, and the oven temperature gradient started at 40°C and held for 3 min, then ramped from 40 to 200°C at a rate of 3°C/min and held for 3 min at 200°C. The system operated in splitless mode with electron ionization (EI), and compound identification was done using the National Institute of Standards and Technology (NIST) database, matching mass spectra with the highest scores to identify the target compound (Shah et al., 2014). Each compound obtained was further reviewed with previous studies for reported bioactivities.

LC-qTOF-MS Analysis

The chloroform crude extract of *C. reinwardti* was reconstituted with methanol, and the concentration was adjusted before the LC-qTOF-MS analysis. A 1.0 µl reconstituted sample was chromatographically separated with an Agilent Zorbax Eclipse XDB-C18 reversed-phase column (Agilent Technologies, USA). The column was maintained at 25°C, and a flow rate of 500 µl/min during analysis. The mobile phases were 0.1% formic acid in water (solvent A) and 0.1% formic acid in acetonitrile (solvent B). The LC gradient followed the previously established program (Shah et al., 2020). Briefly, the gradient started at 5% solvent B for 5 min, progressed to 100% solvent B in 15 min, and was kept for 5 min. Later, the column was conditioned as an initial for 5 min before the subsequent injection. The MS signals were obtained, following the previous methodology with minor modifications (Ling et al., 2018). Data was acquired between an *m/z* of 100 and 1,500, with positive and negative heated electrospray ionization (ESI) deployed at 3,500 and

–3,500 V, respectively. Then, the acquired data was processed with Agilent MassHunter Qualitative Analysis software (version 10), and the compounds were identified with the built-in molecular feature algorithm and matched against the METLIN Metabolomics Database and Library databases. Each compounds obtained were further reviewed with previous studies for reported bioactivities.

RESULTS

Multiple analyses were undertaken in this investigation into the metabolic profiling of *C. reinwardti* sponge chloroform extracts. Initially, TPC and TFC were assessed. Subsequently, the composition of these extracts underwent further elucidation through qualitative biochemical screening, FTIR, GC-MS, and LC-qTOF-MS. The detailed results of these analyses are presented in subsequent sections.

The Percentage Yield, TPC, and TFC

The chloroform extract of *C. reinwardti* yielded 2.45%. The concentration of TPC of *C. reinwardti* chloroform extract was determined according to the equation ($y = 3.5407x + 0.0542$, $R^2 = 0.9962$) as gallic acid equivalent (mg GAE/g extract). The total phenolic content was recorded at 0.117 ± 0.008 mg GAE/g, respectively. The TFC was calculated by the equation ($y = 0.2315x + 0.0024$, $R^2 = 0.9976$), obtained by the calibration curve as catechin equivalents (mg CAE/g extract). The total flavonoid content resulted in 1.320 ± 0.087 mg CAE/g.

Qualitative Metabolites Screening of *C. reinwardti* Extract

The qualitative metabolites screening of *C. reinwardti* chloroform extract indicated the presence of alkaloids and steroids, while anthraquinone and saponins were absent.

FTIR Profile

FTIR analysis (Figure 2) showed a broad and weak absorption band of aliphatic amine stretch (N-H) recorded around 3339.74 cm^{-1}. The strong C-H stretch absorption band was observed around 2920.50 cm^{-1} and the medium band at 2852.89 cm^{-1}. Both these values fall within the reference range of methylene C-H stretch, indicating the presence of aliphatic methylene in the *C. reinwardti* chloroform extract. The adsorption band illustrated the presence of a carbonyl compound (C=O) at 1726.84 cm^{-1}. The co-occurrence of C-H (around 2852.89 cm^{-1}) and C=O stretch (1726.84 cm^{-1}) indicates the presence of an aldehyde group. A weak absorption band at 1636.85 cm^{-1} was attributed to the imine group. In contrast, the weak band around 1545.22 cm^{-1} suggested the presence of amide compound (C=O stretching or N-H bending) vibration in *C. reinwardti* chloroform extract (CONR2). The

fingerprint region (500–1,500 to 1,500 cm^{-1}) was not included as the sample tested was not a pure compound but a crude extract. The reference range was referred to (Nandiyanto et al., 2019; Sadat & Joye, 2020) as listed in Table 1.

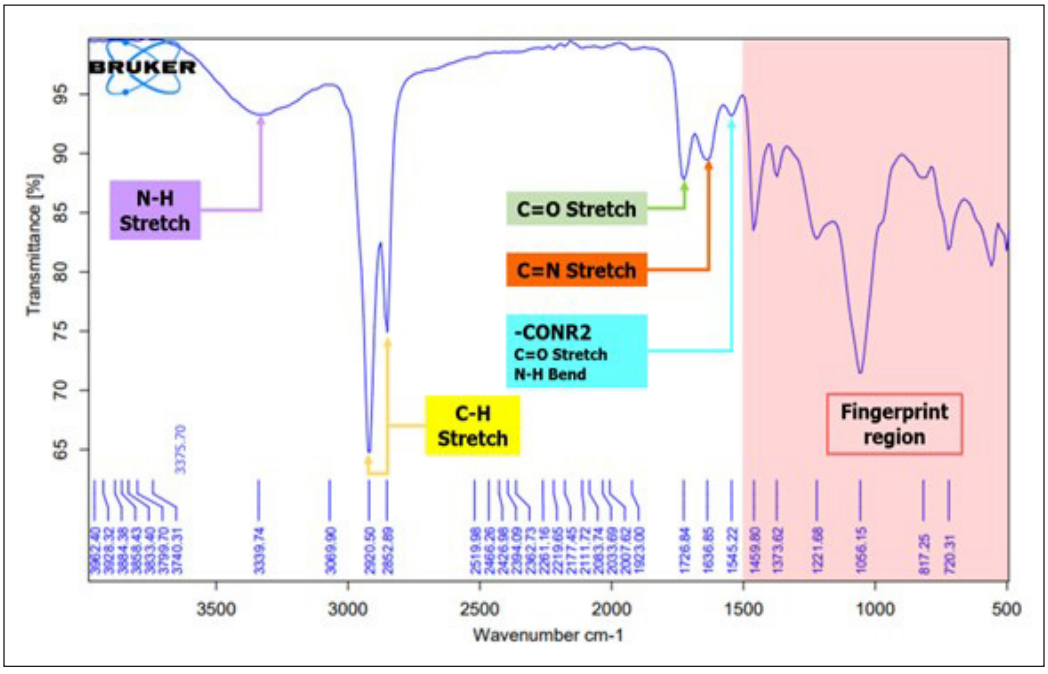

Figure 2. Fourier transform infrared spectroscopy spectrum showing a functional group of *Clathria reinwardti* chloroform extract

Table 1
Identified functional group of the Fourier transform infrared spectroscopy (FTIR) spectrum for Clathria reinwardti *chloroform extract based on the reference range*

Recorded absorption band	Reference range		Functional group
3339.74	3360-3310	N-H	Aliphatic secondary amine
2920.50	2935-2915	C-H	Aliphatic methylene (alkane)
2852.89	2800-2700	C-H	
1728.84	1740-1725	C=O	Carbonyl
1636.85	1690-1590	C=N	Imine
1545.22	1580-1510	-CONR2	Amide
1459.80	Fingerprint region		
1373.62			
1221.68			
1056.15			
817.25			
720.31			

GC-MS Analysis

GC-MS analyses of metabolites carried out in the chloroform extract of *C. reinwardti* are displayed in Table 2. Ten (10) metabolites of various functional groups, such as phenol, alkane, and sterol, are listed. Figure 3 displays the GC-MS chromatogram, while Figure 4 illustrates the structures of the identified metabolites from the chloroform extract.

Table 2
List of metabolites detected in the chloroform extract of Clathria reinwardti *via gas chromatography-mass spectrometry analysis*

No.	Retention time (min)	Metabolites name	Class	Molecular formula	Area (%)
1	26.325	2,5-bis(1,1-Dimethylethyl)phenol	Phenolic	$C_{14}H_{22}O$	1.63
2	34.199	Pentadecane	Alkane	$C_{15}H_{32}$	0.54
3	38.004	Eicosane	Alkane	$C_{20}H_{42}$	2.25
4	39.789	Heneicosane	Alkane	$C_{21}H_{44}$	3.00
5	41.557	Docosane	Alkane	$C_{22}H_{46}$	6.79
6	43.628	Tetracosane	Alkane	$C_{24}H_{50}$	9.16
7	46.306	Pentacosane	Alkane	$C_{25}H_{52}$	10.81
8	47.199	Cholestanol	Steroid	$C_{27}H_{48}0$	9.37
9	49.802	Hexacosane	Alkane	$C_{26}H_{54}$	9.99
10	54.443	Heptacosane	Alkane	$C_{27}H_{56}$	8.10

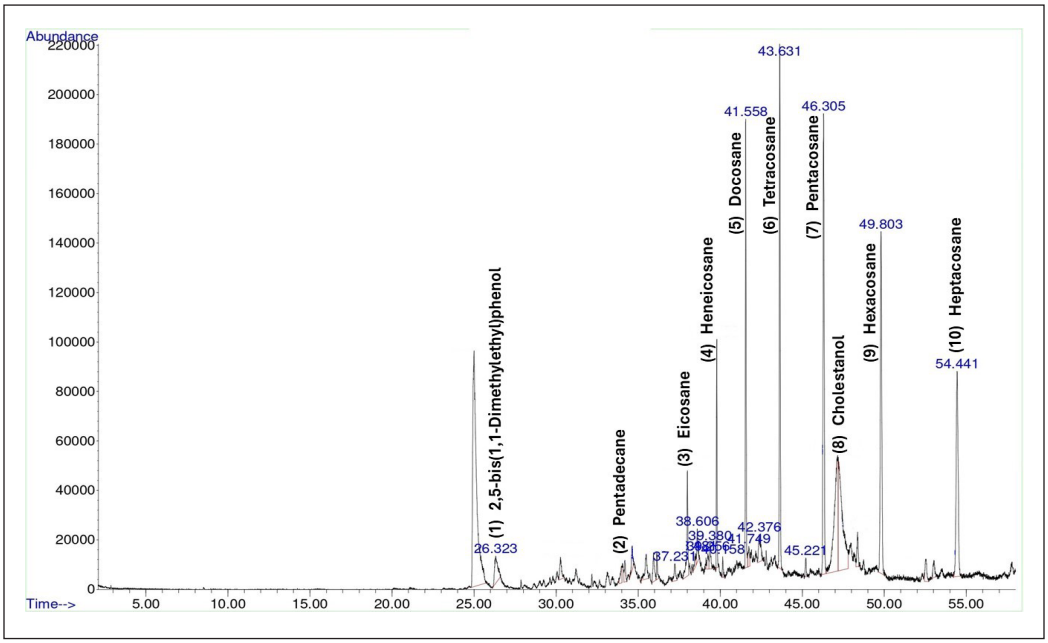

Figure 3. Chromatogram of *Clathria reinwardti* chloroform extract via gas chromatography-mass spectrometry analysis

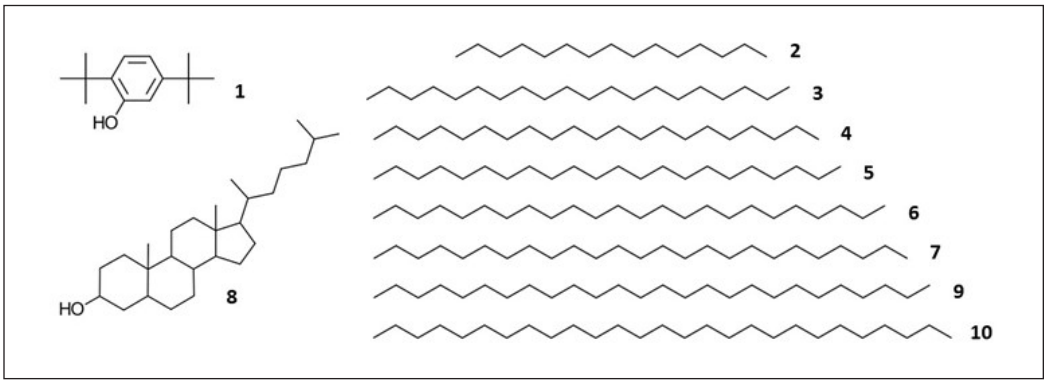

Figure 4. Structures of the detected metabolites in the chloroform extract of *Clathria reinwardti* via gas chromatography-mass spectrometry analysis

The total compounds detected in the chloroform extract of *C. reinwardti via* GC-MS analysis were classified into three chemical classes: phenol (10%), sterol (10%), and predominantly alkane (80%).

LC-qTOF-MS Analysis

(a) Positive Mode of LC-qTOF-MS

LC-qTOF-MS analysis via positive mode carried out in the chloroform extract of *C. reinwardti* is displayed below. Thirty (30) metabolites of different functional groups, such as fatty acids, terpenoids, amino acids, and steroids, are tabulated (Table 3)**.** Figure 5 presents the structure of metabolites identified in the chloroform extract of C. reinwardti using the positive mode of LC-qTOF-MS analysis.

(b) Negative Mode of LC -qTOF-MS

LC-qTOF-MS analysis via negative mode carried out in the chloroform extract of *C. reinwardti* is displayed below. Seven (7) metabolites of different functional groups, such as fatty acids, macrolides, and terpenoids, are tabulated (Table 4). Figure 6 depicts the structure of metabolites detected in the chloroform extract using the negative mode of LC-qTOF-MS analysis.

Overall, thirty (30) and seven (7) metabolites were identified through LC-qTOF-MS analysis via positive and negative modes, respectively. In the positive mode, the compounds can be classified into various chemical classes, dominated by vitamins (24%), followed by steroids (14%). Other reported chemical classes identified include terpenoid (10%), peptide (7%), ketone (7%), fatty amide (7%), aromatic (7%), fatty acid (4%), dicarboxyl acid (4%), amino acid (4%), lactone (3%), flavonoid (3%), sphingolipid (3%), and phenolic (3%).

Table 3
List of metabolites detected in the chloroform extract of Clathria reinwardti *via the positive mode of liquid chromatography-quadrupole time-of-flight mass spectrometry analysis*

No.	Retention time (min)	*m/z*	Metabolites	Class	Molecular formula	Mass error (ppm)
11	1.39	127.0497	Thymine	Purine	$C_5H_6N_2O_2$	1.16
12	7.48	254.1164	Ethyl 3-methyl-9H-carbazole-9-carboxylate	Aromatic	$C_{16}H_{15}NO_2$	4.98
13	12.42	274.273	Hexadecasphinganine	Sphingolipid	$C_{16}H_{35}NO_2$	4.56
14	12.66	181.1204	5-methyl-octanoic acid	Fatty acid	$C_9H_{18}O_2$	-4.61
15	13.16	214.0869	Benzyl nicotinate	Aromatic	$C_{13}H_{11}NO_2$	-1.85
16	13.30	277.1767	Kikkanol A	Terpenoid	$C_{15}H_{26}NO_3$	2.86
17	13.31	295.1874	3-methyl-tetradecanedioic acid	Dicarboxylic acid	$C_{15}H_{28}O_4$	2.87
18	14.97	189.1236	*N*-Alpha-acetyllysine	Amino acid	$C_8H_{16}N_2O_3$	-1.92
19	17.22	279.1537	4-Hydroxy-6-methylpyran-2-one	Lactone	$C_6H_6O_3$	4.12
20	17.23	205.0822	Gly Glu	Peptide	$C_7H_{12}N_2O_5$	-2.02
21	17.27	506.3183	Lys Trp Arg	Peptide	$C_{23}H_{36}N_8O_4$	1.09
22	18.05	600.4635	Hericene B	Phenolic	$C_{37}H_{58}O_5$	-2.34
23	18.28	468.3827	Phylloquinone	Vitamin	$C_{31}H_{46}O_2$	3.18
24	19.37	305.2464	Isoamijiol	Terpenoid	$C_{20}H_{32}O_2$	1.85
25	19.64	395.3284	24-Norcholesterol	Steroid	$C_{26}H_{44}O$	1.88
26	19.75	256.2628	Palmitic amide	Fatty Amide	$C_{16}H_{33}NO$	2.98
27	19.84	282.2779	Oleamide	Fatty Amide	$C_{18}H_{35}NO$	4.52
28	20.12	589.426	Caffeoylcycloartenol	Steroid	$C_{39}H_{56}O_4$	-1.38
29	20.27	398.3415	Solanidine	Steroid	$C_{27}H_{43}NO$	4.73
30	20.30	451.2813	25-Hydroxyvitamin D3-26,23-lactone	Vitamin	$C_{27}H_{40}O_4$	1.24
31	20.32	463.2806	Suillin	Terpenoid	$C_{28}H_{40}NO_4$	1.33
32	20.46	397.3099	25-Hydroxy-23,23,24,24-tetradehydrovitamin D3	Vitamin	$C_{27}H_{40}O_2$	-1.69
33	20.47	419.2959	1α,25-Dihydroxy-3-deoxy-3-thiavitamin D3	Vitamin	$C_{26}H_{42}O_2S$	-0.15
34	20.84	628.1864	Robinetin 3-rutinoside	Flavonoid	$C_{27}H_{30}O_{16}$	-1.12
35	20.96	386.3768	3-Deoxyvitamin D3	Vitamin	$C_{27}H_{44}$	3.80
36	21.04	479.3143	1α,22,25-Trihydroxy-23,24-tetradehydro-24a,24b-dihomo-20-epivitamin D3	Vitamin	$C_{29}H_{44}O_4$	-2.86
37	21.44	413.2655	Apocholic acid	Steroid	$C_{24}H_{38}O_4$	0.92
38	21.71	326.3407	Henicos-6-en-11-one	Ketone	$C_{21}H_{40}O$	4.01
39	21.87	451.3199	24,25-Dihydroxyvitamin D2	Vitamin	$C_{28}H_{44}O_3$	-4.17
40	24.62	338.3402	N-Cyclohexanecarbonylpentadecylamine	Ketone	$C_{22}H_{44}NO$	4.83

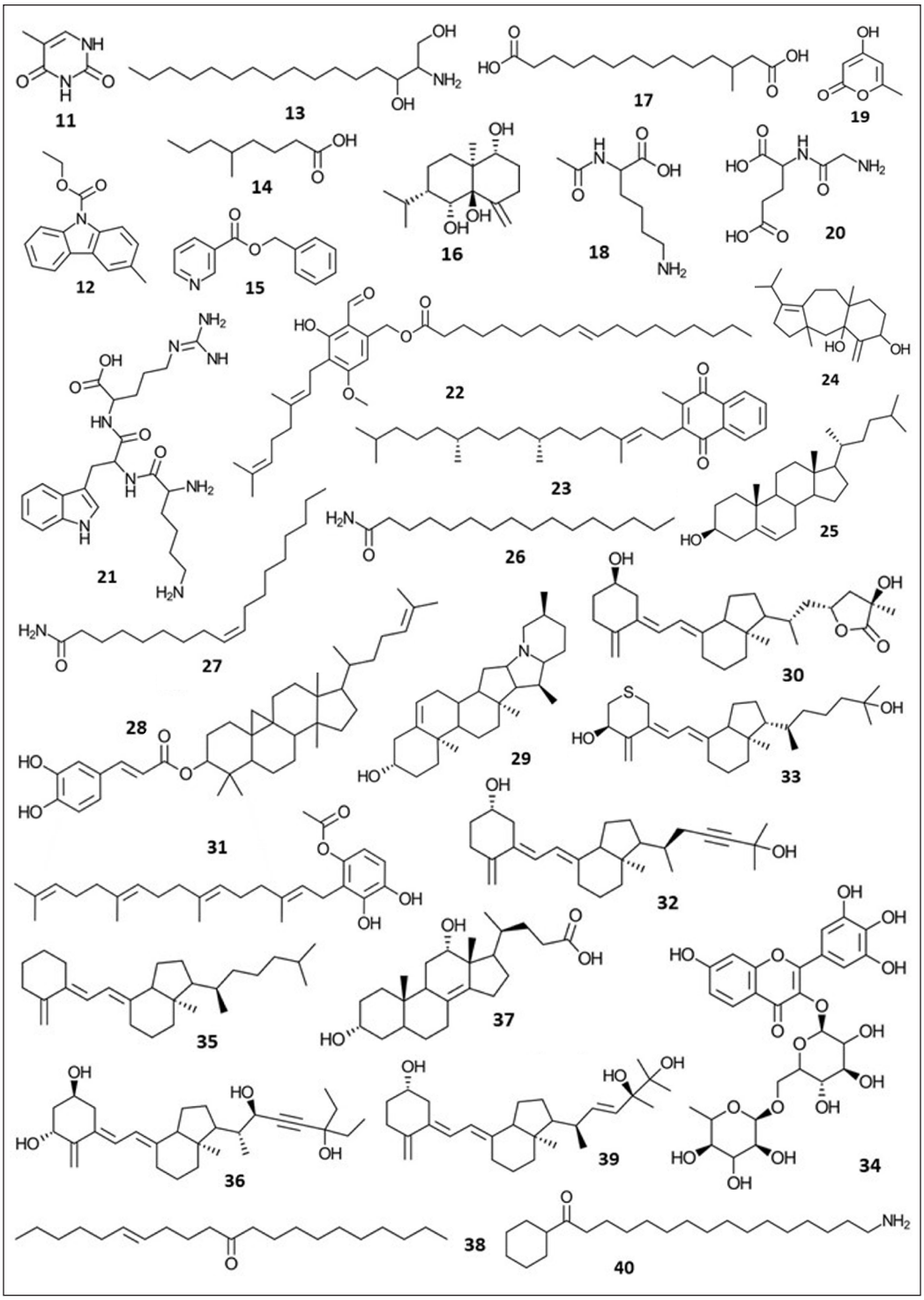

Figure 5. Structure of the metabolites detected in the chloroform extract of *Clathria reinwardti* via the positive mode of liquid chromatography-quadrupole time-of-flight mass spectrometry analysis

Table 4
List of metabolites detected in the chloroform extract of Clathria reinwardti *via the negative mode of liquid chromatography-quadrupole time-of-flight mass spectrometry analyses*

No.	Retenion time (min)	*m/z*	Metabolites name	Class	Molecular formula	Mass error (ppm)
41	14.33	571.3272	6,8a-Seco-6,8a-deoxy-5-oxoavermectin "2b" aglycone	Macrolide	$C_{33}H_{48}O_8$	1.01
42	15.92	317.2137	8-Hydroxyicosa-5,9,11,14,17-pentaenoic acid	Fatty acid	$C_{20}H_{30}O_3$	-4.66
43	16.16	343.2294	13-Hydroxydocosa-4,7,10,14,16,19-hexaenoic acid	Fatty acid	$C_{22}H_{32}O_3$	-4.44
44	16.34	319.2291	11-Hydroxyicosa-5,8,12,14-tetraenoic acid	Fatty acid	$C_{20}H_{32}O_3$	-3.87
45	17.13	599.3212	5-Oxoavermectin "2a" aglycone	Macrolide	$C_{34}H_{48}O_9$	2.04
46	18.54	301.2193	9-Thiastearic acid	Fatty acid	$C_{17}H_{34}O_2S$	4.41
24	19.33	303.2331	Isoamijiol	Terpenoid	$C_{20}H_{32}O_2$	0.03

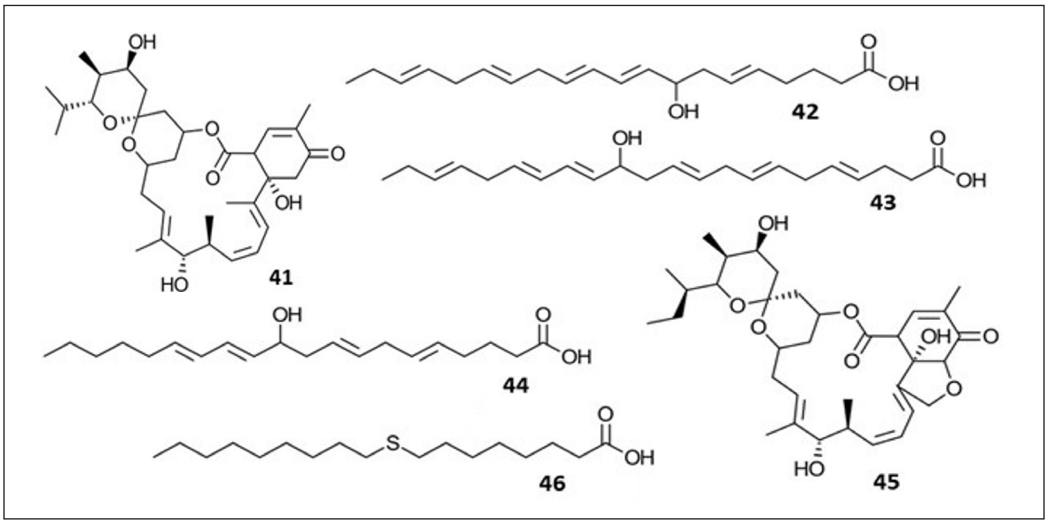

Figure 6. Structure of the metabolites detected in the chloroform extract of *Clathria reinwardti* via the negative mode of liquid chromatography-quadrupole time-of-flight mass spectrometry analysis

Compared to the positive mode, the negative mode of LC-qTOF-MS has detected fewer compounds (7 compounds). The chemical classes of the compounds are also fewer, comprised of terpenoid (14%), macrolide (29%), and dominated by fatty acid (57%).

DISCUSSION

The percentage yield of *C. reinwardti* obtained from chloroform extracts is 2.45%. The yield is lower compared to the methanol extract performed previously (Trang et al.,

2022). It is suggested that the compounds of *C. reinwardti* may have a higher affinity for a high-polarity solvent (methanol). For the chloroform extract, the TPC (0.117 ± 0.008 mg GAE/g) and TFC (1.320 ± 0.087 mg CAE/g) obtained complement the metabolite profiling. The GC-MS analysis (Table 2) has identified a phenol compound, namely, 2,5-bis(1,1-dimethylethyl) phenol, whereas flavonoid (robinetin 3-rutinoside) was identified via LC-qTOF-MS positive mode (Table 3). However, the TPC values of the chloroform extract of *C. reinwardti* are lower compared to the average TPC values (10.02 mg GAE/g extract) reported previously for 47 marine sponges (Oogarah et al., 2020). Aside from the use of different extraction solvents, the variations compared to the reported study may also be attributed to differences in sampling locations and environmental parameters, which can significantly influence the chemical composition of sponge-derived compounds (Melawaty & Pasau, 2015). This discrepancy is plausible, as the previous study collected a sample from Mauritius, located in the southwest Indian Ocean, whereas the present study's sample was obtained from the east side of Sulug Island, Malaysia. These geographic and ecological differences likely contributed to the presence of distinct compounds in sponges, therefore resulting in variation in TPC values. The qualitative screening of the chloroform extract of *C. reinwardti* revealed the presence of alkaloids and steroids, which were further confirmed through metabolite profiling using GC-MS and LC-qTOF-MS analysis. This finding aligns with previous studies, where alkaloids and steroids have been frequently identified in the genus *Clathria* (Capon et al., 2001; Chakraborty & Francis, 2021; Ohta et al., 1993; Woo et al., 2017). However, anthraquinones and saponins were not detected in the chloroform extract. This absence was consistent with subsequent GC-MS and LC-qTOF-MS analyses.

FTIR analysis of chloroform extract revealed absorption bands corresponding to different functional groups, including amine, alkane, carbonyl, imine, and amide. Subsequently, GC-MS analysis indicated that 80% of the compounds detected were alkanes (Figure 4). Additionally, the presence of the carbonyl group might be attributed to the fatty acid, which constitutes 57% of the metabolite class detected via LC-qTOF-MS negative mode.

Furthermore, the chloroform extract of *C. reinwardti* was analyzed through GC-MS for metabolite profiling. Among the 10 detected compounds, nine have demonstrated pharmacological effects, including 2,5-bis(1,1-dimethylethyl) phenol, which has exhibited antibacterial and anti-inflammatory properties (Phillips et al., 2015). Pentadecane has displayed anti-inflammatory, analgesic, and antipyretic activities (Okechuwuo, 2020). Heptacosane has shown antibacterial effects (Khatua et al., 2016). Heneicosane has been recognized for its antimicrobial properties (Vanitha et al., 2020). Eicosane has displayed anti-inflammatory, analgesic, and antipyretic effects (Okechuwuo, 2020). Hexacosane has exhibited antimicrobial properties (Rukaiyat et al., 2015). Tetracosane has displayed cytotoxic and apoptotic effects (Uddin et al., 2012). Pentacosane has shown antimicrobial properties (Carev et al., 2023). Cholestanol has induced apoptosis of corneal endothelial cells and lens epithelial cells and has exhibited cytotoxicity (Inoue et al., 1999; Miyashita et al., 2008).

The positive and negative modes of LC-qTOF-MS analysis indicated 36 metabolites, of which 23 have been reported to have bioactive properties. Some of the important pharmacologically active metabolites include thymine, which has been involved in pyrimidine metabolism (Qu et al., 2024). Hexadeca sphinganine has exhibited anti-cancer, nematocidal, and antibacterial activities (Gao et al., 2016; M. W. Lim et al., 2023; Reid et al., 2019). The 5-methyl-octanoic acid has inhibited α-amino-3-hydroxy-5-methyl-4-isoxazolepropionic acid receptors (AMPAR), a subtype of AMPA-type glutamate receptors, and this inhibition has shown potential therapeutic interventions for Alzheimer's disease (Dunn et al., 2023). Benzyl nicotinate has acted as a vasodilator (Abramović et al., 2008). Kikkanol A has demonstrated inhibitory activity against rat lens aldose reductase (Yoshikawa et al., 1999). N-Alpha-acetyllysine has served as a biomarker for membrane nephropathy (MN) and IgA nephropathy (IgAN) identification (Qu et al., 2024). The 4-Hydroxy-6-methylpyran-2-one has served as a chemical platform (Kim et al., 2023). Hericene B has exhibited anti-diabetic properties and reduced the risk of gastric ulceration (Lv et al., 2021). Phylloquinone has been known for its antihemorrhagic and osteoporosis prevention properties (Bus & Szterk, 2021). Isoamijiol has acted as an antioxidant (M. W. Lim et al., 2023). Palmitic amide has shown antioxidant and anti-neuroinflammatory effects (M. W. Lim et al., 2023; Ngu et al., 2022). Oleamide exhibits anti-inflammatory, hypolipidemic, and chemopreventive effects against Alzheimer's disease, induces deep sleep, and upregulates appetite (Ameamsri et al., 2020; Cheng et al., 2010). Solanidine has acted as an anticancer agent against the Herpes simplex virus, an antitumor, and a protease inhibitor for SARS-CoV-2 (Minorics et al., 2011; Morillo et al., 2020; Zhao et al., 2021). Suillin has inhibited cell proliferation and induced apoptosis in human cancer cells and serves as a chemo-venting agent for the treatment of neurodegenerative diseases like Alzheimer's (Andrade et al., 2022; F.-Y. Liu et al., 2009). Robinetin 3-rutinoside has served as an inhibitor of tyrosinase (Pervaiz et al., 2022). The 3-Deoxyvitamin D3 has exhibited anti-inflammatory properties (Cheema et al., 2017). Apocholic acid demonstrates antimicrobial activity (Chua et al., 2023). The 9-thiastearic acid has inhibited stearoyl-CoA desaturase (G. Liu, 2009). Isoamijiol has displayed antioxidant and insecticidal properties (Kilic et al., 2021; M. W. Lim et al., 2023). Metabolites derived from *C. reinhardtii* may offer benefits to both humans and animals, particularly in aquaculture, which could contribute to enhancing seafood security.

CONCLUSION

Among marine organisms, sponges are an important source of metabolites. *Clathria reinhardt* Vosmaer is a marine sponge belonging to the family Microcionidae. The chloroform extracts displayed total phenolic and total flavonoid content values. The qualitative biochemical screening tests indicated the presence of alkaloids and steroids. The

GC-MS analysis indicated the presence of different metabolites of various natures, which include 2,5-bis(1,1-dimethylethyl) phenol, pentadecane, eicosane, tetracosane, cholestanol, etc. The LC-QTOF-MS analysis indicated the presence of different metabolites, which include thymine, hexadeca sphinganine, hericene B, phylloquinone, 24-norcholesterol, palmitic amide, oleamide, solanidine, suillin, 9-thiastearic acid, and isoamijiol. These compounds have been reported for various pharmacological activities, such as anti-inflammatory, antimicrobial, anti-diabetic, anticancer, antioxidant, anti-hemorrhagic, cytotoxic, neuroprotective, and chemopreventive. Thus, the chloroform extract of *C. reinhardt* is an important source of metabolites. Further isolation, purification, and characterization of the detected metabolites are needed for future studies.

ACKNOWLEDGEMENTS

This work is part of Wan Huey Chan's Marine Science Undergraduate Final Year Project (FYP) Dissertation. We express gratitude to Wei-Ling Ng, Mei Fung Lee, Aiman Haris, and Gilbert Ringgit for assisting in the analysis and sampling. The paper has been funded by the Higher Institution Centre of Excellence (HICoE) Research Grant Scheme (Approval Letter No. JPT(BKPI)1000/016/018/35(2), Grant Code HIC2404), provided by the Ministry of Higher Education, Malaysia and the National Marine Biodiversity Institute of Korea (MABIK) (Grant code: LPA2007).

REFERENCES

Abramović, Z., Šuštaršič, U., Teskač, K., Šentjurc, M., & Kristl, J. (2008). Influence of nanosized delivery systems with benzyl nicotinate and penetration enhancers on skin oxygenation. *International Journal of Pharmaceutics*, *359*(1–2), 220–227. https://doi.org/10.1016/j.ijpharm.2008.03.014

Altaf-Ul-Amin, M., Kanaya, S., & Mohamed-Hussein, Z.-A. (2018). Investigating metabolic pathways and networks. In S. Ranganathan, M. Gribskov, K. Nakai, C. Schönbach (Eds.), *Encyclopedia of bioinformatics and computational biology* (Vol. 3, pp. 489–503). Academic Press. https://doi.org/10.1016/B978-0-12-809633-8.20140-4

Ameamsri, U., Chaveerach, A., Sudmoon, R., Tanee, T., Peigneur, S., & Tytgat, J. (2020). Oleamide in *Ipomoea* and *Dillenia* species and inflammatory activity investigated through ion channel inhibition. *Current Pharmaceutical Biotechnology*, *22*(2), 254–261. https://doi.org/10.2174/1389201021666200607185250

Andrade, J. M., Pachar, P., Trujillo, L., & Cartuche, L. (2022). Suillin: A mixed-type acetylcholinesterase inhibitor from *Suillus luteus* which is used by Saraguros indigenous, southern Ecuador. *PLOS One*, *17*(5), e0268292. https://doi.org/10.1371/journal.pone.0268292

Ashok, A., Arasumuthu, A., K, Diraviya Raj, K., & Patterson Edward, J. K. (2019). *Clathria reinwardtii* - An Active competitor on the coral communities of Gulf of Mannar Marine Biosphere Reserve - Southeast India. *Think India Journal*, *22*(14), 15163–15179.

Bus, K., & Szterk, A. (2021). Relationship between structure and biological activity of various vitamin K forms. *Foods*, *10*(12), 3136. https://doi.org/10.3390/foods10123136

Capon, R. J., Miller, M., & Rooney, F. (2001). Mirabilin G: A new alkaloid from a southern Australian marine sponge, *Clathria* species. *Journal of Natural Products*, *64*(5), 643–644. https://doi.org/10.1021/NP000564G

Carev, I., Gelemanović, A., Glumac, M., Tutek, K., Dželalija, M., Paiardini, A., & Prosseda, G. (2023). *Centaurea triumfetii* essential oil chemical composition, comparative analysis, and antimicrobial activity of selected compounds. *Scientific Reports*, *13*, 7475. https://doi.org/10.1038/s41598-023-34058-2

Chakraborty, K., & Francis, P. (2021). Callypyrones from marine Callyspongiidae sponge *Callyspongia diffusa*: Antihypertensive bis-γ-pyrone polypropionates attenuate angiotensin-converting enzyme. *Natural Product Research*, *35*(24), 5801–5812. https://doi.org/10.1080/14786419.2020.1837819

Cheema, A. K., Mehta, K. Y., Fatanmi, O. O., Wise, S. Y., Hinzman, C. P., Wolff, J., & Singh, V. K. (2017). A metabolomic and lipidomic serum signature from nonhuman primates administered with a promising radiation countermeasure, gamma-tocotrienol. *International Journal of Molecular Sciences*, *19*(1), 79. https://doi.org/10.3390/ijms19010079

Cheng, M.-C., Ker, Y.-B., Yu, T.-H., Lin, L.-Y., Peng, R. Y., & Peng, C.-H. (2010). Chemical synthesis of 9(*Z*)-octadecenamide and its hypolipidemic effect: A bioactive agent found in the essential oil of mountain celery seeds. *Journal of Agricultural and Food Chemistry*, *58*(3), 1502–1508. https://doi.org/10.1021/jf903573g

Chua, R. W., Song, K. P., & Ting, A. S. Y. (2023). Characterization and antimicrobial activities of bioactive compounds from endophytic *Trichoderma asperellum* isolated from *Dendrobium* orchids. *Biologia*, *79*, 569-584. https://doi.org/10.1007/s11756-023-01562-9

Dechsakulwatana, C., Rungsihiranrut, A., Muangchinda, C., Ningthoujam, R., Klankeo, P., & Pinyakong, O. (2022). Biodegradation of petroleum oil using a constructed nonpathogenic and heavy metal-tolerant bacterial consortium isolated from marine sponges. *Journal of Environmental Chemical Engineering*, *10*(6), 108752. https://doi.org/10.1016/J.JECE.2022.108752

Dunn, E., Zhang, B., Sahota, V. K., & Augustin, H. (2023). Potential benefits of medium chain fatty acids in aging and neurodegenerative disease. *Frontiers in Aging Neuroscience*, *15*, 1230467. https://doi.org/10.3389/FNAGI.2023.1230467

Gao, H., Qi, G., Yin, R., Zhang, H., Li, C., & Zhao, X. (2016). *Bacillus cereus* strain S2 shows high nematicidal activity against *Meloidogyne incognita* by producing sphingosine. *Scientific Reports*, *6*, 28756. https://doi.org/10.1038/srep28756

Hamzalioğlu, A., & Gökmen, V. (2016). Interaction between bioactive carbonyl compounds and asparagine and impact on acrylamide. In V. Gökmen (Ed.), *Acrylamide in food: Analysis, content and potential health effects* (pp. 355–376). Academic Press. https://doi.org/10.1016/B978-0-12-802832-2.00018-8

Harborne, A. J. (1998). *Phytochemical methods: A guide to modern techniques of plant analysis* (3rd ed.). Springer.

Inoue, K., Kubota, S., & Seyama, Y. (1999). Cholestanol induces apoptosis of cerebellar neuronal cells. *Biochemical and Biophysical Research Communications*, *256*(1), 198–203. https://doi.org/10.1006/BBRC.1998.9497

Khatua, S., Pandey, A., & Biswas, S. J. (2016). Phytochemical evaluation and antimicrobial properties of *Trichosanthes dioica* root extract. *Journal of Pharmacognosy and Phytochemistry*, *5*(5), 410–413.

Kilic, M., Orhan, I. E., Eren, G., Okudan, E. S., Estep, A. S., Bencel, J. J., & Tabanca, N. (2021). Insecticidal activity of forty-seven marine algae species from the Mediterranean, Aegean, and Sea of Marmara in connection with their cholinesterase and tyrosinase inhibitory activity. *South African Journal of Botany*, *143*, 435–442. https://doi.org/10.1016/j.sajb.2021.06.038

Kim, M. S., Choi, D., Ha, J., Choi, K., Yu, J.-H., Dumesic, J. A., & Huber, G. W. (2023). Catalytic strategy for conversion of triacetic acid lactone to potassium sorbate. *ACS Catalysis*, *13*(21), 14031–14041. https://doi.org/10.1021/ACSCATAL.3C02775

Laport, M. S., Santos, O. C. S., & Muricy, G. (2009). Marine sponges: Potential sources of new antimicrobial drugs. *Current Pharmaceutical Biotechnology*, *10*(1), 86–105. https://doi.org/10.2174/138920109787048625

Lim, M. W., Yow, Y.-Y., & Gew, L. T. (2023). LC-MS profiling-based non-targeted secondary metabolite screening for deciphering cosmeceutical potential of Malaysian algae. *Journal of Cosmetic Dermatology*, *22*(10), 2810–2815. https://doi.org/10.1111/jocd.15794

Lim, S. C. (2008). *A guide to sponges of Singapore*. Science Centre Singapore.

Ling, Y. S., Lim, L. R., Yong, Y. S., Tamin, O., & Puah, P. Y. (2018). MS-based metabolomics revealing Bornean *Sinularia* sp. extract dysregulated lipids triggering programmed cell death in hepatocellular carcinoma. *Natural Product Research*, *34*(12), 1796-1803. https://doi.org/10.1080/14786419.2018.1531288

Liu, F.-Y., Luo, K.-W., Yu, Z.-M., Co, N.-N., Wu, S.-H., Wu, P., Fung, K.-P., & Kwok, T.-T. (2009). Suillin from the mushroom *Suillus placidus* as potent apoptosis inducer in human hepatoma HepG2 cells. *Chemico-Biological Interactions*, *181*(2), 168–174. https://doi.org/10.1016/J.CBI.2009.07.008

Liu, G. (2009). Stearoyl-CoA desaturase inhibitors: Update on patented compounds. *Expert Opinion on Therapeutic Patents*, *19*(9), 1169–1191. https://doi.org/10.1517/13543770903061311

Lu, W., Su, X., Klein, M. S., Lewis, I. A., Fiehn, O., & Rabinowitz, J. D. (2017). Metabolite measurement: pitfalls to avoid and practices to follow. *Annual Review of Biochemistry*, *86*, 277–304. https://doi.org/10.1146/annurev-biochem-061516-044952

Lv, G., Song, X., & Zhang, Z. (2021). Protective effect of the ethanol extract from *Hericium erinaceus* against ethanol-induced gastric ulcers. *Polish Journal of Food and Nutrition Sciences*, *71*(3), 333–341. https://doi.org/10.31883/pjfns/141560

Mayer, A. M. S., Glaser, K. B., Cuevas, C., Jacobs, R. S., Kem, W., Little, R. D., McIntosh, J. M., Newman, D. J., Potts, B. C., & Shuster, D. E. (2010). The odyssey of marine pharmaceuticals: A current pipeline perspective. *Trends in Pharmacological Sciences*, *31*(6), 255–265. https://doi.org/10.1016/j.tips.2010.02.005

Melawaty, L., & Pasau, K. (2015). The profile of secondary metabolites of sponge *Clathria reinwardtii* extract as a result of Fe accumulation in Spermonde Archipelago. *Advances in Biological Chemistry*, *5*, 266–272.

Minorics, R., Szekeres, T., Krupitza, G., Saiko, P., Giessrigl, B., Wölfling, J., Frank, É., & Zupkó, I. (2011). Antiproliferative effects of some novel synthetic solanidine analogs on HL-60 human leukemia cells *in vitro*. *Steroids*, *76*(1–2), 156–162. https://doi.org/10.1016/j.steroids.2010.10.006

Miyashita, H., Kai, Y., Nohara, T., & Ikeda, T. (2008). Efficient synthesis of α- and β-chacotriosyl glycosides using appropriate donors, and their cytotoxic activity. *Carbohydrate Research*, *343*(8), 1309–1315. https://doi.org/10.1016/j.carres.2008.02.012

Morillo, M., Rojas, J., Lequart, V., Lamarti, A., & Martin, P. (2020). Natural and synthetic derivatives of the steroidal glycoalkaloids of *Solanum* genus and biological activity. *Natural Products Chemistry and Research*, *8*, 371.

Nandiyanto, A. B. D., Oktiani, R., & Ragadhita, R. (2019). How to read and interpret ftir spectroscope of organic material. *Indonesian Journal of Science and Technology*, *4*(1), 97–118. https://doi.org/10.17509/ijost.v4i1.15806

Ngu, E.-L., Tan, C.-Y., Lai, N. J.-Y., Wong, K.-H., Lim, S.-H., Ming, L. C., Tan, K.-O., Phang, S.-M., & Yow, Y.-Y. (2022). *Spirulina platensis* suppressed iNOS and proinflammatory cytokines in lipopolysaccharide-induced BV2 microglia. *Metabolites*, *12*(11), 1147. https://doi.org/10.3390/metabo12111147

Ocean Biodiversity Information System. (n.d.). Clathria *(Thalysias)* reinwardti *Vosmaer, 1880*. https://mapper.obis.org/?taxonid=167774

Ohta, S., Okada, H., Kobayashi, H., Oclarit, J. M., & Ikegami, S. (1993). Clathrynamides A, B, and C: Novel amides from a marine sponge *Clathria* sp. that inhibit cell division of fertilized starfish eggs. *Tetrahedron Letters*, *34*(37), 5935–5938. https://doi.org/10.1016/S0040-4039(00)73818-4

Okechuwuo, P. N. (2020). Evaluation of anti-inflammatory, analgesic, antipyretic effect of eicosane, pentadecane, octacosane, and heneicosane. *Asian Journal of Pharmaceutical and Clinical Research*, *13*(4), 29–35. https://doi.org/10.22159/ajpcr.2020.v13i4.36196

Oogarah, P. N., Ramanjooloo, A., Doorga, J. R. S., Meyepa, C., van Soest, R. W. M., & Marie, D. E. P. (2020). Assessing antioxidant activity and phenolic content of marine sponges from Mauritius waters. *International Journal of Pharmacognosy and Phytochemical Research*, *12*(3), 123–131.

Pervaiz, I., Hasnat, M., Ahmad, S., Khurshid, U., Saleem, H., Alshammari, F., Almansour, K., Mollica, A., Rengasamy, K. R. R., Zainal Abidin, S. A., & Anwar, S. (2022). Phytochemical composition, biological propensities, and *in-silico* studies of *Crateva adansonii* DC.: A natural source of bioactive compounds. *Food Bioscience*, *49*, 101890. https://doi.org/10.1016/j.fbio.2022.101890

Phillips, S., Rao, M. R. K., Prabhu, K., Priya, M., Kalaivani, S., Ravi, A., & Dinakar, S. (2015). Preliminary GC-MS analysis of an Ayurvedic medicine "Kulathadi Kashayam". *Journal of Chemical and Pharmaceutical Research*, *7*(9), 393-400.

Qiu, S., Cai, Y., Yao, H., Lin, C., Xie, Y., Tang, S., & Zhang, A. (2023). Small molecule metabolites: Discovery of biomarkers and therapeutic targets. *Signal Transduction and Targeted Therapy*, *8*, 132. https://doi.org/10.1038/s41392-023-01399-3

Qu, Y., Wang, Y., Hu, Z., Su, C., Qian, C., Pan, J., Zhu, Y., & Shi, A. (2024). Role of metabolomic profile as a potential marker to discriminate membranous nephropathy from IgA nephropathy. *International Urology and Nephrology*, *56*, 635-651. https://doi.org/10.1007/s11255-023-03691-1

Reid, T., Kashangura, C., Chidewe, C., Benhura, M. A., Stray-Pedersen, B., & Mduluza, T. (2019). Characterization of anti-*Salmonella typhi* compounds from medicinal mushroom extracts from

Zimbabwe. *International Journal of Medicinal Mushrooms*, *21*(7), 713–724. https://doi.org/10.1615/INTJMEDMUSHROOMS.V21.I7.80

Rukaiyat, M., Garba, S., & Labaran, S. (2015). Antimicrobial activities of hexacosane isolated from *Sanseveria liberica* (Gerome and Labroy) plant. *Advancement in Medicinal Plant Research*, *3*(3), 120–125.

Sadat, A., & Joye, I. J. (2020). Peak fitting applied to fourier transform infrared and raman spectroscopic analysis of proteins. *Applied Sciences*, *10*(17), 5918. https://doi.org/10.3390/APP10175918

Shah, M. D., Venmathi Maran, B. A., Haron, F. K., Ransangan, J., Ching, F. F., Shaleh, S. R. M., Shapawi, R., Yong, Y. S., & Ohtsuka, S. (2020). Antiparasitic potential of *Nephrolepis biserrata* methanol extract against the parasitic leech *Zeylanicobdella arugamensis* (Hirudinea) and LC-QTOF analysis. *Scientific Reports*, *10*, 22091. https://doi.org/10.1038/s41598-020-79094-4

Shah, M. D., Yong, Y. S., & Iqbal, M. (2014). Phytochemical investigation and free radical scavenging activities of essential oil, methanol extract and methanol fractions of *Nephrolepis biserrata*. *International Journal of Pharmacy and Pharmaceutical Sciences*, *6*(9), 269–277.

Sugrani, A., Natsir, H., Djide, M. N., & Ahmad, A. (2019). Antibacterial and anticancer activity of protein sponges collected from the waters of Kapoposang Island of South Sulawesi, Indonesia. *International Research Journal of Pharmacy*, *10*(1), 82–87.

Tai, B. H., Hang, D. T., Trang, D. T., Yen, P. H., Huong, P. T. T., Nhiem, N. X., Thung, D. C., Thao, D. T., Hoai, N. T., & Kiem, P. V. (2021). Conjugated polyene ketones from the Marine sponge *Clathria* (Thalysias) *reinwardti* (Vosmaer, 1880) and their cytotoxic activity. *Natural Product Communications*, *16*(9). https://doi.org/10.1177/1934578X211043732

Trang, D. T., Hang, D. T. T., Dung, D. T., Bang, N. A., Huong, P. T. T., Yen, P. H., Tai, B. H., Cuc, N. T., An, D. H., Nhiem, N. X., Thung, D. C., & Kiem, P. V. (2022). Chemical constituents of *Clathria reinwardti*. *Vietnam Journal of Chemistry*, *60*(S1), 21–26. https://doi.org/10.1002/vjch.202200053

Uddin, S. J., Grice, D., & Tiralongo, E. (2012). Evaluation of cytotoxic activity of patriscabratine, tetracosane and various flavonoids isolated from the Bangladeshi medicinal plant *Acrostichum aureum*. *Pharmaceutical Biology*, *50*(10), 1276–1280. https://doi.org/10.3109/13880209.2012.673628

Vanitha, V., Vijayakumar, S., Nilavukkarasi, M., Punitha, V. N., Vidhya, E., & Praseetha, P. K. (2020). Heneicosane—A novel microbicidal bioactive alkane identified from *Plumbago zeylanica* L. *Industrial Crops and Products*, *154*, 112748. https://doi.org/10.1016/j.indcrop.2020.112748

Varijakzhan, D., Loh, J.-Y., Yap, W.-S., Yusoff, K., Seboussi, R., Lim, S.-H. E., Lai, K.-S., & Chong, C.-M. (2021). Bioactive compounds from marine sponges: Fundamentals and applications. *Marine Drugs*, *19*(5), 246. https://doi.org/10.3390/md19050246

Velioglu, Y. S., Mazza, G., Gao, L., & Oomah, B. D. (1998). Antioxidant activity and total phenolics in selected fruits, vegetables, and grain products. *Journal of Agricultural and Food Chemistry*, *46*(10), 4113–4117. https://doi.org/10.1021/jf9801973

Venkateshwar, G. T., Krishnaiah, P., Malla Reddy, S., Srinivasulu, M., Rama Rao, M., & Venkateswarlu, Y. (2005). Chemical investigation of the marine sponges *Clathria reinwardti* and *Haliclona cribricutis*. *Indian Journal of Chemistry*, *44B*, 607–610.

Wang, Z.-F., You, Y.-L., Li, F.-F., Kong, W.-R., & Wang, S.-Q. (2021). Research progress of NMR in natural product quantification. *Molecules*, *26*(20), 6308. https://doi.org/10.3390/molecules26206308

Woo, J.-K., Ha, T. K. Q., Oh, D.-C., Oh, W.-K., Oh, K.-B., & Shin, J. (2017). Polyoxygenated steroids from the sponge *Clathria gombawuiensis*. *Journal of Natural Products*, *80*(12), 3224–3233. https://doi.org/10.1021/acs.jnatprod.7b00651

Yong, Y. S., Lim, S.-C., Lee, P.-C., & Ling, Y.-S. (2018). Sponges from North Borneo and their bioactivity against human colorectal cancer cells. *Borneo Journal of Marine Science and Aquaculture*, *2*, 40–47. https://doi.org/10.51200/bjomsa.v2i0.1215

Yoshikawa, M., Morikawa, T., Murakami, T., Toguchida, I., Harima, S., & Matsuda, H. (1999). Medicinal medicinal flowers. I. Aldose reductase inhibitors and three new eudesmane-type sesquiterpenes, Kikkanols A, B, and C, from the flowers of *Chrysanthemum indicum* L. *Chemical and Pharmaceutical Bulletin*, *47*(3), 340–345. https://doi.org/10.1248/cpb.47.340

Zhao, D.-K., Zhao, Y., Chen, S.-Y., & Kennelly, E. J. (2021). *Solanum* steroidal glycoalkaloids: Structural diversity, biological activities, and biosynthesis. *Natural Product Reports*, *38*, 1423–1444. https://doi.org/10.1039/d1np00001b

Zou, Y., Lu, Y., & Wei, D. (2004). Antioxidant activity of a flavonoid-rich extract of *Hypericum perforatum* L . *in vitro*. *Journal of Agricultural and Food Chemistry*, *52*(16), 5032–5039. https://doi.org/10.1021/jf049571r

Pertanika J. Sci. & Technol. 33 (5): 2299 - 2316 (2025)

PERTANIKA JOURNALS

SCIENCE & TECHNOLOGY

Journal homepage: http://www.pertanika.upm.edu.my/

Leveraging Portable Digital Microscopes and CNNs for Chicken Meat Quality Evaluation with AlexNet and GoogleNet

Retno Damayanti*, Muhammad Yonanta Cahyo Prabowo, Yusuf Hendrawan, Mitha Sa'diyah, Rut Juniar Nainggolan and Ulfi Dias Nurul Latifah

Department of Biosystems Engineering, Faculty of Agricultural Technology, Universitas Brawijaya, Jl. Veteran, ZIP 65145, Malang, East Java, Indonesia

ABSTRACT

The global consumption of chicken meat has surged due to its affordability, versatility, and perceived health benefits, making quality and safety crucial for public health and consumer trust. This study developed a non-destructive, real-time method for classifying chicken meat quality by integrating portable digital microscopes with Convolutional Neural Networks (CNNs). High-resolution images were captured using a 1,000× WiFi-enabled digital microscope and analyzed with two advanced CNN architectures, AlexNet and GoogLeNet, to categorize chicken meat into four classes: fresh, carrion, rotten, and formalinized. The methodology included systematic sampling and image preprocessing techniques—such as histogram equalization, noise reduction, and color space transformation—to enhance image quality and model performance. A dataset of 2,000 images was split into training and validation sets, with 600 images reserved for testing. Models were optimized using various hyperparameters, including optimizers Stochastic Gradient Descent with Momentum (SGDM), Adaptive Moment Estimation (Adam), Root Mean Square Propagation (RMSProp), and learning rates (0.0001, 0.00005). Results showed that GoogLeNet, optimized with RMSProp and a 0.00005 learning rate, achieved the highest testing accuracy of 99.15%, outperforming AlexNet's 98.65%. The study highlighted that adaptive optimizers and lower learning rates significantly improve model accuracy and stability. Confusion matrix analysis confirmed high precision in classifying most categories, with minor errors in the rotten category. This approach enhances food safety standards, reduces the distribution of low-quality meat, minimizes food waste, and improves supply chain traceability. The CNN-based system offers the poultry industry a rapid, accurate, and cost-effective solution for automating meat quality assessments, boosting consumer confidence, and supporting global sustainability goals.

Keywords: Chicken meat, CNN, digital microscope, image classification

ARTICLE INFO

Article history:
Received: 31 January 2025
Accepted: 08 April 2025
Published: 28 August 2025

DOI: https://doi.org/10.47836/pjst.33.5.12

E-mail addresses:
damayanti@ub.ac.id (Retno Damayanti)
yonanta17@student.ub.ac.id (Muhammad Yonanta Cahyo Prabowo)
yusuf_h@ub.ac.id (Yusuf Hendrawan)
mithasadiyah338@student.ub.ac.id (Mitha Sa'diyah)
niar.1906.rut@gmail.com (Rut Juniar Nainggolan)
ulfidias@student.ub.ac.id (Ulfi Dias Nurul Latifah)
* Corresponding author

e-ISSN: 2231-8526

INTRODUCTION

The global consumption of chicken meat has witnessed a remarkable surge over recent decades, establishing it as the most consumed meat worldwide, surpassing traditional staples such as beef and pork (Gržinić et al., 2023; Rao, 2015; Sporchia et al., 2023). This trend stems from chicken's affordability, versatility in culinary applications, and its perceived health benefits, further bolstered by rising incomes and urbanization in developing countries, making poultry a staple protein source essential for global food security. Consequently, poultry farming has expanded to meet this growing market demand.

However, the escalation in chicken meat consumption has concurrently amplified concerns regarding meat quality and safety. Ensuring the integrity of chicken meat is paramount, as it directly impacts public health and consumer confidence. Pathogenic contamination, largely due to improper handling and processing, poses severe health risks, including foodborne illnesses (Akhlaghi et al., 2024; Gržinić, 2023). Additionally, the widespread use of antibiotics in poultry farming to promote growth and prevent disease has raised alarms about antibiotic resistance, further complicating food safety dynamics (Akhlaghi et al., 2024). Consumers are becoming increasingly vigilant about these issues, demanding greater transparency and assurance regarding the safety and quality of chicken meat products (Akhlaghi et al., 2024; Gržinić, 2023). This heightened awareness underscores the urgent need for effective quality assessment methods that can ensure the safety and reliability of chicken meat in the supply chain.

Traditional methods for assessing meat quality, including sensory evaluation and chemical analysis, present several significant drawbacks. Sensory evaluation, while useful, is inherently subjective and relies heavily on the expertise and consistency of human assessors, which can lead to variability and potential biases in quality assessments (Damez & Clerjon, 2011; Wu et al., 2022). Chemical analysis methods, although objective, are often time-consuming, expensive, and require specialized training and equipment, making them impractical for routine and large-scale quality monitoring (Damez & Clerjon, 2011; Wu et al., 2022). Moreover, these conventional techniques may not sufficiently address the multifaceted nature of meat quality, particularly in detecting microbial contamination or adulterants that can compromise food safety (Adam, 2021; Akhlaghi et al., 2024; Rebezov et al., 2022; Şahin et al., 2025). In contrast, an automated, CNN-based approach offers faster, more accurate evaluations, reducing reliance on intensive labor and subjective judgment.

Recent advancements in machine learning, particularly in the realm of CNNs, coupled with portable imaging technologies, offer promising avenues to address these challenges. CNNs have revolutionized image processing and classification tasks by enabling the extraction of intricate features from visual data without the need for manual intervention (Alzubaidi et al., 2021; Damez & Clerjon, 2011; Mienye & Swart, 2024). Their application in non-destructive food quality assessments has demonstrated significant potential, allowing

for rapid and accurate classification of meat quality based on image data (Alzubaidi et al., 2021; Damez & Clerjon, 2011; Mienye & Swart, 2024). For example, CNNs have been effectively employed to classify the quality of chicken meat through the analysis of hyperspectral images, which capture a broad spectrum of wavelengths and provide detailed insights into the meat's composition (L. Zhou et al., 2019; Mienye & Swart, 2024). These technological innovations not only enhance the precision of quality assessments but also substantially reduce the time and labor associated with traditional methods (Hwang et al., 2025; Suthar et al., 2024). By enabling real-time, high-accuracy detection of quality attributes, CNN-based systems help prevent the distribution of substandard products, thereby minimizing food waste and improving traceability within the supply chain.

The integration of portable digital microscopes with CNNs represents a significant leap forward in the automation and efficiency of meat quality evaluation. Portable digital microscopes are cost-effective, easy to deploy, and capable of capturing high-resolution images that reveal microstructural details of meat samples (Hwang et al., 2025; Xu et al., 2024). When combined with CNNs, these devices facilitate the real-time, non-destructive analysis of chicken meat, enabling the classification of various quality parameters such as freshness, spoilage, and the presence of adulterants (Hwang et al., 2025; Xu et al., 2024). This synergy not only streamlines the quality assessment process but also aligns with broader sustainability goals by reducing the likelihood of sending poor-quality products to market, which in turn curbs unnecessary waste and bolsters trust through transparent tracking of product integrity. The ability to monitor meat quality in real-time ensures that only safe and high-quality products reach consumers, thereby safeguarding public health and reducing environmental impact through more efficient resource utilization (Damez & Clerjon, 2011; Suthar et al., 2024).

Despite the promising advancements, the application of CNNs and portable imaging devices in meat quality assessment is still evolving, with several challenges remaining. One of the primary challenges is ensuring the generalizability of CNN models across different breeds, storage conditions, and imaging devices. Variations in these factors can significantly affect the performance and accuracy of classification models, necessitating extensive training datasets that encompass diverse scenarios (Damez & Clerjon, 2011; Xu et al., 2024). Additionally, the optimization of CNN hyperparameters, such as learning rates and optimizers, is crucial for achieving optimal performance but remains a complex and often trial-and-error process (Mienye & Swart, 2024). Furthermore, the practical implementation of these technologies in real-world settings requires addressing technical challenges related to device calibration, lighting variations, and data standardization to ensure consistent and reliable performance (Hwang et al., 2025; Suthar et al., 2024).

To address these challenges, this study aims to develop a robust CNN-based classification model utilizing images captured by a portable digital microscope to accurately evaluate chicken meat quality. By leveraging advanced CNN architectures such as

AlexNet and GoogleNet, the research seeks to enhance the accuracy and reliability of meat quality assessments while maintaining cost-effectiveness and operational simplicity. The study further investigates the impact of different optimizers and learning rates on model performance, striving to identify the optimal configuration that maximizes classification accuracy and minimizes computational overhead. Through comprehensive evaluation using a substantial dataset, the research endeavors to validate the efficacy of the proposed method in diverse and realistic conditions, thereby contributing to the advancement of non-destructive, automated meat quality assessment technologies.

METHODOLOGY

Sample Collection and Preparation

Chicken meat samples were sourced from local chicken farmers in Malang, East Java, Indonesia, predominantly consisting of commercial broiler chickens (Ross 308) to ensure a diverse representation of quality categories. The sampling procedure adhered to standardized protocols as outlined by the United States Department of Agriculture (USDA) and International Organization for Standardization (ISO), specifically referencing United States Department of Agriculture – Food Safety and Inspection Service (USDA-FSIS) (2021) and ISO 22000:2018 (ISO, 2018), which emphasize systematic sampling from various parts of the poultry carcass to account for variability in quality attributes such as color, texture, and moisture content (Taheri-Garavand et al., 2019). The procedure was organized as follows:

1. Each sample was categorized into one of four quality classes: (a) fresh chicken, (b) carrion chicken, (c) rotten chicken, and (d) formalinized chicken.
2. Fresh chicken was defined as meat cut within 24 hours post-slaughter, exhibiting bright yellowish-white coloration, clean and shiny skin, and no visible blood traces in muscle fibers.
3. Carrion chicken comprised meat from chickens that died without undergoing the slaughter process, displaying red-patched skin, bleeding in the head and neck, and reddish muscle fibers.
4. Rotten chicken was characterized by greenish-gray discoloration indicative of mold and bacterial growth, resulting from storage for six days in a chiller refrigerator at 2–4°C.
5. Formalinized chicken was obtained by immersing fresh chicken meat in a 10% formalin solution (Merck, Germany) for 24 hours at room temperature, resulting in sticky skin and pale meat (Söderqvist et al., 2024).
6. Each sample was filleted to a uniform size (no more than 7 cm in length and 1 cm in thickness) to ensure consistency in image acquisition.
7. A total of 2,000 digital images were captured, with 500 images per quality category. The dataset was then divided into training and validation sets at a ratio of 70:30, and an additional 600 images were reserved for testing. By ensuring a comprehensive

sampling strategy, this methodology establishes a robust foundation for accurate, real-time classification that surpasses traditional subjective or time-consuming methods, ultimately benefiting the poultry industry through more reliable quality assurance.

The types of chicken meat quality categories can be seen in Figure 1, which consists of four classes, namely fresh chicken, carrion chicken, rotten chicken, and formalinized chicken.

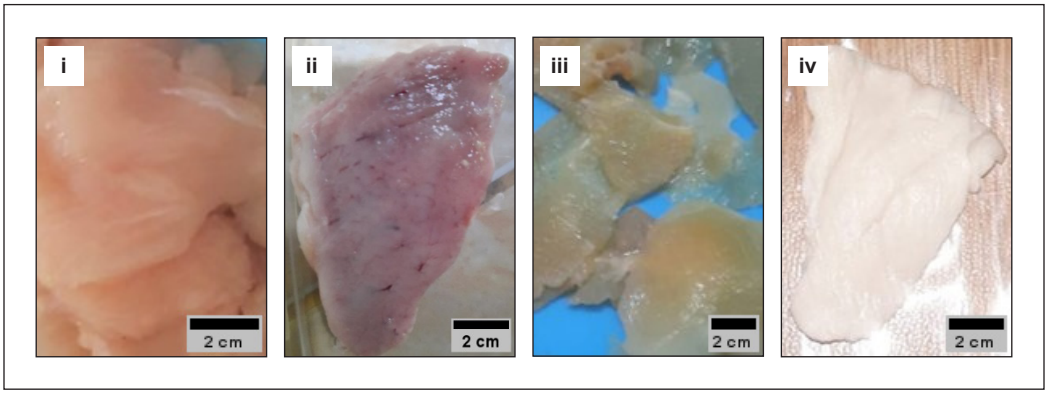

(a)

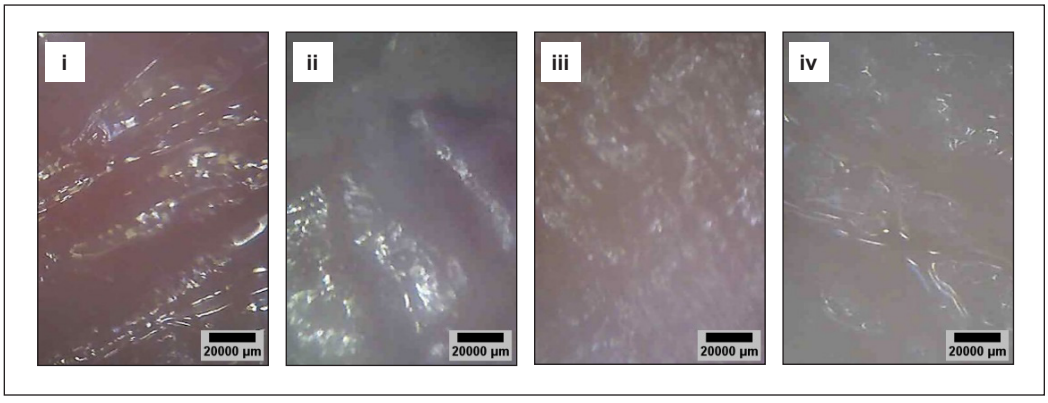

(b)

Figure 1. Image acquisition results in several types of chicken meat quality: (a) Chicken meat before the image acquisition process, (i) fresh sample, (ii) carrion sample, (iii) rotten sample, and (iv) formalinized sample; (b) Image acquisition at 1,000 × magnification level, (i) fresh sample, (ii) carrion sample, (iii) rotten sample, and (iv) formalinized sample

Image Acquisition and Preprocessing

High-resolution images of the chicken meat samples were acquired using an W04 Wi-Fi Portable Digital Microscope (China), Model W04 Wi-Fi Portable Digital Microscope-1000, equipped with a Complementary Metal–Oxide–Semiconductor (CMOS) image sensor, magnification range of 50–1,000×, and a resolution of 960 × 540 pixels. Potential limitations of this microscope include minor variations in magnification accuracy at higher zoom

levels and the possibility of inconsistent focusing under suboptimal lighting conditions. Key steps were as follows:

1. The microscope was connected wirelessly to an Android 5.0 smartphone running HVviewing software, enabling seamless image capture under controlled lighting conditions.
2. An 8 SMD 3528 white light source with a sensitivity of 3V/lux-second was employed to ensure consistent illumination across all samples (Figure 2).
3. CNN models were developed and trained using MATLAB R2021a on an Acer NITRO 5 AN515-52 laptop with an 8th-generation Intel Core i5 processor, 16GB RAM, and a 4GB NVIDIA GeForce GTX 1050 GPU. This setup provided sufficient computational power for high-resolution image data analysis and CNN optimization.
4. Histogram equalization was applied to improve image contrast (Xiong et al., 2021).
5. Noise reduction using Gaussian filters minimized image noise and artifacts (Weli & Abdullah, 2024).
6. Color space transformation converted images from RGB to Lab* color space to facilitate better feature extraction (Lin et al., 2019).
7. Data augmentation (rotation, flipping, scaling) was employed to increase training data diversity, thus preventing overfitting and enhancing model robustness (Dhanya et al., 2022; Natho et al., 2025).

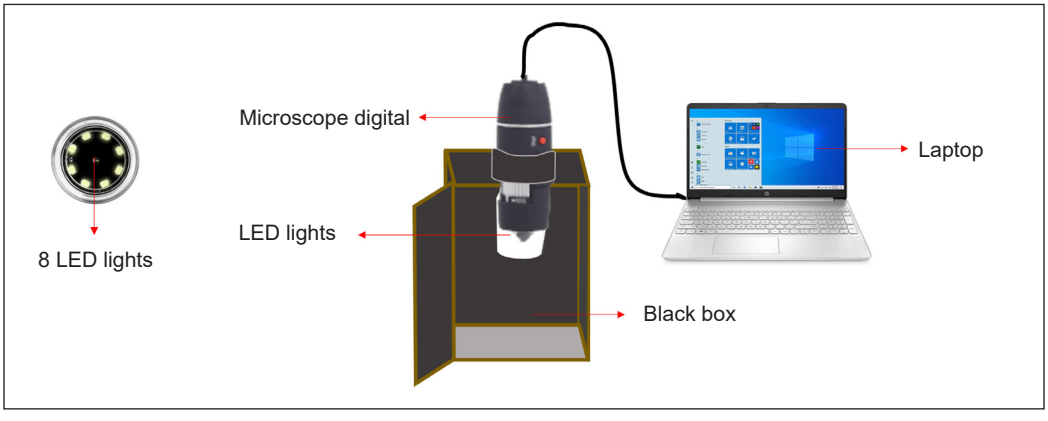

Figure 2. Image acquisition setup using a WiFi digital microscope capturing chicken meat samples under controlled lighting conditions
Note. LED = Light-emitting diode

CNN Model Selection and Hyperparameter Optimization

The study utilized two state-of-the-art CNN architectures, AlexNet and GoogleNet, to perform feature extraction and classification of chicken meat quality. These models were chosen due to their proven efficacy in image classification tasks and their ability to handle

complex feature hierarchies without extensive manual intervention (Alzubaidi et al., 2021; Mienye & Swart, 2024). The architectural models used in this study are AlexNet and GoogleNet. Known for its simplicity and effectiveness in image classification, AlexNet consists of five convolutional layers followed by three fully connected layers, utilizing ReLU activation and dropout for regularization (Alzubaidi et al., 2021). GoogleNet features a more complex architecture with inception modules that allow for parallel convolutional operations, enhancing the network's ability to capture diverse features from the images (Mienye & Swart, 2024).

To optimize the performance of the CNN models, various hyperparameters were systematically tuned, i.e., optimizers, learning rate, epochs and batch size. Three optimizers were evaluated—SGDM, Adam, and RMSProp. Adam was found to perform the best in preliminary studies due to its adaptive learning rate capabilities, which facilitate faster convergence (Li et al., 2022). Two learning rates were tested—0.0001 and 0.00005. A smaller learning rate of 0.00005 was preferred as it provided higher accuracy and stability in the training process (Yoon & Kang, 2023). An optimal epoch of 30 and a batch size of 20 were determined through sensitivity analysis to balance training time and model performance. These careful optimizations ensure that the system can be implemented efficiently in real-world conditions, speeding up decision-making processes and thereby reducing the time window in which suboptimal meat might enter the market.

Evaluation Metrics Analysis

The performance of the CNN models was evaluated using a comprehensive set of metrics to ensure robust and reliable classification results. The primary metrics employed included accuracy, sensitivity, specificity, and confusion matrix. For accuracy, the proportion of correctly classified instances out of the total instances. Sensitivity is needed for the model to correctly identify positive instances within each class, and specificity is needed to correctly identify negative instances. Confusion Matrix provided a detailed breakdown of true positive, false positive, true negative, and false negative classifications for each quality category.

The dataset was split into 70% for training and 30% for validation, ensuring that the model was trained on a diverse set of samples and validated against unseen data to assess generalization. An independent test set of 600 images, not included in the training or validation sets, was used to evaluate the final model performance, thereby providing an unbiased assessment of the model's accuracy and reliability. By leveraging such standardized evaluation protocols, this methodology fosters confidence in the model's real-world applicability, supporting the poultry industry's need for a scalable tool that can be seamlessly integrated into existing quality control workflows.

CNN was used as a modeling method for the classification of chicken meat quality as shown in Figure 3. After the CNN model was built, the CNN model was tested using 600

testing data taken on meat samples outside the training and validation data samples. This study used two pre-trained CNN models, i.e., AlexNet and GoogLeNet. The optimizer variations used in this study included SGDM, Adam, and RMSProp. Variations in learning rate were also carried out at values of 0.0001 and 0.00005. The best CNN model testing process was carried out using the confusion matrix method, using testing data. Such a data-driven, efficient methodology not only surpasses traditional methods in speed and consistency but also supports enhanced traceability and resource management by enabling precise quality checks at critical points in the supply chain.

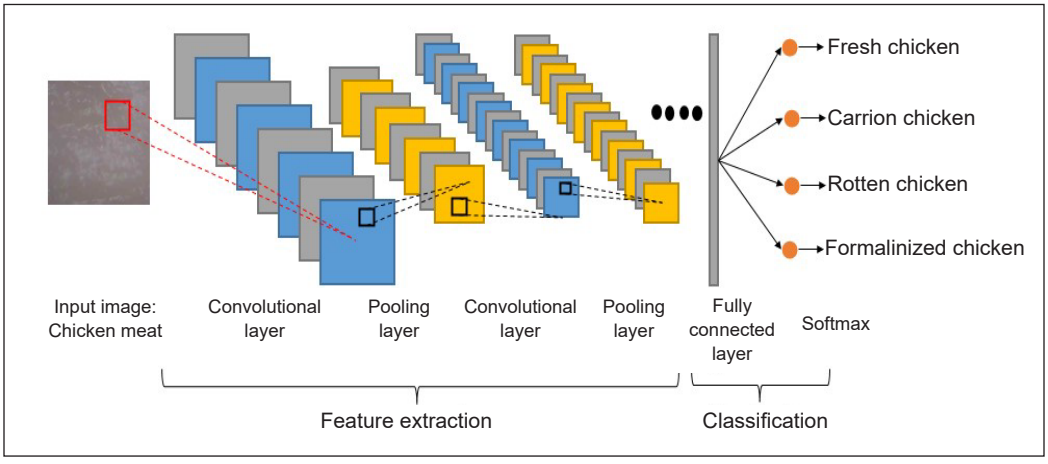

Figure 3. **C**onvolutional **N**eural **N**etwork structure to classify four types of chicken meat quality

RESULTS AND DISCUSSION

Classification Performance

The primary objective of this study was to evaluate the effectiveness of two state-of-the-art CNN architectures, AlexNet and GoogLeNet, in classifying chicken meat quality into four distinct categories: fresh, carrion, rotten, and formalinized. The classification performance was assessed using a comprehensive dataset comprising 2,000 images for training and validation (70:30 split) and an independent test set of 600 images. Table 1 summarizes the validation and testing accuracies achieved by each CNN model combined with different optimizers and learning rates. The highest testing accuracy of 99.15% was achieved using GoogLeNet with the RMSProp optimizer and a learning rate of 0.00005.

The results indicate that both CNN architectures are highly effective in classifying chicken meat quality, with overall testing accuracies exceeding 95% across most configurations. Notably, GoogLeNet outperformed AlexNet in most scenarios, achieving a maximum testing accuracy of 99.15% compared to AlexNet's highest accuracy of 98.65%. This aligns with previous studies highlighting the superior feature extraction capabilities

Table 1
CNN performance based on validation and testing data accuracy

Pre-trained CNN	Optimizer	Learning rate	Validation accuracy (%)	Testing accuracy (%)
GoogLeNet	SGDM	0.0001	96.17	96.82
	SGDM	0.00005	92.00	95.17
	Adam	0.0001	99.00	96.32
	Adam	0.00005	97.17	96.82
	RMSProp	0.0001	98.50	97.85
	RMSProp*	**0.00005**	**97.83**	**99.15**
AlexNet	SGDM	0.0001	97.67	96.50
	SGDM	0.00005	94.50	96.17
	Adam	0.0001	98.00	95.67
	Adam*	**0.00005**	**98.50**	**98.65**
	RMSProp	0.0001	95.50	91.32
	RMSProp	0.00005	94.00	94.50

Note. CNN = **C**onvolutional **N**eural **N**etwork; SGDM = Stochastic Gradient Descent with Momentum; Adam = Adaptive Moment Estimation; RMSProp = Root Mean Square Propagation; * = Optimizer and learning-rate pairing yielded optimal performance

of deeper and more complex architectures like GoogLeNet in image classification tasks (Aguilar et al., 2018; Mienye & Swart, 2024). This level of performance surpasses traditional sensory or chemical assessments, providing the poultry industry with a rapid, objective, and more accurate tool for ensuring product quality.

Comparison of CNN Architecture

The comparative analysis between AlexNet and GoogLeNet reveals significant differences in their classification performances. GoogLeNet consistently achieved higher accuracies across various optimizer and learning rate settings compared to AlexNet. GoogLeNet top performance (99.15%) with RMSProp and a learning rate of 0.00005, along with validation accuracies as high as 99.00%, underscores the advantages of deeper and more complex architectures capable of capturing diverse features (Aguilar et al., 2018; Mienye & Swart, 2024). These improvements mean that producers and processors can identify quality issues earlier and more reliably, allowing them to take corrective action before inferior products reach consumers.

Optimizer and Learning Rates

The study evaluated three different optimizers (SGDM, Adam, and RMSProp) and two learning rates (0.0001 and 0.00005) to determine their effects on the CNN models' performance. Adam and RMSProp, with their adaptive learning rate capabilities, yielded superior results compared to SGDM. RMSProp, in particular, produced the highest

testing accuracy of 99.15%. A lower learning rate of 0.00005 consistently resulted in improved accuracy and training stability, aligning with literature suggesting that fine-tuning hyperparameters enhances model performance (Kingma & Ba, 2014; Loshchilov & Hutter, 2016). Such optimized models can be seamlessly integrated into quality control workflows, improving the speed and consistency of assessments. By ensuring that only top-quality meat moves forward, this reduces the chance of spoilage in the supply chain, thereby minimizing waste and contributing to better traceability as each batch's quality is verified before distribution.

Training and Validation

The training and validation processes were closely monitored to assess the convergence behavior and potential overfitting of the models. Figure 4 illustrates the accuracy and loss curves for the best-performing configurations of GoogLeNet and AlexNet, respectively. Monitoring training and validation processes revealed stable convergence and minimal overfitting. GoogLeNet stabilized around epoch 8 and AlexNet by epoch 5, indicating efficient training. The rapid convergence and stable learning curves attest to the suitability of the chosen architectures and hyperparameters, as well as the efficacy of preprocessing and augmentation steps. This training efficiency also suggests that the system can be deployed in real-world conditions without excessive computational demands, supporting scalability and wider adoption. As a result, even smaller producers or distributors can employ this technology, enhancing industry-wide standards and ensuring high-quality meat reaches consumers.

Confusion Matrix Analysis

Confusion matrices were employed to provide a detailed breakdown of the classification performance across the four meat quality categories. Figure 5 present the confusion matrices for the best-performing GoogLeNet and AlexNet models, respectively. Confusion matrices were used to analyze classification performance across the four categories. GoogLeNet accurately classified 99.30% of fresh, carrion, and formalinized samples, and AlexNet also demonstrated strong performance, albeit with slightly more misclassifications in the rotten category. The primary confusion involved rotten and fresh classes, likely due to subtle visual similarities. Carrion and formalinized classes were occasionally confused, indicating overlapping color and texture features.

These results indicate that both models perform exceptionally well in classifying most categories, with GoogLeNet slightly outperforming AlexNet in overall accuracy. The Rotten category remains the most challenging, particularly for AlexNet, which experienced higher misclassification rates compared to GoogLeNet. This aligns with literature suggesting that more complex architectures like GoogLeNet can better handle subtle differences

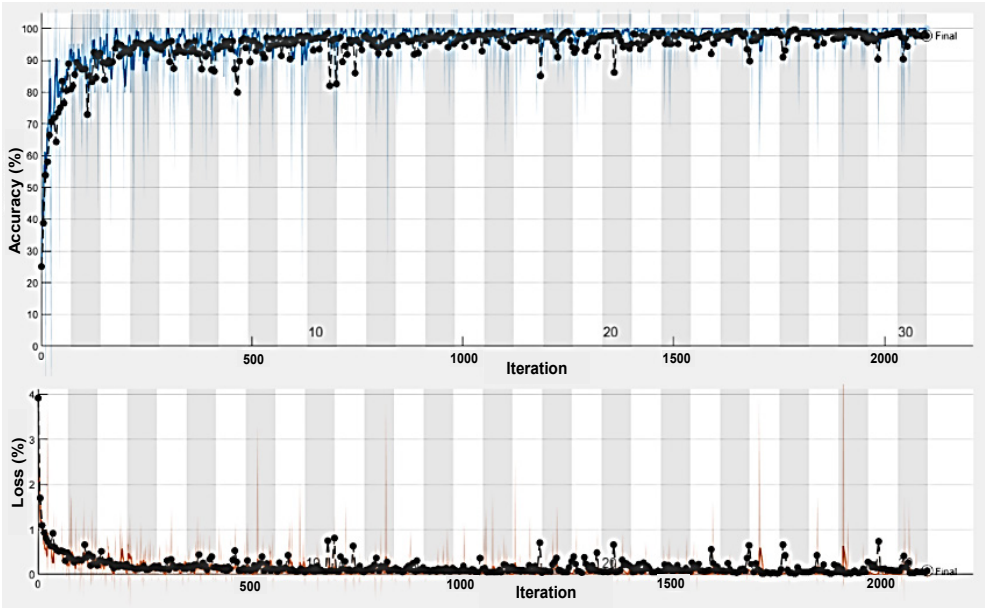

(a)

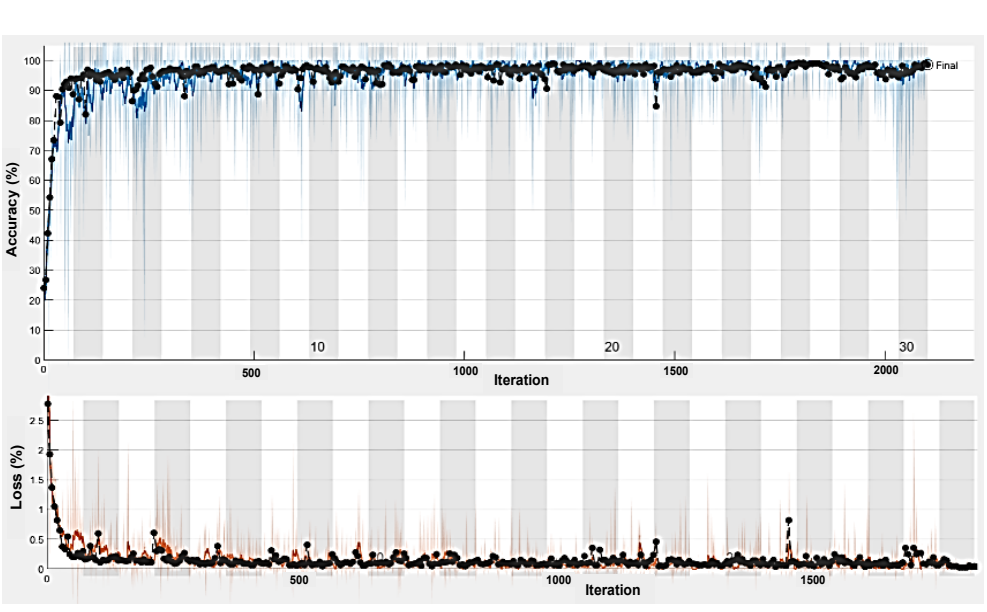

(b)

Figure 4. CNN's learning process for the classification of types of chicken meat quality: (a) GoogLeNet with RMSProp optimizer and learning rate of 0.00005; (b) AlexNet with Adam optimizer and learning rate of 0.00005
Note. CNN = **C**onvolutional **N**eural **N**etwork; RMSProp = Root Mean Square Propagation; Adam = Adaptive Moment Estimation

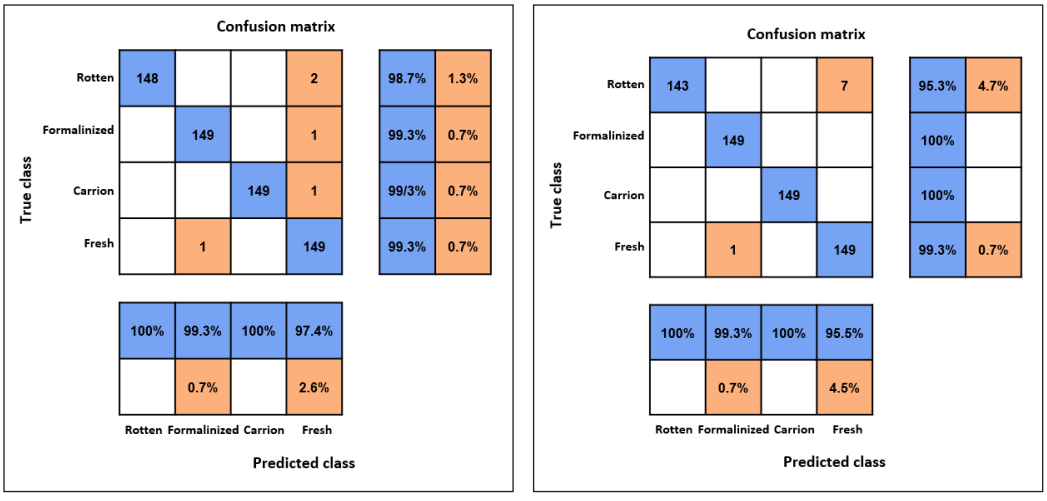

(a) (b)

Figure 5. The results of the confusion matrix on testing data: (a) GoogLeNet with RMSProp optimizer and learning rate of 0.00005; (b) AlexNet with Adam optimizer and learning rate of 0.00005
Note. RMSProp = Root Mean Square Propagation; Adam = Adaptive Moment Estimation

in image features (Aguilar et al., 2018; Mienye & Swart, 2024). Despite these minor misclassifications, the overall high precision of the models ensures that the poultry industry can rely on this tool to maintain quality standards. By flagging questionable products early, the system helps prevent low-quality items from entering the supply chain, reducing waste and enhancing traceability because each product can be monitored, identified, and, if necessary, removed at an earlier stage.

Error Analysis and Misclassification Patterns

An in-depth error analysis was conducted to understand the misclassification patterns and underlying causes. The primary misclassifications observed were between the rotten and fresh categories, as well as between carrion and formalinized categories. For both CNN models, the rotten category had the lowest classification accuracy. In GoogLeNet, 2 out of 150 rotten samples were misclassified as fresh, while in AlexNet, 7 out of 150 were misclassified as fresh. These misclassifications could be attributed to the visual similarities between severely spoiled meat and fresh meat under certain imaging conditions, such as lighting variations or surface moisture levels. This finding is consistent with studies that highlight challenges in distinguishing between similar visual attributes in food quality assessments (Aguilar et al., 2018; Mienye & Swart, 2024). Minor misclassifications occurred between carrion and formalinized categories. For instance, GoogLeNet misclassified 1 carrion sample as formalinized, and AlexNet did not misclassify any carrion samples. These errors may result from overlapping visual features, such as redness in

carrion meat and discoloration in formalinized meat, which can confuse the CNN models. Similar patterns have been observed in other food quality classification studies, where certain quality attributes present overlapping visual characteristics that pose challenges for automated classification systems (Aguilar et al., 2018). Minor misclassifications occurred between carrion and formalinized categories. For instance, GoogLeNet misclassified 1 carrion sample as formalinized, and AlexNet did not misclassify any carrion samples. Minor misclassifications between carrion and formalinized categories may stem from visual similarities in redness and discoloration. Techniques like Gradient-weighted Class Activation Mapping (Grad-CAM) (Saadallah et al., 2022) could further refine the models by highlighting which image features lead to errors, guiding improvements in preprocessing or model architecture. By continually refining and improving model accuracy through such feedback loops, this approach ensures ongoing adaptability and robustness, making it more effective at preventing off-quality products from reaching consumers and sustaining a transparent, trustworthy supply chain.

Model Robustness and Generalization

Testing on an independent dataset validated the model's robustness, with GoogLeNet achieving 99.15% and AlexNet 98.65% accuracy. This indicates strong generalization and suggests that the models can perform well under varied conditions. While the study focused on a single dataset, future work could explore cross-dataset validation to ensure broad applicability. Diversifying the dataset with samples from multiple regions, breeds, and storage conditions could further enhance robustness and make the technology even more attractive for global adoption.

The high performance of the models suggests that the dataset was sufficiently diverse, capturing a wide range of quality attributes and variations within each category. This diversity is crucial for training CNNs to recognize and accurately classify subtle differences in meat quality, enhancing their generalization performance (Elmasry & Abdullah, 2024; L. Zhou et al., 2019). The models' ability to maintain high accuracy on an independent test set indicates their potential for real-world implementation in poultry supply chains. By integrating these CNN models with portable digital microscopes, it is feasible to deploy automated, real-time quality assessment systems that can operate reliably in various environmental conditions, thereby ensuring consistent meat quality and safety (Hwang et al., 2025; Xu et al., 2024). Such systems can be instrumental in enhancing operational efficiency, reducing reliance on labor-intensive traditional methods, and providing immediate feedback for quality control processes.

The training process for both CNN models was efficient, with GoogLeNet converging faster than AlexNet due to its deeper architecture and more sophisticated feature extraction mechanisms. The use of adaptive optimizers like RMSProp and Adam significantly reduced

the number of epochs required for convergence, aligning with findings that adaptive learning rate methods enhance training efficiency and model performance (Szegedy et al., 2015). This efficiency is particularly advantageous for practical deployments where computational resources and time are constrained. Throughout the training process, both models exhibited stable learning curves, with minimal fluctuations in accuracy and loss metrics. This stability is indicative of the models' resilience to overfitting and their ability to consistently learn relevant features from the image data (Alzubaidi et al., 2021; Mienye & Swart, 2024). The balanced training and validation curves suggest that the models maintained a healthy generalization capacity, avoiding the pitfalls of overfitting that can plague complex neural network architectures.

The successful implementation of high-performing models on a relatively modest computational setup (Acer NITRO 5 AN515-52 laptop with an NVIDIA GeForce GTX 1050 GPU) suggests that the proposed system is scalable and can be adapted to various hardware configurations. This scalability is essential for practical deployment in diverse settings, ranging from small-scale farms to large poultry processing facilities (Natho et al., 2025). The use of pre-trained CNN models facilitates transfer learning, allowing for rapid adaptation to new environments and meat types with minimal retraining, thereby enhancing the system's flexibility and applicability (Saadallah et al., 2022). Despite the high accuracies achieved, certain limitations were noted. The rotten category exhibited slightly lower accuracy, particularly in AlexNet, indicating a need for further refinement in distinguishing highly spoiled meat from fresh samples. Additionally, the study was conducted under controlled laboratory conditions, which may not fully replicate the variability encountered in real-world environments (Nayeem et al., 2025).

The models' impressive performance in accurately classifying chicken meat quality has direct implications for the poultry industry. Unlike traditional methods that are subjective, time-intensive, or costly, this CNN-based approach delivers rapid, objective, and repeatable evaluations. By implementing this system, producers can detect low-quality meat at an earlier stage, ensuring that only safe, high-quality products reach the market. This not only builds consumer confidence but also reduces waste by preventing substandard meat from advancing through the supply chain. Moreover, improved traceability results from consistent, documented quality assessments, allowing stakeholders to quickly identify and address issues. These factors collectively support industry-wide upgrades in safety, efficiency, and resource management, ultimately encouraging the technology's scalable and global implementation.

Precise identification of meat quality can significantly reduce food waste by ensuring that only genuinely spoiled or adulterated meat is discarded while retaining consumable products. This efficient utilization of resources aligns with global sustainability goals, promoting environmental stewardship by minimizing the environmental footprint associated with poultry farming and meat processing (Kilibarda et al., 2023; Suthar et al., 2024). By

implementing automated quality assessment systems, the poultry industry can achieve more sustainable operations, reducing both economic and environmental losses linked to food waste. The integration of portable digital microscopes and CNNs facilitates enhanced traceability within the poultry supply chain. Real-time monitoring and documentation of meat quality at various stages of processing and distribution ensure that any issues can be swiftly identified and addressed. This traceability not only enhances food safety by enabling quick identification of contamination sources but also fosters accountability and transparency, thereby increasing stakeholder trust and industry credibility (B. Zhou et al., 2016; El-tahlawy et al., 2025; Suthar et al., 2024).

CONCLUSION

This study successfully demonstrated the integration of portable digital microscopes with advanced CNNs for the accurate classification of chicken meat quality. It provides a robust framework for developing automated, real-time quality assessment systems that align with global food safety and sustainability objectives. By employing two state-of-the-art CNN architectures, AlexNet and GoogLeNet, the research achieved high classification accuracies, with GoogLeNet outperforming AlexNet by attaining a testing accuracy of 99.15% compared to AlexNet's 98.65%. These results affirm that this CNN-based approach surpasses traditional, labor-intensive, and time-consuming methods in both speed and objectivity, providing the poultry industry with a more efficient tool for routine quality assessments. The findings highlight the critical role of optimizer selection and learning rate tuning in enhancing model performance. Adaptive optimizers such as RMSProp and Adam significantly improved classification accuracies and training stability, aligning with existing literature that underscores the effectiveness of these optimizers in complex image processing applications. Additionally, the utilization of a lower learning rate (0.00005) was instrumental in achieving higher accuracy and preventing overfitting, ensuring robust model performance. Beyond mere accuracy improvements, the proposed technology contributes to reducing food waste and improving traceability by quickly identifying low-quality meat before it advances through the supply chain. This early detection prevents substandard products from reaching consumers, thereby minimizing discard rates and enabling stakeholders to maintain detailed quality records that enhance transparency. Implementing such a system not only bolsters consumer confidence and meets regulatory requirements but also fosters a more sustainable and accountable industry. In terms of real-world implementation, the cost-effective, portable nature of the digital microscope-CNN framework supports scalability across different operational scales—from large processing plants to smaller farms. By facilitating timely, data-driven decisions about product quality, this approach is poised to streamline existing workflows, reduce reliance on specialized personnel, and integrate seamlessly into diverse supply chain environments.

ACKNOWLEDGEMENTS

This work was supported by Hibah Professor Research Grant Number 6583, Universitas Brawijaya, Malang, Indonesia, for the year 2024.

REFERENCES

Adam, S. S. M. (2021). Sensory and instrumental methods of meat evaluation: A review. *International Journal of Food Science and Agriculture*, *5*(4), 627–638. https://doi.org/10.26855/ijfsa.2021.12.010

Aguilar, E., Remeseiro, B., Bolaños, M., & Radeva, P. (2018). Grab, pay, and eat: Semantic food detection for smart restaurants. In *IEEE Transactions on Multimedia* (Vol. 20, No. 12, pp. 3266–3275). IEEE. https://doi.org/10.1109/TMM.2018.2831627

Akhlaghi, H., Javan, A. J., & Chashmi, S. H. E. (2024). *Helicobacter pullorum* and *Helicobacter canadensis*: Etiology, pathogenicity, epidemiology, identification, and antibiotic resistance implicating food and public health. *International Journal of Food Microbiology*, *413*, 110573. https://doi.org/10.1016/j.ijfoodmicro.2024.110573

Alzubaidi, L., Zhang, J., Humaidi, A.J., Al-Dujaili, A., Duan, Y., Al-Shamma, O., Santamaría, J. Fadhel, M. A., Al-Amidie, M., & Farham, L. (2021). Review of deep learning: concepts, CNN architectures, challenges, applications, future direction. *Journal of Big Data*, *8*, 53. https://doi.org/10.1186/s40537-021-00444-8

Damez, J.-L., & Clerjon, S. (2011). Recent advances in meat quality assessment. In Y. H. Hui (Ed.), *Handbook of meat and meat processing* (2nd ed.). CRC Press. https://doi.org/10.1201/b11479-12

Dhanya, V. G., Subeesh, A., Kushwaha, N. L., Vishwakarma, D. K., Kumar, T. N., Ritika, G., & Singh, A. N. (2022). Deep learning based computer vision approaches for smart agricultural applications. *Artificial Intelligence in Agriculture*, *6*, 211-299. https://doi.org/10.1016/j.aiia.2022.09.007

Elmasry, A., & Abdullah, W. (2024). An efficient CNN-based model for meat quality assessment: The role of artificial intelligence towards sustainable development. *Precision Livestock*, *1*, 66-74. https://doi.org/10.61356/j.pl.2024.1235

El-tahlawy, A. S., Alawam, A. S., Rudyan, H. A., Allam, A. A., Mahmoud, R., El-Raheem, H. A., & Alahmad, W. (2025). Advanced analytical and digital approaches for proactive detection of food fraud as an emerging contaminant threat. *Talanta Open*, *12*, 100499. https://doi.org/10.1016/j.talo.2025.100499

Gržinić, G., Piotrowicz-Cieślak, A., Klimkowicz-Pawlas, A., Górny, R. L., Ławniczek-Wałczyk, A., Piechowicz, L., Olkowska, E., Potrykus, M., Tankiewicz, M., Krupka, M., Siebielec, G., & Wolska, L. (2023). Review: Intensive poultry farming: A review of the impact on the environment and human health. *Science of The Total Environment*, *858*(Part 3), 160014. https://doi.org/10.1016/j.scitotenv.2022.160014

Hwang, Y.-H., Samad, M., Muazzam, A., Nurul Alam, A. M. M., & Joo, S.-T. (2025). *A comprehensive review of (AI)-driven approaches to meat quality evaluation. Korean Journal for Food Science of Animal Resources, 45*(4), 998-1013. https://doi.org/10.5851/kosfa.2025.e32

International Organization for Standardization. (2018). *ISO 22000:2018: Food safety management systems — Requirements for any organization in the food chain*. ISO. https://www.iso.org/standard/65464.html

Kilibarda, N., Karabasil, N., & Stojanović, J. (2023). Meat matters: Tackling food loss and waste in the meat sector. *Meat Technology*, *64*(2), 177-182. https://doi.org/10.18485/meattech.2023.64.2.32

Kingma, D. P., & Ba, J. (2014). *Adam: A method for stochastic optimization*. arXiv. https://doi.org/10.48550/arXiv.1412.6980

Li, Z., Liu, F., Yang, W., Peng, S., & Zhou, J. (2022). A survey of convolutional neural networks: analysis, applications, and prospects. In *IEEE Transactions on Neural Networks and Learning Systems* (Vol. 33, No. 12, pp. 6999-7019). IEEE. https://doi.org/10.1109/TNNLS.2021.3084827

Lin, P., Xiaoli, L., Li, D., Jiang, S., Zou, Z., Lu, Q., & Chen, Y. (2019). Rapidly and exactly determining postharvest dry soybean seed quality based on machine vision technology, *Scientific Reports*, *9*, 17143. https://doi.org/10.1038/s41598-019-53796-w

Loshchilov, I., & Hutter, F. (2016). *SGDR: Stochastic gradient descent with warm restarts*. arXiv. https://doi.org/10.48550/arXiv.1608.03983

Mienye, I. D., & Swart, T. G. (2024). A comprehensive review of deep learning: Architectures, recent advances, and applications. *Information*, *15*(12), 755. https://doi.org/10.3390/info15120755

Natho, P., Boonying, S., Bonguleaum, P., Tantidontanet, N., & Chamuthai, L. (2025). An enhanced machine vision system for smart poultry farms using deep learning. *Smart Agricultural Technology*, *12*, 101083. https://doi.org/10.1016/j.atech.2025.101083

Nayeem, M., Rahman, M. H., Rhman, M. A., Haque, M. N., & Hashem, M. A. (2025). *Advancing the meat industry with machine learning: A study of progress, challenges, and potential. Meat Research*, *5*(2), 113. https://doi.org/10.55002/mr.5.2.113

Rao, R. S. (2015). Trends and challenges of poultry industry. *International Journal of Engineering and Technologies and Management Research*, *1*(1), 8-13. https://doi.org/10.29121/ijetmr.v1.i1.2015.21

Rebezov, M., Chughtai, M. F. J., Mehmood, T., Khaliq, A., Tanweer, S., Semenova, A., Khayrullin, M., Dydykin, A., Burlankov, S., Thiruvengadam, M., Shariati, M. A., & Lorenzo, J. M. (2022). Novel techniques for microbiological safety in meat and fish industries. *Applied Sciences*, *12*(1), 319. https://doi.org/10.3390/app12010319

Saadallah, A., Büscher, J., Abdulaaty, O., Panusch, T., Deuse, J., & Morik, K. (2022). Explainable predictive quality inspection using deep learning in electronics manufacturing. *Procedia CIRP*, *107*, 594-599. https://doi.org/10.1016/j.procir.2022.05.031

Şahin, D., Torkul, O., Şişci, M., Diren, D. D., Yilmaz, R., & Kibar, A. (2025). Real-time classification of chicken parts in the packaging process using object detection models based on deep learning. *Processes*, *13*(4), 1005. https://doi.org/10.3390/pr13041005

Söderqvist, K., Peterson, M., Johansson, M., Olsson, V., & Boqvist, S. (2024). *A microbiological and sensory evaluation of modified atmosphere-packed (MAP) chicken at use-by date and beyond. Foods*, *13*(13), 2140. https://doi.org/10.3390/foods13132140

Sporchia, F., Galli, A., Kastner T., Pulselli F. M., & Caro, D. (2023). The environmental footprints of the feeds used by the EU chicken meat industry. *Science of the Total Enviroment*, *886*, 163960. https://doi.org/10.1016/j.scitotenv.2023.163960

Suthar, A. P., Shindi, S. H., Kathiriya, J. B., Sharma, A. K., Singh, V. K., & Bhedi, K. R. (2024). Use of artificial intelligence (AI) in ensuring quality and safety of food of animal origin: A review. *International Journal of Veterinary Sciences and Animal Husbandry*, *9*(2S), 240-247. https://doi.org/10.22271/veterinary.2024.v9.i2Sd.1294

Szegedy, C., Liu, W., Jia, Y., Sermanet, P., Reed, S., Anguelov, D., Vanhoucke, V., & Radosavovic, I. (2015). Going deeper with convolutions. In *IEEE Conference on Computer Vision and Pattern Recognition* (pp. 1-9). IEEE. https://doi.org/10.1109/CVPR.2015.7298594

Taheri-Garavand, A., Fatahi, S., Omid, M., & Makino, Y. (2019). Meat quality evaluation based on computer vision technique: A review. *Meat Science*, *156*, 183-195. https://doi.org/10.1016/j.meatsci.2019.06.002

United States Department of Agriculture – Food Safety and Inspection Service. (2021). *USDA food safety and inspection service annual sampling summary report*. https://www.fsis.usda.gov/sites/default/files/media_file/2022-02/FY2021-Sampling-Summary-Report.pdf

Weli, M. M., & Abdullah, O. M. (2024). Digital image noise reduction based on proposed smoothing and sharpening filters. *The Indonesian Journal of Computer Science*, *13*(4), 5001–5021. https://doi.org/10.33022/ijcs.v13i4.4151

Wu, X., Liang, X., Wang, Y., Wu, B., & Sun, J. (2022). Non-destructive techniques for the analysis and evaluation of meat quality and safety: A review. *Foods***,** *11*(22), 3713. https://doi.org/10.3390/foods11223713

Xiong, J., Yu, D., Wang, Q., Shu, L., Cen, J., Liang, Q., Chen, H., & Sun, B. (2021). Application of histogram equalizationfor image enhancement in corrosion areas. *Shock and Vibration*, *2021*, 8883571. https://doi.org/10.1155/2021/8883571

Xu, Z., Han, Y., Zhao, D., Li, K., Li, J., Dong, J., Shi, W., Zhao, H., & Bai, Y. (2024). *Research progress on quality detection of livestock and poultry meat based on machine vision, hyperspectral and multi-source information fusion technologies.* ***Foods*****,** ***13***(3), 469. https://doi.org/10.3390/foods13030469

Yoon, T., & Kang, D. (2023). Multi-modal stacking ensemble for the diagnosis of cardiovascular diseases. *Journal of Personalized Medicine*, *13*(2), 373. https://doi.org/10.3390/jpm13020373

Zhou, B., Khosla, A., Lapedriza, A., Oliva, A., & Torralba, A. (2016). Learning deep features for discriminative localization. In *IEEE Conference on Computer Vision and Pattern Recognition* (pp. 2921–2929). IEEE. https://doi.org/10.1109/CVPR.2016.319

Zhou, L., Zhang, C., Liu, F., Qiu, Z., & He, Y. (2019). Application of deep learning in food: A review. *Comprehensive Reviews in Food Science and Food Safety*, *18*(6), 1793-1811. https://doi.org/10.1111/1541-4337.12492

Pertanika J. Sci. & Technol. 33 (5): 2317 - 2337 (2025)

PERTANIKA JOURNALS

SCIENCE & TECHNOLOGY

Journal homepage: http://www.pertanika.upm.edu.my/

Comparative Analysis of Single and Multiple Change Points Detection for Streamflow Variations

Siti Hawa Mohd Yusoff[1], Firdaus Mohamad Hamzah[2,3,5]*, Othman Jaafar[3], Norshahida Shaadan[4], Lilis Sulistyorini[5] and R. Azizah[5]

[1]Department of Computing, Faculty of Communication, Visual Art and Computing, Universiti Selangor, 45600 Bestari Jaya, Selangor, Malaysia
[2]Department of Mathematics, Centre for Defence Foundation Studies, Universiti Pertahanan Nasional Malaysia, Kem Sungai Besi, 57000 Sungai Besi, Kuala Lumpur, Malaysia
[3]Institute of Climate Change, Universiti Kebangsaan Malaysia, 43600 Bangi, Selangor, Malaysia
[4]School of Mathematical Sciences, College of Computing, Informatics and Mathematics, Universiti Teknologi MARA, 40450 Shah Alam, Selangor, Malaysia
[5]Faculty of Public Health, Universitas Airlangga, Kampus-C, Jalan Mulyorejo, Surabaya 60115, Indonesia

ABSTRACT

Abrupt changes in streamflow patterns significantly affect hydrological systems, making their detection critical for effective water resource management. This study uses the annual maximum streamflow (AMS) data to analyze and identify changes at the Kajang Station in the Langat Basin, Selangor, Malaysia. The objective of research is to determine the precise years of abrupt changes in streamflow and examine the underlying factors causing them. The problem lies in the increasing frequency and intensity of streamflow changes that could be related to factors such as changes in land use and climate variation, which require detailed investigation. This study conducts six complementary statistical tests to identify change points in the streamflow data. Six complementary statistical tests were conducted to identify change points. The Pettitt test (statistic: 276, *p*-value: 0.001), Buishand range test (statistic: 1.5881, *p*-value: 0.034), and standard normal homogeneity test (statistic: 11.349, *p*-value: 0.009) consistently identified 2003 as a significant single change point. For multiple change points, the sequential Mann-Kendall test indicated shifts in 2002 and 2007. The multiple structural change method and classification and regression trees revealed significant change points in 1985, 2003, and 2009. These changes are likely due to the 1982 massive flood event and subsequent changes in land use and river encroachments. The findings

ARTICLE INFO

Article history:
Received: 27 December 2024
Accepted: 11 June 2025
Published: 28 August 2025

DOI: https://doi.org/10.47836/pjst.33.5.13

E-mail addresses:
hawa.yusoff@unisel.edu.my (Siti Hawa Mohd Yusoff)
firdaus.hamzah@upnm.edu.my (Firdaus Mohamad Hamzah)
ojaafar@gmail.com (Othman Jaafar)
shahida@tmsk.uitm.edu.my (Norshahida Shaadan)
l.sulistyorini@fkm.unair.ac.id (Lilis Sulistyorini)
azizah@fkm.unair.ac.id (R. Azizah)
* Corresponding author

underscore the importance of monitoring and managing river systems, especially given the rapidly occurring environmental changes. It is vital to understand these change points to develop more resilient strategies for water resource management.

Keywords: Buishand range test, classification and regression tree, multiple structural change, Pettitt test, sequential Mann-Kendall, standard normal homogeneity test

INTRODUCTION

Streamflow, the flow of water within a river or other watercourse, is a fundamental component of the hydrological cycle, playing a crucial role in shaping landscapes, supporting ecosystems, and sustaining human activities (Dingman, 2015; Wang et al., 2023). Scientifically, streamflow is characterized by a highly nonlinear distribution and dynamic patterns, driven by the complex interplay of climatic, hydrological, and anthropogenic factors (Yaseen et al., 2018). However, hydrological systems globally are increasingly facing profound alterations, with abrupt changes in streamflow patterns posing significant challenges to effective water resource management (Milly et al., 2008; Saad et al., 2020). These shifts can impact water availability, flood risk, sediment transport, and overall riverine health, necessitating a thorough understanding of their occurrence and drivers.

The study of change points, or abrupt shifts, in streamflow is therefore crucial for understanding the dynamics of hydrological systems and the intertwined influence of both natural and anthropogenic factors (Yusoff et al., 2022). Such change points can indicate significant alterations in climatic, hydrologic, or landscape processes. Detecting and characterizing these abrupt changes is critical for developing informed strategies for water allocation, infrastructure planning, environmental protection, and for robust water resource management and flood risk assessment. Ultimately, this understanding is vital for deciphering the complex effects of climate change and human activities on river systems (F. M. Hamzah et al., 2021; Kundzewicz & Robson, 2004).

The frequency and intensity of abrupt changes in streamflow patterns appear to be increasing globally (Intergovernmental Panel on Climate Change [IPCC], 2023). These alterations can be triggered by a complex interplay of factors, including climate variability, land use modifications, and anthropogenic interventions within river basins (e.g., dam construction, diversions) (F. M. Hamzah et al., 2019; Roy et al., 2022). Understanding the specific timing and magnitude of these changes is essential for attributing their causes and predicting future hydrological regimes (Avinash & Dwarakish, 2023; Kamarudin et al., 2023). The potential for such abrupt changes in the Langat Basin, possibly linked to historical events like massive floods and subsequent alterations in land use and river encroachments, necessitates a detailed investigation to quantify these shifts and understand their temporal characteristics. Without a clear identification of these change points, effective water resource management and the development of resilient strategies to cope with

evolving hydrological conditions remain severely challenged. In Malaysia, this urgency is amplified by rapid urbanization, driven by population growth and economic development, which has led to a 30–40% increase in urban land over the past three decades (Hasan et al., 2019), intensifying pressures on river systems and potentially amplifying abrupt streamflow alterations.

While various statistical methods exist for analyzing trends in hydrological time series, identifying the precise timing of abrupt shifts and distinguishing between single and multiple change points requires specific, often complementary, and analytical approaches. Many studies focus on gradual trends, potentially overlooking the critical impacts associated with sudden alterations in streamflow regimes (Danboos et al., 2023). Furthermore, attributing these identified change points to specific underlying factors, such as historical extreme events and long-term changes in land use (Yusoff et al., 2021), requires a robust methodological framework that combines statistical detection with a comprehensive contextual understanding of the basin's history and environmental changes. Therefore, there is a pronounced need for studies that not only pinpoint the years of significant streamflow changes but also explore the potential linkages to specific historical events and evolving basin characteristics.

Recent research has employed a diverse array of methodologies to identify these critical change points in streamflow data across various environments. Nonparametric tests, such as the Pettitt test, have been widely utilized to detect shifts in the central tendency and dispersion of streamflow records, revealing regional and temporal patterns of change (Güçlü, 2020; Kanani et al., 2020; Ryberg et al., 2020). To identify multiple change points and their spatial distribution, spatial clustering techniques have been applied, highlighting the influence of concurrent changes in precipitation and natural climate variability (Ivancic & Shaw, 2017). Other statistical methods, including the Buishand range test (de Jesus et al., 2020), the standard regular homogeneity test (SNHT) for abrupt and gradual trend changes (Pandžić et al., 2020), the sequential Mann-Kendall (SQMK) method for assessing multiple change points (Patakamuri et al., 2020), multiple structural change (MSC) methods (Baltagi et al., 2020), and classification and regression trees (CART) (Yerlikaya-Özkurt & Askan, 2020), further underscore the richness and multidimensionality of change point analysis in environmental and climate variables. For example, CART has been used to analyze the impacts of anthropogenic, climate, and land-use changes on streamflow, as demonstrated in a study in the Talar River basin, Iran, which evaluated the influence of land use changes and climate variations on monthly average streamflow (Ruigar et al., 2023). Their results notably showed that human activities, such as land use changes and point source operations, had a significant impact on streamflow. In specific hydrological settings, such as alpine catchments, wavelet analysis has proven valuable in distinguishing between natural and human-induced breakpoints in streamflow caused by river damming

and hydropower operations (Ciria et al., 2019). Furthermore, copula-based methods have been employed to analyze changes in the dependence structure of flood flow characteristics, providing insights into the non-stationary behavior of streamflow due to human activities (Akbari & Reddy, 2020). The diverse approaches and findings from these studies highlight the importance of employing robust methodologies to accurately detect and interpret abrupt changes in streamflow, paving the way for a more comprehensive understanding of hydrological system dynamics. Understanding the underlying factors causing abrupt changes in streamflow is vital for developing socio-hydrological models and predicting future streamflow scenarios. Studies have shown that human activities, such as reservoir operations and water management policies, significantly impact streamflow patterns, often leading to the disappearance of minor periodicities in runoff records (Lan et al., 2020). These findings underscore the importance of integrating change point detection with an analysis of human and natural influences to better manage and adapt to changing hydrological conditions.

This study aims to identify and characterize abrupt changes in the AMS data at the Kajang Station in the Langat Basin, Selangor, Malaysia. Specifically, it conducted exploratory data analysis to pinpoint any shifts in the recorded data and employed robust methods to determine the break or change points within the time series. To achieve these objectives, the study utilized a multifaceted approach, applying the Pettitt test, Buishand range test, SNHT, SQMK analysis, MSC method, and CART method. This comprehensive suite of techniques ensured a thorough investigation into the structural changes or variations present in the streamflow data for the Kajang Station. The diverse methods employed in this study underscore their commitment to conducting a thorough examination of hydrological dynamics at this critical location in the Langat Basin. By achieving these objectives, this research seeks to provide valuable insights into the dynamics of streamflow regimes in the study area, contributing to a better understanding of hydrological change and informing more effective water resource management strategies in the face of ongoing environmental pressures.

MATERIALS AND METHODS

Study Area

The study was conducted at the Kajang Station (station number 2917401), strategically located within the Langat River Basin in Selangor, Malaysia, as depicted in Figure 1. Situated at a latitude of 02°59′40″ N and a longitude of 101°47′10″ E, this gauging station monitors a significant catchment area of approximately 389.4 km².

The Langat River Basin itself is one of Malaysia's most critical hydrological systems, spanning approximately 1,815 km² between 101°17′E and 101°55′E longitude and 2°40′N and 3°17′N latitude. It originates from the Titiwangsa Range in the northeast of the Hulu Langat District. It ultimately drains into the Straits of Malacca, supplying water to about

two-thirds of Selangor's population. Along its course, the Langat River is monitored by four key gauging stations: Lui, Kajang, Semenyih, and Dengkil stations (F. B. Hamzah et al., 2022; Yusoff et al., 2022).

The Kajang Station is situated explicitly within the city of Kajang, a major urban center in eastern Selangor. Located just 21 km from Malaysia's capital, Kuala Lumpur, Kajang encompasses an area of 60 km² and had a population of approximately 300,000 in 2010. It shares its borders with the Cheras, Ulu Semenyih, Semenyih, and Kajang subdistricts.

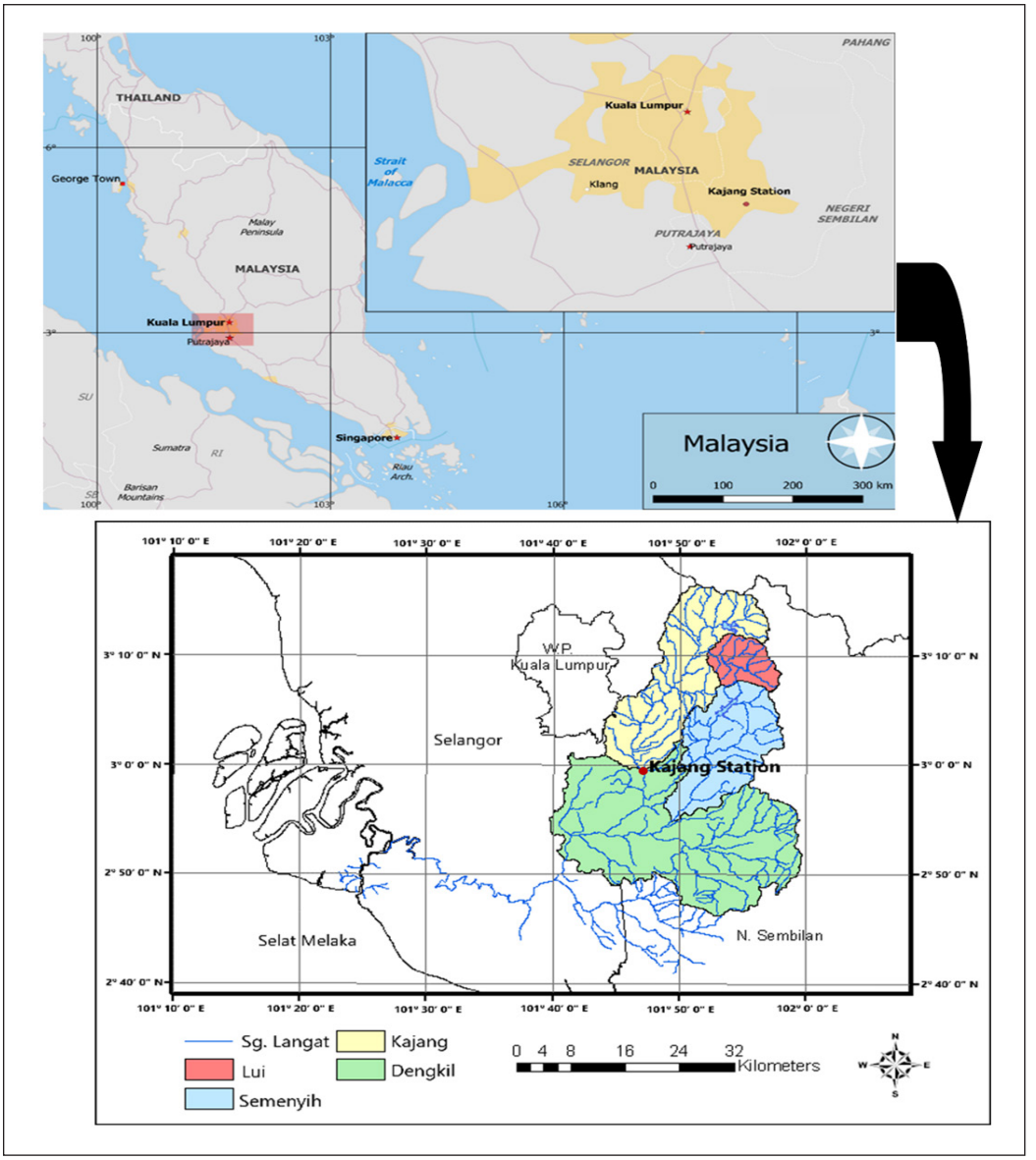

Figure 1. Map of Kajang Station obtained from the Geographic Information System

This area is characterized by high urbanization and dense population. Land use in Kajang is predominantly residential (30.31%), followed by transportation (23.64%), industry (8.13%), public amenities (7.55%), commercial activities (3.03%), and other purposes (1.69%). The extensive urban development in Kajang has notably resulted in the city having a low water retention capacity (Jabatan Perancangan Bandar dan Desa Semenanjung Malaysia [JPBD], 2016), making it particularly susceptible to hydrological changes.

For this research, daily streamflow (m^3/s) data for the Kajang station were analyzed. The streamflow data, spanning the period from 1978 to 2016, were sourced from the Department of Irrigation and Drainage (DID) (Jabatan Pengairan dan Saliran), Malaysia's primary governmental agency responsible for hydrological monitoring. These data, accessed directly from DID, have been subjected to their standard quality control protocols to ensure accuracy and reliability for hydrological analysis.

Single Change Point Detection

Assessment of the change points concerns detecting anomalies in the AMS data. The initial focus is three location-specific tests, the Pettitt test, the Buishand range test, and the SNHT, specifically designed to determine the year a significant break or change is likely to occur in the dataset. The detailed process of change point detection shown in Figure 2 provides a clear and comprehensive overview of the methodology employed to identify and analyze the potential shifts in the streamflow data.

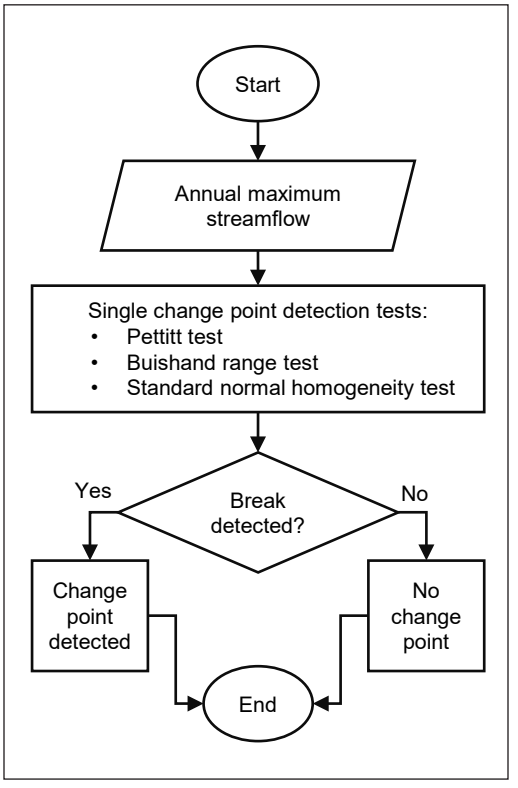

Figure 2. Flowchart for the single change point detection

Pettitt Test

The Pettitt test is a nonparametric tool for examining the homogeneity of a time series and identifying the shifts within the time series. It is specifically formulated to identify breaks in a time series and can efficiently identify the exact year a significant shift occurs. Traditionally used to identify breaks in the middle of a series, the Pettitt test is fundamentally rooted in the rank-based Mann-Whitney two-sample test. It operates on the principle of detecting a shift at an unknown point within a time

series, making it a valuable analytical technique for uncovering temporal shifts or structural changes in the investigated dataset (Pettitt, 1979).

The null hypothesis states there is no change in the distribution of a random variable's sequence. The alternative hypothesis states that the distribution function $F_1(x)$ of the random variables, from X_1 to X_t, differs from the $F_2(x)$ distribution function of the random variables from X_{t+1} to X_T. Given Equation 1:

$$D_{ij} = sgn(X_i - X_j) = \begin{cases} -1 & ,(X_i - X_j) < 0 \\ 0 & ,(X_i - X_j) = 0 \\ +1 & ,(X_i - X_j) > 0 \end{cases} \quad [1]$$

where X_i and X_j are random variables, with X_i following X_j in time. It represents the observed values at two different time points, i and j, in the time series. D_{ij} is a sign function that quantifies the relationship between pairs of observed X_i and X_j. The test statistic $U_{t,T}$ is dependent on D_{ij} (Equation 2).

$$U_{t,T} = \sum_{i=1}^{t} \sum_{j=t+1}^{T} D_{ij} \quad [2]$$

Statistic $U_{t,T}$ is used to analyze samples X_1, ... , X_t and X_{t+1}, ... , X_T from the same population. $U_{i,T}$ is used to assess all random variables from 1 to T and select the critical change point where the $|U_{i,T}|$ value is large (Equation 3).

$$K_T = max_{1 \le t < T} |U_{t,T}| \quad [3]$$

A change point occurs at time t when K_T differs significantly from zero at a particular level given by Equation 4:

$$P = 2exp\left(\frac{-6K_T^2}{T^2+T^3}\right) \quad [4]$$

The null hypothesis is rejected if the p-value is less than the significance level. α, thus allowing the data to be split into two series, each with different distribution functions (Mallakpour & Villarini, 2016).

Buishand Range Test

The Buishand range test is a parametric test that assumes the data values of the test variables are independent and normally and identically distributed (null hypothesis). The research hypothesis suggests the presence of a shift (break). This Buishand range test is suitable for variables with any distribution. It is sensitive to changes in the middle of a time series (AL-Lami et al., 2014; Wijngaard et al., 2003).

$$s_0^* = 0$$

$$s_k^* = \sum_{i=1}^{k}(X_i - \bar{X}),\ k = 1.2 \ldots., N \quad [5]$$

where $\bar{X}$ is the mean of the time series observation; $X_1, X_2, \ldots, X_n$ and k is the number of observations at which a breakpoint occurred.

The rescaled adjusted partial sums are obtained by dividing the s_k^* with the sample standard deviation (Buishand, 1982).

$$D_X = \sqrt{\sum_{i=1}^{N} \frac{(x_i - \bar{x})^2}{N}} \quad [6]$$

$$s_k^{**} = \frac{s_k^*}{D_X}, \qquad k = 1,2, \ldots, N \quad [7]$$

Equation 8 is the statistics for analyzing homogeneity.

$$Q = \max_{0 \le k \le N} |s_k^{**}| \quad [8]$$

The value of $Q/\sqrt{N}$ is compared with the critical value recommended by Buishand (1982). The null hypothesis is rejected if a calculated value is larger than the critical value (Arikan & Kahya, 2019).

Standard Normal Homogeneity Test (SNHT)

Alexandersson (1986) as well as Ahmad and Deni (2013) recommended using $T(d)$ to assess the mean (Stone, 2014) of the initial *d* years of the record relative to the mean of the remaining ($n - d$) years (Equation 9).

$$T_d = d\bar{z}_1^2 + (n-d)\bar{z}_2^2, \quad d = 1,2, \ldots, n \quad [9]$$

where $\bar{z}_1^2 = \frac{1}{d}\sum_{i=1}^{d}(X_i - \bar{X})/s$, $\bar{z}_2^2 = \frac{1}{n-d}\sum_{i=d+1}^{n}(X_i - \bar{X})/s$

are the mean values of z during the first *d* years and the last (*n* - *d*) years, respectively. Equation 10 gives the test statistics.

$$T_0 = \max_{1 \le d \le 0} T(d) \quad [10]$$

The probability of rejecting a null hypothesis when T_0 is greater than a particular critical value depends on the sample size. Therefore, the series is considered inhomogeneous at a given level of significance, such as 95%.

Table 1 presents a comparative analysis of several key characteristics of the Pettitt test, Buishan range test, and SNHT. The Pettitt and Buishand range tests effectively identify the breaks in the middle of the series. In contrast, SNHT identifies the breaks close to the beginning and at the end of the series. The Pettitt test does not require the series to have a normal distribution, but the Buishand range test and SNHT do. Also, unlike the Buishand range test and SNHT, the Pettitt test is less sensitive to outliers.

Table 1
Comparison of the Pettitt test, Buishand range test, and standard normal homogeneity test (SNHT)

Characteristics	Pettitt test	Buishand range test	SNHT
Break	In the middle	In the middle	Near the beginning and at the end of a series
Normality	No normality assumption	Assumes a normally distributed series	Assumes a normally distributed series
Outlier	Less sensitive to outliers	Sensitive to outliers	Sensitive to outliers

Multiple Change Points Detection

This study used specially designed tests, the SQMK, MSC, and CART, to identify the breaks occurring in more than one location in the dataset. These tests efficiently detect shifts across multiple locations. The flowchart in Figure 3 presents the methodology used to identify and analyze the breaks at varying locations.

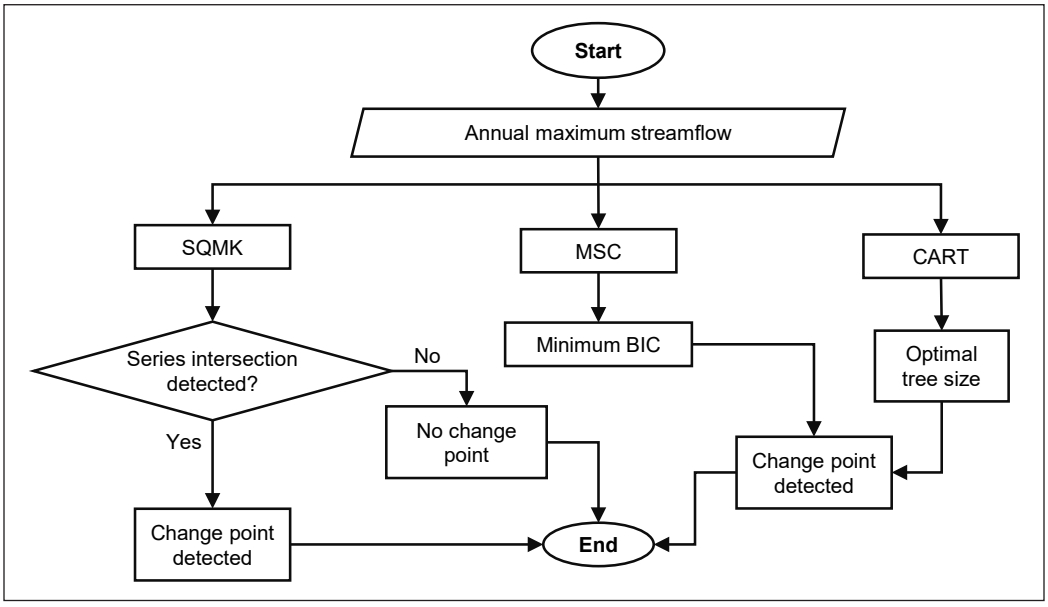

Figure 3. The flowchart for detecting multiple change points
Note. SQMK = Sequential Mann-Kendall; MSC = Multiple structural change; CART = Classification and regression trees; BIC = Bayesian information criterion

Sequential Mann-Kendall Test

Sneyers (1990) introduced the SQMK test, a non-parametric method for identifying a change point or the likely start years for notable trends. The test comprises the forward series $u(t)$ and the backward series $u'(t)$. A trend is statistically significant when the series intersects, separates, and exceeds specific threshold values (± 1.96 for a 95% confidence level). $u(t)$ is a standardized variable with a mean of zero and a standard deviation of one, fluctuating around zero. *u(t)* is the value of the first data point to the last data point. Generally, the SQMK test examines the relative values of the terms in a time series $(x_1, x_2, \dots, x_n)$. The test statistics are calculated as follows:

(i) x_j is the annual mean series $(j = 1, \dots, n)$ evaluated about x_u, (k = 1, … , j−1) and the number of cases where $x_j > x_k$ is counted for each comparison and is designed by n_j.

(ii) The calculation of the test statistics uses the following equation.

$$t_j = \sum_1^j n_j \quad [11]$$

Equations 12 and 13 give the mean and variance.

$$e(t) = \frac{n(n-1)}{4} \quad [12]$$

$$var(t_j) = \frac{j(j-1)(2j+5)}{72} \quad [13]$$

(iii) Equation 14 gives the sequential values of $u(t)$.

$$u(t) = \frac{t_j - e_{(t)}}{\sqrt{var(t_j)}} \quad [14]$$

The values of $u'(t)$ are computed in reverse from the end of the series using a similar approach to $u(t)$. The sequential version of the MK test is an effective tool for detecting the beginning of a trend. The intersection point of the forward and backwards curves indicates the beginning of a trend or change (Zarenistanak, 2019).

Multiple Structural Change Method

Bai (1994) formulated the fundamentals for predicting breaks in time series regression models. Bai and Perron (2003) expanded the equation to account for multiple breaks. They developed an algorithm that allows simultaneous estimation of multiple breakpoints.

Many applications assume the presence of m breakpoints at which the coefficients transition from one stable regression relationship to another. The model consists of m + 1 segments. Each segment has constant regression coefficients written as follows:

$$y_i = x_i^T \beta_j + \mu_i \quad \begin{cases} i = i_{j-1} + 1, \ldots, i_j \\ j = 1, \ldots, m+1 \end{cases} \qquad [15]$$

where, j is the segment index. It is essential to estimate the breakpoints i_j since they are rarely provided externally. The breakpoints estimation is obtained by minimizing the residual sum of squares (RSS) or Bayesian information criterion (BIC) for the above equation (Zeileis et al., 2010).

Classification and Regression Trees

Breiman et al. (1984) developed CART, a recursive algorithm for data mining. It is a non-parametric method that employs input data to develop predictive models. It utilizes historical data to create decision trees. CART builds classification trees when the dependent variable is categorical and a regression tree when the dependent variable is continuous (Choubin et al., 2018). Classification trees classify new observations and organize the dependent variables into the classes specified by the user or calculated using eternal rules. Regression trees aim to predict outcomes. Since they do not have any predefined class, the dependent variables are the response values for the observations within the matrix of independent variables.

This study implemented CART in a structured three-step process. The first step is constructing the maximum tree, which is the most time-intensive phase. The algorithm in regression trees splits and builds the maximum tree by minimizing the squared residuals. Pruning techniques, such as cross-validation and optimization based on the number of points in each node, were used to remove insignificant nodes since the maximum tree, especially the regression tree, can be relatively large. The second step was selecting an optimal tree size using two pruning methods, cross-validation and node point optimization, to determine the appropriate size. In the latter, the splitting process stopped when the number of observations dropped below a predefined minimum. Cross-validation, on the other hand, searched for an optimal balance between misclassification error and tree complexity. The ideal tree size was determined using the complexity parameter (*cp*), where the trial-and-error method was employed to determine the optimal *cp*. Finally, the constructed regression tree predicted the breakpoints for new data to give the response values for each new observation (Choubin et al., 2019; Zhang et al., 2018).

The CART algorithm generates trees with the fewest nodes and cost complexity values to balance simplicity and accuracy. Some of the benefits of this approach are fast computation, easy-to-understand model representation, resistance to irrelevant variables, seamless adaptation to categorical outcomes, single-tuning parameters, and the ability to handle high correlations among variables. However, it is worth noting that CART can sometimes introduce false change points, thus raising false alarms, as observed in a study

Table 2
The advantages of the SQMK, MSC, and CART methods

SQMK	MSC	CART
Detect multiple changes in a time series.	Detect multiple changes in a time series.	Detect multiple changes in a time series.
Non-parametric test.	Use a piecewise linear model.	Fast computations and interpretable model representation
Detect the starting point of trends.	Often applied to data with noise distributions with heavy tails.	Resistant to irrelevant variables and can handle correlation among variables

Note. SQMK = Sequential Mann-Kendall; MSC = Multiple structural change; CART = Classification and regression trees

by Gey and Lebarbier (2008). A notable drawback of the CART method is the potential for error propagation during model construction (Yerlikaya-Özkurt & Askan, 2020). Table 2 compares the advantages and features of the CART, SQMK, and MSC methods.

RESULTS

The Langat Basin has undergone massive changes due to rapid urbanization, industrialization, and intensive agricultural activities. Langat River, an important river in Selangor, is in a fast-transforming area and provides water to 16 intake points in the Langat Basin. The water sources fulfil the diverse water requirements in the region, including industrial, domestic, agricultural, and commercial needs (Abidin et al., 2018). The complex relationship between the river system and the varied demands of a growing urban and industrial area highlights the vital importance of understanding the hydrological dynamics in the Langat Basin in formulating effective management and conservation strategies to preserve the water resources critical for the various sectors in the region.

This study conducted a change point analysis on the AMS data from the Kajang Station in the Langat River Basin. The results of the analysis, as shown in Table 3, indicate that the change point occurred in 2003. Since all methods yielded *p*-values below the significance level of 0.05, the presence of a structural break is considered plausible. The tests suggest that the shift occurred in a single year. However, it would be ideal to investigate whether the change point may have occurred earlier or developed gradually over several years.

The second group of tests, SQMK, MSC, and CART, lasted more than one year.

The first method involved multi-change point analysis and used the AMS data for the Langat River Station in Kajang in the SQMK test. The $u(t)$ sequence represents the forward series, where the AMS data is from the beginning of the series. The $u'(t)$ sequence is the backwards series, where the AMS data is in reverse and begins at the end of the series.

Plotting the $u(t)$ and $u'(t)$ sequences on the same axis gives an intersection point (Figure 4). In the SQMK method, the intersection of $u(t)$ and $u'(t)$ showed that the change points occurred in 2002 and 2007.

Table 3
Results for the change point for the annual maximum streamflow series from 1978 to 2016

Method	Statistic	*p*-value	Shift	Year of shift
Pettitt test	276	0.001	Yes	2003
Buishand range test	1.5881	0.034	Yes	2003
SNHT	11.349	0.009	Yes	2003

Note. SNHT = Standard normal homogeneity test

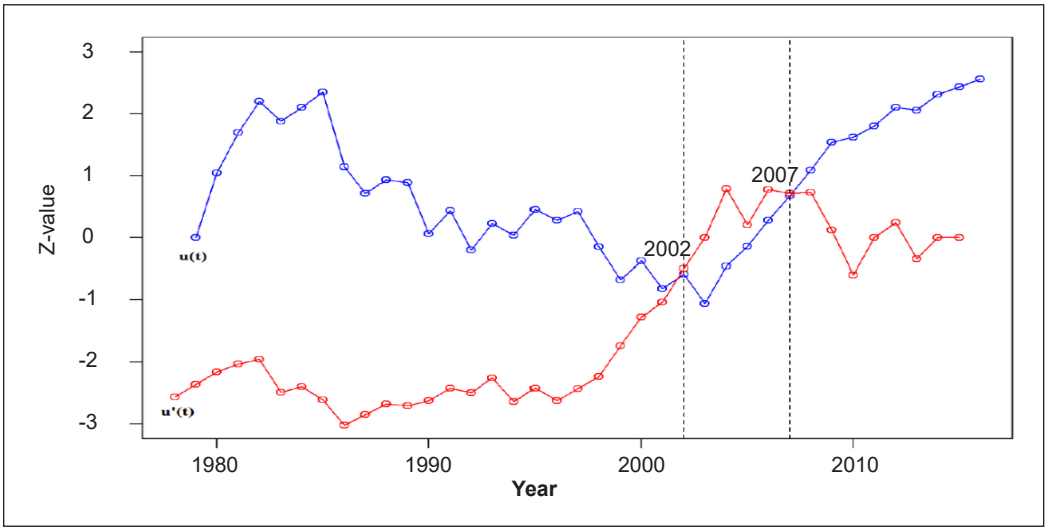

Figure 4. Sequential Mann–Kendall analysis for the Kajang Station

The second method in multichange point analysis uses the MCS methods. The MSC carried out the change point process for the six different breakpoints listed in Table 4 and selected 1985, 2003, and 2009 more frequently than the other years (1982, 1992, and 1997). A comparison of the BIC estimates for different numbers of breakpoints helps determine the optimal number of breakpoints. The BIC selected the lowest value as the optimal number. Table 5 shows the minimum BIC value of 438.8 and two breakpoints. Therefore, the MSC method gives 2003 and 2009 as the years of shift.

The third method, CART, determined that the change points occurred in 1985, 2003, and 2009. Figure 5 shows that the most significant change point was in 2003, and the daily maximum streamflow series comprises two segments. The left tree node is the streamflow series before 2003, and the right tree node is the series after 2003. The left and right nodes represent the second significant change points in 1985 and 2009. The average streamflow values calculated using the change point positions are 67.44, 39.99, 170.80, and 87.58. The primary reason for utilizing the CART method is to detect the change points over time.

Table 4
Number of breakpoints and the respective years

Number of breakpoint	Year					
1					2003	
2					2003	2009
3		1985			2003	2009
4		1985		1997	2003	2009
5		1985	1992	1997	2003	2009
6	1982	1987	1992	1997	2003	2009

Table 5
The Bayesian information criterion (BIC) for selecting the optimal number of breakpoints

Number of breakpoints	0	1	2	3	4	5	6
BIC	445.9	439.3	438.8	444.5	451.6	458.7	466.3

DISCUSSION

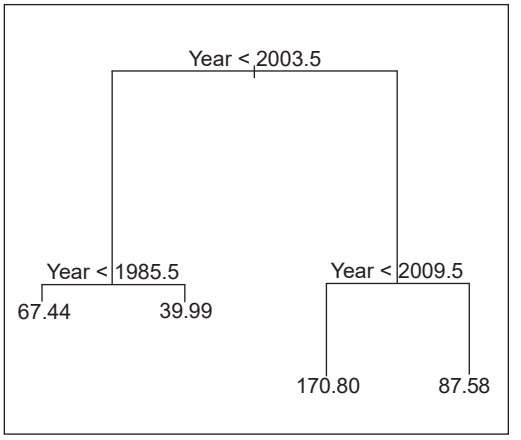

Figure 5. The classification and regression trees

The convergence of results from the single change point detection methods (Pettitt, Buishand range, and SNHT) strongly points to 2003 as a significant year of abrupt change in streamflow characteristics at the Kajang Station. While the SQMK test identified 2002 and 2007 as additional change points, and the MSC method, along with CART, further reinforced the significance of 2003 and 2009, these years collectively indicate a period of pronounced hydrological instability. Notably, CART additionally identified 1985 as a change point. This early identification by CART, coupled with an indication from the analysis that the trend might have begun as early as 1982, aligns critically with the historical flood record for the Langat Basin. Specifically, the flood record details a massive flood event in September 1982, with a stage reading of 26.44 m, almost reaching the dangerous level of 26.50 m. This suggests that the initial abrupt change in streamflow patterns likely commenced around this period, potentially as a direct consequence of or in response to such extreme events. Following this initial shift, the subsequent change points in the early and late 2000s can be linked to the rapid and extensive anthropogenic developments in Kajang. The National Physical Plan (JPBD, 2016) explicitly recognizes Kajang town as an area with a high probability of being inundated. The proliferation of business premises and rapid urbanization in Kajang town have demonstrably

contributed to frequent flash floods, often submerging areas like the Kajang market up to one meter and disrupting daily activities (Wan Mohd Rani et al., 2018). The Kajang city center is identified as the area with the highest risk for flash floods, which typically occur within 30 minutes to two hours of excessive rainfall. Thus, the sequence of detected change points, starting with the immediate aftermath of the 1982 flood and continuing through periods of significant urban expansion, provides a compelling narrative for the drivers of streamflow alteration in the Langat Basin.

Langat River flows through various land uses, including commercial, residential, agricultural, and industrial. According to the land use information obtained by Abidin et al. (2018), 183 km^2 (47%) of the land along the one-kilometer buffer of the Langat River is dominated by commercial crops, primarily rubber and palm oil plantations, in the downstream of the Langat Basin. Seventeen per cent (66 km^2) of the land is dominated by commercial, municipal, residential, and other physical development. There is mixed farming, comprising orchards planted with coconuts, bananas, and other fruit trees, for local consumption and market. Ten percent of the land along the Langat River is allocated for this purpose. Most mixed plantations are along the upper and middle streams of the Langat River. Quarrying and mining activities are carried out in an area of 4.35 km^2 along the Langat River, and about 0.6% is for recreational purposes, especially along the upstream of the Langat River. The rapidly changing land use, especially deforestation for agricultural expansion or urbanization, modifies the hydrological areas and exacerbates flood occurrences (Abdullahi et al., 2018). Flash floods in urban areas are indicative of unplanned development, and this is true in Malaysia, where rapid urbanization in the low-lying areas of major cities such as Kuala Lumpur, George Town, and Kota Bharu has worsened flood occurrences (Chan et al., 2019).

The impervious surfaces gradually replacing the green spaces increase the runoff entering the river within a short period. Sand and mud deposits in most rivers have also reduced their drainage capacity. Besides local geomorphological framework conditions, entry products from the upstream area also influence the channel geometry and fluvial dynamics. In the long term, the transport and disposal of sediment from one side to the other result in the formation of specific channel patterns. Any change in the upstream sediment delivery and discharge regimes will alter local channel adaptations (Hohensinner et al., 2008). Jaafar (2009) reported that one of the factors related to water supply disruptions is the reduced water resources that resulted from a change in the land use in the catchment areas, most notably deforestation for agriculture expansion and urbanization.

Active sand dredging in the Langat River directly impacts river morphology (Abidin et al., 2018). Sand mining activities have been identified as the primary contributors to total suspended solids, sedimentation, and turbidity. The influx of high volumes of suspended solids into the river system exacerbates the river conditions during heavy rainfall. Uncontrolled sand mining can pollute the downstream of rivers and damage their aquatic

flora and fauna. Additionally, river encroachment when developing urban areas close to the river banks narrows the river channels, damages the river reserves, and destroys the buffer zone (Chan et al., 2020). Aling (2020) reported that the encroachment activities on the banks of the Langat River were one of the causes of the worst flash floods in Kajang after the 2016 flood, and affected 141 families.

From a water resources management and flood prevention perspective, these results provide critical insights into the timing and likely causes of hydrological regime shifts. Identifying specific years linked to major changes in streamflow patterns enables water managers and policymakers to correlate these shifts with land development policies and practices. This can support more effective planning and implementation of mitigation strategies, such as improved land-use zoning, sustainable riverbank management, stricter regulation of sand mining, and the integration of green infrastructure to restore natural infiltration and reduce runoff. Moreover, understanding abrupt changes in peak flows can enhance the design of early warning systems, improve flood forecasting accuracy, and inform the development of resilient flood control infrastructure. Ultimately, this research underscores the importance of integrating hydrological data analysis with land-use planning to ensure sustainable and adaptive water resource management in the face of urbanization and climate variability.

LIMITATIONS AND FUTURE WORK

While this study provides robust evidence for significant abrupt changes in streamflow patterns, certain limitations should be acknowledged. The analysis relied on AMS data for a specific period (1978-2016) at a single station (Kajang Station). Future research should extend the time series of streamflow data to capture more recent changes and long-term trends. Incorporating more detailed spatial data on land use and land cover changes over time will allow for a more granular correlation with hydrological responses. Investigating the impact of specific climate variability indices such as El Niño–Southern Oscillation (ENSO) or the Indian Ocean Dipole could provide additional insight into streamflow dynamics. Coupled hydrological-land use models should be developed to simulate the impacts of various development scenarios. Moreover, studies should explore the socio-economic impacts of these streamflow changes on local communities and aim to create integrated socio-hydrologic models that consider both natural and human systems. Applying these robust methodologies to other river basins in Malaysia could help generate broader regional insights and support national water management planning.

CONCLUSION

The application of a suite of complementary statistical tests has provided robust evidence for significant abrupt changes in the AMS patterns within the study area. Specifically, the Pettitt

test, Buishand range test, and SNHT consistently identified 2003 as a key year marking a shift in streamflow characteristics at the analyzed location. Further, the application of methods designed to detect multiple change points, the SQMK test, the MSC method, and CART revealed 2003 and 2009 as significant years of change. The convergence of results across these diverse methodologies underscores the robustness of these identified change points. Notably, the suitability of all employed methods in detecting abrupt shifts within the time series highlights the value of a multi-pronged statistical approach in hydrological change point analysis.

The findings strongly suggest that anthropogenic activities in the vicinity of the Langat River have played a substantial role in altering streamflow behavior and river morphology. The identified change points in 2003 and 2009 appear to coincide with or follow a period of intensified land use activities, including commercial, residential, agricultural, industrial, and sand mining operations. Furthermore, land encroachment on the riverbanks likely contributed to changes in the river's hydraulic characteristics and its response to precipitation events. These activities can lead to increased impervious surfaces, altered infiltration rates, changes in vegetation cover, and modifications to the river channel itself, all of which can significantly impact the magnitude and timing of peak flows.

ACKNOWLEDGMENTS

The authors would like to thank the Earth Observation Centre, Universiti Kebangsaan Malaysia, and the Department of Irrigation and Drainage, Ministry of Natural Resources and Environment, Malaysia, for providing the data for this research. The authors are very grateful to the Universiti Pertahanan Nasional Malaysia and the Ministry of Higher Education Malaysia for their financial assistance under the Fundamental Research Grant Scheme, FRGS/1/2024/STG06/UPNM/01/1.

REFERENCES

Abdullahi, S., Pradhan, B., & Mojaddadi, H. (2018). City compactness: Assessing the influence of the growth of residential land use. *Journal of Urban Technology*, *25*(1), 21–46. https://doi.org/10.1080/10630732.2017.1390299

Abidin, M. Z. A., Kutty, A. A., Lihan, T., & Zakaria, N. A. (2018). Hydrological change effects on Sungai Langat water quality. *Sains Malaysiana*, *47*(7), 1401–1411. https://doi.org/10.17576/jsm-2018-4707-07

Ahmad, N. H., & Deni, S. M. (2013). Homogeneity test on daily rainfall series for Malaysia. *MATEMATIKA*, *29*(1c), 141–150.

Akbari, S., & Reddy, M. J. (2020). Non-stationarity analysis of flood flows using copula based change-point detection method: Application to case study of Godavari river basin. *Science of the Total Environment*, *718*, 134894. https://doi.org/10.1016/j.scitotenv.2019.134894

Alexandersson, H. (1986). A homogeneity test applied to precipitation data. *Journal of Climatology*, *6*(6), 661–675. https://doi.org/10.1002/joc.3370060607

Aling, Y. D. (2020, July 20). *Pencerobohan tebing sungai antara punca banjir kilat* [River bank encroachment among causes of flash floods]. *Harian Metro*. https://www.hmetro.com.my/mutakhir/2020/07/601838/pencerobohan-tebing-sungai-antara-punca-banjir-kilat

AL-Lami, A. M., AL-Timimi, Y. K., & AL-Salihi, A. M. (2014). The homogeneity analysis of rainfall time series for selected meteorological stations in Iraq. *Diyala Journal for Pure Sciences*, *10*(2), 52–63.

Arikan, B. B., & Kahya, E. (2019). Homogeneity revisited: Analysis of updated precipitation series in Turkey. *Theoretical and Applied Climatology*, *135*, 211–220. https://doi.org/10.1007/s00704-018-2368-x

Avinash, R., & Dwarakish, G. S. (2023). Essential climate variables for accurate climate change impact studies on hydrological regime: A comprehensive review. In J. Das, N. V. Umamahesh, J. H. Pu, & M. Pandey (Eds.), *Climate Change Impact on Water Resources: Select Proceedings of HYDRO 2023* (Vol. 561, pp. 339-356). Springer. https://doi.org/10.1007/978-981-97-9180-4_22

Bai, J. (1994). Least squares estimation of a shift in linear processes. *Journal of Time Series Analysis*, *15*(5), 453–472. https://doi.org/10.1007/978-3-319-93549-2_2

Bai, J., & Perron, P. (2003). Computation and analysis of multiple structural change models. *Journal of Applied Econometrics*, *18*(1), 1–22. https://doi.org/10.1002/jae.659

Baltagi, B. H., Kao, C., & Wang, F. (2020). Estimating and testing high dimensional factor models with multiple structural changes. *Journal of Econometrics*, *220*(2), 349-365. https://doi.org/10.1016/j.jeconom.2020.04.005

Breiman, L., Friedman, J., Olshen, R. A., & Stone, C. J. (1984). *Classification and regression trees* (1st ed.). Chapman and Hall/CRC. https://doi.org/10.1201/9781315139470

Buishand, T. A. (1982). Some methods for testing the homogeneity of rainfall records. *Journal of Hydrology*, *58*(1-2), 11–27. https://doi.org/10.1016/0022-1694(82)90066-X

Chan, N. W., Ghani, A. A., Samat, N., Hasan, N. N. N., & Tan, M. L. (2020). Integrating structural and non-structural flood management measures for greater effectiveness in flood loss reduction in the Kelantan River Basin, Malaysia. In F. Mohamed Nazri (Ed.), *Proceedings of AICCE'19: Transforming the Nation for a Sustainable Tomorrow* (Vol. 53, pp. 1151–1162). Springer. https://doi.org/10.1007/978-3-030-32816-0_87

Chan, N. W., Tan, M. L., Ghani, A. A., & Zakaria, N. A. (2019). Sustainable urban drainage as a viable measure of coping with heat and floods due to climate change. In *IOP Conference Series: Earth and Environmental Science* (Vol. 257, No. 1, p. 012013). IOP Publishing. https://doi.org/10.1088/1755-1315/257/1/012013

Choubin, B., Moradi, E., Golshan, M., Adamowski, J., Sajedi-Hosseini, F., & Mosavi, A. (2019). An ensemble prediction of flood susceptibility using multivariate discriminant analysis, classification and regression trees, and support vector machines. *Science of the Total Environment*, *651*(Part 2), 2087–2096. https://doi.org/10.1016/j.scitotenv.2018.10.064

Choubin, B., Zehtabian, G., Azareh, A., Rafiei-Sardooi, E., Sajedi-Hosseini, F., & Kişi, Ö. (2018). Precipitation forecasting using classification and regression trees (CART) model: A comparative study of different approaches. *Environmental Earth Sciences*, *77*, 314. https://doi.org/10.1007/s12665-018-7498-z

Ciria, T. P., Labat, D., & Chiogna, G. (2019). Detection and interpretation of recent and historical streamflow alterations caused by river damming and hydropower production in the Adige and Inn river basins using continuous, discrete and multiresolution wavelet analysis. *Journal of Hydrology*, *578*, 124021. https://doi.org/10.1016/J.JHYDROL.2019.124021

Danboos, A., Sharil, S., Hamzah, F. M., Yafouz, A., Huang, Y. F., Ahmed, A. N., Ebraheem, A. A., Sherif, M., & El-Shafie, A. (2023). Water budget-salt balance model for calculating net water saving considering different non-conventional water resources in agricultural process. *Heliyon*, *9*(4), e15274. https://doi.org/10.1016/j.heliyon.2023.e15274

de Jesus, A. L., Thompson, H., Knibbs, L. D., Kowalski, M., Cyrys, J., Niemi, J. V., Kousa, A., Timonen, H., Luoma, K., Petäjä, T., Beddows, D., Harrison, R. M., Hopke, P., & Morawska, L. (2020). Long-term trends in $PM_{2.5}$ mass and particle number concentrations in urban air: The impacts of mitigation measures and extreme events due to changing climates. *Environmental Pollution*, *263*(Part A), 114500. https://doi.org/10.1016/j.envpol.2020.114500

Dingman, S. L. (2015). *Physical hydrology* (3rd ed.). Waveland Press.

Gey, S., & Lebarbier, E. (2008). *Using CART to detect multiple change points in the mean for large samples*. https://hal.science/hal-00327146v1/document

Güçlü, Y. S. (2020). Improved visualization for trend analysis by comparing with classical Mann-Kendall test and ITA. *Journal of Hydrology*, *584*, 124674. https://doi.org/10.1016/j.jhydrol.2020.124674

Hamzah, F. B., Hamzah, F. M., Mohd Razali, S. F., & El-Shafie, A. (2022). Multiple imputations by chained equations for recovering missing daily streamflow observations: A case study of Langat River basin in Malaysia. *Hydrological Sciences Journal*, *67*(1), 137-149. https://doi.org/10.1080/02626667.2021.2001471

Hamzah, F. M., Tajudin, H., & Jaafar, O. (2021). A comparative flood frequency analysis of high-flow between annual maximum and partial duration series at Sungai Langat basin. *Sains Malaysiana*, *50*(7), 1843-1856. https://doi.org/10.17576/jsm-2021-5007-02

Hamzah, F. M., Yusoff, S. H. M., & Jaafar, O. (2019). L-moment-based frequency analysis of high-flow at Sungai Langat, Kajang, Selangor, Malaysia. *Sains Malaysiana*, *48*(7), 1357-1366. https://doi.org/10.17576/jsm-2019-4807-05

Hasan, H. H., Mohd Razali, S. F., Ahmad Zaki, A. Z. I., & Hamzah, F. M. (2019). Integrated hydrological-hydraulic model for flood simulation in tropical urban catchment. *Sustainability*, *11*(23), 6700. https://doi.org/10.3390/su11236700

Hohensinner, S., Herrnegger, M., Blaschke, A. P., Habereder, C., Haidvogl, G., Hein, T., Jungwirth, M., & Weiβ, M. (2008). Type-specific reference conditions of fluvial landscapes: A search in the past by 3D-reconstruction. *CATENA*, *75*(2), 200-215. https://doi.org/10.1016/j.catena.2008.06.004

Intergovernmental Panel on Climate Change. (2023). *Climate change 2021: The physical science basis*. Cambridge University Press. https://doi.org/10.1017/9781009157896

Ivancic, T. J., & Shaw, S. B. (2017). Identifying spatial clustering in change points of streamflow across the contiguous U.S. between 1945 and 2009. *Geophysical Research Letters*, *44*(5), 2445-2453. https://doi.org/10.1002/2016GL072444

Jabatan Perancangan Bandar dan Desa Semenanjung Malaysia. (2016). *RFN3: Rancangan Fizikal Negara Ke-3*. JPBD. http://myagric.upm.edu.my/id/eprint/16115/1/1%E2%80%A2%20perutusan%20combined.pdf

Jaafar, O., Mastura, S. A. S., & Sood, A. M. (2009). Land use and deforestation modelling of river catchments in Klang Valley, Malaysia. *Sains Malaysiana*, *38*(5), 655-664.

Kanani, R., Fard, A. F., Ghorbani, M. A., & Dinpashoh, Y. (2020). Analysis of the role of climatic and human factors in runoff variations (case study: Lighvan River in Urmia Lake Basin, Iran). *Journal of Water and Climate Change*, *11*(1), 291–302. https://doi.org/10.2166/wcc.2019.186

Kundzewicz, Z. W., & Robson, A. J. (2004). Change detection in hydrological records — A review of the methodology. *Hydrological Sciences Journal*, *49*(1), 7-19. https://doi.org/10.1623/hysj.49.1.7.53993

Lan, T., Zhang, H., Xu, C.-Y., Singh, V. P., & Lin, K. (2020). Detection and attribution of abrupt shift in minor periods in human-impacted streamflow. *Journal of Hydrology*, *584*, 124637. https://doi.org/10.1016/j.jhydrol.2020.124637

Mallakpour, I., & Villarini, G. (2016). A simulation study to examine the sensitivity of the Pettitt test to detect abrupt changes in mean. *Hydrological Sciences Journal*, *61*(2), 245–254. https://doi.org/10.1080/02626667.2015.1008482

Milly, P. C. D., Betancourt, J., Falkenmark, M., Hirsch, R. M., Kundzewicz, Z. W., Lettenmaier, D. P., & Stouffer, R. J. (2008). Stationarity is dead: Whither water management? *Science*, *319*(5863), 573-574. https://doi.org/10.1126/science.1151915

Kamarudin, M. K. A., Toriman, M. E., Abd Wahab, N., Samah, M. A. A., Maulud, K. N. A., Hamzah, F. M., Mohd Saudi, A. S., & Sunardi, S. (2023). Hydrological and climate impacts on river characteristics of Pahang River basin, Malaysia. *Heliyon*, *9*(11), e21573. https://doi.org/10.1016/j.heliyon.2023.e21573

Pandžić, K., Kobold, M., Oskoruš, D., Biondić, B., Biondić, R., Bonacci, O., Likso, T., & Curić, O. (2020). Standard normal homogeneity test as a tool to detect change points in climate-related river discharge variation: Case study of the Kupa River Basin. *Hydrological Sciences Journal*, *65*(2), 227–241. https://doi.org/10.1080/02626667.2019.1686507

Patakamuri, S. K., Muthiah, K., & Sridhar, V. (2020). Long-term homogeneity, trend, and change-point analysis of rainfall in the Arid District of Ananthapuramu, Andhra Pradesh state, India. *Water*, *12*(1), 211. https://doi.org/10.3390/w12010211

Pettitt, A. N. (1979). A non-parametric approach to the change-point problem. *Journal of the Royal Statistics Society*, *28*(2),126–135. https://doi.org/10.2307/2346729

Roy, P. S., Ramachandran, R. M., Paul, O., Thakur, P. K., Ravan, S., Behera, M. D., Sarangi, C., & Kanawade, V. P. (2022). Anthropogenic land use and land cover changes — A review on its environmental consequences and climate change. *Journal of the Indian Society of Remote Sensing*, *50*, 1615-1640. https://doi.org/10.1007/s12524-022-01569-w

Ruigar, H., Emamgholizadeh, S., Gharechelou, S., & Golian, S. (2023). Evaluating the impacts of anthropogenic, climate, and land-use changes on streamflow. *Journal of Water and Climate Change*, *15*(4), 1885-1905. https://doi.org/10.21203/rs.3.rs-3139611/v1

Ryberg, K. R., Hodgkins, G. A., & Dudley, R. W. (2020). Change points in annual peak streamflows: Method comparisons and historical change points in the United States. *Journal of Hydrology*, *583*, 124307. https://doi.org/10.1016/j.jhydrol.2019.124307

Saad, M. H. M., Kamarudin, M. K. A., Saudi, A. S. M., Hamzah, F. M., Hanafiah, M. M., Wahab, N. A., & Bati, S. N. A. M. (2020). Evolution of river characteristics impact on post-flood and normal season in Pinang River Basin, Malaysia. *International Journal of Advanced Science and Technology*, *29*(4s), 2759-2774.

Sneyers, R. (1990). *On the statistical analysis of series of observations*. World Meteorological Organization.

Stone, R. J. (2014). Homogeneity assessment of Trinidad and Tobago's surface air temperature data. *The West Indian Journal of Engineering*, *36*(2), 29–33.

Wan Mohd Rani, W. N. M., Kamarudin, K. H., Razak, K. A., Hasan, R. C., & Mohamad, Z. (2018). Measuring urban resilience using climate disaster resilience index (CDRI). *International Archives of the Photogrammetry, Remote Sensing and Spatial Information Sciences*, *XLII*(4/W9), 237–242. https://doi.org/10.5194/isprs-archives-XLII-4-W9-237-2018

Wang, Q., Deng, H., & Jian, J. (2023). Hydrological processes under climate change and human activities: Status and challenges. *Water*, *15*(23), 4164. https://doi.org/10.3390/w15234164

Wijngaard, J. B., Klein Tank, A. M. G., & Können, G. P. (2003). Homogeneity of 20th century European daily temperature and precipitation series. *International Journal of Climatology*, *23*(6), 679–692. https://doi.org/10.1002/joc.906

Yaseen, Z. M., Allawi, M. F., Yousif, A. A., Jaafar, O., Hamzah, F. M., & El-Shafie, A. (2018). Non-tuned machine learning approach for hydrological time series forecasting. *Neural Computing and Applications*, *30*, 1479-1491. https://doi.org/10.1007/s00521-016-2763-0

Yerlikaya-Özkurt, F., & Askan, A. (2020). Prediction of potential seismic damage using classification and regression trees: A case study on earthquake damage databases from Turkey. *Natural Hazards*, *103*, 3163-3180. https://doi.org/10.1007/s11069-020-04125-2

Yusoff, S. H. M., Hamzah, F. M., Jaafar, O., & Tajudin, H. (2021). Long term trend analysis of upstream and middle-stream river in Langat Basin, Selangor, Malaysia. *Sains Malaysiana*, *50*(3), 629-644. https://doi.org/10.17576/jsm-2021-5003-06

Yusoff, S. H. M., Hamzah, F. M., & Jaafar, O. (2022). Multiparameter probability distributions of at-site L-moment-based frequency analysis in Malaysia. *International Journal of Mechanical Engineering*, *7*(Special Issue 4), 48-58.

Zarenistanak, M. (2019). Historical trend analysis and future projections of precipitation from CMIP5 models in the Alborz mountain area, Iran. *Meteorology and Atmospheric Physics*, *131*, 1259–1280. https://doi.org/10.1007/s00703-018-0636-z

Zeileis, A., Shah, A., & Patnaik, I. (2010). Testing, monitoring, and dating structural changes in exchange rate regimes. *Computational Statistics and Data Analysis*, *54*(6), 1696–1706. https://doi.org/10.1016/j.csda.2009.12.005

Zhang, B., Wei, Z., Ren, J., Cheng, Y., & Zheng, Z. (2018). An empirical study on predicting blood pressure using classification and regression trees. *IEEE Access*, 6, pp. 21758–21768. https://doi.org/10.1109/ACCESS.2017.2787980

Pertanika J. Sci. & Technol. 33 (5): 2339 - 2356 (2025)

PERTANIKA JOURNALS

SCIENCE & TECHNOLOGY

Journal homepage: http://www.pertanika.upm.edu.my/

Field Evaluation of Thermal Behavior of Aerogel-Infused Paint for Building Insulation

Muhammad Fitri Mohd Zulkeple[1], Abd. Rahim Abu Talib[1,2]*, Ezanee Gires[1,2], Syamimi Saadon[1,2], Mohammad Yazdi Harmin[1,2], Rahimi L. Muhamud[3] and Javier Bastan[4]

[1]Aerodynamics, Heat Transfer and Propulsion Group, Department of Aerospace Engineering, Faculty of Engineering, Universiti Putra Malaysia, 43400 Serdang, Selangor, Malaysia
[2]Aerospace Malaysia Research Centre, Faculty of Engineering, Universiti Putra Malaysia, 43400 Serdang, Selangor, Malaysia
[3]Maju Saintifik Sdn Bhd., 35, Jalan Mutiara Subang 1, Taman Mutiara Subang, 47500 Subang Jaya, Selangor, Malaysia
[4]Eika, S. Coop. Urresolo, 47 48277 Etxebarria, Bizkaia, Spain

ABSTRACT

Thermal coatings are highly sought after in both everyday living and industrial manufacturing. The utilization of aerogel in building insulation primarily relies on its low density, thermal insulating properties, flame retardancy, high light transmittance, and other distinctive features. This study investigates the thermal performance of an aerogel-based paint compared to conventional commercial paint for building envelope applications in hot climate conditions. Experimental tests were conducted under outdoor solar irradiation to assess surface temperature behavior, heat absorption characteristics, and effective thermal conductivity. A monitoring infrastructure was established to achieve this goal, allowing the on-site observation of temperature profile using a wireless sensor system called LoRa technology. According to the results, on average, aerogel coating showed a higher thermal reflectivity of 7% than conventional acrylic paint, around 2%. Besides that, the house applied with aerogel paint had a thermal conductivity of $0.019\frac{\mathrm{W}}{\mathrm{m}^2\,^\circ\mathrm{C}}$ while the conventional acrylic paint had a thermal conductivity of $0.131\frac{\mathrm{W}}{\mathrm{m}^2\,^\circ\mathrm{C}}$, representing an 85% improvement in thermal insulation performance. This enhanced performance is attributed to the aerogel's low thermal conductivity and high solar reflectivity, which together limit heat

ARTICLE INFO

Article history:
Received: 26 February 2025
Accepted: 23 June 2025
Published: 28 August 2025

DOI: https://doi.org/10.47836/pjst.33.5.14

E-mail addresses:
fitrizulkeple@gmail.com (Muhammad Fitri Mohd Zulkeple)
abdrahim@upm.edu.my (Abd. Rahim Abu Talib)
ezanee@upm.edu.my (Ezanee Gires)
mimisaadon@upm.edu.my (Syamimi Saadon)
myazdi@upm.edu.my (Mohammad Yazdi Harmin)
salam100269@gmail.com (Rahimi L. Muhamud)
jbaztan@eika.es (Javier Bastan)
* Corresponding author

transfer through the wall. The findings highlight the potential of aerogel-enhanced paints as a passive thermal control strategy for improving indoor comfort and reducing energy demand in hot climate regions.

Keywords: Aerogel, heat transfer, thermal insulation coating

INTRODUCTION

Energy conservation and carbon reduction are two of the most pressing issues confronting human societies nowadays, and the future of humanity depends on how these issues are resolved. Several options have been engineered to address this issue. Thermal coatings are in high demand in domestic and industrial settings to tackle this issue due to excessive energy usage, especially during this post-pandemic era. As society evolves, demands for thermal coating performance in all industries grow. In recent years, thermal insulation has emerged as a popular research area (Ren et al., 2023; Shen et al., 2023; Sun et al., 2021). Thermal insulation materials have been widely applied in multiple sectors. It can be used on components of building construction, such as mortar (Becker et al., 2022), aggregate (L. Chen, 2011), and thermal insulation coating (X. X. Tao et al., 2010; Zhang et al., 2015). Besides that, aerogel has also been employed in aerospace applications (D. He et al., 2022; Pan et al., 2023; Vasile et al., 2020) in addition to the industrial equipment and pipeline usage (Mao et al., 2022). Moreover, the list of sectors or fields that employ the aerogel application has grown over the past decade and is still growing for the upcoming years. Therefore, on a more general note, aerogel has been applied to situations where temperature restrictions or overheating issues are a main concern. However, the insulation requirements vary depending on the application.

For example, buildings generate a lot of carbon dioxide yearly as part of the greenhouse gas emission plan. Though building energy demands increase, the demand for energy-saving materials and systems is rising due to concerns about greenhouse gas emissions (Berardi, 2017a, 2017b). According to the International Energy Agency's Global Buildings Tracker, building operations will account for 30% of global energy consumption in 2021, which is expected to keep rising, particularly in hot climate regions where solar heat gain significantly contributes to indoor thermal discomfort and increases cooling load. According to a study of building energy gain/loss paths, external walls and windows are significant sources of worry for building energy use. External walls gain/lose approximately 23-34% of energy, whereas windows gain/lose around 23-25% (Berardi, 2016; Powell et al., 2016; Raza et al., 2023). Even with the advancement achieved in the construction sector, these values are still worrying and must be reduced further. Due to that, among passive strategies, reflective coatings and thermal insulation paint have a crucial and distinct role in energy-efficient, low-carbon buildings by minimizing heat loss or gain in buildings (Nie et al., 2020; Z. Chen et

al., 2023). Conventional paint, however, often lacks significant thermal resistance, limiting its ability to reduce heat transfer through building walls effectively. Therefore, insulation materials are increasingly being developed with high comfort levels to enhance the longevity of buildings and meet energy-saving requirements (Thapliyal & Singh, 2014).

The thermal properties of buildings depend on the thermal conductivity of the walls and roofs. Specifically, thermal insulation coatings may restrict heat transfer between an object and its environment, preserving a pleasant indoor temperature and less energy wastage. Most coatings employ thermal insulation or reflecting filler to improve thermal insulation capabilities. Thermal insulation coatings typically consist primarily of polymers and fillers (Miao et al., 2023; Wei et al., 2022). The primary role of the polymer is to disperse and secure the filler within the substrate. In contrast, filler is crucial for achieving low thermal conductivity and is indispensable for the thermal insulation coating. Therefore, it is essential to choose a suitable filler while carefully preparing the thermal insulation coating. Aerogel, a material currently being researched, is a strong candidate crucial for reducing building emissions by serving as an effective insulating material (Ganobjak et al., 2020).

Aerogel is a solid material with a definite shape and a complex structure of tiny, linked particles arranged in a three-dimensional network (Adhikary et al., 2021; Mazrouei-Sebdani et al., 2022). Aerogel has some remarkable characteristics because of its distinctive composition, such as a high specific surface area (500–1000 m^2/g), low density (0.003–0.2 g/cm^3), extremely low thermal conductivity (0.013–0.14 W/mK), and a high acoustic impedance (~1.05 MRayl). Aerogel possesses features that make it very suitable for various applications, such as thermal and acoustic barriers and other prospective uses (Hu et al., 2024; J. Tao et al., 2023; Wang et al., 2021).

Aerogel technologies are currently of significant importance in the worldwide insulation market. They are used in the building industry for various applications such as façade systems, plasters, boards, translucent panels, and aerogel panels for ventilation systems (Wakili et al., 2015). The utilization of aerogel in building insulation primarily relies on its low density, thermal insulating properties, flame retardancy, high light transmittance, and other distinctive features. Currently, the application form comprises aerogel glass, aerogel insulating coating, aerogel fiber composite material, and aerogel concrete and mortar. A building envelope insulation system utilizing aerogel material will be designed to achieve this objective, considering its advantages, as illustrated in Figure 1. The wall constitutes the most extensive surface area within the building envelope and contributes to approximately 30% of the building's energy consumption. Therefore, prioritizing insulation for the external wall is crucial for building energy conservation (Yu & Liang, 2016). Silica aerogel panels are also produced using other matrices, such as melamine foam and diverse fiber varieties. Table 1 displays the recorded thermal conductivity of the aerogel panel for several matrix materials and their corresponding densities (Joly et al., 2017; Shanmugam et al., 2020).

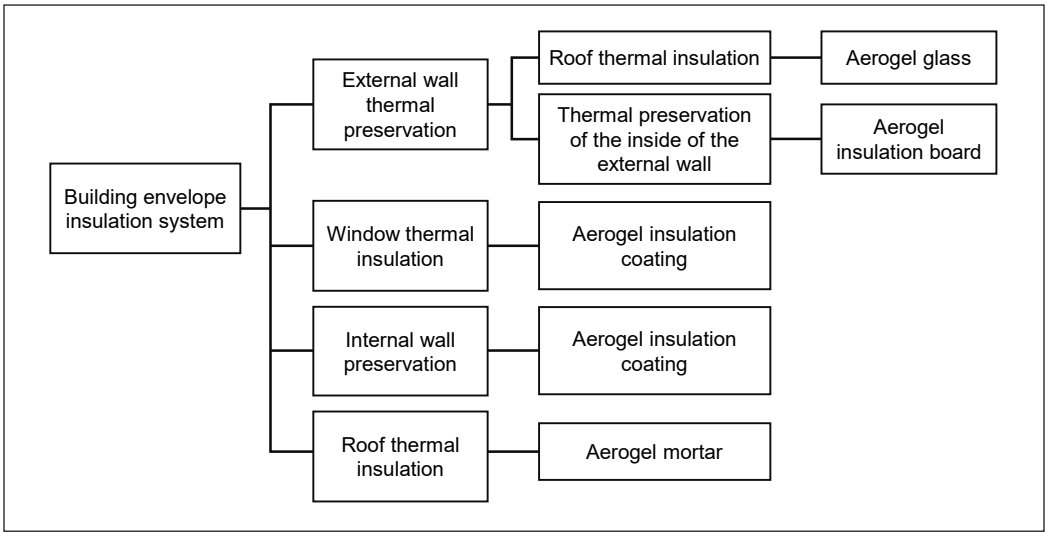

Figure 1. Building envelope insulation system utilizing aerogel material
Note. Reproduced from Yu and Liang (2016)

Table 1
Thermal conductivity of the aerogel matrix materials and their corresponding densities

Reference	Aerogel material	Density, ρ (kg/m^3)	Thermal conductivity, k [W/(m.K)]
Joly et al. (2017)	Aerogel panel with melamine (10 mm)	98.7 - 101.0	0.0137 - 0.0136
	Aerogel panel with PET fiber (13 mm)	118.2 - 116.6	0.0148 - 0.155
	Aerogel panel with glass fiber (30 mm)	98.0 - 106.1	0.0148 - 0.0151
	Aerogel panel with needle glass fiber (7 mm)	182.5 - 194.9	0.0142 - 0.0156
S. He et al. (2025)	Aerogel blanket		0.028
Cuce et al. (2014)	Solid aerogel		0.012 - 0.020
Lu et al. (2018)	Aerogel from fly ash and bottom ash		0.0385
Karim et al. (2023)	Aerogel-based mortar coating	180.0	0.04
Y. X. Chen et al. (2022)	Geopolymer foam aerogel render (GFAR)	715.2	0.133
Zhu et al. (2018)	Aerogel using industrial solid wastes and dislodged sludges		0.03-0.032
Ibrahim et al. (2018)	Aerogel-based plaster	120	0.027

Note. Reproduced from Joly et al. (2017) and Shanmugam et al. (2020)

Due to its seamless adaptability to buildings, the aerogel paint shows promise as a solution for enhancing the thermal performance of buildings without altering their outward appearance. For instance, in a recent year, a study was done by Abdul Halim et al. (2025) developing a method that uses aerogel paint, which is interconnected with many Sustainable Development Goals (SDGs), predominantly by facilitating energy efficiency and mitigating environmental

impact. Yet, despite this potential, the application of aerogel materials in painting formulations remains underexplored, particularly in real-world outdoor conditions. Most existing studies focus on aerogels in bulk form or within composite panels, while limited attention has been given to their behavior in thin-film coatings subjected to solar exposure.

Although aerogel paint offers numerous advantages, it is also essential to consider potential disadvantages. A notable limitation of aerogels is their fragility and rigidity, which can restrict their wide-ranging uses. The application of aerogel coating is reported to be challenging due to inadequate adhesion resulting from either a deficiency in physicochemical bonding or a disparity in the thermal expansion coefficient between the coating and the substrate, especially in real-world applications where paint is exposed to extreme conditions or weather. This ultimately leads to the formation of cracks and spalling. Furthermore, the production of composites may be restricted due to the paint's elevated viscosity. Besides, aerogel paint can be more expensive than conventional acrylic paint, limiting its affordability for many households. Although aerogel paint is expected to reduce heat transmission and indoor temperatures, its effectiveness may be limited in scorching climates or regions with significant humidity. The thermal conductivity of the aerogel might increase as it is exposed to continuous high temperatures, and the hydrophobicity of the aerogel will also disappear after exposure (Gao et al., 2023). In conclusion, although aerogel paint offers numerous advantages, it is crucial to consider these possible disadvantages before selecting it for thermal insulation in a residential setting. Applying a coating made of aerogel is challenging because of the specific characteristics of aerogel powders, such as their granulometric and morphological qualities, which are crucial for successful deposition (Abu Talib & Bheekhun, 2018; Bheekhun et al., 2014, 2018). Therefore, it is necessary to create a paint solution that contains aerogel, specifically focusing on its application in areas with extreme weather conditions or climate, and evaluate the performance for real field conditions.

Furthermore, there is a noticeable lack of comparative experimental studies that directly evaluate the thermal performance of aerogel-based paints against conventional paints. Assessments that combine surface temperature monitoring, solar heat absorption characteristics, and effective thermal conductivity measurement under outdoor environmental conditions are limited. This gap restricts the broader adoption and validation of aerogel-based coatings in practical building applications.

The present study details continuing research into the potential of using aerogel-based paint. A case study was conducted where aerogel-based paint was used to coat the exterior wall of a building located in Pasir Mas, Kelantan, Malaysia. An experimental home model is utilized to conduct a case study evaluating the enhancement of thermal comfort by adding aerogel-infused coatings/paint on the outer surface of the building wall. The study also seeks to assess the potential of aerogel-infused coating and identify anticipated uses for this technology. These coatings, infused with aerogels, were developed through a partnership

with Maju Sainstifik Sdn. Bhd. and Bina Paint Sdn. Bhd., a Nano silica specialist and a paint manufacturing specialist, respectively. The aerogel-infused coating can be applied the same way as regular construction paint, making it highly convenient for application in real-world conditions.

The main goal is to analyze the long-term thermal characteristics of the painted surfaces. A monitoring system was established to achieve this goal, allowing the direct observation of temperature and humidity levels using a wireless sensor system called LoRa technology. These experiments aim to compare the thermal properties of a house building treated with aerogel-based paint and regular paint. In addition, a constant array of sensors monitors the indoor and exterior circumstances and those in the neighboring rooms. The findings of the initial comprehensive in-situ monitoring campaign, which aimed to compare the thermal performance of a house building treated with aerogel-based paint and regular paint, are presented and analyzed.

METHODOLOGY

This section introduces the case study building and outlines the methods used to evaluate the thermal advantages derived from aerogel-infused paint. The section will also encompass a comprehensive depiction of the sensor measuring system, incorporating the utilization of LoRa technology for thermal and humidity measurement and monitoring purposes.

Wall Partitions and Sensor Installation

The advanced aerogel-based paint has been put on the concrete block walls of two test buildings in Pasir Mas, Kelantan (Figure 2). This test aims to evaluate the effects of the thermal properties of the Aerogel-based paint panels examined in this study. The thermal conductivity of the entire wall is measured. The wall's thermal conductivity contributes to the building's comfort level. It was expected that the thermal insulation paint could reduce the heat transfer conducted through the wall, which would reduce the ambient temperature inside the building, increasing the level of comfort for the residents. Applying this thermal coating or paint in "real conditions" might substantially alter the thermal conditions, mainly when used for wall insulation. However, several external factors will affect the performance of the insulator, such as ventilation and weather. These factors, especially the weather, are uncontrollable when conducting actual condition or site testing. Despite concerns about the weather control, this study will concentrate on the potential to enhance the thermal performance of the building by implementing aerogel-enhanced systems.

This study used two identical houses, as shown in Figure 2a with the same orientation to evaluate the effectiveness of wall insulation technologies. Both houses were built based on the standard set by the Syarikat Perumahan Negara Berhad (SPNB) in terms of the brick and material used. Besides that, the paint application procedure also follows the

standard application method, which includes the number of layers and the other preparation requirements before applying the paint. What makes the difference is the paint used to coat the house's external wall. One house had an external wall coated with aerogel-infused paint. In contrast, the other house had its exterior wall coated with the standard wall paint provided by the same manufacturer as the baseline scenario.

The wall partitions were identical in their exposure to sunlight during the afternoon, as one side was entirely exposed without any obstructing structures. The paint was applied with a roller, with the same number of coats and approximately similar thickness in both cases. Besides that, white was chosen for both paints to maximize the thermal reflectivity on the wall. This is because darker hues or even colored paint can increase heat absorption on the wall. A complete thermal performance comparison can be made for aerogel and conventional acrylic paint. The house floor plan is shown in Figure *2*b. Based on the figure, the house has one room facing the sunrise and the other two rooms facing the sunset. The testing wall will be the one that faces the sunset. Therefore, the sensor will be placed on the room wall exposed to the evening sun, as indicated by the cross sign in Figure *2*b. The room was empty without any furniture, and even the fan or heating, ventilation, and air conditioning (HVAC) system was set to be off for the duration of the testing. So, the room was set up to control conditions for both houses.

Sensors are placed on the inner (Figure 3a) and outside surfaces (Figure 3b) of all relevant wall partitions in early October 2023 to assess the thermal characteristics. These sensors are positioned at the same heights and locations to monitor the temperature of the walls, the surrounding temperature, and the relative humidity. This experimental effort aims to gather significant data to comprehend the thermal dynamics within the structure over a five-week data collection period. Furthermore, the external conditions remain beyond our control. This will result in many scenarios and possibilities that the applied paint has encountered. All sensors will be connected to LoRaWAN devices to make them more accessible remotely.

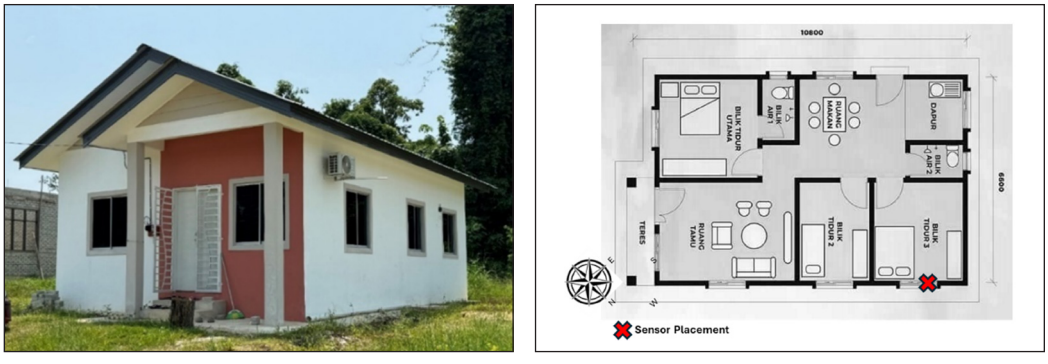

(a) (b)

Figure 2. (a) Test house at Pasir Mas, Kelantan; (b) Floor plan of the houses
Note. Retrieved from SPNB (n.d.)

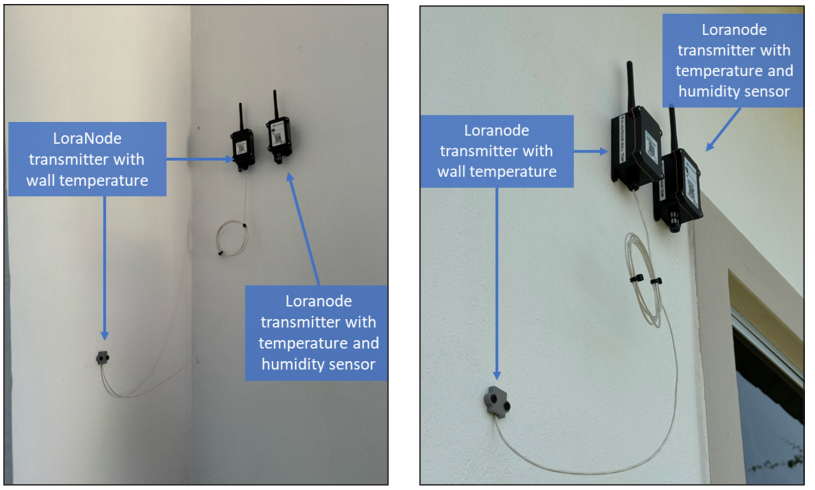

(a) (b)

Figure 3. LoraNode transmitter with temperature and humidity sensor positioning: (a) Indoor; (b) Outdoor

LoRaWAN networks are the preferred choice when there are many devices in a small area, and there is a need for low delays and high dependability, with the ability to adapt to different requirements. Therefore, the monitoring system attempts have chosen the LoRa/LoRaWAN composition due to its various advantageous properties, including bitrate, energy consumption, communication range, simplicity, use of unlicensed bands, and ease of management facilitated by its star-of-stars topology (Beltramelli et al., 2021; Chaudhari et al., 2020). The network will be cost-effective, energy-efficient, and capable of measuring thermal and humidity parameters and facilitating real-time monitoring.

As previously explained, the temperature and relative humidity were remotely monitored and measured using LoRa technology. All the sensors that have been installed will be linked to the LoRaNode transmitter as shown in Figure 4a. Consequently, each house will have a LoraNode transmitter that includes a Temperature and Humidity sensor and a LoraNode transmitter that measures the wall temperature indoors and outdoors. The LoraNode transmitters will consistently transfer the data signal to the LoRaWAN Gateway, Figure 4b located within each residence. The data sampling was transmitted every minute, and the sampling duration was 24 hours daily (total data collected per sensor was 50,400 samples). However, for comparison purposes, only data collected in the evening were considered since the peak exposure of the testing walls is around evening. This consideration was made because heat sources come from the sun's radiation. Therefore, during the early morning, the radiation was not as intense as during the evening. Besides that, it also reduces the uncertainty of the measurement as the measurement was done only on one wall surface, which faces the direction of the evening sun. This helps reduce the data size but also helps focus on the optimum comparison between the paints. The

gateway functions as a relay to provide smooth data transmission between the sensor and the end devices using LoRa frequency bands. The user can access the sensing information through their terminal, which can be done either through a web-based dashboard or an IoT cloud platform. This can be done using laptops, personal computers (PCs), or smartphones. The fundamental operational mechanism of the sensor system is illustrated in Figure 4c. LoRaWAN technology was proven to help remotely monitor real-time data. This has opened new possibilities for testing, such as expanding the range of testing areas from a small area to a much bigger region with different environmental conditions.

The summary of the site testing, which employs the IoT monitoring system using the LoRaWAN technology, is shown in Figure 5. With all the advantages that have been mentioned, these technologies still have some drawbacks, which need proper networking planning. Proper networking planning is critical for LoRaWAN performance because it relies on long-range, low-power radio signals sensitive to surrounding factors. Structures like other buildings, trees, and terrain can disturb the signal of the LoRaWAN. Besides that, gateways must be strategically located to ensure full signal coverage while avoiding dead zones and redundant overlap. Poor networking planning can lead to weak signal strength and frequent retransmissions, which can drain the device's batteries. Therefore, to avoid issues related to this technology, a professional group that was well-versed in this technology reached out for help. The devices were installed by technicians from the Wireless and Photonic Networks (WiPNET) team. Besides the installation, this team also provided help regarding the monitoring process for both houses during the duration of the testing, which was for five weeks.

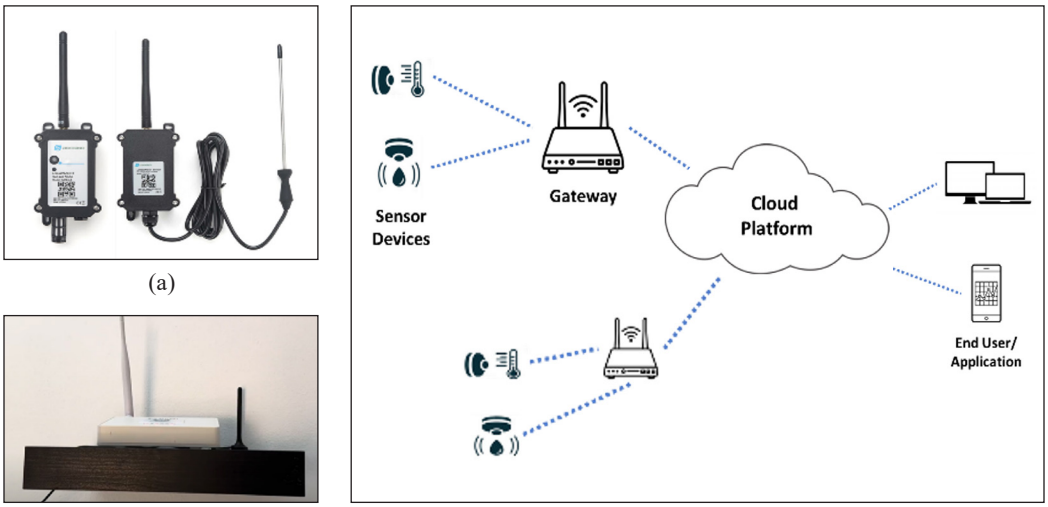

(a) (b) (c)

Figure 4. (a) LoraNode; (b) LoRaWAN Gateway with 4G; (c) The simplified basic working mechanism of the sensor system

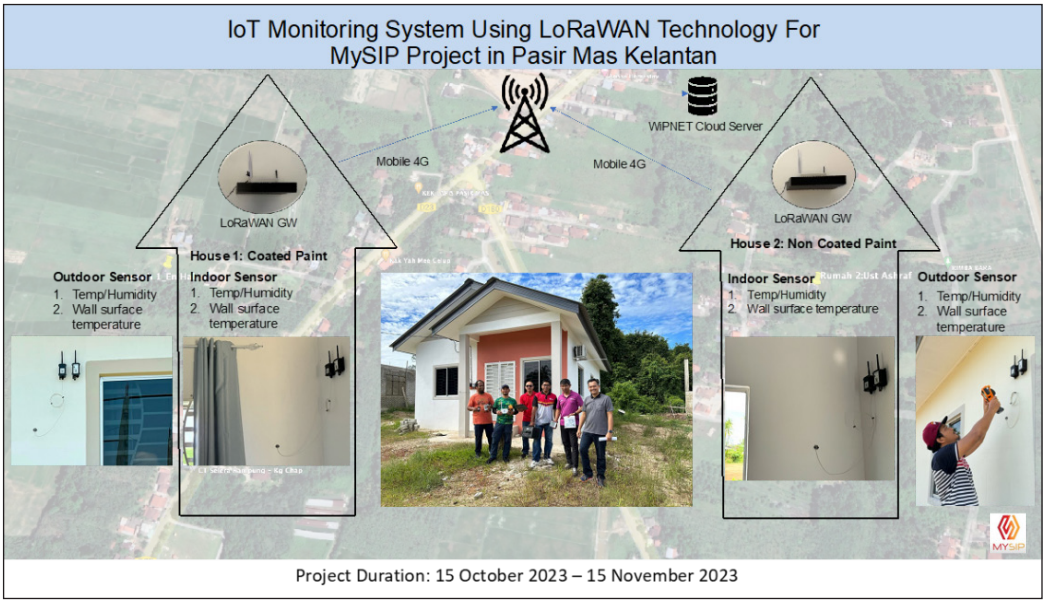

Figure 5. Summary of the Internet of Things (IoT) monitoring system using LoRaWAN technology for the project
Note. WIPNET = Wireless and Photonic Networks; GW = Gateway

RESULTS AND DISCUSSION

The case study is on Pasir Mas, a Kelantan town renowned for its tropical climate. The city is located at a latitude of 6.0424° N and a longitude of 102.1428° E. The weather dataset is from the NASA Prediction of Worldwide Energy Resources, an internet portal with geographic information system (GIS) capabilities. The company provides customized data solutions for three primary user segments: Renewable Energy, Sustainable Buildings, and Agroclimatology. Figure 6 illustrates the cumulative daily solar energy received in the specified climate. Solar radiation increases the temperature of the walls of buildings. As mentioned, walls and windows significantly contribute to the building's rising temperature. Depending on the region, in most buildings, whether residential buildings or industrial ones, the walls and windows are fully exposed to the sun's rays or radiation. In the Malaysian region, where the weather is a tropical climate, Malaysian regions receive about six hours of direct sunlight daily throughout the year since Malaysia is not a four-season country. Based on Figure 6, on average, the solar radiation is at the level of 250 W/m^2, as observed during cloudy days. This number can increase with fewer clouds during a clear sky or good weather. This long exposure to direct sunlight will increase the building's temperature.

An initial observation was done a few weeks before utilizing LoRa technology for thermal and humidity measurement and monitoring purposes using an Infrared sensor camera, as shown in Figure 7. The measurements were made every half an hour for each house from around 10 a.m. until 5 p.m. Even though the camera could capture the whole

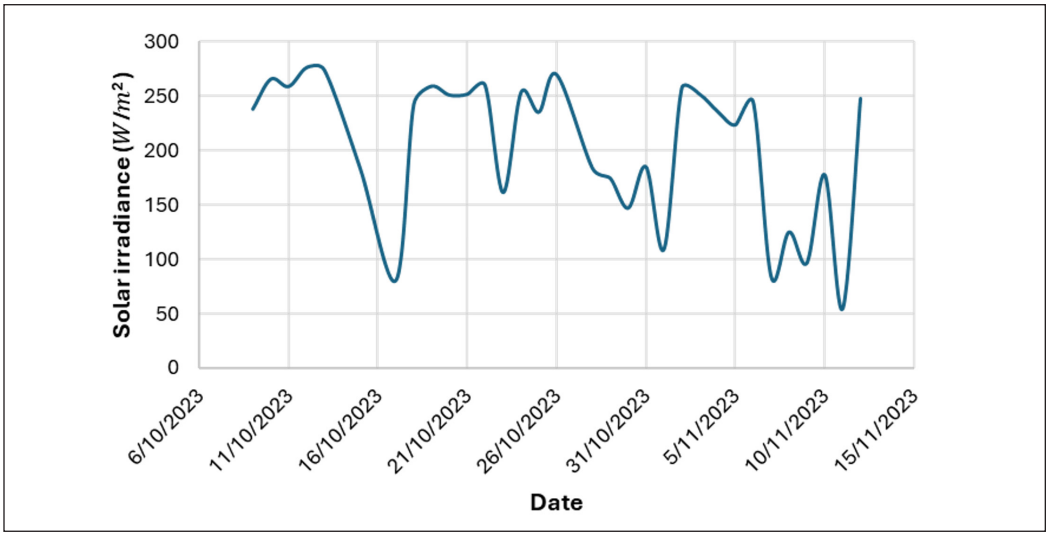

Figure 6. Cumulative daily solar radiation at Pasir Mas, Kelantan

house's thermography, only the interior and outer wall surface temperature was measured and recorded. This means that the temperature of the other parts of the house, such as the window's glass and the house's roof, was not recorded since the region of interest for the current test is the walls that were applied with the aerogel paint. Before the thermograph of the house wall was captured, the emissivity setting of the wall surface was refined accordingly based on the American Society for Testing and Materials (ASTM) E1933 to ensure accurate temperature measurement. For the current case, the emissivity of the wall surface has been estimated using the reference emissive materials method. Based on this method, part of the wall was placed with a piece of electrical tape with known emissivity, which was then used to provide the reference temperature for measuring the emissivity of the wall surface. Based on the thermal images captured, a house coated with aerogel paint shows a significant temperature difference between the indoor and outdoor wall surfaces compared to the conventional acrylic paint. On average, the temperature difference is around 2.1 to 2.4°C for aerogel paint, while it ranges from 0.8 to 1.6°C for conventional acrylic paint. Figure 7a shows the minimum and maximum temperature difference for each house over time. These values indicate that the aerogel-painted house managed to reduce the indoor temperature of the house based on the contribution of the wall alone.

Figure 8 illustrates that the house coated with aerogel paint had a much lower outside wall temperature than the outdoor ambient temperature. This indicates that the insulation effectiveness of the wall will improve, and the influence of the aerogel can become more noticeable. This is because the paint could reduce the absorption of solar radiation. This outcome illustrates the paint's capacity to act as a thermal reflector for the wall. On average, aerogel paint reduces more than 2.5°C, representing about 7% of solar heat reflection

compared to around 2%, as shown by the typical paint in Figure 9. This was contributed by the aerogel properties of high porosity, which have been reported by many previous studies, which reduce the heat transfer by conduction, which leads to a lower level of heat energy being transferred to the outer wall from solar radiation. Besides that, aerogels were engineered to block infrared radiation effectively. For instance, silica aerogel exhibits strong scattering and reflection of infrared waves, which makes it ideal for thermal insulation against radiative heat transfer.

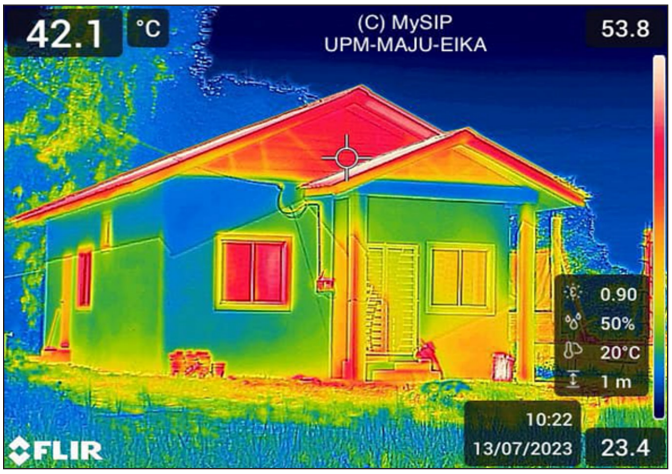

(a)

Aerogarde Paint

Time	Temperature Difference
10:50 am	2.1°C
13:50 pm	2.4°C

(b)

Normal Paint

Time	Temperature Difference
09:45 am	1.6°C
14:00 pm	0.8°C

(c)

Figure 7. (a) Whole house Infrared camera observation sample; (b) House 1 Temperature difference at two different times; (c) House 2 Temperature difference at two different times

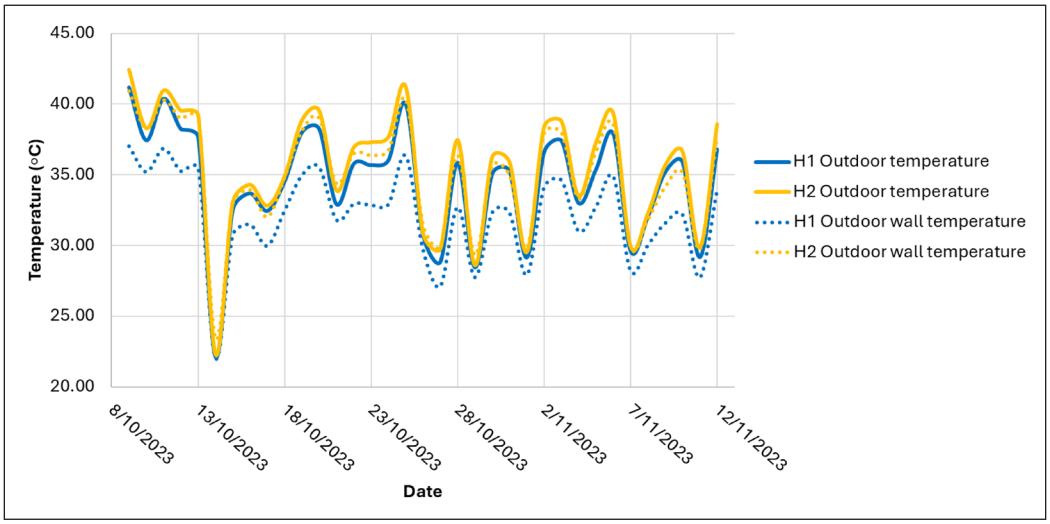

Figure 8. Outside wall temperature in comparison to the outdoor ambient temperature
Note. H1 = House 1; H2 = House 2

Following the analysis of surface temperature differences under solar exposure, where the wall coated with aerogel-based paint consistently exhibits lower surface temperature than the conventional acrylic paint-coated wall, a detailed thermal conductivity assessment was conducted to quantify their insulating performance. The wall coated with aerogel-based paint demonstrates a remarkably low thermal conductivity of $0.019\frac{W}{m^2℃}$, in contrast to $0.131\frac{W}{m^2℃}$ for the conventional acrylic paint. This represents an approximation of an 85% reduction, confirming that the aerogel enhancement formulation effectively suppresses heat transfer through the wall. The reduction in the surface temperature observed is attributed to both the low thermal conductivity and the high solar reflectance of the aerogel coating, which limits the amount of heat absorbed and conducted into the wall. The aerogel's nanoporous structure restricts conductive and convective heat flow, thus enabling the paint to function as a high-performance thermal barrier. These findings underscore the potential of aerogel-based coatings in improving thermal insulation of building envelopes, offering a passive and scalable solution for reducing indoor heat gain in hot climates.

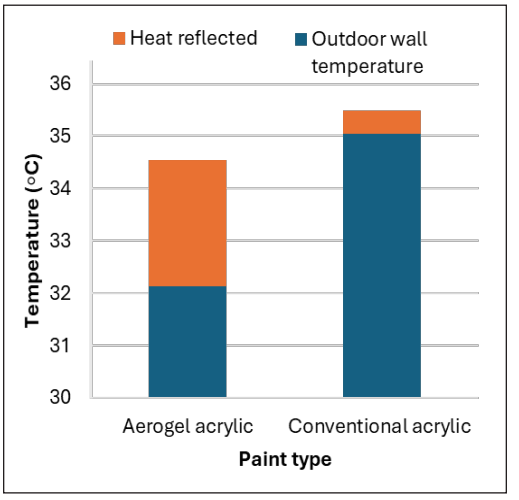

Figure 9. Solar heat reflection by aerogel and conventional acrylic paint

An extensive data analysis was performed to ascertain the variations in the conductivity of the wall structures. To carry out this study, it was essential to monitor the temperature on both the inside and outside sides of the wall (Figure 10).

The thermal resistance, R, was determined using the mean method outlined in the ISO standard 9869 (International Organization for Standardization [ISO], 2014). The standard provides guidelines for determining the thermal performance of building elements (e.g., walls, roofs, floors) under real-world conditions. One key feature and benefit of using ISO 9869 is that, unlike laboratory tests, ISO 9869 captures real-world conditions, including environmental influences like wind, humidity, and temperature fluctuations, and this method does not require damaging the structure, which makes it ideal for assessing existing buildings. Besides that, the standards account for dynamic thermal behaviors such as thermal inertia and transient heat flow by taking long-term measurements, which typically take several days to weeks. To calculate the resistance, one can use this method by dividing the average temperature difference from the wall by the average heat flow density (Equation 1).

$$R = \frac{\sum_{j=1}^{n}\left(T_{si,j} - T_{se,j}\right)}{\sum_{j=1}^{n} q_j} \quad [1]$$

According to the data, it was noticed that home 1, coated with aerogel paint, showed an average thermal resistance of $0.007 \pm 0.0004 \frac{W}{m^{2}\text{°C}}$ while the conventional acrylic paint records around $0.018 \frac{W}{m^{2}\text{°C}}$.

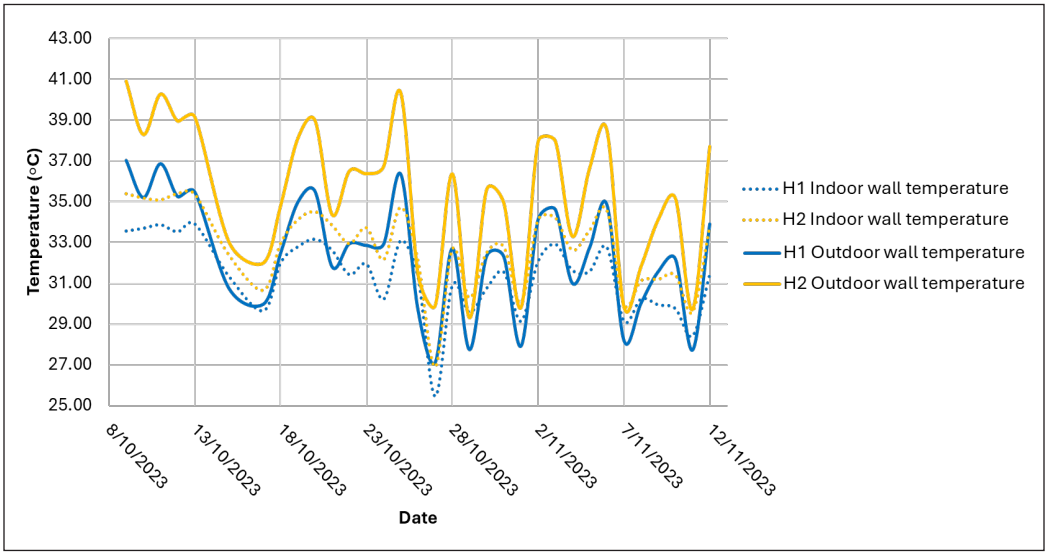

Figure 10. The temperature on both the inside and outside sides of the wall for both houses
Note. H1 = House 1; H2 = House 2

CONCLUSION

This article reported a preliminary study of an elaborate in-situ assessment of the thermal performance of two houses applied with aerogel-infused and regular paint, respectively. This analysis used a monitoring and measuring system that implements LoRa technology. The house coated with aerogel paint had a much lower outside wall temperature than the outdoor ambient temperature. This indicates that the insulation effectiveness of the wall will improve, and the influence of the aerogel can become more noticeable. This is because the paint could reduce the absorption of solar radiation. This outcome illustrates the paint's capacity to act as a thermal reflector for the wall. On average, aerogel paint reduces more than 2.5°C, representing about 7% of solar heat reflection compared to around 2%, as the typical paint shows. Based on the data, it was discovered that the thermal conductivity of the house that was coated with aerogel-infused paint was $0.019 \frac{W}{m^{2}\text{°C}}$ while the conventional

acrylic paint has $0.1\frac{W}{m^2{}^\circ C}$. The aerogel nanoporous structure, combined with high solar reflectance, plays a dual role in minimizing conductive heat transfer and radiative heat gain. These findings confirm that aerogel-infused coating or paint provides a passive thermal barrier that limits solar heat absorption. This contributes to improved indoor thermal comfort and potential reduction in cooling energy demand. As such, aerogel-infused paint represents a promising solution for enhancing the energy efficiency of a building, particularly in hot and sunny climates.

ACKNOWLEDGEMENTS

The authors thank the Ministry of Higher Education (MoHE) for funding this project under the Malaysia-Spain Innovation Programme (MySIP) no. 5540547.

REFERENCES

Abdul Halim, Z. A., Ahmad, N., & Mat Yajid, M. A. (2025). Modifying commercial water-based acrylic paint with rice husk-derived silica aerogel fillers for building thermal insulation. *Progress in Organic Coatings*, *201*, 109114. https://doi.org/10.1016/j.porgcoat.2025.109114

Abu Talib, A. R., & Bheekhun, N. (2018). Feasibility study of a novel aerogel-based thermally sprayed coating. *Journal of Engineering Science and Technology*, *13*, 1-8.

Adhikary, S. K., Ashish, D. K., & Rudžionis, Ž. (2021). Aerogel based thermal insulating cementitious composites: A review. *Energy and Buildings*, *245*, 111058. https://doi.org/10.1016/j.enbuild.2021.111058

Beltramelli, L., Mahmood, A., Österberg, P., & Gidlund, M. (2021). LoRa beyond ALOHA: An investigation of alternative random access protocols. In *IEEE Transactions on Industrial Informatics* (Vol. 17, No. 5, pp. 3544–3554). IEEE. https://doi.org/10.1109/TII.2020.2977046

Berardi, U. (2016). The outdoor microclimate benefits and energy saving resulting from green roofs retrofits. *Energy and Buildings*, *121*, 217–229. https://doi.org/10.1016/j.enbuild.2016.03.021

Berardi, U. (2017a). A cross-country comparison of the building energy consumptions and their trends. *Resources, Conservation and Recycling*, *123*, 230–241. https://doi.org/10.1016/j.resconrec.2016.03.014

Berardi, U. (2017b). The benefits of using aerogel-enhanced systems in building retrofits. *Energy Procedia*, *134*, 626–635. https://doi.org/10.1016/j.egypro.2017.09.576

Becker, P. F. B., Effting, C., & Schackow, A. (2022). Lightweight thermal insulating coating mortars with aerogel, EPS, and vermiculite for energy conservation in buildings. *Cement and Concrete Composites*, *125*, 104283. https://doi.org/10.1016/j.cemconcomp.2021.104283

Bheekhun, N., Abu Talib, A. R., & Hassan, M. R. (2018). Tailoring aerogel for thermal spray applications in aero-engines: A screening study. *Advances in Materials Science and Engineering*, *2018*(1), 5670291. https://doi.org/10.1155/2018/5670291

Bheekhun, N., Abu Talib, A. R., & Hassan, M. R. (2014). Thermal spray coatings for polymer matrix composites in gas turbine engines: A literary preview. *International Review of Aerospace Engineering*, *7*(3), 84-87.

Chaudhari, B. S., Zennaro, M., & Borkar, S. (2020). LPWAN technologies: Emerging application characteristics, requirements, and design considerations. *Future Internet*, *12*(3), 46. https://doi.org/10.3390/fi12030046

Chen, L. (2011). Preparation of environmentally-friendly architectural heat insulation coatings based on polymer emulsions and the heat insulation aggregate. *Journal of Dispersion Science and Technology*, *32*(9), 1273–1278. https://doi.org/10.1080/01932691.2010.505793

Chen, Y. X., Klima, K. M., Brouwers, H. J. H., & Yu, Q. (2022). Effect of silica aerogel on thermal insulation and acoustic absorption of geopolymer foam composites: The role of aerogel particle size. *Composites Part B: Engineering*, *242*, 110048. https://doi.org/10.1016/j.compositesb.2022.110048

Chen, Z., Gao, S., Zhang, J., Liu, D., Zeng, J., Yao, Y., Xu, J.-B., & Sun, R. (2023). Electrospun silicon carbide nanowire film: A highly thermally conductivity and flexible material for advanced thermal management. *Composites Communications*, *41*, 101654. https://doi.org/10.1016/j.coco.2023.101654

Cuce, E., Cuce, P. M., Wood, C. J., & Riffat, S. B. (2014). Toward aerogel based thermal superinsulation in buildings: A comprehensive review. *Renewable and Sustainable Energy Reviews*, *34*, 273–299. https://doi.org/10.1016/j.rser.2014.03.017

Ganobjak, M., Brunner, S., & Wernery, J. (2020). Aerogel materials for heritage buildings: Materials, properties and case studies. *Journal of Cultural Heritage*, *42*, 81–98. https://doi.org/10.1016/j.culher.2019.09.007

Gao, R., Zhou, Z., Zhang, H., Zhang, X., & Wu, Y. (2023). The evolution of insulation performance of fiber-reinforced silica aerogel after high-temperature treatment. *Materials*, *16*(13), 4888. https://doi.org/10.3390/ma16134888

He, D., Jiao, F., Ou, D., Gao, H., & Wu, J. (2022). Thermal insulation and anti-vibration properties evaluation of modified epoxy resin-based thermal protection coatings in arc-jet. *Progress in Organic Coatings*, *173*, 107158. https://doi.org/10.1016/j.porgcoat.2022.107158

He, S., Guo, S., Zhang, Y., & Huang, Y. (2025). High performance thermal insulation blanket integrated with silica aerogel composites. *Ceramics International*, *51*(18), 26879-26890. https://doi.org/10.1016/j.ceramint.2025.03.369

Hu, P., Hu, X., Liu, L., Li, M., Zhao, Z., Zhang, P., Wang, J., & Sun, Z. (2024). Dimensional upgrading of 0D silica nanospheres to 3D networking toward robust aerogels for fire resistance and low-carbon applications. *Materials Science and Engineering: R: Reports*, *161*, 100842. https://doi.org/10.1016/j.mser.2024.100842

Ibrahim, M., Bianco, L., Ibrahim, O., & Wurtz, E. (2018). Low-emissivity coating coupled with aerogel-based plaster for walls' internal surface application in buildings: Energy saving potential based on thermal comfort assessment. *Journal of Building Engineering*, *18*, 454–466. https://doi.org/10.1016/j.jobe.2018.04.008

International Organization for Standardization. (2014). *ISO 9869-1:2014: Thermal insulation — Building elements — In-situ measurement of thermal resistance and thermal transmittance*. ISO. https://www.iso.org/standard/59697.html

Joly, M., Bourdoukan, P., Ibrahim, M., Stipetic, M., Dantz, S., Nocentini, K., Aulagnier, M., Caiazzo, F. G., & Fiorentino, B. (2017). Competitive high performance aerogel-based composite material for the European insulation market. *Energy Procedia*, *122*, 859–864. https://doi.org/10.1016/j.egypro.2017.07.450

Karim, A. N., Kalagasidis, A. S., & Johansson, P. (2023). Moisture absorption of an aerogel-based coating system under different wetting scenarios. *Building and Environment*, *245*, 110905. https://doi.org/10.1016/j.buildenv.2023.110905

Lu, Y., Li, X., Yin, X., Utomo, H. D., Tao, N. F., & Huang, H. (2018). Silica aerogel as super thermal and acoustic insulation materials. *Journal of Environmental Protection*, *9*(4), 295–308. https://doi.org/10.4236/jep.2018.94020

Mao, T., Li, C., Mao, F., Xue, Z., Xu, G., & Amirfazli, A. (2022). A durable anti-corrosion superhydrophobic coating based on carbon nanotubes and SiO_2 aerogel for superior protection for Q235 steel. *Diamond and Related Materials*, *129*, 109370. https://doi.org/10.1016/j.diamond.2022.109370

Mazrouei-Sebdani, Z., Naeimirad, M., Peterek, S., Begum, H., Galmarini, S., Pursche, F., Baskin, E., Zhao, S., Gries, T., & Malfait, W. J. (2022). Multiple assembly strategies for silica aerogel-fiber combinations – A review. *Materials and Design*, *223*, 111228. https://doi.org/10.1016/j.matdes.2022.111228

Miao, J., Shen, Y., Tao, J., Zeng, X., Liu, S., & Wang, Z. (2023). Design and spraying-preparation of the gradient coatings with various diameters and contents of SiO_2 nano-particles for the enhanced anti-impact and thermal insulation performance. *Progress in Organic Coatings*, *179*, 107491. https://doi.org/10.1016/j.porgcoat.2023.107491

Nie, S., Hao, N., Zhang, K., Xing, C., & Wang, S. (2020). Cellulose nanofibrils-based thermally conductive composites for flexible electronics: A mini review. *Cellulose*, *27*, 4173–4187. https://doi.org/10.1007/s10570-020-03103-y

Pan, Y., Han, D., Huang, S., Niu, Y., Liang, B., & Zheng, X. (2023). Thermal insulation performance and thermal shock resistance of plasma-sprayed TiAlCrY/$Gd_2Zr_2O_7$ thermal barrier coating on γ-TiAl alloy. *Surface and Coatings Technology*, *468*, 129715. https://doi.org/10.1016/j.surfcoat.2023.129715

Powell, M. J., Quesada-Cabrera, R., Taylor, A., Teixeira, D., Papakonstantinou, I., Palgrave, R. G., Sankar, G., & Parkin, I. P. (2016). Intelligent multifunctional VO_2/SiO_2/TiO_2 coatings for self-cleaning, energy-saving window panels. *Chemistry of Materials*, *28*(5), 1369–1376. https://doi.org/10.1021/acs.chemmater.5b04419

Raza, M., Al Abdallah, H., Kozal, M., Al Khaldi, A., Ammar, T., & Abu-Jdayil, B. (2023). Development and characterization of polystyrene–date palm surface fibers composites for sustainable heat insulation in construction. *Journal of Building Engineering*, *75*, 106982. https://doi.org/10.1016/j.jobe.2023.106982

Ren, X., Meng, Y., Zhao, Y., Xu, L., Su, J., Han, J., & Dong, J. (2023). Preparation of polyvinylidene fluoride coating modified by well-dispersed MEA-ATO@HNTs and its photocatalytic, antistatic and thermal insulation properties. *Ceramics International*, *49*(12), 20437–20446. https://doi.org/10.1016/j.ceramint.2023.03.172

Shanmugam, G., Gunasekaran, E., Karuppusamy, R. S., Ramesh, R., & Vellaichamy, P. (2020). Utilization of aerogel in building construction – A review. In *IOP Conference Series: Materials Science and Engineering* (Vol. 955, No. 1, p. 012032). IOP Publishing. https://doi.org/10.1088/1757-899X/955/1/012032

Shen, X., Mao, T., Li, C., Mao, F., Xue, Z., Xu, G., & Amirfazli, A. (2023). Durable superhydrophobic coatings based on CNTs-SiO_2 gel hybrids for anti-corrosion and thermal insulation. *Progress in Organic Coatings*, *181*, 107602. https://doi.org/10.1016/j.porgcoat.2023.107602

Sun, G., Yang, L., & Liu, R. (2021). Thermal insulation coatings based on microporous particles from Pickering emulsion polymerization. *Progress in Organic Coatings*, *151*, 106023. https://doi.org/10.1016/j.porgcoat.2020.106023

Syarikat Perumahan Negara Berhad. (n.d.). *Rumah Mesra Rakyat*. SPNB. https://spnb.com.my/rumah-mesra-rakyat/

Tao, J., Yang, F., Wu, T., Shi, J., Zhao, H.-B., & Rao, W. (2023). Thermal insulation, flame retardancy, smoke suppression, and reinforcement of rigid polyurethane foam enabled by incorporating a P/Cu-hybrid silica aerogel. *Chemical Engineering Journal*, *461*, 142061. https://doi.org/10.1016/j.cej.2023.142061

Tao, X. X., Qiao, J., Yin, W. Y., Jin, R. C., Pei, L. Z., Chen, J., & Zhang, Q.-F. (2010). Preparation and characterization of nanoscale silicate composite architectural heat-insulating coatings. *Advanced Materials Research*, *168–170*, 2069–2073. https://doi.org/10.4028/www.scientific.net/AMR.168-170.2069

Thapliyal, P. C., & Singh, K. (2014). Aerogels as promising thermal insulating materials: An overview. *Journal of Materials*, *2014*, 127049. https://doi.org/10.1155/2014/127049

Vasile, B. S., Birca, A. C., Surdu, V. A., Neacsu, I. A., & Nicoară, A. I. (2020). Ceramic composite materials obtained by electron-beam physical vapor deposition used as thermal barriers in the aerospace industry. *Nanomaterials*, *10*(2), 370. https://doi.org/10.3390/nano10020370

Wakili, K. G., Stahl, Th., Heiduk, E., Schuss, M., Vonbank, R., Pont, U., Sustr, C., Wolosiuk, D., & Mahdavi, A. (2015). High performance aerogel containing plaster for historic buildings with structured façades. *Energy Procedia*, *78*, 949–954. https://doi.org/10.1016/j.egypro.2015.11.027

Wang, S., Meng, W., Lv, H., Wang, Z., & Pu, J. (2021). Thermal insulating, light-weight and conductive cellulose/aramid nanofibers composite aerogel for pressure sensing. *Carbohydrate Polymers*, *270*, 118414. https://doi.org/10.1016/j.carbpol.2021.118414

Wei, Z.-Y., Meng, G.-H., Chen, L., Li, G.-R., Liu, M.-J., Zhang, W.-X., Zhao, L.-N., Zhang, Q., Zhang, X.-D., Wan, C.-L., Qu, Z.-X., Chen, L., Feng, J., Liu, L., Dong, H., Bao, Z.-B., Zhao, X.-F., Zhang, X.-F., Guo, L., … Li, C.-J. (2022). Progress in ceramic materials and structure design toward advanced thermal barrier coatings. *Journal of Advanced Ceramics*, *11*, 985–1068. https://doi.org/10.1007/s40145-022-0581-7

Yu, Z., & Liang, D. (2016). Application of SiO_2 aerogel material in building energy saving technology. *Chemical Engineering Transactions*, *55*, 307–312. https://doi.org/10.3303/CET1655052

Zhang, Z., Wang, K., Mo, B., Li, X., & Cui, X. (2015). Preparation and characterization of a reflective and heat insulative coating based on geopolymers. *Energy and Buildings*, *87*, 220–225. https://doi.org/10.1016/j.enbuild.2014.11.028

Zhu, L., Wang, Y., Cui, S., Yang, F., Nie, Z., Li, Q., & Wei, Q. (2018). Preparation of silica aerogels by ambient pressure drying without causing equipment corrosion. *Molecules*, *23*(8), 1935. https://doi.org/10.3390/molecules23081935

Pertanika J. Sci. & Technol. 33 (5): 2357 - 2394 (2025)

PERTANIKA JOURNALS

SCIENCE & TECHNOLOGY

Journal homepage: http://www.pertanika.upm.edu.my/

Review Article

Energy Efficiency and Comfort Performance of Airport Terminal Buildings: A Systematic Review

Lei Wang, Mazran Ismail* and Hazril Sherney Basher

School of Housing, Building and Planning, Universiti Sains Malaysia, 11800 Gelugor, Pulau Pinang, Malaysia

ABSTRACT

Airport terminal buildings (ATBs) exhibit highly dynamic occupancy patterns and extended operating hours, leading to notably higher energy consumption and carbon emissions than other building types. Among the various energy-intensive systems, review findings indicate that heating, ventilation, and air conditioning (HVAC) systems, the most energy-intensive in ATBs, account for approximately 40–60% of total energy consumption, underscoring the need for efficiency improvements, notably during cooling periods. This study systematically reviews 63 studies from 2003 to 2024 to evaluate energy efficiency and thermal comfort performance in ATBs, identifying key research trends and gaps. Despite their significant impact, real-time variations in passenger density and movement patterns pose significant challenges to HVAC optimization, yet existing studies have overlooked mainly their influence on energy performance. The findings reveal that research on ATB energy efficiency has shifted towards integrated approaches that balance energy efficiency and passenger comfort, rather than optimizing either factor independently. Regarding optimization methods, two dominant approaches have been identified: physics-based and data-driven methods, with the latter being the most popular, adopted in 49% of the reviewed studies. Future research should focus on hybrid approaches that integrate physics-based and AI-driven optimization models to improve predictive accuracy and computational efficiency. Additionally, incorporating real-time occupant behaviour into energy optimization strategies is crucial for balancing efficiency and passenger comfort. Advancing robust datasets and enhancing model interpretability will be key to next-generation ATB energy management.

Keywords: Airport terminal building, data-driven energy modeling, energy efficiency, HVAC optimization, systematic review, thermal comfort assessment

ARTICLE INFO

Article history:
Received: 06 November 2024
Accepted: 17 April 2025
Published: 28 August 2025

DOI: https://doi.org/10.47836/pjst.33.5.15

E-mail addresses:
wanglei00826@163.com (Lei Wang)
mazran@usm.my (Mazran Ismail)
hazril@usm.my (Hazril Sherney Basher)
* Corresponding author

INTRODUCTION

Built environments play a crucial role in supporting the Paris Agreement's goal of limiting the increase in the average global temperature to 1.5 °C above pre-industrial levels (International Energy Agency [IEA], 2021) Moreover, achieving the global net-zero emissions goal by 2050. Building

e-ISSN: 2231-8526

operations are responsible for > 30% of global final energy consumption and 26% of global energy-related emissions (i.e., direct emissions constitute 8%, while indirect emissions resulting from electricity generation and heat consumption constitute 18%) (IEA, 2023). Moreover, carbon dioxide emissions account for almost 25% of the global total emissions (González-Torres et al., 2022). Airport terminal buildings (ATBs) are among the most energy-consuming commercial buildings owing to their complicated and multiple space features and operation characteristics (i.e., check-in area, departure area, arrival area, public service area, and baggage handling area) (Xianliang et al., 2021). The average energy consumption per unit of terminal floor area is 180 $kWh/m^2 \cdot yr^{-1}$, roughly 2.9 and 8.0 folds higher than those of normal public buildings and city residential buildings, respectively (Gu, Xie, Huang, Ma, et al., 2022; Xianliang et al., 2021; Z. Li et al., 2023). In addition, Ahn et al. (2015), Kim et al. (2020), and Xianliang et al. (2021) indicated that terminal buildings are one of the most energy-intensive building types. In this context, Strategies to enhance energy efficiency in ATBs while simultaneously maintaining occupant comfort are urgently required.

As essential public infrastructure and transportation hubs (Z. Li et al., 2023). ATBs accommodate a range of stakeholders and activities, accompanied by dynamic occupancy patterns (Mary Reena et al., 2018) and long operational hours (Kotopouleas et al., 2018). Within this context, related equipment operates almost round-the-clock at a constant or maximum capacity, particularly cooling and lighting, to maintain comfortable and satisfactory environments for occupants (Abdallah et al., 2021; Rupcic et al., 2023). In addition, the unique designs of ATBs involve a large window-to-wall ratio, particularly glass curtain walls, resulting in significant solar radiation infiltration and finally exacerbating indoor temperature fluctuations (B. Chen et al., 2024). Moreover, lighting, along with the dynamic passenger occupancy, generates heat, and the cooling system must compensate for this heat gain. These factors contribute to an increased cooling load. Therefore, HVAC systems are the primary sources of power consumption in ATBs, which account for close to 40–60% of the total energy consumption (Xianliang et al., 2021).

In addition, HVAC systems contribute more than 50% of the total carbon dioxide emissions in buildings (Xu et al., 2024). Given this significant impact, extensive research has been conducted to explore strategies for optimizing HVAC systems to enhance energy efficiency and mitigate carbon emissions in airport terminals. Parker et al. (2011) performed a simulation-based analysis on the correlation between HVAC system performance and carbon emissions in East Midlands Airport, United Kingdom, demonstrating that targeted HVAC interventions can substantially reduce carbon dioxide (CO_2) emissions. Similarly, Perdamaian et al. (2013) conducted an energy consumption and emission simulation for Terminal 3 of Soekarno-Hatta International Airport, revealing that HVAC optimization can effectively decrease energy consumption and carbon

emissions. Furthermore, Yıldız et al. (2022) examined the relationship between HVAC energy consumption and CO_2 emissions in Erzurum Airport terminals, highlighting that lowering the heating setpoint temperature not only reduces space heating energy demand but also minimizes the energy consumption of pumps and fans, thereby enhancing overall system efficiency while simultaneously reducing CO_2 emissions. Considering this phenomenon, optimizing HVAC is key to reducing energy demands, energy costs, and CO_2 emissions in ATBs.

In recent years, several efforts have been made to enhance energy efficiency, thermal comfort, and daylighting performance of ATBs, focusing on reducing their total energy demand without compromising the comfort and health of occupants. The parameters for assessing ATB performance are numerous and complex, typically involving three aspects: external environmental, passenger occupancy, and electricity usage, which complicate its energy optimization. However, despite active research in this field, the findings are still fragmented. This study involved a comprehensive review of previous related studies to identify research trends and gaps. To comprehensively review these studies, the following research questions were developed:

1. What are the current widely used strategies and approaches for optimizing the energy performance of ATBs?
2. What are the primary parameters used to evaluate the energy performance of ATBs across different purposes (energy efficiency *vs*. comfort conditions)? How are these parameters measured or estimated?
3. What are the main results observed for energy performance across different purposes (energy efficiency *vs*. comfort conditions)?

Therefore, the expected results will open new research avenues and opportunities for ATB energy strategy optimization, particularly in the post-coronavirus disease pandemic era, as the demand for air passengers could exceed 10 billion journeys by 2050 (International Air Transport Association [IATA], 2025). This study structure allows for a thorough examination of the topics. It began with the screening of high-quality and pertinent research papers for systematic review, followed by examining current research trends using bibliometric analysis, and concluded by assessing the limitations of existing research and delineating potential directions for future research.

MATERIALS AND METHODS

This study employed a systematic literature analysis, following the PRISMA guidelines (Page et al., 2021) to ensure a structured and transparent selection of relevant publications on ATBs. The following sections outline the methodological steps, including literature search, study screening, and data extraction and synthesis.

Literature Search Process

Relevant publications were identified through citation database searches based on predefined eligibility and relevance criteria. The study commenced on 15 July 2024, using Scopus and Web of Science (WoS), two leading academic databases, to ensure a systematic and comprehensive analysis of research on the energy efficiency of ATBs. The search covered studies published up to 15 July 2024. The search involved titles, abstracts, and keywords to attain optimal and maximal retrieval outcomes. In addition, the Boolean operator "AND" included all focus areas, and the operator "OR" was used to gather keywords with equivalent meanings. In addition, wildcards were used to increase flexibility in the search process, i.e., the "*" symbol was used to replace all possible characters when searching for one or more entries, and "?" was used to substitute for a single character. Two keyword sets were used (Table 1).

Table 1
Keywords for literature search on energy efficiency in airport terminal buildings in Scopus and Web of Science

Focus	Keywords
Building type	"airport terminal*" OR "terminal building*" OR "airport terminal building*"
Research purpose	"energy efficien*" OR "energy? saving*" OR "energy consumption*" OR "energy demand*" OR "energy reduction*" OR "energy performance*" OR "energy utili?ation*" OR "energy flexibili*" OR "energy conservation*" OR "energy optimi?ation*" OR "comfort"

Screening Criteria

Overall, 333 records were cumulatively generated based on keyword searches, with 54% from Scopus and 46% from WoS (Figure 1). To ensure relevance and quality, an initial screening was performed based on predefined inclusion and exclusion criteria. The specific criteria applied for filtering and screening the results are as follows:

- English must be the language of publication.
- International Scientific Indexing journal papers (i.e., articles and conference papers) must only be in the final version available or "In Press".
- The chosen research topics must fall within energy, engineering, or environmental science.
- The research must involve either energy efficiency, comfort level, or both.
- The research should focus on systems for end-use energy purposes (therefore, scholarly articles focusing on energy-producing systems, such as photovoltaics or solar energy, were excluded).
- Research should focus on the energy efficiency of the entire ATB, excluding single or isolated components (e.g., glass wall, door and window system, and ceiling system).

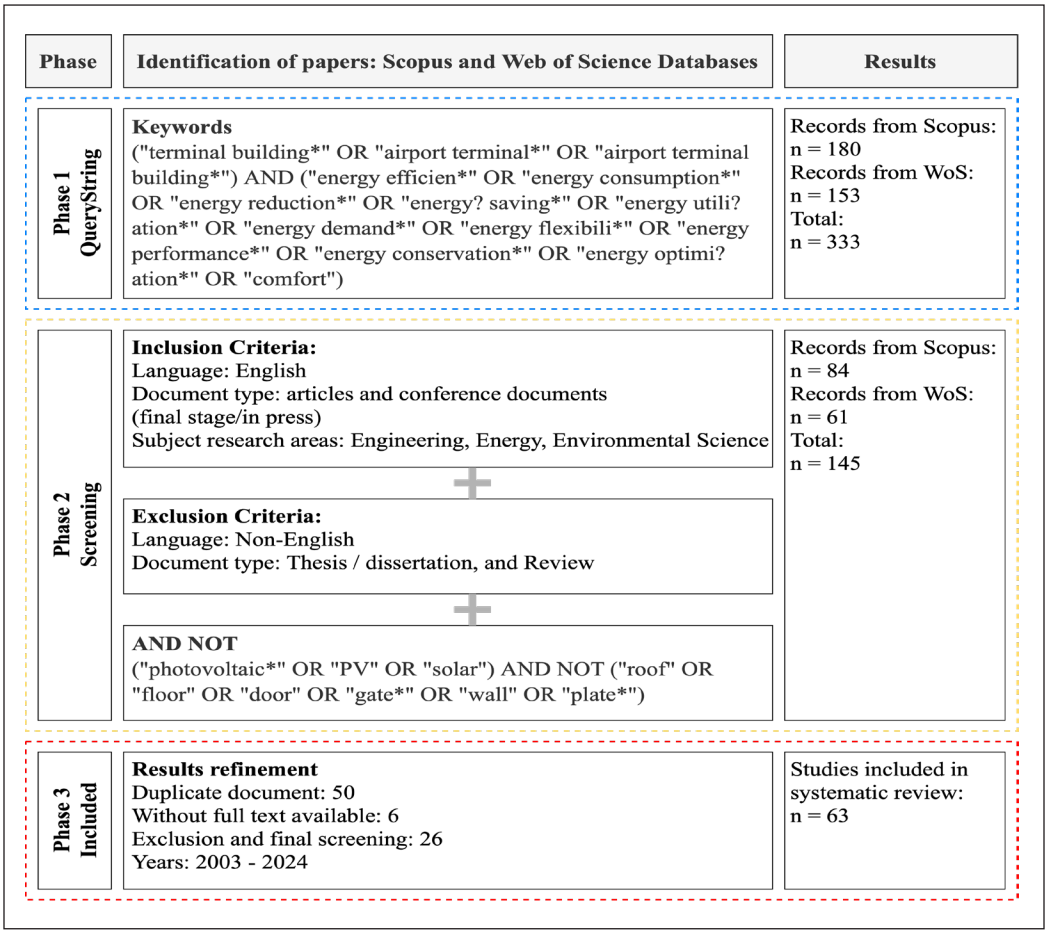

Figure 1. Flow diagram of the systematic review based on the PRISMA guidelines
Note. WoS = Web of Science

- The search engine used the Boolean operator "AND NOT" to eliminate additional specific keywords.

After this phase, 56% of the initial records were excluded based on the filtering and screening criteria, resulting in 145 records being selected for further assessment (84 from Scopus and 61 from WoS).

For further refinement, these records underwent additional screening based on their titles, abstracts, and keywords, leading to the removal of 56 records, including 50 duplicates from both databases and six that lacked full-text availability. A full-text review of the remaining 89 records resulted in the exclusion of 26 papers that did not align with the research scope, since they did not cover ATB's energy consumption. As a result, 63 documents, including 42 research articles (67%) and 21 conference papers (33%), were included in the systematic analysis (Table 2).

Table 2
Overview of authors, publication years, and document types in the systematic review

References	Country	Document type		Building type
		Research article	Conference paper	
B. Chen et al. (2024)	China	✓		Terminal
L. Yang et al. (2024)	China	✓		Terminal
Y. Yang et al. (2024)	China	✓		Terminal
Ma et al. (2024)	China	✓		Terminal
Xu et al. (2024)	China	✓		Terminal
Lin et al. (2023)	China	✓		Terminal
Yue et al. (2023)	China	✓		Terminal
X. Li and Zhao (2023)	China	✓		Terminal
Ma et al. (2023)	China		✓	Terminal
Z. Li et al. (2023)	China	✓		Terminal
Z. Chen et al. (2023)	China		✓	Terminal
Tang et al. (2023)	China	✓		Terminal
Esmaeilzadeh et al. (2023)	United Stated	✓		Terminal
Jia et al. (2022)	China	✓		Terminal
Gu, Xie, Huang, and Liu (2022)	China	✓		Terminal
Jia et al. (2022a)	China	✓		Terminal
Jia et al. (2022b)	China	✓		Terminal
Gu, Xie, Huang, Ma, et al. (2022)	China	✓		Terminal
da Costa et al. (2022)	Brazil	✓		Terminal
Yıldız et al. (2022)	Turkey	✓		Terminal
Yan et al. (2022)	China	✓		Terminal
Hu et al. (2022)	China		✓	Terminal
Akyüz et al. (2021a)	Turkey	✓		Terminal
Xianliang et al. (2021)	China	✓		Terminal
Yıldız et al. (2021)	Turkey	✓		Terminal
Jia et al. (2021)	China	✓		Terminal
Faizah et al. (2021)	Indonesia		✓	Terminal
Akyüz et al. (2021b)	Turkey	✓		Terminal
Dong et al. (2021)	China	✓		Terminal
Liu, Liu, et al. (2021)	China	✓		Terminal
Lin et al. (2021)	China	✓		Terminal
Abdallah et al. (2021)	Egypt	✓		Terminal
Liu, Zhang, et al. (2021)	China	✓		Terminal
Y. Huang et al. (2021)	China	✓		Terminal
Kim et al. (2020)	South Korea	✓		Terminal
Shafei et al. (2020)	Egypt	✓		Terminal
Pasaribu et al. (2019)	Indonesia		✓	Terminal
Sinha et al. (2019)	India		✓	Terminal
Shafei et al. (2019)	Egypt		✓	Terminal

Table 2 *(continue)*

References	Country	Document type		Building type
		Research article	Conference paper	
Lin et al. (2019)	China		✓	Terminal
Liu et al. (2019)	China	✓		Terminal
Mary Reena et al. (2018)	India	✓		Terminal
Kotopouleas et al. (2018)	United Kingdom	✓		Terminal
Miao et al. (2018)	United Stated		✓	Terminal
Malik (2017)	India	✓		Terminal
Weng et al. (2017)	China		✓	Terminal
Zhang et al. (2017)	China	✓		Terminal
B. Li et al. (2017)	China		✓	Terminal
Jiying (2016)	China		✓	Terminal
Kotopouleas et al. (2016)	United Kingdom	✓		Terminal
H. Huang et al. (2015)	Australia	✓		Terminal
Ahn et al. (2015)	United Stated		✓	Terminal
Falvo et al. (2015)	Italy		✓	Terminal
H. Huang et al. (2014)	Australia		✓	Terminal
Wang (2014)	China		✓	Terminal
Gowreesunker and Tassou (2013)	United Kingdom		✓	Terminal
Perdamaian et al. (2013)	Indonesia		✓	Terminal
Sun et al. (2013)	China	✓		Terminal
Danjuma Mambo et al. (2012)	United Kingdom		✓	Terminal
Dai et al. (2012)	China		✓	Terminal
Lau et al. (2011)	Australia		✓	Terminal
Meng et al. (2009)	China	✓		Terminal
Balaras et al. (2003)	Greece	✓		Terminal

RESULTS AND DISCUSSION

Bibliometric Analysis

Based on the bibliometric analysis of the 63 gathered data points (Appendix), summaries of the graphical trend analysis were provided, including publications, countries, variations in paper counts, and network maps generated by VOSviewer.

Publishing Journals

Research Article

Figure 2 and Appendix show that "Building and Environment" was the most prominent journal regarding the topic of energy in ATBs (seven documents), followed by "Energy and Buildings" and "Energy" (each with five documents). While Figure 2 does not provide

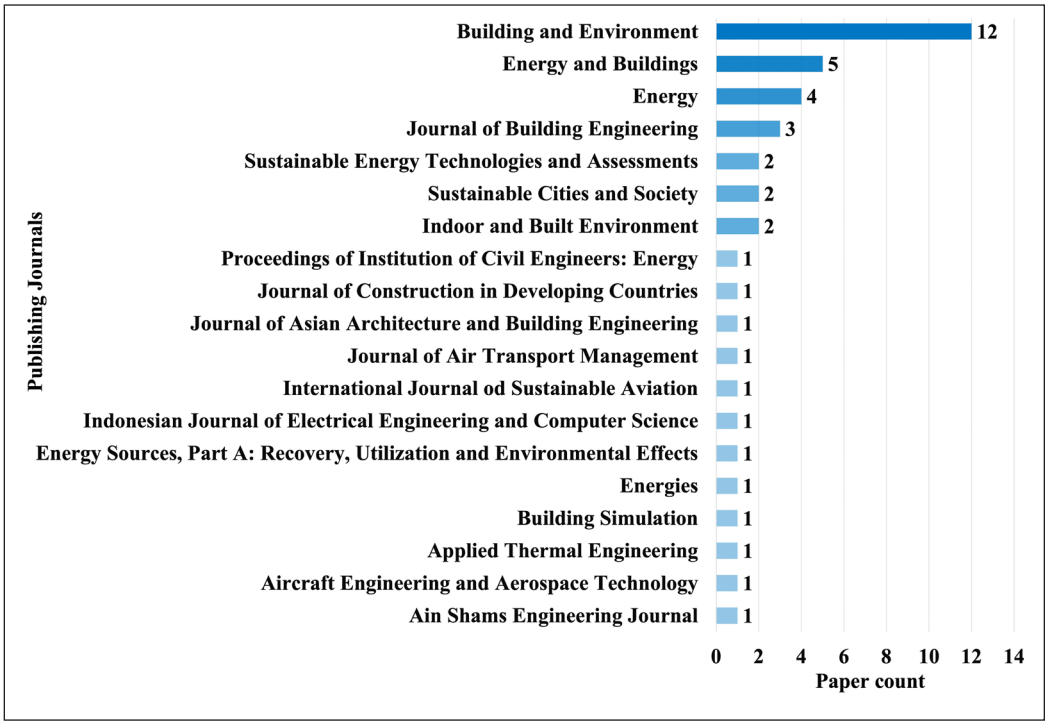

Figure 2. Journal publication distribution of research papers on energy use in airport terminal buildings (up to 15 July 2024)
Note. Darker shades of blue indicate higher values

details on the publisher, most of the selected research articles were published by Elsevier. Refer to the Appendix for further details.

Conference Papers

The International Conference Proceedings contain 21 selected conference papers related to research on ATBs, which span the period from 2011 to 2023. In particular, the International Building Performance Simulation Association (IBPSA) accounts for the highest amount of reviewed conference papers addressing ATBs, close to 24%. The other international conference proceedings, including the International Conference on Environment and Electrical Engineering, the International Symposium on Heating, Ventilation, and Air Conditioning, and the International Conference on Energy, Environment, and Materials Science, account for only one paper each (Appendix).

Study Regions

Figure 3 highlights that publications on the energy efficiency and comfort performance of ATBs are primarily concentrated in countries from the Northern Hemisphere (i.e., eight

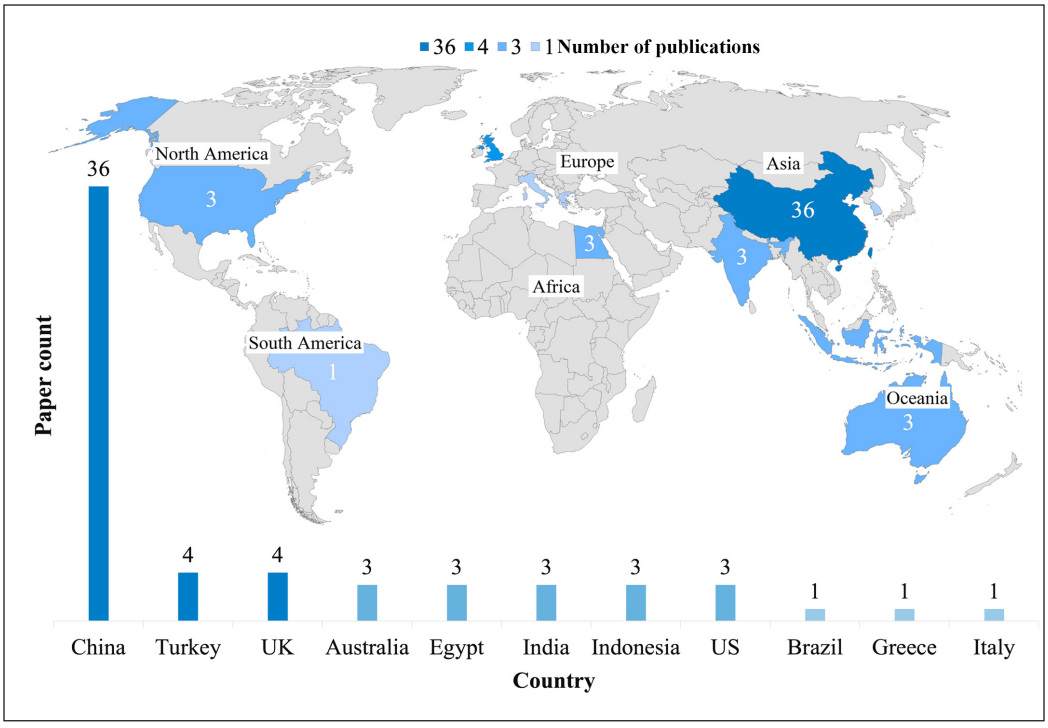

Figure 3. Geographic distribution of research papers on energy use in airport terminal buildings (ATBs) (Up to 15 July 2024)
Note. Darker shades indicate higher numbers of publications; UK = United Kingdom; US = United States

out of eleven published countries). Of the 63 selected studies, 36 (58%) were conducted in China, four (6%) in Turkey, four (6%) in the United Kingdom, and three (5%) in Australia, Egypt, India, Indonesia, and the United States. Only one study was conducted in Brazil, Greece, Italy, and South Korea.

Literature Sources

Figure 4 illustrates the fluctuations in the number of papers published in 2003–2024 (indicated by yellow dashed lines). The starting point of the review paper dates to 2003, as Balaras et al. (2003) was the first relevant and available publication. Additionally, there is currently no single review paper on the energy performance of ATBs. Therefore, this study has covered the past 20 years. Since 2003, the number of research papers on energy and comfort in ATBs has gradually increased, peaking at 12 (11 articles and one conference paper) in 2021. Despite a slight decline in the number of publications since 2021, the overall level remains significantly higher than that recorded in the years prior to 2021. This tendency indicates that there is ongoing interest in the research domain within the academic community, necessitating further in-depth studies in the future.

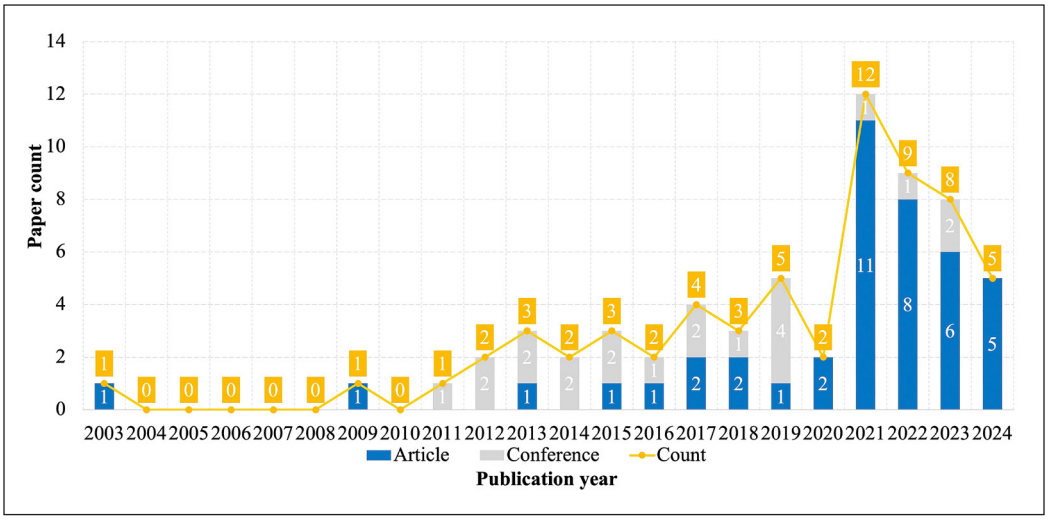

Figure 4. Annual trends in the number of publications on energy performance research of airport terminal buildings (2003–2024)

Keyword Co-Occurrence

Figure 5 presents a keyword co-occurrence analysis map created by VOSviewer, visualizing terms occurring ≥3 times in the keywords and abstracts of 63 reviewed papers. Clusters were identified using the visualization of similarities (VOS) clustering technique, which groups terms with high co-occurrence frequency into distinct categories. In the network map, four colours correspond to four clusters, the node size reflects term recurrence, and terms within the same cluster exhibit strong co-occurrence. The thickness of the links between nodes represents the strength of co-occurrence, with thicker links indicating stronger relationships.

In addition, according to Figure 5, several prominent terms could be identified: "airport terminal building," "energy efficiency," "air conditioning," "thermal comfort", "ventilation" and "cooling" were emphasized and precisely positioned, emphasizing the deep and intrinsic connections between these terms. Moreover, the keyword co-occurrence analysis map offered additional information. The interconnectedness of all the clusters, with the keyword "energy utilization" at the center, suggested that it was the most extensively researched objective purpose in ATB research. Air conditioning was the second focus, and as expected, the energy demand of ATBs was often associated with air conditioning.

Thematic Synthesis

This subsection provides an overview of the relevant literature. First, the identified papers were categorized according to their research objectives, including energy efficiency, occupant comfort, and both energy efficiency and comfort conditions (Figure 6 and

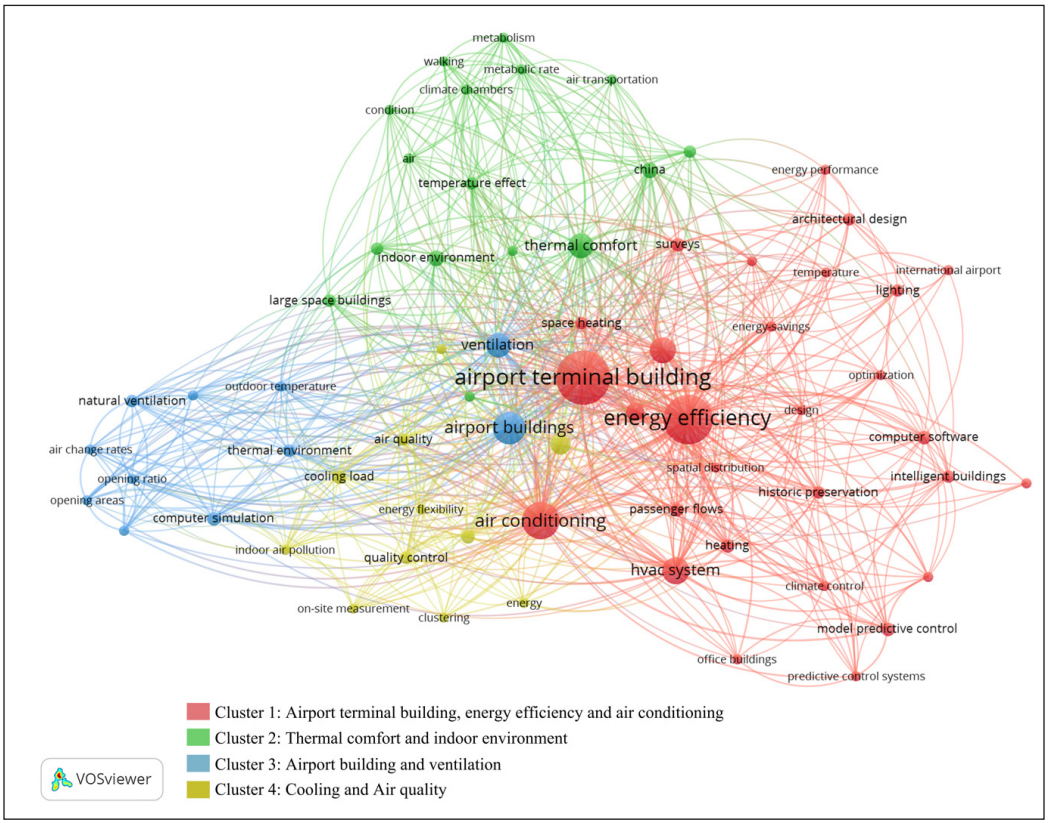

Figure 5. Co-occurrence analysis of keywords (≥3 occurrences) in the reviewed papers using VOSviewer

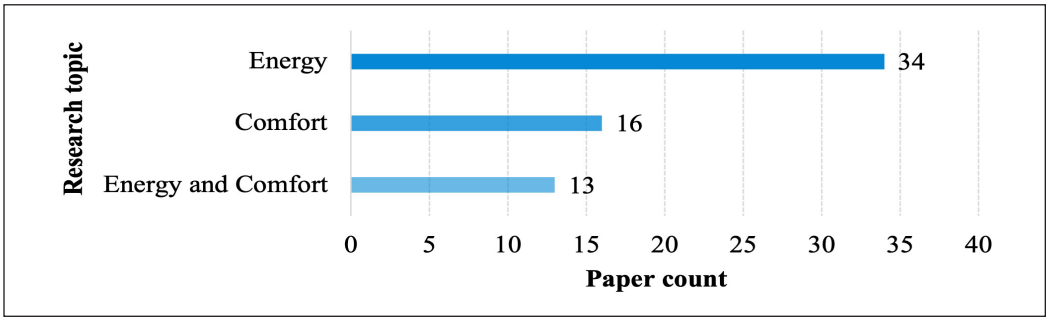

Figure 6. Classification of reviewed papers by research focus: Energy, thermal comfort, and both (n = 63)

Appendix). Among them, 34 (54%) studies concentrated on energy optimization in ATBs, and 16 (25 %) focused on indoor comfort conditions. Only 13 (21%) studies encompassed improved energy efficiency without jeopardizing occupant comfort. Based on the results, we further explored trends in energy performance optimization and the primary parameters evaluated in ATBs in the subsequent section.

Energy Performance Optimization Approach in Terms of Energy Efficiency

Among the 63 studies reviewed, 32 specifically focused on the energy consumption of ATBs, including 22 articles and 11 conference papers (Table 3). Among them, HVAC systems received the most attention, accounting for approximately 40% of the total (25 documents, including 18 articles and seven conference papers). In contrast, only 6% of the reviewed studies (five documents, including one article and four conference papers) examined lighting control systems. Additionally, four studies explored other factors influencing energy consumption.

Besides that, Table 3 presents the energy-saving potential, which varies across different systems. Specifically, previous studies have reported that optimizing the HVAC system can achieve total energy savings between 5 and 57%, depending on the optimization strategies employed. Specifically, these strategies include temperature setpoint adjustments, cooling load parameter optimization, advanced equipment control strategies, fresh air system optimization, and improvements in energy-saving calculation algorithms, among others. For instance, Lin et al. (2023), Malik (2017), and Yıldız et al. (2022) investigated the optimization of air temperature setpoints, with Yıldız et al. (2022) achieving the highest reported energy savings, reaching a 57.24% reduction in energy consumption. Similarly, Lin et al. (2021) and Liu, Liu, et al. (2021) analyzed the impact of adjusting cooling load parameters on overall system performance, with Liu, Liu, et al. (2021) reporting a 34% reduction in HVAC system energy consumption. Additionally, Gowreesunker and Tassou (2013), H. Huang et al. (2014), Liu, Zhang, et al. (2021), Sun et al. (2013), Tang et al. (2023), Z. Li et al. (2023), and Zhang et al. (2017) explored energy-saving strategies for ATBs through advanced control optimizations, among which Tang et al. (2023) reported the highest energy savings, achieving a 38.3% reduction in total energy consumption. Furthermore, Gu, Xie, Huang, and Liu (2022), Gu, Xie, Huang, Ma, et al. (2022), Liu, Zhang, et al. (2021), and Xianliang et al. (2021) optimized cooling load based on passenger distribution, also achieving energy savings. In particular, Gu, Xie, Huang, and Liu (2022) reported a 17.14% reduction in HVAC system energy consumption.

In addition, optimizing the lighting control (LC) system can enhance energy efficiency, particularly with the implementation of an advanced lighting control system. For instance, Wang (2014) reported that adopting such a system led to a total energy consumption reduction of up to 13%. Additionally, Z. Chen (2023) adopted human detection and path planning techniques to adjust terminal internal lighting, ultimately achieving 54.4% energy savings in this system.

Only a limited number of studies (4 out of 63) have explored alternative approaches beyond the two optimization strategies to enhance the overall energy efficiency of ATBs. Among these, Kim (2020) as well as Ahn and Cho (2015) investigated the impact of optimizing relevant parameters on ATB energy consumption, highlighting the critical role

Table 3
Categorization of the reviewed papers by the optimization energy savings factor/system

Optimization factor/system	References	Paper type		Max energy saving (%)			Number of retrieved articles
		Article	Conference	HVAC	LC	Total	
HVAC	B. Chen et al. (2024)	✓		-	-	-	26
	Xu et al. (2024)	✓		-	-	-	
	Lin et al. (2023)	✓		-	-	-	
	Tang et al. (2023)	✓		-	-	38.3	
	Z. Li et al. (2023)	✓		-	-	-	
	Gu, Xie, Huang, and Liu (2022)	✓		17.14	-	-	
	Gu, Xie, Huang, Ma, et al. (2022)	✓		11	-	-	
	da Costa et al. (2022)	✓		-	-	13	
	Yıldız et al. (2022)	✓		-	-	57.24	
	Yıldız et al. (2021)	✓		-	-	11	
	Lin et al. (2021)	✓		-	-	-	
	Liu, Liu, et al. (2021)	✓		34			
	Xianliang et al. (2021)	✓		-	-	-	
	Liu, Zhang, et al. (2021)	✓		-	-	-	
	Liu et al. (2019)	✓		-	-	-	
	Sinha et al. (2019)		✓	-	-	-	
	Miao et al. (2018)		✓	-	-	17	
	Malik (2017)	✓		30	-	-	
	Zhang et al. (2017)	✓		-	-	8	
	Falvo et al. (2015)		✓	77		-	
	H. Huang et al. (2014)		✓	-	-	18	
	Gowreesunker and Tassou (2013)		✓	-	-	30	
	Sun et al. (2013)	✓				19	
	Perdamaian et al. (2013)	✓		-	-	5.16	
	Dai et al. (2012)		✓	-	-	-	
	Lau et al. (2011)		✓	-	-	-	
	Meng et al. (2009)	✓		21	-	-	
LC	Z. Chen et al. (2023)		✓	-	54.4	-	4
	Faizah et al. (2021)		✓	-	-	-	
	Malik (2017)	✓		-	-	-	
	Wang (2014)		✓	-	-	13	
Other	Akyüz et al. (2021a)	✓		-	-	-	4
	Kim et al. (2020)	✓		-	-	-	
	B. Li et al. (2017)		✓	-	-	-	
	Ahn and Cho (2015)		✓	-	-	-	

Note. '-' = No report; HVAC = Heating, ventilation, and air conditioning; LC = Lighting control

of Energy Use Intensity (EUI) in accurately predicting and optimizing energy performance. For instance, Ahn and Cho (2015) conducted a study on United States airports. They demonstrated that EUI optimization could lead to significant cost reductions, with estimated annual electricity savings exceeding $472,000 based on California electricity rates.

Generally, energy efficiency estimates for ATBs cover several aspects, including environmental conditions, passenger occupancy conditions, energy end-use load, and operating costs. Furthermore, an in-depth analysis of the relevant indicator parameters was conducted to understand better and assess their energy-saving potential. Table 4 consolidates the main parameters identified in the reviewed papers for evaluating energy efficiency and shows that air temperatures, passenger distribution, and cooling load were the most frequently assessed parameters in the 34 reviewed energy-related papers, occurring 20, seven, and 14 times, respectively. In addition, the energy analysis mainly focused on the cooling load. Most studies focused on the cooling demands of ATBs; hence, reducing overcooling and energy waste risk during the cooling season is a paramount concern in ATB research.

ATBs typically have an area of several hundred thousand square meters and are larger than general public buildings. Therefore, researchers usually apply simulation model methods to address energy issues. The energy simulation is a mathematical analysis of the physical properties of its elements (Delzendeh et al., 2017). In recent years, two categories of model methods have been widely applied in building load prediction: physical-based and data-driven approaches (B. Chen et al., 2024). Appendix presents an in-depth analysis

Table 4
Overview of main parameters evaluated for the energy savings indicators in airport terminal buildings

References	Main parameters evaluated																
	Environment condition							Passenger behavior				Energy consumption					
	Air temperature	Surface temperature	Relative humidity	Air velocity	Air infiltration	Wind environment	Solar radiation	Illumination level	Passenger distribution	Passenger numbers	Walking speeding	Dwelling time	Cooling load	Heating load	Electricity load	Total energy demand	Coefficient of performance	Energy use intensity
B. Chen et al. (2024)													✓					
Xu et al. (2024)	✓	✓	✓										✓					
Z. Li et al. (2023)									✓									
Lin et al. (2023)	✓		✓	✓			✓						✓					
Tang et al. (2023)	✓		✓															
Z. Chen et al., 2023	✓								✓							✓		

Table 4 *(continue)*

References	Main parameters evaluated															
	Environment condition							Passenger behavior				Energy consumption				
	Air temperature	Surface temperature	Relative humidity	Air velocity	Air infiltration	Wind environment	Solar radiation	Illumination level	Passenger distribution	Passenger numbers	Walking speeding	Dwelling time	Cooling load	Heating load	Electricity load	Total energy demand	Coefficient of performance	Energy use intensity
Gu, Xie, Huang, and Liu (2022)									✓				✓	✓				
Gu, Xie, Huang, Ma, et al. (2022)	✓		✓										✓					
da Costa et al. (2022)	✓																✓	
Yıldız et al. (2022)																✓		
Xianliang et al. (2021)																✓		
Akyüz et al. (2021a)	✓									✓						✓		
Yıldız et al. (2021)	✓					✓								✓		✓		
Liu, Liu, et al. (2021)	✓				✓									✓				
Liu, Zhang, et al. (2021)	✓		✓	✓											✓			
Lin et al. (2021)	✓		✓											✓				
Faizah et al. (2021)								✓							✓			
Kim et al. (2020)	✓												✓					✓
Liu et al. (2019)									✓				✓					
Sinha et al. (2019)									✓		✓	✓	✓					
Miao et al. (2018)													✓	✓				
Malik (2017)	✓		✓													✓		
Zhang et al. (2017)													✓		✓			
B. Li et al. (2017)																✓		
Ahn and Cho (2015)	✓															✓		
Falvo et al. (2015)	✓															✓		
H. Huang et al. (2014)	✓												✓					
Wang (2014)																✓		
Sun et al. (2013)													✓			✓		
Gowreesunker and Tassou (2013)	✓			✓									✓					
Perdamaian et al. (2013)	✓								✓						✓	✓		
Dai et al. (2012)	✓		✓										✓					
Lau et al. (2011)	✓								✓						✓	✓		

Note. Parameters under evaluation must be mentioned at least twice in the selected papers

of the selected papers based on the model method, in which the data-driven approach accounted for 55% and the physical-based approach accounted for 45% (Table 5 and Figure 7). Despite the analysis suggesting less use of the data-driven approach in optimizing ATB rates, it has outperformed the physical-based method regarding energy optimization over the past 5 years, primarily owing to the limitations of the latter. In addition, data-driven approaches have shown greater applicability, computational efficiency, and proficiency in managing nonlinearities (Ala'raj et al., 2022).

Table 5
Summary of energy consumption prediction methods in reviewed studies: Approaches, algorithms, and simulation software

References	Method	Technique/Algorithm	Softerware
B. Chen et al. (2024)	Data-driven method	SSA-CNN-Transformer model	-
Xu et al. (2024)	Physical-based method	Least squares method	-
Lin et al. (2023)	Data-driven method	Clustering analysis (K-means) Uncertainty analysis Bayesian calibration	EnergyPlus DeST
Z. Li et al. (2023)	Data-driven method	PSO	TRNSYS
Z. Chen et al. (2023)	Data-driven method	YOLOv5s algorithm	CAD
Tang et al. (2023)	Data-driven method	U-NSGA-III	Python
da Costa et al. (2022)	Data-driven method	MBE; Cv (RMSE)	AnyLogic IES
Gu, Xie, Huang, and Liu (2022)	Physical-based method	MBE Cv (RMSE)	AnyLogic IES
Gu, Xie, Huang, Ma, et al. (2022)	Physical-based method	Recommissioning	-
Yıldız et al. (2022)	Physical-based method	-	DesignBuilder EnergyPlus
Akyüz et al. (2021a)	Data-driven method	Regression functions	SimaPro
Xianliang et al. (2021)	Data-driven method	Regression functions	Origin
Faizah et al. (2021)	Data-driven method	Energy performance indicators	DesignBuilder EnergyPlus
Liu, Liu, et al. (2021)	Data-driven method	Fuzzy logic	-
Lin et al. (2021)	Data-driven method	Energy performance indicators	-
Liu, Zhang, et al. (2021)	Data-driven method	Monte Carlo method K-means	EnergyPlus Matlab
Yildiz et al. (2021)	Physical-based method	Regression functions	Matlab
Kim et al. (2020)	Data-driven method	Regression functions	EnergyPlus
Sinha et al. (2019)	Data-driven method	Characteristics of the occupancy	AnyLogic OpenStudio EnergyPlus
Liu et al. (2019)	Data-driven method	Characteristics of the occupancy	AnyLogic;
Miao et al. (2018)	Physical-based method	MBE CVRMSE	Trane Trace 700 GLHEPro 5.0

Table 5 *(continue)*

References	Method	Technique/Algorithm	Softerware
Malik (2017)	Data-driven method	Statistical analysis	-
B. Li et al. (2017)	Data-driven method	Sequential Quadratic Programming	Matlab 1stOpt DeST
Zhang et al. (2017)	Physical-based method	Statistical analysis	-
Falvo et al. (2015)	Data-driven method	Regression functions	EnergyPlus
Ahn and Cho (2015)	Physical-based method	Dynamic energy modelling	EnergyPlus Design Builder
Wang (2014)	Data-driven method	ANN	TRNSYS
H. Huang et al. (2014)	Data-driven method	Intelligent control	-
Gowreesunker and Tassou (2013)	Physical-based method		TRNSYS FLUENT
Perdamaian et al. (2013)	Physical-based method	Thermodynamics Principles of matrix algebra	
Sun et al. (2013)	Physical-based method		TRNSYS
Dai et al. (2012)	Physical-based method	Linear regression	-
Lau et al. (2011)	Physical-based method		IES
Meng et al. (2009)	Physical-based method	Thermodynamic principles	DeST PHOENICS

Note. '-' = No report; SSA = Singular Spectrum Analysis; ANN = Artificial neural network; DeST = Designer's Simulation Toolkit; PSO = Particle swarm optimization; TRNSYS = Transient System Simulation Tool; CAD = Computer-aided Design Software; U-NSGA-III = Unified Non-dominated Sorting Genetic algorithm; MBE = Mean bias error; Cv (RMSE) = Coefficient of Variation of root mean square error; IES = Integrated Environmental Solutions Software; SimaPro = Sustainable Product Design and Life Cycle Assessment Software; FLUENT = Fluid Dynamics Software; GLHE = Ground Loop Heat Exchanger Software; PHOENICS = Parabolic Hyperbolic or Elliptic Numerical Integration Code Series

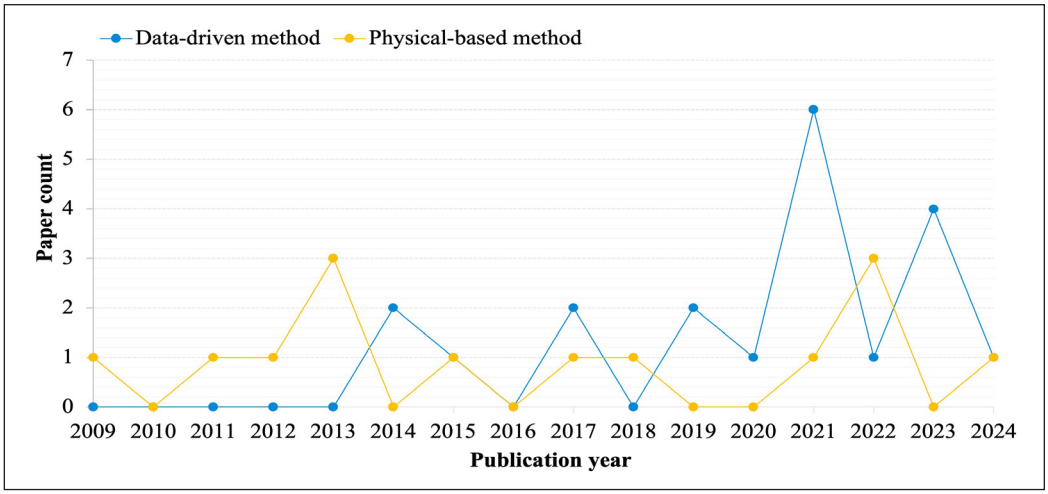

Figure 7. Trends in energy prediction methods for airport terminal buildings (2009-2024): Data-driven vs. physics-based approaches

After analyzing 34 energy-related papers, 18 different types of energy simulation software were identified. As shown in Table 5 and Figure 8, EnergyPlus was primarily used for energy analyses of ATBs, particularly regarding energy issues related to air-conditioning systems (e.g., Kim et al., 2020; Lin et al., 2021, 2023; Sinha et al., 2019; Yıldız et al., 2021, 2022). Although EnergyPlus is a console-based software (Mendes et al., 2024), it also ensures some interoperability with other tools such as DesignBuilder (e.g., Falvo et al., 2015; Yıldız et al., 2021, 2022). In addition, energy analyses of ATBs often used Transient System Simulation Tool (TRNSYS) (e.g., Gowreesunker & Tassou, 2013; H. Huang et al., 2014; Sun et al., 2013; Z. Li et al., 2023) and Anylogicl (e.g., Gu, Xie, Huang, and Liu, 2022; Gu, Xie, Huang, Ma, et al., 2022; Liu et al., 2019; Sinha et al., 2019), and Anylogicl was usually combined with IES-VE to explore passenger distribution and energy consumption relationships (e.g., Gu, Xie, Huang & Liu, 2022; Gu, Xie, Huang, Ma et al., 2022).

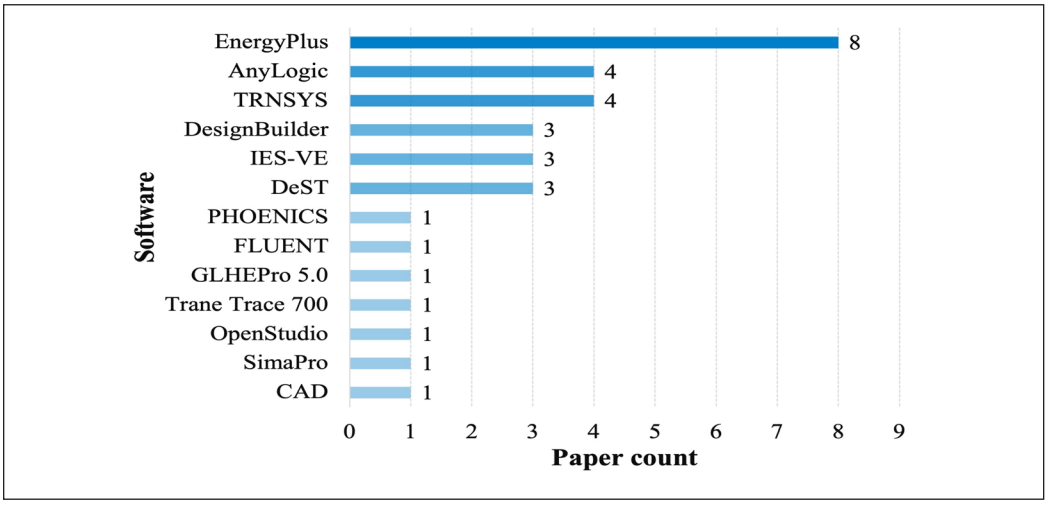

Figure 8. Software usage frequency in the energy simulation of airport terminal buildings (2009–2024): Darker shades indicate higher frequency

Note. TRNSYS = Transient System Simulation Tool; IES-VE = Integrated Environmental Solution-Virtual Environment Software; DeST = Designer's Simulation Toolkit; PHOENICS = Parabolic Hyperbolic or Elliptic Numerical Integration Code Series; FLUENT = Fluid Dynamics Software; GLHE = Ground Loop Heat Exchanger Software; SimaPro = Sustainable Product Design and Life Cycle Assessment Software; CAD = Computer-aided Design Software

Energy Performance Optimization Approach in Terms of Occupant Comfort

The occupant comfort is a key point in architectural design, especially in public buildings. ATB stands out as a complex public transportation facility, characterized by strict service requirements, high passenger densities, and substantial passenger traffic volume (Liu et al., 2018). Consequently, occupant comfort plays a crucial role in determining the degree

of passenger satisfaction and energy demand in ATB. Therefore, improving occupant comfort has become a popular research topic in recent years, and 16 (25%) of the selected papers addressed the topic of occupant comfort (refer to Appendix). Comfort commonly includes thermal, acoustic, visual, and indoor air quality (Ala'raj et al., 2022; Shafei et al., 2020). According to Table 6, thermal comfort has been the most widely considered factor in ATB comfort research, particularly in the summer, accounting for 22% (14 documents). In contrast, acoustic, visual, and indoor air quality received significantly less attention, accounting for 6%.

Within the set of reviewed comfort-related papers, environmental factors and subjective sensations dominated the evaluation of comfort performance indicators in ATBs, closely followed by physiological conditions (Table 7). Regarding environmental conditions, air temperature, relative humidity, and air velocity dominated the main parameter evaluations, with almost all relevant papers mentioning the air temperature parameter and recommending

Table 6
Categorization of reviewed studies on occupant comfort: Analysis by comfort type and season

References	Occupant comfort									
	Studied season					Comfort type				
	Spring	Summer	Autumn	Winter	Not report	Thermal	Acoustic	Visual	Indoor air quality	Other
L. Yang et al. (2024)		✓				✓				
Y. Yang et al. (2024)		✓				✓				
X. Li and Zhao (2023)					✓		✓			
Jia et al. (2022a)		✓				✓				
Jia et al. (2022b)		✓				✓				
Jia et al. (2022)		✓				✓				
Hu et al. (2022)		✓				✓				
Jia et al. (2021)		✓		✓		✓				
Akyüz et al. (2021b)		✓				✓				
Dong et al. (2021)		✓				✓				
Lin et al. (2019)		✓				✓				
Pasaribu et al. (2019)					✓					✓
Kotopouleas and Nikolopoulou (2018)		✓		✓		✓		✓		
Weng et al. (2017)				✓		✓				
Jiying (2015)		✓				✓				
Kotopouleas and Nikolopoulou (2016)		✓		✓		✓				

Note. Other means that personal factors and preferences, indoor physical conditions, external weather conditions, and so on, affect the comfort of occupants

Table 7
Overview of comfort performance indicators in studies on airport terminal buildings: Categorization based on environmental, subjective, and physical conditions

References	Environment condition							Subjective condition					Physical condition			
	Air temperature	Relative humidity	Air velocity	Air infiltration	Wind environment	Lighting	Carbon dioxide concentration	Thermal sensation vote	Thermal performance vote	Thermal comfort vote	Thermal acceptance vote	Sound sensation	Skin Temperature	Metabolic rate	Walking speed	Dwelling time
L. Yang et al. (2024)	✓	✓			✓			✓		✓		✓				
Y. Yang et al. (2024)	✓															
X. Li and Zhao (2023)												✓				
Jia et al. (2022a)	✓	✓	✓					✓	✓	✓	✓		✓	✓	✓	
Jia et al. (2022b)	✓		✓					✓	✓	✓			✓	✓		
Jia et al. (2022)	✓	✓	✓					✓	✓	✓			✓			
Hu et al. (2022)	✓	✓			✓			✓								
Jia et al. (2021)	✓	✓	✓					✓	✓	✓	✓			✓		
Akyüz et al. (2021b)	✓	✓					✓									
Dong et al. (2021)	✓		✓													
Lin et al. (2019)	✓	✓	✓				✓									
Pasaribu et al. (2019)																✓
Kotopouleas and Nikolopoulou (2018)	✓	✓				✓	✓									
Weng et al. (2017)	✓	✓														
Jiying (2015)	✓		✓													
Kotopouleas and Nikolopoulou (2016)	✓	✓					✓	✓	✓							

an indoor set temperature between 24 and 26°C. Additionally, as earlier mentioned, thermal comfort is one of the main focuses; thus, subjective parameters, such as thermal sensation, performance, and comfort, play an important role in evaluating comfort conditions. In ATB, the physiological parameters, such as skin temperature and metabolic rate, are not the primary parameters evaluated, owing to individual differences among passengers; hence, they have not been frequently mentioned.

Figure 9 outlines the standards that the reviewed comfort-related papers frequently apply for the evaluation of the comfort performance of ATBs. As shown in Figure 9, the American Society of Heating, Refrigerating, and Air-conditioning Engineers (ASHRAE) 55 standard, established by the ASHRAE, has emerged as a primary reference in the thermal comfort criteria for ATB. ASHRAE recommends a temperature range of 23–26°C, with

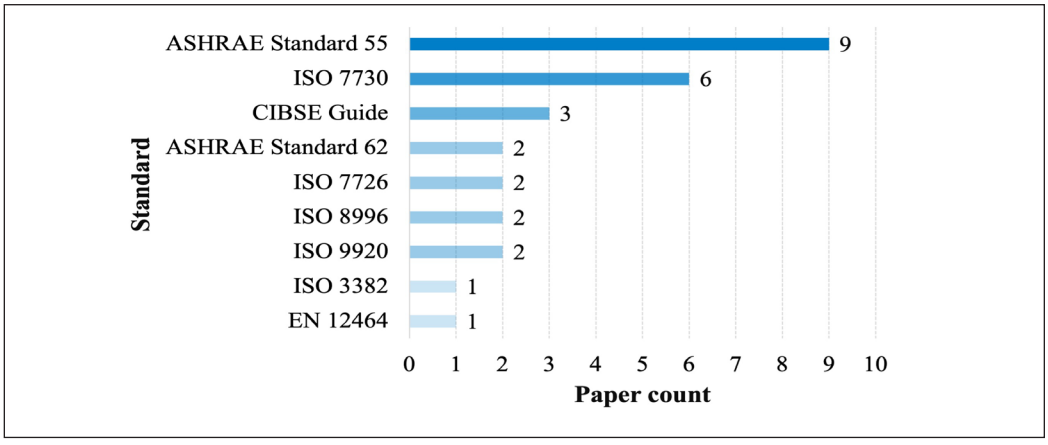

Figure 9. Overview of reference standards adopted in airport terminal buildings thermal comfort studies: Darker shades represent adoption frequency

Note. ASHRAE = American Society of Heating, Refrigerating, and Air-conditioning Engineers; ISO = International Organization for Standardization; CIBSE = Chartered Institution of Building Services Engineers; EN = European Standard

relative humidity values of 30–40% in winter and 40–55% in summer, achieving an 80% comfort acceptability rate (de Dear & Brager, 2002). Previous studies have illustrated the application of this standard (e.g., Akyüz et al., 2021b; Dong et al., 2021; Hu et al., 2022; Jia et al., 2021, 2022, 2022a, 2022b; Kotopouleas & Nikolopoulou, 2016, 2018). In addition, the International Organization for Standardization (ISO) 7730 standard has been widely applied to thermal comfort assessment, with a primary focus on occupant perceptions of the environment (e.g., Akyüz et al., 2021b; Hu et al., 2022; Jia et al., 2021, 2022, 2022a, 2022b). The Chartered Institution of Building Services Engineers (CIBSE) produces CIBSE Guide publications, notably the CIBSE Guide A, another notable authoritative reference standard when evaluating comfort performance.

Energy Performance Optimization Approach in Terms of Energy Savings and Occupant Comfort

Given the nonlinear relationship between energy demand and comfort, 21% (13 documents) of the reviewed papers focused on reducing energy efficiency without jeopardizing occupant comfort, ensuring a suitable trade-off between energy efficiency and comfort performance (Appendix). Therefore, a multi-objective optimization strategy is employed to maximize human comfort, Dual-dimension Strategy (DDS), while minimizing energy consumption. Table 8 demonstrates the application of this strategy, with 19% (12 documents) of the reviewed papers adopting it, attaining energy savings for ATBs between 10 and 40%, while maintaining occupant comfort. Regarding comfort performance, it is noteworthy that almost all the relevant studies address thermal comfort.

Table 8
Categorization of reviewed studies on energy savings and comfort improvement in airport terminal buildings: Optimization strategies and methods

References	Method	Max HVAC system savings (%)	Max total energy savings (%)	Comfort factor	Optimization strategy	Optimization algorithm
Ma et al. (2024)	Data-driven method	10	-	Thermal	OBMPC	GA
Ma et al. (2023)	Data-driven method	13	-	Thermal	OBMPC	GA
Yue et al. (2023)	Data-driven method	34.3	-	Thermal	MPC	BAB
Esmaeilzadeh et al. (2023)	Data-driven method	28	-	Thermal	MPC	GA
Yan et al. (2022)	Data-driven method	44	-	Thermal	SBC	SLSQP
Abdallah et al. (2021)	Data-driven method		24.5	Thermal	MOT	-
Y. Huang et al. (2021)	Physical-based method	-	-	Thermal Acoustic Sound	MOT	OLS
Shafei et al. (2020)	Data-driven method	26.5	13	Thermal	FLC	FA
Shafei et al. (2019)	Data-driven method	-	25	Thermal	DDS	FA
Mary Reena et al. (2018)	Data-driven method	27	-	Thermal	RBC	ANN
H. Huang et al. (2015)	Data-driven method	-	41	Thermal	HMPC	ANN
Danjuma Mambo et al. (2012)	Data-driven method	-	-	Comfort	FLC	FA
Balaras et al. (2003)	Physical-based method	-	40	Thermal	-	-

Note. '-' = No report; OBMPC = Occupant-based model predictive control; GA = Genetic algorithm; MPC = Model predictive control; BAB = Branch and bound; SBC = Scenario-based control; SLSQP = Sequential least squares programming algorithm; MOT = Mathematical optimization technique; OLS = Ordinary Least Squares Algorithm; FLC = Fuzzy logic control; FA = Fuzzy algorithm; DDS = Dual-dimension Strategy; RBC = Rule-based control; ANN = Artificial neural network; HMPC = Hybrid model predictive control

Furthermore, this topic primarily utilizes the data-driven approach, accounting for around 16% (10 documents) of relevant papers on energy and comfort studies, owing to its effectiveness at handling nonlinear relationships. Data-driven approaches typically incorporate various strategies and algorithms to model, control, or optimize energy consumption systems, with model predictive control (MPC) being the most employed approach on ATB energy optimization in the last 5 years (Table 8). Specifically, MPC is a widely recognized approach for managing constrained control based on feedback control and numerical optimization principles (Yaramasu & Wu, 2016). From Table 8, five (8%) of the selected papers (i.e., Esmaeilzadeh et al., 2023; H. Huang et al., 2015; Ma et al., 2023, 2024; Yue et al., 2023) applied MPC-based control approaches combined with different optimization algorithms and achieved energy savings without compromising occupant comfort conditions. Generally, an optimization algorithm aims to minimize or maximize

mathematical objective functions to identify the best possible solution or the most efficient way to solve a problem from available alternatives (Ala'raj et al., 2022). Esmaeilzadeh et al. (2023) and Ma et al. (2023, 2024) employed a genetic algorithm (GA) to achieve 10, 13, and 23% energy savings, respectively. Yue et al. (2023) applied the branch and bound (BAB) algorithm, resulting in energy savings of 34.3%. H. Huang et al. (2015) integrated the artificial neural network (ANN) algorithm, achieving up to 41% energy savings. A comprehensive analysis of the algorithms revealed that the primary approach in this field is a combination of MPC-based strategies and GA (Figure 10). However, this method showed a lower maximum energy savings percentage compared with others. GA, an evolutionary algorithm, has gained widespread use in building energy optimization due to its exceptional accuracy, high sensitivity to parameter variations, and rapid execution speed. Therefore, future research could continue to leverage this advantage along with an MPC-based approach to address the multi-objective optimization challenges of ATBs.

Furthermore, ATB optimization frequently employs the fuzzy logic control strategy, in addition to MPC. Despite the potential ability of this strategy to solve complex control problems, its use in optimizing ATB energy consumption has decreased over the past five years. Besides, researchers have also addressed nonlinear problems in ATB optimization with the ANN-based algorithm, particularly when large amounts of data are involved, but this application is still rarely used today. Considering the previously mentioned information, we found that Swarm Intelligence methods, including particle swarm optimization, ant colony optimization, and grey wolf optimization, have not been applied for ATB energy optimization. This represents a potential direction for future research.

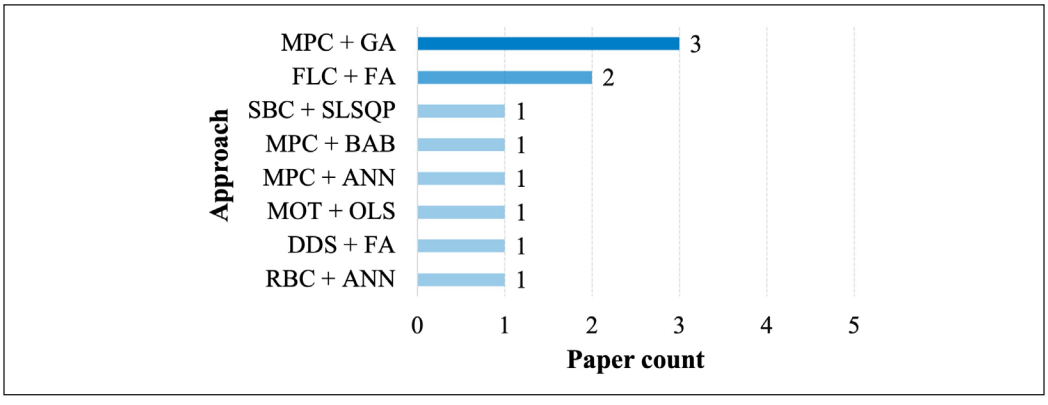

Figure 10. Overview of strategy and algorithm combinations for simultaneous energy optimization and occupant comfort improvement in airport terminal buildings: Darker shades indicate higher adoption frequency

Note. MPC = Model predictive control; GA = Genetic algorithm; FLC = Fuzzy logic control; FA = Fuzzy algorithm; SBC = Scenario-based control; SLSQP = Sequential least squares programming algorithm; BAB = Branch and bound; ANN = Artificial neural network; MOT = Mathematical optimization technique; OLS = Ordinary Least Squares Algorithm; DDS = Dual-dimension strategy; RBC = Rule-based control

DISCUSSION

This study conducts a systematic review of 63 research papers on energy efficiency and occupant comfort in ATBs. Among them, 34 studies specifically examine energy optimization in ATBs, with reported energy savings ranging widely, reaching a maximum of 57% in a single study when occupant comfort is not considered. Additionally, 16 studies explore various aspects of occupant comfort in ATB environments. Furthermore, 13 studies examine energy optimization while preserving occupant comfort, indicating a maximum energy savings of 41%. Notably, the reported minimum and maximum values reflect the global range of findings across the reviewed studies, indicating that energy savings rates are influenced by experimental setups, climatic conditions, and building characteristics, making direct comparisons somewhat limited.

Compared to single-objective energy optimization, multi-objective optimization of both energy consumption and occupant comfort yields a relatively lower energy savings rate (41% vs. 57%). Nevertheless, it ensures occupant comfort while achieving energy savings in ATBs, a factor particularly crucial for buildings with prolonged occupancy, such as airport terminals. This discrepancy can be attributed to the fundamental trade-off between energy efficiency and occupant comfort, as enhanced thermal comfort often requires higher HVAC energy consumption due to increased ventilation rates, stricter temperature controls, and more dynamic system adjustments.

In contrast to data-driven methods, which demonstrate high adaptability in multi-objective optimization, physics-based modeling methods face significant computational and implementation challenges. Among the reviewed studies, 16 papers (25%) employed physics-based modeling methods. However, their application in multi-objective optimization remains limited. Among these 16 studies, physics-based modeling has been predominantly applied to energy consumption minimization, with only two studies attempting to optimize both energy performance and occupant comfort due to the high computational complexity associated with multi-objective simulations.

Physics-based approaches require highly accurate input parameters to ensure reliable simulations. However, compared to conventional buildings, ATBs pose significant challenges in data acquisition. The vast spatial scale limits the feasibility of high-resolution sensor deployment, leading to coarse-grained environmental data. Moreover, dynamic occupant behavior, such as fluctuating passenger density, varying metabolic rates, and diverse clothing insulation levels, introduces uncertainties in thermal comfort modeling. Additionally, ATBs integrate multiple energy systems, including HVAC, lighting, and renewable energy sources, which increases the complexity of energy flow modeling. These factors collectively contribute to parametric uncertainties, potentially leading to deviations between simulated and actual energy performance.

In addition, software limitations further restrict the application of physics-based modeling in optimization. Among the reviewed studies, DesignBuilder is the most used software for physics-based energy simulations, providing a user-friendly graphical interface while integrating EnergyPlus into dynamic thermal modeling. However, it lacks built-in multi-objective optimization capabilities, requiring researchers to integrate external optimization algorithms such as NSGA-II or Python-based solvers, which increase implementation complexity. These factors collectively hinder the feasibility of physics-based methods in optimizing both energy consumption and occupant comfort for ATBs. In contrast, data-driven methods, while highly dependent on data accuracy, have demonstrated high adaptability in optimizing both energy performance and occupant comfort. Given their effectiveness in handling complex multi-objective problems, this approach has shown promising potential in ATB and other large-scale building applications.

Future Research Directions

The primary focus of this review was energy efficiency and comfort performance of ATB. This was achieved by analysing the research methods, evaluated parameters, and energy savings capacity. For future research, recommend the following strategies:

- Most studies highlight that indoor lighting systems have a relatively higher energy demand and that these systems can indirectly help other systems, particularly HVAC systems, reduce cooling loads, and improve indoor thermal comfort. It is worth noting that none of the reviewed studies examined the energy demand and comfort performance of ATB from an indoor lighting conditions perspective. Therefore, future research directions should focus on addressing lighting as a crucial research point for improving energy efficiency and comfort level.
- Because of the design features of ATBs, the facade frequently uses larger-sized glass materials, which usually trigger interior over-illumination during the day, resulting in energy waste and visual discomfort. Therefore, the ATB window-to-wall ratio is worth considering for further research.
- Nowadays, research on ATB energy issues primarily focuses on enhancing energy efficiency while simultaneously improving occupant comfort. However, this topic has only gained wide attention in the last 5 years, which has led to limitations in research methods. Future research could delve into the application of swarm intelligence techniques, specifically Gray Wolf Optimize, given the limited usage of this method in ATB, as suggested by previous findings.
- Currently, research on ATB energy issues primarily focuses on enhancing energy efficiency while improving occupant comfort. However, as this field has gained attention only in the past five years, research methodologies still face limitations, particularly in data availability, model scalability, and evaluation consistency.

Physics-based models offer high interpretability but are computationally intensive, while data-driven approaches are adaptable yet reliant on extensive, high-quality datasets. Future research could explore hybrid modelling approaches that integrate machine learning with physics-based simulations, leveraging both computational efficiency and interpretability. For example, machine learning could assist in parameter tuning and anomaly detection, while physics-based models refine energy flow and occupant behaviour simulations.

- Future research should focus on enhancing data acquisition and real-time monitoring technologies to address the challenges of optimizing energy performance and occupant comfort in ATBs. Given the complexity of ATBs, including their large spatial scale, dynamic occupant behaviour, and multi-system interactions, ensuring the availability of high-resolution, real-time data remains a key challenge. Advancements in IoT-based sensor networks and digital twin technology could enable more precise environmental monitoring. At the same time, AI-driven analytics, such as deep learning and reinforcement learning, can enhance predictive modelling and adaptive control strategies. These developments will be essential in refining data-driven optimization approaches, ultimately improving both energy efficiency and occupant comfort in ATBs and other large-scale buildings.

CONCLUSION

Optimizing energy performance in buildings, especially in ATBs, requires a focus on reducing energy demand and enhancing occupant comfort levels. This study addresses the lack of a review paper focusing on ATB energy performance. Upon adopting a few inclusion and exclusion criteria, 63 research papers spanning 2003–2024 were analyzed and reviewed, with > 50% of the publications emerging within the last 5 years. Further details regarding the conclusions of this study are as follows.

- Bibliometric analysis: Among the reviewed papers, > 55% emerged within the last 5 years, signifying a marked increase in scholarly interest in the energy performance of ATBs; China had the highest number of authors contributing to the reviewed papers, and currently, in the research of ATB energy performance areas, research has mainly concentrated on cooling load and thermal comfort.
- Systematic review: Indoor cooling systems emerged as the predominant factor (68%), with a primary focus on enhancing energy efficiency and thermal comfort; while the evaluation of other systems, such as lighting and acoustic systems, was also aimed at improving the energy efficiency of ATBs, they represented a smaller proportion of the studies (11%).

Studies on the energy performance of ATBs predominantly employed data-driven approaches (49%) because these approaches are easier to compute and better suited for handling nonlinearities than physics-based approaches. Optimal intelligent controls (e.g., MPC) have been widely used in this context.

The parameters evaluated for energy performance indicators mainly focused on three aspects of ATBs: air temperature, passenger flow, and cooling load. According to the systematic review analysis and observed trends in ATB energy performance optimization, significant emphasis was placed on increasing energy efficiency while simultaneously providing thermal comfort based on passenger distribution during the cooling season.

ACKNOWLEDGEMENTS

The authors would like to express sincere gratitude to the School of Housing, Building, and Planning, Universiti Sains Malaysia, Malaysia, for the invaluable support in completing this work.

REFERENCES

Abdallah, A. S. H., Makram, A., & Nayel, M. A. -A. (2021). Energy audit and evaluation of indoor environment condition inside Assiut International Airport terminal building, Egypt. *Ain Shams Engineering Journal*, *12*(3), 3241–3253. https://doi.org/10.1016/j.asej.2021.03.003

American Society of Heating, Refrigerating and Air-Conditioning Engineers. (2017). *ASHRAE Standard 55: Thermal environmental conditions for human occupancy. ASHRAE.*

Ahn, J., & Cho, S. (2015). Energy performance benchmark model for airport terminal buildings. In *Proceedings of Building Simulation 2015: 14th International Conference of the International Building Performance Simulation Association (pp. 2515-2522)*. International Building Performance Simulation Association. https://doi.org/10.26868/25222708.2015.3074

Akyüz, M. K., Kafali, H., & Altuntaş, Ö. (2021a). Investigation of indoor air quality and thermal comfort condition in airport terminal buildings. *Aircraft Engineering and Aerospace Technology: An International Journal*, *93*(1), 25-34. https://doi.org/10.1108/AEAT-06-2020-0118

Akyüz, M. K., Kafalı, H., & Altuntaş, Ö. (2021b). An analysis on energy performance indicator and GWP at airports: A case study. *Energy Sources, Part A: Recovery, Utilization and Environmental Effects*, *43*(19), 2402-2418. https://doi.org/10.1080/15567036.2020.1761483

Ala'raj, M., Radi, M., Abbod, M. F., Majdalawieh, M., & Parodi, M. (2022). Data-driven based HVAC optimisation approaches: A systematic literature review. *Journal of Building Engineering*, *46*, 103678. https://doi.org/10.1016/j.jobe.2021.103678

Balaras, C. A., Dascalaki, E., Gaglia, A., & Droutsa, K. (2003). Energy conservation potential, HVAC installations and operational issues in Hellenic airports. *Energy and Buildings*, *35*(11), 1105-1120. https://doi.org/10.1016/j.enbuild.2003.09.006

Chen, B., Yang, W., Yan, B., & Zhang, K. (2024). An advanced airport terminal cooling load forecasting model integrating SSA and CNN-Transformer. *Energy and Buildings*, *309*, 114000. https://doi.org/10.1016/j.enbuild.2024.114000

Chen, Z., Pan, W., Liao, Z., & Du, J. (2023). Research on intelligent light control system of terminal building based on human detection and path planning. In *6th International Conference on Artificial Intelligence and Big Data* (pp. 357-362). IEEE. https://doi.org/10.1109/ICAIBD57115.2023.10206131

da Costa, W. S., Monteiro, P. R. D., Fortes, M. Z., Colombini, A. C., & de Oliveira, C. M. (2022). Recommissioning methodology for the evaluation of airport air conditioning systems. *Proceedings of Institution of Civil Engineers - Energy*, *176*(3), 142-153. https://doi.org/10.1680/jener.21.00119

Dai, M. H., Zhou, Z. P., & Xue, X. (2012). Test and energy consumption analysis of air-conditioning systems in terminal building of Guilin Liangjiang International Airport. *Applied Mechanics and Materials*, *170-173*, 2652-2656. https://doi.org/10.4028/www.scientific.net/AMM.170-173.2652

Danjuma Mambo, A., Efthekhari, M., & Thomas, S. (2012). Fuzzy supervisory control strategies to minimise energy use of airport terminal buildings. In *18th International Conference on Automation and Computing: Integration of Design and Engineering* (pp. 1-6). IEEE.

Delzendeh, E., Wu, S., Lee, A., & Zhou, Y. (2017). The impact of occupants' behaviours on building energy analysis: A research review. *Renewable and Sustainable Energy Reviews*, *80*, 1061-1071. https://doi.org/10.1016/j.rser.2017.05.264

de Dear, R. J., & Brager, G. S. (2002). Thermal comfort in naturally ventilated buildings: Revisions to ASHRAE Standard 55. *Energy and Buildings*, *34*(6), 549-561. https://doi.org/10.1016/s0378-7788(02)00005-1

Dong, Z., Zhang, L., Yang, Y., Li, Q., & Huang, H. (2021). Numerical study on coupled operation of stratified air distribution system and natural ventilation under multi-variable factors in large space buildings. *Energies*, *14*(23), 8130. https://doi.org/10.3390/en14238130

Esmaeilzadeh, A., Deal, B., Yousefi-Koma, A., & Zakerzadeh, M. R. (2023). How combination of control methods and renewable energies leads a large commercial building to a zero-emission zone - A case study in U.S. *Energy*, *263*(Part D), 125944. https://doi.org/10.1016/j.energy.2022.125944

Faizah, F., Suhanto., Kustori., & Utomo, S. B. (2021). Fuzzy logic for lighting system in eco airport passenger waiting room. *Journal of Physics: Conference Series (Vol. 1845*, No. 1, p. 012050). IOP Publishing. https://doi.org/10.1088/1742-6596/1845/1/012050

Falvo, M. C., Santi, F., Acri, R., & Manzan, E. (2015). Sustainable airports and NZEB: The real case of Rome International Airport. In *15th International Conference on Environment and Electrical Engineering* (pp. 1492-1497). IEEE. https://doi.org/10.1109/EEEIC.2015.7165392

Gowreesunker, L., & Tassou, S. (2013). A TRNSYS-Fluent coupled simulation of the thermal environment of an airport terminal space with a mixing and displacement air conditioning system. In *Proceedings of Building Simulations 2013: 13th Conference of the International Building Performance Simulation Association* (pp. 1568-1575). International Building Performance Simulation Association. https://doi.org/10.26868/25222708.2013.999

Gu, X., Xie, J., Huang, C., & Liu, J. (2022). A spatiotemporal passenger distribution model for airport terminal energy simulation. *Indoor and Built Environment*, *31*(7), 1834-1857. https://doi.org/10.1177/1420326X221074222

Gu, X., Xie, J., Huang, C., Ma, K., & Liu, J. (2022). Prediction of the spatiotemporal passenger distribution of a large airport terminal and its impact on energy simulation. *Sustainable Cities and Society*, *78*, 103619. https://doi.org/10.1016/j.scs.2021.103619

Hu, R., Wang, H., & Li, Y. (2022). Study on human thermal comfort in asymmetric radiant heat environment in large space. *E3S Web of Conferences (Vol. 350*, p. 01015). EDP Sciences. https://doi.org/10.1051/e3sconf/202235001015

Huang, H., Chen, L., & Hu, E. (2014). Model predictive control for energy-efficient buildings: An airport terminal building study. In *11th IEEE International Conference on Control and Automation* (pp. 1025-1030). IEEE. https://doi.org/10.1109/ICCA.2014.6871061

Huang, H., Chen, L., & Hu, E. (2015). A new model predictive control scheme for energy and cost savings in commercial buildings: An airport terminal building case study. *Building and Environment*, *89*, 203-216. https://doi.org/10.1016/j.buildenv.2015.01.037

Huang, Y., Jia, X., Zhu, Y., Zhang, D., & Lin, B. (2021). Research on indoor spaces and passenger satisfaction with terminal buildings in China. *Journal of Building Engineering, 43*, 102873. https://doi.org/10.1016/j.jobe.2021.102873

International Air Transport Association. (2025). *Net zero 2050: Operational and infrastructure improvements*. IATA. https://www.iata.org/en/iata-repository/pressroom/fact-sheets/fact-sheet-netzero-operations-infrastructure/

International Energy Agency. (2021). *Net zero by 2050: A roadmap for the global energy sector*. IEA. https://www.iea.org/reports/net-zero-by-2050

International Energy Agency. (2023). *Buildings*. IEA. https://www.iea.org/energy-system/buildings

Jia, X., Cao, B., & Zhu, Y. (2022). A climate chamber study on subjective and physiological responses of airport passengers from walking to a sedentary status in summer. *Building and Environment, 207*, 108547. https://doi.org/10.1016/j.buildenv.2021.108547

Jia, X., Huang, Y., Cao, B., Zhu, Y., & Wang, C. (2021). Field investigation on thermal comfort of passengers in an airport terminal in the severe cold zone of China. *Building and Environment*, *189*, 107514. https://doi.org/10.1016/j.buildenv.2020.107514

Jia, X., Wang, J., Zhu, Y., Ji, W., & Cao, B. (2022a). Climate chamber study on thermal comfort of walking passengers at different moving speeds. *Building and Environment*, *224*, 109540. https://doi.org/10.1016/j.buildenv.2022.109540

Jia, X., Wang, J., Zhu, Y., Ji, W., & Cao, B. (2022b). Climate chamber study on thermal comfort of walking passengers with elevated ambient air velocity. *Building and Environment*, *218*, 109100. https://doi.org/10.1016/j.buildenv.2022.109100

Jiying, L. (2015). A numerical study of the indoor thermal environment in an air-conditioned large space building. In *8th International Conference on Intelligent Computation Technology and Automation* (pp. 69–72). IEEE. https://doi.org/10.1109/ICICTA.2015.26

Kim, S.-C., Shin, H.-I., & Ahn, J. (2020). Energy performance analysis of airport terminal buildings by use of architectural, operational information, and benchmark metrics. *Journal of Air Transport Management, 83*, 101762. https://doi.org/10.1016/j.jairtraman.2020.101762

Kotopouleas, A., & Nikolopoulou, M. (2016). Thermal comfort conditions in airport terminals: Indoor or transition spaces? *Building and Environment, 99*, 184–199. https://doi.org/10.1016/j.buildenv.2016.01.021

Kotopouleas, A., & Nikolopoulou, M. (2018). Evaluation of comfort conditions in airport terminal buildings. *Building and Environment*, *130*, 162–178. https://doi.org/10.1016/j.buildenv.2017.12.031

Lau, T. C. W., Dally, B. B., & Arjomandi, M. (2011). The application of a dynamic thermal model for the assessment of the energy efficiency of Adelaide Airport Terminal 1. In *Proceedings of Building Simulation 2011: 12th Conference of the International Building Performance Simulation Association* (pp. 1607–1614). International Building Performance Simulation Association. https://doi.org/10.26868/25222708.2011.1537

Li, B., Zhang, W., Wang, J., Xu, J., & Su, J. (2017). Research and analysis on energy consumption features of civil airports. *IOP Conference Series: Earth and Environmental Science (Vol. 94,* **No. 1, p. 012134). IOP Publishing.** https://doi.org/10.1088/1755-1315/94/1/012134

Li, X., & Zhao, Y. (2023). Evaluation of sound environment in departure lounges of a large hub airport. *Building and Environment, 232*, 110046. https://doi.org/10.1016/j.buildenv.2023.110046

Li, Z., Zhang, J., & Mu, S. (2023). Passenger spatiotemporal distribution prediction in airport terminals based on insect intelligent building architecture and its contribution to fresh air energy saving. *Sustainable Cities and Society*, *97*, 104772. https://doi.org/10.1016/j.scs.2023.104772

Lin, L., Chen, G., Liu, X., Liu, X., & Zhang, T. (2023). Characterizing cooling load in multi-area airport terminal buildings: Clustering and uncertainty analysis for energy flexibility. *Journal of Building Engineering*, *79*, 107797. https://doi.org/10.1016/j.jobe.2023.107797

Lin, L., Li, L., Liu, X., Zhang, T., Liu, X., Wei, Q., Gao, X., Wang, T., Tu, S., Zhu, S., Zou, W., & Qu, H. (2019). Performance investigation of indoor thermal environment and air handling unit in a hub airport terminal. *E3S Web of Conferences* (Vol. 111, p. 01024). EDP Sciences. https://doi.org/10.1051/e3sconf/201911101024

Lin, L., Liu, X., Zhang, T., Liu, X., & Rong, X. (2021). Cooling load characteristic and uncertainty analysis of a hub airport terminal. *Energy and Buildings, 231*, 110619. https://doi.org/10.1016/j.enbuild.2020.110619

Liu, X., Li, L., Liu, X., Zhang, T., Rong, X., Yang, L., & Xiong, D. (2018). Field investigation on characteristics of passenger flow in a Chinese hub airport terminal. *Building and Environment*, *133*, 51–61. https://doi.org/10.1016/j.buildenv.2018.02.009

Liu, X., Li, L., Liu, X., & Zhang, T. (2019). Analysis of passenger flow and its influences on HVAC systems: An agent-based simulation in a Chinese hub airport terminal. *Building and Environment*, *154*, 55–67. https://doi.org/10.1016/j.buildenv.2019.03.011

Liu, X., Liu, X., Zhang, T., & Li, L. (2021). An investigation of the cooling performance of air-conditioning systems in seven Chinese hub airport terminals. *Indoor and Built Environment*, *30*(2), 229–244. https://doi.org/10.1177/1420326X19891645

Liu, X., Zhang, T., Liu, X., Li, L., Lin, L., & Jiang, Y. (2021). Energy saving potential for space heating in Chinese airport terminals: The impact of air infiltration. *Energy*, *215*(Part B), 119175. https://doi.org/10.1016/j.energy.2020.119175

Ma, K., Wang, D., Sun, Y., Wang, W., & Gu, X. (2024). Model predictive control for thermal comfort and energy optimization of an air handling unit system in airport terminals using occupant feedback. *Sustainable Energy Technologies and Assessments*, *65*, 103790. https://doi.org/10.1016/j.seta.2024.103790

Ma, K., Wang, D., Wang, W., Zhu, S., & Sun, Y. (2023). Model predictive control strategy of air conditioning system based on dynamic passenger flow: An airport terminal building case study. In *Proceedings of Building Simulation: 18th Conference IBPSA* **(**pp. *3398–3405)*. International Building Performance Simulation Association. https://doi.org/10.26868/25222708.2023.1429

Malik, K. (2017). Assessment of energy consumption pattern and energy conservation potential at Indian airports. *Journal of Construction in Developing Countries*, *22*(Supp. 1), 97-119. https://doi.org/10.21315/jcdc2017.22.supp1.6

Mary Reena, K. E., Mathew, A. T., & Jacob, L. (2018). A flexible control strategy for energy- and comfort-aware HVAC in large buildings. *Building and Environment*, *145*, 330–342. https://doi.org/10.1016/j.buildenv.2018.09.016

Mendes, V. F., Cruz, A. S., Gomes, A. P., & Mendes, J. C. (2024). A systematic review of methods for evaluating the thermal performance of buildings through energy simulations. *Renewable and Sustainable Energy Reviews*, *189*(Part A), 113875. https://doi.org/10.1016/j.rser.2023.113875

Meng, Q., Li, Q., Zhao, L., Li, L., Chen, Z., Chen, Y., & Wang, S. (2009). A case study of the thermal environment in the airport terminal building under natural ventilation. *Journal of Asian Architecture and Building Engineering, 8***(1), 221-227.** https://doi.org/10.3130/jaabe.8.221

Miao, R., Yu, Y., & Audette, R. (2018). Investigation and evaluation of a horizontally bored geothermal heat pump system used in the cold climate of the U.S. *In Proceedings of the 2018 Building Performance Analysis Conference and SimBuild* (pp. 615–622). International Building Performance Simulation Association.

Page, M. J., McKenzie, J. E., Bossuyt, P. M., Boutron, I., Hoffmann, T. C., Mulrow, C. D., Shamseer, L., Tetzlaff, J. M., Akl, E. A., Brennan, S. E., Chou, R., Glanville, J., Grimshaw, J. M., Hróbjartsson, A., Lalu, M. M., Li, T., Loder, E. W., Mayo-Wilson, E., McDonald, S., … Moher, D. (2021). The PRISMA 2020 statement: An updated guideline for reporting systematic reviews. *BMJ***,** *372*, n71. https://doi.org/10.1136/bmj.n71

Pasaribu, M. T. T., Arvanda, E., & Kusuma, N. R. (2019). Active waiting: Potentials of waiting area at airport. *IOP Conference Series: Materials Science and Engineering (Vol. 523,* No. 1, p. 012058). IOP Publishing. https://doi.org/10.1088/1757-899X/523/1/012058

Perdamaian, L. G., Budiarto, R., & Ridwan, M. K. (2013). Scenarios to reduce electricity consumption and CO_2 emission at Terminal 3 Soekarno-Hatta International Airport. *Procedia Environmental Sciences, 17*, 576-585. https://doi.org/10.1016/j.proenv.2013.02.073

Rupcic, L., Pierrat, E., Saavedra-Rubio, K., Thonemann, N., Ogugua, C., & Laurent, A. (2023). Environmental impacts in the civil aviation sector: Current state and guidance. *Transportation Research Part D: Transport and Environment*, *119*, 103717. https://doi.org/10.1016/j.trd.2023.103717

Shafei, M. A. R., Tawfik, M. A., & Ibrahim, D. K. (2020). Fuzzy control scheme for energy efficiency and demand management in airports using 3D simulator. *Indonesian Journal of Electrical Engineering and Computer Science*, *20*(2), 583–592. https://doi.org/10.11591/ijeecs.v20.i2.pp583-592

Shafei, M., Tawfik, M., & Khalil, D. (2019). Improving energy efficiency in Egyptian airports: A case study of Sharm-Elshiekh Airport. *In 21st International Middle East Power Systems Conference* (pp. 289–294). IEEE. https://doi.org/10.1109/MEPCON47431.2019.9008220

Sinha, K., Ali, N., & Elangovan, R. (2019). An agent-based dynamic occupancy schedule model for prediction of HVAC energy demand in an airport terminal building. In *Proceedings of Building Simulation 2019: 16th Conference of IBPSA* (pp. 2063-2070). International Building Performance Simulation Association. https://doi.org/10.26868/25222708.2019.211133

Sun, Y., Wang, S., Cui, B., & Yim, M. S. C. (2013). Energy performance enhancement of Hong Kong International Airport through chilled water system integration and control optimization. *Applied Thermal Engineering*, *60*(1–2), 303–315. https://doi.org/10.1016/j.applthermaleng.2013.06.025

Tang, H., Yu, J., Geng, Y., Wang, Z., Liu, X., Huang, Z., & Lin, B. (2023). Unlocking ventilation flexibility of large airport terminals through an optimal CO_2-based demand-controlled ventilation strategy. *Building and Environment*, *244*, 110808. https://doi.org/10.1016/j.buildenv.2023.110808

Wang, Y. (2014). The application of i-bus intelligent lighting control system in the terminal of Wuhan Tianhe International Airport. In W. Wang (Ed.), *Mechatronics and Automatic Control Systems: Proceedings of the 2013 International Conference on Mechatronics and Automatic Control Systems (Vol. 237*, pp. 393-400). Springer. https://doi.org/10.1007/978-3-319-01273-5_43

Weng, J., Zhao, K., & Ge, J. (2017). Field measurement and numerical simulation of air infiltration from entrances in an airport in winter. *Procedia Engineering, 205*, 2655–2661. https://doi.org/10.1016/j.proeng.2017.10.215

Xianliang, G., Jingchao, X., Zhiwen, L., & Jiaping, L. (2021). Analysis to energy consumption characteristics and influencing factors of terminal building based on airport operating data. *Sustainable Energy Technologies and Assessments*, *44*, 101034. https://doi.org/10.1016/j.seta.2021.101034

Xu, R., Liu, X., Liu, X., & Zhang, T. (2024). Quantifying the energy flexibility potential of a centralized air-conditioning system: A field11 test study of hub airports. *Energy*, *298*, 131313. https://doi.org/10.1016/j.energy.2024.131313

Yan, B., Yang, W., He, F., Huang, K., Zeng, W., Zhang, W., & Ye, H. (2022). Strategical district cooling system operation in hub airport terminals: A research focusing on COVID-19 pandemic impact. *Energy*, *255*, 124478. https://doi.org/10.1016/j.energy.2022.124478

Yang, L., Chen, Z., & Zhen, M. (2024). Effects of thermal-acoustic interaction on airport terminal's indoor thermal comfort: A case study in cold region of China. *Journal of Building Engineering*, *86*, 108834. https://doi.org/10.1016/j.jobe.2024.108834

Yang, Y., Geng, Y., Tang, H., Yuan, M., Yu, J., & Lin, B. (2024). Extraction method of typical IEQ spatial distributions based on low-rank sparse representation and multi-step clustering. *Building Simulation*, *17*, 983-1006. https://doi.org/10.1007/s12273-024-1117-6

Yaramasu, V., & Wu, B. (2017). *Model predictive control of wind energy conversion systems*. Wiley. https://doi.org/10.1002/9781119082989

Yıldız, Ö. F., Yılmaz, M., & Çelik, A. (2021). Energy analysis of cold climate region airports: A case study for airport terminal in Erzurum, Turkey. *International Journal of Sustainable Aviation*, *7*(1), 66–92. https://doi.org/10.1504/IJSA.2021.115343

Yıldız, Ö. F., Yılmaz, M., & Çelik, A. (2022). Reduction of energy consumption and CO_2 emissions of HVAC system in airport terminal buildings. *Building and Environment*, *208*, 108632. https://doi.org/10.1016/j.buildenv.2021.108632

Yue, B., Su, B., Xiao, F., Li, A., Li, K., Li, S., Yan, R., Lian, Q., Li, A., Li, Y., Fang, X., & Liang, X. (2023). Energy-oriented control retrofit for existing HVAC system adopting data-driven MPC – Methodology, implementation and field test. *Energy and Buildings*, *295*, 113286. https://doi.org/10.1016/j.enbuild.2023.113286

Zhang, Y., Si, P., Feng, Y., Rong, X., Wang, X., & Zhang, Y. (2017). Operation strategy optimization of BCHP system with thermal energy storage: A case study for airport terminal in Qingdao, China. *Energy and Buildings*, *154*, 465-478. https://doi.org/10.1016/j.enbuild.2017.08.059

APPENDIX

List of papers included in the systematic review

	Year	Country	Doc type		Focus area		Method				Title	References
			Article	Conference	Energy	Comfort	Field test	Questionnaire	Experiment	Data-driven	Physical-based		
1	2024	China	✓		✓					✓		An advanced airport terminal cooling load forecasting model integrating SSA and CNN-Transformer	B. Chen et al. (2024)
2	2024	China	✓			✓	✓	✓				Effects of thermal-acoustic interaction on airport terminal's indoor thermal comfort: A case study in cold region of China	L. Yang et al. (2024)
3	2024	China	✓			✓	✓	✓				Extraction method of typical IEQ spatial distributions based on low-rank sparse representation and multi-step clustering	Y. Yang et al. (2024)
4	2024	China	✓		✓	✓				✓		Model predictive control for thermal comfort and energy optimization of an air handling unit system in airport terminals using occupant feedback	Ma et al. (2024)
5	2024	China	✓		✓						✓	Quantifying the energy flexibility potential of a centralized air-conditioning system: A field test study of hub airports	Xu et al. (2024)
6	2023	China	✓		✓					✓		Characterizing cooling load in multi-area airport terminal buildings: Clustering and uncertainty analysis for energy flexibility	Lin et al. (2023)
7	2023	China	✓		✓	✓				✓		Energy-oriented control retrofit for existing HVAC system adopting data-driven MPC – Methodology, implementation and field test	Yue et al. (2023)
8	2023	China	✓			✓	✓	✓				Evaluation of sound environment in departure lounges of a large hub airport	Z. Li et al. (2023)
9	2023	China		✓	✓	✓				✓		Model predictive control strategy of air conditioning system based on dynamic passenger flow: An airport terminal building case study	Ma et al. (2023)
10	2023	China	✓		✓					✓		Passenger spatiotemporal distribution prediction in airport terminals based on insect intelligent building architecture and its contribution to fresh air energy saving	Z. Li et al. (2023)
11	2023	China		✓	✓					✓		Research on intelligent light control system of terminal building based on human detection and path planning	Z. Chen et al. (2023)

12	2023	China	✓		✓				✓		Unlocking ventilation flexibility of large airport terminals through an optimal CO_2-based demand-controlled ventilation strategy	Tang et al. (2023)
13	2023	United States	✓		✓	✓			✓		How combination of control methods and renewable energies leads a large commercial building to a zero-emission zone – A case study in U.S.	Esmaeilzadeh et al. (2023)
14	2022	China	✓			✓		✓			A climate chamber study on subjective and physiological responses of airport passengers from walking to a sedentary status in summer	Jia et al. (2022)
15	2022	China	✓		✓					✓	A spatiotemporal passenger distribution model for airport terminal energy simulation	Gu, Xie, Huang, and Liu (2022)
16	2022	China	✓			✓		✓			Climate chamber study on thermal comfort of walking passengers at different moving speeds	Jia et al. (2022a)
17	2022	China	✓			✓		✓			Climate chamber study on thermal comfort of walking passengers with elevated ambient air velocity	Jia et al. (2022b)
18	2022	China	✓		✓					✓	Prediction of the spatiotemporal passenger distribution of a large airport terminal and its impact on energy simulation	Gu, Xie, Huang, Ma, et al. (2022)
19	2022	Brazil	✓		✓				✓		Recommissioning methodology for the evaluation of airport air conditioning systems	Costa et al. (2022)
20	2022	Turkey	✓		✓					✓	Reduction of energy consumption and CO_2 emissions of HVAC system in airport terminal buildings	Yıldız et al. (2022)
21	2022	China	✓		✓	✓			✓		Strategical district cooling system operation in hub airport terminals, a research focusing on COVID-19 pandemic impact	Yan et al. (2022)
22	2022	China		✓		✓	✓	✓			Study on human thermal comfort in asymmetric radiant heat environment in large space	Hu et al. (2022)
23	2021	Turkey	✓		✓					✓	An analysis on energy performance indicator and GWP at Airports; a case study	Akyüz et al. (2021a)
24	2021	China	✓		✓					✓	Analysis to energy consumption characteristics and influencing factors of terminal building based on airport operating data	Xianliang et al. (2021)
25	2021	Turkey	✓		✓				✓		Energy analysis of cold climate region airports: a case study for airport terminal in Erzurum, Turkey	Yıldız et al. (2021)
26	2021	China	✓			✓	✓	✓			Field investigation on thermal comfort of passengers in an airport terminal in the severe cold zone of China	Jia et al. (2021)
27	2021	Indonesia		✓	✓					✓	Fuzzy logic for lighting system in eco airport passenger waiting room	Faizah et al. (2021)

28	2021	Turkey	✓			✓	✓				Investigation of indoor air quality and thermal comfort condition in airport terminal buildings	Akyüz et al. (2021b)
29	2021	China	✓			✓				✓	Numerical study on coupled operation of stratified air distribution system and natural ventilation under multi-variable factors in large space buildings	Dong et al. (2021)
30	2021	China	✓		✓				✓		An investigation of the cooling performance of air-conditioning systems in seven Chinese hub airport terminals	Liu, Liu, et al. (2021)
31	2021	China	✓		✓				✓		Cooling load characteristic and uncertainty analysis of a hub airport terminal	Lin et al. (2021)
32	2021	Egypt	✓		✓	✓				✓	Energy audit and evaluation of indoor environment condition inside Assiut International Airport terminal building, Egypt	Abdallah et al. (2021)
33	2021	China	✓		✓				✓		Energy saving potential for space heating in Chinese airport terminals: The impact of air infiltration	Liu, Zhang, et al. (2021)
34	2021	China	✓		✓	✓	✓	✓			Research on indoor spaces and passenger satisfaction with terminal buildings in China	Y. Huang et al. (2021)
35	2020	South Korea	✓		✓				✓		Energy performance analysis of airport terminal buildings by use of architectural, operational information and benchmark metrics	Kim et al. (2020)
36	2020	Egypt	✓		✓	✓			✓		Fuzzy control scheme for energy efficiency and demand management in airports using 3D simulator	Shafei et al. (2020)
37	2019	Indonesia		✓		✓	✓				Active waiting: Potentials of waiting area at airport	Pasaribu et al. (2019)
38	2019	India		✓	✓				✓		An agent-based dynamic occupancy schedule model for prediction of HVAC energy demand in an airport terminal building	Sinha et al. (2019)
39	2019	Egypt		✓	✓	✓			✓		Improving energy efficiency in Egyptian airports: A case study of Sharm-Elshiekh Airport	Shafei et al. (2019)
40	2019	China		✓		✓	✓				Performance investigation of indoor thermal environment and air handling unit in a hub airport terminal	Lin et al. (2019)
41	2019	China	✓		✓				✓		Analysis of passenger flow and its influences on HVAC systems: An agent based simulation in a Chinese hub airport terminal	Liu et al. (2019)
42	2018	India	✓		✓	✓			✓		A flexible control strategy for energy and comfort aware HVAC in large buildings	Mary Reena et al. (2018)
43	2018	United Kingdom	✓			✓	✓	✓			Evaluation of comfort conditions in airport terminal buildings	Kotopouleas et al. (2018)

44	2018	United States		✓	✓			✓	Investigation and evaluation of a horizontally bored geothermal heat pump system used in the cold climate of the U.S.	Miao et al. (2018)
45	2017	India	✓		✓			✓	Assessment of energy consumption pattern and energy conservation potential at Indian airports	Malik (2017)
46	2017	China		✓		✓		✓	Field Measurement and Numerical Simulation of Air Infiltration from entrances in an Airport in Winter	Weng et al. (2017)
47	2017	China	✓		✓			✓	Operation strategy optimization of BCHP system with thermal energy storage: A case study for airport terminal in Qingdao, China	Zhang et al. (2017)
48	2017	China		✓	✓		✓		Research and analysis on energy consumption features of civil airports	B. Li et al. (2017)
49	2016	China		✓		✓		✓	A numerical study of the indoor thermal environment in an air-conditioned large space building	Jiying (2016)
50	2016	United Kingdom	✓			✓	✓		Thermal comfort conditions in airport terminals: Indoor or transition spaces?	Kotopouleas et al. (2016)
51	2015	Australia	✓		✓	✓		✓	A new model predictive control scheme for energy and cost savings in commercial buildings: An airport terminal building case study	H. Huang et al. (2015)
52	2015	United States		✓	✓			✓	Energy performance benchmark model for airport terminal buildings	Ahn et al. (2015)
53	2015	Italy		✓	✓		✓		Sustainable airports and NZEB: The real case of Rome International Airport	Falvo et al. (2015)
54	2014	Australia		✓	✓		✓		Model predictive control for energy-efficient buildings: An airport terminal building study	H. Huang et al. (2014)
55	2014	China		✓	✓		✓		The application of i-bus intelligent lighting control system in the terminal of Wuhan Tianhe International Airport	Wang (2014)
56	2013	United Kingdom		✓	✓			✓	A TRNSYS-fluent coupled simulation of the thermal environment of an airport terminal space with a mixing and displacement air conditioning system	Gowreesunker et al. (2013)
57	2013	Indonesia		✓	✓			✓	Scenarios to reduce electricity consumption and CO_2 emission at Terminal 3 Soekarno-Hatta International Airport	Laksana Gema Perdamaian et al. (2013)
58	2013	China	✓		✓			✓	Energy performance enhancement of Hong Kong International Airport through chilled water system integration and control optimization	Sun et al. (2013)
59	2012	United Kingdom		✓	✓	✓		✓	Fuzzy supervisory control strategies to minimise energy use of airport terminal buildings	Danjuma Mambo et al. (2012)

60	2012	China		✓	✓			✓	Test and energy consumption analysis of air-conditioning systems in terminal building of Guilin LiangJiang International Airport	Dai et al. (2012)
61	2011	Australia		✓	✓			✓	The application of a dynamic thermal model for the assessment of the energy efficiency of Adelaide airport terminal	Lau et al. (2011)
62	2009	China	✓		✓			✓	A case study of the thermal environment in the airport terminal building under natural ventilation	Meng et al. (2009)
63	2003	Greece	✓		✓	✓	✓	✓	Energy conservation potential, HVAC installations and operational issues in Hellenic airports	Balaras et al. (2003)

Note.

ANN	Artificial neural network
ASHRAE	American Society of Heating, Refrigerating, and Air-Conditioning Engineers
ATB	Airport Terminal Building
BAB	Branch and bound
CAD	Computer-aided design
CIBSE	Chartered Institution of Building Services Engineers
COP	Coefficient of Performance-based Control
DDS	Dual-dimension strategy
FA	Fuzzy algorithm
FLC	Fuzzy logic control
GA	Genetic algorithm
HMPC	Hybrid model predictive control
HVAC	Heating, ventilation, and air conditioning
IEQ	Indoor Environment Quality
IES	Integrated Environmental Solutions Software
ISO	International Organization for Standardization
MBE	Mean bias error
MOT	Mathematical optimization technique
MPC	Model predictive control
OBMPC	Occupant-based model predictive control
OLS	Ordinary Least Squares Algorithm
PSO	Particle swarm optimization
RBC	Rule-based control
PMSE	Root mean square error
SBC	Scenario-based control
SLSQP	Sequential least squares programming algorithm
SR	Systematic review
SSA	Singular Spectrum Analysis
TRNSYS	Transient System Simulation Tool
U.S.	United States

REFEREES FOR THE PERTANIKA
JOURNAL OF SCIENCE & TECHNOLOGY

Vol. 33 (5) Aug. 2025

The Editorial Board of the Pertanika Journal of Science and Technology wishes to thank the following:

Abdul Halin Alfian
(UPM, Malaysia)

Ahmad Yusri Mohamad
(POLISAS, Malaysia)

Aminudin Eeydzah
(UiTM, Malaysia)

Ammayappan Lakshmanan
(NINFET, India)

Athanasios Kiourtis
(UniPi, Greece)

Bahaa El-din Helmy
(BSU, Egypt)

Bilal H. Abed-alguni
(YU, Jordan)

Cheah Wai Shiang
(UNIMAS, Malaysia)

Faradina Merican Mohd Sidik Merican
(USM, Malaysia)

Hatice Citakoglu
(ERU, Turkey)

Hazleen Anuar
(IIUM, Malaysia)

Jiang Chongwen
(CSU, China)

Jidon Janaun
(UMS, Malaysia)

Kopli Bujang
(i-CATS UC, Malaysia)

Kumar Vishal
(Battelle, USA)

Mahirah Jahari
(UPM, Malaysia)

Manjunath Shettar
(MIT, India)

Manoj Kumar Senapati
(GCEKJR, India)

Mohamad Hilmi Ibrahim
(UNIMAS, Malaysia)

Mohamed Abd Rahman
(IIUM, Malaysia)

Mohammad Junaid Khan
(MECW, India)

Mohd Azrizal Fauzi
(UiTM, Malaysia)

Muhamad Saufi Mohd Kassim
(UPM, Malaysia)

Muhammad Azzam Ismail
(AU, United Arab Emirates)

Muhd Ridzuan Mansor
(UTeM, Malaysia)

Mustafa Emienour Muzalina
(UMT, Malaysia)

Natcharee Jirukkakul
(KKU, Thailand)

Nita Merlina
(UNM, Indonesia)

Noor Mohamed Noor Hisyam
(UNIMAS, Malaysia)

Nur Arif Mortadza
(i-CATS UC, Malaysia)

Pertanika Journal of Science & Technology
Vol. 33 (5) Aug. 2025

Content

Pertanika Editorial Office, Journal Division,
Putra Science Park,
1st Floor, IDEA Tower II,
UPM-MTDC Center,
Universiti Putra Malaysia,
43400 UPM Serdang,
Selangor Darul Ehsan
Malaysia

http://www.pertanika.upm.edu.my
Email: executive_editor.pertanika@upm.edu.my
Tel. No.: +603- 9769 1622

PENERBIT UPM UNIVERSITI PUTRA MALAYSIA PRESS

http://penerbit.upm.edu.my
Email: penerbit@upm.edu.my
Tel. No.: +603- 9769 8855

e-ISSN 2231-8526